frontiers | Research Topics

Applying large animals for developmental study and disease modeling

Edited by
Yongye Huang, Jacek Z. Kubiak, Lin Yuan, Sen Wu and Feng Yue

Published in
Frontiers in Cell and Developmental Biology

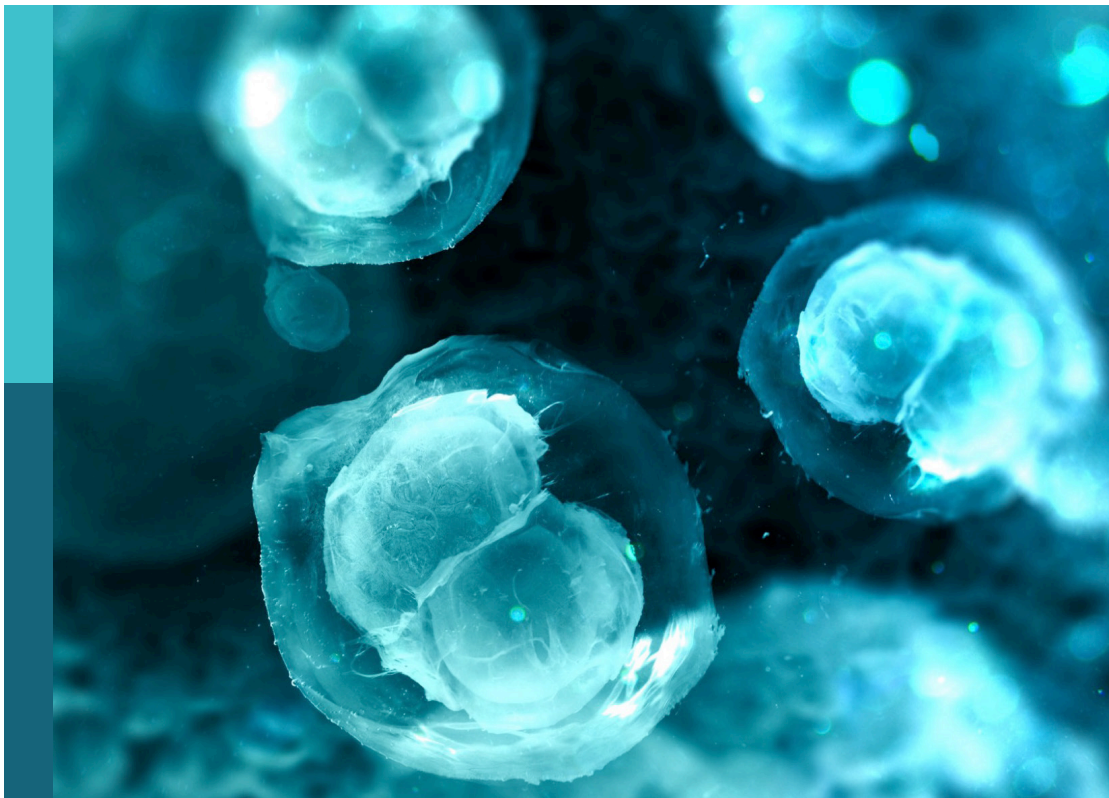

ISSN 1664-8714
ISBN 978-2-8325-2688-0
DOI 10.3389/978-2-8325-2688-0

About Frontiers

Frontiers is more than just an open access publisher of scholarly articles: it is a pioneering approach to the world of academia, radically improving the way scholarly research is managed. The grand vision of Frontiers is a world where all people have an equal opportunity to seek, share and generate knowledge. Frontiers provides immediate and permanent online open access to all its publications, but this alone is not enough to realize our grand goals.

Frontiers journal series

The Frontiers journal series is a multi-tier and interdisciplinary set of open-access, online journals, promising a paradigm shift from the current review, selection and dissemination processes in academic publishing. All Frontiers journals are driven by researchers for researchers; therefore, they constitute a service to the scholarly community. At the same time, the *Frontiers journal series* operates on a revolutionary invention, the tiered publishing system, initially addressing specific communities of scholars, and gradually climbing up to broader public understanding, thus serving the interests of the lay society, too.

Dedication to quality

Each Frontiers article is a landmark of the highest quality, thanks to genuinely collaborative interactions between authors and review editors, who include some of the world's best academicians. Research must be certified by peers before entering a stream of knowledge that may eventually reach the public - and shape society; therefore, Frontiers only applies the most rigorous and unbiased reviews. Frontiers revolutionizes research publishing by freely delivering the most outstanding research, evaluated with no bias from both the academic and social point of view. By applying the most advanced information technologies, Frontiers is catapulting scholarly publishing into a new generation.

What are Frontiers Research Topics?

Frontiers Research Topics are very popular trademarks of the *Frontiers journals series*: they are collections of at least ten articles, all centered on a particular subject. With their unique mix of varied contributions from Original Research to Review Articles, Frontiers Research Topics unify the most influential researchers, the latest key findings and historical advances in a hot research area.

Find out more on how to host your own Frontiers Research Topic or contribute to one as an author by contacting the Frontiers editorial office: frontiersin.org/about/contact

Applying large animals for developmental study and disease modeling

Topic editors

Yongye Huang — Northeastern University, China
Jacek Z. Kubiak — UMR6290 Institut de Genetique et Developpement de Rennes (IGDR), France
Lin Yuan — China Medical University, China
Sen Wu — China Agricultural University, China
Feng Yue — Hainan University, China

Citation

Huang, Y., Kubiak, J. Z., Yuan, L., Wu, S., Yue, F., eds. (2023). *Applying large animals for developmental study and disease modeling*. Lausanne: Frontiers Media SA.
doi: 10.3389/978-2-8325-2688-0

Table of contents

frontiers | Frontiers in Cell and Developmental Biology

TYPE Editorial
PUBLISHED 30 May 2023
DOI 10.3389/fcell.2023.1225060

OPEN ACCESS

EDITED AND REVIEWED BY
Valerie Kouskoff,
The University of Manchester,
United Kingdom

*CORRESPONDENCE
Lin Yuan,
lyuan@cmu.edu.cn
Feng Yue,
fyuee@hotmail.com
Jacek Z. Kubiak,
jacek.kubiak@univ-rennes1.fr
Sen Wu,
swu@cau.edu.cn
Yongye Huang,
huangyongye88@163.com

RECEIVED 18 May 2023
ACCEPTED 24 May 2023
PUBLISHED 30 May 2023

CITATION
Yuan L, Yue F, Kubiak JZ, Wu S and Huang Y (2023), Editorial: Applying large animals for developmental study and disease modeling.
Front. Cell Dev. Biol. 11:1225060.
doi: 10.3389/fcell.2023.1225060

Editorial: Applying large animals for developmental study and disease modeling

Lin Yuan[1]*, Feng Yue[2]*, Jacek Z. Kubiak[3,4]*, Sen Wu[5,6]* and Yongye Huang[7]*

[1]Laboratory of Research in Parkinson's Disease and Related Disorders, Health Sciences Institute, China Medical University, Shenyang, China, [2]Key Laboratory of Biomedical Engineering of Hainan Province, School of Biomedical Engineering, Hainan University, Haikou, China, [3]Faculty of Medicine, Dynamics and Mechanics of Epithelia Group, CNRS, Institute of Genetics and Development of Rennes (IGDR), University Rennes, Rennes, France, [4]Laboratory of Molecular Oncology and Innovative Therapies, Military Institute of Medicine (WIM-PIB), Warsaw, Poland, [5]State Key Laboratory of Animal Biotech Breeding, College of Biological Sciences, China Agricultural University, Beijing, China, [6]Sanya Institute of China Agricultural University, Sanya, China, [7]Key Laboratory of Bioresource Research and Development of Liaoning Province, College of Life and Health Sciences, Northeastern University, Shenyang, China

KEYWORDS

gene editing, CRISPR/Cas9, embryo, development, pig, rabbit, monkey

Editorial on the Research Topic
Applying large animals for developmental study and disease modeling

Introduction

We have a great pleasure to organize the Research Topic "Applying large Animals for Developmental Study and Disease Modeling". It is well known that large animals show similarities in many physical and pathological characteristics with human beings and have numerous advantages in developmental and medical research. In recent years, an important breakthrough has been achieved in gene editing technique, including ZFN, TALEN, CRISPR/Cas9, and so on. Especially for the emergence of CRISPR/Cas9 mediated gene modification strategies, various types of human diseases have been recapitulated in large animal models. It has to be mentioned that the progress in establishing embryonic stem cells and inducible pluripotent stem cells is also critical for the application in diseases modeling and therapies. In our Research Topic more than ten papers have been collected, and most of them focus on pig, monkey, rabbit and horse (Figure 1).

Pig

The pig, as one of the most common livestock, exhibits several advantages in biomedical research. These are: comparable human and pig body sizes, similar anatomical and physiological characteristics, genomic composition and ordinary diets (Hou et al., 2022). It makes the pig a promising alternative animal model for humans. Rapid growth rate, early sexual maturity, short generation intervals, high number of offspring per litter, and standardized breeding techniques, also make easier the application of pigs in the study

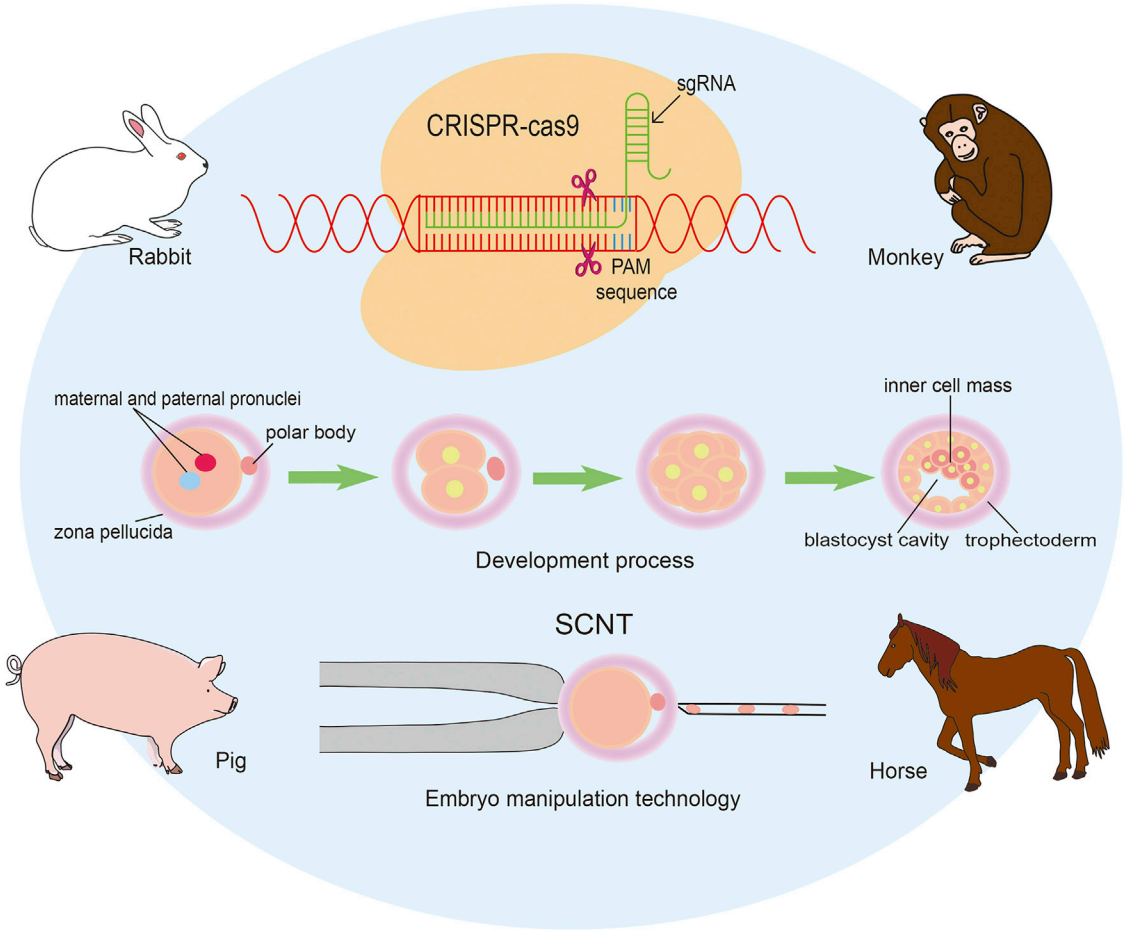

FIGURE 1
Applying genomic editing technology and somatic cell nuclear transfer to generate large animal models.

on human diseases. In recent decades, the advances in technologies contribute to the development of genetically engineered pig models of human diseases. The emergence of somatic cell nuclear transfer (SCNT) and reliable genome editing techniques make possible for the generation of porcine models of human diseases. The efficacy of porcine SCNT has been largely improved and several kinds of small molecular inhibitors have been applied to enhance the developmental competence of SCNT embryos (Ouyang et al., 2021; Hou et al., 2022). CRISPR/Cas9-mediated gene editing strategies are widely used in the establishment of porcine models of human diseases. Various genomic genetically engineered pigs have been generated, including chimeric gene knock in, point mutations, large genome fragment deletions, multifunctional live cell sensors, *etc*. One of the most promising potential application of pigs in the biomedical field is xenotransplantation. In 7 January 2022, the medical school of the University of Maryland in the United States conducted the first-ever life-saving cardiac xenotransplantation and it was successful in extending the patient's life for about 8 weeks (Rothblatt, 2022). The breakthrough sheds light on xenotransplantation using porcine organs as donors. Actually, corneas, lungs, nerve cells, kidneys, livers, and islets of pigs are also potential candidates for xenotransplantation. In the Research Topic, Junliang Li et al. evaluated the methylation status of IG-DMR and gene expression profile in the DLK1-DIO3 region (Li et al.); Lin et al. revealed that intravenous injection of AAV9-GFP could result in widespread expression of transgene in various porcine organs (Lin et al.); Hilansi Rawat et al. found that porcine expanded pluripotent stem cells could differentiate into cardiovascular progenitor cells, functional cardiomyocytes, epicardial cells and epicardial-derived cells, and they established an enhanced system for whole-embryo culture allowing *ex utero* development of porcine post-implantation embryos from ED14 up to ED17 (Hilansi et al.); and many papers review the progress of applying pigs in xenotransplantation and biomedical research.

Nonhuman primates

Nonhuman primates (NHP) emerge increasingly as excellent models for translational research, due to even closer proximity to human beings in terms of physiology, biochemistry, immunology, pathology and genetic evolution. For example, NHP models are widely used in studies on Severe Acute Respiratory Syndrome

Coronavirus 2 (SARS-CoV-2). In fact, NHP models of HIV, ZIKV or Ebola virus infection mirror closely the pathogenesis in human patients. SCNT monkeys have been successfully produced using fetal fibroblasts as donor cells in recent years (Liu et al., 2018). Furthermore, BMAL1 gene-edited monkeys via the CRISPR/Cas9 technique were generated with both intracytoplasmic sperm injection and SCNT method (Liu et al., 2019; Qiu et al., 2019). Cynomolgus monkey blastoids resembling blastocysts in morphology and transcriptomics using naive ESC develop to embryonic disk with the structures of yolk sac, amnion cavity, chorionic cavity and primitive streak via prolonged *in vitro* culture (Li et al., 2023), making it possible to investigate primate embryonic development without the same ethical concerns associated humans. Various NHP models of human diseases have been established in recent years, including bilaterally delivering synthetic Aβ oligomers into the cerebral parenchyma of cynomolgus monkeys to drive early pathological progression of Alzheimer's disease (Yue et al., 2021). However, in the near future, researchers might face monkey shortage crisis (Grimm, 2023). In the Research Topic, Liang et al. summarizes the recent progress in using genomic editing technology in the establishment of NHP models and discusses the factors limiting the wide application of NHP models of human diseases (Liang et al.).

Rabbit

Rabbit is another commonly used experimental model for investigating equivalents of human diseases. With the emergence of microinjecting, SCNT and genomic editing technology, a large number of rabbit models of human diseases were established. The pronuclear microinjection is still the most common method in the generation of transgenic rabbit models. Novel genomic editing technologies, such as CRISPR/Cas9, remarkably promote precision in rabbit genome manipulation (Song et al., 2020). In previous studies, CRISPR/Cas9 technique was applied to introduce mutation of αA-Crystallin or GJA8 gene to induce congenital cataracts in Rabbits (Yuan et al., 2016; Yuan et al., 2017). Recently, SpRY-ABEmax mediated base substitution has been used to generate YIPF5 (p.W218R) mutation to generate rabbit primary microcephaly model, which precisely recapitulate the typical symptoms of human primary microcephaly (Liu et al., 2023). With recent technological innovations in genomic editing techniques, rabbit models will certainly play a much more important role in the study on human diseases. In our Research Topic, a carrageenan-induced abdominal aortic adventitial inflammatory model in hypercholesterolemic rabbits is described (Chen et al.). It determines the role of MMP-12 secreted from adventitial macrophages in the pathogenesis of this diseases (Chen et al.).

Horse

Horses are commonly used as animal models for studying several human diseases, including neurodegenerative diseases, mental and behavioral disorders, neuropsychiatric disorders and spontaneous sepsis. Using SCNT and genomic editing technology to generate horse models of human diseases seems to be less attractive than porcine and rabbit models. However, the rapid development in horse models have been achieved in recent years. A recent report has revealed that a total of 12 SCNT foals were born (Cortez et al., 2023), and gene-edited horse embryos have been generated by CRISPR/Cas9 technology (Maniego et al., 2022). In our Research Topic, Neil Marr et al. utilized immunolabelling for CD146 to determine horse tendon cell population, providing the intrinsic evidences for the relationships between local interfascicular matrix vascular and basement membrane constituents (Marr et al.).

In conclusion, the Research Topic "Applying large Animals for Developmental Study and Disease Modeling" delivers a whole plethora of excellent examples of the fascinating progress made recently in this field of biomedical research.

Author contributions

LY and YH drafted the manuscript, YH revised the draft, FY, JK and SW made substantial contributions to the work through in-depth discussion. All authors contributed to the article and approved the submitted version.

Funding

This study was funded by the National Natural Science Foundation of China (Nos. 82201594 and 81502582). Funding was also provided by the Fundamental Research Funds for the Central Universities (N182004002 and N2220002), Natural Science Foundation of Liaoning Province (2021-MS-104, 2022-YGJC-39 and 2022-MS-228), Fundamental Scientific Research Fund of Liaoning Provincial Education Department (LJKQZ2021002), Key Laboratory of Bioresource Research and Development of Liaoning Province (2022JH13/10200026), Hainan Key Research and Development Project (ZDYF2021SHFZ049), and JK was supported by an internal grant nr. 612/2023 from Wojskowy Instytut Medyczny-Panstwowy Instytut Badawczy, Warsaw, Poland.

Acknowledgments

We would like to thank Wanlu Zhang in Northeastern University for assistance.

Conflict of interest

The authors declare that the research was conducted in the absence of any commercial or financial relationships that could be construed as a potential conflict of interest.

Publisher's note

References

Cortez, J. V., Hardwicke, K., Cuervo-Arango, J., and Grupen, C. G. (2023). Cloning horses by somatic cell nuclear transfer: Effects of oocyte source on development to foaling. *Theriogenology* 203, 99–108. Epub 2023/04/04PubMed PMID: 37011429. doi:10.1016/j.theriogenology.2023.03.018

Grimm, D. U. S. (2023). U.S., European researchers face monkey shortage crisis. *Science* 380 (6645), 567–568. Epub 2023/05/11PubMed PMID: 37167380. doi:10.1126/science.adi6512

Hou, N., Du, X., and Wu, S. (2022). Advances in pig models of human diseases. *Anim. Model Exp. Med.* 5 (2), 141–152. Epub 2022/03/29PubMed PMID: 35343091; PubMed Central PMCID: PMCPMC9043727. doi:10.1002/ame2.12223

Li, J., Zhu, Q., Cao, J., Liu, Y., Lu, Y., Sun, Y., et al. (2023). Cynomolgus monkey embryo model captures gastrulation and early pregnancy. *Cell Stem Cell* 30 (4), 362–377.e7. Epub 2023/04/08PubMed PMID: 37028403. doi:10.1016/j.stem.2023.03.009

Liu, X., Yang, J., Li, Z., Liu, R., Wu, X., Zhang, Z., et al. (2023). YIPF5 (p.W218R) mutation induced primary microcephaly in rabbits. *Neurobiol. Dis.* 182, 106135. Epub 2023/05/05PubMed PMID: 37142085. doi:10.1016/j.nbd.2023.106135

Liu, Z., Cai, Y., Liao, Z., Xu, Y., Wang, Y., Wang, Z., et al. (2019). Cloning of a gene-edited macaque monkey by somatic cell nuclear transfer. *Natl. Sci. Rev.* 6 (1), 101–108. Epub 2019/01/01PubMed PMID: 34691835; PubMed Central PMCID: PMCPMC8291622. doi:10.1093/nsr/nwz003

Liu, Z., Cai, Y., Wang, Y., Nie, Y., Zhang, C., Xu, Y., et al. (2018). Cloning of macaque monkeys by somatic cell nuclear transfer. *Cell* 174 (1), 245. Epub 2018/06/30PubMed PMID: 29958110. doi:10.1016/j.cell.2018.01.036

Maniego, J., Pesko, B., Habershon-Butcher, J., Hincks, P., Taylor, P., Tozaki, T., et al. (2022). Use of mitochondrial sequencing to detect gene doping in horses via gene editing and somatic cell nuclear transfer. *Drug Test. Anal.* 14 (8), 1429–1437. Epub 2022/04/02PubMed PMID: 35362263. doi:10.1002/dta.3267

Ouyang, H., Han, J., and Huang, Y. (2021). Pig cloning using somatic cell nuclear transfer. *Methods Mol. Biol.* 2239, 1–18. Epub 2020/11/24PubMed PMID: 33226609. doi:10.1007/978-1-0716-1084-8_1

Qiu, P., Jiang, J., Liu, Z., Cai, Y., Huang, T., Wang, Y., et al. (2019). BMAL1 knockout macaque monkeys display reduced sleep and psychiatric disorders. *Natl. Sci. Rev.* 6 (1), 87–100. Epub 2019/01/01PubMed PMID: 34691834; PubMed Central PMCID: PMCPMC8291534. doi:10.1093/nsr/nwz002

Rothblatt, M. (2022). Commentary on achievement of first life-saving xenoheart transplant. *Xenotransplantation* 29 (3), e12746. Epub 2022/04/27PubMed PMID: 35471736. doi:10.1111/xen.12746

Song, J., Zhang, J., Xu, J., Garcia-Barrio, M., Chen, Y. E., and Yang, D. (2020). Genome engineering technologies in rabbits. *J. Biomed. Res.* 35 (2), 135–147. Epub 2020/09/17PubMed PMID: 32934190; PubMed Central PMCID: PMCPMC8038526. doi:10.7555/JBR.34.20190133

Yuan, L., Sui, T., Chen, M., Deng, J., Huang, Y., Zeng, J., et al. (2016). CRISPR/Cas9-mediated GJA8 knockout in rabbits recapitulates human congenital cataracts. *Sci. Rep.* 6, 22024. Epub 2016/02/26PubMed PMID: 26912477; PubMed Central PMCID: PMCPMC4766569. doi:10.1038/srep22024

Yuan, L., Yao, H., Xu, Y., Chen, M., Deng, J., Song, Y., et al. (2017). CRISPR/Cas9-Mediated mutation of αa-crystallin gene induces congenital cataracts in rabbits. *Invest. Ophthalmol. Vis. Sci.* 58 (6), BIO34–BIO41. Epub 2017/05/06PubMed PMID: 28475701. doi:10.1167/iovs.16-21287

Yue, F., Feng, S., Lu, C., Zhang, T., Tao, G., Liu, J., et al. (2021). Synthetic amyloid-beta oligomers drive early pathological progression of Alzheimer's disease in nonhuman primates. *iScience* 24 (10), 103207. Epub 2021/10/28PubMed PMID: 34704001; PubMed Central PMCID: PMCPMC8524197. doi:10.1016/j.isci.2021.103207

frontiers | Frontiers in Cell and Developmental Biology

REVIEW
published: 17 May 2022
doi: 10.3389/fcell.2022.919155

Application of CRISPR/Cas9 System in Establishing Large Animal Models

*Yingqi Lin, Jun Li, Caijuan Li, Zhuchi Tu, Shihua Li, Xiao-Jiang Li and Sen Yan**

Guangdong Key Laboratory of Non-human Primate Research, Guangdong-Hongkong-Macau Institute of CNS Regeneration, Jinan University, Guangzhou, China

The foundation for investigating the mechanisms of human diseases is the establishment of animal models, which are also widely used in agricultural industry, pharmaceutical applications, and clinical research. However, small animals such as rodents, which have been extensively used to create disease models, do not often fully mimic the key pathological changes and/or important symptoms of human disease. As a result, there is an emerging need to establish suitable large animal models that can recapitulate important phenotypes of human diseases for investigating pathogenesis and developing effective therapeutics. However, traditional genetic modification technologies used in establishing small animal models are difficultly applied for generating large animal models of human diseases. This difficulty has been overcome to a great extent by the recent development of gene editing technology, especially the clustered regularly interspaced short palindromic repeats (CRISPR)/CRISPR-associated protein 9 (Cas9). In this review, we focus on the applications of CRISPR/Cas9 system to establishment of large animal models, including nonhuman primates, pigs, sheep, goats and dogs, for investigating disease pathogenesis and treatment. We also discuss the limitations of large animal models and possible solutions according to our current knowledge. Finally, we sum up the applications of the novel genome editing tool Base Editors (BEs) and its great potential for gene editing in large animals.

Keywords: Large animals, CRISPR/Cas9, Off-target, Mosaicism, Base editing

OPEN ACCESS

Edited by:
Yongye Huang,
Northeastern University, China

Reviewed by:
Simon Sretenovic,
University of Maryland, United States
Ming Lei,
Sun Yat-Sen Memorial Hospital, China
Desh Deepak Singh,
Amity University Rajasthan, India

****Correspondence:***
Sen Yan
231yansen@163.com

Specialty section:
This article was submitted to Stem Cell Research, a section of the journal Frontiers in Cell and Developmental Biology

Received: *13 April 2022*
Accepted: *02 May 2022*
Published: *17 May 2022*

Citation:
Lin Y, Li J, Li C, Tu Z, Li S, Li X-J and Yan S (2022) Application of CRISPR/Cas9 System in Establishing Large Animal Models. Front. Cell Dev. Biol. 10:919155. doi: 10.3389/fcell.2022.919155

INTRODUCTION

Animal models play an important role in scientific research, including the study of disease mechanisms, medicinal development and the production of agricultural products (McGonigle and Ruggeri, 2014). To create ideal animal models, researchers often genetically modify animals to achieve desirable traits. Gene-modified small rodent models, especially mice and rats, provide a large amount of experimental data and play an important role in the study of disease mechanisms as well as important biology function (Ribitsch et al., 2020). However, these small animal models also have some shortcomings. First, because of considerable differences between small animals and humans in physiological, anatomical, and genomic structures, small animal models are often unable to mimic the disease characteristics of humans, leading to the inability of researchers to fully understand the pathogenesis of diseases. This has also led to the failure of many drugs screened from small animal models in clinical trials (Prabhakar, 2012; Zhao et al., 2019). In addition, small animal models play less roles in agricultural activities, such as the production of animal by-products.

To overcome these limitations, scientists are increasingly focusing on large animal models (including non-human primates (NHPs), pigs, dogs, goats, and sheep). Large animals represented by NHPs are more ideal animal models for human diseases due to their similarities in genetics, physiology, developmental

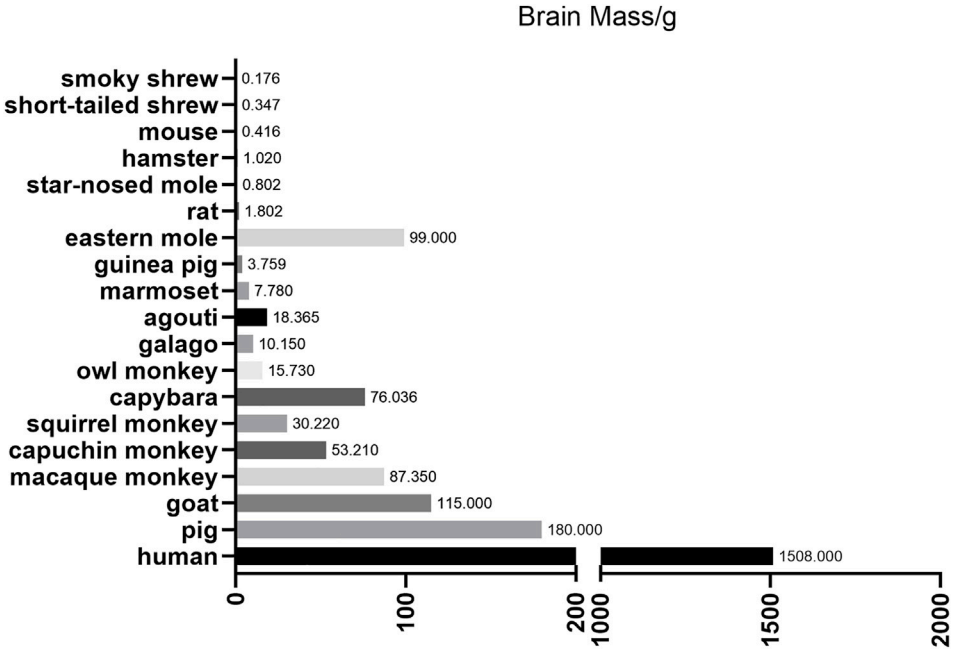

FIGURE 1 | Brain mass for different animals. This figure mainly depicts the brain mass of different large animals and small animals. Notice that large animals, such as pigs and nonhuman primates, are much closer to human beings compared with small animals to some extent.

biology, social behavior and cognition (Shen, 2013). For example, the brain mass of different species, which are depicted in **Figure 1**, are apparently very different. However, many factors, including the difficulties in genome editing, have limited the establishment of gene modified large animal models.

With the development of gene editing technology in recent twodecades, like zinc finger nucleases (ZFNs), transcription activator-like effector nucleases (TALENs) and CRISPR/Cas9, this difficulty has been overcome greatly. The ZFNs system consists of two components, including DNA-binding zinc-finger protein (ZFP) domain at the amino terminus and the Fok I nuclease cleavage domain at the carboxyl terminus. Each Fok I monomer link with a ZFP to form a ZFN that recognizes a specific site. Under certain conditions, two ZFNs can perform enzyme function of cleavage, leading to double-strand breaks (DSBs), thus mediating DNA site-specific cleavage (Durai et al., 2005; Carroll, 2011). ZFNs have been used in a variety of species, including plants, animal and mammalian cells (Carroll, 2011). However, due to the differences between large animals and small animals, it is still difficult to establish a large animal model using ZFNs(Chen et al., 2016). TALENs are gene-editing tools similar to ZFNs(Christian et al., 2010; Mussolino and Cathomen, 2012; Joung and Sander, 2013). They are also made by two structures: a transcription activator-like (TAL) effector DNA-binding domain and a DNA cleavage domain (a nuclease which cuts DNA strands). Thus, TALENs can also be designed to induce site-specific DSBs to target specific gene sequences (Yoshimi and Mashimo, 2018). Compared with ZFNs, the synthesis and design of TALENs components are simpler, so some large animal models are successfully established by TALENs strategy. For example, in 2014, researchers created methyl CpG binding protein 2 (*MECP2*) Mutant Rhesus and Cynomolgus monkeys using TALENs(Liu et al., 2014).

Although ZFNs and TALENs have greatly improved the efficiency of establishing gene editing animal models, CRISPR/Cas9 is the most popular and effective gene editing method at present. The CRISPR/Cas9 system also consists of a recognition component, small RNAs called single-guide RNAs (sgRNAs), and a cleavage component, Cas9 nuclease. CRISPR/Cas9 can target almost any loosened (non-condensed) part of the genomes through base pairing between sgRNAs and DNA as well as the recognition of protospacer adjacent motif (PAM) sequences (Jinek et al., 2012). Cas9 then cleaves the double-strand DNA at the target site to form DSBs. Subsequently, cells repair DSBs sites by non-homologous end joining (NHEJ) or homology-directed repair (HDR). The repair process can go wrong, resulting in mutations at specific genetic loci. Since the discovery of CRISPR/Cas9, researchers have rapidly implemented a series of optimizations to the system, and applied it in the establishment of gene-editing models of small animal, including mice (Wang et al., 2013), rats (Ma et al., 2014) and zebrafishes (Kim and Kim, 2014). As a result, the CRISPR/Cas9 system has greatly accelerated the research of gene editing large animal models, which is what we mainly discuss in this article.

THE APPLICATION OF CRISPR/CAS9 IN NONHUMAN PRIMATE MODELS

Undoubtedly, the nonhuman primate is the most representative animal that is capable of mimicking the human disease for the similarities in terms of genetics, physiology, developmental biology, social behaviors and cognition. However, it is really difficult to create a nonhuman primate transgenic model compared with small animals, such as the mouse because of various factors including the long breeding cycle and ethical factors. The first transgenic mouse model was built as early as 1974 (Jaenisch and Mintz, 1974), but the first genetically modified monkey model did not appear until 2001 (Chan et al., 2001). Afterwards, in 2008, Yang et al. developed a transgenic model of Huntington's disease (HD) in a rhesus macaque that expressed polyglutamine (polyQ)-expanded huntingtin protein (HTT) by injecting lentiviral vector into mature rhesus oocytes followed by fertilization through intracytoplasmic sperm injection and embryo transplantation (Yang et al., 2008). This is the first transgenic nonhuman primate disease model, which could already show some features similar to those found in HD patients, including chorea, dystonia as well as nuclear inclusion and neuropil aggregates in the brains. In the later experiment, they used the same transgenic strategy to introduce mutant huntingtin (*HTT*) genes into monkey oocytes, which also expressed exon1 of *HTT* with a 147Q tract (previous models containing a 65–88Q tract and dying soon) in transgenic monkeys (Wang et al., 2008). These HD monkeys display degeneration of axons and neuronal processes, suggesting that the disruption in axons or dendrites can lead to the neuronal degeneration in HD.

The success of transgenic monkey models of human disease and the advances in gene editing technology inspired scientists to establish genome editing monkey models. The generation of a gene-modified monkey via CRISPR/Cas9 was first reported in 2014 (Niu et al., 2014). By coinjection of Cas9 mRNA and sgRNAs into one-cell-stage embryos, researchers successfully achieved precise gene targeting in cynomolgus monkeys. They also showed that this system enabled simultaneous disruption of two target genes (peroxisome proliferator-activated receptor gamma (*PPARG*) and recombination activating gene 1 (*RAG1*) in one step without detectable off-target effects. They also demonstrated that germline transmission could happen in the Cas9-manipulated monkeys by examining gene targeting in gonads and germ cells (Chen et al., 2015a). However, the resulting transgenic monkey exhibited mosaic mutations accompanied by the presence of wild type allele in different tissues, which left an issue of whether the mosaic mutations could influence the function study. Then, Chen et al. used Cas9 to disrupt the dystrophin gene (*DMD*) in rhesus monkeys, which exhibited markedly depleted dystrophin and muscle degeneration seen in early Duchenne muscular dystrophy (DMD) (Chen et al., 2015b), indicating that CRISPR/Cas9 can efficiently generate monkey models of human diseases regardless of inheritance patterns.

Next, some experiments were conducted aimed at eliminating the mosaic mutations. Researchers showed that biallelic gene mutation can be efficiently generated in monkeys by zygote injection with an optimized Cas9/sgRNA combination in one-step (Wan et al., 2015). After optimization and innovation of the approach, Zuo et al. also showed that a single gene or multiple genes can be completely knocked out in monkey embryos by zygotic injection of Cas9 mRNA and multiple adjacent sgRNAs without mosaicism (Zuo et al., 2017). Apart from that, another research indicated that shortening the half-life of Cas9 in fertilized zygotes reduced mosaic mutations and increased its ability to modify genomes in monkey embryos (Tu et al., 2017). Following this approach, they used the Cas9/sgRNA method to disrupt SH3 and ankyrin repeat domains 3 gene (*SHANK3*) in cynomolgus monkeys, which showed altered neurogenesis and disrupted expression of synaptic proteins in the prefrontal cortex, which was not found in the mouse model (Zhao et al., 2017).

Apart from knockout animals, researchers have also attempted to obtain knock-in nonhuman primates in recent years. Yao et al. first established knock-in monkeys by homology-mediated end joining (HMEJ)-based method. However, monkeys generated by this approach showed mosaicism. Therefore, further serial crossbreeding is required to generate complete gene knock-in monkeys (Yao et al., 2018). A similar work to achieve precise *OCT4*-hr*GFP* (octamer-binding transcription factor 4-humanized recombinant green fluorescent protein) knock-in in cynomolgus monkey model was also tried via CRISPR/Cas9-assisted HR (Cui et al., 2018).

However, a genetically modified nonhuman primate is expensive to maintain and requires the facility that is only available to a small number of laboratories. Thus, researchers have tried to establish the modified embryonic stem cells (ESCs) of rhesus monkey using the CRISPR/Cas9 system, which can undergo unlimited self-renewal while maintaining the potential to give rise to all cell types (Zhu et al., 2015; Kobayashi et al., 2019). Using a dual-guide gene targeting approach, another group achieved biallelic deletions in the *CCR5* gene (C-C motif chemokine receptor 5) of cynomolgus macaque embryos (23–37%) (Schmidt et al., 2020).

Although CRISPR/Cas9 system is the most widely used strategy in the creation of large animal models nowadays, there were also nonhuman primate models using different approaches like TALENs(Liu et al., 2014; Liu et al., 2016; Chen et al., 2017). An obvious issue is the safety of the gene-editing in nonhuman primates due to potential off-target mutations. Using whole-genome sequencing to comprehensively assess on- and off-target mutations in previously produced CRISPR/Cas9 editing monkeys (Chen et al., 2015b), researchers found that CRISPR/Cas9-based gene editing is active on the expected genomic sites without producing off-target modifications in other functional regions of the genome, suggesting that the CRISPR/Cas9 technique could be relatively safe and effective in modeling genetic disease in nonhuman primates (Wang S. et al., 2018; Luo et al., 2019).

CRISPR/Cas9 editing monkeys have already shown better phenotypes in human diseases than mouse models despite a limited number of successfully established models (Seita et al., 2020; Yang et al., 2021; Yin et al., 2022). Yang et al. generated PTEN-induced kinase 1 (*PINK1*, whose mutations

cause early-onset Parkinson's disease (PD) mutant monkeys by targeting two exons in the *PINK1* gene (Yang et al., 2019a; Yang et al., 2019b), which showed remarkable neuronal loss in the cortex, substantia nigra and striatum. However, neuronal loss was not reported in *Pink1* KO mice (Kitada et al., 2007; Dawson et al., 2010) or pigs (Zhou et al., 2015; Wang et al., 2016b). Similar results were confirmed in acute monkey models created by CRISPR/Cas9 system (Li et al., 2021; Sun et al., 2022; Yang et al., 2022). In another example, Kang et al. achieved dosage-sensitive sex reversal, adrenal hypoplasia critical region, on chromosome X, gene 1 (*DAX1*) knockout in the monkey, which could recapitulate the phenotypes of human adrenal hypoplasia congenita (AHC) and hypogonadotropic hypogonadism (HH).

Nonhuman primate models of human diseases were also used for developing therapies. Tu et al. found that abnormal behaviors and brain activities of autism spectrum disorder (ASD) in the previously established monkey models (Zhao et al., 2017) were alleviated by the antidepressant fluoxetine treatment (Tu et al., 2019). This finding demonstrated that the genetically modified non-human primate can be used for translational research of therapeutics for ASD, pointing out that the nonhuman primate models of human disease have a great potential for clinical research like drug tests.

THE APPLICATION OF CRISPR/CAS9 IN PIG MODELS

The pig is also an important animal with several unique features that make it a promising alternative animal model (Prather et al., 2003). Pigs are model animals that are also close to humans (Meurens et al., 2012). Pigs and humans are extremely similar in terms of anatomy, physiology and biochemical metabolism (Roura et al., 2016). Pigs have the advantages of early sexual maturity, short reproductive cycle, high number of offspring per litter (Zou et al., 2019). Moreover, the recent development of somatic cell nuclear transfer (SCNT) technology and genome editing technology has made it possible to generate genetically modified large animals efficiently (Yang et al., 2014). The first genome editing pigs were generated in 1985 using pronuclear DNA microinjection in zygotes (Hammer et al., 1985). With the development of CRISPR/Cas9 technology, the speed of building genome-edited pig models has been greatly accelerated.

Hai et al. first showed that zygotes microinjection of the CRISPR/Cas9 system can efficiently generate genome-modified pigs in one step (Hai et al., 2014), and the mutations can be transmitted into the germline efficiently. Different researchers then reported that single- or double-gene targeted pigs can be effectively achieved by using the CRISPR/Cas9 system combined with SCNT, which avoids mosaic mutation and detectable off-target effects (Whitworth et al., 2014; Zhou et al., 2015). Also, the modification of multiple genes like triple gene-targeted pigs was feasible to be generated (Wang et al., 2016b).

Apart from knockout pigs, CRISPR/Cas system is also used to establish knock-in models that mimic human diseases. Yan et al. used CRISPR/Cas9 to insert a large CAG repeat (150 CAGs) into the endogenous pig *HTT* gene in fibroblast cells and employed the SCNT to generate a HD KI pig model expressing full-length mutant HTT at the endogenous level (Yan et al., 2018), whose brains presented severe and preferential neurodegeneration in the medium spiny neurons like HD patients. Other examples include genes or large fragment knock-in pig models (Ruan et al., 2015; Li G. et al., 2020).

Based on these successful trials in establishing knockout or knock-in animals using CRISPR/Cas9 system, a number of pig models that could recapture the features of human diseases have been created, such as 5-hydroxytryptamine (5-HT) deficiency (Li et al., 2017b), complement protein deficiency (Zhang W. et al., 2017), cardiovascular disease (Huang et al., 2017), cancer (Kang et al., 2016), type II collagenopathy (Zhang et al., 2020), and HD (Yan et al., 2018).

On the other hand, the pig is one of the most important livestock in the agriculture industry. Genetically modified pigs may offer distinct features, such as increased mass of muscle and resistance to the pathogen. As a result, researchers have made great efforts to improve the mass of muscle by using CRISPR/Cas9 system to disrupt genes that hinder the hypertrophy of muscle (Wang K. et al., 2015; Wang et al., 2017; Zou et al., 2018; Liu et al., 2019; Li R. et al., 2020) and improve the resistance to virus (Xie et al., 2020).

Apart from this, the pig is considered to be an important resource of donor organs for transplantation because of the growing demand in the xenotransplantation. A key problem after xenotransplantation is the pig-to-human immunological compatibility. Therefore, a great deal of genome editing pigs has been established to eliminate antigens leading to immunological rejection in human (Petersen et al., 2016; Chuang et al., 2017; Gao et al., 2017; Wu et al., 2017; Joanna et al., 2018). Another problem is the risk of cross-species transmission of porcine endogenous retroviruses (PERVs). Therefore, researchers inactivated all of the PERVs in a porcine primary cell line and generated PERV-inactivated pigs *via* SCNT and CRISPR/Cas9 system (Yang et al., 2015; Niu D. et al., 2017; Yue et al., 2021). These efforts were aimed to make the clinical usage of pig organs safer. Recently, a series of stunning reports have provided the first results showing the feasibility of transplanting organs from transgenic pigs into humans, including the kidney and the heart (2022; Porrett et al., 2022), which marked a great breakthrough in the clinical application.

THE APPLICATION OF CRISPR/CAS9 IN SHEEP AND GOAT MODELS

Sheep and goats have also become important model animals in biomedical research due to their suitable size and short gestation period. Like pigs, sheep and goats also play an important role in agricultural and pharmaceutical field for their meat, milk, fiber, and other by-products. Han et al. reported the successful one-step generation of gene knockout sheep using a one-step zygote injection of the CRISPR/Cas9 system by targeting the myostatin (*MSTN*) gene (Zhengxing et al., 2014), which demonstrated the feasibility of gene targeting in sheep using the CRISPR/Cas9 system at the first time. At the same year, Ni et al. showed for the first time that the CRISPR/Cas9 mediated genome editing can be efficiently

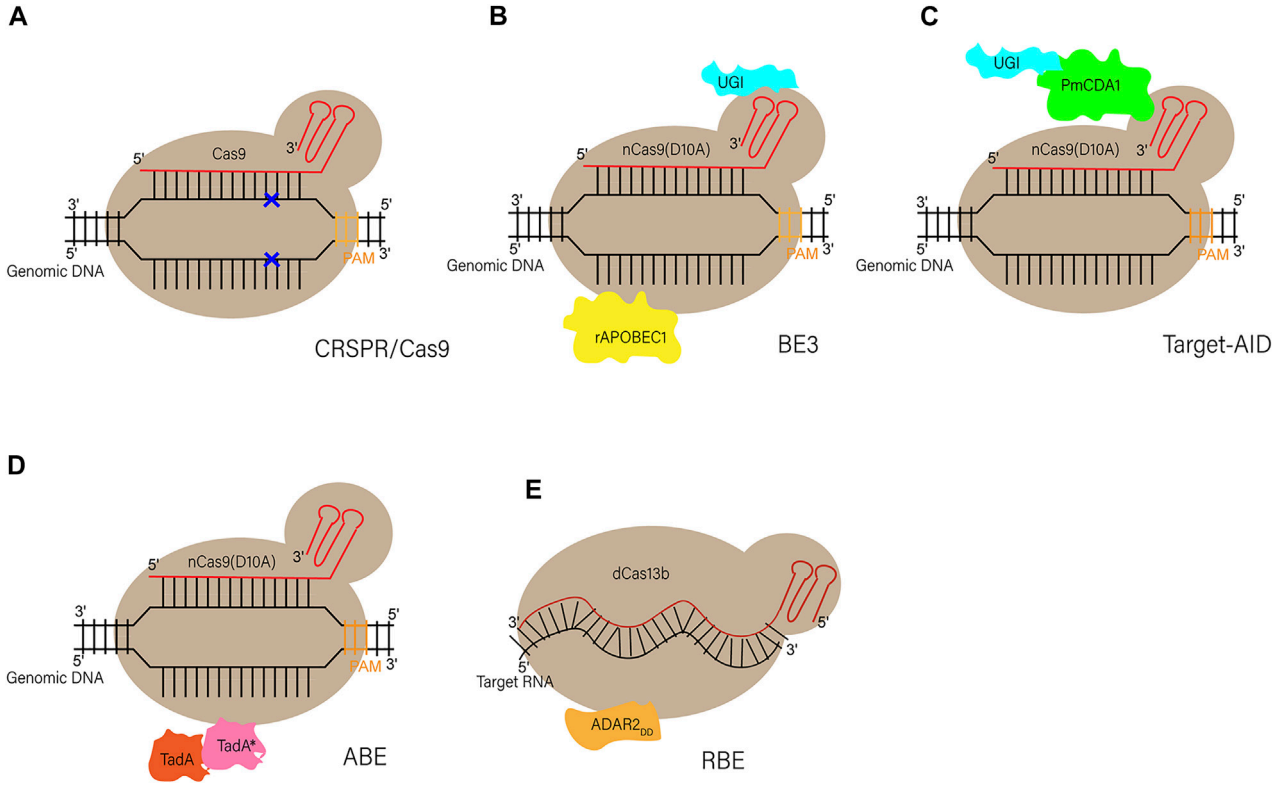

FIGURE 2 | Schematic diagram of CRISPR/Cas9 and different BEs **(A) Schematic diagram of CRISPR/Cas9.** Through base pairing between sgRNAs and DNA as well as the PAM sequence, Cas9 can recognize and cleave the double-strand DNA at the target site to form DSBs **(B,C) Schematic diagram of two original base editors (CBEs).** BE3: a SpCas9 nickase (D10A) is linked to a rat cytidine deaminase (rAPOBEC1) through the N terminus, and to a uracil glycosylase inhibitor (UGI) at the C terminus. Target-AID: the C terminus of SpCas9 nickase (D10A) is linked to both cytidine deaminase from *Petromyzon marinus* (PmCDA1) and UGI **(D) Schematic diagram of adenine base editor (ABEs).** ABEs: fusion of artificially evolved DNA adenine deaminase (TadA*-TadA) with SpCas9 nickase (D10A) generates ABEs (TadA, wildtype *Escherichia* coil tRNA adenosine deaminase; TadA*, mutated TadA) **(E) Schematic diagram of RNA base editor (RBEs).** RBEs: catalytically dead Prevotella sp. Cas13 (dCas13b) is tethered with deaminase domain of human"adenosine deaminase acting on RNA" ($ADAR2_{DD}$) to form RBEs.

accomplished in goats (Ni et al., 2014) and the single-gene knockout fibroblasts were successfully used for SCNT and resulted in live-born goats harboring biallelic mutations.

Apart from the knockout strategy based on the aberrant DNA repair to generate frameshifting insertion-deletion mutations (indels), whether this genomic engineering technique involving HR can be used to introduce defined point mutations is another question. Subsequently, Niu et al. reported a G→A point mutation in the growth differentiation factor 9 (*GDF9*) gene that has a large effect on the litter size of cashmere goats successfully (Niu et al., 2018). Moreover, Wu et al. succeeded in integrating an exogenous t*GFP* (turbo*GFP*) gene into targeted genes in frame with high efficiency (Wu et al., 2016), which was the first gene knock-in sheep via CRISPR/Cas9 system. Another research specifically inserted the thymosin beta 4 (*Tβ4*) gene into the goat *CCR5* locus (Li X. et al., 2019), which also provided an example for the establishment of knock-in goats models.

Sheep and goats have been used as interesting models in biomedical research. Compared to experimental rodents, sheep and goats offer the advantage of being more suitable in mimicking human diseases due to their similar size and anatomy. There have already been some examples of genome editing sheep or goats by CRISPR/Cas9 system to mimic human disease. Fan et al. created the first sheep model of human disease of cystic fibrosis (CF) generated by CRISPR/Cas9 mediated disruption of the cystic fibrosis transmembrane conductance regulator (*CFTR*) gene (Fan et al., 2018). The newborn $CFTR^{-/-}$ sheep developed severe disease phenotypes consistent with CF pathology in humans, like pancreatic fibrosis, intestinal obstruction, and substantial liver and gallbladder disease reflecting CF liver disease that is evident in humans. Another study reported for the first time the generation of otoferlin (*OTOF*) gene disrupted sheep, which provided a model allowing better understanding and development of new therapies for human deafness related to genetic disorders (Menchaca et al., 2020). Additionally, Williams et al. have also reported an interesting sheep model, recapitulating human hypophosphatasia (HPP, a rare metabolic bone disease) by applying CRISPR/Cas9(Williams et al., 2018). In this study, a single point mutation in the tissue-nonspecific alkaline phosphatase gene (*ALPL*) was introduced. Thus, the generated gene-edited lambs accurately phenocopied human HPP, providing a useful large animal model for the study of rare human bone diseases. The results of these reports corroborate the great potential of the CRISPR/Cas9 system to generate gene-edited sheep or goats that recapitulate human diseases (Kalds et al., 2019).

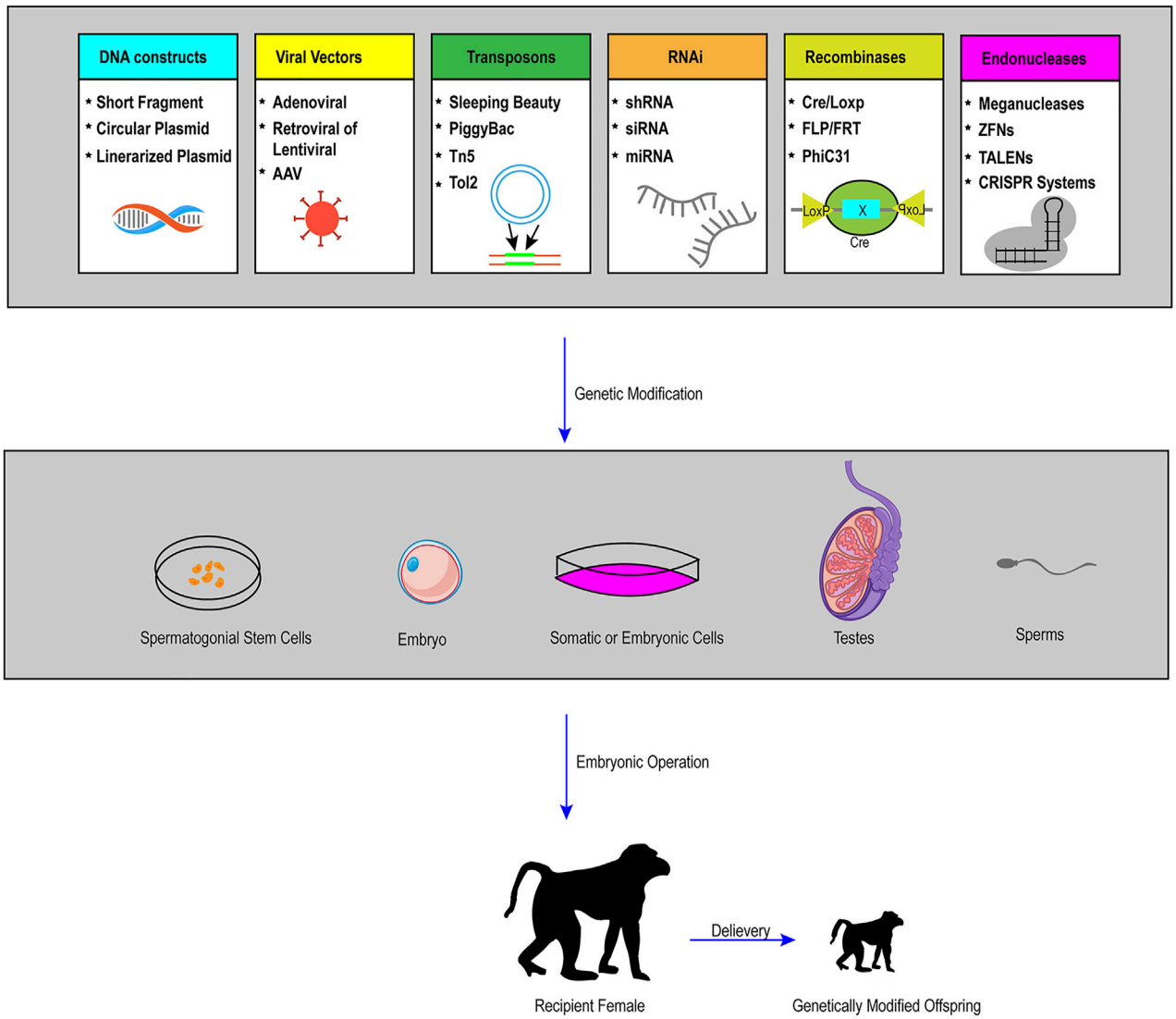

FIGURE 3 | Schematic representation of practical and possible pathways of genetic modification in large animals. To achieve the generation of live founders with desired genetic modifications (pronuclear injection and nuclear transfer are the two primary procedures), the first step is to conduct gene manipulations in a variety of cells or organs, including somatic cells, embryonic cells, embryos, spermatozoa, SSCs and other targeted organs by the use of many tools, such as viral vectors, recombinases, transposons, RNA interference (RNAi), and endonucleases. Through a series of embryonic operations, such as nuclear transfer, genetically modified cells or embryos can produce genetically modified offspring.

Similar to pigs, the sheep or the goat is also one of the most important livestock in agriculture industry, which urges scientists to reform its traits via genome editing from different aspects according to physical demand. Sheep and goats could provide us with donor organs for xenotransplantation by serving as the host for the growth of human organs. As a result, Vilarino et al. created *PDX1*$^{-/-}$ (pancreatic and duodenal homeobox protein 1) fetus lacking a pancreas, which provided the basis for the production of gene-edited sheep as a host for interspecies organ generation (Vilarino et al., 2017). *BMPR-IB* (bone morphogenetic protein receptor type IB, also known as FecB) is a key candidate gene for the genetic control of sheep reproductive performance. Researchers created loss-of-function mutations in the sheep *BMPR-IB* by using the CRISPR/Cas9 system, leading to an increase in ovulation rate and consequently larger litter size (Zhang et al., 2017c). Ma et al. established an *AANAT/ASMT* (aralkylamine N-acetyltransferase/acetylserotonin O-methyltransferase) transgenic animal model constructed with CRISPR/Cas9 system, which served as the mammary gland bioreactor to produce melatonin-enriched milk in the sheep (Ma et al., 2017) or in goats (Zhou et al., 2017; Tian et al., 2018). Another research showed that CRISPR/Cas9-mediated loss of fibroblast growth factor 5 (*FGF5*) activity could promote the wool growth and, consequently, increase the wool length and yield in sheep (Li et al., 2017a; Hu et al., 2017) or in goats (Wang et al., 2016a), and similar research was performed in order to change the coat color of sheep and goats (Zhang et al., 2017b).

TABLE 1 | Examples of genome-edited large animals described in this article.

Species	Genes	Editing type	References
NHPs	*RTT*, *MECP2*	KO	Liu et al. (2014)
	PPARG, *RAG1*	M-KO	Niu et al. (2014)
	DMD	KO	Chen et al. (2015b)
	TP53	KO	Wan et al. (2015)
	ARNTL, *PRRT2*	M-KO	Zuo et al. (2017)
	PINK1, *ASPM*	KO	Tu et al. (2017)
	SHANK3	KO	Zhao et al. (2017)
	mCherry	KI	Yao et al. (2018)
	hr*GFP*	KI	Cui et al. (2018)
	MECP2	KO	Chen et al. (2017)
	PINK1	M-KO	Yang et al. (2019b)
	LMNA	BE	Wang et al. (2020)
Pigs	*VWF*	KO	Zhang et al. (2017a)
	CD1D, *CD163*, *EGFP*	M-KO	Huang et al. (2017)
	PRKN, *DJ-1*, *PINK1*	M-KO	Wang et al. (2016b)
	HTT	KI	Yan et al. (2018)
	Large transgene cassette	KI	Li et al. (2020a)
	F9	KI	Chen et al. (2021)
	Large transgene cassette	KI	Ruan et al. (2015)
	TPH2	KO	Li et al. (2017b)
	C3	KO	Zhang et al. (2017a)
	APOE, *LDLR*	M-KO	Huang et al. (2017)
	RUNX3	KO	Kang et al. (2016)
	MSTN	KO	Wang et al., (2015a) Wang et al., 2017 Li et al. (2020b)
	IGF2	KO	Liu et al. (2019)
	FBX O 40	KO	Zou et al. (2018)
	p*RSAD2*	KI	Xie et al. (2020)
	p*ULBP1*	KO	Joanna et al. (2018)
	PDX1	KO	Wu et al. (2017)
	GGTA1, *CMAH*	M-KO	Gao et al. (2017)
	GGTA1	KO	(Petersen et al., 2016 Chuang et al. (2017)
	GGTA1, *BGALNT2*, *CMAH*	BE	Yuan et al. (2020)
	TWIST2, *TYR*	BE	Li et al. (2018b)
goats	*MSTN*	KO	Ni et al., (2014) Guo et al., 2016 He et al., 2018 Wang et al. (2018b)
	CDF9	PM	Niu et al. (2018)
	Tβ4	KI	Li et al. (2019b)
	SCD1	KO	Tian et al. (2018)
	BLG	KO	Zhou et al. (2017)
	FGF5	KO	Wang et al. (2016a)
	MSTN, *FGF5*	M-KO	Wang et al. (2015b)
	FAT1, *MSTN*	KO/KI	Zhang et al. (2018a)
	FGF5	BE	Li et al. (2019a)
sheep	t*GFP*	KI	Wu et al. (2016)
	CFTR	KO	Fan et al. (2018)
	OTOF	KO	Menchaca et al. (2020)
	ALPL	PM	Williams et al. (2018)
	PDX1	KO	Vilarino et al. (2017)
	BMPR-IB	KO	Zhang et al. (2017c)
	AANAT, *ASMT*	KI	Ma et al. (2017)
	FGF5	KO	Hu et al., (2017) Li et al. (2017a)
	ASIP	KO	Zhang et al. (2017b)
	MSTN	KO	Crispo et al., (2015) Rao et al., 2016

(Continued in next column)

TABLE 1 | (*Continued*) Examples of genome-edited large animals described in this article.

species	Genes	Editing type	References
			Zhang et al. (2018b)
	BC O 2	KO	Niu et al. (2017b)
	SOCS2	BE	Zhou et al. (2019)
dogs	*MSTN*	KO	Zou et al. (2015)
	APOE	KO	Feng et al. (2018)

The table lists genes that have been changed by the way of KO, M-KO, PM or BE or KI. Abbreviations: KO, knockout; M-KO, multiplex knockout; KI, knock-in; PM, point mutation (by HDR); BE, base editing.

To meet the growing demand for the meat product of sheep and goats, many experiments are aimed at improving the yield and quality of the meat production of sheep or goats, most of which were conducted by hindering the muscle producing genes in sheep (Crispo et al., 2015; Niu Y. et al., 2017; Zhang Y. et al., 2018) or in goats (Wang X. et al., 2015; Guo et al., 2016; Zhang J. et al., 2018; Wang X. et al., 2018; He et al., 2018), like *MSTN*. This strategy was also used in the pig.

THE APPLICATION OF CRISPR/CAS9 IN DOG MODELS

The dog is also a typical species used in scientific research, though there are not many labs focusing on the topic of CRISPR/Cas9 system editing dogs. Zou et al. demonstrated for the first time that a single injection of Cas9 mRNA and sgRNA corresponding to a specific gene into zygotes, combined with an auto-embryo transfer strategy, can efficiently generate site-specific genome-modified dogs (Zou et al., 2015). Their team also generated the apolipoprotein E (*APOE*) deficient dogs via similar strategy 3 years later (Feng et al., 2018).

The most exciting breakthrough about gene edited dogs related to CRISPR/Cas9 system happened in the year of 2018. Researchers of Olson lab working with dogs successfully fixed a genetic glitch that causes DMD by further damaging the DNA. They used adeno-associated viruses (AAV) to deliver CRISPR/Cas9 gene editing components to four dogs, which allowed the mutated gene to again make a key muscle protein and greatly alleviated the disease (Amoasii et al., 2018). The feat-achieved for the first time in a large animal-raised hope that such genetic surgery could 1 day prevent or treat this crippling and deadly disease in people, which created a great interest in the field (Cohen, 2018; Duan, 2018; Wasala et al., 2019; Mata Lopez et al., 2020).

DISCUSSION

Limitations of CRISPR/Cas9 System in Large Animal Models

Above all, the progress of genome editing large animal models is accelerated tremendously by CRISPR/Cas9 system because of many aspects of advantages. First, this system is nearly able to

target any locus of the genome in animals theoretically as long as there are PAM sequences near the location (Mali et al., 2013), which really expanded the range of editing genes compared with previous strategy. Next, because the targeting strategy relies on 23 base pair matches, CRISPR/Cas9 can target to virtually any genes in a sequence-dependent manner. As a result, CRISPR/Cas9 can target two alleles to cause a null mutation in the founder animals, which would avoid the procedure of mating heterozygous mutant animals to generate homozygous mutants. This advantage is really critical to large animals because the outcrossing process may take much longer time than mouse models, even several years in nonhuman primates. Third, the CRISPR/Cas9 system can simultaneously manipulate several genes by the co-injection of several sgRNAs with Cas9 into fertilized eggs at the one-cell stage, which makes the establishment of animal models of multigenic disease possible, especially the complex neurodegenerative diseases, such as PD and Alzheimer's disease (AD). As a result, these models may mimic the genetic mutations and the symptoms in patients in a better way.

Although the CRISPR/Cas9 system has brought great hope for the use of large animal models for studying human diseases, several challenges remain. The first one is the off-targeting effect. When the approximate 23 base pairs that enable the specific cutting of Cas9 match other areas of the genomic DNA, nonspecific editing may happen and cause off-targeting mutations. Although the off-target events can be diluted over generations in small animals with short breeding times, this strategy is infeasible for large animals like monkeys because their sexual maturation usually requires 4–5 years (Niu et al., 2014). To eliminate or reduce the side effects of off-target mutations, truncated guide RNAs in the CRISPR/Cas9 system can be used to improve the specificity of Cas9 nucleases or paired nickases (Fu et al., 2013; Sakuma et al., 2014). On the other hand, the use of bioinformatic screening to search for unique genomic targets and the use of paired Cas9 nickases can also reduce off-targets (Tu et al., 2015).

The second problem is the mosaicism in CRISPR/Cas9-mediated genome editing, which means the presence of more than one genotype in one individual. The mechanisms of the mosaicism are still unclear, and there may be several causes. It is possible that the translation of Cas9 mRNA to produce an active enzymatic form is delayed until after the first cell division, and this delay may play a major role in genetic mosaicism. The mosaicism problem may also result from the prolonged expression of Cas9 mRNA. Alternatively, differential DNA repair and non-homozygous recombination activities in zygotes and divided embryonic cells can also influence genetic mutation rates and mosaicism (Tu et al., 2015). In a word, the CRISPR/Cas9 system can continuously target and cleave genes at different stages of embryonic development in different ways, as a result, leading to mosaicism of the introduced mutations. Although the mosaicism is an undesired result in genome editing animals, there may be several advantages, which include enabling animals to survive beyond the lethal phase when manipulated genes are essential to animals. In addition, mosaic animals help us better understand dosage effects of genes on developmental defects, especially those which may mimic human congenital disorders (Zhong et al., 2015). However, the mosaicism caused by CRISPR/Cas9 is undesirable in most cases. The biggest problem of chimeric large animals is that the mutation may be difficult to be transmitted into the offspring (Oliver et al., 2015) because of the long breeding cycle of large animals especially nonhuman primates. There are several possible strategies to reduce the mosaicism. The first way is to speed up the editing process by the introduction of CRISPR/Cas9 components in an appropriate format [Cas9/sgRNA ribonucleoprotein (RNP)] and concentration into very early pronuclear stage zygotes by using electroporation (Mehravar et al., 2019), so the CRISPR/Cas9 system will work at the earliest stage of zygotes. Secondly, as described above, shortening the longevity of Cas9 in combination with embryo splitting to eliminate the delayed function of Cas9 also makes a difference (Tu et al., 2017). The third strategy is to use germline modification. In this way, genetically-modified somatic cells can be used as nuclear donors for SCNT into enucleated germ cells. In another way, generally targeted gene edited spermatogonial stem cells (SSCs) can be used as donors for transplantation into testis directly.

The last problem is the efficiency of the CRISPR/Cas9 system. According to the previous study, the efficiency of gene targeting with CRISPR in large animals (like nonhuman primates) is more variable and lower than that in mice (Chen et al., 2016). Therefore, precise gene editing technologies need to be further improved, to increase the efficiency of gene targeting and the rate of homozygous mutation by using new Cas protein [like Cpf1 (Cas12a)] and new systems (like base editing system).

Base Editing in Large Animals and Prime Editing

Although the CRISPR/Cas9 system has been used to establish gene editing models in multiple species, it is more likely to induce random indels through error-prone NHEJ rather than the error-free HDR during gene editing (Kim and Kim, 2014), which makes indels more likely to occur at the editing site than single-nucleotide substitutions. In addition, DNA sequencing results show that point mutations, not indels, cause the vast majority of human genetic diseases (Yuan et al., 2020), which suggests the importance of the newly developed gene-editing tool base editing in establishing animal models of human disease. Base editing is a gene editing tool developed in recent years, which can lead to gene mutations through changes in a single base pair (Komor et al., 2016; Nishida et al., 2016; Gaudelli et al., 2017). At the genome level, BEs can achieve all four kinds of single base transition, including C to T, G to A, A to G, and T to C (adenine (A), cytosine (C), guanine (G), and thymine (T)). There are several basic base editors, include cytosine base editors (CBEs), adenine base editors (ABEs) and RNA base editors (RBEs). CBEs is capable of converting the base pair C-G to into T-A, while ABEs can achieve the transition from A-T into G-C. RBEs are able to achieve the conversion of A to Inosine (I) in the level of RNA (Molla and Yang, 2019) (the structure of these BEs are depicted in **Figure 2**).

Although there are only several years after the invention of base editing, scientists have used it to achieve gene editing

successfully in many small animals and plants, such as mouse (Ryu et al., 2018), rat (Ma et al., 2018), rabbit (Lee et al., 2018; Liu et al., 2018), zebrafish (Zhang Y. et al., 2017), rice (Hua et al., 2018) and wheat (Li C. et al., 2018).

Apart from these, there are also some examples of gene editing large animal models created by BEs. In the 2018, a group demonstrated the BE3 (one kind of CBEs)-mediated base editing can induce nonsense mutations in the goat *FGF5* gene. They further characterized the phenotypic and genetic changes to investigate the consequence of base pair editing, and provided strong supporting evidence that the BE3 induced off-target mutations were rare at genome-wide level (Li G. et al., 2019). These successful attempts in goats opened up unlimited possibilities of genome engineering by base editing in large animals. Inspired by this, researchers also created BE3-mediated sheep by co-injection of a BE3 mRNA and guide RNA aiming at the *SOCS2* (suppressor of cytokine signaling 2) gene in the next year (Zhou et al., 2019).

By using BE3 to target the *TWIST2* (twist-related protein 2) gene [responsible for the ablepharon macrostomia syndrome (AMS) in human)] and the tyrosinase (*TYR*) gene [the causal gene for oculocutaneous albinism type 1 (OCA1)], researchers created a gene editing pig model successfully in the same year of the first base editing goats (Li Z. et al., 2018), which mimicked the phenotypic characteristics of human diseases well. The group of Liangxue Lai also achieved efficient base editing for several genes in pigs by combining CBEs with SCNT in the next year, including *DMD*, *RAG1* (recombination activating gene 1), *RAG2* (recombination activating gene 1) and *IL2RG* (interleukin 2 receptor subunit gamma) (Xie et al., 2019). Another group also achieved precise base conversion in three genes {[*GGTA1* (glycoprotein alpha-galactosyltransferase 1), *B4GALNT2* (beta-1,4-N-acetyl-galactosaminyltransferase 2), and *CMAH* (cytidine monophospho-N-acetylneuraminic acid hydroxylasegenes)]} in pig genome (Yuan et al., 2020). As for NHPs, researchers generated the first Hutchinson-Gilford progeria syndrome (HGPS) monkey model by delivering a BE mRNA and guide RNA (gRNA) targeting the *LMNA* (lamin A/C) gene via microinjection into monkey zygotes, and the typical HGPS phenotypes including growth retardation, bone alterations, and vascular abnormalities confirmed the reliability of this model (Wang et al., 2020). Since the appearance of BEs, this tool has been applied in some species of large animals, like NHPs, goats, sheep and pigs. It is really convenient to establish disease models or improve the traits in large animals by base editing for its ability of precise single base pair editing.

Although base editing has played a great role in precise genome editing, it is still unable to achieve all base conversions. To solve this problem, researchers created the prime editing. This system consists of a Cas9 nickase (H840A mutation) fused to a reverse transcriptase domain and a modified sgRNA, named prime editing guide RNA (pegRNA). The basic principle is to use nCas9 to nick the non-target strand at the target location, and then use reverse transcriptase to generate the required sequence using the template RNA. Then the FEN1 endonuclease is able to excise the sequence called flap during this process and contributes to the genome repairing (Anzalone et al., 2019; Caso and Davies, 2022). Although this technique has only been reported in the establishment of small animal models (Liu et al., 2020), it is of great significance for the study of diseases caused by various base mutations in large animal models because it can mediate almost all types of base conversions.

Prospects and Challenges

Large animal models can be used in many areas including disease pathogenesis investigation and pre-clinical research. Due to the lack of ESCs from large animals, it has been difficult to use traditional gene targeting technology to establish large animal models of human diseases. Nowadays, the development of precise genome editing tools especially the CRISPR/Cas9 system has greatly advanced this field. Many genome-edited large animals have been created including knockout or knock-in that cover almost all types of currently used experimental animals, such as nonhuman primates, pigs, sheep, goats and dogs. Even so, there are still many limitations in the establishment of large animal models, which may involve the inadequate gene targeting efficiency, mosaicism, and off-targeting. Many strategies and optimized components of the system have been brought up to reduce these drawbacks or to improve efficiency.

The BEs recently provide us with a new tool in the establishment of large animal models with the rapid development and optimization of this new system. Although there are only few successful examples in large animals, the BEs greatly expanded the scope of this area promisingly because the vast majority of human genetic diseases are induced by point mutations. On the other hand, all kinds of other technologies, like somatic cell nuclear transfer, genome editing of SSCs, and tetraploid complementation, have played more and more important roles in the establishment of rodents or even large animal models nowadays. Therefore, the combination of the BEs or optimized CRISPR/Cas9 components with other platforms previously described will make precise genome modification in large animals more efficient and easier (the procedure of gene modified large animal models is depicted in **Figure 3**).

In clinical research, it is a promising direction to use gene therapy to treat inherited human diseases. The FDA has approved some gene therapy products for patients, such as patients with B-cell precursor acute lymphoblastic leukemia (ALL). Before applying the strategy on patients, evaluating the efficacy and safety using genetically modified animal models that can mimic the characteristics of human disease is necessary, which further underscores the importance of the establishment of genome editing large animal models. Xenotransplantation is another promising direction, as the shortage of human organs is a common problem, and model animals can provide a sufficient supply of organ products. Genetic modification of donor animals can eliminate many problems, especially the immunological compatibility, and increase the probability of success

during xenotransplantation. The recent success of transplanting organs from transgenic pigs into the humans is a stunning breakthrough in this field, which will in turn lead to the development of gene-editing large animal models.

In summary, with the development and application of precise genome editing tools represented by CRISPR/Ca9 system, a great number of large animal models will be established (the examples of genome-edited large animals described in this article is listed in **Table 1**). The improvement will create ideal animal models that are more similar to the human, benefit the study of the mechanisms of human diseases, and make important contribution to the clinical application.

AUTHOR CONTRIBUTIONS

Designed the paper: YL, ZT, SY. Wrote the paper: YL, JL. Collected literatures: YL, CL. Edited the paper: SY, SL, X-JL

FUNDING

This work was supported by National Key Research and Development Program of China (2021YFA0805300), The National Natural Science Foundation of China (81922026,82171244), and Guangzhou Key Research Program on Brain Science (202007030008).

REFERENCES

Amoasii, L., Hildyard, J. C. W., Li, H., Sanchez-Ortiz, E., Mireault, A., Caballero, D., et al. (2018). Gene Editing Restores Dystrophin Expression in a Canine Model of Duchenne Muscular Dystrophy. *Science* 362 (6410), 86–91. doi:10.1126/science.aau1549

Anzalone, A. V., Randolph, P. B., Davis, J. R., Sousa, A. A., Koblan, L. W., Levy, J. M., et al. (2019). Search-and-replace Genome Editing without Double-Strand Breaks or Donor DNA. *Nature* 576 (7785), 149–157. doi:10.1038/s41586-019-1711-4

Carroll, D. (2011). Genome Engineering with Zinc-Finger Nucleases. *Genetics* 188 (4), 773–782. doi:10.1534/genetics.111.131433

Caso, F., and Davies, B. (2022). Base Editing and Prime Editing in Laboratory Animals. *Lab. Anim.* 56 (1), 35–49. doi:10.1177/00236772221993895

Chan, A. W. S., Chong, K. Y., Martinovich, C., Simerly, C., and Schatten, G. (2001). Transgenic Monkeys Produced by Retroviral Gene Transfer into Mature Oocytes. *Science* 291 (5502), 309–312. doi:10.1126/science.291.5502.309

Chen, Y., Cui, Y., Shen, B., Niu, Y., Zhao, X., Wang, L., et al. (2015a). Germline Acquisition of Cas9/RNA-Mediated Gene Modifications in Monkeys. *Cell Res.* 25 (2), 262–265. doi:10.1038/cr.2014.167

Chen, Y., Zheng, Y., Kang, Y., Yang, W., Niu, Y., Guo, X., et al. (2015b). Functional Disruption of the Dystrophin Gene in Rhesus Monkey Using CRISPR/Cas9. *Hum. Mol. Genet.* 24 (13), 3764–3774. doi:10.1093/hmg/ddv120

Chen, Y., Niu, Y., and Ji, W. (2016). Genome Editing in Nonhuman Primates: Approach to Generating Human Disease Models. *J. Intern Med.* 280 (3), 246–251. doi:10.1111/joim.12469

Chen, Y., Yu, J., Niu, Y., Qin, D., Liu, H., Li, G., et al. (2017). Modeling Rett Syndrome Using TALEN-Edited MECP2 Mutant Cynomolgus Monkeys. *Cell* 169 (5), 945–955. e910. doi:10.1016/j.cell.2017.04.035

Christian, M., Cermak, T., Doyle, E. L., Schmidt, C., Zhang, F., Hummel, A., et al. (2010). Targeting DNA Double-Strand Breaks with TAL Effector Nucleases. *Genetics* 186 (2), 757–761. doi:10.1534/genetics.110.120717

Chuang, C.-K., Chen, C.-H., Huang, C.-L., Su, Y.-H., Peng, S.-H., Lin, T.-Y., et al. (2017). Generation of GGTA1 Mutant Pigs by Direct Pronuclear Microinjection of CRISPR/Cas9 Plasmid Vectors. *Anim. Biotechnol.* 28 (3), 174–181. doi:10.1080/10495398.2016.1246453

Cohen, J. (2018). In Dogs, CRISPR Fixes a Muscular Dystrophy. *Science* 361 (6405), 835. doi:10.1126/science.361.6405.835

Crispo, M., Mulet, A. P., Tesson, L., Barrera, N., Cuadro, F., dos Santos-Neto, P. C., et al. (2015). Efficient Generation of Myostatin Knock-Out Sheep Using CRISPR/Cas9 Technology and Microinjection into Zygotes. *PLoS One* 10 (8), e0136690. doi:10.1371/journal.pone.0136690

Cui, Y., Niu, Y., Zhou, J., Chen, Y., Cheng, Y., Li, S., et al. (2018). Generation of a Precise Oct4-hrGFP Knockin Cynomolgus Monkey Model via CRISPR/Cas9-assisted Homologous Recombination. *Cell Res.* 28 (3), 383–386. doi:10.1038/cr.2018.10

Dawson, T. M., Ko, H. S., and Dawson, V. L. (2010). Genetic Animal Models of Parkinson's Disease. *Neuron* 66 (5), 646–661. doi:10.1016/j.neuron.2010.04.034

Duan, D. (2018). CRISPR Alleviates Muscular Dystrophy in Dogs. *Nat. Biomed. Eng.* 2 (11), 795–796. doi:10.1038/s41551-018-0320-0

Durai, S., Mani, M., Kandavelou, K., Wu, J., Porteus, M. H., and Chandrasegaran, S. (2005). Zinc Finger Nucleases: Custom-Designed Molecular Scissors for Genome Engineering of Plant and Mammalian Cells. *Nucleic Acids Res.* 33 (18), 5978–5990. doi:10.1093/nar/gki912

Fan, Z., Perisse, I. V., Cotton, C. U., Regouski, M., Meng, Q., Domb, C., et al. (2018). A Sheep Model of Cystic Fibrosis Generated by CRISPR/Cas9 Disruption of the CFTR Gene. *JCI Insight* 3 (19), e123529. doi:10.1172/jci.insight.123529

Feng, C., Wang, X., Shi, H., Yan, Q., Zheng, M., Li, J., et al. (2018). Generation of ApoE Deficient Dogs via Combination of Embryo Injection of CRISPR/Cas9 with Somatic Cell Nuclear Transfer. *J. Genet. Genomics* 45 (1), 47–50. doi:10.1016/j.jgg.2017.11.003

Fu, Y., Foden, J. A., Khayter, C., Maeder, M. L., Reyon, D., Joung, J. K., et al. (2013). High-frequency Off-Target Mutagenesis Induced by CRISPR-Cas Nucleases in Human Cells. *Nat. Biotechnol.* 31 (9), 822–826. doi:10.1038/nbt.2623

Gao, H., Zhao, C., Xiang, X., Li, Y., Zhao, Y., Li, Z., et al. (2017). Production of α1,3-galactosyltransferase and Cytidine Monophosphate-N-Acetylneuraminic Acid Hydroxylase Gene Double-Deficient Pigs by CRISPR/Cas9 and Handmade Cloning. *J. Reproduction Dev.* 63 (1), 17–26. doi:10.1262/jrd.2016-079

Gaudelli, N. M., Komor, A. C., Rees, H. A., Packer, M. S., Badran, A. H., Bryson, D. I., et al. (2017). Programmable Base Editing of at to GC in Genomic DNA without DNA Cleavage. *Nature* 551 (7681), 464–471. doi:10.1038/nature24644

Guo, R., Wan, Y., Xu, D., Cui, L., Deng, M., Zhang, G., et al. (2016). Generation and Evaluation of Myostatin Knock-Out Rabbits and Goats Using CRISPR/Cas9 System. *Sci. Rep.* 6, 29855. doi:10.1038/srep29855

Hai, T., Teng, F., Guo, R., Li, W., and Zhou, Q. (2014). One-step Generation of Knockout Pigs by Zygote Injection of CRISPR/Cas System. *Cell Res.* 24 (3), 372–375. doi:10.1038/cr.2014.11

Hammer, R. E., Pursel, V. G., Rexroad, C. E., Jr., Wall, R. J., Bolt, D. J., Ebert, K. M., et al. (1985). Production of Transgenic Rabbits, Sheep and Pigs by Microinjection. *Nature* 315 (6021), 680–683. doi:10.1038/315680a0

He, Z., Zhang, T., Jiang, L., Zhou, M., Wu, D., Mei, J., et al. (2018). Use of CRISPR/Cas9 Technology Efficiently Targetted Goat Myostatin through Zygotes Microinjection Resulting in Double-Muscled Phenotype in Goats. *Biosci. Rep.* 38 (6), BSR20180742. doi:10.1042/BSR20180742

Hu, R., Fan, Z. Y., Wang, B. Y., Deng, S. L., Zhang, X. S., Zhang, J. L., et al. (2017). RAPID COMMUNICATION: Generation of FGF5 Knockout Sheep via the CRISPR/Cas9 System12. *J. Anim. Sci.* 95 (5), 2019–2024. doi:10.2527/jas.2017.1503

Hua, K., Tao, X., Yuan, F., Wang, D., and Zhu, J.-K. (2018). Precise A·T to G·C Base Editing in the Rice Genome. *Mol. Plant* 11 (4), 627–630. doi:10.1016/j.molp.2018.02.007

Huang, L., Hua, Z., Xiao, H., Cheng, Y., Xu, K., Gao, Q., et al. (2017). CRISPR/Cas9-mediated ApoE-/- and LDLR-/- Double Gene Knockout in Pigs Elevates Serum LDL-C and TC Levels. *Oncotarget* 8 (23), 37751–37760. doi:10.18632/oncotarget.17154

Jaenisch, R., and Mintz, B. (1974). Simian Virus 40 DNA Sequences in DNA of Healthy Adult Mice Derived from Preimplantation Blastocysts Injected with Viral DNA. *Proc. Natl. Acad. Sci. U.S.A.* 71 (4), 1250–1254. doi:10.1073/pnas.71.4.1250

Jiahuan Chen, J., Beiying An, B., Biao Yu, B., Xiaohuan Peng, X., Hongming Yuan, H., and Qiangbing Yang, Q. (2021). CRISPR/Cas9-mediated Knockin of Human Factor IX into Swine Factor IX Locus Effectively Alleviates Bleeding

in Hemophilia B Pigs. *haematol* 106 (3), 829–837. doi:10.3324/haematol.2019.224063

Jinek, M., Chylinski, K., Fonfara, I., Hauer, M., Doudna, J. A., and Charpentier, E. (2012). A Programmable Dual-RNA-Guided DNA Endonuclease in Adaptive Bacterial Immunity. *Science* 337 (6096), 816–821. doi:10.1126/science.1225829

Joanna, Z., Magdalena, H., Agnieszka, N.-T., Jacek, J., Ryszard, S., Zdzisław, S., et al. (2018). The Production of UL16-Binding Protein 1 Targeted Pigs Using CRISPR Technology. *3 Biotech.* 8 (1), 70. doi:10.1007/s13205-018-1107-4

Joung, J. K., and Sander, J. D. (2013). TALENs: a Widely Applicable Technology for Targeted Genome Editing. *Nat. Rev. Mol. Cell Biol.* 14 (1), 49–55. doi:10.1038/nrm3486

Kalds, P., Zhou, S., Cai, B., Liu, J., Wang, Y., Petersen, B., et al. (2019). Sheep and Goat Genome Engineering: From Random Transgenesis to the CRISPR Era. *Front. Genet.* 10, 750. doi:10.3389/fgene.2019.00750

Kang, J.-T., Ryu, J., Cho, B., Lee, E.-J., Yun, Y.-J., Ahn, S., et al. (2016). Generation ofRUNX3knockout Pigs Using CRISPR/Cas9-mediated Gene Targeting. *Reprod. Dom. Anim.* 51 (6), 970–978. doi:10.1111/rda.12775

Kim, H., and Kim, J.-S. (2014). A Guide to Genome Engineering with Programmable Nucleases. *Nat. Rev. Genet.* 15 (5), 321–334. doi:10.1038/nrg3686

Kitada, T., Pisani, A., Porter, D. R., Yamaguchi, H., Tscherter, A., Martella, G., et al. (2007). Impaired Dopamine Release and Synaptic Plasticity in the Striatum of PINK1 -deficient Mice. *Proc. Natl. Acad. Sci. U.S.A.* 104 (27), 11441–11446. doi:10.1073/pnas.0702717104

Kobayashi, K., Tsukiyama, T., Nakaya, M., Kageyama, S., Tomita, K., Murai, R., et al. (2019). Generation of an OCT3/4 Reporter Cynomolgus Monkey ES Cell Line Using CRISPR/Cas9. *Stem Cell Res.* 37, 101439. doi:10.1016/j.scr.2019.101439

Komor, A. C., Kim, Y. B., Packer, M. S., Zuris, J. A., and Liu, D. R. (2016). Programmable Editing of a Target Base in Genomic DNA without Double-Stranded DNA Cleavage. *Nature* 533 (7603), 420–424. doi:10.1038/nature17946

Lee, H. K., Willi, M., Miller, S. M., Kim, S., Liu, C., Liu, D. R., et al. (2018). Targeting Fidelity of Adenine and Cytosine Base Editors in Mouse Embryos. *Nat. Commun.* 9 (1), 4804. doi:10.1038/s41467-018-07322-7

Li, W.-R., Liu, C.-X., Zhang, X.-M., Chen, L., Peng, X.-R., He, S.-G., et al. (2017a). CRISPR/Cas9-mediated Loss of FGF5 Function Increases Wool Staple Length in Sheep. *FEBS J.* 284 (17), 2764–2773. doi:10.1111/febs.14144

Li, C., Zong, Y., Wang, Y., Jin, S., Zhang, D., Song, Q., et al. (2018a). Expanded Base Editing in Rice and Wheat Using a Cas9-Adenosine Deaminase Fusion. *Genome Biol.* 19 (1), 59. doi:10.1186/s13059-018-1443-z

Li, Z., Duan, X., An, X., Feng, T., Li, P., Li, L., et al. (2018b). Efficient RNA-Guided Base Editing for Disease Modeling in Pigs. *Cell Discov.* 4, 64. doi:10.1038/s41421-018-0065-7

Li, G., Zhou, S., Li, C., Cai, B., Yu, H., Ma, B., et al. (2019a). Base Pair Editing in Goat: Nonsense Codon Introgression into FGF 5 Results in Longer Hair. *FEBS J.* 286 (23), 4675–4692. doi:10.1111/febs.14983

Li, X., Hao, F., Hu, X., Wang, H., Dai, B., Wang, X., et al. (2019b). Generation of Tβ4 Knock-In Cashmere Goat Using CRISPR/Cas9. *Int. J. Biol. Sci.* 15 (8), 1743–1754. doi:10.7150/ijbs.34820

Li, G., Zhang, X., Wang, H., Mo, J., Zhong, C., Shi, J., et al. (2020a). CRISPR/Cas9-Mediated Integration of Large Transgene into Pig CEP112 Locus. *G3 (Bethesda)* 10 (2), 467–473. doi:10.1534/g3.119.400810

Li, R., Zeng, W., Ma, M., Wei, Z., Liu, H., Liu, X., et al. (2020b). Precise Editing of Myostatin Signal Peptide by CRISPR/Cas9 Increases the Muscle Mass of Liang Guang Small Spotted Pigs. *Transgenic Res.* 29 (1), 149–163. doi:10.1007/s11248-020-00188-w

Li, H., Wu, S., Ma, X., Li, X., Cheng, T., Chen, Z., et al. (2021). Co-editing PINK1 and DJ-1 Genes via Adeno-Associated Virus-Delivered CRISPR/Cas9 System in Adult Monkey Brain Elicits Classical Parkinsonian Phenotype. *Neurosci. Bull.* 37 (9), 1271–1288. doi:10.1007/s12264-021-00732-6

Liu, H., Chen, Y., Niu, Y., Zhang, K., Kang, Y., Ge, W., et al. (2014). TALEN-mediated Gene Mutagenesis in Rhesus and Cynomolgus Monkeys. *Cell Stem Cell* 14 (3), 323–328. doi:10.1016/j.stem.2014.01.018

Liu, Z., Li, X., Zhang, J.-T., Cai, Y.-J., Cheng, T.-L., Cheng, C., et al. (2016). Autism-like Behaviours and Germline Transmission in Transgenic Monkeys Overexpressing MeCP2. *Nature* 530 (7588), 98–102. doi:10.1038/nature16533

Liu, Z., Chen, M., Chen, S., Deng, J., Song, Y., Lai, L., et al. (2018). Highly Efficient RNA-Guided Base Editing in Rabbit. *Nat. Commun.* 9 (1), 2717. doi:10.1038/s41467-018-05232-2

Liu, X., Liu, H., Wang, M., Li, R., Zeng, J., Mo, D., et al. (2019). Disruption of the ZBED6 Binding Site in Intron 3 of IGF2 by CRISPR/Cas9 Leads to Enhanced Muscle Development in Liang Guang Small Spotted Pigs. *Transgenic Res.* 28 (1), 141–150. doi:10.1007/s11248-018-0107-9

Liu, Y., Li, X., He, S., Huang, S., Li, C., Chen, Y., et al. (2020). Efficient Generation of Mouse Models with the Prime Editing System. *Cell Discov.* 6 (1), 27. doi:10.1038/s41421-020-0165-z

Luo, X., He, Y., Zhang, C., He, X., Yan, L., Li, M., et al. (2019). Trio Deep-Sequencing Does Not Reveal Unexpected Off-Target and On-Target Mutations in Cas9-Edited Rhesus Monkeys. *Nat. Commun.* 10 (1), 5525. doi:10.1038/s41467-019-13481-y

Ma, Y., Zhang, X., Shen, B., Lu, Y., Chen, W., Ma, J., et al. (2014). Generating Rats with Conditional Alleles Using CRISPR/Cas9. *Cell Res.* 24 (1), 122–125. doi:10.1038/cr.2013.157

Ma, T., Tao, J., Yang, M., He, C., Tian, X., Zhang, X., et al. (2017). AnAANAT/ASMTtransgenic Animal Model Constructed with CRISPR/Cas9 System Serving as the Mammary Gland Bioreactor to Produce Melatonin-Enriched Milk in Sheep. *J. Pineal Res.* 63 (1), e12406. doi:10.1111/jpi.12406

Ma, Y., Yu, L., Zhang, X., Xin, C., Huang, S., Bai, L., et al. (2018). Highly Efficient and Precise Base Editing by Engineered dCas9-Guide tRNA Adenosine Deaminase in Rats. *Cell Discov.* 4, 39. doi:10.1038/s41421-018-0047-9

Mali, P., Esvelt, K. M., and Church, G. M. (2013). Cas9 as a Versatile Tool for Engineering Biology. *Nat. Methods* 10 (10), 957–963. doi:10.1038/nmeth.2649

Mata López, S., Balog-Alvarez, C., Vitha, S., Bettis, A. K., Canessa, E. H., Kornegay, J. N., et al. (2020). Challenges Associated with Homologous Directed Repair Using CRISPR-Cas9 and TALEN to Edit the DMD Genetic Mutation in Canine Duchenne Muscular Dystrophy. *PLoS One* 15 (1), e0228072. doi:10.1371/journal.pone.0228072

McGonigle, P., and Ruggeri, B. (2014). Animal Models of Human Disease: Challenges in Enabling Translation. *Biochem. Pharmacol.* 87 (1), 162–171. doi:10.1016/j.bcp.2013.08.006

Mehravar, M., Shirazi, A., Nazari, M., and Banan, M. (2019). Mosaicism in CRISPR/Cas9-mediated Genome Editing. *Dev. Biol.* 445 (2), 156–162. doi:10.1016/j.ydbio.2018.10.008

Menchaca, A., Dos Santos-Neto, P. C., Souza-Neves, M., Cuadro, F., Mulet, A. P., Tesson, L., et al. (2020). Otoferlin Gene Editing in Sheep via CRISPR-Assisted ssODN-Mediated Homology Directed Repair. *Sci. Rep.* 10 (1), 5995. doi:10.1038/s41598-020-62879-y

Meurens, F., Summerfield, A., Nauwynck, H., Saif, L., and Gerdts, V. (2012). The Pig: a Model for Human Infectious Diseases. *Trends Microbiol.* 20 (1), 50–57. doi:10.1016/j.tim.2011.11.002

Molla, K. A., and Yang, Y. (2019). CRISPR/Cas-Mediated Base Editing: Technical Considerations and Practical Applications. *Trends Biotechnol.* 37 (10), 1121–1142. doi:10.1016/j.tibtech.2019.03.008

Mussolino, C., and Cathomen, T. (2012). TALE Nucleases: Tailored Genome Engineering Made Easy. *Curr. Opin. Biotechnol.* 23 (5), 644–650. doi:10.1016/j.copbio.2012.01.013

Ni, W., Qiao, J., Hu, S., Zhao, X., Regouski, M., Yang, M., et al. (2014). Efficient Gene Knockout in Goats Using CRISPR/Cas9 System. *PLoS One* 9 (9), e106718. doi:10.1371/journal.pone.0106718

Nishida, K., Arazoe, T., Yachie, N., Banno, S., Kakimoto, M., Tabata, M., et al. (2016). Targeted Nucleotide Editing Using Hybrid Prokaryotic and Vertebrate Adaptive Immune Systems. *Science* 353 (6305), aaf8729. doi:10.1126/science.aaf8729

Niu, Y., Shen, B., Cui, Y., Chen, Y., Wang, J., Wang, L., et al. (2014). Generation of Gene-Modified Cynomolgus Monkey via Cas9/RNA-Mediated Gene Targeting in One-Cell Embryos. *Cell* 156 (4), 836–843. doi:10.1016/j.cell.2014.01.027

Niu, D., Wei, H.-J., Lin, L., George, H., Wang, T., Lee, I.-H., et al. (2017a). Inactivation of Porcine Endogenous Retrovirus in Pigs Using CRISPR-Cas9. *Science* 357 (6357), 1303–1307. doi:10.1126/science.aan4187

Niu, Y., Jin, M., Li, Y., Li, P., Zhou, J., Wang, X., et al. (2017b). Biallelicβ-carotene Oxygenase 2knockout Results in Yellow Fat in Sheep via CRISPR/Cas9. *Anim. Genet.* 48 (2), 242–244. doi:10.1111/age.12515

Niu, Y., Zhao, X., Zhou, J., Li, Y., Huang, Y., Cai, B., et al. (2018). Efficient Generation of Goats with Defined Point Mutation (I397V) in GDF9 through CRISPR/Cas9. *Reprod. Fertil. Dev.* 30 (2), 307–312. doi:10.1071/RD17068

Oliver, D., Yuan, S., McSwiggin, H., and Yan, W. (2015). Pervasive Genotypic Mosaicism in Founder Mice Derived from Genome Editing through Pronuclear Injection. *PLoS One* 10 (6), e0129457. doi:10.1371/journal.pone.0129457

Petersen, B., Frenzel, A., Lucas-Hahn, A., Herrmann, D., Hassel, P., Klein, S., et al. (2016). Efficient Production of biallelicGGTA1knockout Pigsbycytoplasmic Microinjection of CRISPR/Cas9 into Zygotes. *Xenotransplantation* 23 (5), 338–346. doi:10.1111/xen.12258

Porrett, P. M., Orandi, B. J., Kumar, V., Houp, J., Anderson, D., Cozette Killian, A., et al. (2022). First Clinical-grade Porcine Kidney Xenotransplant Using a Human Decedent Model. *Am. J Transplant.* 22, 1037–1053. doi:10.1111/ajt.16930

Prabhakar, S. (2012). Translational Research Challenges. *J. Investig. Med.* 60 (8), 1141–1146. doi:10.2310/JIM.0b013e318271fb3b

Prather, R. S., Hawley, R. J., Carter, D. B., Lai, L., and Greenstein, J. L. (2003). Transgenic Swine for Biomedicine and Agriculture. *Theriogenology* 59 (1), 115–123. doi:10.1016/s0093-691x(02)01263-3

Rao, S., Fujimura, T., Matsunari, H., Sakuma, T., Nakano, K., Watanabe, M., et al. (2016). Efficient Modification of the Myostatin Gene in Porcine Somatic Cells and Generation of Knockout Piglets. *Mol. Reprod. Dev.* 83 (1), 61–70. doi:10.1002/mrd.22591

Ribitsch, I., Baptista, P. M., Lange-Consiglio, A., Melotti, L., Patruno, M., Jenner, F., et al. (2020). Large Animal Models in Regenerative Medicine and Tissue Engineering: To Do or Not to Do. *Front. Bioeng. Biotechnol.* 8, 972. doi:10.3389/fbioe.2020.00972

Roura, E., Koopmans, S.-J., Lallès, J.-P., Le Huerou-Luron, I., de Jager, N., Schuurman, T., et al. (2016). Critical Review Evaluating the Pig as a Model for Human Nutritional Physiology. *Nutr. Res. Rev.* 29 (1), 60–90. doi:10.1017/S0954422416000020

Ruan, J., Li, H., Xu, K., Wu, T., Wei, J., Zhou, R., et al. (2015). Highly Efficient CRISPR/Cas9-mediated Transgene Knockin at the H11 Locus in Pigs. *Sci. Rep.* 5, 14253. doi:10.1038/srep14253

Ryu, S.-M., Koo, T., Kim, K., Lim, K., Baek, G., Kim, S.-T., et al. (2018). Adenine Base Editing in Mouse Embryos and an Adult Mouse Model of Duchenne Muscular Dystrophy. *Nat. Biotechnol.* 36 (6), 536–539. doi:10.1038/nbt.4148

Sakuma, T., Nishikawa, A., Kume, S., Chayama, K., and Yamamoto, T. (2014). Multiplex Genome Engineering in Human Cells Using All-In-One CRISPR/Cas9 Vector System. *Sci. Rep.* 4, 5400. doi:10.1038/srep05400

Schmidt, J. K., Strelchenko, N., Park, M. A., Kim, Y. H., Mean, K. D., Schotzko, M. L., et al. (2020). Genome Editing of CCR5 by CRISPR-Cas9 in Mauritian Cynomolgus Macaque Embryos. *Sci. Rep.* 10 (1), 18457. doi:10.1038/s41598-020-75295-z

Seita, Y., Morimura, T., Watanabe, N., Iwatani, C., Tsuchiya, H., Nakamura, S., et al. (2020). Generation of Transgenic Cynomolgus Monkeys Overexpressing the Gene for Amyloid-β Precursor Protein. *Jad* 75 (1), 45–60. doi:10.3233/JAD-191081

Shen, H. (2013). Precision Gene Editing Paves Way for Transgenic Monkeys. *Nature* 503 (7474), 14–15. doi:10.1038/503014a

Sun, Z., Ye, J., and Yuan, J. (2022). PINK1 Mediates Neuronal Survival in Monkey. *Protein Cell* 13 (1), 4–5. doi:10.1007/s13238-021-00889-w

Tian, H., Luo, J., Zhang, Z., Wu, J., Zhang, T., Busato, S., et al. (2018). CRISPR/Cas9-mediated Stearoyl-CoA Desaturase 1 (SCD1) Deficiency Affects Fatty Acid Metabolism in Goat Mammary Epithelial Cells. *J. Agric. Food Chem.* 66 (38), 10041–10052. doi:10.1021/acs.jafc.8b03545

Tu, Z., Yang, W., Yan, S., Guo, X., and Li, X.-J. (2015). CRISPR/Cas9: a Powerful Genetic Engineering Tool for Establishing Large Animal Models of Neurodegenerative Diseases. *Mol. Neurodegener.* 10, 35. doi:10.1186/s13024-015-0031-x

Tu, Z., Yang, W., Yan, S., Yin, A., Gao, J., Liu, X., et al. (2017). Promoting Cas9 Degradation Reduces Mosaic Mutations in Non-human Primate Embryos. *Sci. Rep.* 7, 42081. doi:10.1038/srep42081

Tu, Z., Zhao, H., Li, B., Yan, S., Wang, L., Tang, Y., et al. (2019). CRISPR/Cas9-mediated Disruption of SHANK3 in Monkey Leads to Drug-Treatable Autism-like Symptoms. *Hum. Mol. Genet.* 28 (4), 561–571. doi:10.1093/hmg/ddy367

Vilarino, M., Rashid, S. T., Suchy, F. P., McNabb, B. R., van der Meulen, T., Fine, E. J., et al. (2017). CRISPR/Cas9 Microinjection in Oocytes Disables Pancreas Development in Sheep. *Sci. Rep.* 7 (1), 17472. doi:10.1038/s41598-017-17805-0

Wan, H., Feng, C., Teng, F., Yang, S., Hu, B., Niu, Y., et al. (2015). One-step Generation of P53 Gene Biallelic Mutant Cynomolgus Monkey via the CRISPR/Cas System. *Cell Res.* 25 (2), 258–261. doi:10.1038/cr.2014.158

Wang, C.-E., Tydlacka, S., Orr, A. L., Yang, S.-H., Graham, R. K., Hayden, M. R., et al. (2008). Accumulation of N-Terminal Mutant Huntingtin in Mouse and Monkey Models Implicated as a Pathogenic Mechanism in Huntington's Disease. *Hum. Mol. Genet.* 17 (17), 2738–2751. doi:10.1093/hmg/ddn175

Wang, H., Yang, H., Shivalila, C. S., Dawlaty, M. M., Cheng, A. W., Zhang, F., et al. (2013). One-step Generation of Mice Carrying Mutations in Multiple Genes by CRISPR/Cas-mediated Genome Engineering. *Cell* 153 (4), 910–918. doi:10.1016/j.cell.2013.04.025

Wang, K., Ouyang, H., Xie, Z., Yao, C., Guo, N., Li, M., et al. (2015a). Efficient Generation of Myostatin Mutations in Pigs Using the CRISPR/Cas9 System. *Sci. Rep.* 5, 16623. doi:10.1038/srep16623

Wang, X., Yu, H., Lei, A., Zhou, J., Zeng, W., Zhu, H., et al. (2015b). Generation of Gene-Modified Goats Targeting MSTN and FGF5 via Zygote Injection of CRISPR/Cas9 System. *Sci. Rep.* 5, 13878. doi:10.1038/srep13878

Wang, X., Cai, B., Zhou, J., Zhu, H., Niu, Y., Ma, B., et al. (2016a). Disruption of FGF5 in Cashmere Goats Using CRISPR/Cas9 Results in More Secondary Hair Follicles and Longer Fibers. *PLoS One* 11 (10), e0164640. doi:10.1371/journal.pone.0164640

Wang, X., Cao, C., Huang, J., Yao, J., Hai, T., Zheng, Q., et al. (2016b). One-step Generation of Triple Gene-Targeted Pigs Using CRISPR/Cas9 System. *Sci. Rep.* 6, 20620. doi:10.1038/srep20620

Wang, K., Tang, X., Xie, Z., Zou, X., Li, M., Yuan, H., et al. (2017). CRISPR/Cas9-mediated Knockout of Myostatin in Chinese Indigenous Erhualian Pigs. *Transgenic Res.* 26 (6), 799–805. doi:10.1007/s11248-017-0044-z

Wang, S., Ren, S., Bai, R., Xiao, P., Zhou, Q., Zhou, Y., et al. (2018a). No Off-Target Mutations in Functional Genome Regions of a CRISPR/Cas9-generated Monkey Model of Muscular Dystrophy. *J. Biol. Chem.* 293 (30), 11654–11658. doi:10.1074/jbc.AC118.004404

Wang, X., Niu, Y., Zhou, J., Zhu, H., Ma, B., Yu, H., et al. (2018b). CRISPR/Cas9-mediatedMSTNdisruption and Heritable Mutagenesis in Goats Causes Increased Body Mass. *Anim. Genet.* 49 (1), 43–51. doi:10.1111/age.12626

Wang, F., Zhang, W., Yang, Q., Kang, Y., Fan, Y., Wei, J., et al. (2020). Generation of a Hutchinson-Gilford Progeria Syndrome Monkey Model by Base Editing. *Protein Cell* 11 (11), 809–824. doi:10.1007/s13238-020-00740-8

Wasala, N. B., Hakim, C. H., Chen, S.-J., Yang, N. N., and Duan, D. (2019). Questions Answered and Unanswered by the First CRISPR Editing Study in a Canine Model of Duchenne Muscular Dystrophy. *Hum. Gene Ther.* 30 (5), 535–543. doi:10.1089/hum.2018.243

Whitworth, K. M., Lee, K., Benne, J. A., Beaton, B. P., Spate, L. D., Murphy, S. L., et al. (2014). Use of the CRISPR/Cas9 System to Produce Genetically Engineered Pigs from In Vitro-Derived Oocytes and Embryos1. *Biol. Reprod.* 91 (3), 78. doi:10.1095/biolreprod.114.121723

Williams, D. K., Pinzón, C., Huggins, S., Pryor, J. H., Falck, A., Herman, F., et al. (2018). Genetic Engineering a Large Animal Model of Human Hypophosphatasia in Sheep. *Sci. Rep.* 8 (1), 16945. doi:10.1038/s41598-018-35079-y

Wu, M., Wei, C., Lian, Z., Liu, R., Zhu, C., Wang, H., et al. (2016). Rosa26-targeted Sheep Gene Knock-In via CRISPR-Cas9 System. *Sci. Rep.* 6, 24360. doi:10.1038/srep24360

Wu, J., Vilarino, M., Suzuki, K., Okamura, D., Bogliotti, Y. S., Park, I., et al. (2017). CRISPR-Cas9 Mediated One-step Disabling of Pancreatogenesis in Pigs. *Sci. Rep.* 7 (1), 10487. doi:10.1038/s41598-017-08596-5

Xie, J., Ge, W., Li, N., Liu, Q., Chen, F., Yang, X., et al. (2019). Efficient Base Editing for Multiple Genes and Loci in Pigs Using Base Editors. *Nat. Commun.* 10 (1), 2852. doi:10.1038/s41467-019-10421-8

Xie, Z., Jiao, H., Xiao, H., Jiang, Y., Liu, Z., Qi, C., et al. (2020). Generation of pRSAD2 Gene Knock-In Pig via CRISPR/Cas9 Technology. *Antivir. Res.* 174, 104696. doi:10.1016/j.antiviral.2019.104696

Yan, S., Tu, Z., Liu, Z., Fan, N., Yang, H., Yang, S., et al. (2018). A Huntingtin Knockin Pig Model Recapitulates Features of Selective Neurodegeneration in

Huntington's Disease. *Cell* 173 (4), 989–1002. e1013. doi:10.1016/j.cell.2018.03.005

Yang, S.-H., Cheng, P.-H., Banta, H., Piotrowska-Nitsche, K., Yang, J.-J., Cheng, E. C. H., et al. (2008). Towards a Transgenic Model of Huntington's Disease in a Non-human Primate. *Nature* 453 (7197), 921–924. doi:10.1038/nature06975

Yang, H., Wang, G., Sun, H., Shu, R., Liu, T., Wang, C.-E., et al. (2014). Species-dependent Neuropathology in Transgenic SOD1 Pigs. *Cell Res.* 24 (4), 464–481. doi:10.1038/cr.2014.25

Yang, L., Guell, M., Niu, D., George, H., Lesha, E., Grishin, D., et al. (2015). Genome-wide Inactivation of Porcine Endogenous Retroviruses (PERVs). *Science* 350 (6264), 1101–1104. doi:10.1126/science.aad1191

Yang, W., Li, S., and Li, X.-J. (2019a). A CRISPR Monkey Model Unravels a Unique Function of PINK1 in Primate Brains. *Mol. Neurodegener.* 14 (1), 17. doi:10.1186/s13024-019-0321-9

Yang, W., Liu, Y., Tu, Z., Xiao, C., Yan, S., Ma, X., et al. (2019b). CRISPR/Cas9-mediated PINK1 Deletion Leads to Neurodegeneration in Rhesus Monkeys. *Cell Res.* 29 (4), 334–336. doi:10.1038/s41422-019-0142-y

Yang, W., Chen, X., Li, S., and Li, X.-J. (2021). Genetically Modified Large Animal Models for Investigating Neurodegenerative Diseases. *Cell Biosci.* 11 (1), 218. doi:10.1186/s13578-021-00729-8

Yang, W., Guo, X., Tu, Z., Chen, X., Han, R., Liu, Y., et al. (2022). PINK1 Kinase Dysfunction Triggers Neurodegeneration in the Primate Brain without Impacting Mitochondrial Homeostasis. *Protein Cell* 13 (1), 26–46. doi:10.1007/s13238-021-00888-x

Yao, X., Liu, Z., Wang, X., Wang, Y., Nie, Y.-H., Lai, L., et al. (2018). Generation of Knock-In Cynomolgus Monkey via CRISPR/Cas9 Editing. *Cell Res.* 28 (3), 379–382. doi:10.1038/cr.2018.9

Yin, P., Li, S., Li, X.-J., and Yang, W. (2022). New Pathogenic Insights from Large Animal Models of Neurodegenerative Diseases. *Protein Cell* 1, 1. doi:10.1007/s13238-022-00912-8

Yoshimi, K., and Mashimo, T. (2018). Application of Genome Editing Technologies in Rats for Human Disease Models. *J. Hum. Genet.* 63 (2), 115–123. doi:10.1038/s10038-017-0346-2

Yuan, H., Yu, T., Wang, L., Yang, L., Zhang, Y., Liu, H., et al. (2020). Efficient Base Editing by RNA-Guided Cytidine Base Editors (CBEs) in Pigs. *Cell. Mol. Life Sci.* 77 (4), 719–733. doi:10.1007/s00018-019-03205-2

Yue, Y., Xu, W., Kan, Y., Zhao, H.-Y., Zhou, Y., Song, X., et al. (2021). Extensive Germline Genome Engineering in Pigs. *Nat. Biomed. Eng.* 5 (2), 134–143. doi:10.1038/s41551-020-00613-9

Ze, L., Hai-Yuan, Y., Ying, W., Man-Ling, Z., Xiao-Rui, L., Qiang, X., et al. (2017b). Generation of Tryptophan Hydroxylase 2 Gene Knockout Pigs by CRISPR/Cas9-mediated Gene Targeting. *J. Biomed. Res.* 31 (5), 445–452. doi:10.7555/JBR.31.20170026

Zhang, W., Wang, G., Wang, Y., Jin, Y., Zhao, L., Xiong, Q., et al. (2017a). Generation of Complement Protein C3 Deficient Pigs by CRISPR/Cas9-mediated Gene Targeting. *Sci. Rep.* 7 (1), 5009. doi:10.1038/s41598-017-05400-2

Zhang, X., Li, W., Liu, C., Peng, X., Lin, J., He, S., et al. (2017b). Alteration of Sheep Coat Color Pattern by Disruption of ASIP Gene via CRISPR Cas9. *Sci. Rep.* 7 (1), 8149. doi:10.1038/s41598-017-08636-0

Zhang, X., Li, W., Wu, Y., Peng, X., Lou, B., Wang, L., et al. (2017c). Disruption of the Sheep BMPR-IB Gene by CRISPR/Cas9 in *In Vitro* -produced Embryos. *Theriogenology* 91, 163–172. doi:10.1016/j.theriogenology.2016.10.025

Zhang, Y., Qin, W., Lu, X., Xu, J., Huang, H., Bai, H., et al. (2017d). Programmable Base Editing of Zebrafish Genome Using a Modified CRISPR-Cas9 System. *Nat. Commun.* 8 (1), 118. doi:10.1038/s41467-017-00175-6

Zhang, J., Cui, M. L., Nie, Y. W., Dai, B., Li, F. R., Liu, D. J., et al. (2018a). CRISPR /Cas9-mediated Specific Integration of Fat-1 at the Goat MSTN Locus. *FEBS J.* 285 (15), 2828–2839. doi:10.1111/febs.14520

Zhang, Y., Wang, Y., Yulin, B., Tang, B., Wang, M., Zhang, C., et al. (2018b). CRISPR/Cas9-mediated Sheep MSTN Gene Knockout and Promote sSMSCs Differentiation. *J. Cell Biochem.* 120, 1794–1806. doi:10.1002/jcb.27474

Zhang, B., Wang, C., Zhang, Y., Jiang, Y., Qin, Y., Pang, D., et al. (2020). A CRISPR-Engineered Swine Model of COL2A1 Deficiency Recapitulates Altered Early Skeletal Developmental Defects in Humans. *Bone* 137, 115450. doi:10.1016/j.bone.2020.115450

Zhao, H., Tu, Z., Xu, H., Yan, S., Yan, H., Zheng, Y., et al. (2017). Altered Neurogenesis and Disrupted Expression of Synaptic Proteins in Prefrontal Cortex of SHANK3-Deficient Non-human Primate. *Cell Res.* 27 (10), 1293–1297. doi:10.1038/cr.2017.95

Zhao, J., Lai, L., Ji, W., and Zhou, Q. (2019). Genome Editing in Large Animals: Current Status and Future Prospects. *Natl. Sci. Rev.* 6 (3), 402–420. doi:10.1093/nsr/nwz013

Hongbing, H., Yonghe, M., Tao, W., Ling, L., Xiuzhi, T., Rui, H., et al. (2014). One-step Generation of Myostatin Gene Knockout Sheep via the CRISPR/Cas9 System. *Front. Agr. Sci. Eng.* 1 (1), 2. doi:10.15302/j-fase-2014007

Zhong, H., Chen, Y., Li, Y., Chen, R., and Mardon, G. (2015). CRISPR-engineered Mosaicism Rapidly Reveals that Loss of Kcnj13 Function in Mice Mimics Human Disease Phenotypes. *Sci. Rep.* 5, 8366. doi:10.1038/srep08366

Zhou, X., Xin, J., Fan, N., Zou, Q., Huang, J., Ouyang, Z., et al. (2015). Generation of CRISPR/Cas9-mediated Gene-Targeted Pigs via Somatic Cell Nuclear Transfer. *Cell. Mol. Life Sci.* 72 (6), 1175–1184. doi:10.1007/s00018-014-1744-7

Zhou, W., Wan, Y., Guo, R., Deng, M., Deng, K., Wang, Z., et al. (2017). Generation of Beta-Lactoglobulin Knock-Out Goats Using CRISPR/Cas9. *PLoS One* 12 (10), e0186056. doi:10.1371/journal.pone.0186056

Zhou, S., Cai, B., He, C., Wang, Y., Ding, Q., Liu, J., et al. (2019). Programmable Base Editing of the Sheep Genome Revealed No Genome-wide Off-Target Mutations. *Front. Genet.* 10, 215. doi:10.3389/fgene.2019.00215

Zhu, S., Rong, Z., Lu, X., Xu, Y., and Fu, X. (2015). Gene Targeting through Homologous Recombination in Monkey Embryonic Stem Cells Using CRISPR/Cas9 System. *Stem Cells Dev.* 24 (10), 1147–1149. doi:10.1089/scd.2014.0507

Zou, Q., Wang, X., Liu, Y., Ouyang, Z., Long, H., Wei, S., et al. (2015). Generation of Gene-Target Dogs Using CRISPR/Cas9 System. *J. Mol. Cell Biol.* 7 (6), 580–583. doi:10.1093/jmcb/mjv061

Zou, Y., Li, Z., Zou, Y., Hao, H., Li, N., and Li, Q. (2018). An FBXO40 Knockout Generated by CRISPR/Cas9 Causes Muscle Hypertrophy in Pigs without Detectable Pathological Effects. *Biochem. Biophysical Res. Commun.* 498 (4), 940–945. doi:10.1016/j.bbrc.2018.03.085

Zou, X., Ouyang, H., Yu, T., Chen, X., Pang, D., Tang, X., et al. (2019). Preparation of a New Type 2 Diabetic Miniature Pig Model via the CRISPR/Cas9 System. *Cell Death Dis.* 10 (11), 823. doi:10.1038/s41419-019-2056-5

Zuo, E., Cai, Y.-J., Li, K., Wei, Y., Wang, B.-A., Sun, Y., et al. (2017). One-step Generation of Complete Gene Knockout Mice and Monkeys by CRISPR/Cas9-mediated Gene Editing with Multiple sgRNAs. *Cell Res.* 27 (7), 933–945. doi:10.1038/cr.2017.81

Conflict of Interest: The authors declare that the research was conducted in the absence of any commercial or financial relationships that could be construed as a potential conflict of interest.

Publisher's Note: All claims expressed in this article are solely those of the authors and do not necessarily represent those of their affiliated organizations, or those of the publisher, the editors and the reviewers. Any product that may be evaluated in this article, or claim that may be made by its manufacturer, is not guaranteed or endorsed by the publisher.

frontiers | Frontiers in Cell and Developmental Biology

TYPE Original Research
PUBLISHED 10 August 2022
DOI 10.3389/fcell.2022.964045

OPEN ACCESS

EDITED BY
Lin Yuan,
China Medical University, China

REVIEWED BY
Shoulong Deng,
Chinese Academy of Medical Sciences and Peking Union Medical College, China
Xiangpeng Dai,
Jilin University, China

*CORRESPONDENCE
Dawei Yu,
ydw023@163.com
Huabin Zhu,
zhuhuabin@caas.cn
Shijie Li,
lishijie20005@163.com
Huiying Zou,
zouhuiying@caas.cn

†These authors have contributed equally to this work

SPECIALTY SECTION
This article was submitted to Stem Cell Research, a section of the journal Frontiers in Cell and Developmental Biology

RECEIVED 08 June 2022
ACCEPTED 12 July 2022
PUBLISHED 10 August 2022

CITATION
Li J, Yu D, Wang J, Li C, Wang Q, Wang J, Du W, Zhao S, Pang Y, Hao H, Zhao X, Zhu H, Li S and Zou H (2022), Identification of the porcine IG-DMR and abnormal imprinting of DLK1-DIO3 in cloned pigs.
Front. Cell Dev. Biol. 10:964045.
doi: 10.3389/fcell.2022.964045

Identification of the porcine IG-DMR and abnormal imprinting of *DLK1-DIO3* in cloned pigs

Junliang Li[1,2†], Dawei Yu[1,3*†], Jing Wang[4†], Chongyang Li[4], Qingwei Wang[4], Jing Wang[5], Weihua Du[1], Shanjiang Zhao[1], Yunwei Pang[1], Haisheng Hao[1], Xueming Zhao[1], Huabin Zhu[1*], Shijie Li[2*] and Huiying Zou[1*]

[1]Institute of Animal Sciences, Chinese Academy of Agricultural Sciences, Beijing, China, [2]College of Life Sciences, Hebei Agricultural University, Baoding, Hebei, China, [3]National Germplasm Center of Domestic Animal Resources, Institute of Animal Sciences, Chinese Academy of Agricultural Sciences, Beijing, China, [4]State Key Laboratory of Stem Cell and Reproductive Biology, Institute of Zoology, Chinese Academy of Sciences, Beijing, China, [5]Department of Human Genetics David Geffen School of Medicine University of California Los Angeles, Los Angeles, CA, United States

Correct reprogramming of the *DLK1-DIO3* imprinted region is critical for the development of cloned animals. However, in pigs, the imprinting and regulation of the *DLK1-DIO3* region has not been systematically analyzed. The objective of this study was to investigate the imprinting status and methylation regulation of the *DLK1-DIO3* region in wild-type and cloned neonatal pigs. We mapped the imprinting control region, IG-DMR, by homologous alignment and validated it in sperm, oocytes, fibroblasts, and parthenogenetic embryos. Subsequently, single nucleotide polymorphism-based sequencing and bisulfite sequencing polymerase chain reaction were conducted to analyze imprinting and methylation in different types of fibroblasts, as well as wild-type and cloned neonatal pigs. The results showed that Somatic cell nuclear transfer (SCNT) resulted in hypermethylation of the IG-DMR and aberrant gene expression in the *DLK1-DIO3* region. Similar to wild-type pigs, imprinted expression and methylation were observed in the surviving cloned pigs, whereas in dead cloned pigs, the IG-DMR was hypermethylated and the expression of *GTL2* was nearly undetectable. Our study reveals that abnormal imprinting of the *DLK1-DIO3* region occurs in cloned pigs, which provides a theoretical basis for improving the cloning efficiency by gene editing to correct abnormal imprinting.

KEYWORDS

pig, IG-DMR, DNA methylation, genomic imprinting, SCNT

Introduction

Somatic cell nuclear transfer (SCNT) is an assisted reproduction technology applied in the production of genetically modified (transgenic) animals, multiplication of elite animals, and protection of endangered species. Although the SCNT technology has been well developed in most domesticated and laboratory animals, the efficiency remains low, which limits its widespread application. Cloned animals show high rates of abortion

during the perinatal period and reduced neonatal viability due to obesity, immunodeficiency, and respiratory defects (Ogura et al., 2013; Loi et al., 2016). A growing number of studies have demonstrated that cloned animals often undergo epigenetic modification errors, with gene imprinting being a major cause of developmental disorders in cloned animals (Matoba and Zhang 2018). The erasure and reconstruction of gene imprinting during somatic cell nuclear transfer cannot fully mimic normal gamete fertilization and embryo development, resulting in the loss of gene imprinting, which in turn affects the development of cloned embryos.

Imprinted genes are usually present in clusters, and the *delta-like homolog one* gene and the *type III iodothyronine deiodinase* gene (*DLK1-DIO3*) imprinted domains are located on chromosomes 12 (Schmidt et al., 2000) and 14 (Miyoshi et al., 2000) in mouse and human, respectively. The *DLK1-DIO3* imprinting domain spans a region of 825 kb in the mouse and contains multiple coding and non-coding transcripts (da Rocha et al., 2008). The main genes are the paternally expressed imprinted genes *DLK1*, *RTL1*, and *DIO3,* and the maternally expressed imprinted gene *GTL2*. The genetic spacer region DMR (intergenic DMR, IG-DMR) located between *GTL2* and *DLK1* has been demonstrated to regulate the expression of the entire DLK1-DIO3 region. The *GTL2* gene has been shown to repress the expression of the maternally expressed gene *DLK1* in cis-regulation by recruiting polycomb repressive complex II (PRC2) in mice (Zhao et al., 2010; Kaneko et al., 2014; Das et al., 2015; Sanli et al., 2018). Previous studies have reported that the control of *GTL2* expression by the IG-DMR is essential for the maintenance of imprinting in the *DLK1-DIO3* domain (Lin et al., 2003; Kota et al., 2014; Das et al., 2015; Luo et al., 2016).

Loss of imprinting of *DLK1-DIO3* is associated with severe developmental defects and malignant tumorigenesis (da Rocha et al., 2008; Jelinic and Shaw 2007; Khoury et al., 2010; Manodoro et al., 2014). The *DLK1-DIO3* imprinted domain plays an important role in the derivation and culture of induced pluripotent stem cells and embryonic stem cells in mice (Liu et al., 2010; Carey et al., 2011; Stadtfeld et al., 2012; Mo et al., 2015). A recent study successfully generated bimaternal and bipaternal mice by knocking out three maternal imprinting regions (including the IG-DMR) and seven paternal imprinting regions in parthenogenetic haploid stem cells and parthenogenetic haploid stem cells, respectively. The bimaternal mice survived to adulthood, while the bipaternal mice survived more than 48 h (Li et al., 2018). These results suggest that proper maintenance of imprinting in the *DLK1-DIO3* region is critical for embryonic development.

The expression of imprinting genes is controlled by DNA methylation marks that are established in germ cells in a sex-specific manner by cis-regulated differentially methylated regions (DMRs) called imprinting control regions (ICRs). Differentially methylated regions within imprinted loci undergo binding of specific transcription factors and modification by chromatin modifiers, ultimately establishing single allele expression patterns (Ferguson-Smith and Bourc'his 2018). Countless reports in the human and mouse have shown that the IG-DMR is the ICR of the *DLK1-DIO3* imprinting region. (Rocha et al., 2008; Saito et al., 2017; Tucci et al., 2019), but there are no reports in large mammals such as the pig.

Previous studies have demonstrated that the *DLK1-DIO3* region is silenced in cloned pig embryos, and the survival rate of cloned pigs is significantly improved by dosage compensation of the *RTL1* gene, indicating that the imprinting of the *DLK1-DIO3* region is abnormal in cloned pigs (Yu et al., 2018). Currently, there are few studies on the *DLK1-DIO3* region. In addition, the location of the IG-DMR imprinting regulatory region in the *DLK1-DIO3* region and the imprinting state of the *DLK1-DIO3* region in pigs remain unknown. Therefore, a detailed and systematic study of the porcine *DLK1-DIO3* imprinting region is necessary to provide a theoretical basis for improving the efficiency of pig cloning.

In the present study, the conserved sequences of the IG-DMRs in the mouse, human, and sheep were used for a comparative analysis of the porcine genome, and the location of the IG-DMR in the pig was localized. Methylation analysis of the IG-DMR showed that the methylation of cloned fetal fibroblasts and neonatal cloned dead pigs was higher than that of corresponding donor cells and wild-type neonates. In addition, the expression of the *DLK1-DIO3* region was aberrant, and the expression of *GTL2* was nearly completely lost in neonatal cloned dead pigs, indicating abnormal imprinting in the *DLK1-DIO3* imprinted domain.

Materials and methods

Primary cell isolation and culture

Porcine fetal fibroblasts (PEFs) were isolated from 20 to 30-day-old embryos of forward and backward crosses of laboratory minipigs, Duroc and Rongchang. Porcine fetal fibroblasts were cultured in Dulbecco's modified Eagle medium containing 10% fetal bovine serum, 1% non-essential amino acids (Invitrogen), and 1% penicillin–streptomycin (Gibco) in a constant temperature and humidified incubator at 37.5 ˚C and 5% CO_2.

Collection and *in vitro* maturation of porcine oocytes

The bilateral ovaries of slaughterhouse sows were harvested within 30 min of slaughtering and dried with sterilized gauzes. The ovaries were placed in wide-mouth thermos flasks filled in sterilized saline (containing both antibiotics) at a temperature of 30–35˚C and transported back to the laboratory within 2 h. The follicular fluid from follicles of 3–6 mm in diameter was collected with an 18-gauge needle connected to a filter pump in a 50-ml centrifuge tube and undisturbed for 45–60 min. The supernatant

was discarded, and Poly (vinyl alcohol)-Phosphate Buffered Saline (PVA-PBS) solution was added to the precipitate, followed by resuspension in a 60-mm cell culture dish. The intact cumulus and oocytes (COCs) were collected with a mouth pipette under a body view microscope and cultured in an incubator at 38.5°C with 5% CO_2 for approximately 40 h. The matured COCs were transferred into T2 solution containing l mg/ml hyaluronidase pre-warmed to 38.5°C, followed by gentle pipetting. The oocytes with clear perivitelline gaps and homogenized cytoplasm were selected under the body view microscope and placed in T2 solution pre-warmed to 38.5°C.

Nuclear transfer

The mature oocytes were removed by micro-manipulation. Next, the individual donor cells were injected into the perivitelline space, and fusion was completed with two 1.2 kV/cm DC pulses (1-s interval) of 30 μs in fusion medium [0.3 M mannitol, 1.0 mM $CaCl_2$, 0.1 mM $MgCl_2$, 0.5 mM HEPES (pH 7.0–7.4)] using a BTX electronic cell manipulator. The oocytes were then incubated for 30 min in porcine zygote medium-3 (PZM-3), and the fusion percentage was calculated under a stereomicroscope. Fifty fused embryos were placed into a four-well dish (Nunc) containing 500 μl of PZM-3 pre-warmed to 38.5°C and incubated at 5% CO_2 with maximum humidity.

Embryo transfer

The day-1 NT zygotes were surgically transferred into surrogate mothers (250–300 zygotes per surrogate). Approximately 25 days later, the pregnancy status of each surrogate was determined by ultrasonography.

Sample collection

The pregnant sows were executed on gestational day 114, and the skin, fat, muscle, and peritoneum were incised sequentially in the lower abdomen. The uterine body and uterine horns were ligated with hemostats, and the uterus was removed for dissection. An incision in the uterus was made to detach the placenta containing the fetus from the uterus. Finally, the fetus was removed for anatomical sampling. These tissues are subsequently used to extract RNA or DNA.

RNA and DNA extraction

Fetuses and placentae were frozen in liquid N_2 and grounded in a mortar with a pestle. Half of each tissue was used for RNA extraction, and the remaining half was used for DNA extraction. RNA was extracted using the RNeasy Mini Kit (Qiagen), according to the manufacturer's protocol. To eliminate contamination of RNA with DNA, genomic DNA was removed by treatment with DNase I. The RNA was eluted in RNase free water and stored at −80°C. The DNA samples were extracted using the QIAamp DNA Mini Kit (Qiagen), according to the manufacturer's protocol. The DNA was eluted in sterile RNase-free water and stored at -20 °C until use.

RNA reverse transcription and quantitative polymerase chain reaction analysis

One microgram of total RNA was converted to a final volume of 20 μl of cDNA using the HiScript®III First Strand cDNA Synthesis Kit. The universal SYBR qPCR Master Mix was used for quantitative polymerase chain reactions. The procedure included 40 cycles of pre-denaturation (95°C, 30 s) and amplification (95°C, 10 s; 60°C, 30 s), followed by melting curve analysis (95°C, 15 s; 60°C, 1 min; 95°C, 15 s). The expression of the housekeeping gene glyceraldehyde-3-phosphate dehydrogenase (GAPDH) was used as a control. The primer information is provided in Supplementary Table S1. Statistical analyses were performed using Excel and graphs were prepared using GraphPad Prism 5, and the statistical significance was set at 0.05.

Bisulfite genomic sequencing analysis

Genomic DNA was extracted from tissue samples using the TIANamp Genomic DNA Kit. For bisulfite genomic sequencing, 1 μg of gDNA was subjected to bisulfite treatment using the EpiTect Bisulfite Kit (Qiagen, Germany), according to the manufacturer's protocol. Bisulfite sequencing PCR primers were designed using a web-based methylation primer tool (http://www.urogene.org/cgi-bin/methprimer/methprimer.cgi). The PCR products were cloned into the pMD19-T vector. At least ten randomly selected clones were sequenced. The sequences were aligned using a web-based quantification tool for methylation analysis (QUMA; http://quma.cdb.riken.jp/).

Examination of the allelic expression status of *DLK1*, *GTL2*, and *DIO3*

All heterozygous individuals corresponding to each SNP were used to analyze the allelic expression of *DLK1*, *GTL2*, and *DIO3* by quantitative PCR. The cDNA templates were reverse transcribed from fetal and placental samples by random hexamer priming. The primers DK-F and DK-R were used for *DLK1* expression analysis, the primers GT-F and GT-R were used for *GTL2* expression analysis, and the primers DO-F and DO-R were used for *DIO3* expression analysis. The cDNA

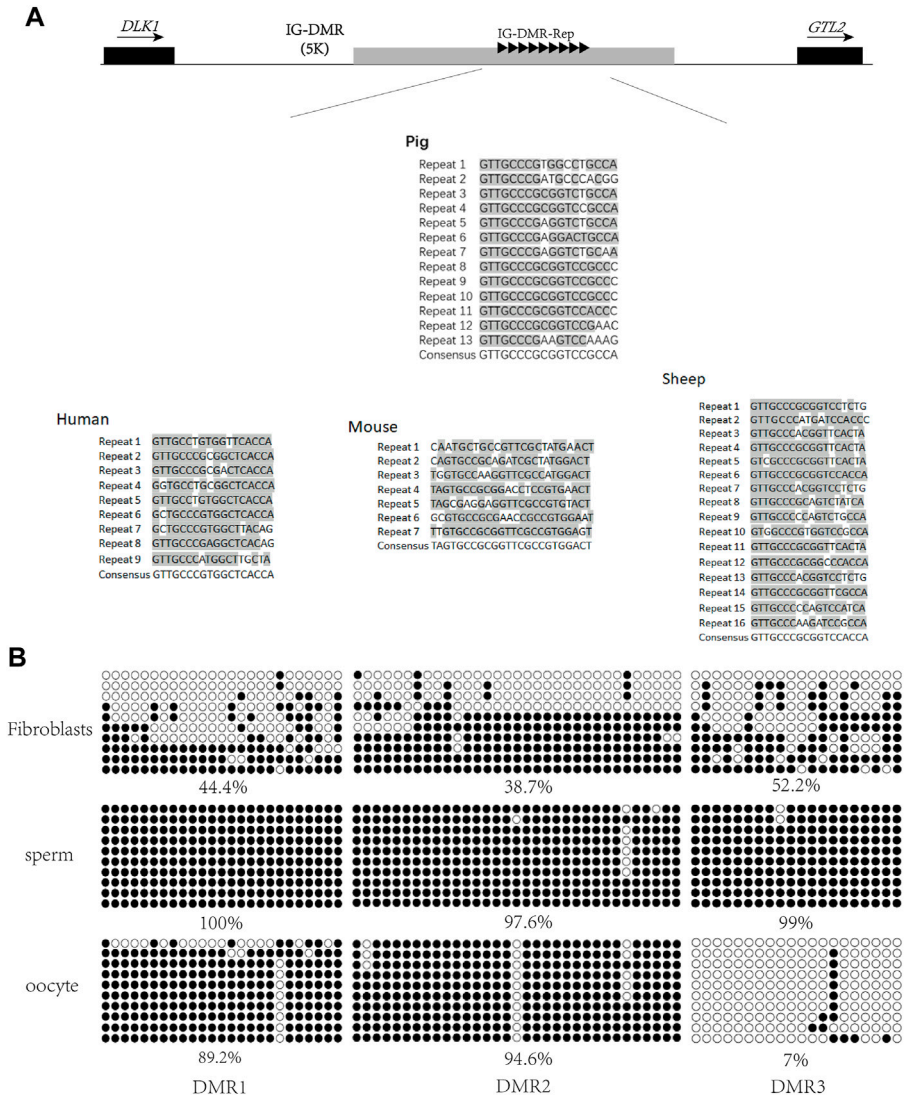

FIGURE 1
Screening of porcine IG-DMR. **(A)** Analysis of the IG-DMR tandem repeat sequences in pigs by interspecies conserved sequences. The black squares represent the positions of *DLK1* and *GTL2*, respectively. The arrow direction is the gene transcription direction. The gray rectangle represents the IG-DMR candidate region (5 kb). The black triangle represents the conserved interspecies tandem repeat sequence, and the gray areas of the tandem repeat sequences in human, mouse, sheep, and pig are the conserved sequence dinucleotides. **(B)** Analysis of methylation in porcine fibroblasts, sperm, and oocytes Each circle represents a CpG dinucleotide. The degree of methylation (%) is based on methylated CpGs/all CpGs; open circles indicate unmethylated CpGs and filled circles indicate methylated CpGs.

templates were amplified for 35 cycles. The PCR products were extracted from agarose gels using the Gel Recovery Kit (Sangon, Shanghai, China) and subjected to direct sequencing.

Results

Identification of the porcine IG-DMR

A previous study has reported that conserved repeats exist in the IG-DMRs of the human, mouse, and sheep (Paulsen et al., 2001). To investigate whether such repeats exist in the porcine IG-DMR, the conserved repeats from the human, mouse, and sheep were aligned with the porcine *DLK1-GTL2* region. As a result, conserved repeats were observed 5 kb upstream of *GTL2* in the pig (Figure 1A). The repeat sequence of the pig included 13 repeats, and the conserved sequence was GTTGCCCGCGGT CCGCCA.

To map the porcine IG-DMR, we used a website tool (MethPrimer) to predict the three DMRs around the repeats and designed methylation primers to analyze this region. The methylation detection of the three DMRs was carried

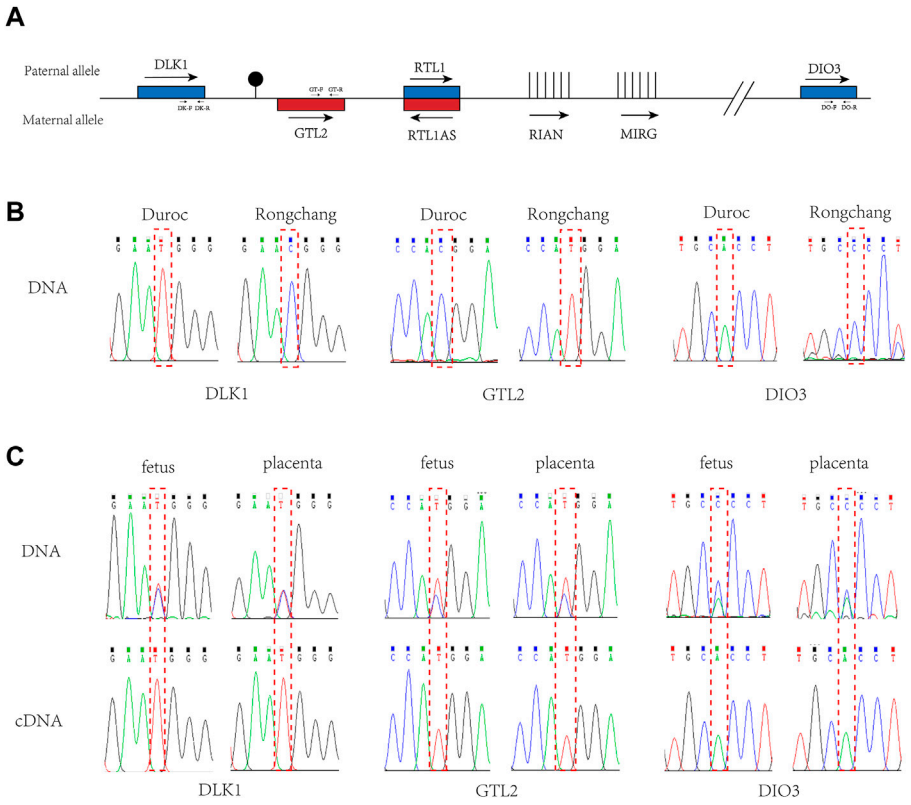

FIGURE 2
Imprinted expression of DLK1, GTL2, and DIO3 in the DLK1-DIO3 region. **(A)**. Structure diagram of the *DLK1-DIO3* imprinted domain. Blue squares represent paternal expression imprinted genes, and red squares represent maternal expression imprinted bases. The arrow direction is the transcription direction, and vertical lines represent non-coding RNA. Primer positions and directions are marked on the corresponding genes. **(B)**. Validation of SNPs in Rongchang and Duroc pig genomes. **(C)**. Allele-specific expression analysis of *DLK1*, *GTL2*, and *DIO3* in the fetus and placenta of the three crossbred pigs. The above sequencing results used the genome as a template for PCR, and the following sequencing results used cDNA as a template for PCR. The red-dashed boxes indicate SNP loci.

out in sperm, oocytes, and fibroblasts. The results showed that DMR3 was hypomethylated in oocytes, hypermethylated in sperm, and half hypermethylated and half hypomethylated in fibroblasts, suggesting DMR3 is the IG-DMR regulating imprinting in the *DLK1-GTL2* region (Figure 1B).

Conserved imprinting of the porcine *DLK1-DIO3* region

To examine the imprinting status of the *DLK1-DIO3* region (Figure 2A), we performed allele-specific expression analysis in 20-days (20-d) Rongchang (mother) and Duroc (father) crossbred pigs. To distinguish the expression between paternal and maternal alleles, we searched for SNPs in the *DLK1-DIO3* region between the two pig breeds using the UCSC database (UCSC Genome Browser Home). Three SNPs (rs81211138, rs325797437, and rs343094622) were identified in *DLK1*, *GTL2*, and *RTL1*, respectively, and verified in the genomes of the female parent Rongchang pig and the male parent Duroc pig (Table 1; Figure 2B). The SNP rs81211138 in *DLK1* was C in Rongchang and T in Duroc. The SNP rs325797437 in *GTL2* was T in Rongchang and C in Duroc. The SNP rs343094622 in *DIO3* was C in Rongchang and A in Duroc (Figure 2C). Quantitative polymerase chain reactions were performed to detect the expression of the three genes in fetuses and placentae of 20-d crossbred pigs. The PCR products were sequenced and showed monoallelic expression of *DLK1*, *GTL2*, and *DIO3* in the three crossbred pigs.

Combined with SNP analysis, *DLK1* and *DIO3* were determined to be expressed by the paternal chromosome and *GTL2* was determined to be expressed by the maternal chromosome. The results indicated that *DLK1* and *DIO3* in the porcine *DLK1-DIO3* imprinted domain were maternally imprinted genes and *GTL2* was paternally imprinted, consistent with the imprinting status of the mouse *DLK1-DIO3* imprinted domain (Edwards et al., 2008; Li et al., 2008;

TABLE 1 *DLK1*, *GTL2*, and *DIO3* gene SNPs in both Rongchang and Duroc minipigs.

Gene	dbSNP	SNP position	Duroc	Rongchang
DLK1	rs81211138	chr7:132345395-132345395	T	C
GTL2	rs325797437	chr7:132161133-132161133	C	T
DIO3	rs343094622	chr7:130203103-130203103	A	C

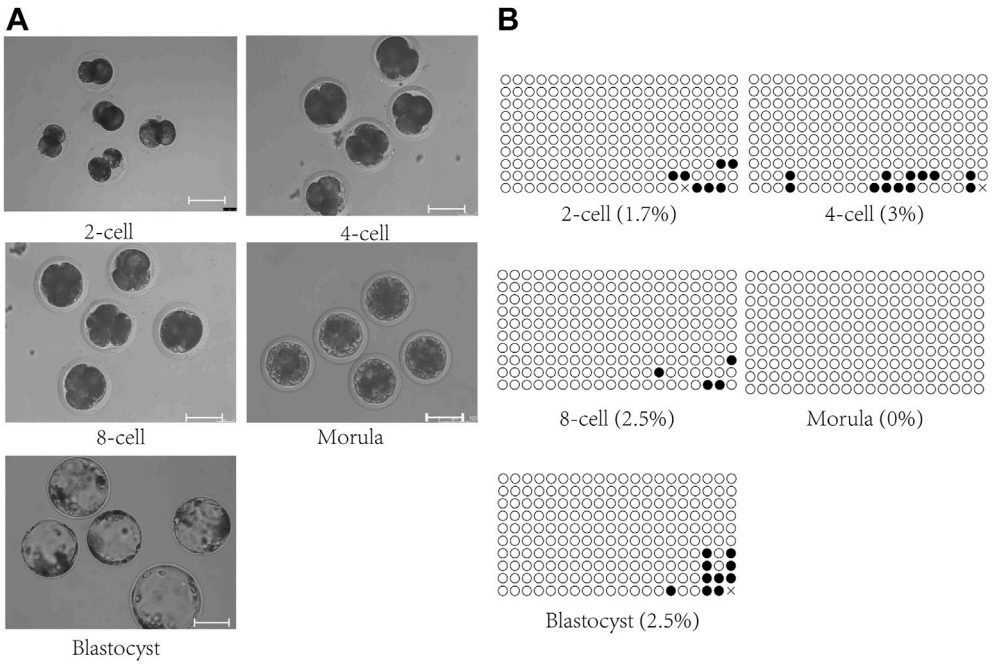

FIGURE 3
Methylation analysis of the IG-DMR in parthenogenetic embryos. **(A)**. Parthenogenetic embryos at different developmental stages. Scale bars, 100 μm. **(B)**. Methylation analysis of the IG-DMR in parthenogenetic embryos. Each circle represents a CpG dinucleotide. The degree of methylation (%) is based on methylated CPGs/all CPGs; open circles indicate unmethylated CpGs, and filled circles indicate methylated CpGs.

Coster et al., 2012). These results reveal that imprinting of the *DLK1-DIO3* domain is conserved in mammals (Coster et al., 2012; Kalish et al., 2014).

IG-DMR is hypomethylated in porcine parthenogenetic embryos

The genome of parthenogenetic embryos is derived from oocytes. Methylation analysis of the IG-DMR was conducted on parthenogenetic embryos at different developmental stages (Figure 3). The results showed that the IG-DMR in parthenogenetic embryos remained hypomethylated from the two-cell stage to the blastocyst stage, consistent with the hypomethylation of the IG-DMR in the female parent.

SCNT alters imprinting and methylation of the *DLK1-DIO3* region

The data from mice and some pigs showed that the methylation of the IG-DMR and the gene expression of the *DLK1-DIO3* imprinted domain were abnormal in unisexual embryos and cloned animals (Wei et al., 2010; Aronson et al., 2021; Wei et al., 2022). Therefore, we initially performed methylation analysis of the IG-DMR and examined gene imprinting expression of the *DLK1-DIO3* region in porcine fetal fibroblasts (pEF-1, pEF-2) (Figure 4A), fetal fibroblasts derived from porcine somatic cell nuclear transfer embryos (pEF-1-NT, pEF-2-NT) (Figure 4B), and fetal fibroblasts derived from porcine parthenogenetic embryos (PApEF-1, PApEF-2, PApEF-3) (Figure 4C). PEF-1 and PEF-2 were

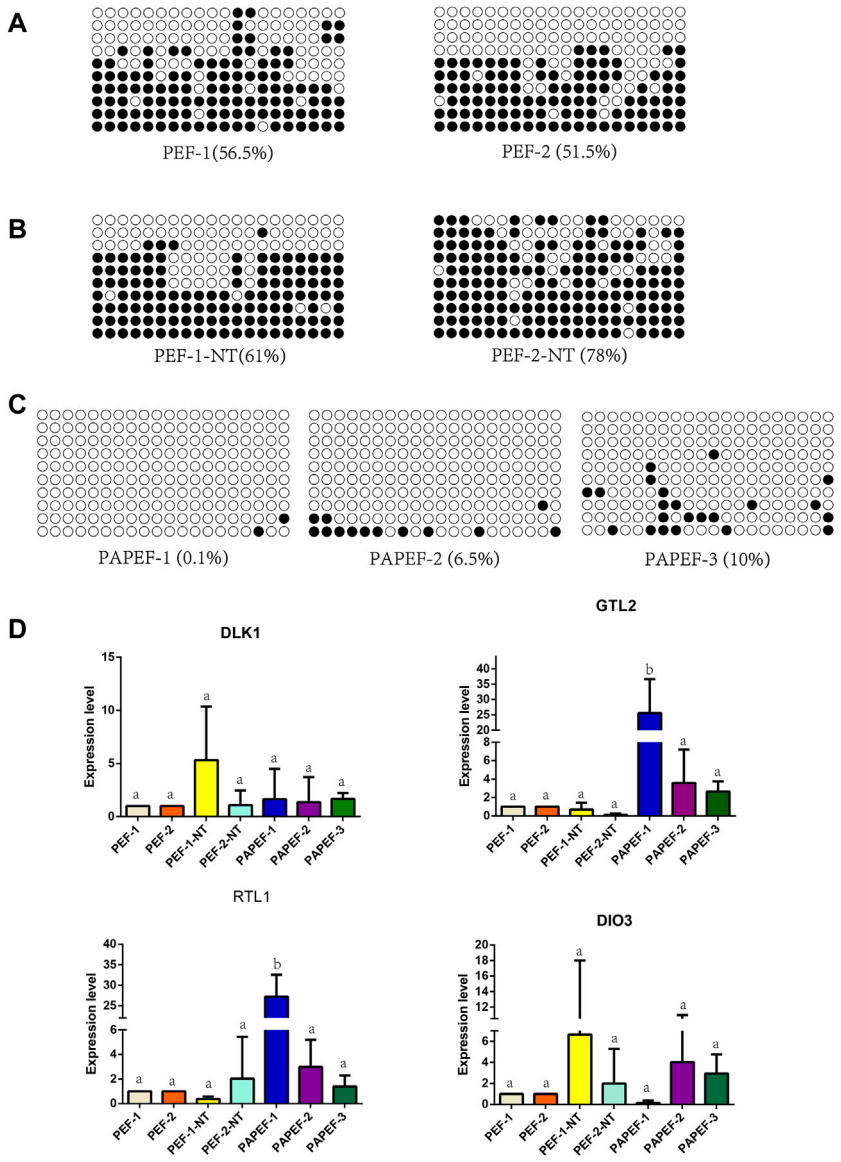

FIGURE 4
Methylation analysis of IG-DMR gene imprinting expression of the DLK1-DIO3 region in pEF, NTpEF, and PApEF. **(A)** Analysis of IG-DMR methylation levels in pEF, **(B)** NTpEF, and **(C)** PApEF. Each circle represents one CpG dinucleotide. The degree of methylation (%) is based on methylated CPGs/all CPGs; open circles indicate unmethylated CpGs, and filled circles indicate methylated CpGs. **(D)** Analysis of *DLK1*, *GTL2*, *RTL1*, and *DIO3* gene expression in pEF, NTpEF, and PApEF. Horizontal coordinates are samples, and vertical coordinates are gene expression levels. Different letters **(A,B)** indicate significant differences ($p < 0.05$).

donor cells for nuclear transfer embryos of PEF-1-NT and PEF-2-NT, respectively. The IG-DMR methylation levels of PEF-1-NT and PEF-2-NT were higher than those of PEF-1 and PEF-2. The IG-DMRs of PApEF-1, PApEF-2, and PApEF-3 were hypomethylated, consistent with previous results in early parthenogenetic embryos (Sato et al., 2011). Correspondingly, the *GTL2* expression level was decreased in pEF-1-NT and pEF-2-NT, whereas it was increased in PApEF-1, PApEF-2, and PApEF-3, indicating the IG-DMR regulates the expression of *GTL2*. The expression levels of maternally imprinted genes *DLK1*, *RTL1*, and *DIO3* were not significantly different among the three types of cells (Figure 4D). These results reveal that the methylation status of the IG-DMR is abnormal in cloned and parthenogenetic embryos, which affects the expression of the paternally imprinted gene *GTL2*.

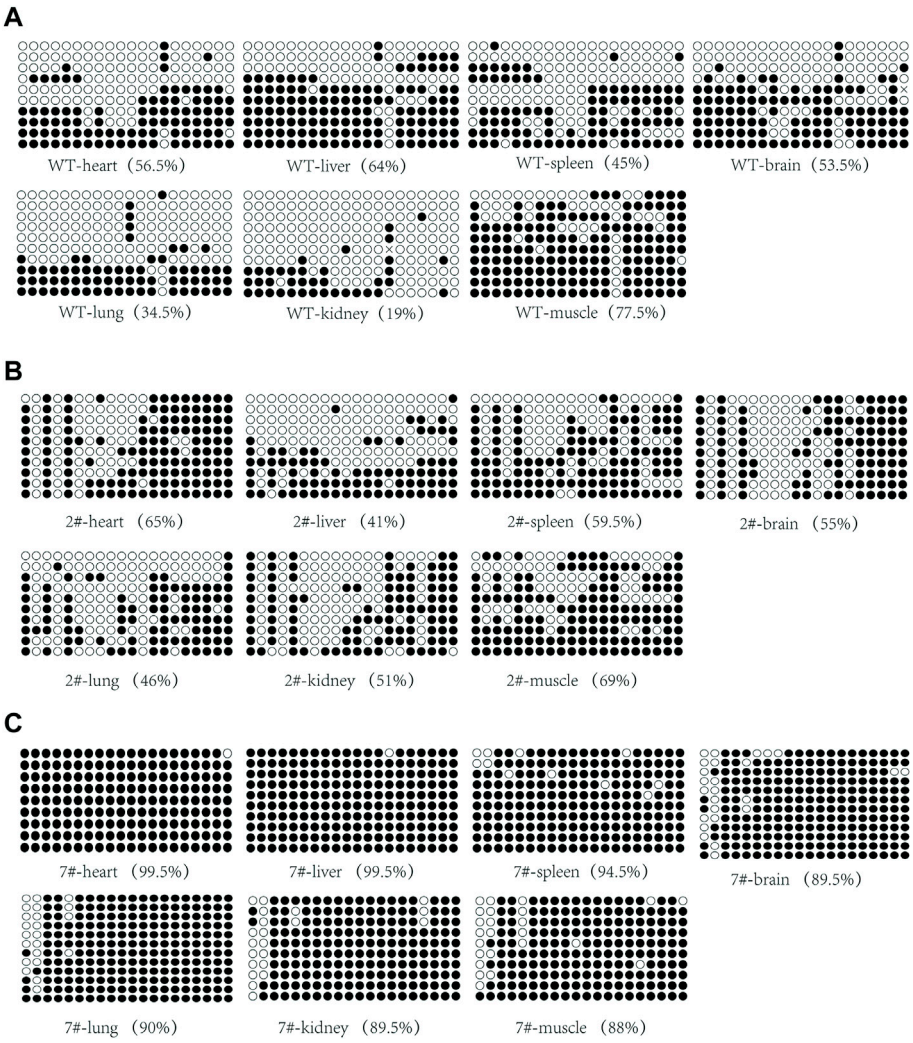

FIGURE 5
Analysis of IG-DMR methylation in wild-type neonatal pigs and cloned neonatal pigs. **(A)** Analysis of IG-DMR methylation in wild-type neonatal pigs. **(B)** Analysis of methylation in the surviving cloned piglet #2. **(C)** Analysis of methylation in dead cloned piglet #7. Each circle represents a CpG dinucleotide. The degree of methylation (%) is based on methylated CpGs/all CpGs; open circles indicate unmethylated CpGs, and filled circles indicate methylated CpGs.

IG-DMR is abnormally methylated in cloned pigs

To investigate in detail the methylation status of the IG-DMR in cloned pigs, we performed methylation assays on various tissues from wild-type neonatal and cloned neonatal pigs. Wild-type pigs are born naturally at term. The newborn cloned pigs were obtained by caesarean section at term, of which #7 died during birth, while #2 and #28503 survived at birth. IG-DMR methylation analysis was performed on various tissues (heart, liver, spleen, lung, kidney, muscle, and brain) from these pigs. The methylation level in cloned pig #2 was not significantly different from that in wild-type pigs (Figures 5A,B; Supplementary Figure S1A), and the methylation degree of each tissue was approximately 50%, whereas the IG-DMR in cloned pig #7 was abnormally hypermethylated, and the methylation level of each tissue was higher than 88% (Figure 5C). Therefore, we hypothesize that reprogramming errors occur in the methylation of the IG-DMR during somatic reprogramming.

Abnormal imprinted expression in cloned pigs

We analyzed the gene expression of the *DLK1-DIO3* imprinted domain in wild-type neonatal pigs and cloned neonatal pigs. The results of quantitative PCR showed that

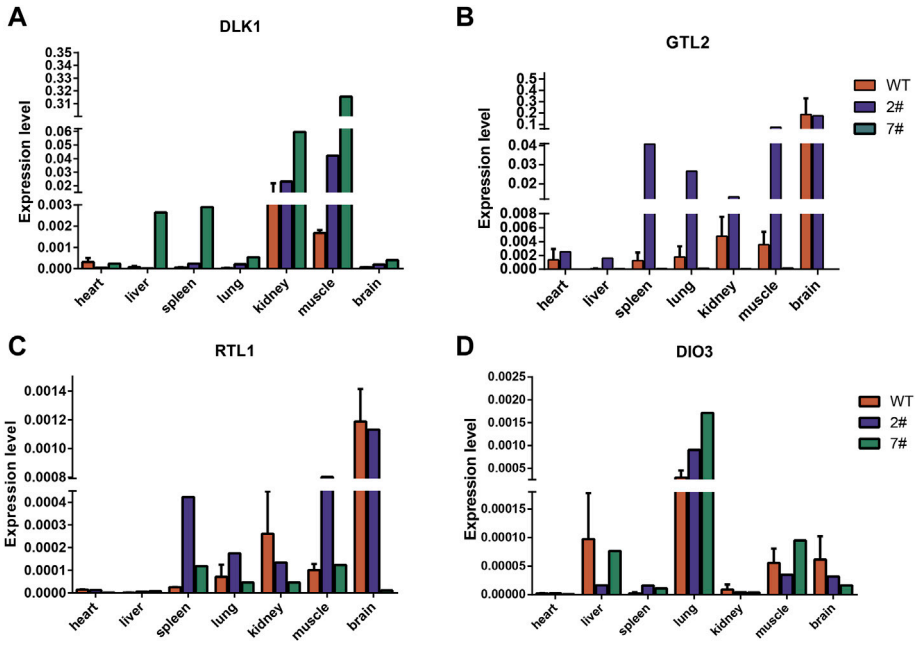

FIGURE 6
Analysis of DLK1-DIO3 imprinted domain gene expression in wild-type neonatal pigs and cloned neonatal pigs. **(A)** The expression of *DLK1* in wild-type neonatal pigs and cloned neonatal pigs. **(B)** The expression of *GTL2* in wild-type neonatal pigs and cloned neonatal pigs. **(C)** The expression of *RTL1* in wild-type neonatal pigs and cloned neonatal pigs. **(D)** The expression of *DIO3* in wild-type neonatal pigs and cloned neonatal pigs. The quantitative results are presented for tissue samples at horizontal coordinates and gene expression levels at vertical coordinates.

DLK1 was highly expressed in the muscle (Figures 6A; Supplementary Figure S1B), *DIO3* was highly expressed in the lungs (Figure 6D), and *GTL2* and *RTL1* were highly expressed in the brain (Figures 6B,C). The expression level of *GTL2* in cloned pig #2 was higher than that in wild-type pigs, with no significant differences in the expression levels of maternally imprinted genes in most tissues. However, *GTL2* expression was nearly undetectable in cloned pig #7, and *DLK1* expression was elevated in most tissues. The hypermethylation of the IG-DMR in cloned pig #7 inhibited the expression of *GTL2*, indicating aberrant methylation of the IG-DMR was an important cause of death of cloned pig #7.

Discussion

Genomic imprinting is critical for several life processes. The *DLK1-DIO3* imprinted domain is a cluster of genes essential for mammalian development. Numerous studies performed in the human and mouse have demonstrated that the IG-DMR is a key regulatory element of *DLK1-DIO3* and that it can also control maternally imprinted gene expression by regulating *GTL2* expression (Lin et al., 2003; Nowak et al., 2011; Kota et al., 2014; Luo et al., 2016; Wang et al., 2017; Saito et al., 2018). However, the imprinting of the *DLK1-DIO3* region in the pig and the location of the IG-DMR remain unknown. We examined the expression of *DLK1*, *GTL2*, and *DIO3* in Rongchang and Duroc crossbred pigs. The expression of male and female alleles was analyzed by SNPs in both pig breeds. The results showed that *DLK1* and *DIO3* were paternally expressed in the fetus and placenta, while *GTL2* was maternally expressed, consistent with the results observed in the human and mouse. Thus, the imprinting of the *DLK1-DIO3* region is well conserved in mammals.

Furthermore, we identified the tandem repeats in the pig based on the intermediate conserved repeat sequences in the human, mouse, and sheep IG-DMR and located it in the pig IG-DMR (Engemann et al., 2000; Okamura et al., 2000; Onyango et al., 2000; Paulsen et al., 2000). These tandem repeats are highly conserved, thus verifying the reliability of the pig IG-DMR locus. Nine tandem repeats were found in the human, seven conserved tandem repeats in the mouse, 16 conserved tandem repeats in the sheep, and 13 conserved tandem repeats, which spanned approximately 2.5 kb, in the pig.

The analysis of the methylation of the IG-DMR and the expression of each gene in the imprinted domain of *DLK1-DIO3* in cloned pigs showed abnormal hypermethylation of the IG-DMR in dead cloned pigs and the loss of *GTL2* expression in various tissues. *GTL2* is widely involved in various cell processes, including transcriptional repression and RNA interference-mediated mRNA degradation (Charlier et al., 2001) *GTL2* is expressed in the embryo and placenta, as well as in the adult, and the brain is the main site of its expression (Rocha et al., 2008).

Maternal deletion of *GTL2* and its DMR in the mouse leads to death due to alveolar hypoplasia and hepatocyte necrosis. We speculate that the loss of *GTL2* expression in various tissues may affect the growth and development of cloned pigs.

Previous studies in the mouse have indicated that *Gtl2* suppresses the expression of the parental allele (Rocha et al., 2008). In our study, the expression levels of the maternal imprinting genes *DLK1* and *DIO3* were higher in the tissues of cloned surviving and dead pigs than those in wild-type pigs, whereas the *DLK1* expression level was significantly higher in the muscle and kidneys and that of *DIO3* was significantly higher in the lungs of wild-type pigs and cloned surviving pigs. However, the *RTL1* expression level was unchanged. *RTL1* is mainly expressed in embryonic and placental tissues, where it is essential for normal placental development, and both paternal and maternal *RTL1* deletion can lead to growth retardation and prenatal death (Yu et al., 2018). The antisense strand of the *RTL1* gene encodes an RNA transcript and two maternally expressed microRNAs that are complementary to *RTL1* (Seitz et al., 2003). We speculate that *RTL1* was not elevated like the other maternally imprinted genes in cloned dead pigs because *RTL1as*, which is expressed by the antisense strand, also participates in the regulation of *RTL1* expression.

In conclusion, we have localized the porcine IG-DMR and demonstrated that the porcine *DLK1-DIO3* region was imprinted. In addition, abnormal *DLK1-DIO3* region imprinting was observed in cloned dead pigs by methylation and quantitative PCR analyses. Our study provides a theoretical basis for the future correction of aberrant methylation in the IG-DMR by epigenetic editing and provides new directions for improving the cloning efficiency in pigs.

Data availability statement

The original contributions presented in the study are included in the article/Supplementary Material, further inquiries can be directed to the corresponding authors.

Ethics statement

The animal study was reviewed and approved by The Institute of Animal Sciences, Chinese Academy of Agricultural Sciences, Beijing, China IAS 2021-240.

Author contributions

HYZ, DY, HBZ, and SL designed the research; JL, DY, JW, CL, QL, JW, WD, SZ, YP, HH, and XZ performed the experiments and analyzed the data. JL, HYZ, DY, JW, HBZ, and SL wrote the manuscript. All authors read and approved the final manuscript.

Funding

This study was funded by the Agricultural Science and Technology Innovation Program (ASTIP-IAS04-1, ASTIP-IAS06) and the Hebei Province Natural Science Foundation of China (C2020204004).

Acknowledgments

We would like to thank all those who helped us during the study and the writing of this manuscript.

Conflict of interest

The authors declare that the research was conducted in the absence of any commercial or financial relationships that could be construed as a potential conflict of interest.

Publisher's note

Supplementary material

The Supplementary Material for this article can be found online at: https://www.frontiersin.org/articles/10.3389/fcell.2022.964045/full#supplementary-material

References

Aronson, B. E., Scourzic, L., Shah, V., Swanzey, E., Kloetgen, A., Polyzos, A., et al. (2021). A bipartite element with allele-specific functions safeguards DNA methylation imprints at the Dlk1-Dio3 locus. *Dev. Cell* 56 (22), 3052–3065.e5. doi:10.1016/j.devcel.2021.10.004.e3055

Carey, B. W., Markoulaki, S., Hanna, J. H., Faddah, D. A., Buganim, Y., Kim, J., et al. (2011). Reprogramming factor stoichiometry influences the epigenetic state and biological properties of induced pluripotent stem cells. *Cell Stem Cell* 9 (6), 588–598. doi:10.1016/j.stem.2011.11.003

Charlier, C., Segers, K., Wagenaar, D., Karim, L., Berghmans, S., Jaillon, O., et al. (2001). Human-ovine comparative sequencing of a 250-kb imprinted domain encompassing the callipyge (clpg) locus and identification of six imprinted transcripts: DLK1, DAT, GTL2, PEG11, antiPEG11, and MEG8. *Genome Res.* 11 (5), 850–862. doi:10.1101/gr.172701

Coster, A., Madsen, O., Heuven, H. C., Dibbits, B., Groenen, M. A., van Arendonk, J. A., et al. (2012). The imprinted gene DIO3 is a candidate gene for litter size in pigs. *PLoS One* 7 (2), e31825. doi:10.1371/journal.pone.0031825

da Rocha, S. T., Edwards, C. A., Ito, M., Ogata, T., and Ferguson-Smith, A. C. (2008). Genomic imprinting at the mammalian Dlk1-Dio3 domain. *Trends Genet.* 24 (6), 306–316. doi:10.1016/j.tig.2008.03.011

Das, P. P., Hendrix, D. A., Apostolou, E., Buchner, A. H., Canver, M. C., Beyaz, S., et al. (2015). PRC2 is required to maintain expression of the maternal gtl2-rian-mirg locus by preventing de novo DNA methylation in mouse embryonic stem cells. *Cell Rep.* 12 (9), 1456–1470. doi:10.1016/j.celrep.2015.07.053

Edwards, C. A., Mungall, A. J., Matthews, L., Ryder, E., Gray, D. J., Pask, A. J., et al. (2008). The evolution of the DLK1-DIO3 imprinted domain in mammals. *PLoS Biol.* 6 (6), e135. doi:10.1371/journal.pbio.0060135

Engemann, S., Strödicke, M., Paulsen, M., Franck, O., Reinhardt, R., Lane, N., et al. (2000). Sequence and functional comparison in the beckwith-wiedemann region: Implications for a novel imprinting centre and extended imprinting. *Hum. Mol. Genet.* 9 (18), 2691–2706. doi:10.1093/hmg/9.18.2691

Ferguson-Smith, A. C., and Bourc'his, D. (2018). The discovery and importance of genomic imprinting. *Elife* 7, e42368. doi:10.7554/eLife.42368

Jelinic, P., and Shaw, P. (2007). Loss of imprinting and cancer. *J. Pathol.* 211 (3), 261–268. doi:10.1002/path.2116

Kalish, J. M., Jiang, C., and Bartolomei, M. S. (2014). Epigenetics and imprinting in human disease. *Int. J. Dev. Biol.* 58 (2-4), 291–298. doi:10.1387/ijdb.140077mb

Kaneko, S., Son, J., Bonasio, R., Shen, S. S., and Reinberg, D. (2014). Nascent RNA interaction keeps PRC2 activity poised and in check. *Genes Dev.* 28 (18), 1983–1988. doi:10.1101/gad.247940.114

Khoury, H., Suarez-Saiz, F., Wu, S., and Minden, M. D. (2010). An upstream insulator regulates DLK1 imprinting in AML. *Blood* 115 (11), 2260–2263. doi:10.1182/blood-2009-03-212746

Kota, S. K., Llères, D., Bouschet, T., Hirasawa, R., Marchand, A., Begon-Pescia, C., et al. (2014). ICR noncoding RNA expression controls imprinting and DNA replication at the Dlk1-Dio3 domain. *Dev. Cell* 31 (1), 19–33. doi:10.1016/j.devcel.2014.08.009

Li, X. P., Do, K. T., Kim, J. J., Huang, J., Zhao, S. H., Lee, Y., et al. (2008). Molecular characteristics of the porcine DLK1 and MEG3 genes. *Anim. Genet.* 39 (2), 189–192. doi:10.1111/j.1365-2052.2007.01693.x

Li, Z. K., Wang, L. Y., Wang, L. B., Feng, G. H., Yuan, X. W., Liu, C., et al. (2018). Generation of bimaternal and bipaternal mice from hypomethylated haploid ESCs with imprinting region deletions. *Cell Stem Cell* 23 (5), 665–676. doi:10.1016/j.stem.2018.09.004

Lin, S.-P., Youngson, N., Takada, S., Seitz, H., Reik, W., Paulsen, M., et al. (2003). Asymmetric regulation of imprinting on the maternal and paternal chromosomes at the Dlk1-Gtl2 imprinted cluster on mouse chromosome 12. *Nat. Genet.* 35 (1), 97–102. doi:10.1038/ng1233

Liu, L., Luo, G. Z., Yang, W., Zhao, X., Zheng, Q., Lv, Z., et al. (2010). Activation of the imprinted Dlk1-Dio3 region correlates with pluripotency levels of mouse stem cells. *J. Biol. Chem.* 285 (25), 19483–19490. doi:10.1074/jbc.M110.131995

Loi, P., Iuso, D., Czernik, M., and Ogura, A. (2016). A new, dynamic era for somatic cell nuclear transfer? *Trends Biotechnol.* 34 (10), 791–797. doi:10.1016/j.tibtech.2016.03.008

Luo, Z., Lin, C., Woodfin, A. R., Bartom, E. T., Gao, X., Smith, E. R., et al. (2016). Regulation of the imprinted Dlk1-Dio3 locus by allele-specific enhancer activity. *Genes Dev.* 30 (1), 92–101. doi:10.1101/gad.270413.115

Manodoro, F., Marzec, J., Chaplin, T., Miraki-Moud, F., Moravcsik, E., Jovanovic, J. V., et al. (2014). Loss of imprinting at the 14q32 domain is associated with microRNA overexpression in acute promyelocytic leukemia. *Blood* 123 (13), 2066–2074. doi:10.1182/blood-2012-12-469833

Matoba, S., and Zhang, Y. (2018). Somatic cell nuclear transfer reprogramming: Mechanisms and applications. *Cell Stem Cell* 23 (4), 471–485. doi:10.1016/j.stem.2018.06.018

Miyoshi, N., Wagatsuma, H., Wakana, S., Shiroishi, T., Nomura, M., Aisaka, K., et al. (2000). Identification of an imprinted gene, Meg3/Gtl2 and its human homologue MEG3, first mapped on mouse distal chromosome 12 and human chromosome 14q. *Genes cells.* 5 (3), 211–220. doi:10.1046/j.1365-2443.2000.00320.x

Mo, C. F., Wu, F. C., Tai, K. Y., Chang, W. C., Chang, K. W., Kuo, H. C., et al. (2015). Loss of non-coding RNA expression from the DLK1-DIO3 imprinted locus correlates with reduced neural differentiation potential in human embryonic stem cell lines. *Stem Cell Res. Ther.* 6 (1), 1. doi:10.1186/scrt535

Nowak, K., Stein, G., Powell, E., He, L. M., Naik, S., Morris, J., et al. (2011). Establishment of paternal allele-specific DNA methylation at the imprinted mouse Gtl2 locus. *Epigenetics* 6 (8), 1012–1020. doi:10.4161/epi.6.8.16075

Ogura, A., Inoue, K., and Wakayama, T. (2013). Recent advancements in cloning by somatic cell nuclear transfer. *Philos. Trans. R. Soc. Lond. B Biol. Sci.* 368 (1609), 20110329. doi:10.1098/rstb.2011.0329

Okamura, K., Hagiwara-Takeuchi, Y., Li, T., Vu, T. H., Hirai, M., Hattori, M., et al. (2000). Comparative genome analysis of the mouse imprinted gene impact and its nonimprinted human homolog IMPACT: Toward the structural basis for species-specific imprinting. *Genome Res.* 10 (12), 1878–1889. doi:10.1101/gr.139200

Onyango, P., Miller, W., Lehoczky, J., Leung, C. T., Birren, B., Wheelan, S., et al. (2000). Sequence and comparative analysis of the mouse 1-megabase region orthologous to the human 11p15 imprinted domain. *Genome Res.* 10 (11), 1697–1710. doi:10.1101/gr.161800

Paulsen, M., El-Maarri, O., Engemann, S., Strödicke, M., Franck, O., Davies, K., et al. (2000). Sequence conservation and variability of imprinting in the Beckwith-Wiedemann syndrome gene cluster in human and mouse. *Hum. Mol. Genet.* 9 (12), 1829–1841. doi:10.1093/hmg/9.12.1829

Paulsen, M., Takada, S., Youngson, N. A., Benchaib, M., Charlier, C., Segers, K., et al. (2001). Comparative sequence analysis of the imprinted dlk1–gtl2 locus in three mammalian species reveals highly conserved genomic elements and refines comparison with the Igf2–H19 region. *Genome Res.* 11 (12), 2085–2094. doi:10.1101/gr.206901

Rocha, S. T. d., Edwards, C. A., Ito, M., Ogata, T., and Ferguson-Smith, A. C. (2008). Genomic imprinting at the mammalian Dlk1-Dio3 domain. *Trends Genet.* 24 (6), 306–316. doi:10.1016/j.tig.2008.03.011

Saito, T., Hara, S., Kato, T., Tamano, M., Muramatsu, A., Asahara, H., et al. (2018). A tandem repeat array in IG-DMR is essential for imprinting of paternal allele at the Dlk1-Dio3 domain during embryonic development. *Hum. Mol. Genet.* 27 (18), 3283–3292. doi:10.1093/hmg/ddy235

Saito, T., Hara, S., Tamano, M., Asahara, H., and Takada, S. (2017). Deletion of conserved sequences in IG-DMR at Dlk1-Gtl2 locus suggests their involvement in expression of paternally expressed genes in mice. *J. Reprod. Dev.* 63 (1), 101–109. doi:10.1262/jrd.2016-135

Sanli, I., Lalevée, S., Cammisa, M., Perrin, A., Rage, F., Llères, D., et al. (2018). Meg3 non-coding RNA expression controls imprinting by preventing transcriptional upregulation in cis. *Cell Rep.* 23 (2), 337–348. doi:10.1016/j.celrep.2018.03.044

Sato, S., Yoshida, W., Soejima, H., Nakabayashi, K., and Hata, K. (2011). Methylation dynamics of IG-DMR and Gtl2-DMR during murine embryonic and placental development. *Genomics* 98 (2), 120–127. doi:10.1016/j.ygeno.2011.05.003

Schmidt, J. V., Matteson, P. G., Jones, B. K., Guan, X. J., and Tilghman, S. M. (2000). The Dlk1 and Gtl2 genes are linked and reciprocally imprinted. *Genes Dev.* 14 (16), 1997–2002. doi:10.1101/gad.14.16.1997

Seitz, H., Youngson, N., Lin, S. P., Dalbert, S., Paulsen, M., Bachellerie, J. P., et al. (2003). Imprinted microRNA genes transcribed antisense to a reciprocally imprinted retrotransposon-like gene. *Nat. Genet.* 34 (3), 261–262. doi:10.1038/ng1171

Stadtfeld, M., Apostolou, E., Ferrari, F., Choi, J., Walsh, R. M., Chen, T., et al. (2012). Ascorbic acid prevents loss of Dlk1-Dio3 imprinting and facilitates generation of all-iPS cell mice from terminally differentiated B cells. *Nat. Genet.* 44 (4), 398–392. doi:10.1038/ng.1110

Tucci, V., Isles, A. R., Kelsey, G., and Ferguson-Smith, A. C. (2019). Genomic imprinting and physiological processes in mammals. *Cell* 176 (5), 952–965. doi:10.1016/j.cell.2019.01.043

Wang, Y., Shen, Y., Dai, Q., Yang, Q., Zhang, Y., Wang, X., et al. (2017). A permissive chromatin state regulated by ZFP281-AFF3 in controlling the imprinted Meg3 polycistron. *Nucleic Acids Res.* 45 (3), 1177–1185. doi:10.1093/nar/gkw1051

Wei, Y., Yang, C. R., and Zhao, Z. A. (2022). Viable offspring derived from single unfertilized mammalian oocytes. *Proc. Natl. Acad. Sci. U. S. A.* 119 (12), e2115248119. doi:10.1073/pnas.2115248119

Wei, Y., Zhu, J., Huan, Y., Liu, Z., Yang, C., Zhang, X., et al. (2010). Aberrant expression and methylation status of putatively imprinted genes in placenta of cloned piglets. *Cell. Reprogr.* 12 (2), 213–222. doi:10.1089/cell.2009.0090

Yu, D., Wang, J., Zou, H., Feng, T., Chen, L., Li, J., et al. (2018). Silencing of retrotransposon-derived imprinted gene RTL1 is the main cause for postimplantational failures in mammalian cloning. *Proc. Natl. Acad. Sci. U. S. A.* 115 (47), E11071–E11080. doi:10.1073/pnas.1814514115

Zhao, J., Ohsumi, T. K., Kung, J. T., Ogawa, Y., Grau, D. J., Sarma, K., et al. (2010). Genome-wide identification of polycomb-associated RNAs by RIP-seq. *Mol. Cell* 40 (6), 939–953. doi:10.1016/j.molcel.2010.12.011

frontiers | Frontiers in Cell and Developmental Biology

TYPE Review
PUBLISHED 08 September 2022
DOI 10.3389/fcell.2022.913996

OPEN ACCESS

EDITED BY
Lin Yuan,
China Medical University, China

REVIEWED BY
Suhas Sureshchandra,
University of California, Irvine, United States
Yongchang Chen,
Kunming University of Science and Technology, China
Nagarajan Perumal,
National Institute of Immunology (NII), India

*CORRESPONDENCE
Weizheng Liang,
jmbb1203@126.com
Shanliang Li,
lisl2019@gxtcmu.edu.cn
Yukai Wang,
wangyukai@ioz.ac.cn
Hongyang Yi,
yhyyysm@126.com

†These authors have contributed equally to this work and share the first authorship

SPECIALTY SECTION
This article was submitted to Stem Cell Research, a section of the journal Frontiers in Cell and Developmental Biology

RECEIVED 06 April 2022
ACCEPTED 15 August 2022
PUBLISHED 08 September 2022

CITATION
Liang W, He J, Mao C, Yu C, Meng Q, Xue J, Wu X, Li S, Wang Y and Yi H (2022), Gene editing monkeys: Retrospect and outlook.
Front. Cell Dev. Biol. 10:913996.
doi: 10.3389/fcell.2022.913996

Gene editing monkeys: Retrospect and outlook

Weizheng Liang[1†*], Junli He[2†], Chenyu Mao[3†], Chengwei Yu[4], Qingxue Meng[1], Jun Xue[5], Xueliang Wu[5], Shanliang Li[6*], Yukai Wang[7,8,9,10*] and Hongyang Yi[11*]

[1]Central Laboratory, The First Affiliated Hospital of Hebei North University, Zhangjiakou, China, [2]Department of Pediatrics, Shenzhen University General Hospital, Shenzhen, China, [3]University of Pennsylvania, Philadelphia, PA, United States, [4]School of Future Technology, University of Chinese Academy of Sciences, Beijing, China, [5]Department of General Surgery, The First Affiliated Hospital of Hebei North University, Zhangjiakou, China, [6]Department of Pharmacology, Guangxi University of Chinese Medicine, Nanning, Guangxi, China, [7]State Key Laboratory of Stem Cell and Reproductive Biology, Institute of Zoology, Chinese Academy of Sciences, Beijing, China, [8]Institute for Stem Cell and Regeneration, Chinese Academy of Sciences, Beijing, China, [9]Beijing Institute for Stem Cell and Regenerative Medicine, Beijing, China, [10]National Stem Cell Resource Center, Chinese Academy of Sciences, Beijing, China, [11]National Clinical Research Centre for Infectious Diseases, The Third People's Hospital of Shenzhen and The Second Affiliated Hospital of Southern University of Science and Technology, Shenzhen, China

Animal models play a key role in life science research, especially in the study of human disease pathogenesis and drug screening. Because of the closer proximity to humans in terms of genetic evolution, physiology, immunology, biochemistry, and pathology, nonhuman primates (NHPs) have outstanding advantages in model construction for disease mechanism study and drug development. In terms of animal model construction, gene editing technology has been widely applied to this area in recent years. This review summarizes the current progress in the establishment of NHPs using gene editing technology, which mainly focuses on rhesus and cynomolgus monkeys. In addition, we discuss the limiting factors in the applications of genetically modified NHP models as well as the possible solutions and improvements. Furthermore, we highlight the prospects and challenges of the gene-edited NHP models.

KEYWORDS

nonhuman primates, gene editing, rhesus monkeys, cynomolgus monkeys, CRISPR/Cas9, human diseases

Introduction

With the development of human medical research, a broader and deeper understanding of disease pathology and identification of therapeutic strategies has become quite urgent. The establishment of genetically modified animal models is an important aspect of human disease studies. The validity of the animal model is based on its evolutionary similarity to humans. So far, a lot of research has been conducted on the construction of rodent models such as mice models (Gurney, 2000; Wong et al., 2002). Though mice models have played a big role in clinical research, models with higher similarity to humans are needed to study pathogenesis, especially in neurological diseases

(Wong et al., 2019). Compared to other animal models, primates are more similar to humans in terms of genetic background and physiological characteristics (Zhao et al., 2019). With up to 93% homologous genome between monkeys and humans, the NHP model has become irreplaceable in studying human diseases (Gibbs et al., 2007; Yan et al., 2011; Higashino et al., 2012; Brasó-Vives et al., 2020).

Though scientists have obtained primate models by screening natural mutations, drug induction, and traditional genetic engineering methods previously (Chan, 2004; Chen et al., 2012; Forny-Germano et al., 2014), it was difficult to obtain by spontaneous mutation. Traditional transgenic methods are not only inefficient but also require many embryonic stem cells, which is time consuming and laborious. In addition, other methods such as retroviral or lentivirus-mediated gene modification methods, RNA interference techniques, and sperm vector-mediated methods are subject to large exogenous random insertion of foreign genes with unstable expression and low operability accompanied by significant chimerism. Until recent years, with the development of gene editing technologies, researchers can use TALEN and CRISPR technology to achieve precise genetic modification on monkeys with the advantage of higher efficiency and accuracy which are unmatched by other methods. Here, we will present recent developments of gene-modified rhesus and cynomolgus monkeys and discuss the factors limiting the application of NHP models and highlight their future applications prospects.

Traditional transgenic methods to establish NHP models

The classical method of constructing transgenic primates mainly depends on the retrovirus vector-mediated approach, which recombines the target gene into the retroviral vector and integrates the exogenous target gene into the host genome by infecting the host cells. This method has been applied to mice for a long time (Gordon et al., 1980). In 2001, Chan et al. (2001) successfully established a transgenic rhesus monkey termed ANDi by transducing oocytes with high-titer lentivirus followed by sperm injection and embryo transfer, which is the first genetically modified primate in the world. Although the expression of the exogenous gene *GFP* was detected in only one of the three births obtained, this pioneering work marked the birth of transgenic NHP technology. In the same year, another group also constructed the transgenic rhesus monkeys with exogenous *eGFP* integrated into the placental tissue (Wolfgang et al., 2001). Taken together, these two studies provide the basis for the feasibility of exogenous gene integration and lay the foundation for future functional gene studies. Seven years later, scientists successfully obtained the transgenic macaque model expressing the human *HTT* gene to study Huntington's disease (HD) (Yang et al., 2008). This is the first transgenic primate model with human disease-causing gene integration, which not only helps to study the pathogenic mechanism of HD and explores corresponding treatment options but also makes it possible for studying other genetic diseases such as Parkinson's disease and Alzheimer's disease. Subsequently, Sasaki et al. (2009) successfully generated germline-transmissible *GFP* transgenic marmosets through lentiviral vector transfection. For the first time, this study demonstrated germline inheritance of transgenic traits in primates. In addition, people from other countries also established transgenic monkey models (Niu et al., 2010; Liu et al., 2016a).

Although some progress has been made in the construction of NHP models through the retroviral vector methods (Figure 1; Tables 1, 2), these gene modification sites are random and uncertain, and precise genetically modified NHP models cannot be obtained. In addition, the length of the fragment inserted is also limited since lentiviral vectors can only carry fragments no larger than 10 kb, which also brings many uncertainties and limitations to the research. Finally, the low efficiency of transgenic methods also restricts their application. Therefore, more precise and efficient gene editing methods are needed to overcome these limitations.

ZFN and TALEN gene editing technology to build NHP models

Zinc finger endonucleases (ZFNs) structurally comprise a zinc finger DNA-binding domain and a Fok I DNA-cleavage domain (Carroll, 2011; Wood et al., 2011). Transcription activator-like effector nucleases (TALENs) are gene editing tools made by TAL effector DNA-binding domains and FokI DNA-cleavage domains (Cermak et al., 2011; Wood et al., 2011). After recognizing DNA sequences through DNA-binding domains, the DNA-cleavage domains will target specific DNA sequences to introduce double-strand breaks, which subsequently induce cell repair mechanisms to achieve gene knockout or knock-in by non-homologous end joining (NHEJ) or homologous recombination (HR). The ZFN is time consuming and costly in construction and design, with severe off-target effects. So far, there are no reports on the application of ZFNs on rhesus and cynomolgus monkeys. Compared to ZFNs, TALENs technology is relatively simple to design, less costly, and has high DNA sequence specificity and fewer off-target events, which make it a useful and effective tool to achieve gene modification. Previous studies have witnessed its successful application in many species, including mice, rats, zebrafish, Xenopus, Iberian ribbed newts, zebrafish, and maize (Lei et al., 2012; Qiu et al., 2013; Hayashi et al., 2014; Hisano et al., 2014; Liang et al., 2014; Chen et al., 2017a). Recently, more scientists have started to turn their attention to primates. In 2014, one group successfully generated *MeCP2* gene mutated female cynomolgus monkeys with Rett syndrome (RTT) using

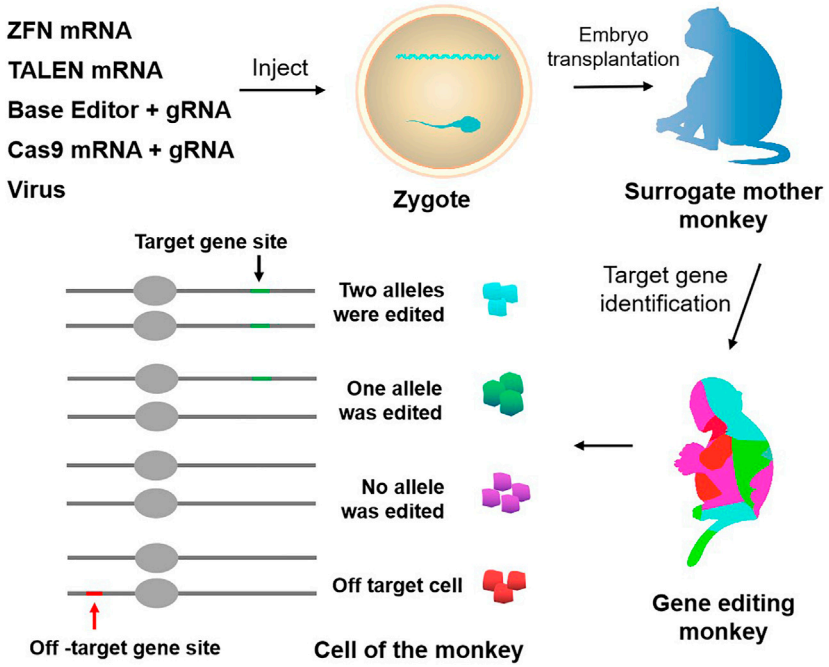

FIGURE 1
Approaches to genetically modify monkeys. Current techniques to genetically modify monkeys include virus, ZFN, TALEN, CRISPR-Cas9, and base editor. Chimerism exists in gene editing monkeys, and there is the potential for off-targeting.

TABLE 1 Rhesus monkey models established by various gene editing technologies.

Modified gene	Method	Success rate	Disease model	Year	References
GFP	Retrovirus-mediated gene transfer	20%	None	2001	Chan et al. (2001)
HTT-84Q, GFP	Lentivirus-mediated gene transfer	22%	Huntington's disease	2008	Yang et al. (2008)
EGFP	Simian Immunodeficiency Virus (SIV)-based lentivirus-mediated gene transfer	50%	None	2010	Niu et al. (2010)
MeCP2	TALEN	67%	Rett syndrome	2014	Liu et al. (2014a)
Dystrophin	CRISPR/Cas9	61%	Duchenne muscular dystrophy	2015	Chen et al. (2015b)
α-Syn	Lentivirus-mediated gene transfer	85%	Parkinson's disease	2015	Niu et al. (2015)
MCPH1	Lentivirus-mediated gene transfer	100%	Brain development	2019	Shi et al. (2019)
PINK1	CRISPR/Cas9	73%	Parkinson's disease	2019	Yang et al. (2019)
MeCP2	CBE	30% (embryo)	Rett syndrome	2020	Qin et al. (2020)

Success rate: number of transgenic monkeys/number of pregnancies (birth).

TALENs technology (Liu et al., 2014a). RTT cynomolgus monkeys have many similarities with RTT patients in both genotype and phenotype, which is of great significance for human research on the pathogenesis and treatment of RTT. Afterward, other groups also obtained *MeCP2* gene-modified monkeys by using TALENs technology (Liu et al., 2014b; Chen et al., 2017b). In 2016, Ke et al. reported another case that constructed an *MCPH1* gene-modified cynomolgus monkey model mimicking human microcephaly using TALENs-based method (Ke et al., 2016).

In sum, the application of TALENs technology has been widely reported in various studies (Figure 1; Tables 1, 2). However, the gene editing technique requires the design of different recognition proteins for different target sites, which

TABLE 2 Cynomolgus monkey models established by various gene editing technologies.

Modified gene	Method	Success rate	Disease model	Year	References
MeCP2	TALEN	16.7%	Rett syndrome	2014	Liu et al. (2014a)
Pparg, Rag1	CRISPR/Cas9	100%	None	2014	Niu et al. (2014)
P53	CRISPR/Cas9	66.7%	*P53* related tumor	2015	Wan et al. (2015)
Dax1	CRISPR/Cas9	25%	adrenal hypoplasia congenita, hypogonadotropic hypogonadism	2015	Kang et al. (2015)
GFP	Embryo stem cell transplantation	—	None	2015	Chen et al. (2015c)
MeCP2	Lentivirus-mediated gene transfer	100%	Rett syndrome	2016	Liu et al. (2016a)
GFP	Lentivirus-mediated gene transfer	50%	None	2016	Seita et al. (2016)
MCPH1	TALEN	33%	Microcephaly	2016	Ke et al. (2016)
SHANK3	CRISPR/Cas9	100%	Autism spectrum disorders	2017	Zhao et al. (2017)
MeCP2	TALEN	81%	Rett syndrome	2017	Chen et al. (2017b)
mCherry	CRISPR/Cas9	—	None	2017	Yao et al. (2017)
SIRT6	CRISPR/Cas9	100%	developmental retardation	2018	Zhang et al. (2018)
Oct4-GFP	CRISPR/Cas9	62%	None	2018	Cui et al. (2018)
SHANK3	CRISPR/Cas9	55%	Autism spectrum disorders	2019	Zhou et al. (2019)
BMAL1	CRISPR/Cas9	62%	Circadian disruption	2019	Qiu et al. (2019)
PKD1	CRISPR/Cas9	80%	Autosomal dominant polycystic kidney disease	2019	Tsukiyama et al. (2019)
HBB	CRISPR/Cas9	100%	β-Thalassemia	2019	Huang et al. (2019)
LMNA	CBE	83%	Hutchinson-Gilford progeria syndrome	2020	Wang et al. (2020)
Multiple targets	CBE, ABE	—	None	2020	Zhang et al. (2020b)
Pten, p53	CRISPR/Cas9	87%	Primary and metastatic liver tumors	2021	Zhong et al. (2021)

— means no data for live monkeys.

involves huge protein modification work and is time consuming, labor intensive, and costly. These limitations seriously restrict the wide application of TALENs.

Application of CRISPR/Cas9 gene editing technology in NHPs

The CRISPR/Cas system, which is short for clustered regularly interspaced short palindromic repeats and CRISPR-associated protein, was originally characterized as a defense mechanism that bacteria use against viruses (Horvath and Barrangou, 2010). It was subsequently engineered to cleave DNA in eukaryotes (Cong et al., 2013; Mali et al., 2013). Due to its simplicity, efficiency, and technical flexibility, CRISPR/Cas technologies became strong tools in biological and biomedical studies of various cell types and living organisms.

As for primates, there are also gratifying results. In 2014, for the first time, the researchers obtained twin cynomolgus monkeys carrying targeted mutation genes and achieved simultaneous knockout of two genes *PPARγ* and *RAG1* by using CRISPR/Cas9 technology (Niu et al., 2014), and it's important for studying immune system related diseases. This was the first application of CRISPR gene editing technology in primates. More importantly, this study achieved the simultaneous knockout of two target genes in one step. In addition, the DNA samples extracted from the umbilical cord and placenta of newborn monkeys were detected and analyzed, and no off-target phenomenon was found. Finally, they also found the mutation appeared in germ cells, which demonstrated that genetic mutations mediated by CRISPR technology can enable germline transmission (Chen et al., 2015a). The success of this study makes it possible to establish animal models of some complex diseases controlled by multiple genes. Duchenne muscular dystrophy (DMD) is a genetic disorder characterized by muscle degeneration due to the mutant muscle protein dystrophin. In order to study this disease, Chen et al. generated mutant rhesus monkeys by using CRISPR/Cas9 technology to target the dystrophin gene (Chen et al., 2015b). They analyzed the muscle tissue of monkeys who died of dystocia, finding that the expression of dystrophin protein was significantly decreased, which was similar to that of DMD patients. And the degeneration of muscle cells at an early stage was observed in both monkey

models and DMD. In the same year, one group obtained a *P53* gene (tumor suppressor gene) biallelic mutant cynomolgus monkey model without germline mating by optimizing the CRISPR/Cas9 technology (Wan et al., 2015). Meanwhile, another group generated a cynomolgus monkey model with *DAX1* gene deletion via CRISPR/Cas9 technology (Kang et al., 2015). This *DAX1* mutant monkey exhibited adrenal developmental defects and aberrant testicular architecture which were very similar to the clinical features of AHC-HH patients. Another study reported a rhesus monkey model with hemoglobin beta gene modified by CRISPR/Cas9 technology, and they found a way to improve the gene editing efficiency and reduced unfavorable outcomes such as off-target effects by optimization of sgRNAs concentrations (Midic et al., 2017). In 2019, scientists utilized CRISPR/Cas9 to establish *SHANK3* gene mutated cynomolgus macaques and their F1 offspring (Zhou et al., 2019), which could lead to sleep disorders, movement disorders, increased repetitive behaviors, and social and learning disabilities similar to what happened in autism spectrum disorders. Another example is the *SIRT6* gene, the scientists successfully generated *SIRT6* gene-modified cynomolgus monkeys, which showed a deficiency in *SIRT6* function (Zhang et al., 2018). SIRT6 has been identified as a longevity protein in mice (Mostoslavsky et al., 2006). As expected, the model monkey died shortly after birth and displayed severe developmental retardation. A recent study reported a new method to generate gene-modified monkeys by *in situ* CRISPR-mediated technique (Zhong et al., 2021). This study utilized CRISPR/Cas9 to knock down *Pten* and *p53* genes in adult cynomolgus, thus modeling primary and metastatic liver tumors rapidly, which was effective *in situ* gene editing approach. Other groups also generated gene-edited monkeys using this method (Figure 1; Tables 1, 2).

Limitation factors affecting the application of gene-edited NHP models

Whether it is transgenic monkeys obtained by lentiviral vector transduction or gene-edited monkeys generated by targeting nucleases, most of the founder monkeys exist in the form of chimeras. For surviving chimeric founder monkeys, it is difficult to precisely map the transgene or target gene mutation to the underlying phenotype. When using lentiviral vectors to construct transgenic monkeys, various numbers of lentiviral vector sequences can be integrated into the monkey genome at different time points in early embryos, accompanied by the randomness of integration numbers and time. This leads to the possibility that the number of transgene copies and the transgene integration sites of individuals obtained from different embryos injected with the same batch of viral vectors may vary greatly, and the number of transgenes and integration sites contained in different cells of the same transgenic individual may also be different (Liu et al., 2016a). Then the same batch of transgenic founder monkeys obtained by the same lentivirus may have phenotypic differences. To overcome this problem, a non-integrating lentiviral vector (NILV) has been developed by integrase mutation to reduce the risks of random insertion (Wanisch and Yáñez-Muñoz, 2009). Currently, NILVs have shown efficacy in different preclinical mice models, such as Parkinson's disease and Hemophilia B, with relatively lower expression levels than integrating lentiviral vectors though (Lu-Nguyen et al., 2014; Suwanmanee et al., 2014). So, whether NILV can construct transgenic NHP models with fewer random insertion risks still remains to be seen.

Similarly, when using targeted nucleases such as ZFN, TALENs, and CRISPR/Cas9 to construct gene editing monkeys, the founder monkeys obtained always exist in the form of chimeras (Niu et al., 2014; Chen et al., 2015b; Guo and Li, 2015) (Figure 1). Due to the long growth cycle of NHPs, it takes a lot of time and money to screen animal models with purely targeted gene modification through multi-generational mating. Chimeric mutations can also seriously affect the functional studies of target genes and the pathological analysis of related diseases, so it is particularly necessary to reduce the generation of chimeras. Two main reasons account for chimeric mutation. First, after Cas9 modifies the target site, the DNA repair activity between dividing cells may differ, resulting in different degrees of mutation of the target gene between different cells and tissues. Second, random insertion and deletion (Insertion/deletion, indel) will occur in the process of the NHEJ-mediated DNA repairing, resulting in various indels at the target site, leading to the formation of multi-genotype chimeric mutants.

Another problem in constructing gene editing monkeys using targeted nucleases such as ZFNs, TALENs, and CRISPR/Cas9 is off-targeting (Figure 1; Tables 3, 4). Previous studies did by multiple groups showed significant off-target activity in the CRISPR/Cas9 system (Fu et al., 2013; Pattanayak et al., 2013; Cho et al., 2014). Although no off-target effects have been found in NHPs models built by the CRISPR/Cas9 system which may be due to the limitation of the number of detection sites, it is difficult to conclude that these founder monkeys did not have off-target mutations. Therefore, the existence of the off-target phenomenon is also one of the unavoidable factors that potentially limit the in-depth study of gene editing monkeys as animal models.

The third problem is the low efficiency of gene knock-in. The incidence of HR repair for gene editing is very low in the current use of the CRISPR/Cas9 system for NHPs. The only successful results are the knock-in of small DNA sequences (Wan et al., 2015). However, no successful knock-in of large segments of gene sequences has been reported in NHPs.

TABLE 3 Comparison of the three main used genome editing technologies in monkeys: ZFN, TALEN, and CRISPR.

	ZFN	TALEN	CRISPR
Target recognition	Protein-DNA	Protein-DNA	RNA-DNA
Number of target sequence (bp)	18–36 bp	24–40 bp	~23 bp
Sequence recognition	3 bp as a unit	Requires a T at 5′-end of the target sequence	Requires NGG sequence at 3′-end
Build difficulty	Difficult	Easy	Very easy
Editing RNA	No	No	Yes
Off-target	High	High	Low
Cytotoxicity	High	Low	Low

TABLE 4 The advantage and disadvantages of the three main used gene editing technologies.

	ZFN	TALEN	CRISPR
Advantage	Mature technology	High specificity, simpler design than ZFN, high success rate	Low off-target effects, low cytotoxicity, cheap
Disadvantage	Low success rate, high off-target effects, high cytotoxicity	Cumbersome process, heavy workload, high cost	The possibility of off-target

Refinement of strategies to overcome these deficiencies

All the factors mentioned above strictly limited the broad application of NHPs as animal models for human diseases. So, there is an urgent need for some improvements to overcome these deficiencies. With the development of technology, some effective methods start to appear. As for chimerism, current researches show that the continuous expression of Cas9 protein may increase chimeric mutation. So, it is easy to imagine that restricting Cas9 expression only at the one-cell stage may be an effective method to reduce chimeric mutation. One group established a new method in which they linked ubiquitin-proteasome to the N-terminus of Cas9 protein, which can facilitate the degradation of Cas9 protein in cynomolgus monkey embryos whereby reducing the mosaic mutations (Tu et al., 2017). Similarly, other ways of controlling the Cas9 activity can also be applied in the future establishment of gene-edited NHPs models such as small molecules, light, inhibitors, and degraders (González et al., 2014; Nihongaki et al., 2015a; Nihongaki et al., 2015b; Zhou et al., 2018; Gangopadhyay et al., 2019; Maji et al., 2019). Another alternative approach to avoid mosaic mutations is the F1 offspring. As is well known, no matter what form of chimerism it is in the founder monkey, the F1 offspring can only get a specific edited genotype. Since the sexual maturation cycle of NHPs is very long, which takes about 4–5 years to reach sexual maturity for commonly used rhesus and cynomolgus monkeys, the development of methods to shorten the sexual maturation cycle of NHPs to achieve accelerated reproduction will promote the application of NHPs research. For this purpose, one group has developed testis xenotransplantation to accelerate spermatogenesis. By transplanting juvenile cynomolgus monkey testis tissue blocks to the back of adult male nude mice, the spermatogenesis time of cynomolgus monkeys was successfully shortened to 24 months, and the obtained sperm was used for embryo construction and transplantation to obtain healthy offspring of cynomolgus monkeys (Liu et al., 2016b). Therefore, the development of other methods to accelerate the reproduction cycle of NHPs will also be an important research direction for future NHP genetic modification models. Finally, one group generated complete gene knockout monkeys in one step by multiple sgRNAs, which provides another method to reduce the chimerism rate (Zuo et al., 2017).

In addition, for the off-target phenomenon, some improvements have been made to avoid this. One method is to screen and predict potential off-target sites in silico and optimize the gRNA design accordingly to minimize the off-target effects. Sangsu et al. developed a tool termed Cas-OFFinder, which can search for potential off-target sites in a given genome or user-defined sequences (Bae et al., 2014). Another method is Cas9 protein optimization. People from various groups have utilized different ways to optimize the Cas9 protein including fusion protein and mutated protein to achieve lower or no off-target efficiency (Koo et al., 2015; Anders et al., 2016; Kleinstiver et al., 2016; Slaymaker et al., 2016). In addition, controlling Cas9 protein expression can be used as another strategy to circumvent the off-target. Some groups have used inducible Cas9 protein and Cas9 inhibitory protein to achieve this goal (Nihongaki et al., 2015a; Rauch et al., 2017). All these methods are worth trying on monkeys in the future.

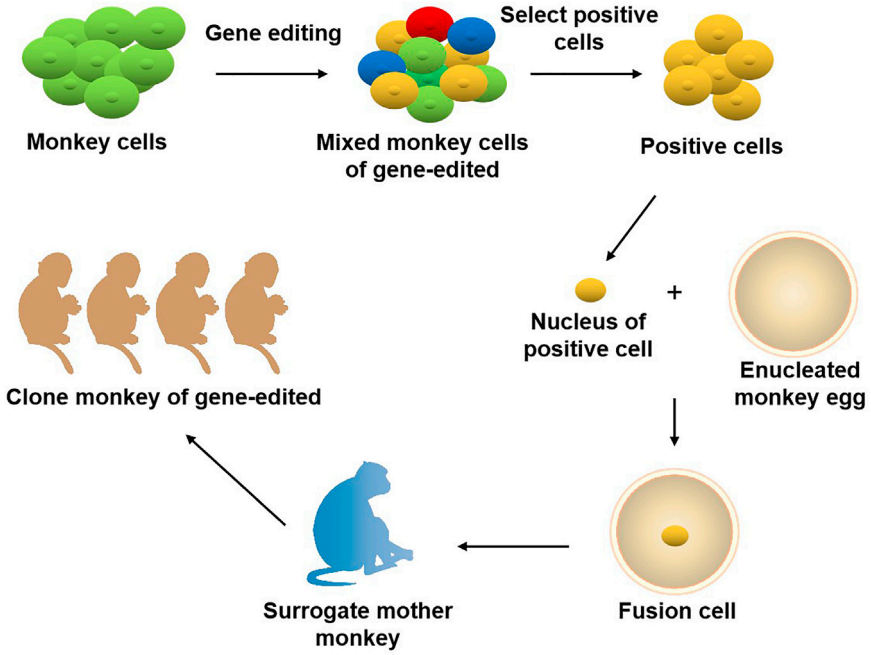

FIGURE 2
Joint application of gene editing and nuclear transfer technique in producing gene-modified monkeys. Using gene editing technology to modify the genome of monkey cells, and screen out specific types of positive cells. The nuclei of the positive cells are transferred to the enucleated monkey eggs, and the fusion cells are transferred to the surrogate mother monkey to obtain the gene-edited cloned monkeys.

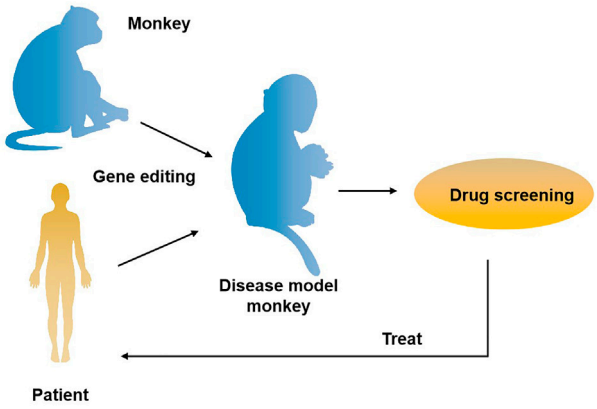

FIGURE 3
The application of gene-edited monkey models in drug development and treatment for the disease. A transgenic monkey model constructed by gene editing can be applied to drug screening for human diseases such as neurodegenerative diseases and cancer, thus providing an opportunity for disease treatment.

As for low knock-in efficiency, there are also some promising results. In principle, two ways can be used to improve the knock-in efficiency, one is to block non-homologous end joining, and the other is to increase homologous repair. Previous studies have shown that Scr7 which can bind to Ligase IV, a key component in the NHEJ process, can be used to block the NHEJ pathway whereby improving the precise repair (Chu et al., 2015; Vartak and Raghavan, 2015; Maruyama et al., 2016). In addition, another group enhanced the HR efficiency by optimizing donor DNA (Richardson et al., 2016).

Lastly, base editor systems can also be used to achieve precise gene editing, by which one base can be converted to another base precisely without requiring DNA cleavage, thus decreasing insertion or deletion events that happened randomly at the specific sites caused by DSB.

Single-base editing technology mainly realizes gene editing through the complex formed by deaminase, Cas9 variant, and sgRNA, in which sgRNA is responsible for guiding the complex to target the target sequence, and deaminase is responsible for deamination to achieve single-base editing (Komor et al., 2016; Gaudelli et al., 2017). According to different editing sequences and editors, the developed single-base editing technologies can be divided into two categories, namely cytosine base editing (CBE) technology and purine base editing (ABE) technology. CBE technology mainly realizes C→T or G→A conversion through sgRNA, inactive Cas9 protein (dCas9), and cytosine deaminase (Komor et al., 2016), there are various types of CBEs such as CBE1, CBE2, CBE3, CBE4, HF-CBE, SaBE4, CBE4-Gam, eCBE et al. ABE technology mainly realizes A→G or T→C base editing through sgRNA, adenosine deaminase and Cas9n, in which

sgRNA is responsible for guiding the complex to target the target sequence, and adenosine deaminase is responsible for catalyzing the deamination of adenine in the target sequence (Gaudelli et al., 2017). Various types of ABEs have been developed such as xABE, SaABE, VRER-ABE, ScCas9-ABE, et al. Until now, there are different types of base editor systems developed and applied (Komor et al., 2016; Gaudelli et al., 2017; Komor et al., 2017; Koblan et al., 2018; Molla and Yang, 2019; Zhang et al., 2020a). In addition, point mutation is a key cause of genetic diseases. Therefore, the base editor systems can be used in constructing gene-edited monkeys mimicking the diseases caused by point mutations. One group successfully generated base-edited cynomolgus monkeys with multiple target sites simultaneously modified using cytidine- and adenine-base editors (Zhang et al., 2020b).

Conclusion and perspectives

The role primates play in the field of biomedical research is unmatched by other species. It is well known that the odds for a newly discovered drug to come to the market are lower than 10%. The primary cause for this situation is that there are no ideal animal models available that mimic human diseases, such as cancer. Currently, two animal models are commonly used clinically for drug and vaccinee valuation in the antitumor market, which in rodents and NHPs. The former is preferred by many scientists due to its short reproduction cycle, cheap, small, clean genetic background, and genetic operability. However, the large species divergences between humans and rodents render many failures in clinical trials though the drug has shown satisfying safety and efficacy in preclinical trials. NHPs, however, such as cynomolgus monkeys and rhesus monkeys, display considerable similarities to humans in terms of genetic background, physiological composition, and immunological nature. As such, NHP has an advantage over other animal models to be applied in drug research and development and preclinical animal trials for safety and efficacy evaluation. Monkeys and chimpanzees share many cancer genes with humans. However, they are seldomly used in cancer research and drug development because of high costs and ethical issues. Furthermore, generating loss-of-function or gain-of-function mutations in NHPs by breeding remains cumbersome and challenging compared to rodents due to their longer sexual maturity cycle. On the other hand, using nuclear transfer (NT) technology to obtain cloned transgenic animals is the most direct and reliable method, which is a very mature technology in some species (Zhou et al., 2015). One group successfully obtained healthy cloned monkeys using somatic cell nuclear transfer technology, which provides important technical support for gene editing and model construction of NHPs (Liu et al., 2018). Therefore, combining gene editing technology with nuclear transfer and other technologies in the future is expected to contribute to constructing primate disease models more efficiently (Figure 2). Meanwhile, with the continuous updating and improvement of technology, the establishment of primate models of human diseases will eventually provide more possibilities for scientists to deeply study disease mechanisms and explore new disease treatments, which will eventually bring a boon to human health (Figure 3).

Author contributions

WL, HY, YW, and SL contributed directly to this review. WL designed and wrote the preliminary version of the manuscript. JH and CM collected literature and drew the figures with the help of CY and QM. JX and XW helped in the article revision. All authors reviewed and discussed the results and contributed to the article preparation. All authors have read and approved the final manuscript.

Funding

This study was funded by Inheritance and innovation team of Guangxi Traditional Chinese Medicine (2022B005) and the Doctoral Research Start-up Fund of Guangxi University of Chinese Medicine (2019BS008).

Conflict of interest

The authors declare that the research was conducted in the absence of any commercial or financial relationships that could be construed as a potential conflict of interest.

Publisher's note

References

Anders, C., Bargsten, K., and Jinek, M. (2016). Structural plasticity of PAM recognition by engineered variants of the RNA-guided endonuclease Cas9. *Mol. Cell* 61, 895–902. doi:10.1016/j.molcel.2016.02.020

Bae, S., Park, J., and KimCas-OFFinder, J.-S. (2014). Cas-OFFinder: A fast and versatile algorithm that searches for potential off-target sites of Cas9 RNA-guided endonucleases. *Bioinformatics* 30, 1473–1475. doi:10.1093/bioinformatics/btu048

Brasó-Vives, M., Povolotskaya, I. S., Hartasanchez, D. A., Farre, X., Fernandez-Callejo, M., Raveendran, M., et al. (2020). Copy number variants and fixed duplications among 198 rhesus macaques (*Macaca mulatta*). *PLoS Genet.* 16, e1008742. doi:10.1371/journal.pgen.1008742

Carroll, D. (2011). Genome engineering with zinc-finger nucleases. *Genetics* 188, 773–782. doi:10.1534/genetics.111.131433

Cermak, T., Doyle, E. L., Christian, M., Wang, L., Zhang, Y., Schmidt, C., et al. (2011). Efficient design and assembly of custom TALEN and other TAL effector-based constructs for DNA targeting. *Nucleic Acids Res.* 39, e82. doi:10.1093/nar/gkr218

Chan, A. W., Chong, K. Y., Martinovich, C., Simerly, C., and Schatten, G. (2001). Transgenic monkeys produced by retroviral gene transfer into mature oocytes. *Science* 291, 309–312. doi:10.1126/science.291.5502.309

Chan, A. W. (2004). Transgenic nonhuman primates for neurodegenerative diseases. *Reprod. Biol. Endocrinol.* 2, 39. doi:10.1186/1477-7827-2-39

Chen, Y., Cui, Y., Shen, B., Niu, Y., Zhao, X., Wang, L., et al. (2015). Germline acquisition of Cas9/RNA-mediated gene modifications in monkeys. *Cell Res.* 25, 262–265. doi:10.1038/cr.2014.167

Chen, Y., Lu, W., Gao, N., Long, Y., Shao, Y., Liu, M., et al. (2017). Generation of obese rat model by transcription activator-like effector nucleases targeting the leptin receptor gene. *Sci. China. Life Sci.* 60, 152–157. doi:10.1007/s11427-016-5049-y

Chen, Y., Niu, Y., and Ji, W. (2012). Transgenic nonhuman primate models for human diseases: Approaches and contributing factors. *J. Genet. Genomics* 39, 247–251. doi:10.1016/j.jgg.2012.04.007

Chen, Y., Niu, Y., Li, Y., Ai, Z., Kang, Y., Shi, H., et al. (2015). Generation of cynomolgus monkey chimeric fetuses using embryonic stem cells. *Cell Stem Cell* 17, 116–124. doi:10.1016/j.stem.2015.06.004

Chen, Y., Yu, J., Niu, Y., Qin, D., Liu, H., Li, G., et al. (2017). Modeling Rett syndrome using TALEN-edited MECP2 mutant cynomolgus monkeys. *Cell* 169, 945–955. e910. doi:10.1016/j.cell.2017.04.035

Chen, Y., Zheng, Y., Kang, Y., Yang, W., Niu, Y., Guo, X., et al. (2015). Functional disruption of the dystrophin gene in rhesus monkey using CRISPR/Cas9. *Hum. Mol. Genet.* 24, 3764–3774. doi:10.1093/hmg/ddv120

Cho, S. W., Kim, S., Kim, Y., Kweon, J., Kim, H. S., Bae, S., et al. (2014). Analysis of off-target effects of CRISPR/Cas-derived RNA-guided endonucleases and nickases. *Genome Res.* 24, 132–141. doi:10.1101/gr.162339.113

Chu, V. T., Weber, T., Wefers, B., Wurst, W., Sander, S., Rajewsky, K., et al. (2015). Increasing the efficiency of homology-directed repair for CRISPR-Cas9-induced precise gene editing in mammalian cells. *Nat. Biotechnol.* 33, 543–548. doi:10.1038/nbt.3198

Cong, L., Ran, F. A., Cox, D., Lin, S., Barretto, R., Habib, N., et al. (2013). Multiplex genome engineering using CRISPR/Cas systems. *Science* 339, 819–823. doi:10.1126/science.1231143

Cui, Y., Niu, Y., Zhou, J., Chen, Y., Cheng, Y., Li, S., et al. (2018). Generation of a precise Oct4-hrGFP knockin cynomolgus monkey model via CRISPR/Cas9-assisted homologous recombination. *Cell Res.* 28, 383–386. doi:10.1038/cr.2018.10

Forny-Germano, L., Lyra e Silva, N. M., Batista, A. F., Brito-Moreira, J., Gralle, M., Boehnke, S. E., et al. (2014). Alzheimer's disease-like pathology induced by amyloid-β oligomers in nonhuman primates. *J. Neurosci.* 34, 13629–13643. doi:10.1523/jneurosci.1353-14.2014

Fu, Y., Foden, J. A., Khayter, C., Maeder, M. L., Reyon, D., Joung, J. K., et al. (2013). High-frequency off-target mutagenesis induced by CRISPR-Cas nucleases in human cells. *Nat. Biotechnol.* 31, 822–826. doi:10.1038/nbt.2623

Gangopadhyay, S. A., Cox, K. J., Manna, D., Lim, D., Maji, B., Zhou, Q., et al. (2019). Precision control of CRISPR-cas9 using small molecules and light. *Biochemistry* 58, 234–244. doi:10.1021/acs.biochem.8b01202

Gaudelli, N. M., Komor, A. C., Rees, H. A., Packer, M. S., Badran, A. H., Bryson, D. I., et al. (2017). Programmable base editing of A● T to G● C in genomic DNA without DNA cleavage. *Nature* 551, 464–471. doi:10.1038/nature24644

Gibbs, R. A., Rogers, J., Katze, M. G., Bumgarner, R., and Weinstock, G. M. (2007). Evolutionary and biomedical insights from the rhesus macaque genome. *Science* 316, 222–234. doi:10.1126/science.1139247

González, F., Zhu, Z., Shi, Z. D., Lelli, K., Verma, N., Li, Q. V., et al. (2014). An iCRISPR platform for rapid, multiplexable, and inducible genome editing in human pluripotent stem cells. *Cell Stem Cell* 15, 215–226. doi:10.1016/j.stem.2014.05.018

Gordon, J. W., Scangos, G. A., Plotkin, D. J., Barbosa, J. A., and Ruddle, F. H. (1980). Genetic transformation of mouse embryos by microinjection of purified DNA. *Proc. Natl. Acad. Sci. U. S. A.* 77, 7380–7384. doi:10.1073/pnas.77.12.7380

Guo, X., and Li, X. J. (2015). Targeted genome editing in primate embryos. *Cell Res.* 25, 767–768. doi:10.1038/cr.2015.64

Gurney, M. E. (2000). What transgenic mice tell us about neurodegenerative disease. *Bioessays* 22, 2972–3304. doi:10.1002/(SICI)1521-1878(200003)22:3<297::AID-BIES12>3.0.CO;2-I

Hayashi, T., Sakamoto, K., Sakuma, T., Yokotani, N., Inoue, T., Kawaguchi, E., et al. (2014). Transcription activator-like effector nucleases efficiently disrupt the target gene in Iberian ribbed newts (*Pleurodeles waltl*), an experimental model animal for regeneration. *Dev. Growth Differ.* 56, 115–121. doi:10.1111/dgd.12103

Higashino, A., Sakate, R., Kameoka, Y., Takahashi, I., Hirata, M., Tanuma, R., et al. (2012). Whole-genome sequencing and analysis of the Malaysian cynomolgus macaque (*Macaca fascicularis*) genome. *Genome Biol.* 13, R58. doi:10.1186/gb-2012-13-7-r58

Hisano, Y., Ota, S., and Kawahara, A. (2014). Genome editing using artificial site-specific nucleases in zebrafish. *Dev. Growth Differ.* 56, 26–33. doi:10.1111/dgd.12094

Horvath, P., and Barrangou, R. (2010). CRISPR/Cas, the immune system of bacteria and archaea. *Science* 327, 167–170. doi:10.1126/science.1179555

Huang, Y., Ding, C., Liang, P., Li, D., Tang, Y., Meng, W., et al. (2019). HBB-deficient *Macaca fascicularis* monkey presents with human β-thalassemia. *Protein Cell* 10, 538–542. doi:10.1007/s13238-019-0627-y

Kang, Y., Zheng, B., Shen, B., Chen, Y., Wang, L., Wang, J., et al. (2015). CRISPR/Cas9-mediated Dax1 knockout in the monkey recapitulates human AHC-HH. *Hum. Mol. Genet.* 24, 7255–7264. doi:10.1093/hmg/ddv425

Ke, Q., Li, W., Lai, X., Chen, H., Huang, L., Kang, Z., et al. (2016). TALEN-based generation of a cynomolgus monkey disease model for human microcephaly. *Cell Res.* 26, 1048–1061. doi:10.1038/cr.2016.93

Kleinstiver, B. P., Pattanayak, V., Prew, M. S., Tsai, S. Q., Nguyen, N. T., Zheng, Z., et al. (2016). High-fidelity CRISPR-Cas9 nucleases with no detectable genome-wide off-target effects. *Nature* 529, 490–495. doi:10.1038/nature16526

Koblan, L. W., Doman, J. L., Wilson, C., Levy, J. M., Tay, T., Newby, G. A., et al. (2018). Improving cytidine and adenine base editors by expression optimization and ancestral reconstruction. *Nat. Biotechnol.* 36, 843–846. doi:10.1038/nbt.4172

Komor, A. C., Kim, Y. B., Packer, M. S., Zuris, J. A., and Liu, D. R. (2016). Programmable editing of a target base in genomic DNA without double-stranded DNA cleavage. *Nature* 533, 420–424. doi:10.1038/nature17946

Komor, A. C., Zhao, K. T., Packer, M. S., Gaudelli, N. M., Waterbury, A. L., Koblan, L. W., et al. (2017). Improved base excision repair inhibition and bacteriophage Mu Gam protein yields C:G-to-T:A base editors with higher efficiency and product purity. *Sci. Adv.* 3, eaao4774. doi:10.1126/sciadv.aao4774

Koo, T., Lee, J., and Kim, J. S. (2015). Measuring and reducing off-target activities of programmable nucleases including CRISPR-cas9. *Mol. Cells* 38, 475–481. doi:10.14348/molcells.2015.0103

Lei, Y., Guo, X., Liu, Y., Cao, Y., Deng, Y., Chen, X., et al. (2012). Efficient targeted gene disruption in Xenopus embryos using engineered transcription activator-like effector nucleases (TALENs). *Proc. Natl. Acad. Sci. U. S. A.* 109, 17484–17489. doi:10.1073/pnas.1215421109

Liang, Z., Zhang, K., Chen, K., and Gao, C. (2014). Targeted mutagenesis in Zea mays using TALENs and the CRISPR/Cas system. *J. Genet. Genomics* 41, 63–68. doi:10.1016/j.jgg.2013.12.001

Liu, H., Chen, Y., Niu, Y., Zhang, K., Kang, Y., Ge, W., et al. (2014). TALEN-mediated gene mutagenesis in rhesus and cynomolgus monkeys. *Cell Stem Cell* 14, 323–328. doi:10.1016/j.stem.2014.01.018

Liu, Z., Cai, Y., Wang, Y., Nie, Y., Zhang, C., Xu, Y., et al. (2018). Cloning of macaque monkeys by somatic cell nuclear transfer. *Cell* 174, 881–887. doi:10.1016/j.cell.2018.01.020

Liu, Z., Li, X., Zhang, J. T., Cai, Y. J., Cheng, T. L., Cheng, C., et al. (2016). Autism-like behaviours and germline transmission in transgenic monkeys overexpressing MeCP2. *Nature* 530, 98–102. doi:10.1038/nature16533

Liu, Z., Nie, Y. H., Zhang, C. C., Cai, Y. J., Wang, Y., Lu, H. P., et al. (2016). Generation of macaques with sperm derived from juvenile monkey testicular xenografts. *Cell Res.* 26, 139–142. doi:10.1038/cr.2015.112

Liu, Z., Zhou, X., Zhu, Y., Chen, Z. F., Yu, B., Wang, Y., et al. (2014). Generation of a monkey with MECP2 mutations by TALEN-based gene targeting. *Neurosci. Bull.* 30, 381–386. doi:10.1007/s12264-014-1434-8

Lu-Nguyen, N. B., Broadstock, M., Schliesser, M. G., Bartholomae, C. C., von Kalle, C., Schmidt, M., et al. (2014). Transgenic expression of human glial cell line-derived neurotrophic factor from integration-deficient lentiviral vectors is neuroprotective in a rodent model of Parkinson's disease. *Hum. Gene Ther.* 25, 631–641. doi:10.1089/hum.2014.003

Maji, B., Gangopadhyay, S. A., Lee, M., Shi, M., Wu, P., Heler, R., et al. (2019). A high-throughput platform to identify small-molecule inhibitors of CRISPR-cas9. *Cell* 177, 1067–1079. e1019. doi:10.1016/j.cell.2019.04.009

Mali, P., Yang, L., Esvelt, K. M., Aach, J., Guell, M., DiCarlo, J. E., et al. (2013). RNA-guided human genome engineering via Cas9. *Science* 339, 823–826. doi:10.1126/science.1232033

Maruyama, T., Dougan, S. K., Truttmann, M. C., Bilate, A. M., Ingram, J. R., and Ploegh, H. L. (2016). Corrigendum: Increasing the efficiency of precise genome editing with CRISPR-Cas9 by inhibition of nonhomologous end joining. *Nat. Biotechnol.* 34, 210. doi:10.1038/nbt0216-210c

Midic, U., Hung, P. H., Vincent, K. A., Goheen, B., Schupp, P. G., Chen, D. D., et al. (2017). Quantitative assessment of timing, efficiency, specificity and genetic mosaicism of CRISPR/Cas9-mediated gene editing of hemoglobin beta gene in rhesus monkey embryos. *Hum. Mol. Genet.* 26, 2678–2689. doi:10.1093/hmg/ddx154

Molla, K. A., and Yang, Y. (2019). CRISPR/Cas-Mediated base editing: Technical considerations and practical applications. *Trends Biotechnol.* 37, 1121–1142. doi:10.1016/j.tibtech.2019.03.008

Mostoslavsky, R., Chua, K. F., Lombard, D. B., Pang, W. W., Fischer, M. R., Gellon, L., et al. (2006). Genomic instability and aging-like phenotype in the absence of mammalian SIRT6. *Cell* 124, 315–329. doi:10.1016/j.cell.2005.11.044

Nihongaki, Y., Kawano, F., Nakajima, T., and Sato, M. (2015). Photoactivatable CRISPR-Cas9 for optogenetic genome editing. *Nat. Biotechnol.* 33, 755–760. doi:10.1038/nbt.3245

Nihongaki, Y., Yamamoto, S., Kawano, F., Suzuki, H., and Sato, M. (2015). CRISPR-Cas9-based photoactivatable transcription system. *Chem. Biol.* 22, 169–174. doi:10.1016/j.chembiol.2014.12.011

Niu, Y., Guo, X., Chen, Y., Wang, C. E., Gao, J., Yang, W., et al. (2015). Early Parkinson's disease symptoms in α-synuclein transgenic monkeys. *Hum. Mol. Genet.* 24, 2308–2317. doi:10.1093/hmg/ddu748

Niu, Y., Shen, B., Cui, Y., Chen, Y., Wang, J., Wang, L., et al. (2014). Generation of gene-modified cynomolgus monkey via Cas9/RNA-mediated gene targeting in one-cell embryos. *Cell* 156, 836–843. doi:10.1016/j.cell.2014.01.027

Niu, Y., Yu, Y., Bernat, A., Yang, S., He, X., Guo, X., et al. (2010). Transgenic rhesus monkeys produced by gene transfer into early-cleavage-stage embryos using a simian immunodeficiency virus-based vector. *Proc. Natl. Acad. Sci. U. S. A.* 107, 17663–17667. doi:10.1073/pnas.1006563107

Pattanayak, V., Lin, S., Guilinger, J. P., Ma, E., Doudna, J. A., and Liu, D. R. (2013). High-throughput profiling of off-target DNA cleavage reveals RNA-programmed Cas9 nuclease specificity. *Nat. Biotechnol.* 31, 839–843. doi:10.1038/nbt.2673

Qin, W. S., Shuang, W., Ting, Z., Shang-gang, L., and Chen, Y. C. (2020). T158M single base editing of *MECP2* gene in murine and rhesus monekey's embryos. *China Biotechnol.* 40, 31–39. doi:10.13523/j.cb.2001063

Qiu, P., Jiang, J., Liu, Z., Cai, Y., Huang, T., Wang, Y., et al. (2019). BMAL1 knockout macaque monkeys display reduced sleep and psychiatric disorders. *Natl. Sci. Rev.* 6, 87–100. doi:10.1093/nsr/nwz002

Qiu, Z., Liu, M., Chen, Z., Shao, Y., Pan, H., Wei, G., et al. (2013). High-efficiency and heritable gene targeting in mouse by transcription activator-like effector nucleases. *Nucleic Acids Res.* 41, e120. doi:10.1093/nar/gkt258

Rauch, B. J., Silvis, M. R., Hultquist, J. F., Waters, C. S., McGregor, M. J., Krogan, N. J., et al. (2017). Inhibition of CRISPR-cas9 with bacteriophage proteins. *Cell* 168, 150–158. e110. doi:10.1016/j.cell.2016.12.009

Richardson, C. D., Ray, G. J., DeWitt, M. A., Curie, G. L., and Corn, J. E. (2016). Enhancing homology-directed genome editing by catalytically active and inactive CRISPR-Cas9 using asymmetric donor DNA. *Nat. Biotechnol.* 34, 339–344. doi:10.1038/nbt.3481

Sasaki, E., Suemizu, H., Shimada, A., Hanazawa, K., Oiwa, R., Kamioka, M., et al. (2009). Generation of transgenic non-human primates with germline transmission. *Nature* 459, 523–527. doi:10.1038/nature08090

Seita, Y., Tsukiyama, T., Iwatani, C., Tsuchiya, H., Matsushita, J., Azami, T., et al. (2016). Generation of transgenic cynomolgus monkeys that express green fluorescent protein throughout the whole body. *Sci. Rep.* 6, 24868. doi:10.1038/srep24868

Shi, L., Luo, X., Jiang, J., Chen, Y., Liu, C., Hu, T., et al. (2019). Transgenic rhesus monkeys carrying the human MCPH1 gene copies show human-like neoteny of brain development. *Natl. Sci. Rev.* 6, 480–493. doi:10.1093/nsr/nwz043

Slaymaker, I. M., Gao, L., Zetsche, B., Scott, D. A., Yan, W. X., and Zhang, F. (2016). Rationally engineered Cas9 nucleases with improved specificity. *Science* 351, 84–88. doi:10.1126/science.aad5227

Suwanmanee, T., Hu, G., Gui, T., Bartholomae, C. C., Kutschera, I., von Kalle, C., et al. (2014). Integration-deficient lentiviral vectors expressing codon-optimized R338L human FIX restore normal hemostasis in Hemophilia B mice. *Mol. Ther.* 22, 567–574. doi:10.1038/mt.2013.188

Tsukiyama, T., Kobayashi, K., Nakaya, M., Iwatani, C., Seita, Y., Tsuchiya, H., et al. (2019). Monkeys mutant for PKD1 recapitulate human autosomal dominant polycystic kidney disease. *Nat. Commun.* 10, 5517. doi:10.1038/s41467-019-13398-6

Tu, Z., Yang, W., Yan, S., Yin, A., Gao, J., Liu, X., et al. (2017). Promoting Cas9 degradation reduces mosaic mutations in non-human primate embryos. *Sci. Rep.* 7, 42081. doi:10.1038/srep42081

Vartak, S. V., and Raghavan, S. C. (2015). Inhibition of nonhomologous end joining to increase the specificity of CRISPR/Cas9 genome editing. *Febs J.* 282, 4289–4294. doi:10.1111/febs.13416

Wan, H., Feng, C., Teng, F., Yang, S., Hu, B., Niu, Y., et al. (2015). One-step generation of p53 gene biallelic mutant Cynomolgus monkey via the CRISPR/Cas system. *Cell Res.* 25, 258–261. doi:10.1038/cr.2014.158

Wang, F., Zhang, W., Yang, Q., Kang, Y., Fan, Y., Wei, J., et al. (2020). Generation of a Hutchinson-Gilford progeria syndrome monkey model by base editing. *Protein Cell* 11, 809–824. doi:10.1007/s13238-020-00740-8

Wanisch, K., and Yáñez-Muñoz, R. J. (2009). Integration-deficient lentiviral vectors: A slow coming of age. *Mol. Ther.* 17, 1316–1332. doi:10.1038/mt.2009.122

Wolfgang, M. J., Eisele, S. G., Browne, M. A., Schotzko, M. L., Garthwaite, M. A., DurningM., et al. (2001). Rhesus monkey placental transgene expression after lentiviral gene transfer into preimplantation embryos. *Proc. Natl. Acad. Sci. U. S. A.* 98, 10728–10732. doi:10.1073/pnas.181336098

Wong, C. H., Siah, K. W., and Lo, A. W. (2019). Corrigendum: Estimation of clinical trial success rates and related parameters. *Biostatistics* 20, 366. doi:10.1093/biostatistics/kxy072

Wong, P. C., Cai, H., Borchelt, D. R., and Price, D. L. (2002). Genetically engineered mouse models of neurodegenerative diseases. *Nat. Neurosci.* 5, 633–639. doi:10.1038/nn0702-633

Wood, A. J., Lo, T. W., Zeitler, B., Pickle, C. S., Ralston, E. J., Lee, A. H., et al. (2011). Targeted genome editing across species using ZFNs and TALENs. *Science* 333, 307. doi:10.1126/science.1207773

Yan, G., Zhang, G., Fang, X., Zhang, Y., Li, C., Ling, F., et al. (2011). Genome sequencing and comparison of two nonhuman primate animal models, the cynomolgus and Chinese rhesus macaques. *Nat. Biotechnol.* 29, 1019–1023. doi:10.1038/nbt.1992

Yang, S. H., Cheng, P. H., Banta, H., Piotrowska-Nitsche, K., Yang, J. J., Cheng, E. C. H., et al. (2008). Towards a transgenic model of Huntington's disease in a non-human primate. *Nature* 453, 921–924. doi:10.1038/nature06975

Yang, W., Liu, Y., Tu, Z., Xiao, C., Yan, S., Ma, X., et al. (2019). CRISPR/Cas9-mediated PINK1 deletion leads to neurodegeneration in rhesus monkeys. *Cell Res.* 29, 334–336. doi:10.1038/s41422-019-0142-y

Yao, X., Wang, X., Hu, X., Liu, Z., Liu, J., Zhou, H., et al. (2017). Homology-mediated end joining-based targeted integration using CRISPR/Cas9. *Cell Res.* 27, 801–814. doi:10.1038/cr.2017.76

Zhang, W., Aida, T., Del Rosario, R. C. H., Wilde, J. J., Ding, C., Zhang, X., et al. (2020). Multiplex precise base editing in cynomolgus monkeys. *Nat. Commun.* 11, 2325. doi:10.1038/s41467-020-16173-0

Zhang, W., Wan, H., Feng, G., Qu, J., Wang, J., Jing, Y., et al. (2018). SIRT6 deficiency results in developmental retardation in cynomolgus monkeys. *Nature* 560, 661–665. doi:10.1038/s41586-018-0437-z

Zhang, X., Chen, L., Zhu, B., Wang, L., Chen, C., Hong, M., et al. (2020). Increasing the efficiency and targeting range of cytidine base editors through fusion of a single-stranded DNA-binding protein domain. *Nat. Cell Biol.* 22, 740–750. doi:10.1038/s41556-020-0518-8

Zhao, H., Tu, Z., Xu, H., Yan, S., Yan, H., Zheng, Y., et al. (2017). Altered neurogenesis and disrupted expression of synaptic proteins in prefrontal cortex of SHANK3-deficient non-human primate. *Cell Res.* 27, 1293–1297. doi:10.1038/cr.2017.95

Zhao, J., Lai, L., Ji, W., and Zhou, Q. (2019). Genome editing in large animals: Current status and future prospects. *Natl. Sci. Rev.* 6, 402–420. doi:10.1093/nsr/nwz013

Zhong, L., Huang, Y., He, J., Yang, N., Xu, B., Ma, Y., et al. (2021). Generation of *in situ* CRISPR-mediated primary and metastatic cancer from monkey liver. *Signal Transduct. Target. Ther.* 6, 411. doi:10.1038/s41392-021-00799-7

Zhou, X., Xin, J., Fan, N., Zou, Q., Huang, J., Ouyang, Z., et al. (2015). Generation of CRISPR/Cas9-mediated gene-targeted pigs via somatic cell nuclear transfer. *Cell. Mol. Life Sci.* 72, 1175–1184. doi:10.1007/s00018-014-1744-7

Zhou, X. X., Zou, X., Chung, H. K., Gao, Y., Liu, Y., Qi, L. S., et al. (2018). A single-chain photoswitchable CRISPR-cas9 architecture for light-inducible gene editing and transcription. *ACS Chem. Biol.* 13, 443–448. doi:10.1021/acschembio.7b00603

Zhou, Y., Sharma, J., Ke, Q., Landman, R., Yuan, J., Chen, H., et al. (2019). Atypical behaviour and connectivity in SHANK3-mutant macaques. *Nature* 570, 326–331. doi:10.1038/s41586-019-1278-0

Zuo, E., Cai, Y. J., Li, K., Wei, Y., Wang, B. A., Sun, Y., et al. (2017). One-step generation of complete gene knockout mice and monkeys by CRISPR/Cas9-mediated gene editing with multiple sgRNAs. *Cell Res.* 27, 933–945. doi:10.1038/cr.2017.81

frontiers | Frontiers in Cell and Developmental Biology

TYPE Review
PUBLISHED 10 October 2022
DOI 10.3389/fcell.2022.1033197

OPEN ACCESS

EDITED BY
Feng Yue,
Hainan University, China

REVIEWED BY
Tao Li,
Second Affiliated Hospital of Hainan Medical University, China
Cara Ellis,
University of Alberta, Canada
Yifan Dai,
Nanjing Medical University, China

*CORRESPONDENCE
Hongming Yuan,
yuanhongming@jlu.edu.cn
Daxin Pang,
pdx@jlu.edu.cn

†These authors have contributed equally to this work

SPECIALTY SECTION
This article was submitted to Stem Cell Research, a section of the journal Frontiers in Cell and Developmental Biology

RECEIVED 31 August 2022
ACCEPTED 26 September 2022
PUBLISHED 10 October 2022

CITATION
Deng J, Yang L, Wang Z, Ouyang H, Yu H, Yuan H and Pang D (2022), Advance of genetically modified pigs in xeno-transplantation.
Front. Cell Dev. Biol. 10:1033197.
doi: 10.3389/fcell.2022.1033197

Advance of genetically modified pigs in xeno-transplantation

Jiacheng Deng[1†], Lin Yang[1†], Ziru Wang[1], Hongsheng Ouyang[1,2,3], Hao Yu[1], Hongming Yuan[1,2,3]* and Daxin Pang[1,2,3]*

[1]College of Animal Sciences, Jilin University, Changchun, China, [2]Chongqing Research Institute, Jilin University, Chongqing, China, [3]Chongqing Jitang Biotechnology Research Institute, Chongqing, China

As the standard of living improves, chronic diseases and end-stage organ failure have been a regular occurrence in human beings. Organ transplantation has become one of the hopes in the fight against chronic diseases and end-stage organ failure. However, organs available for transplantation are far from sufficient to meet the demand, leading to a major organ shortage crisis. To solve this problem, researchers have turned to pigs as their target since pigs have many advantages as xenograft donors. Pigs are considered the ideal organ donor for human xenotransplantation, but direct transplantation of porcine organs to humans faces many obstacles, such as hyperacute rejection, acute humoral xenograft rejection, coagulation dysregulation, inflammatory response, coagulation dysregulation, and endogenous porcine retroviral infection. Many transgenic strategies have been developed to overcome these obstacles. This review provides an overview of current advances in genetically modified pigs for xenotransplantation. Future genetic engineering-based delivery of safe and effective organs and tissues for xenotransplantation remains our goal.

KEYWORDS

gene editing, pigs, xeno-transplantation, xenograft donors, xenograft rejection

Introduction

In recent years, the incidence of vital organ failure has increased(Abouna, 2008). Different types of diseases progress to the end stage, and organs are no longer able to meet the most basic needs of the body. Despite the use of drugs and conventional surgery, organ transplantation has become one of the most viable solutions to this problem. To date, more than 106,120 patients have required organ transplants in the United States, while only approximately 40,000 transplants were performed in 2021 (data from URL: https://www.organdonor.gov/statistics-stories/statistics.html). Based on urgent clinical needs, replacing human organs with fully functional animal organs for xenotransplantation therapy is an effective method to address the shortage of donor organs.

Compared with nonhuman primates, pigs have characteristics such as fast reproduction, easy breeding, lower cost, and closer anatomical characteristics and physiological indices to humans, and the use of pigs can avoid the ethical problems caused by the use of nonhuman primate organs (Gao et al., 2021). The use of pigs as

donors for pig-to-nonhuman primate (NHP) organ transplantation has become a standard model for preclinical xenotransplantation studies(Klymiuk et al., 2010). However, the clinical application of xenotransplantation still faces many problems: immune rejection of xenotransplantation, abnormal coagulation due to endothelial damage caused by rejection and abnormal growth of transplant donors and biosafety. Gene editing technology has been widely used to solve these problems and prolong the survival rate of organ transplantation. This article reviews the status of xenotransplant organ development and future perspectives.

Antigens existing in porcine cells that introduce xenograft rejection

The major carbohydrate antigen on porcine vascular endothelial cells has been identified as galactose-α1,3-galactose (α-Gal), to which humans and nonhuman primates have anti-pig antibodies(Cooper et al., 2016). Activation of natural antibodies and the complement cascade mediated by α-Gal (α-1,3-galactosyl) epitopes on the pig cell surface is the main cause of hyperacute rejection (HAR), which leads to severe immune rejection in xenotransplantation (Cowan et al., 2000; Bucher et al., 2005). In 2002, Lai et al. (2002) generated α-1,3-galactosyltransferase knockout pigs, which significantly reduced HAR in pig-to-primate organ transplantation. Subsequently, many research groups have deleted the porcine α-1,3-galactosyltransferase gene and have shown that transplantation of organs from α-1,3-galactosyltransferase knockout (GTKO) pigs significantly prolonged the survival of transplants(Dai et al., 2002; Phelps et al., 2003; Chen et al., 2005; Kuwaki et al., 2005).

Furthermore, previous studies(Chen et al., 2005; Kuwaki et al., 2005; Ezzelarab et al., 2009) have shown that antibody binding to non-Gal antigens and complement activation also lead to xenograft rejection. Acute humoral xenograft rejection (AHXR) caused by non-Gal antibodies and complement activation are obstacles at present. Non-Gal antigens that have been identified to cause AHXR include N-acetylneuraminic acid (Neu5Gc) synthesized by cytidine monophosphate-N-acetylneuraminic acid hydroxylase (CMAH) and Sd^a produced by β4GalNT2 glycosyltransferase(Byrne et al., 2015; Wang et al., 2018). Several research groups(Estrada et al., 2015; Martens et al., 2017; Zhang et al., 2018; Tanihara et al., 2021) have developed GGTA1/CMAH/β4GalNT2 knockout pigs, which greatly reduced HAR and AHXR. In 2021, Tanihara's group(Tanihara et al., 2021) generated GGTA1/CMAH double gene-edited pigs and GGTA1/CMAH/B4GALNT2 triple gene-edited pigs using the CRISPR/Cas9 system, which was the first time that multiple gene-edited pigs had been generated from CRISPR/Cas9-mediated gene-edited zygotes using electroporation. However, there is also some basal reactivity in the TKO (triple knockout) background, leading to poor pig-to-NHP xenotransplantation (Firl and Markmann, 2022).

Martens et al. (2017) revealed SLA class I as an additional target for gene editing in xenotransplantation by screening for human antibody binding using flow cytometric crossmatch (FCXM) in 2017. HLA is a protein complex expressed on human tissue that stimulates the production of new antibodies in allotransplantation. These antibodies can lead to graft failure through hyperacute, acute, or chronic rejection(Ladowski et al., 2021).

In 2014, Reyes et al. (2014) produced piglets lacking the expression of class I SLA proteins, which developed normally. However, class I SLA antigens are critical for viral control in pigs(Ambagala et al., 2000), and class I SLA antigen knockout in pigs still requires long-term evaluation to determine the susceptibility of these animals to infectious diseases and cancer. In 2019, Fischer et al. (2020) produced pigs carrying four gene knockouts of GGTA1, CMAH, B4GALNT2 and either the SLA-I heavy α-chain or light β-chain (B2M), which showed functional knockdown of B2M in animals as well as a lack of SLA-I molecules on the cell surface. However, one group reported negative effects of B2M knockout in mice(Santos et al., 1996). Although the absence of SLA expression is possible, it makes pigs susceptible to infectious complications. A potential alternative effective strategy is to screen key amino acids in SLA by base editor-mediated screening to produce pigs that eliminate cross-reactive binding in the future.

Human proteins involved in alleviating xenograft rejection

Although knockdown of antigens in pigs helps to reduce graft rejection, there are still other factors that affect graft survival, such as human complement-mediated injury, inflammatory response, and coagulation dysregulation. The expression of human C-reactive proteins (hCRPs) has been reported to prevent damage to pig cells by complement activation(Lin et al., 2009). A number of attempts have been made to deplete or inhibit the complement cascade, generating pigs expressing hCRPs (human C-reactive proteins), hDAF (human decay-accelerating factor, also known as CD55) (Cozzi and White, 1995), hMCP (human membrane cofactor protein, also known as CD46) (Diamond et al., 2001) and hCD59(Fodor et al., 1994). A series of studies have shown that organs from pigs expressing hCRPs effectively resist complement-mediated cytolysis, thereby increasing the survival time after xenotransplantation(Diamond et al., 1996; Ramirez et al., 2000).

However, several other immunological and nonimmunological barriers remain. In 2008, Sprangers et al. (2008) noted that humoral and cellular immune-mediated acute vascular rejection (AVR) mechanisms play key roles in

xenotransplantation. The human A20 gene (hA20) is considered to be potentially involved in AVR regulation (Opipari et al., 1990; Daniel et al., 2004; Ferran, 2006). AVR is characterized by endothelial cell (EC) activation and coagulation disorder. In 2009, Oropeza et al. (2009) successfully prepared pigs expressing hA20. The expression of hA20 protects cells against TNF-mediated apoptosis and cell damage caused by inflammation. In addition to A20, haem oxygenase-1 (HO-1) is also a potential factor in the regulation of acute vascular rejection (AVR). HO-1 and its derivatives have anti-apoptotic and anti-inflammatory effects and can resist reactive oxygen species(Nath et al., 1992; Ramackers et al., 2008). In 2011, Petersen et al. (2011) reported hHO-1 gene-modified pigs, and hHO-1 expression was detected in various organs and cells cultured *in vitro*, such as heart, kidney, endothelial and fibroblast cells. Moreover, their results demonstrate that HO-1 plays a protective role in TNF-α-mediated apoptosis(Houser et al., 2004; Shimizu et al., 2005; Shimizu et al., 2008; Shimizu et al., 2012).

It has also been shown that thrombotic microangiopathy occurs in most pig grafts, which may induce the recipient to develop consumptive coagulopathy, leading to graft failure. hTM (human thrombomodulin) is a natural anticoagulant. TM inhibits thrombosis by suppressing direct prothrombinase activity through binding to prothrombinase and enhances its activation of protein C, which is an anticoagulant when activated(Conway, 2012; Yazaki et al., 2012). In 2014, Wuensch et al. (2014) created a genetically modified pig expressing hTM and proved that hTM-expressing pig endothelial cells had anticoagulant properties in a human whole-blood assay. In addition, the biological efficacy of hTM indicated that hTM gene-modified pigs could overcome the coagulation incompatibility in pig-to-primate xenotransplantation.

In addition, the expression of other human coagulation-regulatory proteins (endothelial protein C receptor, tissue factor pathway inhibitor, CD39, CD73) has undergone extensive testing (Lee et al., 2008; Roussel et al., 2008; Petersen et al., 2009; Miwa et al., 2010; Mohiuddin et al., 2014c; Iwase et al., 2014; Mohiuddin et al., 2016). It has been demonstrated that human coagulation proteins greatly minimize coagulation-related problems after xenotransplantation, and coexpression of these coagulation proteins can further improve graft survival (Mohiuddin et al., 2014a; Mohiuddin et al., 2014b; Mohiuddin et al., 2014c). CD47 is a negative regulator of macrophages and is widely expressed in many cells(Oldenborg et al., 2000). The production of CD47 gene-edited pigs is an approach to reduce intrinsic and inflammatory responses and thus improve xenograft survival(Navarro-Alvarez and Yang, 2011). Porcine CD47 does not induce SIRPα tyrosine phosphorylation in human macrophage-like cell lines, and the expression of soluble human CD47-Fc fusion protein induces SIRPα tyrosine phosphorylation, thereby inhibiting phagocytosis of porcine cells by human macrophages. Ide et al. expressed human CD47 in porcine cells and fundamentally demonstrated that it reduced phagocytosis (Ide et al., 2007). Subsequent groups have reported prolonged skin graft survival after the use of human CD47-expressing porcine cells, as well as a substantial protective effect of porcine cell expression of human CD47 on xenografts(Tena et al., 2014; Tena et al., 2017; Chen et al., 2019). Inhibiting the activation of human macrophages through the CD47-SIRP-α signaling pathway is a feasible approach to improve the success rate of xenotransplantation.

Advance of genetically modified pigs in xenotransplantation

In recent years, the application of gene editing technology has become increasingly common, which has led to prolonged survival of transplanted pig organs in nonhuman primates (NHPs) and a reduced risk of pathogen transfer in organs. Xenotransplantation has made breakthroughs in many fields, especially in heart (see Figure 1 and Table 1), liver (see Figure 2 and Table 2), kidney (see Figure 3 and Table 3), and islet transplantation.

Advances in heart xenotransplantation

In 1964, Hardy performed the first clinical orthotopic cardiac xenotransplantation (CXTx) when he implanted a chimpanzee's heart into a 64-year-old male patient who died within 2 h of transplantation(Hardy and Chavez, 1969). Histopathological examination showed that antibody-mediated rejection was the primary cause of the patient's death(Murthy et al., 2016). In 1968, Donald performed the first clinical heterotopic abdominal CXTx by implanting a wild-type porcine heart into a patient who died of hyperacute rejection (HAR) within minutes after receiving the xenotransplanted heart (Figure 1; Table 1) (Adams et al., 2000), which was intended to confirm the feasibility of human heart transplantation and to provide experience for subsequent human xenotransplantation. In 1998, the Waterworth group(Waterworth et al., 1998) attempted to transplant transgenic porcine hearts to NHPs. They transplanted hCD55 gene-modified pig hearts into baboons, and histological studies showed acute vascular rejection resulting in graft failure (Figure 1; Table 1). Expression of the hCD55 gene extended survival to 21 days and abrogated hyperacute rejection. In 2005, the Kuwaki group(Kuwaki et al., 2005) used alpha1,3-galactosyltransferase knockout pigs as donors for heart transplantation in baboons, which further prevented hyperacute rejection and prolonged survival time to 2–6 months, though xenograft injury due to thrombotic microangiopathy occurred. The transplantation of hearts from galactosyltransferase gene knockout pigs increases graft survival

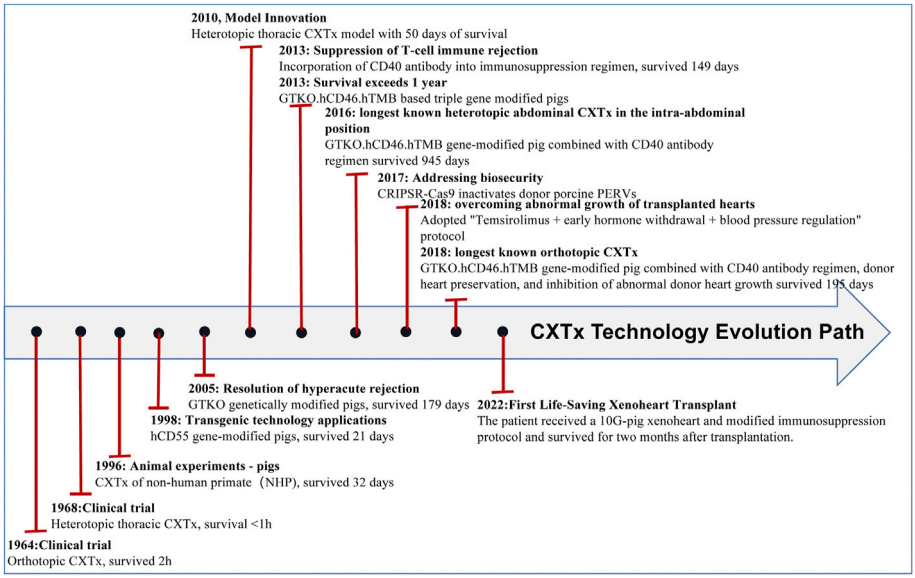

FIGURE 1
CXTx technology evolution path.

TABLE 1 Progress in transgenic porcine heart xenotransplantation.

Year	Recipient	Genetic modifications	Survival	Reason of experiment termination	References
1968	human	WT	<1 h	hyperacute rejection	Adams et al. (2000)
1998	baboon	hCD55	21 d	acute vascular rejection	Baldan et al. (2004)
2005	baboon	GTKO	179 d	thrombotic microangiopathy	Kuwaki et al. (2005)
2010	baboon	GGTA1KO/hCD46	50 d	no signs of infection and active rejection	Bauer et al. (2010)
2013	baboon	GTKO/hCD46/hTBM	499 d	heart xenografts were explanted after rejection and recipient baboons were survived	Mohiuddin et al. (2014a)
2016	baboon	GTKO/hCD46/hTBM	945 d	anti-CD40 significantly prolongs graft survival	Mohiuddin et al. (2016)
2018	baboon	GTKO/hCD46/hTBM	195 d	consistent life-supporting function	Längin et al. (2018)
2022	human	G10	8weeks	multiple organ failure and a porcine virus	Rothblatt, (2022)

compared to previous studies. In 2010, Bauer's group(Bauer et al., 2010) performed the first heterotopic thoracic pig-baboon heart transplantation, where the recipient heart could assist the donor heart during rejection episodes, and the recipient eventually survived for 50 days compared to the orthotopic transplant.

An immunosuppressive regimen of co-stimulation blockade *via* anti-CD154 antibodies significantly prolonged cardiac xenograft survival, but many coagulation disorders were observed with the use of anti-CD154 antibodies. In 2013, Mohiuddin's group(Mohiuddin et al., 2014b) replaced anti-CD154 antibody with anti-CD40 antibody in a GTKO/hCD46 Tg pig-to-baboon heterotopic allograft model, and graft survival was prolonged, with a maximum survival of 146 days. To solve the issue of thrombus formation, GTKO/hCD46 Tg pigs were engineered to express hTBM. In 2013, Mohiuddin's group transplanted GTKO/hCD46/hTBM pig hearts into baboons, and recipient survival occurred after 1 year(Mohiuddin et al., 2014a). In 2016, the Mohiuddin group(Mohiuddin et al., 2016) achieved recipient survival of 945 days based on a GTKO/hCD46/hTBM modified pig conjugated CD40 antibody regimen. In 2018, the Längin group(Längin et al., 2018) achieved allograft transplantation based on GTKO/hCD46/hTBM combined with nonischemic preservation, continuous perfusion and controlled

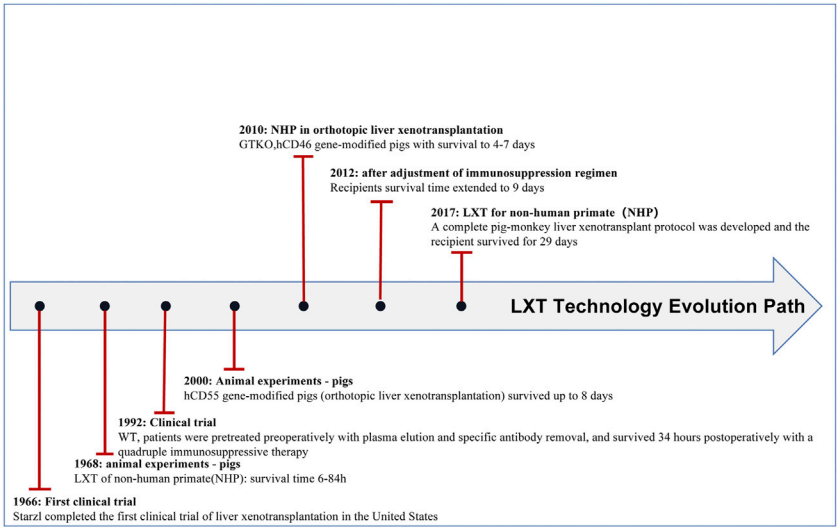

FIGURE 2
Lxt technology evolution path.

TABLE 2 Progress in transgenic porcine liver xenotransplantation.

Year	Recipient	Genetic modifications	Survival	Reason of experiment termination	References
1968	baboon	WT	6–84 h	hyperacute rejection	Calne et al. (1968)
1992	human	WT	34 h	hyperacute rejection	Starzl et al. (1999)
2000	baboon	hCD55	8 d	development of sepsis and coagulopathy	Ramirez et al. (2000)
2010	baboon	GTKO/hCD46	4-7 d	thrombocytopenia	Ekser et al. (2010)
2012	baboon	GTKO	9 d	bleeding and enterococcal infection	Kim et al. (2012)
2017	baboon	GTKO	29 d	minimal inflammation	Shah et al. (2017)

posttransplant growth of the heart and maintained stable life support function for up to 195 days. Furthermore, on 7 January 2022, Baltimore reported the first-ever life-saving cardiac xenotransplantation. The procedure was successful in extending the patient's life for 8 weeks. The patient received a 10G-pig xeno-heart (6 human genes knocked-in: CD55, CD46, CD47, human hemeoxygenase-1, human endothelial protein C receptor, hTM; four pig genes knocked-out: Alpha-Gal, Beta4GalNT2, CMAH, growth hormone receptor) and a modified immunosuppression protocol, including costimulation blockade (anti-CD40) maintenance(Rothblatt, 2022). Early published results of posttransplant survival showed that the heart performed very well in the absence of rejection. In the eighth week posttransplant, the patient's status started to decline, and 2 months after posttransplant, the patient died of multiple organ failure. It is encouraging to see that hyperacute rejection has been defeated. A porcine virus was detected in the transplanted heart and may have been the cause of the patient's death(Kuehn, 2022).

Advances in liver xenotransplantation

To address the insufficient supply of living donor livers, liver xenotransplantation is an attractive approach. In 1968, Calne's group(Calne et al., 1968) performed the first trial of liver xenotransplantation using wild-type pigs as donors, with a maximum survival time of 3.5 days for the recipients, and the longest surviving recipient was treated with an immunosuppressive therapy of glucocorticoids (GC) and azathioprine (AZA). With the application of gene editing, hDAF transgenic pigs with hearts and kidneys that prolong survival and suppress hyperacute rejection have been reported. In 2000, the Ramirez group(Ramirez et al., 2000) first

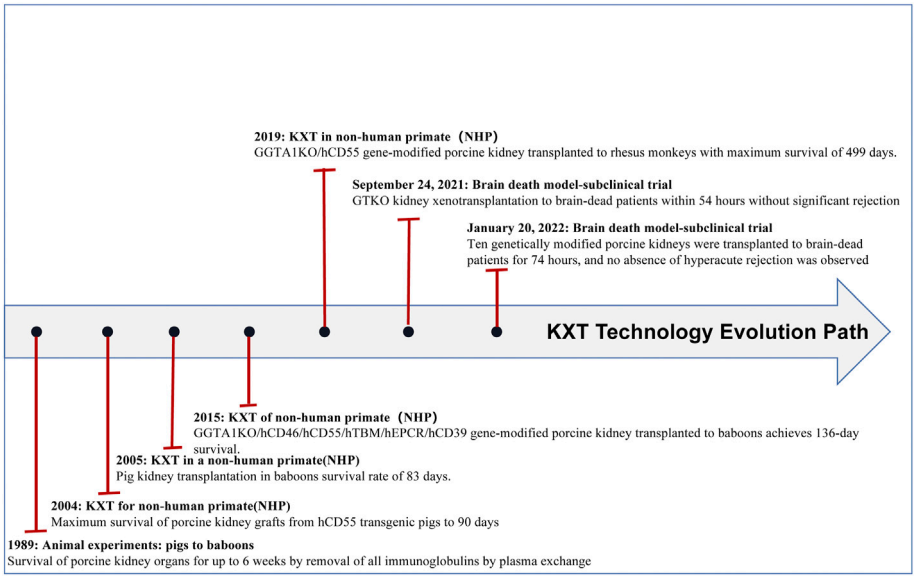

FIGURE 3
Kxt technology evolution path.

TABLE 3 Progress in transgenic porcine kidney xenotransplantation.

Year	Recipient	Genetic modifications	Survival	Reason of experiment termination	References
1968	baboon	WT	6–84 h	hyperacute rejection	Calne et al. (1968)
1992	human	WT	34 h	hyperacute rejection	Starzl et al. (1999)
2000	baboon	hCD55	8 d	development of sepsis and coagulopathy	Ramirez et al. (2000)
2010	baboon	GTKO/hCD46	4-7 d	thrombocytopenia	Ekser et al. (2010)

orthotopically transplanted h-DAF gene-modified porcine livers into baboons, which survived up to 8 days postoperatively. The results showed that HAR was abrogated. In 2010, Ekser's group(Ekser et al., 2010) performed the first orthotopic liver xenotransplantation in baboons using GTKO minipigs transfected with hCD46 as donors, and the baboons survived 4–7 days before dying of abdominal hemorrhage. Baboon survival was prolonged, and hyperacute rejection was further eliminated after transplantation using GTKO. hCD46 pigs as donors compared to hCD46 pigs as donors.

With the elimination of the major obstacle (hyperacute rejection), the current obstacle to the clinical application of liver transplantation is severe thrombocytopenia(Rees et al., 2002; Ekser et al., 2010). Burlak and his colleagues found binding and phagocytosis of human platelets by sinusoidal endothelial cells and Kupffer cells in an *ex vivo* perfusion system. ASGR1 is a receptor expressed by Kupffer cells and hepatocytes that mediates platelet phagocytosis based on the carbohydrate profile of platelets. Paris and his colleagues(Paris et al., 2011) knocked down ASGR1 to reduce ASGR1 expression in asynchronous primary enriched liver sinusoidal endothelial cells (eLSEC) and cripple the ability of primary porcine eLSEC to bind and phagocytose human platelets. Xie's group(Xie et al., 2021) produced ASGR1-deficient pigs using the CRISPR/Cas9 system. The ASGR1-deficient pigs unexpectedly exhibited mild to moderate liver injury, which has not been reported in humans with ASGR1 variants.

One of the possible approaches to address liver damage resulting from ASGR1 defects in pigs is to screen key amino acid functional loci of proteins at the individual level using base editing techniques. The approach aims to eliminate the liver damage caused by ASGR1 defects in pigs and to effectively alleviate thrombocytopenia in liver xenografts as much as possible.

Shah's group(Shah et al., 2017) developed a complete pig-to-NHP liver xenotransplantation protocol based on the long-term survival of kidney and heart xenotransplants using GTKO pigs, which do not carry cytomegalovirus, as the organ source. Then, the pigs were supplemented with human clotting factors, followed by applying anti-CD40 monoclonal antibodies to block activation of the recipient costimulatory pathway. For the first time, the protocol allowed for recipient survival following pig-to-primate liver xenotransplantation (LXT) for nearly 1 month. Amino acid and lipid profiles following pig-to-primate liver xenotransplantation suggest that most of the biochemical profiles of porcine liver can be maintained postoperatively in baboons and that supplementation with arginine after LXT may be a potential option to further extend the survival of xenografts(Shah et al., 2019). Based on costimulation blockade with posttransplant administration of human coagulation factors, the team effectively circumvented consumptive coagulopathy and prevented the development of thrombotic microangiopathy (TMA).

Liver xenotransplantation still has a long way to go before undergoing clinical trials, with thrombocytopenia and coagulation dysregulation remaining major hurdles(Li et al., 2021). Gene editing techniques and the combination of tailored immunosuppression and coagulation factor support will likely accelerate the arrival of clinical trials for pig-to-human liver xenotransplantation.

Advances in kidney xenotransplantation

The rapid development of genome editing technologies such as CRISPR–Cas9 technology has led to significant progress in kidney transplantation from pigs to NHPs. To date, some groups have achieved more than 6 months of survival in life-supporting pig-to-baboon kidney transplants(Iwase et al., 2017). Recently, the Kim group(Kim et al., 2019) even achieved more than 1 year of survival in life-supporting pig-to-macaque kidney transplants. These recent experiments confirmed the feasibility of kidney transplantation from pigs to NHPs. On 24 September 2021, Robert's group transplanted a GTKO experimental porcine kidney xenograft into a brain-dead patient, and it functioned immediately after transplantation, urinating and clearing creatinine with no obvious signs of rejection. On 20 January 2022, Porrett's group(Porrett et al., 2022) performed bilateral native nephrectomies in a human brain-dead decedent. They transplanted a TKO pig kidney with seven additional genetic modifications (ten genetic modifications or 10G-pigs) into a brain-dead patient. The absence of hyperacute rejection (HAR) and the fact that the kidneys remained viable until termination after 74 h suggested that the major barriers to human xenotransplantation had been overcome (Figure 3; Table 3). However, the biopsy revealed thrombotic microangiopathy, which may have been caused by brain death rather than antibody-mediated rejection (AMR). Because the brain death model has many flaws, the next step is expected to be transplanting kidneys from genetically engineered pigs into patients who cannot wait for an allogeneic liver donor.

Advances in islet xenotransplantation

Pig islet xenotransplantation is a potential approach to patients with type 1 diabetes. In 1994, Groth et al. (1994) performed the first clinical islet xenotransplantation using foetal porcine islet cell-like clusters (ICCs), providing preliminary data for subsequent clinical islet xenotransplantation. There has also been some work in islet xenotransplantation from pigs to NHPs and successful reversal of recipient diabetes and achievement of long-term normoglycemia(Dufrane et al., 2006; Hering et al., 2006; Cardona et al., 2007). Moreover, in some clinical trials(Yang and Yoon, 2015), xenografts were performed using encapsulated neonatal porcine islets, and the grafts were maintained for more than 2 years with a significant reduction in the number of hypoglycemic episodes. In islet xenotransplantation, islet encapsulation and gene editing technologies are currently used to alleviate rejection(Dhanasekaran et al., 2017). Targeted specific removal of porcine endogenous retroviruses from the genomes of porcine cell lines using CRISPR/Cas9 can improve islet xenotransplantation safety. The production of pigs with multiple genetic modifications for xenotransplantation using the targeted specificity of CRISPR/Cas9 has been discussed in this paper and will not be discussed here.

Discussion

Although the current work has effectively reduced the occurrence of immune rejection, the cross-species infection of pathogens between pigs and humans remains a difficult problem to be solved. This difficulty arises from two aspects: first, overexpression of human genes may increase the risk of human pathogens infecting genetically engineered pigs; second, transplanting pig organs into human bodies may also increase the risk of infection by pig pathogens.

Knock-in of certain human proteins in pigs may enhance the susceptibility of certain viruses to the organism. In engineering genetically modified pigs to overcome immune rejection, human CD46 was introduced into porcine cells to inhibit complement-mediated graft injury(Lu et al., 2019). CD46 not only regulates complement activation and T-cell immunity but is also especially able to control inflammation(Diamond et al., 2001; Astier, 2008; Griffiths et al., 2009). However, CD46 has been shown to be the receptor for measles virus(Okada et al., 1995; Pérez De La Lastra et al., 1999). In addition, hCD55 has been shown to be a receptor for pathogens(Bergelson et al., 1995). Knocking out porcine genomic PERV sequences is a feasible solution to avoid cross-species

transmission of PERV and improve the safety of xenotransplantation. Certain groups have performed a large amount of work in this area. Yang et al.(Yang et al., 2015) disrupted all copies of the PERV pol gene in porcine PK-15 at the genome-wide level by using CRISPR/Cas9, reducing the risk of human PERV infection during xenotransplantation by approximately 1000 times. Niu et al. (2017) successfully inactivated all PERV copies in primary pig cell lines using CRISPR/Cas9 and generated PERV-inactivated pigs. Not only are these pigs healthy, but their genome changes are heritable. All of these efforts have effectively addressed the problem of transmission of swine pathogens to humans. In the transplantation of porcine organs into humans, a number of other roseoloviruses may be transmitted and pose a risk in xenografts, such as porcine cytomegalovirus(Denner et al., 2019). Increased viral replication occurs in xenografts during immunosuppression(Mueller et al., 2004). Porcine cytomegalovirus is responsible for a significant reduction in the survival time of transplanted porcine organs. PCMV-negative piglets can be obtained for PCMV elimination through a number of early weaning strategies(Denner, 2022). Eliminating the safety concerns associated with viral infections during xenotransplantation is an essential safety consideration for xenotransplantation.

Furthermore, to further reduce the incidence of immune rejection that is still an issue in current xenotransplants, researchers could try to produce pigs with different genetic modifications using different gene-editing combinations, including knocking in human genes and knocking out pig immunogenicity-related genes(Hinrichs et al., 2021; Yue et al., 2021), to test whether immune rejection is further effectively reduced. Adopting new editing tools is still a good option. Several groups have attempted to use base editors, such as CBE and ABE, to construct better xenograft model pigs(Yuan et al., 2020; Zhu et al., 2022). CRISPR screening of new factors is also a promising option. The emergence of CRISPR genetic screening tools offers hope for screening for new antigenic factors in xenotransplantation. Zhao's group(Zhao et al., 2020) constructed the first genome-scale CRISPR/Cas9 libraries for screening studies in pigs. A porcine genome-scale CRISPR/Cas9 knockout (PigGeCKO) library was designed, and key host factors promoting JEV infection in porcine cells were identified. It is theoretically feasible to use a porcine genome-scale CRISPR/Cas9 knockout (PigGeCKO) library to identify novel antigens in xenotransplantation.

From the recent first-ever life-saving cardiac xenotransplantation, patients died of multiple organ failure, and organ grafts died from porcine virus infection(Kuehn, 2022). Therefore, with the hope of the eventual implementation of clinical cardiac xenotransplantation, we think it is important to eliminate porcine virus infections to prolong the lifespan of these clinical grafts. The molecular mechanisms associated with rejection involved in pig liver xenotransplantation are more complex than those in cardiac xenotransplantation(Lu et al., 2019). Thrombotic microangiopathy and systemic consumptive coagulopathy are more severe in grafts after liver xenotransplantation than in xenotransplantations of other organs(Zhou et al., 2022). Therefore, addressing thrombotic microangiopathy and systemic consumptive coagulopathy remains a priority for breakthroughs in liver xenotransplantation. In the field of kidney xenotransplantation, which has recently been performed successfully in a brain-dead patient, NYU porcine kidney transplantation is just the beginning. More clinical data are still needed, and the next step may be to initiate a pig kidney transplant trial in patients with end-stage renal failure. More clinical organ xenotransplantation may begin within a few years, with clinical kidney xenotransplantation going first. This is because in the event of a failed transplant, patients could also be put back on dialysis to stay alive(Porrett et al., 2022). In islet xenotransplantation, a current hot spot is the use of cell encapsulation techniques to protect islets from host immune rejection during the initial stages of transplantation. Additionally, there are now some groups trying to transplant porcine islets into different recipient sites(Zhou et al., 2022).

Author contributions

Writing—original draft preparation, J.D and L.Y.; writing and revision, H.Y., D.P., and H.O.; Figure preparation, L.Y.; H.Y and Z.W.; manuscript revision and supervision, H.O and D.P.; and funding acquisition, D.P. All authors have read and agreed to the published version of the manuscript.

Funding

This work was supported by the National Key Research and Development Program of China—Stem Cell and Translational Research (2019YFA0110702) and the Special Funds for Cultivation and Breeding of New Transgenic Organisms (No. 2016ZX08006003).

Conflict of interest

The authors declare that the research was conducted in the absence of any commercial or financial relationships that could be construed as a potential conflict of interest.

Publisher's note

References

Abouna, G. M. (2008). Organ shortage crisis: Problems and possible solutions. *Transpl. Proc.* 40, 34–38. doi:10.1016/j.transproceed.2007.11.067

Adams, D. H., Chen, R. H., and Kadner, A. (2000). Cardiac xenotransplantation: Clinical experience and future direction. *Ann. Thorac. Surg.* 70, 320–326. doi:10.1016/s0003-4975(00)01281-9

Ambagala, A. P., Hinkley, S., and Srikumaran, S. (2000). An early pseudorabies virus protein down-regulates porcine MHC class I expression by inhibition of transporter associated with antigen processing (TAP). *J. Immunol.* 164, 93–99. doi:10.4049/jimmunol.164.1.93

Astier, A. L. (2008). T-cell regulation by CD46 and its relevance in multiple sclerosis. *Immunology* 124, 149–154. doi:10.1111/j.1365-2567.2008.02821.x

Baldan, N., Rigotti, P., Calabrese, F., Cadrobbi, R., Dedja, A., Iacopetti, I., et al. (2004). Ureteral stenosis in HDAF pig-to-primate renal xenotransplantation: A phenomenon related to immunological events? *Am. J. Transpl.* 4, 475–481. doi:10.1111/j.1600-6143.2004.00407.x

Bauer, A., Postrach, J., Thormann, M., Blanck, S., Faber, C., Wintersperger, B., et al. (2010). First experience with heterotopic thoracic pig-to-baboon cardiac xenotransplantation. *Xenotransplantation* 17, 243–249. doi:10.1111/j.1399-3089.2010.00587.x

Bergelson, J. M., Mohanty, J. G., Crowell, R. L., St John, N. F., Lublin, D. M., and Finberg, R. W. (1995). Coxsackievirus B3 adapted to growth in RD cells binds to decay-accelerating factor (CD55). *J. Virol.* 69, 1903–1906. doi:10.1128/JVI.69.3.1903-1906.1995

Bucher, P., Morel, P., and Bühler, L. H. (2005). Xenotransplantation: An update on recent progress and future perspectives. *Transpl. Int.* 18, 894–901. doi:10.1111/j.1432-2277.2005.00124.x

Byrne, G. W., Mcgregor, C. G. A., and Breimer, M. E. (2015). Recent investigations into pig antigen and anti-pig antibody expression. *Int. J. Surg.* 23, 223–228. doi:10.1016/j.ijsu.2015.07.724

Calne, R. Y., White, H. J., Herbertson, B. M., Millard, P. R., Davis, D. R., Salaman, J. R., et al. (1968). Pig-to-baboon liver xenografts. *Lancet* 1, 1176–1178. doi:10.1016/s0140-6736(68)91869-2

Cardona, K., Milas, Z., Strobert, E., Cano, J., Jiang, W., Safley, S. A., et al. (2007). Engraftment of adult porcine islet xenografts in diabetic nonhuman primates through targeting of costimulation pathways. *Am. J. Transpl.* 7, 2260–2268. doi:10.1111/j.1600-6143.2007.01933.x

Chen, G., Qian, H., Starzl, T., Sun, H., Garcia, B., Wang, X., et al. (2005). Acute rejection is associated with antibodies to non-Gal antigens in baboons using Gal-knockout pig kidneys. *Nat. Med.* 11, 1295–1298. doi:10.1038/nm1330

Chen, M., Wang, Y., Wang, H., Sun, L., Fu, Y., and Yang, Y. G. (2019). Elimination of donor CD47 protects against vascularized allograft rejection in mice. *Xenotransplantation* 26, e12459. doi:10.1111/xen.12459

Conway, E. M. (2012). Thrombomodulin and its role in inflammation. *Semin. Immunopathol.* 34, 107–125. doi:10.1007/s00281-011-0282-8

Cooper, D. K., Ekser, B., Ramsoondar, J., Phelps, C., and Ayares, D. (2016). The role of genetically engineered pigs in xenotransplantation research. *J. Pathol.* 238, 288–299. doi:10.1002/path.4635

Cowan, P. J., Aminian, A., Barlow, H., Brown, A. A., Chen, C. G., FisicaroN., et al. (2000). Renal xenografts from triple-transgenic pigs are not hyperacutely rejected but cause coagulopathy in non-immunosuppressed baboons. *Transplantation* 69, 2504–2515. doi:10.1097/00007890-200006270-00008

Cozzi, E., and White, D. J. (1995). The generation of transgenic pigs as potential organ donors for humans. *Nat. Med.* 1, 964–966. doi:10.1038/nm0995-964

Dai, Y., Vaught, T. D., Boone, J., Chen, S. H., Phelps, C. J., Ball, S., et al. (2002). Targeted disruption of the alpha1, 3-galactosyltransferase gene in cloned pigs. *Nat. Biotechnol.* 20, 251–255. doi:10.1038/nbt0302-251

Daniel, S., Arvelo, M. B., Patel, V. I., Longo, C. R., Shrikhande, G., Shukri, T., et al. (2004). A20 protects endothelial cells from TNF-Fas-and NK-mediated cell death by inhibiting caspase 8 activation. *Blood* 104, 2376–2384. doi:10.1182/blood-2003-02-0635

Denner, J., Bigley, T. M., Phan, T. L., Zimmermann, C., Zhou, X., and Kaufer, B. B. (2019). Comparative analysis of roseoloviruses in humans, pigs, mice, and other species. *Viruses* 11 (12), 1108. doi:10.3390/v11121108

Denner, J. (2022). The porcine cytomegalovirus (PCMV) will not stop xenotransplantation. *Xenotransplantation* 29, e12763. doi:10.1111/xen.12763

Dhanasekaran, M., George, J. J., Loganathan, G., Narayanan, S., Hughes, M. G., Williams, S. K., et al. (2017). Pig islet xenotransplantation. *Curr. Opin. Organ Transpl.* 22, 452–462. doi:10.1097/MOT.0000000000000455

Diamond, L. E., Mccurry, K. R., Martin, M. J., McClellan, S. B., Oldham, E. R., Platt, J. L., et al. (1996). Characterization of transgenic pigs expressing functionally active human CD59 on cardiac endothelium. *Transplantation* 61, 1241–1249. doi:10.1097/00007890-199604270-00021

Diamond, L. E., Quinn, C. M., Martin, M. J., Lawson, J., Platt, J. L., and Logan, J. S. (2001). A human CD46 transgenic pig model system for the study of discordant xenotransplantation. *Transplantation* 71, 132–142. doi:10.1097/00007890-200101150-00021

Dufrane, D., Goebbels, R. M., Saliez, A., Guiot, Y., and Gianello, P. (2006). Six-month survival of microencapsulated pig islets and alginate biocompatibility in primates: Proof of concept. *Transplantation* 81, 1345–1353. doi:10.1097/01.tp.0000208610.75997.20

Ekser, B., Long, C., Echeverri, G. J., Hara, H., EzzelarabM.Lin, C. C., et al. (2010). Impact of thrombocytopenia on survival of baboons with genetically modified pig liver transplants: Clinical relevance. *Am. J. Transpl.* 10, 273–285. doi:10.1111/j.1600-6143.2009.02945.x

Estrada, J. L., Martens, G., Li, P., Adams, A., Newell, K. A., Ford, M. L., et al. (2015). Evaluation of human and non-human primate antibody binding to pig cells lacking GGTA1/CMAH/β4GalNT2 genes. *Xenotransplantation* 22, 194–202. doi:10.1111/xen.12161

Ezzelarab, M., Garcia, B., Azimzadeh, A., Sun, H., Lin, C. C., Hara, H., et al. (2009). The innate immune response and activation of coagulation in alpha1, 3-galactosyltransferase gene-knockout xenograft recipients. *Transplantation* 87, 805–812. doi:10.1097/TP.0b013e318199c34f

Ferran, C. (2006). Protective genes in the vessel wall: Modulators of graft survival and function. *Transplantation* 82, S36–S40. doi:10.1097/01.tp.0000231445.62162.d5

Firl, D. J., and Markmann, J. F. (2022). Measuring success in pig to non-human-primate renal xenotransplantation: Systematic review and comparative outcomes analysis of 1051 life-sustaining NHP renal allo- and xeno-transplants. *Am. J. Transpl.* 22, 1527–1536. doi:10.1111/ajt.16994

Fischer, K., Rieblinger, B., Hein, R., Sfriso, R., Zuber, J., Fischer, A., et al. (2020). Viable pigs after simultaneous inactivation of porcine MHC class I and three xenoreactive antigen genes GGTA1, CMAH and B4GALNT2. *Xenotransplantation* 27, e12560. doi:10.1111/xen.12560

Fodor, W. L., Williams, B. L., Matis, L. A., Madri, J. A., Rollins, S. A., Knight, J. W., et al. (1994). Expression of a functional human complement inhibitor in a transgenic pig as a model for the prevention of xenogeneic hyperacute organ rejection. *Proc. Natl. Acad. Sci. U. S. A.* 91, 11153–11157. doi:10.1073/pnas.91.23.11153

Gao, M., Zhu, X., Yang, G., Bao, J., and Bu, H. (2021). CRISPR/Cas9-Mediated gene editing in porcine models for medical research. *DNA Cell Biol.* 40, 1462–1475. doi:10.1089/dna.2020.6474

Griffiths, M. R., Gasque, P., and Neal, J. W. (2009). The multiple roles of the innate immune system in the regulation of apoptosis and inflammation in the brain. *J. Neuropathol. Exp. Neurol.* 68, 217–226. doi:10.1097/NEN.0b013e3181996688

Groth, C. G., Korsgren, O., Tibell, A., Tollemar, J., Möller, E., Bolinder, J., et al. (1994). Transplantation of porcine fetal pancreas to diabetic patients. *Lancet* 344, 1402–1404. doi:10.1016/s0140-6736(94)90570-3

Hardy, J. D., and Chavez, C. M. (1969). The first heart transplant in man: Historical reexamination of the 1964 case in the light of current clinical experience. *Transpl. Proc.* 1, 717–725.

Hering, B. J., Wijkstrom, M., Graham, M. L., Hardstedt, M., Aasheim, T. C., Jie, T., et al. (2006). Prolonged diabetes reversal after intraportal xenotransplantation of wild-type porcine islets in immunosuppressed nonhuman primates. *Nat. Med.* 12, 301–303. doi:10.1038/nm1369

Hinrichs, A., Riedel, E. O., Klymiuk, N., Blutke, A., Kemter, E., Langin, M., et al. (2021). Growth hormone receptor knockout to reduce the size of donor pigs for preclinical xenotransplantation studies. *Xenotransplantation* 28, e12664. doi:10.1111/xen.12664

Houser, S. L., Kuwaki, K., Knosalla, C., Dor, F. J. M. F., Gollackner, B., Cheng, J., et al. (2004). Thrombotic microangiopathy and graft arteriopathy in pig hearts following transplantation into baboons. *Xenotransplantation* 11, 416–425. doi:10.1111/j.1399-3089.2004.00155.x

Ide, K., Wang, H., Tahara, H., Liu, J., Wang, X., Asahara, T., et al. (2007). Role for CD47-SIRPalpha signaling in xenograft rejection by macrophages. *Proc. Natl. Acad. Sci. U. S. A.* 104, 5062–5066. doi:10.1073/pnas.0609661104

Iwase, H., Ekser, B., Hara, H., Phelps, C., Ayares, D., Cooper, D. K. C., et al. (2014). Regulation of human platelet aggregation by genetically modified pig endothelial cells and thrombin inhibition. *Xenotransplantation* 21, 72–83. doi:10.1111/xen.12073

Iwase, H., Hara, H., Ezzelarab, M., Li, T., Zhang, Z., Gao, B., et al. (2017). Immunological and physiological observations in baboons with life-supporting genetically engineered pig kidney grafts. *Xenotransplantation* 24, e12293. doi:10.1111/xen.12293

Kim, K., Schuetz, C., Elias, N., Veillette, G. R., Wamala, I., Varma, M., et al. (2012). Up to 9-day survival and control of thrombocytopenia following alpha1, 3-galactosyl transferase knockout swine liver xenotransplantation in baboons. *Xenotransplantation* 19, 256–264. doi:10.1111/j.1399-3089.2012.00717.x

Kim, S. C., Mathews, D. V., Breeden, C. P., Higginbotham, L. B., Ladowski, J., Martens, G., et al. (2019). Long-term survival of pig-to-rhesus macaque renal xenografts is dependent on CD4 T cell depletion. *Am. J. Transpl.* 19, 2174–2185. doi:10.1111/ajt.15329

Klymiuk, N., Aigner, B., Brem, G., and Wolf, E. (2010). Genetic modification of pigs as organ donors for xenotransplantation. *Mol. Reprod. Dev.* 77, 209–221. doi:10.1002/mrd.21127

Kuehn, B. M. (2022). First pig-to-human heart transplant marks a milestone in xenotransplantation. *Circulation* 145, 1870–1871. doi:10.1161/CIRCULATIONAHA.122.060418

Kuwaki, K., Tseng, Y. L., Dor, F. J., Shimizu, A., Houser, S. L., Sanderson, T. M., et al. (2005). Heart transplantation in baboons using alpha1, 3-galactosyltransferase gene-knockout pigs as donors: Initial experience. *Nat. Med.* 11, 29–31. doi:10.1038/nm1171

Ladowski, J. M., Hara, H., and Cooper, D. K. C. (2021). The role of SLAs in xenotransplantation. *Transplantation* 105, 300–307. doi:10.1097/TP.0000000000003303

Lai, L., Kolber-Simonds, D., Park, K. W., Cheong, H. T., Greenstein, J. L., Im, G. S., et al. (2002). Production of alpha-1, 3-galactosyltransferase knockout pigs by nuclear transfer cloning. *Science* 295, 1089–1092. doi:10.1126/science.1068228

Längin, M., Mayr, T., Reichart, B., Michel, S., Buchholz, S., Guethoff, S., et al. (2018). Consistent success in life-supporting porcine cardiac xenotransplantation. *Nature* 564, 430–433. doi:10.1038/s41586-018-0765-z

Lee, K. F., Salvaris, E. J., Roussel, J. C., Robson, S. C., d'Apice, A. J. F., and Cowan, P. J. (2008). Recombinant pig TFPI efficiently regulates human tissue factor pathways. *Xenotransplantation* 15, 191–197. doi:10.1111/j.1399-3089.2008.00476.x

Li, X., Wang, Y., Yang, H., and Dai, Y. (2021). Liver and hepatocyte transplantation: What can pigs contribute? *Front. Immunol.* 12, 802692. doi:10.3389/fimmu.2021.802692

Lin, C. C., Cooper, D. K., and Dorling, A. (2009). Coagulation dysregulation as a barrier to xenotransplantation in the primate. *Transpl. Immunol.* 21, 75–80. doi:10.1016/j.trim.2008.10.008

Lu, T., Yang, B., Wang, R., and Qin, C. (2019). Xenotransplantation: Current status in preclinical research. *Front. Immunol.* 10, 3060. doi:10.3389/fimmu.2019.03060

Martens, G. R., Reyes, L. M., Li, P., Butler, J. R., Ladowski, J. M., Estrada, J. L., et al. (2017). Humoral reactivity of renal transplant-waitlisted patients to cells from GGTA1/CMAH/B4GalNT2, and SLA class I knockout pigs. *Transplantation* 101, e86–e92. doi:10.1097/TP.0000000000001646

Miwa, Y., Yamamoto, K., Onishi, A., Iwamoto, M., Yazaki, S., Haneda, M., et al. (2010). Potential value of human thrombomodulin and DAF expression for coagulation control in pig-to-human xenotransplantation. *Xenotransplantation* 17, 26–37. doi:10.1111/j.1399-3089.2009.00555.x

Mohiuddin, M. M., Singh, A. K., Corcoran, P. C., Hoyt, R. F., Thomas, M. L., Ayares, D., et al. (2014a). Genetically engineered pigs and target-specific immunomodulation provide significant graft survival and hope for clinical cardiac xenotransplantation. *J. Thorac. Cardiovasc. Surg.* 148, 1106–1113. doi:10.1016/j.jtcvs.2014.06.002

Mohiuddin, M. M., Singh, A. K., Corcoran, P. C., Hoyt, R. F., Thomas, M. L., Lewis, B. G. T., et al. (2014c). One-year heterotopic cardiac xenograft survival in a pig to baboon model. *Am. J. Transpl.* 14, 488–489. doi:10.1111/ajt.12562

Mohiuddin, M. M., Singh, A. K., Corcoran, P. C., Hoyt, R. F., Thomas, M. L., Lewis, B. G. T., et al. (2014b). Role of anti-CD40 antibody-mediated costimulation blockade on non-Gal antibody production and heterotopic cardiac xenograft survival in a GTKO.hCD46Tg pig-to-baboon model. *Xenotransplantation* 21, 35–45. doi:10.1111/xen.12066

Mohiuddin, M. M., Singh, A. K., Corcoran, P. C., Thomas Iii, M. L., Clark, T., Lewis, B. G., et al. (2016). Chimeric 2C10R4 anti-CD40 antibody therapy is critical for long-term survival of GTKO.hCD46.hTBM pig-to-primate cardiac xenograft. *Nat. Commun.* 7, 11138. doi:10.1038/ncomms11138

Mueller, N. J., Livingston, C., Knosalla, C., Barth, R. N., Yamamoto, S., Gollackner, B., et al. (2004). Activation of porcine cytomegalovirus, but not porcine lymphotropic herpesvirus, in pig-to-baboon xenotransplantation. *J. Infect. Dis.* 189, 1628–1633. doi:10.1086/383351

Murthy, R., Bajona, P., Bhama, J. K., and Cooper, D. K. C. (2016). Heart xenotransplantation: Historical background, experimental progress, and clinical prospects. *Ann. Thorac. Surg.* 101, 1605–1613. doi:10.1016/j.athoracsur.2015.10.017

Nath, K. A., Balla, G., Vercellotti, G. M., Balla, J., Jacob, H. S., Levitt, M. D., et al. (1992). Induction of heme oxygenase is a rapid, protective response in rhabdomyolysis in the rat. *J. Clin. Invest.* 90, 267–270. doi:10.1172/JCI115847

Navarro-Alvarez, N., and Yang, Y. G. (2011). CD47: A new player in phagocytosis and xenograft rejection. *Cell. Mol. Immunol.* 8, 285–288. doi:10.1038/cmi.2010.83

Niu, D., Wei, H. J., Lin, L., George, H., Wang, T., Lee, I. H., et al. (2017). Inactivation of porcine endogenous retrovirus in pigs using CRISPR-Cas9. *Science* 357, 1303–1307. doi:10.1126/science.aan4187

Okada, N., Liszewski, M. K., Atkinson, J. P., and CaparonM. (1995). Membrane cofactor protein (CD46) is a keratinocyte receptor for the M protein of the group A streptococcus. *Proc. Natl. Acad. Sci. U. S. A.* 92, 2489–2493. doi:10.1073/pnas.92.7.2489

Oldenborg, P. A., Zheleznyak, A., Fang, Y. F., Gresham, H. D., and Lindberg, F. P. (2000). Role of CD47 as a marker of self on red blood cells. *Science* 288, 2051–2054. doi:10.1126/science.288.5473.2051

Opipari, A. W., JR., Boguski, M. S., and Dixit, V. M. (1990). The A20 cDNA induced by tumor necrosis factor alpha encodes a novel type of zinc finger protein. *J. Biol. Chem.* 265, 14705–14708. doi:10.1016/s0021-9258(18)77165-2

Oropeza, M., Petersen, B., Carnwath, J. W., Lucas-Hahn, A., Lemme, E., Hassel, P., et al. (2009). Transgenic expression of the human A20 gene in cloned pigs provides protection against apoptotic and inflammatory stimuli. *Xenotransplantation* 16, 522–534. doi:10.1111/j.1399-3089.2009.00556.x

Paris, L. L., Chihara, R. K., Reyes, L. M., Sidner, R. A., Estrada, J. L., Downey, S. M., et al. (2011). ASGR1 expressed by porcine enriched liver sinusoidal endothelial cells mediates human platelet phagocytosis *in vitro*. *Xenotransplantation* 18, 245–251. doi:10.1111/j.1399-3089.2011.00639.x

Pérez De La Lastra, J. M., Hanna, S. M., and Morgan, B. P. (1999). Distribution of membrane cofactor protein (MCP/CD46) on pig tissues. Relevance to xenotransplantation. *Immunology* 98, 144–151. doi:10.1046/j.1365-2567.1999.00830.x

Petersen, B., Ramackers, W., Lucas-Hahn, A., Lemme, E., Hassel, P., Queisser, A. L., et al. (2011). Transgenic expression of human heme oxygenase-1 in pigs confers resistance against xenograft rejection during *ex vivo* perfusion of porcine kidneys. *Xenotransplantation* 18, 355–368. doi:10.1111/j.1399-3089.2011.00674.x

Petersen, B., Ramackers, W., Tiede, A., Lucas-Hahn, A., Herrmann, D., Barg-Kues, B., et al. (2009). Pigs transgenic for human thrombomodulin have elevated production of activated protein C. *Xenotransplantation* 16, 486–495. doi:10.1111/j.1399-3089.2009.00537.x

Phelps, C. J., Koike, C., Vaught, T. D., Boone, J., Wells, K. D., Chen, S. H., et al. (2003). Production of alpha 1, 3-galactosyltransferase-deficient pigs. *Science* 299, 411–414. doi:10.1126/science.1078942

Porrett, P. M., Orandi, B. J., Kumar, V., Houp, J., Anderson, D., Cozette Killian, A., et al. (2022). First clinical-grade porcine kidney xenotransplant using a human decedent model. *Am. J. Transpl.* 22, 1037–1053. doi:10.1111/ajt.16930

Ramackers, W., Friedrich, L., Tiede, A., Bergmann, S., Schuettler, W., Schuerholz, T., et al. (2008). Effects of pharmacological intervention on coagulopathy and organ function in xenoperfused kidneys. *Xenotransplantation* 15, 46–55. doi:10.1111/j.1399-3089.2008.00443.x

Ramirez, P., Chavez, R., Majado, M., Munitiz, V., Munoz, A., Hernandez, Q., et al. (2000). Life-supporting human complement regulator decay accelerating factor transgenic pig liver xenograft maintains the metabolic function and coagulation in the nonhuman primate for up to 8 days. *Transplantation* 70, 989–998. doi:10.1097/00007890-200010150-00001

Rees, M. A., Butler, A. J., Chavez-Cartaya, G., Wight, D. G. D., Casey, N. D., Alexander, G., et al. (2002). Prolonged function of extracorporeal hDAF transgenic pig livers perfused with human blood. *Transplantation* 73, 1194–1202. doi:10.1097/00007890-200204270-00003

Reyes, L. M., Estrada, J. L., Wang, Z. Y., Blosser, R. J., Smith, R. F., Sidner, R. A., et al. (2014). Creating class I MHC-null pigs using guide RNA and the Cas9 endonuclease. *J. Immunol.* 193, 5751–5757. doi:10.4049/jimmunol.1402059

Rothblatt, M. (2022). Commentary on achievement of first life-saving xenoheart transplant. *Xenotransplantation* 29, e12746. doi:10.1111/xen.12746

Roussel, J. C., Moran, C. J., Salvaris, E. J., Nandurkar, H. H., d'Apice, A. J. F., and Cowan, P. J. (2008). Pig thrombomodulin binds human thrombin but is a poor cofactor for activation of human protein C and TAFI. *Am. J. Transpl.* 8, 1101–1112. doi:10.1111/j.1600-6143.2008.02210.x

Santos, M., Schilham, M. W., Rademakers, L. H., Marx, J. J., de SousaM.and Clevers, H. (1996). Defective iron homeostasis in beta 2-microglobulin knockout mice recapitulates hereditary hemochromatosis in man. *J. Exp. Med.* 184, 1975–1985. doi:10.1084/jem.184.5.1975

Shah, J. A., Patel, M. S., Elias, N., Navarro-AlvarezN.Rosales, I., Wilkinson, R. A., et al. (2017). Prolonged survival following pig-to-primate liver xenotransplantation utilizing exogenous coagulation factors and costimulation blockade. *Am. J. Transpl.* 17, 2178–2185. doi:10.1111/ajt.14341

Shah, J. A., Patel, M. S., Louras, N., Sachs, D. H., and Vagefi, P. A. (2019). Amino acid and lipid profiles following pig-to-primate liver xenotransplantation. *Xenotransplantation* 26, e12473. doi:10.1111/xen.12473

Shimizu, A., Hisashi, Y., Kuwaki, K., Tseng, Y. L., Dor, F. J. M. F., Houser, S. L., et al. (2008). Thrombotic microangiopathy associated with humoral rejection of cardiac xenografts from alpha1, 3-galactosyltransferase gene-knockout pigs in baboons. *Am. J. Pathol.* 172, 1471–1481. doi:10.2353/ajpath.2008.070672

Shimizu, A., Yamada, K., Robson, S. C., Sachs, D. H., and Colvin, R. B. (2012). Pathologic characteristics of transplanted kidney xenografts. *J. Am. Soc. Nephrol.* 23, 225–235. doi:10.1681/ASN.2011040429

Shimizu, A., Yamada, K., Yamamoto, S., Lavelle, J. M., Barth, R. N., Robson, S. C., et al. (2005). Thrombotic microangiopathic glomerulopathy in human decay accelerating factor-transgenic swine-to-baboon kidney xenografts. *J. Am. Soc. Nephrol.* 16, 2732–2745. doi:10.1681/ASN.2004121148

Sprangers, B., Waer, M., and Billiau, A. D. (2008). Xenotransplantation: Where are we in 2008? *Kidney Int.* 74, 14–21. doi:10.1038/ki.2008.135

Starzl, T. E., Rao, A. S., Murase, N., Demetris, A. J., Thomson, A., and Fung, J. J. (1999). Chimerism and xenotransplantation. New concepts. *Surg. Clin. North Am.* 79, 191–205. doi:10.1016/s0039-6109(05)70014-1

Tanihara, F., Hirata, M., Nguyen, N. T., Sawamoto, O., Kikuchi, T., and Otoi, T. (2021). One-step generation of multiple gene-edited pigs by electroporation of the CRISPR/Cas9 system into zygotes to reduce xenoantigen biosynthesis. *Int. J. Mol. Sci.* 22, 2249. doi:10.3390/ijms22052249

Tena, A. A., Sachs, D. H., Mallard, C., Yang, Y. G., Tasaki, M., Farkash, E., et al. (2017). Prolonged survival of pig skin on baboons after administration of pig cells expressing human CD47. *Transplantation* 101, 316–321. doi:10.1097/TP.0000000000001267

Tena, A., Kurtz, J., Leonard, D. A., Dobrinsky, J. R., Terlouw, S. L., Mtango, N., et al. (2014). Transgenic expression of human CD47 markedly increases engraftment in a murine model of pig-to-human hematopoietic cell transplantation. *Am. J. Transpl.* 14, 2713–2722. doi:10.1111/ajt.12918

Wang, R. G., Ruan, M., Zhang, R. J., Chen, L., Li, X. X., Fang, B., et al. (2018). Antigenicity of tissues and organs from GGTA1/CMAH/β4GalNT2 triple gene knockout pigs. *J. Biomed. Res.* 33, 235–243. doi:10.7555/JBR.32.20180018

Waterworth, P. D., Dunning, J., Tolan, M., Cozzi, E., LanGford, G., Chavez, G., et al. (1998). Life-supporting pig-to-baboon heart xenotransplantation. *J. Heart Lung Transpl.* 17, 1201–1207.

Wuensch, A., Baehr, A., Bongoni, A. K., Kemter, E., Blutke, A., Baars, W., et al. (2014). Regulatory sequences of the porcine THBD gene facilitate endothelial-specific expression of bioactive human thrombomodulin in single- and multitransgenic pigs. *Transplantation* 97, 138–147. doi:10.1097/TP.0b013e3182a95cbc

Xie, B., Shi, X., Li, Y., Xia, B., Zhou, J., Du, M., et al. (2021). Deficiency of ASGR1 in pigs recapitulates reduced risk factor for cardiovascular disease in humans. *PLoS Genet.* 17, e1009891. doi:10.1371/journal.pgen.1009891

Yang, H. K., and Yoon, K. H. (2015). Current status of encapsulated islet transplantation. *J. Diabetes Complicat.* 29, 737–743. doi:10.1016/j.jdiacomp.2015.03.017

Yang, L., GüELL, M., Niu, D., George, H., Lesha, E., Grishin, D., et al. (2015). Genome-wide inactivation of porcine endogenous retroviruses (PERVs). *Science* 350, 1101–1104. doi:10.1126/science.aad1191

Yazaki, S., Iwamoto, M., Onishi, A., Miwa, Y., Hashimoto, M., Oishi, T., et al. (2012). Production of cloned pigs expressing human thrombomodulin in endothelial cells. *Xenotransplantation* 19, 82–91. doi:10.1111/j.1399-3089.2012.00696.x

Yuan, H., Yu, T., Wang, L., Yang, L., Zhang, Y., Liu, H., et al. (2020). Efficient base editing by RNA-guided cytidine base editors (CBEs) in pigs. *Cell. Mol. Life Sci.* 77, 719–733. doi:10.1007/s00018-019-03205-2

Yue, Y., Xu, W., Kan, Y., Zhao, H. Y., Zhou, Y., Song, X., et al. (2021). Extensive germline genome engineering in pigs. *Nat. Biomed. Eng.* 5, 134–143. doi:10.1038/s41551-020-00613-9

Zhang, R., Wang, Y., Chen, L., Wang, R., Li, C., Li, X., et al. (2018). Reducing immunoreactivity of porcine bioprosthetic heart valves by genetically-deleting three major glycan antigens, GGTA1/β4GalNT2/CMAH. *Acta Biomater.* 72, 196–205. doi:10.1016/j.actbio.2018.03.055

Zhao, C., Liu, H., Xiao, T., Wang, Z., Nie, X., Li, X., et al. (2020). CRISPR screening of porcine sgRNA library identifies host factors associated with Japanese encephalitis virus replication. *Nat. Commun.* 11, 5178. doi:10.1038/s41467-020-18936-1

Zhou, Q., Li, T., Wang, K., Zhang, Q., Geng, Z., Deng, S., et al. (2022). Current status of xenotransplantation research and the strategies for preventing xenograft rejection. *Front. Immunol.* 13, 928173. doi:10.3389/fimmu.2022.928173

Zhu, X. X., Pan, J. S., Lin, T., Yang, Y. C., Huang, Q. Y., Yang, S. P., et al. (2022). Adenine base-editing-mediated exon skipping induces gene knockout in cultured pig cells. *Biotechnol. Lett.* 44, 59–76. doi:10.1007/s10529-021-03214-x

frontiers | Frontiers in Cell and Developmental Biology

TYPE Mini Review
PUBLISHED 17 October 2022
DOI 10.3389/fcell.2022.1031812

OPEN ACCESS

EDITED BY
Yongye Huang,
Northeastern University, China

REVIEWED BY
Rodolfo Gabriel Gatto,
Mayo Clinic, United States
Yuning Song,
Jilin University, China

*CORRESPONDENCE
Ye Jin,
jy_ccucm@163.com
Zhidong Qiu,
qzdcczy@163.com

SPECIALTY SECTION
This article was submitted to Stem Cell Research,
a section of the journal
Frontiers in Cell and Developmental Biology

RECEIVED 30 August 2022
ACCEPTED 26 September 2022
PUBLISHED 17 October 2022

CITATION
Wei J, Zhang W, Li J, Jin Y and Qiu Z (2022), Application of the transgenic pig model in biomedical research: A review. *Front. Cell Dev. Biol.* 10:1031812. doi: 10.3389/fcell.2022.1031812

Application of the transgenic pig model in biomedical research: A review

Jialin Wei, Wen Zhang, Jie Li, Ye Jin* and Zhidong Qiu*

School of Pharmacy, Changchun University of Chinese Medicine, Changchun, China

The large animal model has gradually become an essential part of preclinical research studies, relating to exploring the disease pathological mechanism, genic function, pharmacy, and other subjects. Although the mouse model has already been widely accepted in clinical experiments, the need for finding an animal model with high similarity compared with a human model is urgent due to the different body functions and systems between mice and humans. The pig is an optimal choice for replacement. Therefore, enhancing the production of pigs used for models is an important part of the large animal model as well. Transgenic pigs show superiority in pig model creation because of the progress in genetic engineering. Successful cases of transgenic pig models occur in the clinical field of metabolic diseases, neurodegenerative diseases, and genetic diseases. In addition, the choice of pig breed influences the effort and efficiency of reproduction, and the mini pig has relative obvious advantages in pig model production. Indeed, pig models in these diseases provide great value in studies of their causes and treatments, especially at the genetic level. This review briefly outlines the method used to create transgenic pigs and species of producing transgenic pigs and provides an overview of their applications on different diseases and limitations for present pig model developments.

KEYWORDS

pig model, transgenetic pigs, biomedicine, engineering editing, disease model

1 Introduction

Animal models for human diseases commonly include the kind of animals that imitate traits of a certain disease, which is an essential technique to learn the pathogenesis and treatment of a disease. It can help researchers gain a better understanding of pharmaceutical development and toxicological or safety screening technologies (Robl et al., 2007). Indeed, disease animal models are always regarded as a basis for life science research studies. Animal models have a long history in body function observation, which began in ancient Greece (Ericsson et al., 2013). With the growing need for *in vivo* experiments, specific species were chosen as animal models including rabbits, sheep, and pigs (Hammer et al., 1985). However, considering finance conditions and characteristics of specific species, the production of animal models has become a challenge to scientific research studies. Tissue and organ structures and cellular function of mice are similar to those of humans, which makes mice a suitable

option for imitating the body of humans (Kobayashi et al., 2012; Hryhorowicz et al., 2020; Lunney et al., 2021). In the 1980s, since the dramatic development of genetic techniques, mice with deleted genetic material were accepted widely. Such a model could produce a stable and quick process of reproduction (Ericsson et al., 2013). An animal whose genome has been altered by the inclusion of foreign genetic material can be called a transgenic animal, aiming to add new genes to an organism's genome to produce a new protein or set of proteins that has not been presented before (Tadesse and Koricho, 2017). Although mouse models are widely used in biomedical research, less similarity between mice and humans in pathological mechanisms of diseases and medical safety raises strong worries and challenges in biomedical research studies. Combining with the superiority of high similarity of humans in body size, organ size and structure, physiology, and pathophysiology (Flisikowska et al., 2014), the pig is thought to be a better model than mice and the transgenic pig has been used with sophisticated technology in diseases such as cardiovascular diseases, cancers, diabetes mellitus, Alzheimer's disease, cystic fibrosis, and Duchenne muscular dystrophy (Flisikowska et al., 2014). This article will provide an overview of techniques to create transgenic pigs, breeds of mini pigs for transgenic technique applications, and diseases that used transgenic pig models to explore relative mechanisms and treatments. In the end, a discussion of worries about pig models would be mentioned, including the large-scale production of models and applications on potential gene targets. The ways of researching transgenic pigs may provide inspiration for exploring other big animal models.

2 Techniques for building trans genetic pigs

2.1 Microinjection

Microinjection has a long history in biomedical research. This well-developed technology involves the injection of the DNA material into the male pronucleus, the RNA material into the cytoplasm, or proteins into the cytoplasm or pronucleus (Stout et al., 2009a; Hryhorowicz et al., 2020). The technique for adding a transgene by using pronuclear injection was pioneered in mice (Gordon et al., 1980) and then in pigs. Conventionally, gene-editing pigs were produced first by pronuclear injection (Xu, 2019). The random feature of integration can be viewed as an advantage or a disadvantage due to the fact that genome integration occurs randomly (Lavitrano et al., 1989; Stout et al., 2009b), which could lead to less efficiency on a specific structure, function, and expression regulation of genes. The effects of microinjection depend greatly on many aspects including the solution purity, its concentration (Piedrahita, 2000), material form (DNA/RNA/protein) (Le et al., 2021), the length or size of the introduced structure (with increasing length/size, the efficiency decreases), and embryo development (Le et al., 2021).

2.2 Sperm-mediated gene transfer (SMGT)

Sperm-mediated gene transfer (SMGT) is a kind of method that enhances the intrinsic ability of sperm cells to bind and internalize exogenous DNA molecules and to transfer them into the oocyte at fertilization. This technique first appeared in 1989, gaining a result of transgenetic rats with 30% integration degree and stable inheritance and expression in the next generation (Sperandio et al., 1996). Obvious advantages of this method include the high rate of integration with the natural combining process and less damage to the embryo caused by the machine (Umeyama et al., 2012). On the other hand, due to the differences between species, large efficiency gaps occurred among species. Sperm-mediated gene transfer has been used successfully in mice (Lavitrano et al., 2003), pigs (Harel-Markowitz et al., 2009), and chickens (García-Vázquez et al., 2010) The first transgenetic pig was developed by recombinase-mediated DNA transfer and the ICSI-SGMT technique (Perry et al., 1999). Intracytoplasmic sperm injection-mediated gene transfer is one way of SMGT which is widely used to create the transgenic pig model by controlling stable integration and gene expression of reproduction at the embryonic level (Lai et al., 2002; Watanabe et al., 2012; Dicks et al., 2015).

2.3 Somatic cell nuclear transfer

SCNT is a technique that transfers somatic nuclei into mature denucleated oocytes by using denucleated oocytes as the recipient and single cell nuclei as the donor. This technique first appeared in 1996 when Dolly sheep was cloned successfully (Wilmut et al., 2007). Since then, SCNT entered into an era of dramatic development. Theoretically, SCNT is a simple technique, involving the removal of nuclear DNA from an oocyte and its replacement with a somatic cell nucleus (Czernik et al., 2019). However, this process is influenced by the quality of oocytes and their ages, and high fetal mortality resulting primarily from genetic defects shows a great challenge in the colon process (Campbell, 2002). However, the efficiency of genome-edited somatic cells is only 0.5%–1.0% in livestock animals (Tan et al., 2016). Mature techniques of building gene-editing pigs have already been applied in large animal models. SCNT played great roles in editing the CRISPR/Cas9 system without detectable off-target effects to improve the convenience and efficacy of generating genetically modified pigs (Wilmut et al., 1997), tackling the

TABLE 1 Techniques, working mechanisms, and features for transgene pig model creation.

Technique		Mechanism	Feature	Reference
Microinjection		Injecting the DNA material into the male pronucleus	Random feature of integration	(Lavitrano et al., 1989; Stout et al., 2009a)
		Injecting the RNA material into the cytoplasm	Low efficiency on a specific structure, function, and expression regulation of genes	
		Injecting proteins into the cytoplasm or pronucleus	Depends greatly on many aspects	Piedrahita, (2000)
				Le et al. (2021)
Sperm-mediated gene transfer (SMGT)		Using exogenous DNA molecules to transfer them into the oocyte at fertilization	High rate of integration with the natural combining process	Umeyama et al. (2012)
			Less damage to the embryo caused by the machine	
			Large efficiency gaps occurred among species	
Somatic cell nuclear transfer (SCNT)		Injecting the RNA material into the cytoplasm	Low efficiency on a specific structure, function, and expression regulation of genes	Campbell, (2002)
		Injecting proteins into the cytoplasm or pronucleus	Depends greatly on many aspects	Piedrahita, (2000)
		Injecting the RNA material into the cytoplasm	Low efficiency of genome-edited somatic cells	Le et al. (2021)
			Low efficiency on a specific structure, function, and expression regulation of genes	
Gene-targeted technique	Homologous recombination	Homologous recombination between DNA sequences residing in the chromosome and newly introduced, cloned DNA sequences (gene targeting)	Allowing the transfer of any modification of the cloned gene into the genome of a living cell	(Watanabe et al., 2010; Zhou et al., 2015)
	Zinc-finger nucleases (ZFNs)		Knockout genes	Watanabe et al. (2010)
				Cermak et al. (2011)
	Transcription activator-like effector nucleases, (TALENs)		Knockout genes	Li et al. (2015)
	CRISPR/Cas9		Multiple knockout genes	(Cong et al., 2013; Ding et al., 2013; Mali et al., 2013)

barrier of low efficiency of homologous recombination (HR) in somatic cells in genetic pigs (Hammer et al., 1985).

2.4 Gene-targeting technique

The development of the gene-targeting technique dramatically fastens the speed of reproducing pig models. Several methods have significant functions in the process of developing gene targeting, including HR, zinc-finger nucleases (ZFNs), transcription activator-like effector nucleases (TALENs), and the CRISPR/Cas9 system (Hai et al., 2014). HR between DNA sequences residing in the chromosome and newly introduced, cloned DNA sequences (gene targeting) allows the transfer of any modification of the cloned gene into the genome of a living cell (Watanabe et al., 2010; Zhou et al., 2015). The first gene-targeting pig model was produced in 2002, α-1,3-galactosyltransferase (GGTA1)-knockout pigs, which produced an ideal animal model for xenotransplantation. ZFN is a method with high efficiency of knockout genes in many species. This method first appeared in 2010, and now, knockout pigs have been produced containing GGTA1 biallelic-knockout pigs (Watanabe et al., 2010) and PPARγ mono-allelic-knockout pigs (Cermak et al., 2011). TALENs have been proved to achieve site-directed modification of the target sequence (Li et al., 2015). Other pig models made by TALEN were GGTA1-knockout pigs (Li et al., 2014) and Rosa26-targeted swine models (Wang et al., 2013). The CRISPR/Cas9 system is an easier and more advanced method since the appearance of ZFN and TALEN (Hai et al., 2014). The CRISPR/Cas9 system has validated its gene knocking on multiple species with the unique advantage of multiple editing genes (including embryos and cells) with high efficiency (Cong et al., 2013; Ding et al., 2013; Mali et al., 2013). Hai et al. (2014) first used CRISPR/Cas9 to gain a vWF gene-knockout pig, combining with microinjection of fertilized eggs. The PRSAD2 gene-knock-in pig (Tanihara et al., 2021) and CD163-edited pig (Stumvoll et al., 2005) are also developed by the CRISPR/Cas9 system. Table 1 concludes the techniques, their

working mechanisms, and features for transgene pig model creations.

3 Breeds of transgenic pigs

Several features should have occurred in a proper animal model: pathogenesis homology, behavioral image consistency, and drug treatment predictability (Deslauriers et al., 2018). Features like convenience, reputation, and finance should also be considered in building an animal model. Rodent animals account for the largest proportion and the most significant function in animal models. It plays essential roles in exploring biological activities, disease pathogenesis, and drug development in human beings due to advanced and sophisticated gene techniques in mouse models (Nakamura et al., 2004; Kim et al., 2020). Furthermore, it has high similarity in physiological, biochemical, and developmental processes. In addition, the availability of embryonic stem cell (ESC) lines highlighted mice's significance in animal model usage (Bronson and Smithies, 1994; Rogers, 2016b; a). This is why mouse models can intimate drug functions when a disease occurs in them. Nevertheless, failing to recreate important aspects of human diseases such as fewer genetic similarities and significant differences in hereditation and lifespan could limit utilities as translational research tools (Tammen et al., 2006). In order to clarify the pathogenesis of human diseases specifically, especially those that are serious, animal models in higher evolutionary positions are really needed (Mclean et al., 2020). Research related to human safety, such as curative effects and disease treatments, demands more on large animal models, even non-human primate models. Indeed, narrowing the genetic differences between animals and humans can lead to the real condition of human physiology (Van Dam and De Deyn, 2017), which could provide a basic guarantee to human beings.

Pigs have been the predominant choice when modeling most human diseases (Min et al., 2014), owing to their high productivity, finance, and abundant resources. Since the development of hybridizing techniques, mini pigs were used more than farmyard pigs because of their remarkable smaller size, taking advantage of the growing process to be more controllable, reducing the compound that needs consequential prohibitive costs for the experiments, and making animal handling easier (Min et al., 2014). Nevertheless, compared with breeding mini pigs in the way of hybridization, transgenic pigs show benefits in shortening the breeding period and reducing limitations like provenance to introduce new traits, which greatly affects the improvement of pig models at the genetic level.

In view of the superiority of mini pigs, researchers from America, Europe, and Japan have started breeding new pig varieties with the goal of minimizing expenditure on building pig models as early as the 1940s and successively bred several breeds including Yucatan mini pigs, Gottingen mini pigs, and many other miniature pig breeds and strains. China followed the step and self-developed domestic species such as WZS pigs and Bama mini pigs that have already been widely accepted by medical institutions and organizations all over the world.

One of the cases for the Yucatan transgenic pig is generating male and female LDLR+/-pigs with techniques of recombinant adeno-associated virus-mediated gene targeting and somatic cell nuclear transfer in 2014, providing a better model of large animals in familial hypercholesterolemia and atherosclerosis (Wells and Prather, 2017). In addition, genetic inheritable GGTA1-knockout Yucatan miniature pigs were produced by combining transcription activator-like effector nuclease (TALEN) and nuclear transfer in 2020 by Choi. They concluded that TALEN could be a precise and safe tool for generating gene-edited pigs, and the TALEN-mediated GGTA1-knockout Yucatan miniature pig model in this study can serve as a safe and effective organ and tissue resource for clinical applications (Choi et al., 2020). Another Yucatan miniature pig with a gene knockout technique that should be mentioned was reported by Shim in 2021. Triple knockout of the genes occurred on GGTA1, cytidine monophosphate-N-acetylneuraminic acid hydroxylase (CMAH), and alpha 1,3-galactosyltransferase 2 (A3GALT2) in Yucatan miniature pigs on human immune reactivity (Shim et al., 2021). Although many cases lacking in the use of *in vitro* testing restrained a whole conclusion from being explored, studies on characterizations of Yucatan miniature pigs and the effects of genetically modified pig-to-nonhuman primate organ transplantation would be focused (Li et al., 2015).

Apart from Yucatan miniature pigs, Gottingen minipig, a small, white miniature pig with good fertility and stable genetics, is also a widely used mini-pig model (Eriksson et al., 2018). Crossing the Minnesota mini pig with the Vietnamese potbelly swine and the German Landrace, the Institute of Animal Breeding and Genetics of the University of Gottingen in Germany produced the Gottingen minipig between 1961 and 1962 (Bollen and Ellegaard, 1997). Gottingen miniature pigs are generally used as a model for neurodegenerative diseases, such as Alzheimer's disease (Norris et al., 2021). A double-transgenic Gottingen minipig model was created by Jakobsen in 2016. PSEN1, the gene for Alzheimer's disease, was induced in double-transgenic Gottingen minipig and triggered Met146Ile (PSEN1M146I) mutation (Jakobsen et al., 2016). This model could clarify the pathogenesis of Alzheimer's disease at an early stage (Shim et al., 2021).

Although China started late, the development had been rapid in Bama and Wuzhishan minipigs to obtain multiple genetically modified pigs and had even cultivated inbred minipigs (Renner et al., 2013). Wuzhishan pigs were on edge of extinction in the 1980s, found by Chinese scientists when performing animal species research. They inhabited isolated tropical areas in Hainan province, an island in southern China. In the

TABLE 2 Overview of mini pig species used for transgenic pig models.

Species	Species of origin	Application/target gene	Year	Technique	Reference
Yucatan miniature pig	One breed of native wild pigs in Península de Yucatán of Mexico	Creating male and female LDLR+/−pigs	2014	Adeno-associated virus-mediated gene targeting SCNT	Wells and Prather, (2017)
		GGTA1-knockout Yucatan miniature pigs	2020	TALEN Nuclear transfer	Pan et al. (2019)
		GGTA1 Cytidine monophosphate-N-acetylneuraminic acid hydroxylase (CMAH) Alpha 1,3-galactosyltransferase 2 (A3GALT2)	2021	Triple knockout of genes	Li et al. (2015)
Gottingen minipig	Crossing German Landrace, Vietnamese potbelly swine	Double-transgenic Gottingen minipig model for Alzheimer's disease	2016	SCNT	Shim et al. (2021)
WZS pig	One breed of Hainan province	Models with GH functions in relation to cancer, diabetes, and longevity	2015	Handmade cloning with impaired systemic GHR activity	Panepinto and Phillips, (1986)
Bama minipig	One breed of Guangxi province	Providing assessment and establishment of producing pig transgenic models	2015	SCNT	Jakobsen et al. (2016)

beginning, this breed was used to enlarge reproduction and then, was found to be a proper species for the mini pig model. One case of transgenic Wuzhishan mini pigs was produced by handmade cloning with impaired systemic GHR activity, and research studies assessed their growth profile and glucose metabolism. The studies concluded that this model could be valuable in growth hormone functions in relation to cancer, diabetes, and longevity (Panepinto and Phillips, 1986).

The Bama mini-pig is a miniature porcine species from the Guangxi province of China. A study reported an optimization of the efficiency of production of transgenic Bama mini-pigs through SCNT, concluding that the *in vitro* and *in vivo* developmental competence of transgenic Bama mini-pig embryos was improved using roscovitine-treated donor cells for SCNT (Jakobsen et al., 2016). The result provided both assessment and establishment of producing pig transgenic models for biomedical uses. Table 2 provides an overview of mini pig species used for transgenic pig models.

4 Diseases of applying transgenetic pig models

4.1 Alzheimer's disease

Alzheimer's disease (AD) is an age-related, progressive neurodegenerative disorder with the characteristics of memory dysfunction, presenting symptoms such as disorientation cognitive decline and cognitive decline (Hoffe and Holahan, 2019). Alzheimer's disease at the early stage is caused by increased production of the AβPP-derived peptide Aβ42 with the growth in mutations in the amyloid-β protein precursor gene (AβPP), the presenilin 1 gene (PSEN1), or the presenilin 2 gene (PSEN2) (Younkin, 1998; Renner et al., 2010; Hansson et al., 2019). The targeted genes that are generally chosen for transgene usage are the APP695sw-human transgene, PSEN1M1461-human transgene (Al-Mashhadi et al., 2013), APP695sw and PSEN1M1461human transgenes (Shim et al., 2021), and hAPP, hTau, and hPS1n human transgenes (Donninger et al., 2015). A kind of Göttingen minipigs was created for carrying the genome of one copy of a human PSEN1 cDNA with the Met146Ile (PSEN1M146I) mutation and three copies of a human AβPP695 cDNA with the Lys670Asn/Met671Leu (AβPPsw) double-mutation, to accumulate Aβ42 in brains (Denner et al., 2020). The accumulation could be detected by staining with Aβ42-specific antibodies in the intraneuronal system to reflect the pathogenesis of Alzheimer's disease at the beginning period of its developing process (Shim et al., 2021). The AD transgenic pig by SCNT 47 was produced for preclinical research for drug treatment. Through research studies, six well-characterized mutations were observed: hAPP (K670N/M671L, I716V, and V717I), hTau (P301L), and hPS1 (M146V and L286P). The result demonstrated that compared to the wild-type, the AD transgenic pig could express a higher level in brain tissue and a two-fold increase in Aβ levels in the brain (Donninger et al.,

2015), which shows the transgenic pig is more suitable for Alzheimer's disease research.

4.2 Diabetes mellitus

Diabetes mellitus (DM) is a group of metabolic disorders with the result of deficiency or ineffectiveness of insulin featuring hyperglycemia. It mainly classifies DM into three types: type I, type II, and gestational diabetes. Type II, thereinto, is explored more widely than the other two types. Although many studies have been made, most of the transgenic pig models used in type II DM are single-gene variant models due to their feature of polygenic complex disease. At present, targeting porcine InsC94Y (Kong et al., 2016), human HNF-1αP291fsinsC (Yamagata et al., 1996; Umeyama et al., 2009), and glucose-dependent insulinotropic polypeptide (GIP) Rdn (Jakobsen et al., 2016) are mostly used in diabetic transgenic pigs. Renner created the INSC94Y transgenic pig, meaning a permanent neonatal diabetic pig model was developed successfully (Kong et al., 2016). However, as the age grows, associated cataracts became more and more serious. A total of 29 transgenic pigs expressing a dominant-negative GIP receptor (GIPR [dn]) in pancreatic islets were generated, demonstrating an essential role of GIP30 for insulin secretion, the proliferation of β-cells, and physiological expansion of β-cell mass. These pigs are good models to study the role of GIP in glucose homeostasis and pancreatic development due to the obvious insulin resistance to exogenous GIP (Jakobsen et al., 2016). This finding may provide direction for analyzing the influences of GIP in different stages of pancreatic development.

4.3 Cystic fibrosis

Cystic fibrosis (CF) is caused by dysfunction of the CF transmembrane conductance regulator (CFTR), which is a recessive genetic disease with a single gene mutation (Bobadilla et al., 2002; Rogers et al., 2008a). The disease can affect many tissues and organs (Dinwiddie, 2000; Rogers et al., 2008b). Targets of editing genes of the CF pig model include the homozygous stop in CFTR exon 10 (Uc et al., 2012) and homozygous ΔF508 in CFTR (Cheng et al., 1990; Li et al., 2016). Stoltz et al. established a corrected model for intestinal expression based on studies of the pigs CFTR−/− (Flisikowska et al., 2012) in 2013, which alleviated meconium obstruction successfully. This result gives inspiration for CF treatments from the intestinal aspect.

4.4 Muscular dystrophy

Muscular dystrophy is a genetic disorder whose symptoms are progressive muscle weakness, wasting, and muscle degeneration. These diseases mainly include Duchenne muscular dystrophy (DMD) (Sheikh and Yokota, 2021), Becker muscular dystrophy (BMD) (Slatkovska et al., 2010), limb-girdle muscular dystrophy (LGMD) (Nallamilli et al., 2018), congenital muscular dystrophy (CMD) (CMD et al., 2012), and Emery–Dreifuss muscular dystrophy (EDMD) (Bushby et al., 2007; Fröhlich et al., 2016). DMD is an incurable X-linked genetic disease caused by deletion, point mutation, or duplication of the DMD gene (Klymiuk et al., 2013). Indeed, DND is essential for muscular dystrophy model building and relative treatments. Through gene targeting and SCNT, a pig model with a deletion of exon 52 of DMD was generated by Klymiuk et al. (2013). A high similarity occurred between this pig model and human DMD patients (Yu et al., 2016). Nevertheless, the problem of the rates of pig neonatal death needed to be considered, which could restrain the use of DMD pig models. Although an updated technique (accurate edit exon 27 of DMD) was used, this problem had not been solved yet (Chiappalupi et al., 2019). A truncated DMDΔ51–52 pig model was found with a lower neonatal death rate. This model not only enhanced skeletal muscle function and heart rhythm but also limited the inflammatory response and the expression of dystrophin through injecting porcine Sertoli cells (Walsh et al., 2005; Renner et al., 2010). The model is regarded to be useful to patients with d52DMD.

4.5 Cancer

Transgenic pig models have been developed for several kinds of cancer, such as porcine cancer models, breast cancer, colorectal cancer, and pancreatic cancer models. Targeted gene usage contains BRCA1' BRCA1+/Δ, APC, RUNX 3, TP53, KRASG12D, and TP53R167H. In 2010, a pig model with a knockout of the breast cancer-associated gene (BRCA1) mediated by adenovirus was reported. This model was the first pig model for breast cancer, with features of breast cancer stem cells. Through mutating adenomatous polyposis coli (APC) at sites 1,311 and 1,016, abnormal lesions and adenomas occurred in large intestines of pigs, which was regarded as impossible in the mouse model because it led to similar growths between the model and patients with familial adenomatous polyposis in human colorectal lesions. In 2016, Kang et al. created RUNX 3-knockout pigs to push gastric cancer research move forward a large step (Wang et al., 2017). Saalfrank et al. produced targeted TP53-knockout pigs, which developed multiple tumors at the same time (Hou et al., 2022). Combining TALEN and SCNT techniques, pigs simulating human non-small cell lung cancer were developed and achieved time–space and site-specific expression of the mutant proteins through rearrangement of echinoderm microtubule-associated protein 4 (EML4) and anaplastic lymphoma kinase (ALK) genes.

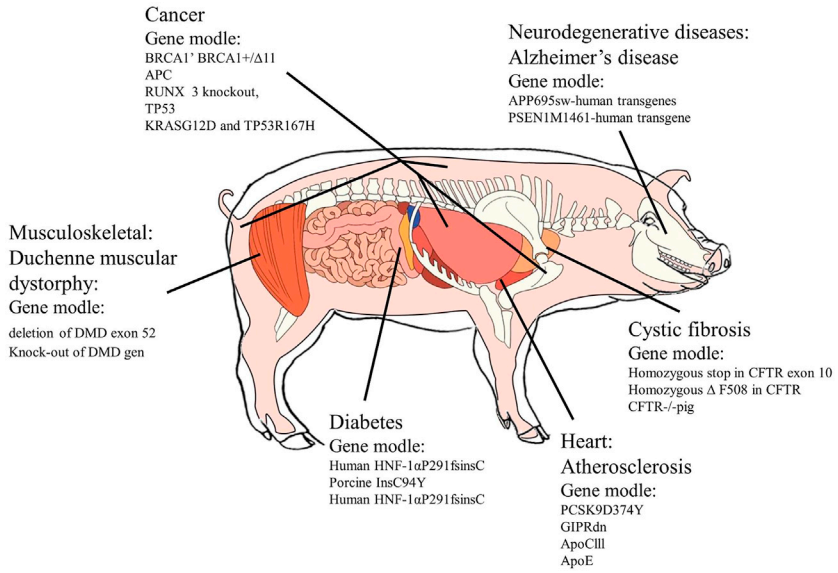

FIGURE 1
Diseases of transgenic pig model application. Source: Section 4.

4.6 Cardiovascular diseases

Atherosclerosis is one of the major causes of cardiovascular diseases, with symptoms of narrowing of arteries because of the accumulation of lipid and plaque formation (Gofman and Lindgren, 1950; Rogers, 2016b). Its features generally contain the deposition of lipids, cholesterol, and sugar complexes beginning from the intima and histiocytosis, leading to calcification (Crowther, 2005; Poirier et al., 2006). In research studies until now, four kinds of genes were used to produce transgenic pig models related to cardiovascular diseases. Proprotein convertase subtilisin/kexin type 9 (PCSK 9) mutation pigs could decrease low-density lipoprotein receptor (LDLR) levels and become a suitable model with obvious atherosclerosis symptoms (Renner et al., 2010). In 2013, al-Mashhadi et al. generated proprotein convertase subtilisin/kexin type 9 (PCSK 9) mutation pigs, which exhibited reduced low-density lipoprotein receptor (LDLR) levels and developed severe hypercholesterolemia and spontaneous atherosclerosis (Renner et al., 2010). Large animal models with impaired incretin function were proved to have a crucial function for GIP for insulin secretion, the proliferation of $^{N}_{L}$-cells, and physiological expansion of $^{N}_{L}$-cell mass. Although human ApoCIII transgenic pigs were ideal models for hypertriglyceridemia-associated diseases and drug treatments, their relation with atherosclerosis had not been cleared in 2010 (Renner et al., 2010). In 2012, a pig model of hypertriglyceridemia was created by targeting a key apolipoprotein in triglyceride metabolism-apolipoprotein (Apo) CIII (Wei et al., 2012). However, 6 years later, the success of apolipoprotein E (ApoE)-knockout pigs reproduced the human-like atherosclerotic lesions induced by a high-fat, high-cholesterol diet when the model had severe hypercholesterolemia (Fang et al., 2018), making a better representation of atherosclerosis in transgenic pig models. Figure 1 summarizes applications of the transgenic pig model for specific diseases.

5 Discussion

In summary, techniques for developing genetic pig models showed a trend of advanced level with a rapid speed. Apart from methods and diseases that used transgenic pig models, this review introduces the breeds for creating transgenic pigs that could provide another direction for producing pig models from a biological and physical aspect, including considering skin colors and size of viscera. Indeed, such a model with obvious natural features could help disease symptoms to be represented in a better way. Although many similar characteristics to human physiological and biological distinctions had been mentioned, several challenges still need to be tackled.

Developing the scale of transgenic pigs as an industrialized model is a suitable option to solve the issues of the shortage of animal resources and the high cost of building models. It is obvious that gene-editing accounts for the largest amount of pig model production but lacking a stable and fixed procedure for a breed of pig and low efficiency of success targeting are

still barriers to the industrialization of the transgenic pig model.

In addition, with the growing number of potential targeted genes and pathogenesis of human diseases that have been discovered, using gene editing technology to explore functions of the genome, realizing genetic improvement in reproduction traits, and overcoming species differences to simulate human diseases accurately still need further research. Moreover, models of large animals for human diseases have already been developed well in species like sheep (Banstola and Reynolds, 2022), monkeys (Khampang et al., 2021), and horses (Metrangolo et al., 2021) that covered genetic diseases like Batten disease (Karageorgos et al., 2011) and Gaucher disease (Kawabata et al., 2021), hypophyseal dysfunction (Koch and Betts, 2007), joint problems (Harman et al., 2021), and cutaneous wounds (Rogers, 2016b). Although the system of a species can differ from another, the ways of creating transgenic pig may provide new directions for other large animal models.

Author contributions

JW was responsible for the writing of the manuscript, WZ for the editing of the graphs and charts, JL for the editing and recording of the tables, and JW for the revision and final review of the manuscript. All authors were involved in the creation and were responsible for the content of the work.

Funding

The study was supported by the National Natural Science Foundation of China (Grant No. 81973712, 82003985), the Jilin Province Science and Technology Development Project in China (Grant No. 20210204013YY), the Jilin Province Science and Technology Development Plan Project (Grant No. 20200708081YY), and the Jilin Provincial Development and Reform Commission Innovation Capacity Building Project (Grant No. 2021C035-5).

Conflict of interest

The authors declare that the research was conducted in the absence of any commercial or financial relationships that could be construed as a potential conflict of interest.

Publisher's note

All claims expressed in this article are solely those of the authors and do not necessarily represent those of their affiliated organizations, or those of the publisher, the editors, and the reviewers. Any product that may be evaluated in this article, or claim that may be made by its manufacturer, is not guaranteed or endorsed by the publisher.

References

Al-Mashhadi, R. H., Sørensen, C. B., Kragh, P. M., Christoffersen, C., Mortensen, M. B., Tolbod, L. P., et al. (2013). Familial hypercholesterolemia and atherosclerosis in cloned minipigs created by DNA transposition of a human PCSK9 gain-of-function mutant. *Sci. Transl. Med.* 5 (166), 166ra1. doi:10.1126/scitranslmed.3004853

Banstola, A., and Reynolds, J. N. J. (2022). The sheep as a large animal model for the investigation and treatment of human disorders. *Biology* 11 (9), 1251. doi:10.3390/biology11091251

Bobadilla, J. L., Macek, M., Jr, Fine, J. P., and Farrell, P. M. (2002). Cystic fibrosis: A worldwide analysis of CFTR mutations—correlation with incidence data and application to screening. *Hum. Mutat.* 19 (6), 575–606. doi:10.1002/humu.10041

Bollen, P., and Ellegaard, L. (1997). The Göttingen minipig in pharmacology and toxicology. *Pharmacol. Toxicol.* 80, 3–4. doi:10.1111/j.1600-0773.1997.tb01980.x

Bronson, S. K., and Smithies, O. (1994). Altering mice by homologous recombination using embryonic stem cells. *J. Biol. Chem.* 269 (44), 27155–27158. doi:10.1016/s0021-9258(18)46959-1

Bushby, K., Norwood, F., and Straub, V. (2007). The limb-girdle muscular dystrophies--diagnostic strategies. *Biochim. Biophys. Acta* 1772 (2), 238–242. doi:10.1016/j.bbadis.2006.09.009

Campbell, K. H. (2002). A background to nuclear transfer and its applications in agriculture and human therapeutic medicine. *J. Anat.* 200, 267–275. doi:10.1046/j.1469-7580.2002.00035.x

Cermak, T., Doyle, E. L., Christian, M., Wang, L., Zhang, Y., Schmidt, C., et al. (2011). Efficient design and assembly of custom TALEN and other TAL effector-based constructs for DNA targeting. *Nucleic Acids Res.* 39 (12), e82. doi:10.1093/nar/gkr218

Cheng, S. H., Gregory, R. J., Marshall, J., Paul, S., Souza, D. W., White, G. A., et al. (1990). Defective intracellular transport and processing of CFTR is the molecular basis of most cystic fibrosis. *Cell* 63 (4), 827–834. doi:10.1016/0092-8674(90)90148-8

Chiappalupi, S., Salvadori, L., Luca, G., Riuzzi, F., Calafiore, R., Donato, R., et al. (2019). Do porcine Sertoli cells represent an opportunity for Duchenne muscular dystrophy? *Cell Prolif.* 52 (3), e12599. doi:10.1111/cpr.12599

Choi, K., Shim, J., Ko, N., and Park, J. (2020). No excessive mutations in transcription activator-like effector nuclease-mediated α-1, 3-galactosyltransferase knockout Yucatan miniature pigs. *Asian-Australas. J. Anim. Sci.* 33 (2), 360–372. doi:10.5713/ajas.19.0480

Cmd, L. Z., Cmd, S. X., Cmd, C. J., Cmd, J. H., Cmd, D. H., Han, D. X., et al. (2012). An effectiveness study comparing acupuncture, physiotherapy, and their combination in poststroke rehabilitation: A multicentered, randomized, controlled clinical trial. *Altern. Ther. Health Med.* 18 (3), 8–14.

Cong, L., Ran, F. A., Cox, D., Lin, S., Barretto, R., Habib, N., et al. (2013). Multiplex genome engineering using CRISPR/Cas systems. *Science* 339 (6121), 819–823. doi:10.1126/science.1231143

Crowther, M. A. (2005). Pathogenesis of atherosclerosis. *Hematology Am Soc Hematol Educ Program*, America, 436–441. doi:10.1182/asheducation-2005.1.436

Czernik, M., Anzalone, D. A., Palazzese, L., Oikawa, M., and Loi, P. (2019). Somatic cell nuclear transfer: Failures, successes and the challenges ahead. *Int. J. Dev. Biol.* 63 (3-4-5), 123–130. doi:10.1387/ijdb.180324mc

Denner, J., Tanzi, R., and Jacobson, S. (2020). Animal models of Alzheimer's disease should Be controlled for roseolovirus. *J. Alzheimers Dis.* 77 (2), 543–545. doi:10.3233/jad-200591

Deslauriers, J., Toth, M., Der-Avakian, A., and Risbrough, V. B. (2018). Current status of animal models of posttraumatic stress disorder: Behavioral and biological phenotypes, and future challenges in improving translation. *Biol. Psychiatry* 83 (10), 895–907. doi:10.1016/j.biopsych.2017.11.019

Dicks, N., Agellon, L. B., and Bordignon, V. (2015). "Somatic cell nuclear transfer and the creation of transgenic large animal models," in *Somatic genome manipulation* (Springer), 123–143.

Ding, Q., Regan, S. N., Xia, Y., Oostrom, L. A., Cowan, C. A., and Musunuru, K. (2013). Enhanced efficiency of human pluripotent stem cell genome editing through replacing TALENs with CRISPRs. *Cell Stem Cell* 12 (4), 393–394. doi:10.1016/j.stem.2013.03.006

Dinwiddie, R. (2000). Pathogenesis of lung disease in cystic fibrosis. *Respiration.* 67 (1), 3–8. doi:10.1159/000029453

Donninger, H., Hobbing, K., Schmidt, M. L., Walters, E., Rund, L., Schook, L., et al. (2015). A porcine model system of BRCA1 driven breast cancer. *Front. Genet.* 6, 269. doi:10.3389/fgene.2015.00269

Ericsson, A. C., Crim, M. J., and Franklin, C. L. (2013). A brief history of animal modeling. *Mo. Med.* 110 (3), 201–205.

Eriksson, S., Jonas, E., Rydhmer, L., and Röcklinsberg, H. (2018). Invited review: Breeding and ethical perspectives on genetically modified and genome edited cattle. *J. Dairy Sci.* 101 (1), 1–17. doi:10.3168/jds.2017-12962

Fang, B., Ren, X., Wang, Y., Li, Z., Zhao, L., Zhang, M., et al. (2018). Apolipoprotein E deficiency accelerates atherosclerosis development in miniature pigs. *Dis. Model. Mech.* 11 (10), dmm036632. doi:10.1242/dmm.036632

Flisikowska, T., Kind, A., and Schnieke, A. (2014). Genetically modified pigs to model human diseases. *J. Appl. Genet.* 55 (1), 53–64. doi:10.1007/s13353-013-0182-9

Flisikowska, T., Merkl, C., Landmann, M., Eser, S., Rezaei, N., Cui, X., et al. (2012). A porcine model of familial adenomatous polyposis. *Gastroenterology* 143 (5), 1173–1175. e1177. doi:10.1053/j.gastro.2012.07.110

Fröhlich, T., Kemter, E., Flenkenthaler, F., Klymiuk, N., Otte, K. A., Blutke, A., et al. (2016). Progressive muscle proteome changes in a clinically relevant pig model of Duchenne muscular dystrophy. *Sci. Rep.* 6, 33362. doi:10.1038/srep33362

García-Vázquez, F. A., Ruiz, S., Matás, C., Izquierdo-Rico, M. J., Grullón, L. A., De Ondiz, A., et al. (2010). Production of transgenic piglets using ICSI-sperm-mediated gene transfer in combination with recombinase RecA. *Reproduction* 140 (2), 259–272. doi:10.1530/rep-10-0129

Gofman, J. W., and Lindgren, F. (1950). The role of lipids and lipoproteins in atherosclerosis. *Science* 111 (2877), 166–171. doi:10.1126/science.111.2877.166

Gordon, J. W., Scangos, G. A., Plotkin, D. J., Barbosa, J. A., and Ruddle, F. H. (1980). Genetic transformation of mouse embryos by microinjection of purified DNA. *Proc. Natl. Acad. Sci. U. S. A.* 77 (12), 7380–7384. doi:10.1073/pnas.77.12.7380

Hai, T., Teng, F., Guo, R., Li, W., and Zhou, Q. (2014). One-step generation of knockout pigs by zygote injection of CRISPR/Cas system. *Cell Res.* 24 (3), 372–375. doi:10.1038/cr.2014.11

Hammer, R. E., Pursel, V. G., Rexroad, C. E., Jr., Wall, R. J., Bolt, D. J., Ebert, K. M., et al. (1985). Production of transgenic rabbits, sheep and pigs by microinjection. *Nature* 315 (6021), 680–683. doi:10.1038/315680a0

Hansson, O., Lehmann, S., Otto, M., Zetterberg, H., and Lewczuk, P. (2019). Advantages and disadvantages of the use of the CSF Amyloid β (Aβ) 42/40 ratio in the diagnosis of Alzheimer's Disease. *Alzheimers Res. Ther.* 11 (1), 34–15. doi:10.1186/s13195-019-0485-0

Harel-Markowitz, E., Gurevich, M., Shore, L. S., Katz, A., Stram, Y., and Shemesh, M. (2009). Use of sperm plasmid DNA lipofection combined with REMI (restriction enzyme-mediated insertion) for production of transgenic chickens expressing eGFP (enhanced green fluorescent protein) or human follicle-stimulating hormone. *Biol. Reprod.* 80 (5), 1046–1052. doi:10.1095/biolreprod.108.070375

Harman, R. M., Theoret, C. L., and Van de Walle, G. R. (2021). The horse as a model for the study of cutaneous wound healing. *Adv. Wound Care* 10 (7), 381–399. doi:10.1089/wound.2018.0883

Hoffe, B., and Holahan, M. R. (2019). The use of pigs as a translational model for studying neurodegenerative diseases. *Front. Physiol.* 10, 838. doi:10.3389/fphys.2019.00838

Hou, N., Du, X., and Wu, S. (2022). Advances in pig models of human diseases. *Anim. Model. Exp. Med.* 5 (2), 141–152. doi:10.1002/ame2.12223

Hryhorowicz, M., Lipiński, D., Hryhorowicz, S., Nowak-Terpiłowska, A., Ryczek, N., and Zeyland, J. (2020). Application of genetically engineered pigs in biomedical research. *Genes (Basel)* 11 (6), E670. doi:10.3390/genes11060670

Jakobsen, J. E., Johansen, M. G., Schmidt, M., Liu, Y., Li, R., Callesen, H., et al. (2016). Expression of the Alzheimer's disease mutations AβPP695sw and PSEN1M146I in double-transgenic göttingen minipigs. *J. Alzheimers Dis.* 53 (4), 1617–1630. doi:10.3233/jad-160408

Karageorgos, L., Lancaster, M. J., Nimmo, J. S., and Hopwood, J. J. (2011). Gaucher disease in sheep. *J. Inherit. Metab. Dis.* 34 (1), 209–215. doi:10.1007/s10545-010-9230-3

Kawabata, T., Suga, H., Takeuchi, K., Nagata, Y., Sakakibara, M., Ushida, K., et al. (2021). A new primate model of hypophyseal dysfunction. *Sci. Rep.* 11 (1), 10729. doi:10.1038/s41598-021-90209-3

Khampang, S., Parnpai, R., Mahikul, W., Easley, C. A. t., Cho, I. K., and Chan, A. W. S. (2021). CAG repeat instability in embryonic stem cells and derivative spermatogenic cells of transgenic Huntington's disease monkey. *J. Assist. Reprod. Genet.* 38 (5), 1215–1229. doi:10.1007/s10815-021-02106-3

Kim, J., Koo, B.-K., and Knoblich, J. A. (2020). Human organoids: Model systems for human biology and medicine. *Nat. Rev. Mol. Cell Biol.* 21 (10), 571–584. doi:10.1038/s41580-020-0259-3

Klymiuk, N., Blutke, A., Graf, A., Krause, S., Burkhardt, K., Wuensch, A., et al. (2013). Dystrophin-deficient pigs provide new insights into the hierarchy of physiological derangements of dystrophic muscle. *Hum. Mol. Genet.* 22 (21), 4368–4382. doi:10.1093/hmg/ddt287

Kobayashi, E., Hishikawa, S., Teratani, T., and Lefor, A. T. (2012). The pig as a model for translational research: Overview of porcine animal models at jichi medical university. *Transpl. Res.* 1 (1), 8. doi:10.1186/2047-1440-1-8

Koch, T. G., and Betts, D. H. (2007). Stem cell therapy for joint problems using the horse as a clinically relevant animal model. *Expert Opin. Biol. Ther.* 7 (11), 1621–1626. doi:10.1517/14712598.7.11.1621

Kong, S., Ruan, J., Xin, L., Fan, J., Xia, J., Liu, Z., et al. (2016). Multi-transgenic minipig models exhibiting potential for hepatic insulin resistance and pancreatic apoptosis. *Mol. Med. Rep.* 13 (1), 669–680. doi:10.3892/mmr.2015.4582

Lai, L., Kolber-Simonds, D., Park, K. W., Cheong, H. T., Greenstein, J. L., Im, G. S., et al. (2002). Production of alpha-1, 3-galactosyltransferase knockout pigs by nuclear transfer cloning. *Science* 295 (5557), 1089–1092. doi:10.1126/science.1068228

Lavitrano, M., Camaioni, A., Fazio, V. M., Dolci, S., Farace, M. G., and Spadafora, C. (1989). Sperm cells as vectors for introducing foreign DNA into eggs: Genetic transformation of mice. *Cell* 57 (5), 717–723. doi:10.1016/0092-8674(89)90787-3

Lavitrano, M., Forni, M., Bacci, M. L., Di Stefano, C., Varzi, V., Wang, H., et al. (2003). Sperm mediated gene transfer in pig: Selection of donor boars and optimization of DNA uptake. *Mol. Reprod. Dev.* 64 (3), 284–291. doi:10.1002/mrd.10230

Le, Q. A., Tanihara, F., Wittayarat, M., Namula, Z., Sato, Y., Lin, Q., et al. (2021). Comparison of the effects of introducing the CRISPR/Cas9 system by microinjection and electroporation into porcine embryos at different stages. *BMC Res. Notes* 14 (1), 7. doi:10.1186/s13104-020-05412-8

Li, F., Li, Y., Liu, H., Zhang, X., Liu, C., Tian, K., et al. (2015). Transgenic Wuzhishan minipigs designed to express a dominant-negative porcine growth hormone receptor display small stature and a perturbed insulin/IGF-1 pathway. *Transgenic Res.* 24 (6), 1029–1042. doi:10.1007/s11248-015-9912-6

Li, X., Tang, X. X., Vargas Buonfiglio, L. G., Comellas, A. P., Thornell, I. M., Ramachandran, S., et al. (2016). Electrolyte transport properties in distal small airways from cystic fibrosis pigs with implications for host defense. *Am. J. Physiol. Lung Cell. Mol. Physiol.* 310 (7), L670–L679. doi:10.1152/ajplung.00422.2015

Li, X., Yang, Y., Bu, L., Guo, X., Tang, C., Song, J., et al. (2014). Rosa26-targeted swine models for stable gene over-expression and Cre-mediated lineage tracing. *Cell Res.* 24 (4), 501–504. doi:10.1038/cr.2014.15

Lunney, J. K., Van Goor, A., Walker, K. E., Hailstock, T., Franklin, J., and Dai, C. (2021). Importance of the pig as a human biomedical model. *Sci. Transl. Med.* 13 (621), eabd5758. doi:10.1126/scitranslmed.abd5758

Mali, P., Yang, L., Esvelt, K. M., Aach, J., Guell, M., DiCarlo, J. E., et al. (2013). RNA-guided human genome engineering via Cas9. *Science* 339 (6121), 823–826. doi:10.1126/science.1232033

Mclean, Z., Oback, B., and Laible, G. (2020). Embryo-mediated genome editing for accelerated genetic improvement of livestock. *Front. Agric. Sci. Eng.* 7 (148), 148–15302. doi:10.15302/j-fase-2019305

Metrangolo, V., Ploug, M., and Engelholm, L. H. (2021). The urokinase receptor (uPAR) as a "trojan horse" in targeted cancer therapy: Challenges and opportunities. *Cancers (Basel)* 13 (21), 5376. doi:10.3390/cancers13215376

Min, F., Pan, J., Wang, X., Chen, R., Wang, F., Luo, S., et al. (2014). Biological characteristics of captive Chinese wuzhishan minipigs (*Sus scrofa*). *Int. Sch. Res. Not.* 2014, 761257. doi:10.1155/2014/761257

Nakamura, T., Xi, G., Hua, Y., Schallert, T., Hoff, J. T., and Keep, R. F. (2004). Intracerebral hemorrhage in mice: Model characterization and application for genetically modified mice. *J. Cereb. Blood Flow. Metab.* 24 (5), 487–494. doi:10.1097/00004647-200405000-00002

Nallamilli, B. R. R., Chakravorty, S., Kesari, A., Tanner, A., Ankala, A., Schneider, T., et al. (2018). Genetic landscape and novel disease mechanisms from a large LGMD cohort of 4656 patients. *Ann. Clin. Transl. Neurol.* 5 (12), 1574–1587. doi:10.1002/acn3.649

Norris, C., Lisinski, J., McNeil, E., VanMeter, J. W., VandeVord, P., and LaConte, S. M. (2021). MRI brain templates of the male Yucatan minipig. *Neuroimage* 235, 118015. doi:10.1016/j.neuroimage.2021.118015

Pan, D., Liu, T., Lei, T., Zhu, H., Wang, Y., and Deng, S. (2019). Progress in multiple genetically modified minipigs for xenotransplantation in China. *Xenotransplantation* 26 (1), e12492. doi:10.1111/xen.12492

Panepinto, L. M., and Phillips, R. W. (1986). The yucatan miniature pig: Characterization and utilization in biomedical research. *Lab. Anim. Sci.* 36 (4), 344–347.

Perry, A. C., Wakayama, T., Kishikawa, H., Kasai, T., Okabe, M., Toyoda, Y., et al. (1999). Mammalian transgenesis by intracytoplasmic sperm injection. *Science* 284 (5417), 1180–1183. doi:10.1126/science.284.5417.1180

Piedrahita, J. A. (2000). Targeted modification of the domestic animal genome. *Theriogenology* 53 (1), 105–116. doi:10.1016/s0093-691x(99)00244-7

Poirier, P., Giles, T. D., Bray, G. A., Hong, Y., Stern, J. S., Pi-Sunyer, F. X., et al. (2006). Obesity and cardiovascular disease: Pathophysiology, evaluation, and effect of weight loss. *Arterioscler. Thromb. Vasc. Biol.* 26 (5), 968–976. doi:10.1161/01.ATV.0000216787.85457.f3

Renner, S., Braun-Reichhart, C., Blutke, A., Herbach, N., Emrich, D., Streckel, E., et al. (2013). Permanent neonatal diabetes in INS(C94Y) transgenic pigs. *Diabetes* 62 (5), 1505–1511. doi:10.2337/db12-1065

Renner, S., Fehlings, C., Herbach, N., Hofmann, A., von Waldthausen, D. C., Kessler, B., et al. (2010). Glucose intolerance and reduced proliferation of pancreatic beta-cells in transgenic pigs with impaired glucose-dependent insulinotropic polypeptide function. *Diabetes* 59 (5), 1228–1238. doi:10.2337/db09-0519

Robl, J. M., Wang, Z., Kasinathan, P., and Kuroiwa, Y. (2007). Transgenic animal production and animal biotechnology. *Theriogenology* 67 (1), 127–133. doi:10.1016/j.theriogenology.2006.09.034

Rogers, C. S., Abraham, W. M., Brogden, K. A., Engelhardt, J. F., Fisher, J. T., McCray, P. B., Jr., et al. (2008a). The porcine lung as a potential model for cystic fibrosis. *Am. J. Physiol. Lung Cell. Mol. Physiol.* 295 (2), L240–L263. doi:10.1152/ajplung.90203.2008

Rogers, C. S. (2016a). Engineering large animal species to model human diseases. *Curr. Protoc. Hum. Genet.* 90, 1–15. doi:10.1002/cphg.18

Rogers, C. S. (2016b). Genetically engineered livestock for biomedical models. *Transgenic Res.* 25 (3), 345–359. doi:10.1007/s11248-016-9928-6

Rogers, C. S., Stoltz, D. A., Meyerholz, D. K., Ostedgaard, L. S., Rokhlina, T., Taft, P. J., et al. (2008b). Disruption of the CFTR gene produces a model of cystic fibrosis in newborn pigs. *Science* 321 (5897), 1837–1841. doi:10.1126/science.1163600

Sheikh, O., and Yokota, T. (2021). Developing DMD therapeutics: A review of the effectiveness of small molecules, stop-codon readthrough, dystrophin gene replacement, and exon-skipping therapies. *Expert Opin. Investig. Drugs* 30 (2), 167–176. doi:10.1080/13543784.2021.1868434

Shim, J., Ko, N., Kim, H. J., Lee, Y., Lee, J. W., Jin, D. I., et al. (2021). Human immune reactivity of GGTA1/CMAH/A3GALT2 triple knockout Yucatan miniature pigs. *Transgenic Res.* 30 (5), 619–634. doi:10.1007/s11248-021-00271-w

Slatkovska, L., Alibhai, S., Beyene, J., and Cheung, A. (2010). Effect of whole-body vibration on BMD: A systematic review and meta-analysis. *Osteoporos. Int.* 21 (12), 1969–1980. doi:10.1007/s00198-010-1228-z

Sperandio, S., Lulli, V., Bacci, M., Forni, M., Maione, B., Spadafora, C., et al. (1996). Sperm-mediated DNA transfer in bovine and swine species. *Anim. Biotechnol.* 7 (1), 59–77. doi:10.1080/10495399609525848

Stout, J. R., Rizk, R. S., and Walczak, C. E. (2009a). Protein inhibition by microinjection and RNA-mediated interference in tissue culture cells: Complementary approaches to study protein function. *Methods Mol. Biol.* 518, 77–97. doi:10.1007/978-1-59745-202-1_7

Stout, J. R., Rizk, R. S., and Walczak, C. E. (2009b). "Protein inhibition by microinjection and RNA-mediated interference in tissue culture cells: Complementary approaches to study protein function," in *Microinjection* (Springer), 77–97.

Stumvoll, M., Goldstein, B. J., and van Haeften, T. W. (2005). Type 2 diabetes: Principles of pathogenesis and therapy. *Lancet* 365 (9467), 1333–1346. doi:10.1016/s0140-6736(05)61032-x

Tadesse, T., and Koricho, D. (2017). Biomedical application and future prospects of transgenic animal: Review. *J. Nat. Sci. Res.* 7 (23), 82–88.

Tammen, I., Houweling, P. J., Frugier, T., Mitchell, N. L., Kay, G. W., Cavanagh, J. A., et al. (2006). A missense mutation (c.184C>T) in ovine CLN6 causes neuronal ceroid lipofuscinosis in Merino sheep whereas affected South Hampshire sheep have reduced levels of CLN6 mRNA. *Biochim. Biophys. Acta* 1762 (10), 898–905. doi:10.1016/j.bbadis.2006.09.004

Tan, W., Proudfoot, C., Lillico, S. G., and Whitelaw, C. B. (2016). Gene targeting, genome editing: From dolly to editors. *Transgenic Res.* 25 (3), 273–287. doi:10.1007/s11248-016-9932-x

Tanihara, F., Hirata, M., Nguyen, N. T., Le, Q. A., Wittayarat, M., Fahrudin, M., et al. (2021). Generation of CD163-edited pig via electroporation of the CRISPR/Cas9 system into porcine *in vitro*-fertilized zygotes. *Anim. Biotechnol.* 32 (2), 147–154. doi:10.1080/10495398.2019.1668801

Uc, A., Giriyappa, R., Meyerholz, D. K., Griffin, M., Ostedgaard, L. S., Tang, X. X., et al. (2012). Pancreatic and biliary secretion are both altered in cystic fibrosis pigs. *Am. J. Physiol. Gastrointest. Liver Physiol.* 303 (8), G961–G968. doi:10.1152/ajpgi.00030.2012

Umeyama, K., Saito, H., Kurome, M., Matsunari, H., Watanabe, M., Nakauchi, H., et al. (2012). Characterization of the ICSI-mediated gene transfer method in the production of transgenic pigs. *Mol. Reprod. Dev.* 79 (3), 218–228. doi:10.1002/mrd.22015

Umeyama, K., Watanabe, M., Saito, H., Kurome, M., Tohi, S., Matsunari, H., et al. (2009). Dominant-negative mutant hepatocyte nuclear factor 1alpha induces diabetes in transgenic-cloned pigs. *Transgenic Res.* 18 (5), 697–706. doi:10.1007/s11248-009-9262-3

Van Dam, D., and De Deyn, P. P. (2017). Non human primate models for Alzheimer's disease-related research and drug discovery. *Expert Opin. Drug Discov.* 12 (2), 187–200. doi:10.1080/17460441.2017.1271320

Walsh, D. M., Klyubin, I., Shankar, G. M., Townsend, M., Fadeeva, J. V., Betts, V., et al. (2005). The role of cell-derived oligomers of Abeta in Alzheimer's disease and avenues for therapeutic intervention. *Biochem. Soc. Trans.* 33, 1087–1090. doi:10.1042/bst20051087

Wang, H., Yang, H., Shivalila, C. S., Dawlaty, M. M., Cheng, A. W., Zhang, F., et al. (2013). One-step generation of mice carrying mutations in multiple genes by CRISPR/Cas-mediated genome engineering. *Cell* 153 (4), 910–918. doi:10.1016/j.cell.2013.04.025

Wang, K., Jin, Q., Ruan, D., Yang, Y., Liu, Q., Wu, H., et al. (2017). Cre-dependent Cas9-expressing pigs enable efficient *in vivo* genome editing. *Genome Res.* 27 (12), 2061–2071. doi:10.1101/gr.222521.117

Watanabe, M., Kurome, M., Matsunari, H., Nakano, K., Umeyema, K., Shiota, A., et al. (2012). The creation of transgenic pigs expressing human proteins using BAC-derived, full-length genes and intracytoplasmic sperm injection-mediated gene transfer. *Transgenic Res.* 21 (3), 605–618. doi:10.1007/s11248-011-9561-3

Watanabe, M., Umeyama, K., Matsunari, H., Takayanagi, S., Haruyama, E., Nakano, K., et al. (2010). Knockout of exogenous EGFP gene in porcine somatic cells using zinc-finger nucleases. *Biochem. Biophys. Res. Commun.* 402 (1), 14–18. doi:10.1016/j.bbrc.2010.09.092

Wei, J., Ouyang, H., Wang, Y., Pang, D., Cong, N. X., Wang, T., et al. (2012). Characterization of a hypertriglyceridemic transgenic miniature pig model expressing human apolipoprotein CIII. *Febs J.* 279 (1), 91–99. doi:10.1111/j.1742-4658.2011.08401.x

Wells, K. D., and Prather, R. S. (2017). Genome-editing technologies to improve research, reproduction, and production in pigs. *Mol. Reprod. Dev.* 84 (9), 1012–1017. doi:10.1002/mrd.22812

Wilmut, I., Schnieke, A. E., McWhir, J., Kind, A. J., and Campbell, K. H. (1997). Viable offspring derived from fetal and adult mammalian cells. *Nature* 385 (6619), 810–813. doi:10.1038/385810a0

Wilmut, I., Schnieke, A. E., McWhir, J., Kind, A. J., and Campbell, K. H. (2007). Viable offspring derived from fetal and adult mammalian cells. *Cloning Stem Cells* 9 (1), 3–7. doi:10.1089/clo.2006.0002

Xu, W. (2019). Microinjection and micromanipulation: A historical perspective. *Methods Mol. Biol.* 1874, 1–16. doi:10.1007/978-1-4939-8831-0_1

Yamagata, K., Oda, N., Kaisaki, P. J., Menzel, S., Furuta, H., Vaxillaire, M., et al. (1996). Mutations in the hepatocyte nuclear factor-1alpha gene in maturity-onset diabetes of the young (MODY3). *Nature* 384 (6608), 455–458. doi:10.1038/384455a0

Younkin, S. G. (1998). The role of Aβ42 in Alzheimer's disease. *J. Physiol. Paris* 92 (3-4), 289–292. doi:10.1016/s0928-4257(98)80035-1

Yu, H. H., Zhao, H., Qing, Y. B., Pan, W. R., Jia, B. Y., Zhao, H. Y., et al. (2016). Porcine zygote injection with cas9/sgRNA results in DMD-modified pig with muscle dystrophy. *Int. J. Mol. Sci.* 17 (10), E1668. doi:10.3390/ijms17101668

Zhou, X., Xin, J., Fan, N., Zou, Q., Huang, J., Ouyang, Z., et al. (2015). Generation of CRISPR/Cas9-mediated gene-targeted pigs via somatic cell nuclear transfer. *Cell. Mol. Life Sci.* 72 (6), 1175–1184. doi:10.1007/s00018-014-1744-7

frontiers | Frontiers in Cell and Developmental Biology

TYPE Review
PUBLISHED 25 October 2022
DOI 10.3389/fcell.2022.1031638

OPEN ACCESS

EDITED BY
Yongye Huang,
Northeastern University, China

REVIEWED BY
Haijiao Mao,
Ningbo University, China
Yang Han,
RWTH Aachen University, Germany

*CORRESPONDENCE
Ye Jin,
jy_ccucm@163.com
Zhidong Qiu,
qzdcczy@163.com

SPECIALTY SECTION
This article was submitted to Stem Cell Research,
a section of the journal
Frontiers in Cell and Developmental Biology

RECEIVED 30 August 2022
ACCEPTED 12 October 2022
PUBLISHED 25 October 2022

CITATION
Zhang G, Zhou X, Hu S, Jin Y and Qiu Z (2022), Large animal models for the study of tendinopathy.
Front. Cell Dev. Biol. 10:1031638.
doi: 10.3389/fcell.2022.1031638

Large animal models for the study of tendinopathy

Guorong Zhang[1,2], Xuyan Zhou[2], Shuang Hu[2], Ye Jin[2]* and Zhidong Qiu[2]*

[1]School of Clinical Medicine, Changchun University of Chinese Medicine, Changchun, China, [2]School of Pharmacy, Changchun University of Chinese Medicine, Changchun, China

Tendinopathy has a high incidence in athletes and the aging population. It can cause pain and movement disorders, and is one of the most difficult problems in orthopedics. Animal models of tendinopathy provide potentially efficient and effective means to develop understanding of human tendinopathy and its underlying pathological mechanisms and treatments. The selection of preclinical models is essential to ensure the successful translation of effective and innovative treatments into clinical practice. Large animals can be used in both micro- and macro-level research owing to their similarity to humans in size, structure, and function. This article reviews the application of large animal models in tendinopathy regarding injuries to four tendons: rotator cuff, patellar ligament, Achilles tendon, and flexor tendon. The advantages and disadvantages of studying tendinopathy with large animal models are summarized. It is hoped that, with further development of animal models of tendinopathy, new strategies for the prevention and treatment of tendinopathy in humans will be developed.

KEYWORDS

large animal model, tendinopathy, rotator cuff injury, patellar tendon injury, Achilles tendon injury, flexor tendon injury

Introduction

Tendons are dense connective tissues that connect muscle to bone and transmit the forces created by muscles to the bones, which causes movement. Trauma, strenuous exercise, or overuse can lead to acute tendon rupture or chronic degenerative disease, resulting in pain, movement disorders and other clinical symptoms (Dean et al., 2017). Tendon injuries often occur in areas with frequent movements and high stress. The frequent sites of tendon injuries in humans are demonstrated the schematic diagram in Figure 1. Tendon injury is very common and can be debilitating, but tendon repair remains a clinical challenge for orthopedic medicine.

Tendon biology is poorly understood compared to other components of the musculoskeletal system (Gaut and Duprez, 2016). Development of effective therapeutics is hindered by the lack of fundamental guiding data on the biology of tendon development, signal transduction, mechanotransduction, and the basic mechanisms underlying tendon pathogenesis and healing (Andarawis-Puri et al., 2015). The ability to perform invasive assays in animal models provides researchers

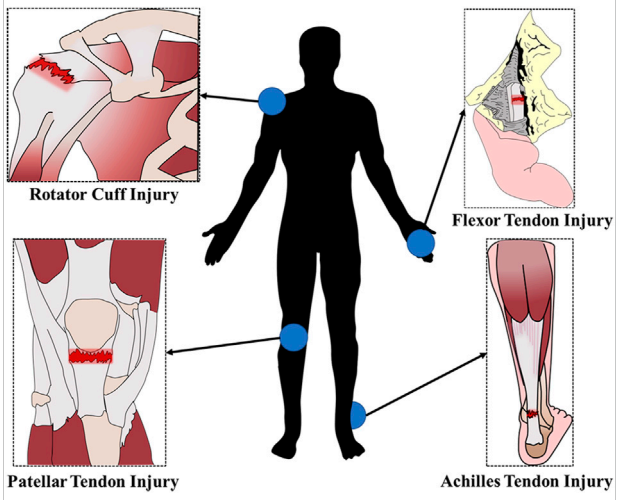

FIGURE 1
Schematic diagram of the sites of tendon injuries that frequently occur in humans.

with powerful opportunities to improve understanding of many aspects of tendinopathy (Warden, 2007). The efficacy and safety of stem cells, growth factors, drugs, tissue-engineered tendons, and other therapeutic methods must be validated in animal models before using them in clinical trials. Therefore, to study the pathogenesis and treatment of tendinopathy, animal models are indispensable (Habets et al., 2018; Longo et al., 2018).

The pathology and pathophysiology of tendinopathy in humans is currently poorly understood, meaning that the validation of animal models is difficult. Two common and established features associated with tendinopathy in humans are histopathological changes and mechanical weakening of the tendon (Warden, 2007). The prominent histological and molecular features of tendinopathy include increased immune cells and inflammatory mediators, enhanced cellular apoptosis, dysregulated extracellular matrix homeostasis, disorganization of collagen fibers, an increase in the microvasculature, and sensory nerve innervation (Millar et al., 2021). The most reasonable way to generate tendinopathy in animal models is to introduce known and potential causative factors. At present, the most used methods of modeling tendinopathy include mechanical stimulation, chemical induction, and surgical operation.

The principal animals used in the study of tendinopathy include rats, mice, chickens, rabbits, sheep, horses, dogs, pigs, and so on. The research objectives of tendinopathy are stratified by two main concerns (Liu et al., 2021). One is at the micro level, such as the biological characteristics of tendon-bone healing, the potential signaling pathway and the genetic mechanism of the disease, *etc.*; verified small animal models can usually meet the needs of such research. The second is at the macro level, such as biomechanical modeling, optimization of surgical techniques, evaluation of new instruments or devices, *etc.* This type of research requires animal models to be highly similar to humans in structure and function, so large animal models, especially non-human primate models, are usually more suitable. In most cases, these two goals are not separate; both micro and macro levels need to be considered. Large animals have more prospects for application because they can be used for both microscopic and macroscopic research.

This article reviews and analyzes the large animal models used in the study of tendinopathy in recent years with respect to four aspects: rotator cuff injury, patellar ligament injury, Achilles tendon injury and flexor tendon injury. The article aims to provide reference for further research.

Rotator cuff injury model

Rotator cuff injury is the most common shoulder injury. After injury, the tissue often presents with irreversible muscle atrophy, stiffness and fatty infiltration (Derwin et al., 2007). The ideal animal model of rotator cuff injury should have a similar anatomical structure and function to humans to be able to simulate the local microenvironment and histological changes after tendon injury. Previous studies have evaluated the application of various experimental animals in rotator cuff injury modeling (Takase et al., 2017; Lebaschi et al., 2018). But, in fact, except for humans, most animals rely on limbs for support. Even if there is occasional standing behavior supported on double hind limbs for a short time, the double forelimbs still have more weight-bearing functions than humans. Thus, the anatomy of the shoulder is different between humans and most other animals. The shoulder structure of nonhuman primates is the closest anatomical and physiological analog to that of humans. A schematic diagram of the scapula structure of human and different animals is shown in Figure 2. Large animal models of rotator cuff injury are mainly rabbits, sheep, dogs and cattle, which are suitable for studying the mechanisms of muscle degeneration, stent repair technology and improved surgical methods (Bisson et al., 2008; Liu et al., 2018; Smith et al., 2018; Roßbach et al., 2020).

Rabbits are one of the commonly used animal models in orthopedic studies. Hyman et al. presented a detailed architectural and physiological analysis of chronic tear and repair compared with age-matched control rabbit supraspinatus muscles (Hyman et al., 2021). Previous studies have used rabbit supraspinatus tendon or infraspinatus tendon tear models to analyze the tendon-bone healing effects of platelet-rich plasma and ozone therapy (Gurger et al., 2021), microfracture apertures (Sun et al., 2020), decellularized tendon sheets (Liu et al., 2018), preservation of native enthesis (Su et al., 2018) and nano-calcium silicate mineralized fish scale scaffolds (Han et al., 2023). Lee et al. studied the histological and biomechanical changes in a rabbit model of chronic rotator

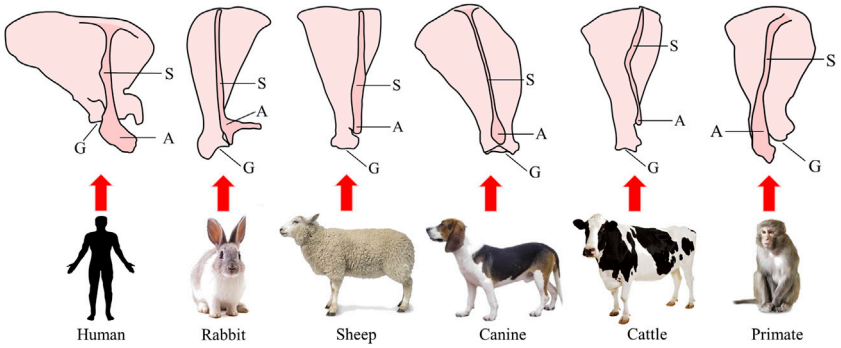

FIGURE 2
Schematic diagram of the structure of the scapula in humans and different animals. S, scapular spine; A, acromion; G, glenoid cavity.

cuff tears repaired by human dermal fibroblasts (Lee et al., 2021). Yildiz et al. used a rabbit irreparable rotator cuff tear model to compare the healing of two types of upper joint capsule reconstruction grafts (Yildiz et al., 2019). Xu et al. explored the in vivo biomechanical and histological processes of the rerouting biceps tendon to treat chronic irreparable rotator cuff tears in a rabbit model (Xu et al., 2022). In addition, Grumet et al. proposed that the rabbit subscapularis muscle model could be used for the study of rotator cuff lesions. They found that the rabbit glenohumeral joint had a bone channel formed by the supraglenoid tubercle, coracoid process and infraglenoid tubercle. The rabbit subscapularis muscle passes through this bone channel and to the lesser tubercle of the humerus, similar to the human supraspinatus tendon that passes under the acromion to the greater tubercle of the humerus. More importantly, the structure traversed within this bone tunnel is the tendon part of the subscapularis muscle. Another advantage of this model is the presence of fatty infiltration of the muscle after the tendon is severed (Grumet et al., 2009). Vargas-Vila et al. studied the progression of muscle loss and fat accumulation in a rabbit model of rotator cuff tear (Vargas-Vila et al., 2022). Wang et al. studied that adipose stem cell-derived exosomes decreased fatty infiltration and enhanced rotator cuff healing in a rabbit model of chronic tears (Wang et al., 2020).

Sheep can be used as a practical, large animal model. This model has been gradually used in various orthopedic studies, including studies on rotator cuff repair, due to its easy availability, ease of rearing, and relatively low cost. The large size of the infraspinatus tendon in sheep makes them particularly suitable for *in vitro* biomechanical studies (Camenzind et al., 2016; Guo et al., 2016). In addition, the sheep model has also been used to investigate the effect on rotator cuff repair of engineered tissue grafting (Novakova et al., 2018), perforated anchors, or collagen scaffolds loaded with tenocytes (Roßbach et al., 2020). Coleman et al. successfully constructed a chronic rotator cuff injury repair model by wrapping the broken end of the ovine infraspinatus tendon with a membrane (Coleman et al., 2003). Sener et al. used two different fixation methods to investigate the biomechanical and histological characteristics of patellar tendon-bone autografting and free flexor-tendon autografting in reconstruction of an infraspinatus defect in sheep (Sener et al., 2004). Romeo et al. evaluated the mechanical, structural, and histologic quality of rotator cuff repairs augmented with an interposition electrospun nanofiber scaffold in an acute sheep model (Romeo et al., 2022). Luan et al. found that muscle fatty infiltration and fibrosis would also occur after repair of acute rotator cuff injury in sheep (Luan et al., 2015). In a sheep rotator cuff model, tenotomy predominantly induces fatty infiltration, and denervation induces mostly muscle atrophy (Wieser et al., 2021). Some scholars have further revealed the possible mechanisms of muscle atrophy and degeneration after rotator cuff injury through sheep models, which is expected to provide a new target for clinical treatment (Gerber et al., 2017; Ruoss et al., 2018a; Ruoss et al., 2018b).

The canine rotator cuff injury model has been used to study a variety of rotator cuff repair materials or surgical methods (Adams et al., 2006; Derwin et al., 2007; Roller et al., 2018; Smith et al., 2018). Adams et al. used a full-thickness tear model of the Canis infraspinatus tendon to evaluate the effect of using human acellular dermal matrix grafting to enhance rotator cuff repair (Adams et al., 2006). Smith et al. compared the augmentation of partial rotator cuff tears of biologic scaffolds in a canine model (Smith et al., 2020). Derwin et al. evaluated the applicability of the canine rotator cuff acute full-thickness injury repair model; their results demonstrated that the repair strength immediately after surgery depended on the suture type and method, although all repaired tendons had retears shortly after surgery (Derwin et al., 2007). Derwin et al. evaluated the extent to which augmentation of acute repair of rotator cuff tendons with a newly designed poly-L-lactide repair device would improve functional and biomechanical outcomes in a canine

model (Derwin et al., 2009). In addition, the canine model can replicate muscle atrophy and fatty infiltration following rotator cuff injury in humans. Safran et al. developed a canine rotator cuff chronic injury model to explore the dynamic performance, muscle volume, and fat infiltration of infraspinatus muscles over time (Safran et al., 2005). The canine rotator cuff injury repair model can also tolerate various postoperative rehabilitation programs, such as plaster fixation, suspension fixation, and treadmill exercises (Lebaschi et al., 2016). Ji et al. tested a non-weight-bearing (NWB) canine model for rotator cuff repair research. In this model, the extensor muscles of the elbow and wrist were denervated by cutting the radial nerve proximal to the innervation region of the triceps brachii, to prevent weight bearing and muscle contraction of the affected limb after surgery (Ji et al., 2015). Liu et al. reported a novel biomaterial with engineered tendon-fibrocartilage-bone composite and bone marrow-derived mesenchymal stem cell sheet; the construct was tested for augmentation of rotator cuff repair using a canine NWB model (Liu et al., 2019).

The rotator cuff injury model of cattle is used in biomechanical research. Previous studies have investigated the biomechanical differences between single-row and double-row rotator cuff repairs (Mahar et al., 2007), the initial fixation strength of different suture methods under cyclic loading (Anderl et al., 2012), the influence of suture materials on the biomechanics of the suture–tendon interface (Bisson et al., 2008), and the pull out strength of different stitches (Bisson and Manohar, 2010). Park et al. evaluated the interface pressure of the rotator cuff tendon to the greater tuberosity for different rotator cuff repair techniques. Simulated rotator cuff tears over a 1 x 2 cm infraspinatus insertion footprint were created in 25 bovine shoulders. A transosseous tunnel simple suture technique, suture anchor simple technique, and suture anchor mattress technique were used for repair. Their results showed that the transosseous tunnel rotator cuff repair technique created significantly more contact and greater overall pressure distribution over a defined footprint when compared with suture anchor techniques (Park et al., 2005). The main advantage of the bovine rotator cuff injury model is that there is little difference in rotator cuff size and quality of tissue between different individuals, which helps to ensure the consistency of the replication model (Liu et al., 2021).

From the perspective of translational medicine, nonhuman primates are undoubtedly the most ideal species for shoulder joint research, as they are the most similar to humans in anatomical structure and physiology. Plate et al. studied age-related degenerative functional, radiographic, and histological changes of the shoulder in nonhuman primates (Plate et al., 2013). Sonnabend et al. stated that baboons make the best animal model for rotator cuff repair research based on their shoulders' similarity to the human shoulder joint (Sonnabend et al., 2010). Xu et al. used the African green monkey rotator cuff injury model to evaluate the repair effect and immune response of a non-cross-linked porcine dermal extracellular matrix graft; the results of this study demonstrated that the graft integrated well with the host tendon tissue and did not cause significant inflammatory reactions (Xu et al., 2012). However, the high cost of primate rearing, complexity of management, and difficulties in ethical approval limit its experimental application (Warden, 2007).

Patellar tendon injury model

The patellar tendon is located on the surface of the knee joint, connecting the patella and the tibia of the lower leg. It is one of the knee extensor devices. Due to the constant movement of the human knee joint, the patellar tendon is under periodic load for a long time, and the patellar tendon has become a common and frequent site of tendinopathy (Hast et al., 2014). In general, the patellar tendon is relatively large and its anatomical position is superficial and easy to access (Longo et al., 2011). The animal model of this part is convenient for biomechanical testing and research because the dual osseous attachment of the patellar tendon can be pulled without direct injury to the tendon material. However, the patellar tendon is wide and thin, which makes it difficult to inject drugs into. It requires delicate local operations, which require higher technical requirements for operators. Large animal models used in the study of tendinopathy include rabbit, sheep, dog, cow, and pig.

Patellar tendinitis in athletes is a chronic injury caused by repeated pulling on the patellar tip attachment of the patellar tendon due to excessive training, which can overload the patella and patellar tendon. To study the pathogenesis and development of patellar tendon fibrosis, a rabbit model of patellar tendon fibrosis was established by electrical stimulation-induced jumping (Liu et al., 2020). Intense exercise can cause acute injury to the proximal patella. Wang et al. detected the effect of the time of training after injury on healing (Wang et al., 2017). Xu et al. established a rabbit model of partial patellar resection to verify whether combined magnetic field technology can promote the healing of the bone–tendon junction through endochondral ossification (Xu et al., 2014). Kim et al. evaluated the healing capacity of injected atelocollagen as a treatment scaffold for patellar tendon defects (Kim et al., 2021). Other studies have compared the effects of human recombinant epidermal growth factor and platelet-rich plasma on the histological healing process and gene expression profile using a rabbit patellar tendon incision model (Lyras et al., 2016; Sarıkaya et al., 2017).

The sheep knee joint is often used as a model in orthopedic research. Kayser et al. provided ultrasound images of the sheep knee joint that were relevant in musculoskeletal research (Kayser et al., 2019). The biomechanical characteristics of the patellar tendon, such as elasticity and stiffness, are of paramount importance and constitute major outcome measures in research. Kayser et al. assessed whether the stiffness of the healthy ovine patellar tendon changed with age and weight in

a population of normal animals (Kayser et al., 2022). Thangarajah et al. used a sheep model of acute tendon contraction to study the role of the demineralized bone matrix in the treatment of tendon tear retractions. The patellar tendon was detached from the tibial tuberosity and a complete distal tendon transverse defect measuring 1 cm was created. The tendon was reconnected with suture anchors, and the defect was bridged with a demineralized bone matrix and minimally invasive mesenchymal stem cells (Thangarajah et al., 2016). Enea et al. performed surgery on the right hind leg of 48 Welsh goats, removed the central third of the patellar tendon, replaced it with an implant, and studied the effect of implanted collagen on tendon and ligament tissue regeneration *in vivo* (Enea et al., 2013).

One study examined the biomechanical and histological properties of the medial third of the patellar tendon in dogs; the results found a direct contrast to those of the central third (Linder et al., 1994). Gersoff et al. used the canine patellar tendon defect model to perform full-thickness proximal and distal flap defects of the patellar tendon in eight purpose-bred research mongrel dogs, and compared the healing of the Artelon patch-augmented tendon and tendon repair alone (Gersoff et al., 2019). A total of 27 patellar tendons in male Beagles were surgically subjected to stretching by a small diameter or a large diameter rod to induce damage due to strain, and were evaluated at 4- and 8-week intervals using quantitative magnetic resonance imaging, biomechanical testing, and histology (Pownder et al., 2021). de Moya and Kim quantified changes in the patellar tendon length following surgical correction of medial patellar luxation in dogs and evaluated the potential risk factors associated with patellar tendon elongation using dogs that underwent surgery for medial patellar luxation correction and had 2–3 months follow ups (de Moya and Kim, 2020).

In animal models of tendinopathy, the main *ex vivo* measurements of interest are the mechanical properties of the tendon. Reduced mechanical properties leading to an increased likelihood of spontaneous rupture is the result of clinical tendinopathy. The bovine patellar tendon is often used in biomechanical studies owing to its large size. Flanigan et al. evaluated the biomechanical properties of FiberWire, a novel suture material, compared with standard Ethibond sutures for tendon injury repair in the bovine knee joint (Flanigan et al., 2011). A three-step tensile stress-relaxation test was conducted on the patellar tendons of bovines, and the result revealed that long-term relaxation behavior is affected or implied by proteoglycans and crimp angle, possibly relating to slow structural reorganization of the tissue (Ristaniemi et al., 2021). To describe and compare the characteristics and coordination between knee ligaments and patellar tendons, dumbbell-shaped tensile specimens were cut from bovine knee ligament and patellar tendon for tensile testing. This study improved the understanding of the elasticity, viscoelasticity and failure characteristics of knee ligaments and patellar tendons (Ristaniemi et al., 2018).

Neovascular embolization is a therapeutic strategy for chronic musculoskeletal pain. Ghelfi et al. established a large animal model of patellar tendinopathy with neovascularization by percutaneous injection of increased doses of collagenase in nine 3-month-old male piglets. The model is feasible, safe and reproducible, which is helpful for the study of a new treatment for direct endovascular embolization of neovascularization (Ghelfi et al., 2021).

Achilles tendon injury model

As the largest and longest tendon of the human body, the Achilles tendon can typically bear more than 12.5 times the weight of the individual. Long-term, high-intensity load increases the incidence of Achilles tendinopathy (Komi, 1990). The Achilles tendon is also one of the most thoroughly researched elements of animal models of tendinopathy. It is advantageous to study because of its superficial parts, convenience of operation, and ease of sampling, which are conducive to the study of the mechanisms of tendinopathy. The Achilles tendon has been widely used in a variety of animal models (Hast et al., 2014; Loiselle et al., 2016). Large animals such as sheep or cattle are popular due to the appropriate size of their Achilles tendon, the weight bearing similar to humans, and their suitability for clinical evaluation. Rabbits are also suitable for Achilles tendon injury models because their Achilles tendon size allows for surgical approaches and accurate specimen examination (Doherty et al., 2006).

Skalec et al. conducted an anatomical and histological analysis on eight female New Zealand rabbits and comprehensively described the macroscopic and microscopic morphology of their Achilles tendon and its related structures (Skalec et al., 2019). The Achilles tendon transection model is a common model of injury that is used to study the biomechanical properties of healed tendons and the degree of adhesion formation (Meier Bürgisser et al., 2016), as well as the time-dependent changes of strain ratios (SRs) and the correlation between SRs and mechanical and histological properties of healed tissue (Yamamoto et al., 2017). It was also used to compare the effects of early activity and fixation on postoperative healing of rabbit Achilles tendon rupture (Jielile et al., 2016). The healing of tendons through open and percutaneous repair techniques was compared by histological, electron microscopic and biomechanical investigation (Yılmaz et al., 2014). Achilles tendon defects occur frequently in traumatic injuries. The rabbit Achilles tendon defect model was used to evaluate the repair effect of decellularized bovine tendon sheets (Zhang et al., 2018), polyethylene terephthalate artificial ligaments (Li et al., 2016), and collagen implants with or without a polydioxanone sheath for Achilles tendon defect reconstruction (Meimandi-Parizi et al., 2013). The Achilles tendinopathy model induced by bilateral Achilles tendon

injection of collagenase in rabbits accurately represents the progressive histological and biomechanical characteristics of human chronic Achilles tendinopathy (de Cesar Netto et al., 2018). A rabbit model of ischemic injury caused by Achilles tendon ligation was used to compare a series of changes in Achilles tendon morphology and strain in the early stage of Achilles tendinopathy (Ahn et al., 2017).

Achilles tendon rupture is common in sheep Achilles tendon injury models. Previous studies have evaluated the repair effect of cross-linked acellular porcine dermal patches, platelet-rich plasma fibrin matrixes (Sarrafian et al., 2010), exogenous growth differentiation factor CDMP-2 (Virchenko et al., 2008) and plasma rich in growth factors (Fernández-Sarmiento et al., 2013) on sheep Achilles tendon ruptures. Bruns et al. studied the spontaneous healing process of sheep Achilles tendons after transection and partial resection by means of histological and biomechanical analyses (Bruns et al., 2000). Dündar et al. used the sheep Achilles tendon tear model to compare the biomechanical properties of modified Kessler, Bunnell and Tsuge technology in repairing sheep Achilles tendon tears (Dündar et al., 2020). Leung et al. simulated bone–bone, bone–tendon and tendon–tendon repairs with osteotomy of the calcaneus, reattachment of Achilles tendon to the calcaneus after removal of the insertion, and tenotomy of the Achilles tendon resection in 47 goats (Leung et al., 2015). There have also been studies using collagenase injections to create Achilles tendon injury models. Serrani et al. used real-time elastosonography to monitor the progress of Achilles tendon healing after an experimentally induced tendinopathy (Serrani et al., 2021). Facon-Poroszewska et al. compared the efficacy of radial pressure wave therapy with injections of autologous adipose-derived stem cells or platelet rich plasma in the therapeutic procedure for collagenase-induced Achilles tendinopathy in sheep (Facon-Poroszewska et al., 2019).

Cattle Achilles tendons are larger and are often used for improvements in surgical suture techniques. Tian et al. designed the Locking Block Modified Krackow (LBMK) peri-tendon fixation technique for minimally invasive surgery and then compared the biomechanics of LBMK with Kessler and percutaneous Achilles repair system techniques with a simulated early rehabilitation program (Tian et al., 2020b).Tian et al. used 20 fresh bovine Achilles tendon specimens and randomly divided them into two groups, which were respectively sutured by open Giftbox Achilles tendon repair and minimally invasive LBMK techniques. The early rehabilitation simulation scheme was used to compare the biomechanics of the two techniques (Tian et al., 2020a).

There are few studies on pigs as animal models for Achilles tendon injury. Previous studies used pigs to study the biological characteristics of Achilles tendons or collected the Achilles tendons of pigs as materials for tendon injury repair. Zhang et al. characterized the structural components, vascularity, and resident tendon cells of the porcine Achilles tendon (Zhang et al., 2021). Lohan et al. achieved tendon-like tissue formation by implanting decellularized porcine Achilles tendons that were recellularized with human hamstring tendon-derived tenocytes into nude mice (Lohan et al., 2018).

Flexor tendon injury model

Animal models involving flexor tendons include the superficial flexor digitorum and flexor digitorum profunda tendons. The tendon healing process here is very slow due to the presence of ischemic and cell deficiency, which is consistent with the healing characteristics of tendinopathy (Adams and Habbu, 2015). Flexor tendons are relatively small, limiting their use in small animals. At the same time, large animals have the advantage of naturally occurring tendinopathy (Longo et al., 2011). At present, large mammals such as sheep and horses are the main animal models of flexor tendon injuries. However, large animals cost more, and rabbits offer a good compromise. Moreover, rabbit flexor tendons are more like human tendons in diameter and the presence of a perceptible synovial sheath (Bottagisio and Lovati, 2017).

To understand the repair process of flexor tendon injuries, studies have used the rabbit flexor tendon injury model to detect the expression of mast cells, fibroblasts, neuropeptides (Berglund et al., 2010) and growth response factor-1 (Derby et al., 2012). Progressive tendon adhesion is a major challenge in flexor tendon repair. Liao et al. developed an anti-adhesion scaffold for surgical repair of the flexor tendon in a rabbit model (Liao et al., 2018). Chen et al. investigated the preventive effects and mechanism of chitosan on tendon repair adhesion in rabbit flexor tendons (Chen et al., 2015). Previous studies have explored the effects on the healing of flexor tendon injury in rabbits investigated fibrin glue (He et al., 2013), autologous platelet-rich fibrin (Liao et al., 2017), bone marrow mesenchymal stem cells (He et al., 2015), adipose-derived stem cells (de Lima Santos et al., 2019), growth differentiation factor-5 (Henn et al., 2010), and lactoferrin peptide (Håkansson et al., 2012). A reinforced tubular, medicated electrospun construct was developed for rabbit deep flexor tendon repair that combines mechanical strength with the release of anti-inflammatory and anti-adhesion drugs (Peeters et al., 2022).

Sheep flexor tendon injury models include flexor tendon transection, collagenase induction, and partial tendon resection to create defects. To explore the mechanism of flexor tendon injury, Biasutti et al. recorded the gene expression, and histopathology and biomechanical changes that occur throughout the superficial digital flexor tendon up to 16 weeks post-injury in a sheep surgical model (Biasutti et al., 2017). Previous studies have investigated the repair effects of synovial multipotent cells (Khan et al., 2020), peripheral blood-derived mesenchymal stromal cells, and platelet-rich plasma (Martinello et al., 2013) on experimentally injured

TABLE 1 Advantages and disadvantages of large animal models in studying tendinopathy.

Species	Advantages	Disadvantages
Rabbit	Low cost and easy to access and manage	Strong self-healing ability, not easy to simulate the disease process
	Cytological and histological levels similarities to humans	Diarrhea occurs easily due to fright Lui et al. (2011)
	Medium somatotype is convenient for surgical operation	
	Biomechanical testing can be performed	
	In vivo imaging can be performed	
	Commercial reagents are available for molecular research	
	The rabbit subscapularis muscle model, which has a similar structure with humans, can be used for the study of rotator cuff injury Grumet et al. (2009)	
Sheep	Easily available and feeding	High costs of feeding and management
	Biomechanical and anatomical similarities to humans	Long growth period
	Big dimensions and easy to perform surgical procedures	Not useful for rehabilitation programs
	Biomechanical testing can be performed	
	Model transformation can be carried out	
	In vivo imaging can be performed	
	It is mainly used in the study of chronic tendon injuries and various suture techniques to reduce postoperative adverse conditions Gerber et al. (2004)	
Canine	Easy to access and manage	Higher costs of purchase and breeding
	Similar biomechanical environments	Difficulty unfolding large sample experimental studies
	Large dimensions and easy to perform surgical procedures	Significant differences from the anatomy of humans
	Biomechanical testing can be performed	Cases with spontaneous rotator cuff degeneration, not conducive to control variables Fransson et al. (2005)
	Model transformation can be carried out	Ethical concerns
	Better tolerance of multiple postoperative rehabilitation programs	
	In vivo imaging can be performed	
	It is used to explore the repair effect of tendon injury mediated by some internal factors and postoperative rehabilitation plan	
Cattle	Offer great potential for long-term functional studies	High feeding costs
	It is used in biomechanical research	Lack of reagents for molecular studies
Horse	The flexor digitorum superficialis tendon of horse is functionally equivalent to the human Achilles tendon	High feeding costs
	Tendinopathy occurs naturally Longo et al. (2011)	Lack of reagents for molecular studies
Primate	The anatomical structure and physiological functions are closest to those of humans	The cost of purchasing, feeding and management is extremely high
	Larger tissues allow for easier examination	Ethical concerns
	The structure of the shoulder is very similar to that of humans. Baboons may be the best animals to study rotator cuff damage Sonnabend et al. (2010)	

deep digital flexor tendons of sheep. The effects of the multiwave locked system were investigated in the acute phase of collagenase-induced tendon lesions in six adult sheep (Iacopetti et al., 2015). De Mattos et al. examined the effect of nano light emitting diode phototherapy on tendinopathy by partial tenotomies measuring 0.2 × 0.5 cm on the second third of the superficial flexor tendons of 10 healthy sheep (de Mattos et al., 2015). The sheep flexor tendon injury model is also used to improve surgical suture techniques. Uslu et al. randomly divided 60 fresh sheep forelimb flexor digitorum profundus tendons into three groups, and used two-, four-, and eight-strand suture techniques, respectively, to investigate the biomechanical relationship between the diameter of the core suture and the final repair strength of the surrounding suture with an increase of the number of suture lines (Uslu et al., 2014). Doğramaci et al. used 20 fresh flexor digitorum profundus tendons from the forelimbs of healthy adult sheep to improve suture techniques and evaluate their mechanical properties after repair (Doğramaci et al., 2009).

The flexor digitorum superficialis tendon of horses is a frequently injured structure that is functionally equivalent to the human Achilles tendon. Both play a key role in energy storage systems during high-speed exercise and can accumulate microdamage related to exercise and age, and are prone to rupture during strenuous activities (Patterson-Kane et al., 2012). To study the biological mechanism of age-related tendon injury, some studies have performed qualitative and quantitative analyses on the gene expression and collagen fiber

diameters of the flexor digitorum superficially and the flexor digitorum profunda tendons of horses at different ages (Ribitsch et al., 2020). Some researchers studied the therapeutic effect of fetal-derived embryonic-like stem cells using a collagenase gel-physical defect model in the mid-metacarpal region of the superficial digital flexor tendon of horses (Watts et al., 2011). Durgam et al. described the value of intralesional tendon-derived progenitor cell injections in equine flexor tendinitis using collagenase-induced tendinitis in both front superficial digital flexor tendons of horses (Durgam et al., 2016). Some studies examined superficial flexor tendon injuries in both horse forelimbs to explore the safety and effectiveness of equine allogeneic tenogenic primed mesenchymal stem cells in the treatment of tendon injury (Depuydt et al., 2021), and compared the changes of imaging, histology, and biochemical and biomechanical parameters (Johnson et al., 2021). Nelson et al. compared the intra- and postoperative clinical features of desmotomy of the accessory ligament of the superficial digital flexor tendon using a Saber radiofrequency electrosurgical probe *versus* sharp transection with a tenotomy knife (Nelson et al., 2015). With in-depth research on equine tendinopathy in recent years, the application of flexor tendon modeling is more common, and further promotes the translation of research results from large animal models to clinical practice on humans.

Conclusion

The selection of preclinical models is essential to ensure that the efficacy and safety of studied treatments is successfully translated into clinical practice. The selection of animal models requires consideration of scientific criteria, economics, and ethical issues. Indeed, the costs associated with animal rearing and management significantly influence the selection of animal species because an adequate sample size is necessary to obtain reliable results. Therefore, the selection of animal models for proof-of-concept studies needs to balance the ethical justification, cost-effectiveness, and appropriateness of the model itself, such as anatomical location, size, surgical approach, and biomechanical properties. When considering the efficacy of a new therapy, for the validity of preclinical models, the identification of appropriate controls, optimal study duration and intermediate time points, and the provision of the most in-depth analysis must be considered (Bottagisio and Lovati, 2017).

Rodents are the most used animal model for the study of the genetic and molecular mechanisms of tendinopathy due to their minimal cost and ethical compliance. Rats are often used to explore the factors affecting tendon-bone healing (Degen et al., 2016; Arimura et al., 2017; Nakagawa et al., 2017; Yonemitsu et al., 2019), the molecular mechanisms underlying ectopic ossification in tendinopathy (Geng et al., 2020) and inflammation and scar formation in the injury tendon healing (Wang et al., 2019; Geng et al., 2020). The advantage of mouse model is the ability to examine the role of specific signal transduction pathways and molecules in tendon degeneration and repair by gene knockout (Kuenzler et al., 2017; Jensen et al., 2018). Despite their low cost and ease of rearing, the small size of rats and mice has an impact on surgical approaches, non-invasive imaging techniques, and biomechanical testing. Moreover, the relevant results still need to be applied to large animals and clinical trials to ensure safety and effectiveness.

Compared with small animals, large animals share many similar characteristics with humans in genetics, anatomy, physiology, pathology, and so on. Therefore, large animals are more suitable for macroscopic research on topics such as tendon biomechanics, scaffold repair technology, and surgical method optimization. The advantages and disadvantages of large animal models in tendinopathy research are summarized in Table 1. However, due to the prohibitive cost of rearing and managing large animals and the difficulty of ethical approval, typically only small sample studies can be conducted. Rabbits offer a satisfactory compromise. The size and biomechanical properties of rabbit tendons are similar to those of human flexor tendons (Goodman and Choueka, 2005; Nagasawa et al., 2008), allowing for surgical and *in vivo* imaging analysis. The docility of rabbits allows evaluation of postoperative rehabilitation effects by immobilization or active loading. Rabbit models can also be used to evaluate the role of autologous cell therapy and regenerative medicine (Chong et al., 2007). Sheep are readily available, moderately expensive, and are used to study chronic tendon injuries and various suture techniques to reduce postoperative adverse conditions. Dogs are used to explore the repair effect of tendon injury mediated by internal factors and postoperative rehabilitation schemes, owing to their high degree of cooperation. However, public opinion pressure against the animal testing dogs hinders the selection of this species. Some experiments have used specially bred dogs as models of tendinopathy. The horse is a natural tendon injury model due to its frequent sports. Horses can be used to study the mechanisms and repair methods of tendon injury. Porcine tendons and ligaments are the best animal sources for xenogeneic tendon transplantation.

The application of animal models has promoted the progress of tendinopathy research but, given the complexity of human tendinopathy, there are still significant differences between animal experimental models and clinical human tendon injuries. In addition, more validated animal models are needed, as no single model can answer all the questions (Warden, 2007). It is hoped that, with the further development of animal models of tendinopathy, new strategies for the prevention and treatment of human tendinopathy can be provided.

Author contributions

GZ was responsible for the writing of the manuscript, XZ for the editing of the graphs and charts, SH for the editing and recording of the tables, YJ and ZQ for the revision and final review of the manuscript. All authors were involved in the creation and were responsible for the content of the work.

Funding

This work was supported by the National Natural Science Foundation of China (Grant No. 81973712, 82003985). Jilin Province Science and Technology Development Project in China (Grant No. 20210204013YY, 20200504005YY). Jilin Province Science and Technology Development Plan Project (Grant No. 20200708081YY). Jilin Province Traditional Chinese Medicine Science and Technology Project (Grant No. 2022012). Jilin Provincial Development and Reform Commission Innovation Capacity Building Project (Grant No. 2021C035-5).

Conflict of interest

The authors declare that the research was conducted in the absence of any commercial or financial relationships that could be construed as a potential conflict of interest.

Publisher's note

All claims expressed in this article are solely those of the authors and do not necessarily represent those of their affiliated organizations, or those of the publisher, the editors and the reviewers. Any product that may be evaluated in this article, or claim that may be made by its manufacturer, is not guaranteed or endorsed by the publisher.

References

Adams, J. E., and Habbu, R. (2015). Tendinopathies of the hand and wrist. *J. Am. Acad. Orthop. Surg.* 23 (12), 741–750. doi:10.5435/jaaos-d-14-00216

Adams, J. E., Zobitz, M. E., Reach, J. S., Jr., An, K. N., and Steinmann, S. P. (2006). Rotator cuff repair using an acellular dermal matrix graft: an in vivo study in a canine model. *Arthroscopy* 22 (7), 700–709. doi:10.1016/j.arthro.2006.03.016

Ahn, K. S., Lee, N. J., Kang, C. H., Lee, Y. H., and Jeon, H. J. (2017). Serial changes of tendon histomorphology and strain elastography after induced achilles tendinopathy in rabbits: An in vivo study. *J. Ultrasound Med.* 36 (4), 767–774. doi:10.7863/ultra.16.02059

Andarawis-Puri, N., Flatow, E. L., and Soslowsky, L. J. (2015). Tendon basic science: Development, repair, regeneration, and healing. *J. Orthop. Res.* 33 (6), 780–784. doi:10.1002/jor.22869

Anderl, W., Heuberer, P. R., Laky, B., Kriegleder, B., Reihsner, R., and Eberhardsteiner, J. (2012). Superiority of bridging techniques with medial fixation on initial strength. *Knee Surg. Sports Traumatol. Arthrosc.* 20 (12), 2559–2566. doi:10.1007/s00167-012-1922-9

Arimura, H., Shukunami, C., Tokunaga, T., Karasugi, T., Okamoto, N., Taniwaki, T., et al. (2017). TGF-β1 improves biomechanical strength by extracellular matrix accumulation without increasing the number of tenogenic lineage cells in a rat rotator cuff repair model. *Am. J. Sports Med.* 45 (10), 2394–2404. doi:10.1177/0363546517707940

Berglund, M. E., Hildebrand, K. A., Zhang, M., Hart, D. A., and Wiig, M. E. (2010). Neuropeptide, mast cell, and myofibroblast expression after rabbit deep flexor tendon repair. *J. Hand Surg. Am.* 35 (11), 1842–1849. doi:10.1016/j.jhsa.2010.06.031

Biasutti, S., Dart, A., Smith, M., Blaker, C., Clarke, E., Jeffcott, L., et al. (2017). Spatiotemporal variations in gene expression, histology and biomechanics in an ovine model of tendinopathy. *PLoS One* 12 (10), e0185282. doi:10.1371/journal.pone.0185282

Bisson, L. J., and Manohar, L. M. (2010). A biomechanical comparison of the pullout strength of No. 2 FiberWire suture and 2-mm FiberWire tape in bovine rotator cuff tendons. *Arthroscopy* 26 (11), 1463–1468. doi:10.1016/j.arthro.2010.04.075

Bisson, L. J., Manohar, L. M., Wilkins, R. D., Gurske-Deperio, J., and Ehrensberger, M. T. (2008). Influence of suture material on the biomechanical behavior of suture-tendon specimens: a controlled study in bovine rotator cuff. *Am. J. Sports Med.* 36 (5), 907–912. doi:10.1177/0363546508314793

Bottagisio, M., and Lovati, A. B. (2017). A review on animal models and treatments for the reconstruction of Achilles and flexor tendons. *J. Mater. Sci. Mater. Med.* 28 (3), 45. doi:10.1007/s10856-017-5858-y

Bruns, J., Kampen, J., Kahrs, J., and Plitz, W. (2000). Achilles tendon rupture: experimental results on spontaneous repair in a sheep-model. *Knee Surg. Sports Traumatol. Arthrosc.* 8 (6), 364–369. doi:10.1007/s001670000149

Camenzind, R. S., Wieser, K., Fessel, G., Meyer, D. C., and Snedeker, J. G. (2016). Tendon collagen crosslinking offers potential to improve suture pullout in rotator cuff repair: An *ex vivo* sheep study. *Clin. Orthop. Relat. Res.* 474 (8), 1778–1785. doi:10.1007/s11999-016-4838-8

Chen, Q., Lu, H., and Yang, H. (2015). Chitosan prevents adhesion during rabbit flexor tendon repair via the sirtuin 1 signaling pathway. *Mol. Med. Rep.* 12 (3), 4598–4603. doi:10.3892/mmr.2015.4007

Chong, A. K., Ang, A. D., Goh, J. C., Hui, J. H., Lim, A. Y., Lee, E. H., et al. (2007). Bone marrow-derived mesenchymal stem cells influence early tendon-healing in a rabbit achilles tendon model. *J. Bone Jt. Surg. Am.* 89 (1), 74–81. doi:10.2106/jbjs.E.01396

Coleman, S. H., Fealy, S., Ehteshami, J. R., MacGillivray, J. D., Altchek, D. W., Warren, R. F., et al. (2003). Chronic rotator cuff injury and repair model in sheep. *J. Bone Jt. Surg. Am.* 85 (12), 2391–2402. doi:10.2106/00004623-200312000-00018

de Cesar Netto, C., Godoy-Santos, A. L., Augusto Pontin, P., Natalino, R. J. M., Pereira, C. A. M., Lima, F. D. O., et al. (2018). Novel animal model for Achilles tendinopathy: Controlled experimental study of serial injections of collagenase in rabbits. *PLoS One* 13 (2), e0192769. doi:10.1371/journal.pone.0192769

de Lima Santos, A., Silva, C. G. D., de Sá Barretto, L. S., Franciozi, C., Tamaoki, M. J. S., de Almeida, F. G., et al. (2019). Biomechanical evaluation of tendon regeneration with adipose-derived stem cell. *J. Orthop. Res.* 37 (6), 1281–1286. doi:10.1002/jor.24182

de Mattos, L. H., Álvarez, L. E., Yamada, A. L., Hussni, C. A., Rodrigues, C. A., Watanabe, M. J., et al. (2015). Effect of phototherapy with light-emitting diodes (890 nm) on tendon repair: an experimental model in sheep. *Lasers Med. Sci.* 30 (1), 193–201. doi:10.1007/s10103-014-1641-1

de Moya, K., and Kim, S. (2020). Radiographic evaluation of patellar tendon length following corrective surgical procedures for medial patellar luxation in dogs. *PLoS One* 15 (9), e0238598. doi:10.1371/journal.pone.0238598

Dean, B. J. F., Dakin, S. G., Millar, N. L., and Carr, A. J. (2017). Review: Emerging concepts in the pathogenesis of tendinopathy. *Surgeon* 15 (6), 349–354. doi:10.1016/j.surge.2017.05.005

Degen, R. M., Carbone, A., Carballo, C., Zong, J., Chen, T., Lebaschi, A., et al. (2016). The effect of purified human bone marrow-derived mesenchymal stem cells on rotator cuff tendon healing in an athymic rat. *Arthroscopy* 32 (12), 2435–2443. doi:10.1016/j.arthro.2016.04.019

Depuydt, E., Broeckx, S. Y., Van Hecke, L., Chiers, K., Van Brantegem, L., van Schie, H., et al. (2021). The evaluation of equine allogeneic tenogenic primed mesenchymal stem cells in a surgically induced superficial digital flexor tendon lesion model. *Front. Vet. Sci.* 8, 641441. doi:10.3389/fvets.2021.641441

Derby, B. M., Reichensperger, J., Chambers, C., Bueno, R. A., Suchy, H., and Neumeister, M. W. (2012). Early growth response factor-1: expression in a rabbit

flexor tendon scar model. *Plast. Reconstr. Surg.* 129 (3), 435e–442e. doi:10.1097/PRS.0b013e3182402d81

Derwin, K. A., Baker, A. R., Codsi, M. J., and Iannotti, J. P. (2007). Assessment of the canine model of rotator cuff injury and repair. *J. Shoulder Elb. Surg.* 16, S140–S148. doi:10.1016/j.jse.2007.04.002

Derwin, K. A., Codsi, M. A., Baker, A. R., and McCarron, J. A. (2009). Rotator cuff repair augmentation in a canine model with use of a woven poly-L-lactide device. *J. Bone Joint Surg. Am.* 91 (5), 1159–1171. doi:10.2106/jbjs.H.00775

Doğramaci, Y., Kalaci, A., Sevinç, T. T., Süner, G., Emir, A., and Yanat, A. N. (2009). Single side locking on the opposite of the modified kessler tendon repair prevents gap formation and suture pull-out: a biomechanical evaluation in sheep tendons. *Eklem Hast. Cerrahisi* 20 (2), 102–106.

Doherty, G. P., Koike, Y., Uhthoff, H. K., Lecompte, M., and Trudel, G. (2006). Comparative anatomy of rabbit and human achilles tendons with magnetic resonance and ultrasound imaging. *Comp. Med.* 56 (1), 68–74.

Dündar, N., Güneri, B., Uzel, M., and Doğaner, A. (2020). Biomechanical comparison of Bunnell, modified Kessler, and Tsuge tendon repair techniques using two suture types. *Acta Orthop. Traumatol. Turc.* 54 (1), 104–113. doi:10.5152/j.aott.2020.01.411

Durgam, S. S., Stewart, A. A., Sivaguru, M., Wagoner Johnson, A. J., and Stewart, M. C. (2016). Tendon-derived progenitor cells improve healing of collagenase-induced flexor tendinitis. *J. Orthop. Res.* 34 (12), 2162–2171. doi:10.1002/jor.23251

Enea, D., Gwynne, J., Kew, S., Arumugam, M., Shepherd, J., Brooks, R., et al. (2013). Collagen fibre implant for tendon and ligament biological augmentation. in vivo study in an ovine model. *Knee Surg. Sports Traumatol. Arthrosc.* 21 (8), 1783–1793. doi:10.1007/s00167-012-2102-7

Facon-Poroszewska, M., Kiełbowicz, Z., and Prządka, P. (2019). Influence of radial pressure wave therapy (RPWT) on collagenase-induced achilles tendinopathy treated with platelet rich plasma and autologous adipose derived stem cells. *Pol. J. Vet. Sci.* 22 (4), 743–751. doi:10.24425/pjvs.2019.131405

Fernández-Sarmiento, J. A., Domínguez, J. M., Granados, M. M., Morgaz, J., Navarrete, R., Carrillo, J. M., et al. (2013). Histological study of the influence of plasma rich in growth factors (PRGF) on the healing of divided Achilles tendons in sheep. *J. Bone Jt. Surg. Am.* 95 (3), 246–255. doi:10.2106/jbjs.K.01659

Flanigan, D. C., Bloomfield, M., and Koh, J. (2011). A biomechanical comparison of patellar tendon repair materials in a bovine model. *Orthopedics* 34 (8), e344–e348. doi:10.3928/01477447-20110627-13

Fransson, B. A., Gavin, P. R., and Lahmers, K. K. (2005). Supraspinatus tendinosis associated with biceps brachii tendon displacement in a dog. *J. Am. Vet. Med. Assoc.* 227 (9), 1429–1433. doi:10.2460/javma.2005.227.1429

Gaut, L., and Duprez, D. (2016). Tendon development and diseases. *Wiley Interdiscip. Rev. Dev. Biol.* 5 (1), 5–23. doi:10.1002/wdev.201

Geng, Y., Zhao, X., Xu, J., Zhang, X., Hu, G., Fu, S. C., et al. (2020). Overexpression of mechanical sensitive miR-337-3p alleviates ectopic ossification in rat tendinopathy model via targeting IRS1 and Nox4 of tendon-derived stem cells. *J. Mol. Cell Biol.* 12 (4), 305–317. doi:10.1093/jmcb/mjz030

Gerber, C., Meyer, D. C., Schneeberger, A. G., Hoppeler, H., and von Rechenberg, B. (2004). Effect of tendon release and delayed repair on the structure of the muscles of the rotator cuff: an experimental study in sheep. *J. Bone Jt. Surg. Am.* 86 (9), 1973–1982. doi:10.2106/00004623-200409000-00016

Gerber, C., Meyer, D. C., Flück, M., Valdivieso, P., von Rechenberg, B., Benn, M. C., et al. (2017). Muscle degeneration associated with rotator cuff tendon release and/or denervation in sheep. *Am. J. Sports Med.* 45 (3), 651–658. doi:10.1177/0363546516677254

Gersoff, W. K., Bozynski, C. C., Cook, C. R., Pfeiffer, F. M., Kuroki, K., and Cook, J. L. (2019). Evaluation of a novel degradable synthetic biomaterial patch for augmentation of tendon healing in a large animal model. *J. Knee Surg.* 32 (5), 434–440. doi:10.1055/s-0038-1646930

Ghelfi, J., Bacle, M., Stephanov, O., de Forges, H., Soulairol, I., Roger, P., et al. (2021). Collagenase-induced patellar tendinopathy with neovascularization: First results towards a piglet model of musculoskeletal embolization. *Biomedicines* 10 (1), 2. doi:10.3390/biomedicines10010002

Goodman, H. J., and Choueka, J. (2005). Biomechanics of the flexor tendons. *Hand Clin.* 21 (2), 129–149. doi:10.1016/j.hcl.2004.11.002

Grumet, R. C., Hadley, S., Diltz, M. V., Lee, T. Q., and Gupta, R. (2009). Development of a new model for rotator cuff pathology: the rabbit subscapularis muscle. *Acta Orthop.* 80 (1), 97–103. doi:10.1080/17453670902807425

Guo, Q., Li, C., Qi, W., Li, H., Lu, X., Shen, X., et al. (2016). A novel suture anchor constructed of cortical bone for rotator cuff repair: a biomechanical study on sheep humerus specimens. *Int. Orthop.* 40 (9), 1913–1918. doi:10.1007/s00264-016-3185-4

Gurger, M., Once, G., Yilmaz, E., Demir, S., Calik, I., Say, Y., et al. (2021). The effect of the platelet-rich plasma and ozone therapy on tendon-to-bone healing in the rabbit rotator cuff repair model. *J. Orthop. Surg. Res.* 16 (1), 202. doi:10.1186/s13018-021-02320-w

Habets, B., van den Broek, A. G., Huisstede, B. M. A., Backx, F. J. G., and van Cingel, R. E. H. (2018). Return to sport in athletes with midportion achilles tendinopathy: A qualitative systematic review regarding definitions and criteria. *Sports Med.* 48 (3), 705–723. doi:10.1007/s40279-017-0833-9

Håkansson, J., Mahlapuu, M., Ekström, L., Olmarker, K., and Wiig, M. (2012). Effect of lactoferrin peptide (PXL01) on rabbit digit mobility after flexor tendon repair. *J. Hand Surg. Am.* 37 (12), 2519–2525. doi:10.1016/j.jhsa.2012.09.019

Han, F., Li, T., Li, M., Zhang, B., Wang, Y., Zhu, Y., et al. (2023). Nano-calcium silicate mineralized fish scale scaffolds for enhancing tendon-bone healing. *Bioact. Mater.* 20, 29–40. doi:10.1016/j.bioactmat.2022.04.030

Hast, M. W., Zuskov, A., and Soslowsky, L. J. (2014). The role of animal models in tendon research. *Bone Jt. Res.* 3 (6), 193–202. doi:10.1302/2046-3758.36.2000281

He, M., Gan, A. W., Lim, A. Y., Goh, J. C., Hui, J. H., Lee, E. H., et al. (2013). The effect of fibrin glue on tendon healing and adhesion formation in a rabbit model of flexor tendon injury and repair. *J. Plast. Surg. Hand Surg.* 47 (6), 509–512. doi:10.3109/2000656x.2013.789037

He, M., Gan, A. W., Lim, A. Y., Goh, J. C., Hui, J. H., and Chong, A. K. (2015). Bone marrow derived mesenchymal stem cell augmentation of rabbit flexor tendon healing. *Hand Surg.* 20 (3), 421–429. doi:10.1142/s0218810415500343

Henn, R. F., 3rd, Kuo, C. E., Kessler, M. W., Razzano, P., Grande, D. P., and Wolfe, S. W. (2010). Augmentation of zone II flexor tendon repair using growth differentiation factor 5 in a rabbit model. *J. Hand Surg. Am.* 35 (11), 1825–1832. doi:10.1016/j.jhsa.2010.08.031

Hyman, S. A., Wu, I. T., Vasquez-Bolanos, L. S., Norman, M. B., Esparza, M. C., Bremner, S. N., et al. (2021). Supraspinatus muscle architecture and physiology in a rabbit model of tenotomy and repair. *J. Appl. Physiol.* 131 (6), 1708–1717. doi:10.1152/japplphysiol.01119.2020

Iacopetti, I., Perazzi, A., Maniero, V., Martinello, T., Patruno, M., Glazar, M., et al. (2015). Effect of MLS(®) laser therapy with different dose regimes for the treatment of experimentally induced tendinopathy in sheep: pilot study. *Photomed. Laser Surg.* 33 (3), 154–163. doi:10.1089/pho.2014.3775

Jensen, A. R., Kelley, B. V., Mosich, G. M., Ariniello, A., Eliasberg, C. D., Vu, B., et al. (2018). Neer Award 2018: Platelet-derived growth factor receptor α co-expression typifies a subset of platelet-derived growth factor receptor β-positive progenitor cells that contribute to fatty degeneration and fibrosis of the murine rotator cuff. *J. Shoulder Elb. Surg.* 27 (7), 1149–1161. doi:10.1016/j.jse.2018.02.040

Ji, X., Bao, N., An, K. N., Amadio, P.C., Steinmann, S. P., and Zhao, C. (2015). A canine non-weight-bearing model with radial neurectomy for rotator cuff repair. *PLoS One* 10 (6), e0130576. doi:10.1371/journal.pone.0130576

Jielile, J., Asilehan, B., Wupuer, A., Qianman, B., Jialihasi, A., Tangkejie, W., et al. (2016). Early ankle mobilization promotes healing in a rabbit model of achilles tendon rupture. *Orthopedics* 39 (1), e117–e126. doi:10.3928/01477447-20160106-01

Johnson, S. A., Valdés-Martínez, A., Turk, P. J., Wayne McIlwraith, C., Barrett, M. F., McGilvray, K. C., et al. (2021). Longitudinal tendon healing assessed with multi-modality advanced imaging and tissue analysis. *Equine Vet. J.* 54, 766–781. doi:10.1111/evj.13478

Kayser, F., Hontoir, F., Clegg, P., Kirschvink, N., Dugdale, A., and Vandeweerd, J. M. (2019). Ultrasound anatomy of the normal stifle in the sheep. *Anat. Histol. Embryol.* 48 (1), 87–96. doi:10.1111/ahe.12414

Kayser, F., Bori, E., Fourny, S., Hontoir, F., Clegg, P., Dugdale, A., et al. (2022). *Ex vivo* study correlating the stiffness of the ovine patellar tendon to age and weight. *Int. Biomech.* 9 (1), 1–9. doi:10.1080/23335432.2022.2108899

Khan, M. R., Smith, R. K., David, F., Lam, R., Hughes, G., De Godoy, R., et al. (2020). Evaluation of the effects of synovial multipotent cells on deep digital flexor tendon repair in a large animal model of intra-synovial tendinopathy. *J. Orthop. Res.* 38 (1), 128–138. doi:10.1002/jor.24423

Kim, D. K., Ahn, J., Kim, S. A., Go, E. J., Lee, D. H., Park, S. C., et al. (2021). Improved healing of rabbit patellar tendon defects after an atelocollagen injection. *Am. J. Sports Med.* 49 (11), 2924–2932. doi:10.1177/03635465211030508

Komi, P. V. (1990). Relevance of in vivo force measurements to human biomechanics. *J. Biomech.* 23, 23–34. doi:10.1016/0021-9290(90)90038-5

Kuenzler, M. B., Nuss, K., Karol, A., Schär, M. O., Hottiger, M., Raniga, S., et al. (2017). Neer award 2016: reduced muscle degeneration and decreased fatty infiltration after rotator cuff tear in a poly(ADP-ribose) polymerase 1 (PARP-1) knock-out mouse model. *J. Shoulder Elb. Surg.* 26 (5), 733–744. doi:10.1016/j.jse.2016.11.009

Kwon, J., Kim, Y. H., Rhee, S. M., Kim, T. I., Lee, J., Jeon, S., et al. (2018). Effects of allogenic dermal fibroblasts on rotator cuff healing in a rabbit model of chronic tear. *Am. J. Sports Med.* 46 (8), 1901–1908. doi:10.1177/0363546518770428

Lebaschi, A., Deng, X. H., Zong, J., Cong, G. T., Carballo, C. B., Album, Z. M., et al. (2016). Animal models for rotator cuff repair. *Ann. N. Y. Acad. Sci.* 1383 (1), 43–57. doi:10.1111/nyas.13203

Lebaschi, A. H., Deng, X. H., Camp, C. L., Zong, J., Cong, G. T., Carballo, C. B., et al. (2018). Biomechanical, histologic, and molecular evaluation of tendon healing in a new murine model of rotator cuff repair. *Arthroscopy* 34 (4), 1173–1183. doi:10.1016/j.arthro.2017.10.045

Lee, J. H., Kim, Y. H., Rhee, S. M., Han, J., Jeong, H. J., Park, J. H., et al. (2021). Rotator cuff tendon healing using human dermal fibroblasts: Histological and biomechanical analyses in a rabbit model of chronic rotator cuff tears. *Am. J. Sports Med.* 49 (13), 3669–3679. doi:10.1177/03635465211041102

Leung, K. S., Chong, W. S., Chow, D. H., Zhang, P., Cheung, W. H., Wong, M. W., et al. (2015). A comparative study on the biomechanical and histological properties of bone-to-bone, bone-to-tendon, and tendon-to-tendon healing: An achilles tendon-calcaneus model in goats. *Am. J. Sports Med.* 43 (6), 1413–1421. doi:10.1177/0363546515576904

Li, S., Ma, K., Li, H., Jiang, J., and Chen, S. (2016). The effect of sodium hyaluronate on ligamentation and biomechanical property of tendon in repair of achilles tendon defect with polyethylene terephthalate artificial ligament: A rabbit tendon repair model. *Biomed. Res. Int.* 2016, 8684231. doi:10.1155/2016/8684231

Liao, J. C. Y., He, M., Gan, A. W. T., and Chong, A. K. S. (2017). The effects of autologous platelet-rich fibrin on flexor tendon healing in a rabbit model. *J. Hand Surg. Am.* 42 (11), 928.e921–928. doi:10.1016/j.jhsa.2017.06.098

Liao, J. C. Y., He, M., Gan, A. W. T., Wen, F., Tan, L. P., and Chong, A. K. S. (2018). The effects of bi-functional anti-adhesion scaffolds on flexor tendon healing in a rabbit model. *J. Biomed. Mater. Res. B Appl. Biomater.* 106 (7), 2605–2614. doi:10.1002/jbm.b.34077

Linder, L. H., Sukin, D. L., Burks, R. T., and Haut, R. C. (1994). Biomechanical and histological properties of the canine patellar tendon after removal of its medial third. *Am. J. Sports Med.* 22 (1), 136–142. doi:10.1177/036354659402200121

Liu, G. M., Pan, J., Zhang, Y., Ning, L. J., Luo, J. C., Huang, F. G., et al. (2018). Bridging repair of large rotator cuff tears using a multilayer decellularized tendon slices graft in a rabbit model. *Arthroscopy* 34 (9), 2569–2578. doi:10.1016/j.arthro.2018.04.019

Liu, P., Zhu, W., and Liu, Q. (2021). Animal models for study on rotator cuff injury. *Zhong Nan Da Xue Xue Bao Yi Xue Ban* 46 (4), 426–431. doi:10.11817/j.issn.1672-7347.2021.200064

Liu, Q., Yu, Y., Reisdorf, R. L., Qi, J., Lu, C. K., Berglund, L. J., et al. (2019). Engineered tendon-fibrocartilage-bone composite and bone marrow-derived mesenchymal stem cell sheet augmentation promotes rotator cuff healing in a non-weight-bearing canine model. *Biomaterials* 192, 189–198. doi:10.1016/j.biomaterials.2018.10.037

Liu, H., Gao, F., Liang, X., Chen, X., Qu, Y., and Wang, L. (2020). Pathogenesis and development of patellar tendon fibrosis in a rabbit overuse model. *Am. J. Sports Med.* 48 (5), 1141–1150. doi:10.1177/0363546520902447

Lohan, A., Kohl, B., Meier, C., and Schulze-Tanzil, G. (2018). Tenogenesis of decellularized porcine achilles tendon matrix reseeded with human tenocytes in the nude mice xenograft model. *Int. J. Mol. Sci.* 19 (7), E2059. doi:10.3390/ijms19072059

Loiselle, A. E., Kelly, M., and Hammert, W. C. (2016). Biological augmentation of flexor tendon repair: A challenging cellular landscape. *J. Hand Surg. Am.* 41 (1), 144–149. quiz 149. doi:10.1016/j.jhsa.2015.07.002

Longo, U. G., Forriol, F., Campi, S., Maffulli, N., and Denaro, V. (2011). Animal models for translational research on shoulder pathologies: from bench to bedside. *Sports Med. Arthrosc. Rev.* 19 (3), 184–193. doi:10.1097/JSA.0b013e318205470e

Longo, U. G., Ronga, M., and Maffulli, N. (2018). Achilles tendinopathy. *Sports Med. Arthrosc. Rev.* 26 (1), 16–30. doi:10.1097/jsa.0000000000000185

Luan, T., Liu, X., Easley, J. T., Ravishankar, B., Puttlitz, C., and Feeley, B. T. (2015). Muscle atrophy and fatty infiltration after an acute rotator cuff repair in a sheep model. *Muscle Ligaments Tendons J.* 5 (2), 106–112. doi:10.32098/mltj.02.2015.09

Lui, P. P., Maffulli, N., Rolf, C., and Smith, R. K. (2011). What are the validated animal models for tendinopathy? *Scand. J. Med. Sci. Sports* 21 (1), 3–17. doi:10.1111/j.1600-0838.2010.01164.x

Lyras, D. N., Kazakos, K., Tilkeridis, K., Kokka, A., Ververidis, A., Botaitis, S., et al. (2016). Temporal and spatial expression of TGF-b1 in the early phase of patellar tendon healing after application of platelet rich plasma. *Arch. Bone Jt. Surg.* 4 (2), 156–160.

Mahar, A., Tamborlane, J., Oka, R., Esch, J., and Pedowitz, R. A. (2007). Single-row suture anchor repair of the rotator cuff is biomechanically equivalent to double-row repair in a bovine model. *Arthroscopy* 23 (12), 1265–1270. doi:10.1016/j.arthro.2007.07.010

Martinello, T., Bronzini, I., Perazzi, A., Testoni, S., De Benedictis, G. M., Negro, A., et al. (2013). Effects of in vivo applications of peripheral blood-derived mesenchymal stromal cells (PB-MSCs) and platlet-rich plasma (PRP) on experimentally injured deep digital flexor tendons of sheep. *J. Orthop. Res.* 31 (2), 306–314. doi:10.1002/jor.22205

Meier Bürgisser, G., Calcagni, M., Bachmann, E., Fessel, G., Snedeker, J. G., Giovanoli, P., et al. (2016). Rabbit Achilles tendon full transection model - wound healing, adhesion formation and biomechanics at 3, 6 and 12 weeks post-surgery. *Biol. Open* 5 (9), 1324–1333. doi:10.1242/bio.020644

Meimandi-Parizi, A., Oryan, A., and Moshiri, A. (2013). Tendon tissue engineering and its role on healing of the experimentally induced large tendon defect model in rabbits: a comprehensive in vivo study. *PLoS One* 8 (9), e73016. doi:10.1371/journal.pone.0073016

Millar, N. L., Silbernagel, K. G., Thorborg, K., Kirwan, P. D., Galatz, L. M., Abrams, G. D., et al. (2021). Tendinopathy. *Nat. Rev. Dis. Prim.* 7 (1), 1. doi:10.1038/s41572-020-00234-1

Nagasawa, K., Noguchi, M., Ikoma, K., and Kubo, T. (2008). Static and dynamic biomechanical properties of the regenerating rabbit Achilles tendon. *Clin. Biomech.* 23 (6), 832–838. doi:10.1016/j.clinbiomech.2008.02.002

Nakagawa, H., Morihara, T., Fujiwara, H., Kabuto, Y., Sukenari, T., Kida, Y., et al. (2017). Effect of footprint preparation on tendon-to-bone healing: A histologic and biomechanical study in a rat rotator cuff repair model. *Arthroscopy* 33 (8), 1482–1492. doi:10.1016/j.arthro.2017.03.031

Nelson, B. B., Kawcak, C. E., Ehrhart, E. J., and Goodrich, L. R. (2015). Radiofrequency probe and sharp transection for tenoscopic-guided desmotomy of the accessory ligament of the superficial digital flexor tendon. *Vet. Surg.* 44 (6), 713–722. doi:10.1111/vsu.12328

Novakova, S. S., Mahalingam, V. D., Florida, S. E., Mendias, C. L., Allen, A., Arruda, E. M., et al. (2018). Tissue-engineered tendon constructs for rotator cuff repair in sheep. *J. Orthop. Res.* 36 (1), 289–299. doi:10.1002/jor.23642

Park, M. C., Cadet, E. R., Levine, W. N., Bigliani, L. U., and Ahmad, C.S. (2005). Tendon-to-bone pressure distributions at a repaired rotator cuff footprint using transosseous suture and suture anchor fixation techniques. *Am. J. Sports Med.* 33 (8), 1154–1159. doi:10.1177/0363546504273053

Patterson-Kane, J. C., Becker, D. L., and Rich, T. (2012). The pathogenesis of tendon microdamage in athletes: the horse as a natural model for basic cellular research. *J. Comp. Pathol.* 147 (2-3), 227–247. doi:10.1016/j.jcpa.2012.05.010

Peeters, I., Pien, N., Mignon, A., Van Damme, L., Dubruel, P., Van Vlierberghe, S., et al. (2022). Flexor tendon repair using a reinforced tubular, medicated electrospun construct. *J. Orthop. Res.* 40 (3), 750–760. doi:10.1002/jor.25103

Plate, J. F, Bates, C. M., Mannava, S., Smith, T. L., Jorgensen, M. J., Register, T. C., et al. (2013). Age-related degenerative functional, radiographic, and histological changes of the shoulder in nonhuman primates. *J. Shoulder Elbow Surg.* 22 (8), 1019–1029. doi:10.1016/j.jse.2012.11.004

Pownder, S. L., Hayashi, K., Lin, B. Q., Meyers, K. N., Caserto, B. G., Breighner, R. E., et al. (2021). Differences in the magnetic resonance imaging parameter T2* may be identified during the course of canine patellar tendon healing: a pilot study. *Quant. Imaging Med. Surg.* 11 (4), 1234–1246. doi:10.21037/qims-20-684

Ribitsch, I., Gueltekin, S., Keith, M. F., Minichmair, K., Peham, C., Jenner, F., et al. (2020). Age-related changes of tendon fibril micro-morphology and gene expression. *J. Anat.* 236 (4), 688–700. doi:10.1111/joa.13125

Ristaniemi, A., Stenroth, L., Mikkonen, S., and Korhonen, R. K. (2018). Comparison of elastic, viscoelastic and failure tensile material properties of knee ligaments and patellar tendon. *J. Biomech.* 79, 31–38. doi:10.1016/j.jbiomech.2018.07.031

Ristaniemi, A., Regmi, D., Mondal, D., Torniainen, J., Tanska, P., Stenroth, L., et al. (2021). Structure, composition and fibril-reinforced poroviscoelastic properties of bovine knee ligaments and patellar tendon. *J. R. Soc. Interface* 18 (174), 20200737. doi:10.1098/rsif.2020.0737

Roller, B. L., Kuroki, K., Bozynski, C. C., Pfeiffer, F. M., and Cook, J. L. (2018). Use of a novel magnesium-based resorbable bone cement for augmenting anchor and tendon fixation. *Am. J. Orthop.* 47 (2). doi:10.12788/ajo.2018.0010

Romeo, A., Easley, J., Regan, D., Hackett, E., Johnson, J., Johnson, J., et al. (2022). Rotator cuff repair using a bioresorbable nanofiber interposition scaffold: a biomechanical and histologic analysis in sheep. *J. Shoulder Elbow Surg.* 31 (2), 402–412. doi:10.1016/j.jse.2021.07.018

Roßbach, B. P., Gülecyüz, M. F., Kempfert, L., Pietschmann, M. F., Ullamann, T., Ficklscherer, A., et al. (2020). Rotator cuff repair with autologous tenocytes and

biodegradable collagen scaffold: A histological and biomechanical study in sheep. *Am. J. Sports Med.* 48 (2), 450–459. doi:10.1177/0363546519892580

Ruoss, S., Kindt, P., Oberholzer, L., Rohner, M., Jungck, L., Abdel-Aziz, S., et al. (2018a). Inhibition of calpain delays early muscle atrophy after rotator cuff tendon release in sheep. *Physiol. Rep.* 6 (21), e13833. doi:10.14814/phy2.13833

Ruoss, S., Möhl, C. B., Benn, M. C., von Rechenberg, B., Wieser, K., Meyer, D. C., et al. (2018b). Costamere protein expression and tissue composition of rotator cuff muscle after tendon release in sheep. *J. Orthop. Res.* 36 (1), 272–281. doi:10.1002/jor.23624

Safran, O., Derwin, K. A., Powell, K., and Iannotti, J. P. (2005). Changes in rotator cuff muscle volume, fat content, and passive mechanics after chronic detachment in a canine model. *J. Bone Jt. Surg. Am.* 87 (12), 2662–2670. doi:10.2106/jbjs.D.02421

Sarıkaya, B., Yumuşak, N., Yigin, A., Sipahioğlu, S., Yavuz, Ü., and Altay, M. A. (2017). Comparison of the effects of human recombinant epidermal growth factor and platelet-rich plasma on healing of rabbit patellar tendon. *Eklem Hast. Cerrahisi* 28 (2), 92–99. doi:10.5606/ehc.2017.55396

Sarrafian, T. L., Wang, H., Hackett, E. S., Yao, J. Q., Shih, M. S., Ramsay, H. L., et al. (2010). Comparison of Achilles tendon repair techniques in a sheep model using a cross-linked acellular porcine dermal patch and platelet-rich plasma fibrin matrix for augmentation. *J. Foot Ankle Surg.* 49 (2), 128–134. doi:10.1053/j.jfas.2009.12.005

Sener, M., Altay, M. A., Baki, C., Turhan, A. U., and Cobanoglu, U. (2004). The comparison of patellar tendon-bone autografting and free flexor-tendon autografting in infraspinatus defect of the shoulder: biomechanical and histological evaluation in a sheep model. *Knee Surg. Sports Traumatol. Arthrosc.* 12 (3), 235–240. doi:10.1007/s00167-003-0473-5

Serrani, D., Volta, A., Cingolani, F., Pennasilico, L., Di Bella, C., Bonazzi, M., et al. (2021). Serial ultrasonographic and real-time elastosonographic assessment of the ovine common calcaneal tendon, after an experimentally induced tendinopathy. *Vet. Sci.* 8 (4), 54. doi:10.3390/vetsci8040054

Skalec, A., Janeczek, M., and Czerski, A. (2019). Anatomy and histology of the rabbit common calcanean tendon. *Anat. Histol. Embryol.* 48 (5), 466–475. doi:10.1111/ahe.12468

Smith, M. J., Pfeiffer, F. M., Cook, C. R., Kuroki, K., and Cook, J. L. (2018). Rotator cuff healing using demineralized cancellous bone matrix sponge interposition compared to standard repair in a preclinical canine model. *J. Orthop. Res.* 36 (3), 906–912. doi:10.1002/jor.23680

Smith, M. J., Bozynski, C. C., Kuroki, K., Cook, C. R., Stoker, A. M., and Cook, J. L. (2020). Comparison of biologic scaffolds for augmentation of partial rotator cuff tears in a canine model. *J. Shoulder Elb. Surg.* 29 (8), 1573–1583. doi:10.1016/j.jse.2019.11.028

Sonnabend, D. H., Howlett, C. R., and Young, A. A. (2010). Histological evaluation of repair of the rotator cuff in a primate model. *J. Bone Jt. Surg. Br.* 92 (4), 586–594. doi:10.1302/0301-620x.92b4.22371

Su, W., Li, X., Zhao, S., Shen, P., Dong, S., Jiang, J., et al. (2018). Native enthesis preservation versus removal in rotator cuff repair in a rabbit model. *Arthroscopy* 34 (7), 2054–2062. doi:10.1016/j.arthro.2018.03.005

Suh, D. S., Lee, J. K., Yoo, J. C., Woo, S. H., Kim, G. R., Kim, J. W., et al. (2017). Atelocollagen enhances the healing of rotator cuff tendon in rabbit model. *Am. J. Sports Med.* 45 (9), 2019–2027. doi:10.1177/0363546517703336

Sun, Y., Kwak, J. M., Kholinne, E., Zhou, Y., Tan, J., Koh, K. H., et al. (2020). Small subchondral drill holes improve marrow stimulation of rotator cuff repair in a rabbit model of chronic rotator cuff tear. *Am. J. Sports Med.* 48 (3), 706–714. doi:10.1177/0363546519896350

Takase, F., Inui, A., Mifune, Y., Sakata, R., Muto, T., Harada, Y., et al. (2017). Effect of platelet-rich plasma on degeneration change of rotator cuff muscles: In vitro and in vivo evaluations. *J. Orthop. Res.* 35 (8), 1806–1815. doi:10.1002/jor.23451

Thangarajah, T., Shahbazi, S., Pendegrass, C. J., Lambert, S., Alexander, S., and Blunn, G. W. (2016). Tendon reattachment to bone in an ovine tendon defect model of retraction using allogenic and xenogenic demineralised bone matrix incorporated with mesenchymal stem cells. *PLoS One* 11 (9), e0161473. doi:10.1371/journal.pone.0161473

Tian, J., Rui, R., Xu, Y., Yang, W., Chen, X., Zhang, X., et al. (2020a). Achilles tendon rupture repair: Biomechanical comparison of the locking block modified Krackow technique and the Giftbox technique. *Injury* 51 (2), 559–564. doi:10.1016/j.injury.2019.10.019

Tian, J., Rui, Y., Xu, Y., Yang, W., Xu, T., Chen, X., et al. (2020b). A biomechanical comparison of Achilles tendon suture repair techniques: Locking Block Modified Krackow, Kessler, and Percutaneous Achilles Repair System with the early rehabilitation program in vitro bovine model. *Arch. Orthop. Trauma Surg.* 140 (11), 1775–1782. doi:10.1007/s00402-020-03535-y

Uslu, M., Isik, C., Ozsahin, M., Ozkan, A., Yasar, M., Orhan, Z., et al. (2014). Flexor tendons repair: effect of core sutures caliber with increased number of suture strands and peripheral sutures. A sheep model. *Orthop. Traumatol. Surg. Res.* 100 (6), 611–616. doi:10.1016/j.otsr.2014.05.009

Vargas-Vila, M. A., Gibbons, M. C., Wu, I. T., Esparza, M. C., Kato, K., Johnson, S. D., et al. (2022). Progression of muscle loss and fat accumulation in a rabbit model of rotator cuff tear. *J. Orthop. Res.* 40 (5), 1016–1025. doi:10.1002/jor.25160

Virchenko, O., Fahlgren, A., Rundgren, M., and Aspenberg, P. (2008). Early Achilles tendon healing in sheep. *Arch. Orthop. Trauma Surg.* 128 (9), 1001–1006. doi:10.1007/s00402-008-0691-x

Wang, C., Hu, Q., Song, W., Yu, W., and He, Y. (2020). Adipose stem cell-derived exosomes decrease fatty infiltration and enhance rotator cuff healing in a rabbit model of chronic tears. *Am. J. Sports Med.* 48 (6), 1456–1464. doi:10.1177/0363546520908847

Wang, L., Xiong, K., Wang, B., Liang, X., Li, H., Liu, H., et al. (2017). Effects of time to start training after acute patellar tendon enthesis injuries on healing of the injury in a rabbit model. *Am. J. Sports Med.* 45 (10), 2405–2410. doi:10.1177/0363546517712223

Wang, Y., He, G., Tang, H., Shi, Y., Kang, X., Lyu, J., et al. (2019). Aspirin inhibits inflammation and scar formation in the injury tendon healing through regulating JNK/STAT-3 signalling pathway. *Cell Prolif.* 52 (4), e12650. doi:10.1111/cpr.12650

Warden, S. J. (2007). Animal models for the study of tendinopathy. *Br. J. Sports Med.* 41 (4), 232–240. doi:10.1136/bjsm.2006.032342

Watts, A. E., Yeager, A. E., Kopyov, O. V., and Nixon, A. J. (2011). Fetal derived embryonic-like stem cells improve healing in a large animal flexor tendonitis model. *Stem Cell Res. Ther.* 2 (1), 4. doi:10.1186/scrt45

Wieser, K., Grubhofer, F., Hasler, A., Götschi, T., Beeler, S., Meyer, D., et al. (2021). Muscle Degeneration Induced by Sequential Release and Denervation of the Rotator Cuff Tendon in Sheep. *J. Sports Med.* 9 (8), 23259671211025302. doi:10.1177/23259671211025302

Xu, H., Sandor, M., Qi, S., Lombardi, J., Connor, J., McQuillan, D. J., et al. (2012). Implantation of a porcine acellular dermal graft in a primate model of rotator cuff repair. *J. Shoulder Elb. Surg.* 21 (5), 580–588. doi:10.1016/j.jse.2011.03.014

Xu, J., Li, Y., Zhang, X., Han, K., Ye, Z., Wu, C., et al. (2022). The Biomechanical and Histological Processes of Rerouting Biceps to Treat Chronic Irreparable Rotator Cuff Tears in a Rabbit Model. *Am. J. Sports Med* . 50 (2), 347–361. doi:10.1177/03635465211062914

Xu, D., Zhang, T., Qu, J., Hu, J., and Lu, H. (2014). Enhanced patella-patellar tendon healing using combined magnetic fields in a rabbit model. *Am. J. Sports Med.* 42 (10), 2495–2501. doi:10.1177/0363546514541539

Yamamoto, Y., Yamaguchi, S., Sasho, T., Fukawa, T., Akatsu, Y., Akagi, R., et al. (2017). Quantitative US elastography can Be used to quantify mechanical and histologic tendon healing in a rabbit model of achilles tendon transection. *Radiology* 283 (2), 408–417. doi:10.1148/radiol.2016160695

Yildiz, F., Bilsel, K., Pulatkan, A., Kapicioglu, M., Uzer, G., Çetindamar, T., et al. (2019). Comparison of two different superior capsule reconstruction methods in the treatment of chronic irreparable rotator cuff tears: a biomechanical and histologic study in rabbit models. *J. Shoulder Elb. Surg.* 28 (3), 530–538. doi:10.1016/j.jse.2018.08.022

Yılmaz, G., Doral, M. N., Turhan, E., Dönmez, G., Atay, A., and Kaya, D. (2014). Surgical treatment of achilles tendon ruptures: the comparison of open and percutaneous methods in a rabbit model. *Ulus. Travma Acil Cerrahi Derg.* 20 (5), 311–318. doi:10.5505/tjtes.2014.42716

Yonemitsu, R., Tokunaga, T., Shukunami, C., Ideo, K., Arimura, H., Karasugi, T., et al. (2019). Fibroblast growth factor 2 enhances tendon-to-bone healing in a rat rotator cuff repair of chronic tears. *Am. J. Sports Med.* 47 (7), 1701–1712. doi:10.1177/0363546519836959

Yoon, J. P., Lee, C. H., Jung, J. W., Lee, H. J., Lee, Y. S., Kim, J. Y., et al. (2018). Sustained delivery of transforming growth factor β1 by use of absorbable alginate scaffold enhances rotator cuff healing in a rabbit model. *Am. J. Sports Med.* 46 (6), 1441–1450. doi:10.1177/0363546518757759

Zhang, C. H., Jiang, Y. L., Ning, L. J., Li, Q., Fu, W. L., Zhang, Y. J., et al. (2018). Evaluation of decellularized bovine tendon sheets for achilles tendon defect reconstruction in a rabbit model. *Am. J. Sports Med.* 46 (11), 2687–2699. doi:10.1177/0363546518787515

Zhang, J., Li, F., Williamson, K. M., Tan, S., Scott, D., Onishi, K., et al. (2021). Characterization of the structure, vascularity, and stem/progenitor cell populations in porcine Achilles tendon (PAT). *Cell Tissue Res.* 384 (2), 367–387. doi:10.1007/s00441-020-03379-3

frontiers | Frontiers in Cell and Developmental Biology

TYPE Original Research
PUBLISHED 09 January 2023
DOI 10.3389/fcell.2022.1094124

OPEN ACCESS

EDITED BY
Yongye Huang,
Northeastern University, China

REVIEWED BY
Jaroslava Halper,
University of Georgia, United States
Julia Etich,
University Hospital of Cologne, Germany

*CORRESPONDENCE
Neil Marr,
nmarr@rvc.ac.uk

SPECIALTY SECTION
This article was submitted to Stem Cell Research,
a section of the journal
Frontiers in Cell and Developmental Biology

RECEIVED 09 November 2022
ACCEPTED 23 December 2022
PUBLISHED 09 January 2023

CITATION
Marr N, Zamboulis DE, Werling D, Felder AA, Dudhia J, Pitsillides AA and Thorpe CT (2023), The tendon interfascicular basement membrane provides a vascular niche for CD146+ cell subpopulations.
Front. Cell Dev. Biol. 10:1094124.
doi: 10.3389/fcell.2022.1094124

The tendon interfascicular basement membrane provides a vascular niche for CD146+ cell subpopulations

Neil Marr[1]*, Danae E. Zamboulis[1], Dirk Werling[2], Alessandro A. Felder[3], Jayesh Dudhia[4], Andrew A. Pitsillides[1] and Chavaunne T. Thorpe[1]

[1]Comparative Biomedical Sciences, Royal Veterinary College, London, United Kingdom, [2]Pathobiology and Population Sciences, Centre for Vaccinology and Regenerative Medicine, Royal Veterinary College, Hatfield, United Kingdom, [3]Research Software Development Group, Advanced Research Computing, University College London, London, United Kingdom, [4]Clinical Sciences and Services, Royal Veterinary College, Hatfield, United Kingdom

Introduction: The interfascicular matrix (IFM; also known as the endotenon) is critical to the mechanical adaptations and response to load in energy-storing tendons, such as the human Achilles and equine superficial digital flexor tendon (SDFT). We hypothesized that the IFM is a tendon progenitor cell niche housing an exclusive cell subpopulation.

Methods: Immunolabelling of equine superficial digital flexor tendon was used to identify the interfascicular matrix niche, localising expression patterns of CD31 (endothelial cells), Desmin (smooth muscle cells and pericytes), CD146 (interfascicular matrix cells) and LAMA4 (interfascicular matrix basement membrane marker). Magnetic-activated cell sorting was employed to isolate and compare in vitro properties of CD146+ and CD146– subpopulations.

Results: Labelling for CD146 using standard histological and 3D imaging of large intact 3D segments revealed an exclusive interfascicular cell subpopulation that resides in proximity to a basal lamina which forms extensive, interconnected vascular networks. Isolated CD146+ cells exhibited limited mineralisation (osteogenesis) and lipid production (adipogenesis).

Discussion: This study demonstrates that the interfascicular matrix is a unique tendon cell niche, containing a vascular-rich network of basement membrane, CD31+ endothelial cells, Desmin+ mural cells, and CD146+ cell populations that are likely essential to tendon structure and/or function. Contrary to our hypothesis, interfascicular CD146+ subpopulations did not exhibit stem cell-like phenotypes. Instead, our results indicate CD146 as a pan-vascular marker within the tendon interfascicular matrix. Together with previous work demonstrating that endogenous tendon CD146+ cells migrate to sites of injury, our data suggest that their mobilisation to promote intrinsic repair involves changes in their relationships with local interfascicular matrix vascular and basement membrane constituents.

KEYWORDS

tendon, interfascicular matrix, tendon progenitors, CD146, basement membrane

1 Introduction

Tendons are fundamental components of the musculoskeletal system, acting as connections between muscle and bone. The predominant function of tendon is to transfer the forces exerted by skeletal muscle contractions to bone, positioning the limb for locomotion (Alexander, 1991; Benjamin et al., 2008). However, specialised energy-storing tendons, such as the equine superficial digital flexor tendon (SDFT) and human Achilles tendon, enhance the functional adaptation of tendon by lowering the energetic cost of locomotion through their mechanical properties, such as greater extensibility, elasticity and fatigue resistance (Biewener, 1998; Alexander, 2002; Thorpe et al., 2015). Much like skeletal muscle, these specialised mechanical properties of energy-storing tendons are provided by their hierarchical structure of subunits predominantly composed of type I collagen, forming fascicles and fascicle bundles. Both fascicles and fascicle bundles are surrounded and bound by a non-collagenous interfascicular matrix (IFM, also known as the endotenon) which governs the high-strain behaviour of energy-storing SDFT by facilitating sliding between fascicles (Kannus, 2000; Thorpe and Screen, 2016; Handsfield et al., 2016). While the mechanical role of IFM in the function of energy storing tendons is well defined, less is known regarding its biological role in developing, adult and ageing tendon, particularly regarding the identity and function of IFM localised cell populations and their niche, defined as the anatomical microenvironment in which specific cell populations reside.

Histological analyses of tendon have revealed regional morphological differences in cell populations, with rounder cells within the IFM, present in greater number compared to those within the fascicles which are highly aligned with the long axis of the tendon (Thorpe and Screen, 2016; Thorpe et al., 2016). In addition, seminal studies have alluded to an endogenous tendon stem/progenitor cell (TSPC) population and niche, both of which remain largely undefined but have been speculated to reside within the IFM (Bi et al., 2007; Richardson et al., 2007; Godwin et al., 2012). In other tissues, the stem cell niche is maintained by mechanically unique microenvironments, similar to the high shear environment within the IFM, which may therefore be the location of the tendon stem/progenitor cell niche (Evans et al., 2013; Ivanovska et al., 2015; Smith et al., 2018).

Tendon development is driven by stem/progenitor cell populations which express Mohawk homeobox (MKX) and Scleraxis (SCX) transcription factors (Schweitzer et al., 2001; Anderson et al., 2006; Kimura et al., 2011); unfortunately, their intracellular localisation impedes cell sorting techniques required for *in vitro* study of stem/progenitor cell populations. In adult tissues, cell surface markers, such as CD44 and CD90 (THY1), are members of a number of canonical marker panels routinely used in the characterisation and isolation of specific stromal/stem cell populations (Horwitz et al., 2005; Morath et al., 2016). Recent studies have also reported resident CD146 populations in tendon (Yin et al., 2016; Gumucio et al., 2020). CD146 or melanoma adhesion molecule (MCAM; MUC18; Gicerin; OMIM:155735) is a transmembrane glycoprotein belonging to the IgG superfamily of cell adhesion molecules (Shih, 1999). Originally characterised as a marker of tumour progression and metastasis, CD146 has since been reported as a marker of endothelial cell lineages, both haematopoietic and mesenchymal stem cell lineages, as well as synovial fibroblasts and periosteal cells (Johnson et al., 1993; Sers et al., 1993; Schlagbauer-Wadl et al., 1999; Schrage et al., 2008; Kaltz et al., 2010; Russell et al., 2010; Tormin et al., 2011). Our laboratory has recently reported that these CD146 subpopulations are present within the IFM of the rat Achilles and recruited to injury sites from their IFM niche *via* the CD146 ligand Laminin α4 (LAMA4) (Marr et al., 2021). However, to the authors' knowledge, no studies have attempted to comprehensively characterise CD146 tendon cells and their *in vivo* cell niche composition.

In this study, we tested the hypothesis that the IFM is a tendon progenitor cell niche housing an exclusive cell subpopulation. We report novel markers of interfascicular cells and basement membrane, and identify CD146 as an optimal marker for use in IFM cell sorting procedures. We also demonstrate that the lineage potential and clonogenicity of interfascicular CD146 cells is limited, which may be indicative of a differentiated vascular population rather than resident tendon stem/progenitor cells.

2 Materials and methods

2.1 Ethical statement

The collection of animal tissues was approved by the Royal Veterinary College Ethics and Welfare Committee (URN-2016-1627b). All tissues were sourced from horses euthanised for reasons unrelated to this study, and other than tendon injury at a commercial equine abattoir.

2.2 Tissue acquisition

Superficial digital flexor tendons (SDFT) were harvested from forelimbs taken from young, skeletally mature horses (age = 3–8 years, $n = 5$, exercise history unknown). Prior to isolation, the forelimbs were clipped to remove hair and the skin sterilised by several applications of 4% chlorhexidine (HiBiScrub®; Mölnlycke Health Care). Portions of mid-metacarpal SDFT (6–10 cm) were dissected free of the limb and stored immediately in standard growth medium consisting of pyruvate and low glucose Dulbecco's modified eagle medium (DMEM) supplemented with 1% (v/v) penicillin/streptomycin and 10% (v/v) qualified, heat-inactivated foetal bovine serum (FBS) until tissue processing (all from Gibco™). Excised tendons presenting with previously reported definitions of macroscopic evidence of injury were excluded from all experiments (Webbon, 1977; Dakin et al., 2012), and all tendons had a normal histological appearance. Dissections and subsequent cell processing were completed within 24 h of euthanasia.

2.3 Cryosectioning

SDFT frozen sections were prepared as previously described (Godinho et al., 2017). Tissues were briefly washed in Dulbecco's phosphate-buffered saline (calcium and magnesium free, embedded with optimal cutting temperature compound (OCT; Cell Path, Newtown, United Kingdom) embedding matrix and snap-frozen in pre-cooled hexane on dry ice. Serial longitudinal (6–20 μm thickness) and transverse (30 μm thickness) sections

were prepared using a cryostat microtome (OTF5000, Bright Instruments) equipped with MX35 Premier Disposable Low-Profile Microtome Blades (3052835, Fisher Scientific). Tissue sections were mounted on SuperFrost™ Plus Slides (10149870, Fisher Scientific), air-dried at room temperature (RT) for a maximum of 2 h and stored at −80 °C.

2.4 Periodic acid-Schiff staining

Periodic acid-Schiff (PAS) staining was used to detect mucins and basement membrane proteins. Staining was performed using an Alcian Blue (pH 2.5)/PAS staining kit according to manufacturer guidelines (Atomic Scientific). SDFT cryosections (20 µm) were thawed and fixed with 4% PFA/10% NBF for 10 min at RT. Slides were rinsed thoroughly with distilled water, stained with 1% Alcian blue in 3% acetic acid (pH 2.5) for 10 min, and washed thoroughly in distilled water. Slides were treated with 1% periodic acid solution for 10 min at RT, washed with distilled water, then treated with Schiff reagent (Feulgen) for 10 min at RT. Sections were then washed under running tap water until sections presented a magenta colour macroscopically. Sections were then counter-stained with haematoxylin, dehydrated and cleared using an automated slide stainer (Varistain™ Gemini ES), and mounted with glass coverslips using DPX mountant. Slides were cured at RT overnight and imaged using brightfield microscopy (DM4000B upright microscope) in Leica Application Suite software version 2.6 (Leica Microsystems).

2.5 Network-based predictions of CD146 interactions

Proteins of interest for immunolabelling were selected based on their expression by tendon progenitor cell subpopulations in previous reports (Yin et al., 2016) and their predicted interactions in *Equus caballus* (NCBI taxid: 9796) using STRING (version 10.5) network-based predictions for CD146 and LAMA4 (Szklarczyk et al., 2017; Gumucio et al., 2020).

2.6 Immunolabelling

SDFT cryosections were thawed and fixed with acetone (pre-cooled at −20°C) for 10 min, washed three times for 5 min at RT with tris-buffered saline (TBS), incubated in "blocking" buffer (TBS supplemented with 1% (w/v) bovine serum albumin (Scientific Laboratory Supplies), 5% (v/v) goat serum (Sigma), and 5% (v/v) horse serum (Sigma) for 2 h. Horse serum was used to saturate Fc receptors on the surface of cells within the tissue. Sections were incubated with primary antibodies overnight at 4°C (details regarding primary and secondary antibodies are provided in Supplementary Table S1). For negative controls, sections were treated with blocking buffer only. For isotype controls, sections were treated with mouse and rabbit IgG isotype-matched controls diluted in blocking buffer at identical concentration to primary antibodies used. For fluorescent detection (10 µm sections), secondary antibodies diluted in blocking buffer were applied to sections and incubated for 1 h at RT under dark conditions. Sections were washed three times with TBS for 5 min, and mounted with glass coverslips using ProLong™ Diamond antifade mountant with 4′,6-diamidino-2-phenylindole (DAPI) as a nuclei counterstain. Slides were cured for 24 h at RT under dark conditions, prior to imaging. Negative and isotype matched control images for fluorescent labelling are provided in Supplementary Figure S1. Immunohistochemical labelling (6 µm sections) was performed in a similar manner to fluorescent detection, using an EnVision®+ Dual Link System-HRP DAB+ system (Dako), with the inclusion of an of EnVision dual endogenous enzyme block for 15 min at RT under dark conditions prior to treatment with blocking buffer, and wash steps were performed using .05% (v/v) TBS-TWEEN20. For immunohistochemical detection, sections were incubated in EnVision peroxidase labelled polymer (conjugated to goat anti-mouse and goat anti-rabbit immunoglobulins) for 30 min at RT. Sections were then washed three times and incubated with EnVision DAB+ substrate buffer-3,3′-diaminobenzidine (DAB) chromogen solution for 3 min, rinsed three times with deionised water (diH_2O), counter-stained using haematoxylin according to Delafield, dehydrated and cleared using standard procedures on a Varistain™ Gemini ES automated slide stainer, then finally mounted with glass coverslips using DPX mountant. Slides were cured at RT overnight and imaged using brightfield microscopy (DM4000B upright microscope) in Leica Application Suite software version 2.6 (Leica Microsystems). Regions clearly showing IFM vascular morphology and positively labelled structures were chosen to demonstrate protein localisation. Negative control images for immunohistochemistry are provided in Supplementary Figure S2.

2.7 Fluorescent labelling analyses

To distinguish between regions of IFM and fascicular matrix (FM), boundaries between both phases were determined by light refraction in phase contrast images, as well as gross identification by nuclei number and cell morphology (Supplementary Figure S3). For quantification, all settings remained constant between samples including exposure, pixel size, z-step size, and laser settings with all images taken in one single session. For each sample, two distinct areas were imaged in two separate serial tissue sections (2 × sections per horse donor, n = 5). Confocal images are presented as maximum intensity projections from z-stacks containing image slices at a resolution of 512 × 512 × 40 pixels (227.9 × 227.9 × 13.09 µm; .34 µm z-step size) to fully capture tissue depths. Image processing and analysis was performed using Fiji/ImageJ software (Schindelin et al., 2012). For IFM measurements, an area fraction (%) of positively stained pixels were recorded in 8-bit binary images (black = negative, white = positive) to measure expression of markers of interest. To generate binary images for each marker, a background correction was performed to remove noise, followed by a median filter and threshold (Triangle for CD146/MKX = 555 nm, Huang for CD44/CD90 = 633 nm). The lookup table (LUT) of colour channels within images was changed for visualisation purposes.

2.8 3D immunolabelling

3D immunolabelling of SDFT segments was performed as previously described (Marr et al., 2020). All steps were performed with orbital agitation. SDFT segments (5 mm × 5 mm × 2 mm, n = 2)

were washed twice for 12 h with TBS at RT, and permeabilised sequentially in 50% (v/v) methanol:TBS, 80% (v/v) methanol: diH_2O, and 100% methanol for 2 h at 4°C. Samples were washed sequentially for 40 min at 4°C with 20% (v/v) DMSO:methanol, 80% (v/v) methanol:diH_2O, 50% (v/v) methanol:TBS, TBS, and TBS supplemented with .2% (v/v) Triton X-100. Prior to blocking, samples were incubated with a pre-blocking penetration buffer containing .2% TBS-TX100, .3 M glycine, and 20% DMSO for 6 h at 37°C. Equine SDFT segments were blocked for 80 h at 37°C in .2% TBS-TX100 supplemented with 6% (v/v) goat and 6% (v/v) donkey serum and 10% (v/v) DMSO. Primary antibody incubations for CD146 (1:100) were performed at 37°C for 80 h in wash buffer (TBS supplemented with .2% (v/v) TWEEN20), 3% (v/v) goat serum, 3% (v/v) donkey serum, and 5% (v/v) DMSO. Segments were washed 3 × 2 h with wash buffer, incubated with secondary antibodies (1:250, goat anti-rabbit Alexa Fluor® 594) for 36 h at 37°C, washed 5 × 5 min with wash buffer, and counterstained overnight with DAPI (1:2000) diluted in wash buffer. Segments were dehydrated with increasing concentration of methanol, and tissue cleared with immersion in Visikol® HISTO™-1 for 36 h, followed by immersion in HISTO™-2 for at least 36 h at RT. Samples were stored in HISTO™-2 at 4°C prior to confocal imaging. Confocal imaging of regions (approx. 1 mm × 1 mm × .2 mm) within each sample was performed using a Leica TCS SP8 laser scanning confocal microscope with a motorised stage. Images were captured using lasers emitting light at 405 (blue channel; DAPI) and 561 (red channel; Alexa Fluor 594) nm with laser power <10% and scanning speed = 600 Hz with a HC PL FLUOTAR 10x/.32 dry objective lens, resolution = 1,024 × 1,024 px, pinhole size = 1 Airy unit, frame average = 1, line average = 8, and electronic zoom = .75. 3D renderings were captured in Leica LAS X software (version 3.5.5) within the 3D module.

2.9 Primary tendon cell culture

SDFTs collected under sterile conditions were placed in Petri dishes containing Gibco™ Dulbecco's PBS (without phenol red, calcium and magnesium) supplemented with 1% (v/v) antibiotic-antimycotic solution. Surrounding peritenon was removed to isolate the tendon core (6 g), which was diced into approximately 4 mm^3 pieces, rinsed with DPBS, and digested with 1 mg/mL pronase E (39052, VWR) per 1 g tissue for 6–8 h at 37°C and 5% CO_2 under constant agitation. Following pronase digestion, tissue was digested for a further 24 h with .5 mg/ml collagenase type IV (CLS-4, Lorne Laboratories) and 1 mg/mL dispase II (17105041, Invitrogen) at 37°C and 5% CO_2 with constant agitation (Garvican et al., 2017).

2.10 Magnet-activated cell sorting (MACS) of CD146 cells

Previous studies have shown that >50% expression of cell membrane proteins can be restored post-digestion by 24 h *in vitro* culture (Autengruber et al., 2012). Hence, to enhance antigen recovery, freshly digested tendon-derived cells (TDCs) were cultured overnight to maximise CD146 cell isolations. Following this recovery phase, adherent cells were dissociated at 37°C for 10 min using Accutase® solution according to manufacturer's guidelines. Cells remaining in suspension (i.e. non-adherent populations) were also collected alongside dissociated cells (adherent populations). Cell isolates were washed by resuspension in fresh growth medium and centrifuged at 300 × g for 10–20 min depending on pellet formation. Cell pellets (passage 1; p1) were resuspended in growth medium and separated into single-cell suspensions (SCSs) by passing through a 70 µm cell strainer. SCSs were resuspended in freshly prepared, ice-cold MACS buffer containing sterile-filtered FACSFlow™ (342003, BD Biosciences) supplemented with 1% (w/v) BSA. SCSs were centrifuged for 10 min at 300 × g, resuspended in MACS buffer, and both cell viability and numbers determined by trypan blue (T8154, Sigma-Aldrich) and a haemocytometer. Suspensions with <90% viability were discarded. SCSs were incubated with anti-CD146 antibodies (ab75769, Abcam, Cambridge, United Kingdom) at a concentration of 1 µg/mL for 30 min at 4°C on ice. Following primary antibody incubation, SCSs were washed three times by centrifugation at 300 × g, resuspended in MACS buffer, and incubated with anti-rabbit IgG micro-beads (130-048-602, Miltenyi biotec) diluted in MACS buffer for 15 min at 4°C. SCSs were washed three times by centrifugation at 300 × g and resuspended in MACS buffer. MidiMACS™ LS columns (130-042-401, Miltenyi biotec) were mounted to a MidiMACS™ Separator and multistand (130-042-301, Miltenyi biotec) and washed with MACS buffer according to manufacturer guidelines. MACS-ready SCSs were passed through MidiMACS™ columns and washed with MACS buffer twice. All wash elutions containing negatively selected cells (i.e. $CD146^-$ TDCs) were collected on ice until processing of sub-cultures. Following negative cell depletion, $CD146^+$ cells were collected by removing the MACS column from the MACS magnet and eluting the column with MACS buffer and a plunger. All sub-cultures were maintained until a maximum of three passages (p3) to limit phenotypic drift. For downstream assays, cells were dissociated using Accutase® solution (A6964, Sigma-Aldrich). n = 9 (biological replicates).

2.11 Flow cytometry

For direct flow cytometry, .1–.2 × 10^6 cells were resuspended in DPBS. For $CD146^+$ cells, lower concentrations were used according to yields following MACS isolation. All tubes were stored on ice immediately prior to and during flow cytometry. Cell suspensions (50 µl) were incubated with a phycoerythrin (PE)-conjugated variant of the EPR3208 anti-CD146 antibody (1:100, ab209298, Abcam, Cambridge, United Kingdom) on ice for 30 min, washed with DPBS and spun at 400 × g. Supernatant was removed, and pellets resuspended in 500 µl DPBS for immediate flow cytometry analyses.

All flow cytometry acquisition was performed using an air-cooled 3-laser BD FACSCanto II™ flow cytometer (BD Biosciences) equipped with BD FACSDiva (version 8.0.1, BD Biosciences). Acquisition equipment and software were calibrated daily or immediately prior to acquisition using BD FACSDiva™ CS&T Research Beads (BD Biosciences). Data analyses was performed in FlowJo software (version 10, FlowJo LLC). Unstained controls (fluorescence minus one control) were used to gate and discriminate positively and negatively labelled populations (see Supplementaty Figure S4). The percentage of positive cells gated in unstained samples (i.e., autofluorescent cells) was subtracted from stained samples (i.e. experimental cells) to give an overall percentage of immunoreactivity.

All experiments recorded a minimum of 10,000 total events (i.e. cells). n = 2 (biological replicates) per cell fraction.

2.12 Immunocytochemistry

For detection of CD146 in unsorted TDCs, .1–.2 × 10^6 cells were seeded on sterile 16 mm borosilicate glass circle coverslips coated with poly-L-lysine solution (.01%, sterile-filtered, P4832, Sigma-Aldrich) until 70%–80% confluence. To detect CD146 within MACS-enriched $CD146^+$ cells, immunocytochemistry was performed directly on cells (.1–.2 × 10^6 seeding density) in non-coated culture vessels at 70%–80% confluence. Cells were washed 3 times with DPBS, fixed with pre-chilled (−20°C) acetone:methanol (1:1) for 20 min on ice, then washed three times with DPBS. Cells were blocked for 1 h with blocking buffer as described above. Cells were incubated overnight with primary antibodies overnight at 4°C as described above, washed three times with DPBS, incubated for 1 h with secondary antibodies (1:500, goat anti-rabbit Alexa Fluor® 488 and goat anti-mouse Alexa Fluor® 594).

For direct CD146 labelling in MACS-sorted populations, cells were incubated overnight at 4 °C with phycoerythrin (PE)-conjugated anti-CD146 antibodies (1:100, ab209298, Abcam, Cambridge, United Kingdom). Cells were washed three times with DPBS, labelled with DAPI (1 µg/mL) for 2 min, washed three times with DPBS and mounted using Prolong™ Diamond, cured at RT under dark conditions for 24 h before storing at 4°C until imaging. Fluorescent imaging of TDCs was performed using a Leica SP5 (40 × HCX PL FLUOTAR PH2 NA = .75 objective). For $CD146^+$ cells, imaging was performed on a DMIRB inverted microscope (Leica Microsystems, Wetzlar, Germany; 40 × N PLAN L corr PH2 NA = .55 objective). n = 3 (biological replicates).

2.13 Clonogenic assay

Bone marrow-derived mesenchymal stromal cells (MSCs) isolated as described previously were kindly provided by Dr Giulia Sivelli (Godwin et al., 2012). MSCs, unsorted TDCs, sorted $CD146^-$ cells and $CD146^+$ cells were seeded in 6-well plates at a density of 100 cells cm^{-3} (approx. 900 cells) and cultured for 7 d. At termination of cultures, cells were washed 3× with DPBS, fixed with 2.5% glutaraldehyde for 10 min, then washed 3× DBPS (all steps at RT). Cells were stained with .1% (v/v) crystal violet for 30 min at RT. Cells were washed 3x with DBPS and left to air dry at RT. Images were acquired using a flat-bed scanner (Epson Perfection 4990, Epson) at a resolution of 800 dpi. n = 3 for each cell type (biological replicates). n = 2–3 wells for each condition (technical replicates).

2.14 Adipogenesis assay

MSCs, unsorted TDCs, sorted $CD146^-$ cells and $CD146^+$ cells were seeded into 12-well plates at a density of .4 × 10^5 cells per well and cultured for 48 h until adherence in standard growth medium. To induce adipogenesis, standard growth media was removed, and cells were cultured with StemPro® Adipogenesis differentiation media for a further 14 d. Cells were fed induction media every 72 h. Upon termination of culture, monolayers were washed once with DPBS before fixation with 4% PFA/10% NBF for 30 min at RT. To assess intracellular lipid vesicles produced by adipogenic conditions, cells were stained with Oil Red O. Fixed monolayers were rinsed once with distilled water then washed with 60% isopropanol for 5 min at RT. Monolayers were stained for 15 min at RT with a 3:2 working solution of 3-parts .3% (w/v) Oil Red O diluted in isopropanol and 1-part distilled water. Cells were washed repeatedly with distilled water until rinsed clear of precipitating Oil Red O, then counterstained with Harris haematoxylin for 1 min at RT. Imaging was performed on an Axiovert 135TV inverted microscope (Zeiss) using Image Pro Insight version 9.1.4 (Media Cybernetics). n = 3 for each cell type (biological replicates). n = 2-3 wells for each condition (technical replicates).

2.15 Osteogenesis assay

Following dissociation, MSCs, unsorted TDCs, sorted $CD146^+$ and $CD146^-$ cells were seeded into 12-well plates a density of .1 × 10^6 cells per well with osteogenic media containing 2 mM sodium phosphate dibasic (DiP) or standard growth medium as a control with each condition supplemented with 50 µg/ml ascorbic acid to promote collagen synthesis (Barnes, 1975; Patel et al., 2019). DiP (free phosphate donor) is essential for bone/mineralised extracellular matrix metabolism during osteogenesis (Robey and Termine, 1985). Monolayers were fed with fresh half-media changes corresponding to each condition every 72 h. Cell cultures were terminated after 21 days to assess mineralisation with Alizarin Red S staining (Taylor et al., 2014). Monolayers were rinsed once with DPBS then fixed for 10 min at RT with 2.5% (v/v) glutaraldehyde. Fixed cells were rinsed once with DBPS then three times with 70% ethanol and air-dried at RT overnight. Dried monolayers were subsequently stained with 1% (w/v) Alizarin Red S in diH_2O for 5 min at RT, then washed three times with 50% ethanol and left to air-dry overnight. Imaging was performed as described above. n = 3 for each cell type (biological replicates). n = 2-3 wells for each condition (technical replicates).

2.16 Statistical analyses

Statistical analyses and graphs were produced using GraphPad Prism (version 9.1). Normality tests were performed according to Shapiro-Wilk tests (α = .05). All datasets passed normality tests and were analysed using unpaired two-tailed t-test (significance set to p < .05). Graphs were plotted as mean (μ) ± standard deviation (SD).

3 Results

3.1 CD146 is a marker of interfascicular cell populations

PAS staining demonstrated that the IFM contains mucin-rich basement membrane (Figure 1A). Using both CD146 and the IFM basement membrane marker LAMA4 in STRING predictions identified several potential interfascicular cell surface markers including CD44, CD90 (THY1) and CD133 (PROM1), as well as a

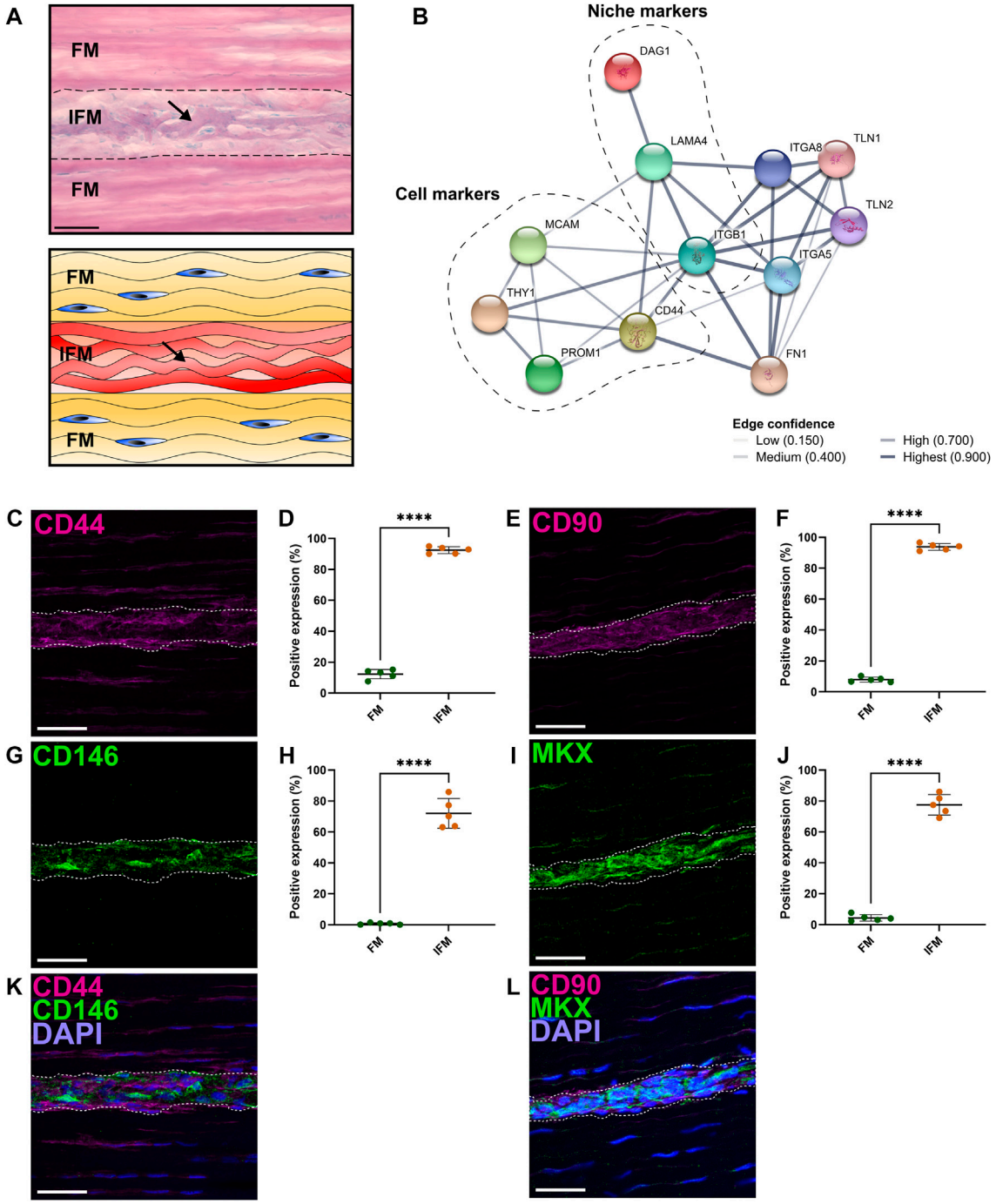

FIGURE 1
Analyses of regional differences in tendon cell marker expression demonstrated that CD146 is exclusively expressed by interfascicular cells within an interfascicular niche. **(A)** PAS-staining and schematic of SDFT sections highlighted mucin-rich basement membrane (arrow; purple, schematic; red) within the interfascicular matrix (IFM). Nuclei = blue. Scale bar = 50 μm. **(B)** STRING-predicted protein-protein interactions revealed potential targets for novel tendon cell populations using validated interfascicular niche markers CD146 and LAMA4. Interactions based on CD146 (MCAM) and LAMA4 demonstrated a protein neighborhood consisting of cell markers CD44, CD90 (THY1), CD133 (PROM1), as well as cell niche components such as ITGB1, DAG1 and FN1. **(C–J)** Image analyses comparing the positive labelling (area fraction; %) of longitudinal SDFT sections immunolabelled with CD44 **(C,D)**, CD90 **(E,F)**, CD146 **(G,H)** and MKX **(I,J)** overlayed with DAPI [blue = nuclei; **(K,L)**] in both fascicular matrix (FM) and IFM regions. The IFM is outlined by dotted lines. Scale bar = 50 μm. Biological replicates (*n*) = 5 per tendon region. Technical replicates = 3-4 per individual sample. Graphs were plotted as mean (μ) ± SD. Statistical significance: **** ($p \leq .0001$).

broader network of interfascicular niche and basement membrane components, including dystroglycan 1 (DAG1), integrin subunit β1 (ITGB1) and fibronectin 1 (FN1) (Figure 1B). To validate these proposed interfascicular cell markers, fluorescent labelling of CD44, CD90, CD146 and MKX was quantified in both fascicular and interfascicular regions. All markers were

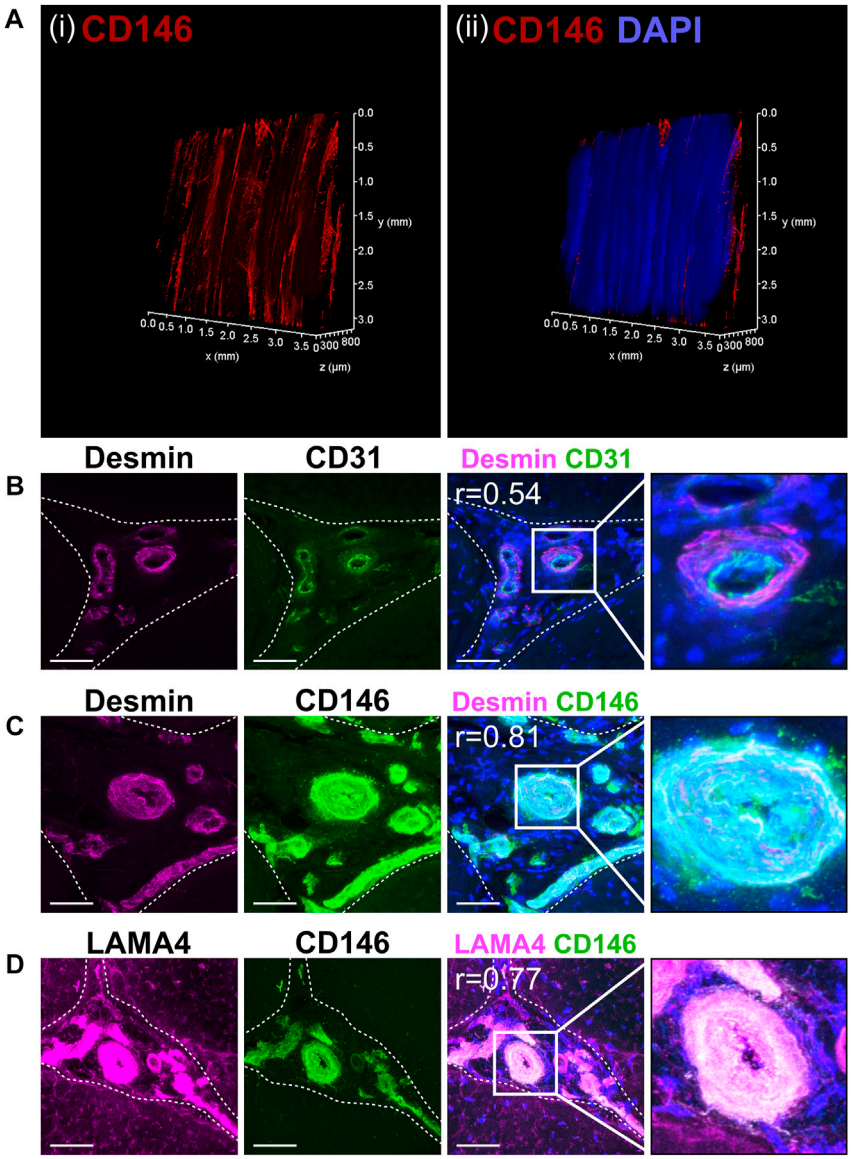

FIGURE 2
CD146 cell populations demarcated a vascular network indicative of a vascular cell niche within the interfascicular matrix. **(A)** 3D imaging of (i) CD146 and (ii) CD146 and nuclei (DAPI, blue) confirmed that the IFM was enriched with CD146 cell populations as part of an interconnected vessel network. Images of labelled transverse SDFT sections demonstrating colocalisation of Desmin with CD31 and CD146 **(B,C)** and CD146 with LAMA4 **(D)** indicating that CD146 represents a marker of interfascicular vascular cell populations resident within laminin-rich vessels. Nuclei = DAPI (blue). IFM is demarcated by dashed lines in transverse images. Scale bar = 50 μm. Images represent maximum projection of 30 μm section.

enriched within IFM (72%–94% positive expression) and had significantly less expression within fascicles; fascicular CD146 expression was less than 1% whereas CD44, CD90 and MKX expression was between 4% and 15% (Figures 1C–J). Using 3D imaging of SDFT labelled with CD146, we identified an interfascicular network of vascular structures within which CD146 cells were localised (Figure 2A). The colocalisation of Desmin (mural cell marker) with CD31 (endothelial marker) and CD146 (pan-vascular marker), alongside LAMA4 (basement membrane; Figures 2B–D) observed in transverse sections confirmed that the structures were vascular, and often found in regions of IFM connecting 3 adjacent fascicles. Within IFM, we observed distinct CD31 endothelium surrounded by Desmin-rich layers, whilst CD146 and Desmin colocalised in smooth muscle and pericyte layers. Labelling of CD31, CD146 and Desmin was also confirmed in vascular layers of larger blood vessels within epitendinous regions (Supplementary Figure S5).

3.2 Tendon interfascicular matrix is enriched in an endothelial basement membrane

To characterise the distribution of the major components of interfascicular basement membrane, we performed immunolabelling of basement membrane proteins in longitudinal tendon sections, including full-length laminin (pan-laminin), type

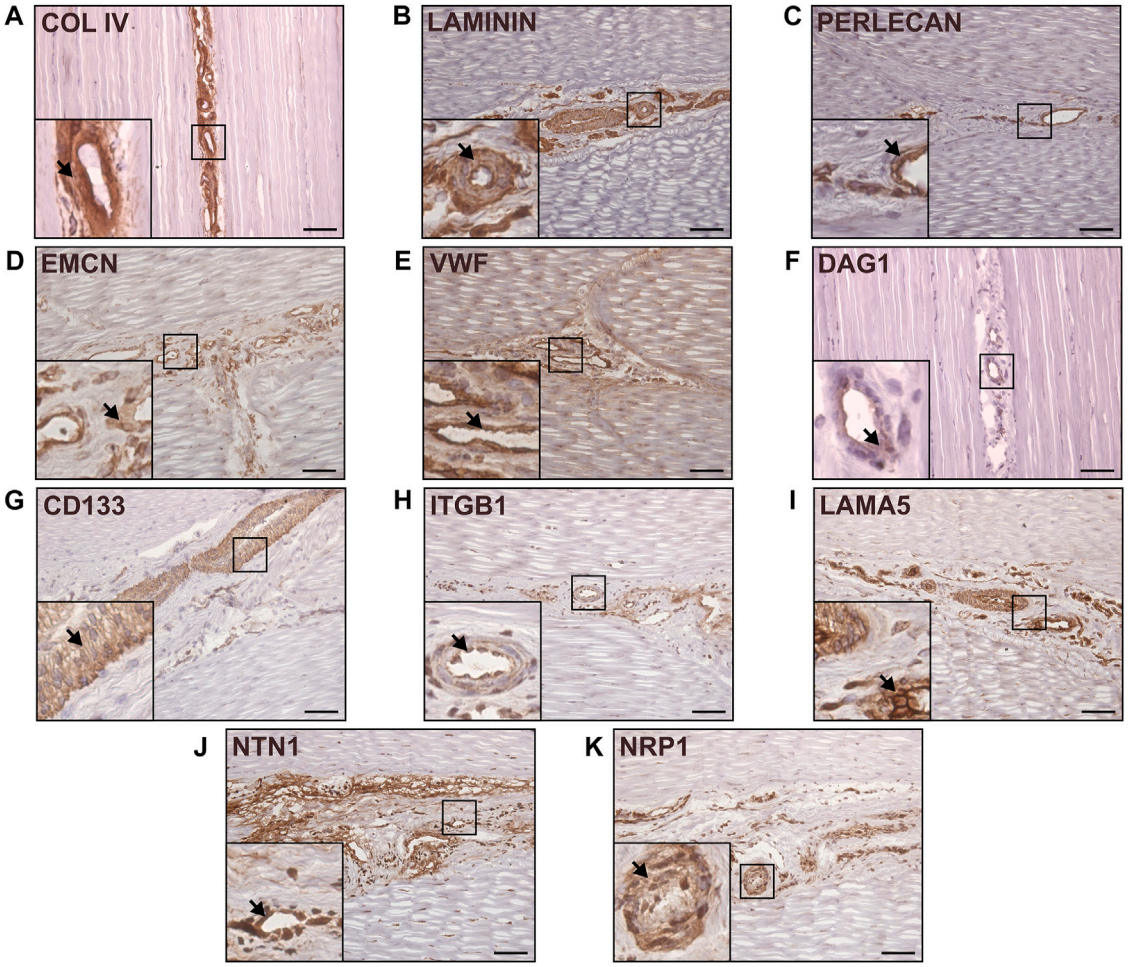

FIGURE 3
Canonical and network-predicted vascular and basement membrane components were enriched within the interfascicular matrix. Immunohistochemical labelling of longitudinal sections confirmed interfascicular expression of Type IV collagen **(A)**, full-length laminin **(B)**, Perlecan **(C)**, as well as vascular markers EMCN **(D)** and VWF **(E)**. Immunolabelling validation also confirmed enrichment within interfascicular vasculature with network-predicted markers DAG1 (IIH6; **(F)**, CD133 **(G)**, ITGB1 **(H)**, laminin isoform LAMA5 **(I)**, and angiogenic mediators NTN1 **(J)** and NRP1 **(K)**. Scale bar = 75 μm. Representative images shown.

IV collagen, and Perlecan (Figures 3A–C), all of which localised to the vasculature within IFM. Further labelling with endothelial markers endomucin (EMCN) and von Willebrand factor (VWF) demonstrated abundant expression within the IFM (Figures 3D, E). STRING predictions in *Equus caballus* identified canonical basement membrane components integrin β1 (ITGB1) and dystroglycan 1 (DAG1), as part of the CD146-LAMA4 interaction network. Hence, we performed labelling of α-dystroglycan (IIH6) and ITGB1 (Figures 3F, H), in addition to network-predicted cell surface marker CD133 (Figure 3G) with all three labelled abundantly within the IFM. As LAMA4/LAMA5 ratios are critical for basement membrane integrity (Galatenko et al., 2018), we also demonstrated labelling for laminin α5 (LAMA5) within the IFM (Figure 3I). We also examined other reported angiogenic mediators, Netrin-1 (NTN1); a reported ligand of CD146, and Neuropilin-1 (NRP1), both of which also localised to the IFM (Figures 3J, K). In addition to demonstrating the presence of these vascular and basement membrane markers in the IFM, our results highlight the variability in IFM vasculature and morphology in the mid-metarcarpal region of the SDFT, with a complex vascular network distinguishable in transverse and longitudinal sections, as well as 3D imaging (Figure 2).

3.3 Interfascicular CD146$^+$ cells are a rare subpopulation requiring enrichment for *in vitro* isolation

Upon isolation from the SDFT, *in vitro* labelling of cell surface markers demonstrated that the majority of TDCs exhibited abundant CD44 and CD90 labelling and limited CD146 expression (Figures 4A–C). To study CD146 cells *in vitro*, we therefore developed a MACS procedure for the enrichment of CD146 cells. Immunocytochemistry of positively sorted CD146 cells confirmed enrichment for cells expressing CD146 (Figure 4D). A single application of MACS was able to yield CD146 cells with enrichment of approximately 64% as determined by flow cytometry (Figures 4E, F). Comparison of cell

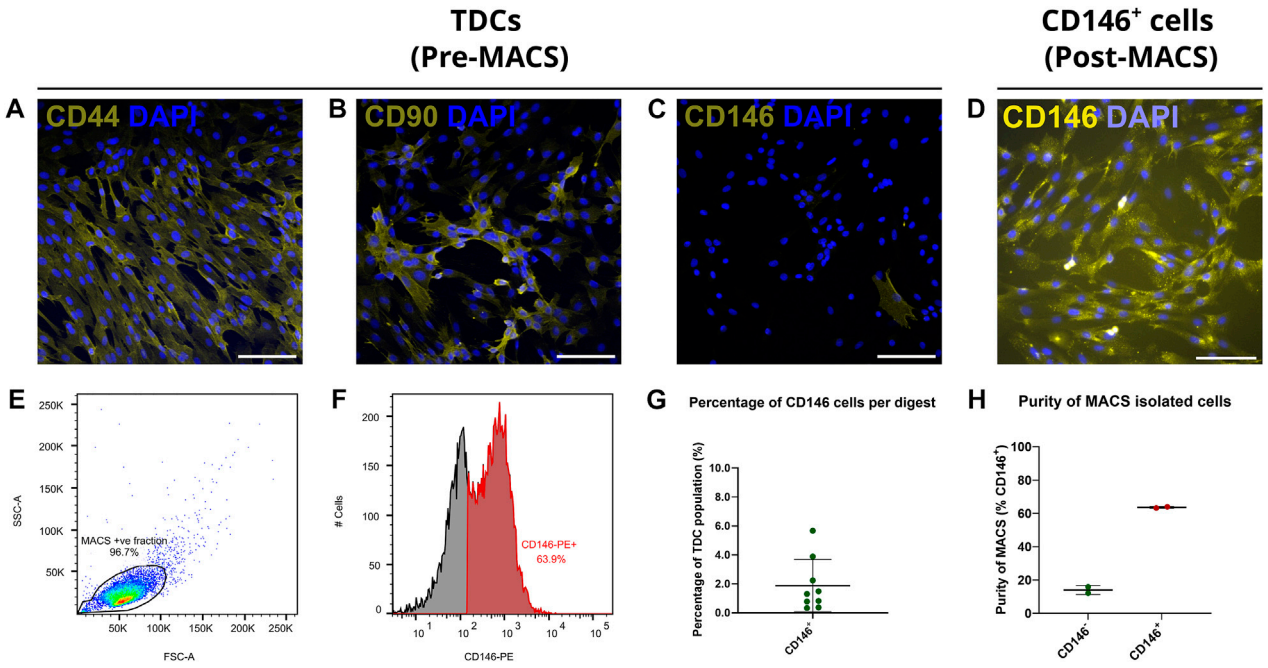

FIGURE 4
Immunocytochemical labelling confirms CD146$^+$ cells are a rare subpopulation when expanded *in vitro,* and can be enriched *via* MACS. Tendon cell-surface markers CD44 **(A)**, CD90 **(B)** and CD146 **(C)** demonstrate that CD146 cells are a rare subpopulation amongst cultured TDCs (passage 1) when compared to cells expressing CD44 or CD90. n = 3 (biological replicates). Scale bar = 100 μm. Immunocytochemically labelled CD146 cells (D; passage 2) labelled with CD146 reaffirmed that expression persisted once expanded *in vitro*. n = 3 (biological replicates). Scale bar = 100 μm. Flow cytometry **(E,F)** confirmed CD146 expression in CD146$^+$ cell populations. Total events = 10,000. **(G)** The percentage of CD146 cells (approx. 2%) yields by MACS from the original tendon-derived cell suspensions as determined by cell counting, reiterated the rarity of CD146 cells. n = 9 (biological replicates). Across MACS isolations **(H)**, flow cytometry confirms CD146 enrichment, albeit approximately 15% of cells in the CD146$^-$ negative fraction were positive for CD146. n = 2 (biological replicates) per cell fraction. Graphs were plotted as mean (μ) ± SD.

numbers pre and post MACS showed that approximately 2% of unsorted cells were CD146 positive (Figure 4G), providing further emphasis on the rarity of CD146 cell subpopulations and requirements for optimal enrichment procedures. However, some CD146 positive cells were detected in negative fractions (approx. 14%; Figure 4H).

3.4 Interfascicular CD146 cells have limited differentiation potential

To assess their clonogenicity and multi-lineage potential, unsorted TDCs, CD146$^+$, CD146$^-$ cells were subjected to clonogenic, osteogenic and adipogenic assays using MSCs as a positive control. CD146$^+$ cells showed no enhanced clonogenicity compared to CD146-negative cells or heterogenous TDCs (Figures 5A–D). For adipogenesis, TDCs, CD146$^+$ and CD146$^-$ cells all showed limited adipogenic potential when stimulated (Figures 5E–H). Under osteogenic conditions, unsorted TDCs displayed extensive calcium deposition with some mineralised nodules present, however virtually no calcium deposition nor mineralisation was detected in either CD146$^+$ and CD146$^-$ sorted cell populations (Figures 5M–P).

4 Discussion

In this study, we have characterised CD146$^+$ cell populations and their niche within the tendon IFM. We demonstrate that CD146$^+$ cells exclusively localise to the IFM in healthy tendon, forming extensive interconnected 3D networks, comprising a niche containing vascular basement membrane and vascular-associated cells and proteins, several of which have been identified in the IFM for the first time. In contrast to our hypothesis that the IFM is a progenitor cell niche, CD146$^+$ cells exhibited limited differentiation potential, indicating they are unlikely to be stem/progenitor cells, and are instead likely of vascular derivation.

The presence of CD146$^+$ cells in tendon has been demonstrated previously; with immunolabelling of the human Achilles showing CD146 within the IFM (Yin et al., 2016). Our results support these findings. In addition, single-cell RNA sequencing of human tendon revealed three cell populations that express CD146; one of which was an endothelial population which co-expressed CD31 (Kendal et al., 2020). Furthermore, in single-cell analyses of mouse tendon, CD146$^+$ tendon cells, identified as haematopoietic cells, represented around 9% of TDCs (De Micheli et al., 2020). In other tissues such as bone, CD31 and CD146 expression can be used to delineate endosteal and vascular populations which remodel the haematopoietic niche (Sacchetti et al., 2007; Tormin et al., 2011). Previous research from our group has highlighted CD31 as an IFM-localised vascular marker (Godinho et al., 2017) whilst other studies have reported Desmin as a pericyte and muscle cell marker (Chan-Ling et al., 2004; Piercy et al., 2007). The localisation of CD146 and CD31 with Desmin we report herein suggests that CD146$^+$ delineates IFM endothelial and mural populations, whilst CD31 distinguishes endothelial cells from Desmin$^+$ smooth muscle cells and pericytes. Indeed, the

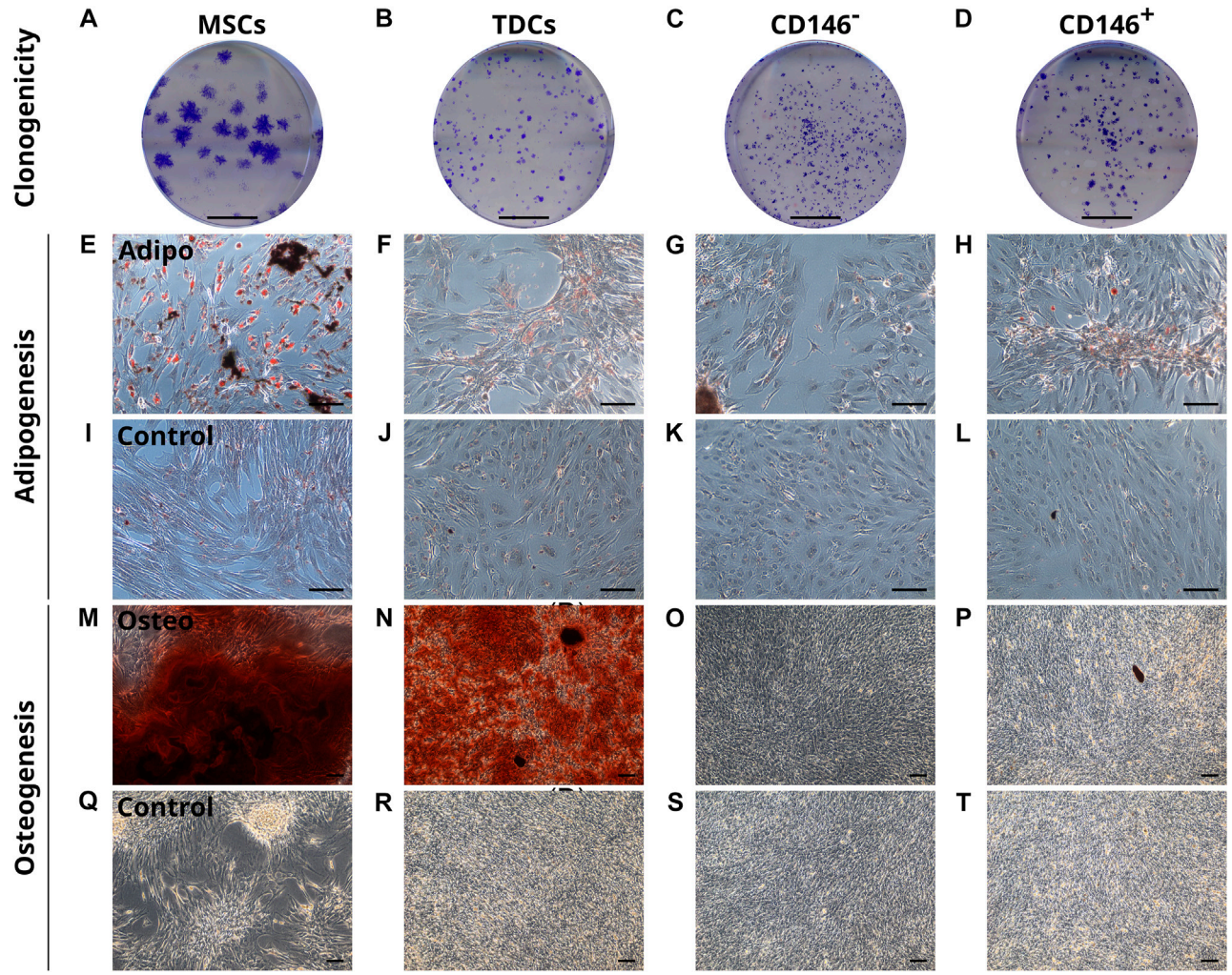

FIGURE 5
CD146$^+$ cells exhibit limited clonogenicity and lineage potential. Representative images of colonies formed by MSCs, TDCs, CD146$^-$ and CD146$^+$ populations **(A–D)**. Scale bar = 1 cm. Oil Red O staining of MSCs, TDCs, CD146$^-$ and CD146$^+$ cells **(E–L)** under adipogenic conditions using StemPro® Adipogenesis differentiation media **(E–H)** and control conditions **(I–L)** demonstrate that TDCs, CD146$^+$ and CD146$^-$ cells produce a limited number of lipid vesicles. Lipid vesicles = red. *n* = 3 per cell type (biological replicates). *n* = 3 per condition (technical replicates). Scale bar = 100 μm. Alizarin Red S staining of MSCs, TDCs, CD146$^-$ and CD146$^+$ cells **(M–T)** under osteogenic conditions containing 2 mM DiP **(M–P)** and control conditions **(Q–T)** demonstrate that tendon cells exhibit limited mineralisation capacity when separated. Mineralised nodules = black. Calcium deposits = red. Unmineralised matrix = reflective/white. Scale bar = 100 μm. Images shown are representative of each condition.

interconnected network of CD146 positivity detected demonstrates the presence of an interconnected IFM vascular network, which is likely continuous throughout the entire tendon. While studies have demonstrated vascularization of the IFM in both the SDFT and Achilles (Kraus-Hansen et al., 1992; Ahmed et al., 1998), the abundance and complexity of these vessels has not been appreciated previously. Further, epitendinous vessels (i.e., arteries and veins) are distinct when compared to interfascicular arterioles, capillaries or venules, given the observed differences in smooth muscle layers and whole vessel. Future studies are therefore required to improve classification of tendinous vasculature and the role of vasculature-associated cells in tendon homeostasis and repair.

In addition, our recent studies have established that CD146$^+$ cells migrate to sites of injury in the rat Achilles tendon, which is accompanied by increased LAMA4 expression (Marr et al., 2021). In the current study, 3D imaging of the SDFT revealed an extensive interconnected network of CD146 labelling within the IFM; together these findings suggest that CD146$^+$ cells are found both within, and separate from the vasculature. However it is yet to be established whether these are two distinct cell populations, or whether vascular-associated CD146 cells are able to migrate away from the vasculature. The interconnected network of CD146 forms structures which were similar those seen in 3D imaging of LAMA4 in SDFT (Marr et al., 2020). The colocalisation of CD146 and LAMA4 in the current study further reinforces the putative ligand-receptor interaction that CD146 and LAMA4 share, which has been demonstrated in previous studies (Ishikawa et al., 2014; Wragg et al., 2016). In chondrocytes, blocking of LAMA4 inhibited cluster formation, which is typical of pathological cartilage, and also resulted in downregulation of Claudin-1 (previously identified as a tendon IFM protein) and MMP3 (Fuerst et al., 2011; Moazedi-Fuerst et al., 2016). Recent studies have already established that loss of LAMA4 results in reduced CD146 cell expression and loss of basement membrane/niche maintenance in both mesenchymal and

haematopoietic environments (Cai et al., 2022). Therefore, LAMA4 may act as a homing receptor for migrating interfascicular CD146$^+$ tenocytes, however the chemokines that facilitate this are yet to be identified.

Here, we demonstrate that both LAMA4 and LAMA5 are abundant within the IFM niche, alongside other vascular components ITGB1, VWF, EMCN, NTN1 and NRP1. It has been shown previously that the early stage deletion of the laminin α4-chain is not functionally compensated for by other laminin chains leading to failed angiogenic development. Yet, in contrast, compensatory upregulation of LAMA5 as a result of LAMA4 loss results in a relatively milder vascular phenotype during postnatal maturation, which suggests that the balance between laminin subunits LAMA4/LAMA5 ratios is critical for maintaining a healthy vascular network and vascular niche (Thyboll et al., 2002). Given the abundant expression of both LAMA4 and LAMA5 found in our studies, it is likely that both chains and their full-length laminin isoforms 411 and 511 are essential to IFM endothelial basement membrane function, due to their previously reported role in shear-stress response and mechanotransduction (Di Russo et al., 2017; Beguin et al., 2020).

In situ, IFM cells were also positive for CD44 and CD90. Although their expression is likely acquired at later stages of differentiation and proliferation. These markers have been used to label putative stem/progenitor cell populations in tendon and other tissues (Leonardi et al., 2021). However, given that both markers were widely expressed throughout the IFM and fascicles, it is unlikely that they specifically label tendon stem cells in the equine SDFT and instead label several populations within tendon, including the tenocytes resident within fascicles. This assertion is supported by single-cell RNA sequencing data from the mouse Achilles tendon showing that both CD44 and CD90 are expressed by tenocytes and other tendon cell populations (De Micheli et al., 2020).

The identification of multiple vascular structures using markers of endothelial/vascular cell lineages demonstrates that the IFM houses a specialised vascular niche, rich in basement membrane proteins. This builds on our previous proteomics data showing enrichment of basement membrane proteins in the IFM, including perlecan, laminins and collagen type IV (Thorpe et al., 2016). The identification of perlecan-rich vascular networks in tendon IFM has major implications for the study of tendon. During development, perlecan is integral for tight packaging of interstitial tissues, which house vasculature, to ensure that maturation of endothelial tissues proceeds (Gustafsson et al., 2013). In addition, lymphangiogenesis within interstitial tissues is defined by the expression of perlecan and interstitial fluid flow (Rutkowski et al., 2006). In tendons, fascicular sliding may therefore be integral to IFM lymphatic and vascular remodelling. Moreover, VWF is likely to act as an endothelial cell ligand within the interfascicular basement membrane. The assembly of vascular basement membranes are regulated by β1-integrins and dystroglycans, and are typically formed of type IV collagens, proteoglycans such as perlecan, as well as vascular laminin isoforms comprised of LAMA4 and LAMA5 (Nikolova et al., 2006; Thomsen et al., 2017). Previous studies have reported vascular cell niches housing CD146-expressing stem/progenitor populations (Castrechini et al., 2010). Furthermore, the angiogenic capacity of CD146 is controlled by signalling molecules such as Netrin-1 and Neuropilin-1; both of which are critical for vascular cell patterning (Melani and Weinstein, 2010; Tu et al., 2015; Chen et al., 2018). It is notable that several of the above mentioned proteins, most of which are predicted to interact with CD146, localise to the IFM, indicating tethering of CD146 cells to a vascular basement membrane.

In vitro, tendon derived cells showed similar protein expression to that seen *in situ*, with abundant labelling of CD44 and CD90, and limited labelling for CD146 in only 2% of TDC. This is somewhat lower than the 9% of cells in the mouse Achilles that expressed CD146 as determined by single cell sequencing (De Micheli et al., 2020); this discrepancy may be explained by species-specific differences. The equine model is a highly relevant and well-accepted model for tendon research as the SDFT and human Achilles share similar function, structure and injury risk (Innes and Clegg, 2010; Patterson-Kane and Rich, 2014). Another explanation for this discrepancy in population proportions is the removal of the epitenon in the current study, which is known to house CD146$^+$ cells (Marr et al., 2020). MACS was successfully employed to enrich CD146 populations, with approximately 65% of cells positive for CD146 post-sorting as determined by flow cytometry. This percentage is likely an under-representation, as CD146$^+$ cells were detected using flow cytometry immediately post MACS-enrichment. This suggests that some CD146 antigens may still be bound to the magnetic label used during MACS, rendering them unavailable for binding to fluorescently tagged antibodies and hence non-detected by flow cytometry. Indeed, immunocytochemistry of CD146$^+$ cells showed that virtually all cells labelled positively for CD146 post-MACS enrichment. However, a proportion of negatively selected cells expressed CD146 following cell sorting, likely due to a small number of CD146$^+$ cells not binding to the column and therefore being eluted with the negative fraction. Enrichment could have been improved by additional rounds of sorting; however, this would have resulted in insufficient cell numbers for downstream experiments.

While previous studies have reported CD146 as a marker of mesenchymal stem cell lineages, tendon-derived CD146 populations exhibited similar clonogenicity to other TDCs, as well as limited differentiation potential. These findings agree with previous studies that demonstrated equine SDFT-derived TSPCs have limited clonogenicity and differentiation potential; this study utilised low density plating as opposed to cell sorting procedures to obtain TSPCs yet still failed to detect adipogenesis following stimulation (Williamson et al., 2015). In the current study, a limited number of lipid vesicles were however produced in adipogenic-induced TDCs, CD146$^+$ and CD146$^-$ cells. Unfortunately, we were unable to assess chondrogenesis after sorting due to the insufficient number of CD146$^+$ cells for micromass survival during chondrogenic pellet induction. Together, these results indicate that CD146$^+$ tendon-derived cells do not exhibit stem cell plasticity and instead CD146 is a pan-vascular marker in tendon, labelling both mural and endothelial cells. While the multipotency of pericytes has been demonstrated in a range of species (Esteves and Donadeu, 2018), other studies have shown that pericyte plasticity varies between tissue types, with some pericytes having limited differentiation potential (Herrmann et al., 2016). It is possible that, while tendon pericytes have a limited multipotency, they can differentiate down a tenogenic lineage, and indeed single cell sequencing data indicate that pericytes are a source of progenitor cells for adult tenocytes in murine tendon (De Micheli et al., 2020). However, as we did not assess tenogenesis in CD146 subpopulations, we are unable to confirm this and therefore future studies will need to fully characterize CD146 subpopulations. As tendon CD146$^+$ populations have been shown to migrate to sites of injury, establishing further understanding of their local microenvironment, lineage origins, *in vitro* characteristics, and

the effects of ageing will aid future research aimed at establishing if mobilising these populations can enhance intrinsic repair.

5 Conclusion

CD146 demarcates an IFM-specific cell population that reside in a niche rich in basement membrane and vascular proteins in tendons. Contrary to our hypothesis, CD146$^+$ cells have limited clonogenicity and differentiation potential indicating they are unlikely to be stem/progenitor cells. Instead, co-localisation of Desmin with CD31 and CD146 indicates that CD146 is a pan-vascular marker within tendon. As previous studies have shown that CD146 cells migrate to sites of injury, establishing regenerative strategies that utilise endogenous tendon cell populations to promote intrinsic repair could act as a viable and effective method for improving healing responses and preventing tendon re-injury.

Data availability statement

The original contributions presented in the study are included in the article/Supplementary Material, further inquiries can be directed to the corresponding author.

Author contributions

Conceptualization, NM and CT; methodology, NM, AF, DW and CT; investigation, NM and DZ; writing—original draft preparation, NM and CT; writing—review and editing, NM, DZ, AF, DW, CT, JD and AP; supervision, CT, JD and AP; project administration, CT; funding acquisition, CT. All authors have read and agreed to the published version of the manuscript.

Funding

This research was funded by Versus Arthritis (grant numbers 21216 and 22607).

Acknowledgments

The authors would like to thank Dr Isabel Orris and Dr Lucie Bourne for support and guidance on mineralisation cultures.

Conflict of interest

The authors declare that the research was conducted in the absence of any commercial or financial relationships that could be construed as a potential conflict of interest.

Publisher's note

All claims expressed in this article are solely those of the authors and do not necessarily represent those of their affiliated organizations, or those of the publisher, the editors and the reviewers. Any product that may be evaluated in this article, or claim that may be made by its manufacturer, is not guaranteed or endorsed by the publisher.

Supplementary material

The Supplementary Material for this article can be found online at: https://www.frontiersin.org/articles/10.3389/fcell.2022.1094124/full#supplementary-material

References

Ahmed, I. M., Lagopoulos, M., McConnell, P., Soames, R. W., and Sefton, G. K. (1998). Blood supply of the achilles tendon. *J. Orthop. Res.* 16 (5), 591–596. doi:10.1002/jor.1100160511

Alexander, R. M. (1991). Energy-saving mechanisms in walking and running. *J. Exp. Biol.* 160 (1), 55–69. doi:10.1242/jeb.160.1.55

Alexander, R. M. (2002). Tendon elasticity and muscle function. *Comp. Biochem. Physiol. A Mol. Integr. Physiol.* 133 (4), 1001–1011. doi:10.1016/s1095-6433(02)00143-5

Anderson, D. M., Arredondo, J., Hahn, K., Valente, G., Martin, J. F., Wilson-Rawls, J., et al. (2006). Mohawk is a novel homeobox gene expressed in the developing mouse embryo. *Dev. Dyn.* 235 (3), 792–801. doi:10.1002/dvdy.20671

Autengruber, A., Gereke, M., Hansen, G., Hennig, C., and Bruder, D. (2012). Impact of enzymatic tissue disintegration on the level of surface molecule expression and immune cell function. *Eur. J. Microbiol. Immunol. (Bp)* 2 (2), 112–120. doi:10.1556/EuJMI.2.2012.2.3

Barnes, M. J. (1975). Function of ascorbic acid in collagen metabolism. *Ann. N. Y. Acad. Sci.* 258 (1), 264–277. doi:10.1111/j.1749-6632.1975.tb29287.x

Beguin, E. P., Janssen, E. F. J., Hoogenboezem, M., Meijer, A. B., Hoogendijk, A. J., and van den Biggelaar, M. (2020). Flow-induced reorganization of laminin-integrin networks within the endothelial basement membrane uncovered by proteomics. *Mol. Cell. Proteomics* 19 (7), 1179–1192. doi:10.1074/mcp.RA120.001964

Benjamin, M., Kaiser, E., and Milz, S. (2008). Structure-function relationships in tendons: A review. *J. Anat.* 212 (3), 211–228. doi:10.1111/j.1469-7580.2008.00864.x

Bi, Y., Ehirchiou, D., Kilts, T. M., Inkson, C. A., Embree, M. C., Sonoyama, W., et al. (2007). Identification of tendon stem/progenitor cells and the role of the extracellular matrix in their niche. *Nat. Med.* 13 (10), 1219–1227. doi:10.1038/nm1630

Biewener, A. A. (1998). Muscle-tendon stresses and elastic energy storage during locomotion in the horse. *Comp. Biochem. Physiol. B Biochem. Mol. Biol.* 120 (1), 73–87. doi:10.1016/s0305-0491(98)00024-8

Cai, H., Kondo, M., Sandhow, L., Xiao, P., Johansson, A. S., Sasaki, T., et al. (2022). Critical role of Lama4 for hematopoiesis regeneration and acute myeloid leukemia progression. *Blood* 139 (20), 3040–3057. doi:10.1182/blood.2021011510

Castrechini, N. M., Murthi, P., Gude, N. M., Erwich, J. J. H. M., Gronthos, S., Zannettino, A., et al. (2010). Mesenchymal stem cells in human placental chorionic villi reside in a vascular Niche. *Placenta* 31 (3), 203–212. doi:10.1016/j.placenta.2009.12.006

Chan-Ling, T., Page, M. P., Gardiner, T., Baxter, L., Rosinova, E., and Hughes, S. (2004). Desmin ensheathment ratio as an indicator of vessel stability: Evidence in normal development and in retinopathy of prematurity. *Am. J. Pathology* 165 (4), 1301–1313. doi:10.1016/s0002-9440(10)63389-5

Chen, J., Luo, Y., Huang, H., Wu, S., Feng, J., Zhang, J., et al. (2018). CD146 is essential for PDGFRβ-induced pericyte recruitment. *Protein & Cell.* 9 (8), 743–747. doi:10.1007/s13238-017-0484-5

Dakin, S. G., Werling, D., Hibbert, A., Abayasekara, D. R., Young, N. J., Smith, R. K., et al. (2012). Macrophage sub-populations and the lipoxin A4 receptor implicate active inflammation during equine tendon repair. *PLoS One* 7 (2), e32333. doi:10.1371/journal.pone.0032333

De Micheli, A. J., Swanson, J. B., Disser, N. P., Martinez, L. M., Walker, N. R., Oliver, D. J., et al. (2020). Single-cell transcriptomic analysis identifies extensive heterogeneity in the cellular composition of mouse Achilles tendons. *Am. J. Physiol. Cell. Physiol.* 319 (5), C885–C894. doi:10.1152/ajpcell.00372.2020

Di Russo, J., Luik, A. L., Yousif, L., Budny, S., Oberleithner, H., Hofschroer, V., et al. (2017). Endothelial basement membrane laminin 511 is essential for shear stress response. *EMBO J.* 36 (2), 183–201. doi:10.15252/embj.201694756

Esteves, C. L., and Donadeu, F. X. (2018). Pericytes and their potential in regenerative medicine across species. *Cytom. Part A* 93 (1), 50–59. doi:10.1002/cyto.a.23243

Evans, N. D., Oreffo, R. O. C., Healy, E., Thurner, P. J., and Man, Y. H. (2013). Epithelial mechanobiology, skin wound healing, and the stem cell niche. *J. Mech. Behav. Biomed. Mater.* 28, 397–409. doi:10.1016/j.jmbbm.2013.04.023

Fuerst, F. C., Gruber, G., Stradner, M. H., Jones, J. C., Kremser, M. L., Angerer, H., et al. (2011). Regulation of MMP3 by laminin alpha 4 in human osteoarthritic cartilage. *Scand. J. Rheumatol.* 40 (6), 494–496. doi:10.3109/03009742.2011.605392

Galatenko, V. V., Maltseva, D. V., Galatenko, A. V., Rodin, S., and Tonevitsky, A. G. (2018). Cumulative prognostic power of laminin genes in colorectal cancer. *BMC Med. Genomics* 11 (1), 9. doi:10.1186/s12920-018-0332-3

Garvican, E. R., Salavati, M., Smith, R. K. W., and Dudhia, J. (2017). Exposure of a tendon extracellular matrix to synovial fluid triggers endogenous and engrafted cell death: A mechanism for failed healing of intrathecal tendon injuries. *Connect. Tissue Res.* 58 (5), 438–446. doi:10.1080/03008207.2016.1245726

Godinho, M. S. C., Thorpe, C. T., Greenwald, S. E., and Screen, H. R. C. (2017). Elastin is localised to the interfascicular matrix of energy storing tendons and becomes increasingly disorganised with ageing. *Sci. Rep.* 7 (1), 9713–9811. doi:10.1038/s41598-017-09995-4

Godwin, E. E., Young, N. J., Dudhia, J., Beamish, I. C., and Smith, R. K. (2012). Implantation of bone marrow-derived mesenchymal stem cells demonstrates improved outcome in horses with overstrain injury of the superficial digital flexor tendon. *Equine Vet. J.* 44 (1), 25–32. doi:10.1111/j.2042-3306.2011.00363.x

Gumucio, J. P., Schonk, M. M., Kharaz, Y. A., Comerford, E., and Mendias, C. L. (2020). Scleraxis is required for the growth of adult tendons in response to mechanical loading. *JCI Insight* 5 (13), e138295. doi:10.1172/jci.insight.138295

Gustafsson, E., Almonte-Becerril, M., Bloch, W., and Costell, M. (2013). Perlecan maintains microvessel integrity *in vivo* and modulates their formation *in vitro*. *PLoS One* 8 (1), e53715. doi:10.1371/journal.pone.0053715

Handsfield, G. G., Slane, L. C., and Screen, H. R. C. (2016). Nomenclature of the tendon hierarchy: An overview of inconsistent terminology and a proposed size-based naming scheme with terminology for multi-muscle tendons. *J. Biomech.* 49 (13), 3122–3124. doi:10.1016/j.jbiomech.2016.06.028

Herrmann, M., Bara, J. J., Sprecher, C. M., Menzel, U., Jalowiec, J. M., Osinga, R., et al. (2016). Pericyte plasticity - comparative investigation of the angiogenic and multilineage potential of pericytes from different human tissues. *Eur. Cell. Mater* 31, 236–249. doi:10.22203/ecm.v031a16

Horwitz, E. M., Le Blanc, K., Dominici, M., Mueller, I., Slaper-Cortenbach, I., Marini, F. C., et al. (2005). Clarification of the nomenclature for MSC: The international society for cellular therapy position statement. *Cytotherapy* 7 (5), 393–395. doi:10.1080/14653240500319234

Innes, J. F., and Clegg, P. (2010). Comparative rheumatology: What can be learnt from naturally occurring musculoskeletal disorders in domestic animals? *Rheumatol. Oxf.* 49 (6), 1030–1039. doi:10.1093/rheumatology/kep465

Ishikawa, T., Wondimu, Z., Oikawa, Y., Gentilcore, G., Kiessling, R., Egyhazi Brage, S., et al. (2014). Laminins 411 and 421 differentially promote tumor cell migration via α6β1 integrin and MCAM (CD146). *Matrix Biol.* 38, 69–83. doi:10.1016/j.matbio.2014.06.002

Ivanovska, I. L., Shin, J. W., Swift, J., and Discher, D. E. (2015). Stem cell mechanobiology: Diverse lessons from bone marrow. *Trends Cell. Biol.* 25 (9), 523–532. doi:10.1016/j.tcb.2015.04.003

Johnson, J. P., Rothbacher, U., and Sers, C. (1993). The progression associated antigen MUC18: A unique member of the immunoglobulin supergene family. *Melanoma Res.* 3 (5), 337–340. doi:10.1097/00008390-199310000-00006

Kaltz, N., Ringe, J., Holzwarth, C., Charbord, P., Niemeyer, M., Jacobs, V. R., et al. (2010). Novel markers of mesenchymal stem cells defined by genome-wide gene expression analysis of stromal cells from different sources. *Exp. Cell. Res.* 316 (16), 2609–2617. doi:10.1016/j.yexcr.2010.06.002

Kannus, P. (2000). Structure of the tendon connective tissue. *Scand. J. Med. Sci. Sports* 10 (6), 312–320. doi:10.1034/j.1600-0838.2000.010006312.x

Kendal, A. R., Layton, T., Al-Mossawi, H., Appleton, L., Dakin, S., Brown, R., et al. (2020). Multi-omic single cell analysis resolves novel stromal cell populations in healthy and diseased human tendon. *Sci. Rep.* 10 (1), 13939. doi:10.1038/s41598-020-70786-5

Kimura, W., Machii, M., Xue, X., Sultana, N., Hikosaka, K., Sharkar, M. T., et al. (2011). Irxl1 mutant mice show reduced tendon differentiation and no patterning defects in musculoskeletal system development. *Genesis* 49 (1), 2–9. doi:10.1002/dvg.20688

Kraus-Hansen, A. E., Fackelman, G. E., Becker, C., Williams, R. M., and Pipers, F. S. (1992). Preliminary studies on the vascular anatomy of the equine superficial digital flexor tendon. *Equine Veterinary J.* 24 (1), 46–51. doi:10.1111/j.2042-3306.1992.tb02778.x

Leonardi, E. A., Xiao, M., Murray, I. R., Robinson, W. H., and Abrams, G. D. (2021). Tendon-derived progenitor cells with multilineage potential are present within human patellar tendon. *Orthop. J. Sports Med.* 9 (8), 23259671211023452. doi:10.1177/23259671211023452

Marr, N., Hopkinson, M., Hibbert, A. P., Pitsillides, A. A., and Thorpe, C. T. (2020). Bimodal whole-mount imaging of tendon using confocal microscopy and X-ray micro-computed tomography. *Biol. Proced. Online* 22 (1), 13. doi:10.1186/s12575-020-00126-4

Marr, N., Meeson, R., Kelly, E. F., Fang, Y., Peffers, M. J., Pitsillides, A. A., et al. (2021). CD146 delineates an interfascicular cell sub-population in tendon that is recruited during injury through its ligand laminin-α4. *Int. J. Mol. Sci.* 22 (18), 9729. doi:10.3390/ijms22189729

Melani, M., and Weinstein, B. M. (2010). Common factors regulating patterning of the nervous and vascular systems. *Annu. Rev. Cell. Dev. Biol.* 26 (1), 639–665. doi:10.1146/annurev.cellbio.093008.093324

Moazedi-Fuerst, F. C., Gruber, G., Stradner, M. H., Guidolin, D., Jones, J. C., Bodo, K., et al. (2016). Effect of Laminin-A4 inhibition on cluster formation of human osteoarthritic chondrocytes. *J. Orthop. Res.* 34 (3), 419–426. doi:10.1002/jor.23036

Morath, I., Hartmann, T. N., and Orian-Rousseau, V. (2016). CD44: More than a mere stem cell marker. *Int. J. Biochem. Cell. Biol.* 81, 166–173. doi:10.1016/j.biocel.2016.09.009

Nikolova, G., Jabs, N., Konstantinova, I., Domogatskaya, A., Tryggvason, K., Sorokin, L., et al. (2006). The vascular basement membrane: A niche for insulin gene expression and β cell proliferation. *Dev. Cell.* 10 (3), 397–405. doi:10.1016/j.devcel.2006.01.015

Patel, J. J., Bourne, L. E., Davies, B. K., Arnett, T. R., MacRae, V. E., Wheeler-Jones, C. P. D., et al. (2019). Differing calcification processes in cultured vascular smooth muscle cells and osteoblasts. *Exp. Cell. Res.* 380 (1), 100–113. doi:10.1016/j.yexcr.2019.04.020

Patterson-Kane, J. C., and Rich, T. (2014). Achilles tendon injuries in elite athletes: Lessons in pathophysiology from their equine counterparts. *ILAR J.* 55 (1), 86–99. doi:10.1093/ilar/ilu004

Piercy, R. J., Zhou, H., Feng, L., Pombo, A., Muntoni, F., and Brown, S. C. (2007). Desmin immunolocalisation in autosomal dominant Emery-Dreifuss muscular dystrophy. *Neuromuscul. Disord.* 17 (4), 297–305. doi:10.1016/j.nmd.2007.01.003

Richardson, L. E., Dudhia, J., Clegg, P. D., and Smith, R. (2007). Stem cells in veterinary medicine--attempts at regenerating equine tendon after injury. *Trends Biotechnol.* 25 (9), 409–416. doi:10.1016/j.tibtech.2007.07.009

Robey, P. G., and Termine, J. D. (1985). Human bone cells*in vitro*. *Calcif. Tissue Int.* 37 (5), 453–460. doi:10.1007/BF02557826

Russell, K. C., Phinney, D. G., Lacey, M. R., Barrilleaux, B. L., Meyertholen, K. E., and O'Connor, K. C. (2010). *In vitro* high-capacity assay to quantify the clonal heterogeneity in trilineage potential of mesenchymal stem cells reveals a complex hierarchy of lineage commitment. *Stem Cells* 28 (4), 788–798. doi:10.1002/stem.312

Rutkowski, J. M., Boardman, K. C., and Swartz, M. A. (2006). Characterization of lymphangiogenesis in a model of adult skin regeneration. *Am. J. Physiol. Heart Circ. Physiol.* 291 (3), H1402–H1410. doi:10.1152/ajpheart.00038.2006

Sacchetti, B., Funari, A., Michienzi, S., Di Cesare, S., Piersanti, S., Saggio, I., et al. (2007). Self-renewing osteoprogenitors in bone marrow sinusoids can organize a hematopoietic microenvironment. *Cell.* 131 (2), 324–336. doi:10.1016/j.cell.2007.08.025

Schindelin, J., Arganda-Carreras, I., Frise, E., Kaynig, V., Longair, M., Pietzsch, T., et al. (2012). Fiji: An open-source platform for biological-image analysis. *Nat. Methods* 9 (7), 676–682. doi:10.1038/nmeth.2019

Schlagbauer-Wadl, H., Jansen, B., Muller, M., Polterauer, P., Wolff, K., Eichler, H. G., et al. (1999). Influence of MUC18/MCAM/CD146 expression on human melanoma growth and metastasis in SCID mice. *Int. J. Cancer* 81 (6), 951–955. doi:10.1002/(sici)1097-0215(19990611)81:6<951::aid-ijc18>3.0.co;2-v

Schrage, A., Loddenkemper, C., Erben, U., Lauer, U., Hausdorf, G., Jungblut, P. R., et al. (2008). Murine CD146 is widely expressed on endothelial cells and is recognized by the monoclonal antibody ME-9F1. *Histochem Cell. Biol.* 129 (4), 441–451. doi:10.1007/s00418-008-0379-x

Schweitzer, R., Chyung, J. H., Murtaugh, L. C., Brent, A. E., Rosen, V., Olson, E. N., et al. (2001). Analysis of the tendon cell fate using Scleraxis, a specific marker for tendons and ligaments. *Development* 128 (19), 3855–3866. doi:10.1242/dev.128.19.3855

Sers, C., Kirsch, K., Rothbacher, U., Riethmuller, G., and Johnson, J. P. (1993). Genomic organization of the melanoma-associated glycoprotein MUC18: Implications for the evolution of the immunoglobulin domains. *Proc. Natl. Acad. Sci. U. S. A.* 90 (18), 8514–8518. doi:10.1073/pnas.90.18.8514

Shih, I. M. (1999). The role of CD146 (Mel-CAM) in biology and pathology. *J. Pathol.* 189 (1), 4–11. doi:10.1002/(SICI)1096-9896(199909)189:1<4::AID-PATH332>3.0.CO;2-P

Smith, L. R., Cho, S., and Discher, D. E. (2018). Stem cell differentiation is regulated by extracellular matrix mechanics. *Physiology* 33 (1), 16–25. doi:10.1152/physiol.00026.2017

Szklarczyk, D., Morris, J. H., Cook, H., Kuhn, M., Wyder, S., Simonovic, M., et al. (2017). The STRING database in 2017: Quality-controlled protein-protein association networks, made broadly accessible. *Nucleic Acids Res.* 45 (D1), D362–D368. doi:10.1093/nar/gkw937

Taylor, S. E., Shah, M., and Orriss, I. R. (2014). Generation of rodent and human osteoblasts. *Bonekey Rep.* 3, 585. doi:10.1038/bonekey.2014.80

Thomsen, M. S., Routhe, L. J., and Moos, T. (2017). The vascular basement membrane in the healthy and pathological brain. *J. Cereb. Blood Flow Metabolism* 37 (10), 3300–3317. doi:10.1177/0271678x17722436

Thorpe, C. T., Godinho, M. S. C., Riley, G. P., Birch, H. L., Clegg, P. D., and Screen, H. R. C. (2015). The interfascicular matrix enables fascicle sliding and recovery in tendon, and

behaves more elastically in energy storing tendons. *J. Mech. Behav. Biomed. Mater* 52, 85–94. doi:10.1016/j.jmbbm.2015.04.009

Thorpe, C. T., Peffers, M. J., Simpson, D., Halliwell, E., Screen, H. R., and Clegg, P. D. (2016). Anatomical heterogeneity of tendon: Fascicular and interfascicular tendon compartments have distinct proteomic composition. *Sci. Rep.* 6 (1), 20455. doi:10.1038/srep20455

Thorpe, C. T., and Screen, H. R. C. (2016b). "Tendon structure and composition," in *Metabolic influences on risk for tendon disorders*. Editors P. W. Ackermann and D. A. Hart (Cham: Springer International Publishing), 3–10.

Thorpe, C. T., and Screen, H. R. (2016a). Tendon structure and composition. *Adv. Exp. Med. Biol.* 920, 3–10. doi:10.1007/978-3-319-33943-6_1

Thyboll, J., Kortesmaa, J., Cao, R., Soininen, R., Wang, L., Iivanainen, A., et al. (2002). Deletion of the laminin alpha4 chain leads to impaired microvessel maturation. *Mol. Cell. Biol.* 22 (4), 1194–1202. doi:10.1128/MCB.22.4.1194-1202.2002

Tormin, A., Li, O., Brune, J. C., Walsh, S., Schutz, B., Ehinger, M., et al. (2011). CD146 expression on primary nonhematopoietic bone marrow stem cells is correlated with *in situ* localization. *Blood* 117 (19), 5067–5077. doi:10.1182/blood-2010-08-304287

Tu, T., Zhang, C., Yan, H., Luo, Y., Kong, R., Wen, P., et al. (2015). CD146 acts as a novel receptor for netrin-1 in promoting angiogenesis and vascular development. *Cell. Res.* 25 (3), 275–287. doi:10.1038/cr.2015.15

Webbon, P. M. (1977). A post mortem study of equine digital flexor tendons. *Equine Vet. J.* 9 (2), 61–67. doi:10.1111/j.2042-3306.1977.tb03981.x

Williamson, K. A., Lee, K. J., Humphreys, W. J., Comerford, E. J., Clegg, P. D., and Canty-Laird, E. G. (2015). Restricted differentiation potential of progenitor cell populations obtained from the equine superficial digital flexor tendon (SDFT). *J. Orthop. Res.* 33 (6), 849–858. doi:10.1002/jor.22891

Wragg, J. W., Finnity, J. P., Anderson, J. A., Ferguson, H. J., Porfiri, E., Bhatt, R. I., et al. (2016). MCAM and LAMA4 are highly enriched in tumor blood vessels of renal cell carcinoma and predict patient outcome. *Cancer Res.* 76 (8), 2314–2326. doi:10.1158/0008-5472.CAN-15-1364

Yin, Z., Hu, J. J., Yang, L., Zheng, Z. F., An, C. R., Wu, B. B., et al. (2016). Single-cell analysis reveals a nestin(+) tendon stem/progenitor cell population with strong tenogenic potentiality. *Sci. Adv.* 2 (11), e1600874. doi:10.1126/sciadv.1600874

frontiers | Frontiers in Cell and Developmental Biology

TYPE Original Research
PUBLISHED 10 January 2023
DOI 10.3389/fcell.2022.1097137

OPEN ACCESS

EDITED BY
Feng Yue,
Hainan University, China

REVIEWED BY
JiaMing Wang,
California State University, Sacramento, United States
Xian Wu Cheng,
Yanbian University Hospital, China
Xiang-An Li,
University of Kentucky, United States

*CORRESPONDENCE
Haizhao Yan,
yan_haizhao@gibh.ac.cn
Jianglin Fan,
jianglin@yamanashi.ac.jp

†These authors have contributed equally to this work

SPECIALTY SECTION
This article was submitted to Stem Cell Research, a section of the journal Frontiers in Cell and Developmental Biology

RECEIVED 13 November 2022
ACCEPTED 26 December 2022
PUBLISHED 10 January 2023

CITATION
Chen Y, Yang X, Kitajima S, Quan L, Wang Y, Zhu M, Liu E, Lai L, Yan H and Fan J (2023), Macrophage elastase derived from adventitial macrophages modulates aortic remodeling.
Front. Cell Dev. Biol. 10:1097137.
doi: 10.3389/fcell.2022.1097137

Macrophage elastase derived from adventitial macrophages modulates aortic remodeling

Yajie Chen[1,2†], Xiawen Yang[1†], Shuji Kitajima[3†], Longquan Quan[4†], Yao Wang[1], Maobi Zhu[1], Enqi Liu[5], Liangxue Lai[1,6], Haizhao Yan[1,2,6*] and Jianglin Fan[1,2*]

[1]Guangdong Province Key Laboratory, Southern China Institute of Large Animal Models for Biomedicine, School of Biotechnology and Health Sciences, Wuyi University, Jiangmen, China, [2]Department of Molecular Pathology, Interdisciplinary Graduate School of Medicine, University of Yamanashi, Yamanashi, Japan, [3]Analytical Research Center for Experimental Sciences, Saga University, Saga, Japan, [4]College of Animal Science and Technology, China Agricultural University, Beijing, China, [5]Research Institute of Atherosclerotic Disease and Laboratory Animal Center, Xi'an Jiaotong University School of Medicine, Xi'an, China, [6]Key Laboratory of Regenerative Biology, South China Institute for Stem Cell, Biology and Regenerative Medicine, Guangzhou Institutes of Biomedicine and Health, Chinese Academy of Sciences, Guangzhou, China

Abdominal aortic aneurysm (AAA) is pathologically characterized by intimal atherosclerosis, disruption and attenuation of the elastic media, and adventitial inflammatory infiltrates. Although all these pathological events are possibly involved in the pathogenesis of AAA, the functional roles contributed by adventitial inflammatory macrophages have not been fully documented. Recent studies have revealed that increased expression of matrix metalloproteinase-12 (MMP-12) derived from macrophages may be particularly important in the pathogenesis of both atherosclerosis and AAA. In the current study, we developed a carrageenan-induced abdominal aortic adventitial inflammatory model in hypercholesterolemic rabbits and evaluated the effect of adventitial macrophage accumulation on the aortic remodeling with special reference to the influence of increased expression of MMP-12. To accomplish this, we compared the carrageenan-induced aortic lesions of transgenic (Tg) rabbits that expressed high levels of MMP-12 in the macrophage lineage to those of non-Tg rabbits. We found that the aortic medial and adventitial lesions of Tg rabbits were greater in degree than those of non-Tg rabbits, with the increased infiltration of macrophages and prominent destruction of elastic lamellae accompanied by the frequent appearance of dilated lesions, while the intimal lesions were slightly increased. Enhanced aortic lesions in Tg rabbits were focally associated with increased dilation of the aortic lumens. RT-PCR and Western blotting revealed high levels of MMP-12 in the lesions of Tg rabbits that were accompanied by elevated levels of MMP-2 and -3, which was caused by increased number of macrophages. Our results suggest that adventitial inflammation constitutes a major stimulus to aortic remodeling and increased expression of MMP-12 secreted from adventitial macrophages plays an important role in the pathogenesis of vascular diseases such as AAA.

KEYWORDS

MMP-12, macrophage, elastin, abdominal aortic aneurysm, transgenic rabbits, atherosclerosis

1 Introduction

Abdominal aortic aneurysm (AAA) is thought to be a degenerative process affecting the aortic wall; however, its cause remains unclear (Thompson et al., 2006; Wassef et al., 2007). Regardless of etiology, the basic pathologic features of most AAA are quite similar: intimal atherosclerosis and marked destruction of the aortic wall characterized by the degradation of elastin and collagen in medial and adventitial lesions. Accumulating evidence has suggested that increased activity of matrix metalloproteinases (MMPs) derived from vascular cells such as macrophages and smooth muscle cells plays a major role in the pathogenesis of AAA (Thompson and Parks, 1996; Shah, 1997; Liapis and Paraskevas, 2003). So far, many MMPs have been detected in the lesions of AAA and it seems that many of them, either predominantly or collaboratively, are involved in the process of aneurysm's formation. In the aortic wall, elastin and collagen constitute most of the extracellular matrix (ECM), and therefore increased elastolytic activity has been suggested to be critical in the cascade of MMP-mediated degradation of ECM. Curci and coworkers first reported that the levels of macrophage elastase (MMP-12), the major elastin-degrading enzyme in the arterial wall is remarkably increased in the lesions of AAA patients, suggesting MMP-12 to be an important MMP that is involved in the pathogenesis of AAA (Curci et al., 1998). In MMP-12 knock-out mice, a deficiency of MMP-12 attenuated calcium chloride-induced AAA (Longo et al., 2005).

MMP-12, also called macrophage metalloelastase, was first identified as a potent elastolytic metalloproteinase specifically secreted by macrophages (Banda and Werb, 1981; Shapiro et al., 1993). In addition to elastin, MMP-12 is also able to degrade a broad spectrum of components of the ECM in the arterial wall such as collagen type IV, fibronectin, laminin, vitronectin, proteoglycans and plasminogen (Chandler et al., 1996; Gronski et al., 1997). Therefore, it is very likely that in the arterial wall, MMP-12 degrade not only elastin but also collagen directly or through interaction with other MMPs. Several lines of evidence show that MMP-12 can activate other MMPs such as MMP-2 and MMP-3 (Matsumoto et al., 1998) thus, MMP-12 has a pivotal role in the activation of other MMPs in the arterial wall.

To elucidate the functional roles of MMP-12, our laboratory generated transgenic rabbits with high levels of human MMP-12 specifically in tissue macrophages (Fan et al., 2004). Using this unique model, we have demonstrated that increased MMP-12 expression enhances the development of atherosclerosis (Liang et al., 2006) and inflammatory arthritis (Wang et al., 2004). We postulated that abnormal expression of macrophage-derived MMP-12, in concert with other MMPs, may also play a central role in the abdominal aortic remodeling. Rabbits are an appropriate model to study hyperlipidemia and atherosclerosis because they are sensitive to a cholesterol diet and rapidly develop atherosclerosis (Fan et al., 2015). In addition, our previous study revealed that many MMPs are upregulated in the lesions of aortic atherosclerosis of hypercholesterolemic rabbits (Fan et al., 2018). However, cholesterol-diet manipulation alone in rabbits usually induces prominent atherosclerotic lesions initiated in the aortic arch and thoracic aorta rather than abdominal aorta, which hampers examination of the effect of MMP-12 on AAA and aortic remodeling. In the current study, we produced a model of abdominal aortic injury in rabbits fed a cholesterol diet. Through embedding carrageenan, chronic adventitial inflammation of the abdominal aorta was induced to examine whether the adventitial inflammation is involved in aortic remodeling. Here we report that MMP-12 derived from adventitial inflammatory macrophages significantly modulates the formation of aortic lesions and aortic remodeling.

2 Materials and methods

2.1 Animals

MMP-12 transgenic (Tg) rabbits expressing human MMP-12 were generated in our laboratory as described previously (Fan et al., 2004). The Tg construct consisted of human MMP-12 cDNA (catalytic domain sequence) under the control of the human scavenger receptor A enhancer/promoter, which directs the expression of the transgene in the macrophage lineage (Fan et al., 2004) and foam cells of atherosclerotic lesions (Horvai et al., 1995). A total of 18 male Tg and 18 non-Tg littermates (5–6 months old) were used for the current study. They were fed a diet containing .3–.8% cholesterol and 3% soybean oil for 4 weeks and then, the abdominal aortic adventitial lesions were produced as described below (Figure 1). During the period of feeding, we maintained the plasma total cholesterol levels in these rabbits at a constant 800–1,000 mg/dL (Supplemental Fig.1) (similar to levels in homozygous familial hypercholesterolemic patients) by adjusting the cholesterol content of the diet.

2.2 Carrageenan-induced abdominal aortic adventitial lesions

To produce the abdominal aortic adventitial inflammation, we embedded carrageenan (a polysaccharide) around the isolated abdominal aorta segment (2.5 cm between inferior mesenteric artery and lumbar artery) as shown in Figure 1. Carrageenan is a potent chemoattractant for monocytes and can induce the focal accumulation of inflammatory macrophages (Wang et al., 2004). For this undertaking, rabbits were anesthetized by intramuscular injection of ketamine (25 mg/kg BW) + medetomidine hydrochloride (.5 mg/kg BW) and the abdominal aortas were exposed. A piece of sterilized gauze was pre-soaked in 10 mg/mL of λ-carrageenan (Wako Chemicals, Osaka, Japan) in .9% NaCl (w/v) at 40°C overnight, laid around the isolated abdominal aorta without any arterial branches, and gently covered with a sheet of polyethylene film to prevent inflammatory adhesion to the surrounding tissue. All rabbits were sacrificed at 24 weeks after surgery by intravenous injection of an overdose of sodium pentobarbital solution. The whole abdominal aortas were carefully collected for histological examination, immunostaining, and RNA and protein extraction (see below). This study was approved by the Animal Care Committee of the University of Yamanashi and Saga University and conformed to the Guide for the Care and Use of Laboratory Animals published by the NIH.

2.3 Histological examinations and immunohistochemical staining

The abdominal aortas were divided into 10 segments, fixed in 10% neutral buffered formalin, and embedded in paraffin. The sections (3 μm thick) were stained with hematoxylin and eosin (H&E) and Elastica van Gieson (EVG) for histological examination and morphometric analysis. To assess the degree to which elastic fibers were degraded, we quantified the contents of elastic fibers (expressed as elastic staining area μm (Wassef et al., 2007) per section) and the aortic diameter (expressed as μm calculated by

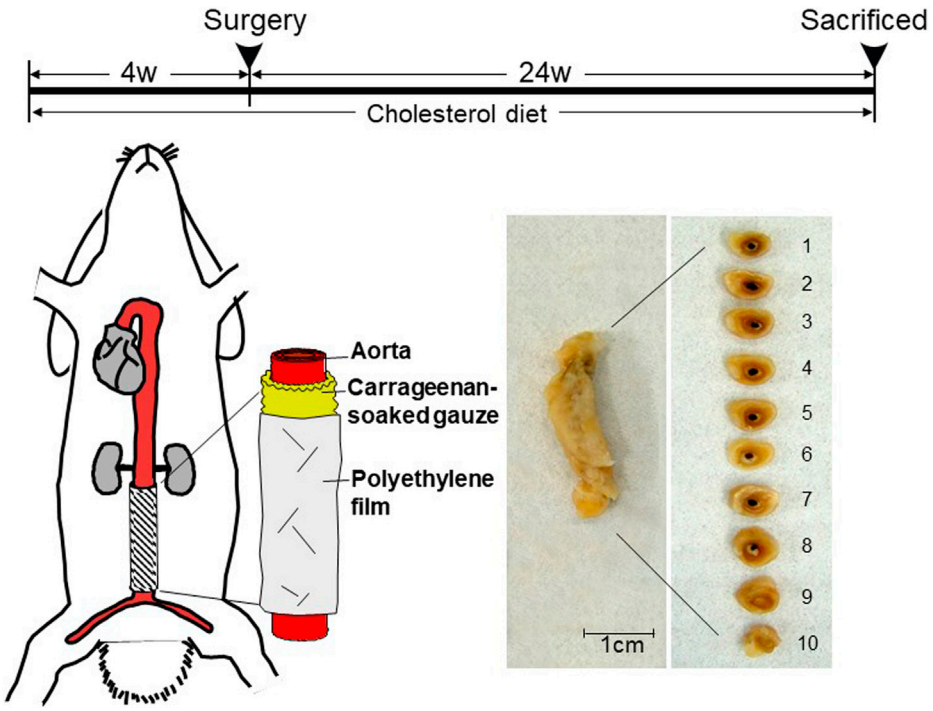

FIGURE 1
Schematic illustration of carrageenan-induced abdominal aortic lesions. Rabbits were fed a cholesterol-diet for 4 weeks before the surgery. A piece of sterilized gauze pre-soaked with λ-carrageenan was placed along the isolated abdominal aorta between the inferior mesenteric artery and lumbar artery and wrapped with a piece of polyethylene film. At the end of experiments, aortic rings were sectioned as shown on the right. The abdominal aorta was cut into 10 cross-sections.

area of the internal elastic lamina) using EVG-stained specimens and an image analysis system (Liang et al., 2006). The number of focal micro-dilated lesions in each aorta was calculated by two independent researchers. Immunohistochemical staining was performed using labeled streptavidin biotin kits (Nichirei Co, Tokyo, Japan) according to the manufacturer's instructions. After hydration and the blocking of endogenous peroxidase activity, the sections were incubated with monoclonal antibodies (mAbs) against rabbit macrophages (RAM11, 1:200) from Dako Corporation (Carpineteria, CA), and against smooth muscle α-actin (HHF35, 1:400) and the human MMP-12 catalytic domain (MAB 919, 1:20) from R&D System (Minneapolis, MN). Non-specific mouse IgG was used to stain the sections as a negative control. Macrophage infiltration in the peri-adventitial area was quantitated using an image analysis system after immunohistochemical staining. The positive staining area of the whole adventitial granulomatous lesion was measured and expressed as the percentages of the lesions. In addition, *in situ* β-casein zymography was performed using selected frozen sections to confirm MMP enzymatic activity in adventitial macrophages (Yu et al., 2008).

2.4 Real-time reverse-transcription polymerase chain reaction

A 1.0 μg sample of total RNA isolated from the aortas of three non-Tg and three Tg rabbits was transcribed into cDNA using QuantiTect® reverse transcription kit (Qiagen K.K., Tokyo). Amplification was conducted in a total reaction volume of 20 μL containing 5 μL of cDNA, 10 μL of 2X SYBR Green PCR Master Mix, and .5 μL of each primer (10 μM). Primers for real-time reverse-transcription (RT) polymerase chain reaction (PCR) was used as shown in Table 1. Rabbit endogenous glyceraldehyde-3-phosphate dehydrogenase (GAPDH) gene expression was measured as an internal control and changes in each gene expression were expressed as the fold-increase relative to the control. All analyses were performed in triplicate. Amplifications were performed on a DNA Engine Opticon (MJ Research, Tokyo, Japan) using a DyNAmo™ SYBR® Green qPCR kit (Finnzymes, MJ Bioworks, Inc., Espoo, Finland) according to the manufacturer's instructions. The absence of non-specific amplification products was confirmed in a melting-curve analysis.

2.5 Western blot analysis

The abdominal aortic segments from 3 non-Tg and 3 Tg rabbits were homogenized in an ice-cold suspension buffer (10 mM Tris-HCl, pH7.6, 100 mM NaCl) supplemented with a proteinase inhibitor cocktail (Sigma, St. Louis, MO). The supernatant was collected, and the protein content was measured using a Bio-Rad protein assay kit (Bio-Rad Japan, Tokyo). Ten-microgram aliquots of the crude proteins from the artery were separated by 10% SDS-PAGE for Western blotting and probed with a panel of Abs against MMP-2, −3, −9, and −12 (Liang et al., 2006).

TABLE 1 Primer sequences and amplification conditions for real-time RT-PCR.

Gene	Primer sequence (5′-3′)	Annealing temperature (°C)	Product size (bp)
MMP-2	Gaaggtcaagtggtccgtgt ccgtacttgccatccttctc	68	167
MMP-3	Cgttcctgatgttggtcacttc ttggcagatccggtgtgtaa	63	100
MMP-9	aaactggatgacgatgtctgcgtcccg acctgttccgctatggttacacccgcgta	58	362
MMP-12	tggcagaggtggtgtcatag tggtcacaggcagttggttc	60	326
MCP-1	Ttcagctcccatgtgctt ctggacccacttctg	62	204
TIMP-1	gtcatcagggccaagtttgt tccagcgatgagaaactcct	58	209
GAPDH	acggtgcacgccatcactgcc gcctgcttcaccaccttcttg	63	266

2.6 Statistical analyses

All values were expressed as the mean ± SE and statistical significance was analyzed using Student's t-test or Mann-Whitney's *U* test for non-parametric analysis. Statistical significance was set at $p < .05$.

3 Results

By embedding carrageenan, we produced chronic inflammatory lesions around the abdominal aorta in rabbits fed a cholesterol diet. As shown in Figure 2, the peri-aortic lesions were mainly composed of infiltrating macrophages, many of which had a foamy appearance, resembling granulomatous lesions. We examined whether adventitial chronic inflammation influences aortic remodeling and intimal lesions or whether increased MMP-12 (derived from macrophages) is instrumental in these processes.

3.1 Adventitial lesions

At first glance, the abdominal aortas were surrounded by numerous infiltrating macrophages with few intimal lesions (see below). The adventitial accumulation of macrophages was markedly and significantly increased in Tg compared to non-Tg rabbits and was associated with strong staining intensity of MMP-12 (Figure 2). *In situ* zymography confirmed that there was MMP-degrading activity around the aorta (data not shown). Furthermore, the lesions of Tg rabbits were characterized by remarkable disruption of the elastic fibers of both medial and

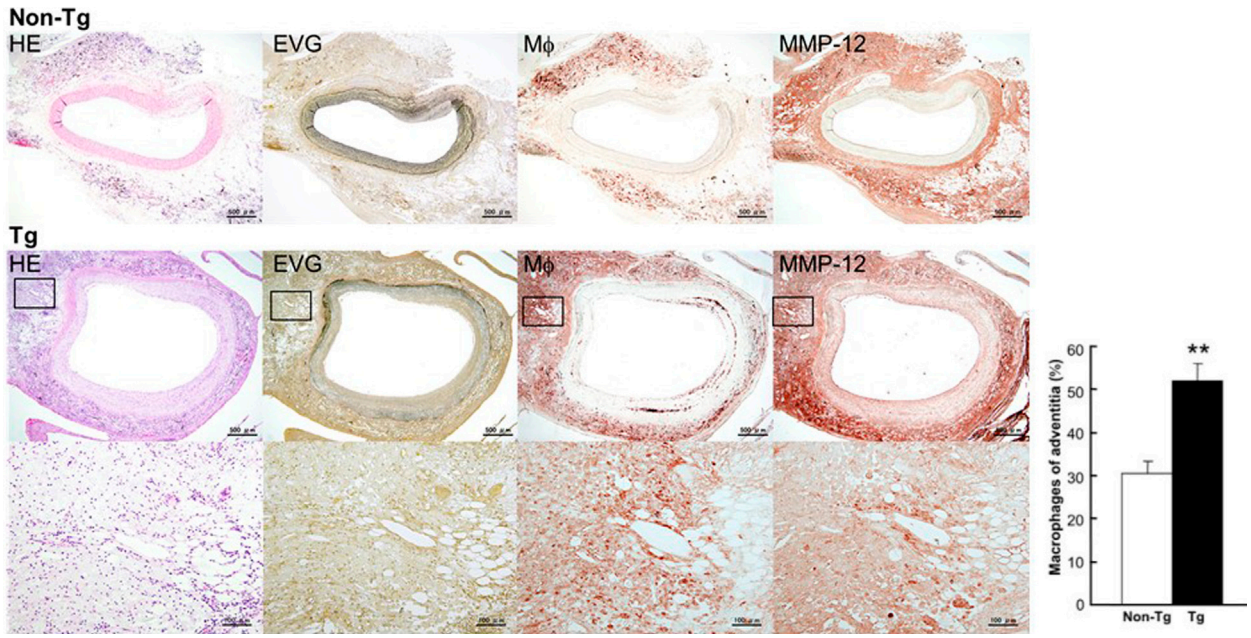

FIGURE 2
Micrographs of abdominal aortic lesions from non-Tg and Tg rabbits. Cross-sections were stained with H&E, with EVG, or immunohistochemically with Abs against macrophages and MMP-12. Adventitial macrophage infiltration and MMP-12 staining of a Tg rabbit aorta are shown at higher magnification at the bottom. Macrophage infiltration was quantitated and showed as percentage. 4–10 immunostained sections from each rabbit ($n = 8$ for non-Tg and 9 for Tg) were used. The data were expressed as the mean ± SE. $^{**}p < .01$ vs. non-Tg.

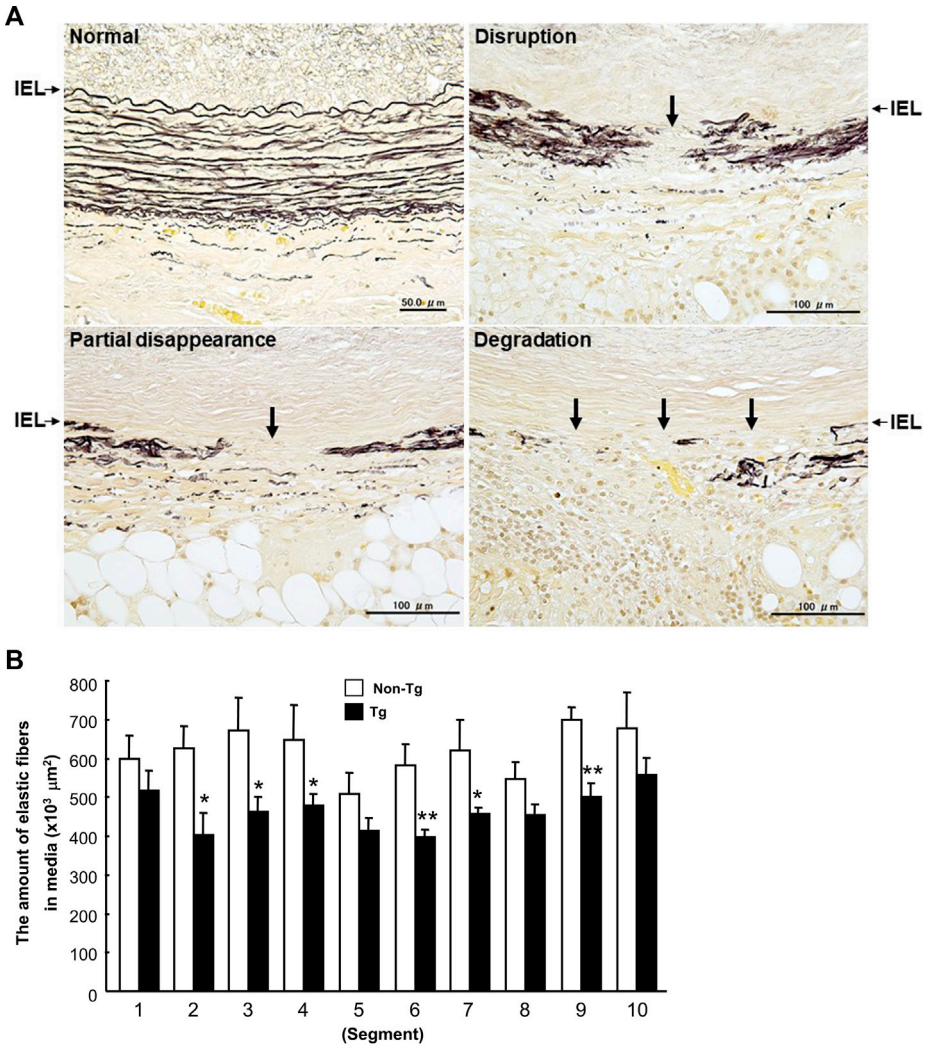

FIGURE 3
Disruption of elastin fibers of the aortic wall **(A)** and quantitation of the elastin contents of each section **(B)**. A: Histological features of destroyed elastic fibers in carrageenan-induced lesions. Cross-sections were stained with EVG. IEL (arrows): internal elastic lamina. B: The data were expressed as the mean ± SE (n = 12 for each group). *p < .05 **p < .01 vs. non-Tg.

adventitial lamellae as visualized with the EVG staining. The destruction of aortic elastin was histologically characterized by a partial or complete disappearance or degradation, or loss as shown in Figure 3A. In areas where the destruction occurred, there were many macrophages intermingled. To quantitate these changes, we measured the amount of elastin in each segment using EVG-stained specimens and compared Tg rabbits with non-Tg rabbits. The elastin content was significantly and consistently reduced throughout the segments of the abdominal aorta in Tg rabbits (Figure 3B). Of note, loss of the elastin was colocalized with MMP-12 immunoreactive proteins (Supplemental Fig.2) and associated with aortic remodeling in Tg rabbits. Under microscopic observation, we found that the aortic lumen focally protruded outwards and formed partially dilated (Figure 4A). We calculated the number of such lesions from all segments of the abdominal aorta and found that Tg rabbits had a 2-fold higher frequency of the dilated lesions than did non-Tg rabbits (4.0 ± .9 lesions/aorta in Tg vs. 2.2 ± .5 lesions/aorta in non-Tg, p < .05). We also measured the aortic diameter of each segment and found that 1–3rd and 7–10th of the segments of Tg rabbits were dilated compared to non-Tg aortas (Figure 4B) although average diameter of 10 segments were not statistically significant between two groups. Taken together, these results revealed that increased expression of MMP-12 in Tg rabbits resulted in more lesions and augmented degradation of the elastin in the aortic wall.

3.2 Intimal atherosclerosis

To examine whether the adventitial inflammation also affects the abdominal aortic intima, we analyzed the intimal atherosclerotic lesions. The intimal lesions in the abdominal aortas were essentially characterized by intimal thickening and mainly

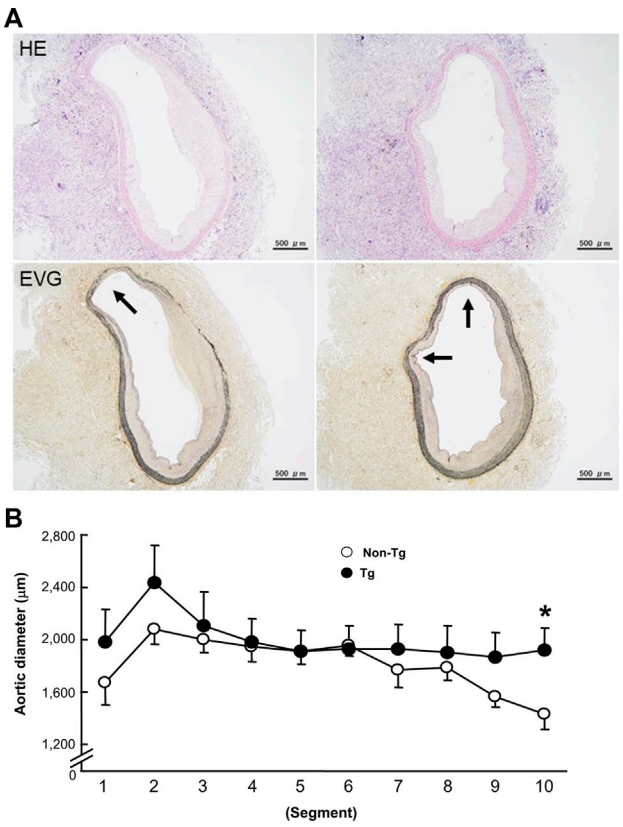

FIGURE 4
Representative micrographs of the focal dilation in the abdominal aortas of Tg rabbits **(A)** and quantitation of aortic dilation **(B)**. A: The lesions were stained with either H&E or EVG. Arrows indicate the protruded lumens. B: The aortic dilation was evaluated by measuring a defined area of the internal elastic lamina and calculating the diameter in each segment of the aorta. The data were expressed as the mean ± SE (n = 12 for each group). *p < .05 vs. non-Tg.

composed of proliferating smooth muscle cells (SMCs) and extracellular matrix with very few macrophages at the surface (Figure 5A). We measured the area occupied by intimal lesions in each segment. As shown in Figure 5B, in all segments, the lesions tended to be larger in Tg than non-Tg rabbits.

3.3 Analysis of MMP expression

To investigate the status of MMPs in the lesions, we measured the MMPs expression at both the protein and mRNA levels using Western blotting and real-time RT-PCR. As shown in Figures 6A, B, levels of MMP-12 along with MMP-2 and -3 were significantly increased in Tg rabbits compared to non-Tg rabbits. The mRNA expression of monocyte chemoattractant protein-1 (MCP-1) was also increased but that of MMP-9 and TIMP-1 were not significantly changed in Tg rabbits.

4 Discussion

Although it is generally accepted that aortic atherosclerosis is the main risk factor for AAA (Alcorn et al., 1996; Golledge et al., 2006), the role of adventitial inflammatory macrophages, while involved in many vascular diseases (Michel et al., 2007), has not been fully appreciated. In this study, we developed a rabbit model of adventitial inflammation to investigate the influence of inflammatory macrophages and MMP-12 on abdominal aortic remodeling. We found that embedding carrageenan around the abdominal aorta for 24 weeks resulted in a marked accumulation of macrophages, many of which had a foamy appearance, histologically resembling granulomatous lesions. These macrophages could be possibly originated from the peritoneal cavity where many resident macrophages were normally present. It should be pointed out that the lesions produced by carrageenan differ from other models of AAA such as the periarterial application of calcium chloride in rabbit carotid arteries and aortas (Gertz et al., 1988; Freestone et al., 1997) because the carrageen treatment cannot lead to the formation of typical AAA lesions. However, this adventitial inflammation model allowed us to examine the potential role of inflammatory macrophages in the (1) destruction of the elastic lamellae of the aortic wall; (2) aortic remodeling (depicted as aortic dilation); (3) the formation of micro-aneurysm-like lesions; and (4) intimal thickening. In this respect, we were specifically interested in the role of MMP-12, an important elastase secreted from macrophages, which has been shown to play diverse roles in inflammatory processes such as arthritis (Wang et al., 2004), atherosclerosis (Johnson et al., 2005; Liang et al., 2006), and AAA (Curci et al., 1998; Longo et al., 2005).

Compared to non-Tg rabbits, Tg rabbits showed a greater infiltration of macrophages along with a greater reduction of the elastin content of the aortic wall, suggesting that MMP-12 derived from macrophages is indeed involved in the enhanced degradation of elastin. The decrease in elastin content of the aortic wall led to a partial dilation of aortic lumens. All these changes suggest that increased MMP-12 activity enhances aortic remodeling. Several possible mechanisms exist for these pathological changes in Tg rabbits. First, increased elastolytic activity of MMP-12 derived from adventitial macrophages may directly lead to the degradation of aortic elastin and other extracellular matrices. More importantly, in addition to MMP-12, other MMPs such as MMP-2 and -3 also derived from increased infiltrating macrophages may be upregulated in the lesions as shown by the results of Western blotting and real-time RT-PCR. Thus, it is likely that increased activity of MMP-12 may trigger the activation of other MMPs (Matsumoto et al., 1998) which work together in aortic remodeling. Second, increased MMP-12 may also result in increased macrophage infiltration through the generation of elastin peptide, which can induce monocyte chemotaxis (Senior et al., 1980). Of note, MCP-1, a potent chemoattractant for monocytes, was highly expressed in the lesions, which may indirectly indicate a high degree of inflammation. Lanone et al. (2002) demonstrated that MMP-12 can accelerate IL-13-induced inflammatory infiltration whereas MMP-12-deficient macrophages showed diminished proteolytic activity and migration (Shipley et al., 1996). Consistent with these observations, a deficiency in MMP-12 gene attenuated calcium chloride-induced aneurysm growth with less infiltration by macrophages in MMP-12 KO mice (Longo et al., 2005) although there was no effect on the elastase-infusion model (Pyo et al., 2000).

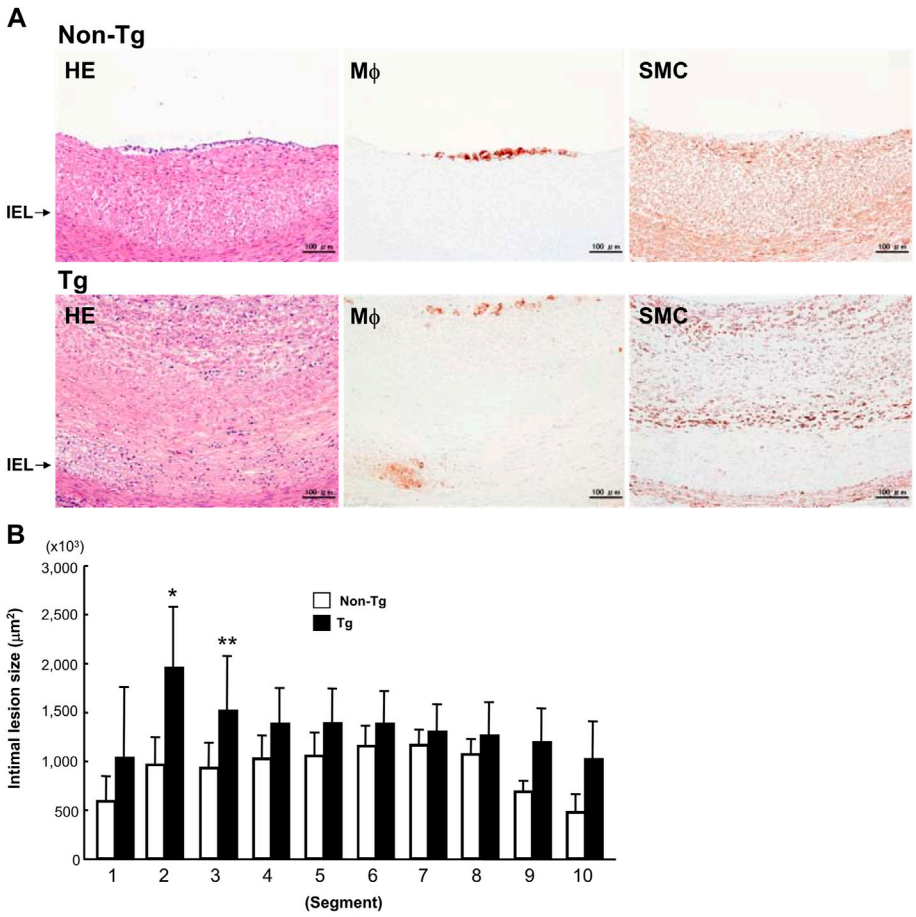

FIGURE 5
Representative intimal atherosclerotic lesions of Tg and non-Tg rabbits **(A)** and quantitation of intimal lesions **(B)**. A: Cross-sections of the aorta were stained with H&E or immunohistochemically stained with Abs against macrophages (Mϕ) and smooth muscle cells (SMC). B: The area occupied by intimal lesions was measured using an image analysis system as described in the Materials and Methods. The data were expressed as the mean ± SE (n = 12 for each group). *p < .05, **p < .01 vs. non-Tg.

As mentioned above, we failed to observe gross aneurysms in the damaged abdominal aortas though we did observe dilated lesions under the microscope. This may be because in the current model, we covered the carrageenan-induced peri-aortic lesions with a sheet of polyethylene film to prevent inflammatory adhesion to the adjacent tissues, which may limit remarkable dilation of the aortic wall or aneurysms. Alternatively, the period of observation was not long enough for AAAs to form. Therefore, this model is merely an adventitial inflammatory model rather than a true AAA model. While having such a flaw, we could assess the influence of MMP-12 on aortic remodeling, which is closely associated with the formation of AAA. Recently, we also generated transgenic rabbits expressed high levels of MMP-1 and MMP-9 in macrophages (Niimi et al., 2019; Chen et al., 2020). It seems that MMP-1 is also involved in the formation of AAA but MMP-9 contributes the vascular calcification formation. In future, it needs to compare these MMPs in terms of AAA development.

In addition to the medial and adventitial lesions, we found that intimal atherosclerotic lesions were also more frequent in Tg rabbits than non-Tg rabbits. However, these intimal lesions were essentially characterized by the proliferation of SMCs whereas macrophage infiltration was less prominent. This result was surprising because the SMC-rich lesions induced by adventitial inflammation were sharply different from the foam cell-rich lesions often observed in the aortic arch and thoracic aortas of cholesterol-fed rabbits (Liang et al., 2006). It seems that the SMC-rich lesions seen in these rabbits are more like injury-induced (balloon or cuff) lesions (Booth et al., 1989; Kockx et al., 1993). It has been reported that enhanced elastin fragmentation is required for the migration and proliferation of SMCs (Zempo et al., 1994; Southgate et al., 1996). Because we merely examined the aortic lesions at 24 weeks after surgery, it is also possible that macrophage-rich lesions are present in the early stages.

In conclusion, we have demonstrated that adventitial inflammation can affect aortic remodeling, and increased activity of MMP-12 derived from infiltrating macrophages leads to the enhanced formation of lesions. These results suggest that adventitial inflammation is a crucial stimulus for the development of vascular lesions and remodeling. Our findings clearly support the hypothesis that MMP-12 derived from adventitial macrophages plays an important role in the pathogenesis of atherosclerotic disease such as AAA. It would be interesting to examine whether the

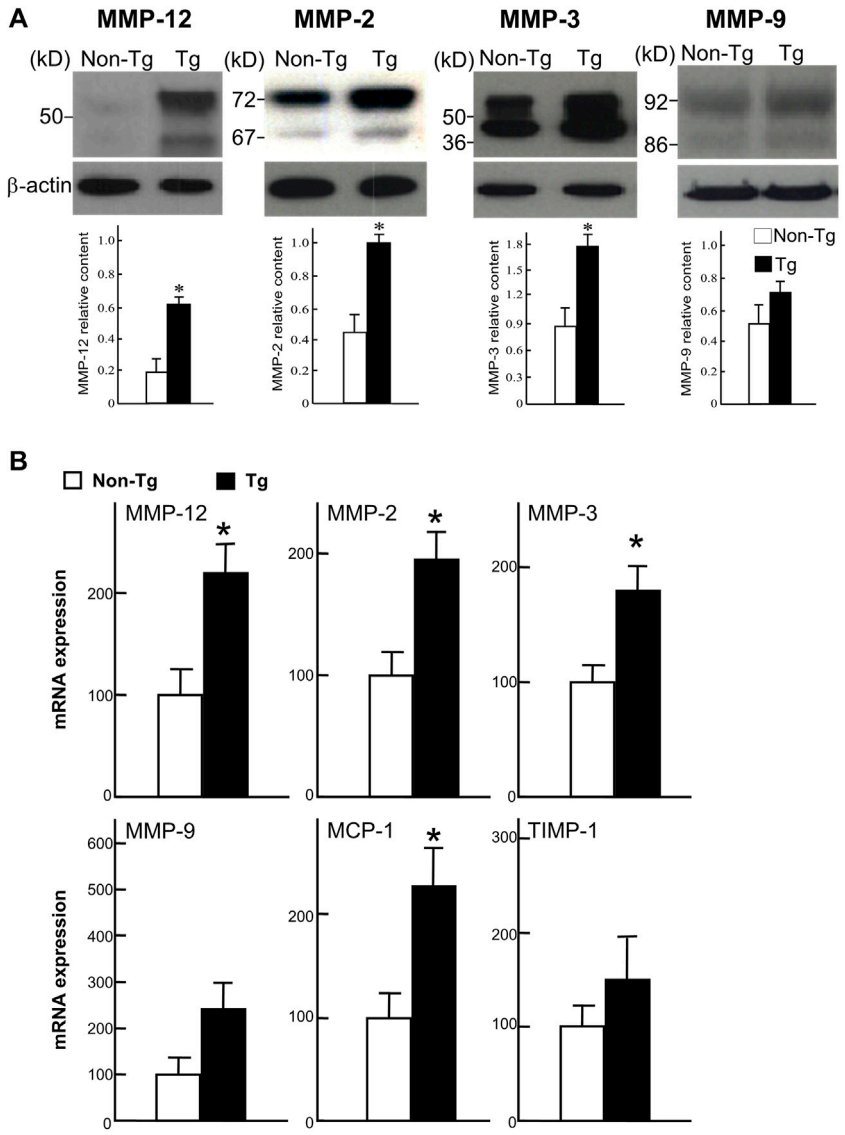

FIGURE 6
Western blot analysis **(A)** and real-time RT-PCR analysis **(B)**. A: Proteins isolated from the aortic lesions were subjected to 10% SDS-PAGE under reducing conditions, and probed with Abs against MMP-12, MMP-2, MMP-3, and MMP-9. The same membrane was re-probed with mAb against β-actin to indicate that equal amounts of proteins were loaded. The relative level of each MMP was quantitated by calculating the optical density (OD) of each signal on the films using a densitometer (GS-700, Bio-Rad) and normalized relative to the amount of protein for β-actin. All analyses were performed in triplicate and the values are expressed as the mean ± SE (n = 3 for each group). *p < .05 vs. non-Tg. B: Expression of MMP-12, -2, -3, and -9, MCP-1, and TIMP-1 were analyzed with real-time RT-PCR. Expression levels of each gene are expressed as a percentage of the control value. Data are expressed as the mean ± SE (n = 5 for each group). *p < .05 vs. non-Tg.

administration of a MMP-12 specific inhibitor (Devel et al., 2006) prevents the formation of atherosclerosis *in vivo*.

Data availability statement

The raw data supporting the conclusion of this article will be made available by the authors, without undue reservation.

Ethics statement

The animal study was reviewed and approved by University of Yamanashi.

Author contributions

YC, XY, HY, and JF designed this study. YC, XY, SK, and LQ performed most of the experiments and data analysis. YW and MZ provided assistance in molecular experiments. EL and HY performed the histological examinations and analysis. LL, HY, and JF prepared the manuscript. HY and JF supervised this study.

Funding

This work was supported the National Natural Science Foundation of China (No. 81941001, 82100482, and

82200504), National Key Research and Development Program of China (2022YFA1105403), Science and Technology Planning Project of Guangdong Province (2021A1515110916, 2020A1515110213, 2021A1515110008), and Innovation team program supported by Guangdong Province (2020KCXTD038). Application Foundation Project Support by Jiangmen City (2021030103170007301), Guangdong Province Key Program of Discipline (2021ZDJS091).

Conflict of interest

The authors declare that the research was conducted in the absence of any commercial or financial relationships that could be construed as a potential conflict of interest.

Publisher's note

Supplementary material

The Supplementary Material for this article can be found online at: https://www.frontiersin.org/articles/10.3389/fcell.2022.1097137/full#supplementary-material

References

Alcorn, H. G., Wolfson, S. K., Jr., Sutton-Tyrrell, K., Kuller, L. H., and O'Leary, D. (1996). Risk factors for abdominal aortic aneurysms in older adults enrolled in the Cardiovascular Health Study. *Arterioscler. Thromb. Vasc. Biol.* 16, 963–970. doi:10.1161/01.atv.16.8.963

Banda, M. J., and Werb, Z. (1981). Mouse macrophage elastase. Purification and characterization as a metalloproteinase. *Biochem. J.* 193, 589–605. doi:10.1042/bj1930589

Booth, R. F., Martin, J. F., Honey, A. C., Hassall, D. G., Beesley, J. E., and Moncada, S. (1989). Rapid development of atherosclerotic lesions in the rabbit carotid artery induced by perivascular manipulation. *Atherosclerosis* 76, 257–268. doi:10.1016/0021-9150(89)90109-3

Chandler, S., Cossins, J., Lury, J., and Wells, G. (1996). Macrophage metalloelastase degrades matrix and myelin proteins and processes a tumour necrosis factor-alpha fusion protein. *Biochem. Biophys. Res. Commun.* 228, 421–429. doi:10.1006/bbrc.1996.1677

Chen, Y., Waqar, A. B., Nishijima, K., Ning, B., Kitajima, S., Matsuhisa, F., et al. (2020). Macrophage-derived MMP-9 enhances the progression of atherosclerotic lesions and vascular calcification in transgenic rabbits. *J. Cell Mol. Med.* n/a, 4261–4274. doi:10.1111/jcmm.15087

Curci, J. A., Liao, S., Huffman, M. D., Shapiro, S. D., and Thompson, R. W. (1998). Expression and localization of macrophage elastase (matrix metalloproteinase-12) in abdominal aortic aneurysms. *J. Clin. Invest.* 102, 1900–1910. doi:10.1172/JCI2182

Devel, L., Rogakos, V., David, A., Makaritis, A., Beau, F., Cuniasse, P., et al. (2006). Development of selective inhibitors and substrate of matrix metalloproteinase-12. *J. Biol. Chem.* 281, 11152–11160. doi:10.1074/jbc.M600222200

Fan, J., Chen, Y., Yan, H., Liu, B., Wang, Y., Zhang, J., et al. (2018). Genomic and transcriptomic analysis of hypercholesterolemic rabbits: Progress and perspectives. *Int. J. Mol. Sci.* 19, 3512–3523. doi:10.3390/ijms19113512

Fan, J., Kitajima, S., Watanabe, T., Xu, J., Zhang, J. F., Liu, E. Q., et al. (2015). Rabbit models for the study of human atherosclerosis: From pathophysiological mechanisms to translational medicine. *Pharmacol. Ther.* 146, 104–119. doi:10.1016/j.pharmthera.2014.09.009

Fan, J., Wang, X., Wu, L., Matsumoto, S. I., Liang, J., Koike, T., et al. (2004). Macrophage-specific overexpression of human matrix metalloproteinase-12 in transgenic rabbits. *Transgenic Res.* 13, 261–269. doi:10.1023/b:trag.0000034717.70729.61

Freestone, T., Turner, R. J., Higman, D. J., Lever, M. J., and Powell, J. T. (1997). Influence of hypercholesterolemia and adventitial inflammation on the development of aortic aneurysm in rabbits. *Arterioscler. Thromb. Vasc. Biol.* 17, 10–17. doi:10.1161/01.atv.17.1.10

Gertz, S. D., Kurgan, A., and Eisenberg, D. (1988). Aneurysm of the rabbit common carotid artery induced by periarterial application of calcium chloride *in vivo*. *J. Clin. Invest.* 81, 649–656. doi:10.1172/JCI113368

Golledge, J., Muller, J., Daugherty, A., and Norman, P. (2006). Abdominal aortic aneurysm: Pathogenesis and implications for management. *Arterioscler. Thromb. Vasc. Biol.* 26, 2605–2613. doi:10.1161/01.ATV.0000245819.32762.cb

Gronski, T. J., Jr., Martin, R. L., Kobayashi, D. K., Walsh, B. C., Holman, M. C., Huber, M., et al. (1997). Hydrolysis of a broad spectrum of extracellular matrix proteins by human macrophage elastase. *J. Biol. Chem.* 272, 12189–12194. doi:10.1074/jbc.272.18.12189

Horvai, A., Palinski, W., Wu, H., Moulton, K. S., Kalla, K., and Glass, C. K. (1995). Scavenger receptor A gene regulatory elements target gene expression to macrophages and to foam cells of atherosclerotic lesions. *Proc. Natl. Acad. Sci. U. S. A.* 92, 5391–5395. doi:10.1073/pnas.92.12.5391

Johnson, J. L., George, S. J., Newby, A. C., and Jackson, C. L. (2005). Divergent effects of matrix metalloproteinases 3, 7, 9, and 12 on atherosclerotic plaque stability in mouse brachiocephalic arteries. *Proc. Natl. Acad. Sci. U. S. A.* 102, 15575–15580. doi:10.1073/pnas.0506201102

Kockx, M. M., De Meyer, G. R., Andries, L. J., Bult, H., Jacob, W. A., and Herman, A. G. (1993). The endothelium during cuff-induced neointima formation in the rabbit carotid artery. *Arterioscler. Thromb.* 13, 1874–1884. doi:10.1161/01.atv.13.12.1874

Lanone, S., Zheng, T., Zhu, Z., Liu, W., Lee, C. G., Ma, B., et al. (2002). Overlapping and enzyme-specific contributions of matrix metalloproteinases-9 and -12 in IL-13-induced inflammation and remodeling. *J. Clin. Invest.* 110, 463–474. doi:10.1172/JCI14136

Liang, J., Liu, E., Yu, Y., Kitajima, S., Koike, T., Jin, Y., et al. (2006). Macrophage metalloelastase accelerates the progression of atherosclerosis in transgenic rabbits. *Circulation* 113, 1993–2001. doi:10.1161/CIRCULATIONAHA.105.596031

Liapis, C. D., and Paraskevas, K. I. (2003). The pivotal role of matrix metalloproteinases in the development of human abdominal aortic aneurysms. *Vasc. Med.* 8, 267–271. doi:10.1191/1358863x03vm504ra

Longo, G. M., Buda, S. J., Fiotta, N., Xiong, W., Griener, T., Shapiro, S., et al. (2005). MMP-12 has a role in abdominal aortic aneurysms in mice. *Surgery* 137, 457–462. doi:10.1016/j.surg.2004.12.004

Matsumoto, S., Kobayashi, T., Katoh, M., Saito, S., Ikeda, Y., Kobori, M., et al. (1998). Expression and localization of matrix metalloproteinase-12 in the aorta of cholesterol-fed rabbits: Relationship to lesion development. *Am. J. Pathol.* 153, 109–119. doi:10.1016/s0002-9440(10)65551-4

Michel, J. B., Thaunat, O., Houard, X., Meilhac, O., Caligiuri, G., and Nicoletti, A. (2007). Topological determinants and consequences of adventitial responses to arterial wall injury. *Arterioscler. Thromb. Vasc. Biol.* 27, 1259–1268. doi:10.1161/ATVBAHA.106.137851

Niimi, M., Nishijima, K., Kitajima, K., Matsuhisa, F., Koike, Y., Koike, K., et al. (2019). Macrophage-derived matrix metalloproteinase-1 accelerates aortic aneurysm formation in transgenic rabbits. *J. Biomed. Res.* 33, 271–279. doi:10.7555/JBR.33.20180097

Pyo, R., Lee, J. K., Shipley, J. M., Curci, J. A., Mao, D., Ziporin, S. J., et al. (2000). Targeted gene disruption of matrix metalloproteinase-9 (gelatinase B) suppresses development of experimental abdominal aortic aneurysms. *J. Clin. Invest.* 105, 1641–1649. doi:10.1172/JCI8931

Senior, R. M., Griffin, G. L., and Mecham, R. P. (1980). Chemotactic activity of elastin-derived peptides. *J. Clin. Invest.* 66, 859–862. doi:10.1172/JCI109926

Shah, P. K. (1997). Inflammation, metalloproteinases, and increased proteolysis: An emerging pathophysiological paradigm in aortic aneurysm. *Circulation* 96, 2115–2117. doi:10.1161/01.cir.96.7.2115

Shapiro, S. D., Kobayashi, D. K., and Ley, T. J. (1993). Cloning and characterization of a unique elastolytic metalloproteinase produced by human alveolar macrophages. *J. Biol. Chem.* 268, 23824–23829. doi:10.1016/s0021-9258(20)80459-1

Shipley, J. M., Wesselschmidt, R. L., Kobayashi, D. K., Ley, T. J., and Shapiro, S. D. (1996). Metalloelastase is required for macrophage-mediated proteolysis and matrix invasion in mice. *Proc. Natl. Acad. Sci. U. S. A.* 93, 3942–3946. doi:10.1073/pnas.93.9.3942

Southgate, K. M., Fisher, M., Banning, A. P., Thurston, V. J., Baker, A. H., Fabunmi, R. P., et al. (1996). Upregulation of basement membrane-degrading metalloproteinase secretion after balloon injury of pig carotid arteries. *Circ. Res.* 79, 1177–1187. doi:10.1161/01.res.79.6.1177

Thompson, R. W., Curci, J. A., Ennis, T. L., Mao, D., Pagano, M. B., and Pham, C. T. (2006). Pathophysiology of abdominal aortic aneurysms: Insights from the elastase-induced model in mice with different genetic backgrounds. *Ann. N. Y. Acad. Sci.* 1085, 59–73. doi:10.1196/annals.1383.029

Thompson, R. W., and Parks, W. C. (1996). Role of matrix metalloproteinases in abdominal aortic aneurysms. *Ann. N. Y. Acad. Sci.* 800, 157–174. doi:10.1111/j.1749-6632.1996.tb33307.x

Wang, X., Liang, J., Koike, T., Sun, H., Ichikawa, T., Kitajima, S., et al. (2004). Overexpression of human matrix metalloproteinase-12 enhances the development of inflammatory arthritis in transgenic rabbits. *Am. J. Pathol.* 165, 1375–1383. doi:10.1016/S0002-9440(10)63395-0

Wassef, M., Upchurch, G. R., Jr., Kuivaniemi, H., Thompson, R. W., and Tilson, M. D., 3rd (2007). Challenges and opportunities in abdominal aortic aneurysm research. *J. Vasc. Surg.* 45, 192–198. doi:10.1016/j.jvs.2006.09.004

Yu, Y., Koike, T., Kitajima, S., Liu, E., Morimoto, M., Shiomi, M., et al. (2008). Temporal and quantitative analysis of expression of metalloproteinases (MMPs) and their endogenous inhibitors in atherosclerotic lesions. *Histology Histopathol.* 23, 1503–1516. doi:10.14670/HH-23.1503

Zempo, N., Kenagy, R. D., Au, Y. P., Bendeck, M., Clowes, M. M., Reidy, M. A., et al. (1994). Matrix metalloproteinases of vascular wall cells are increased in balloon-injured rat carotid artery. *J. Vasc. Surg* 20, 209–217. doi:10.1016/0741-5214(94)90008-6

frontiers | Frontiers in Cell and Developmental Biology

TYPE Mini Review
PUBLISHED 12 January 2023
DOI 10.3389/fcell.2022.1093534

OPEN ACCESS

EDITED BY
Feng Yue,
Hainan University, China

REVIEWED BY
Jiaojiao Huang,
Qingdao Agricultural University, China
Ling Shuai,
Nankai University, China
Yongchang Chen,
Kunming University of Science and Technology, China

*CORRESPONDENCE
Chengcheng Tang,
wyuchemtcc@126.com
Xiaoqing Zhou,
wyuchemzxq@126.com

SPECIALTY SECTION
This article was submitted to Stem Cell Research, a section of the journal Frontiers in Cell and Developmental Biology

RECEIVED 09 November 2022
ACCEPTED 31 December 2022
PUBLISHED 12 January 2023

CITATION
Xi J, Zheng W, Chen M, Zou Q, Tang C and Zhou X (2023), Genetically engineered pigs for xenotransplantation: Hopes and challenges.
Front. Cell Dev. Biol. 10:1093534.
doi: 10.3389/fcell.2022.1093534

Genetically engineered pigs for xenotransplantation: Hopes and challenges

Jiahui Xi, Wei Zheng, Min Chen, Qingjian Zou, Chengcheng Tang* and Xiaoqing Zhou*

Guangdong Provincial Key Laboratory of Large Animal Models for Biomedicine, South China Institute of Large Animal Models for Biomedicine, School of Biotechnology and Health Science, Wuyi University, Jiangmen, China

The shortage of donor resources has greatly limited the application of clinical xenotransplantation. As such, genetically engineered pigs are expected to be an ideal organ source for xenotransplantation. Most current studies mainly focus on genetically modifying organs or tissues from donor pigs to reduce or prevent attack by the human immune system. Another potential organ source is interspecies chimeras. In this paper, we reviewed the progress of the genetically engineered pigs from the view of immunologic barriers and strategies, and discussed the possibility and challenges of the interspecies chimeras.

KEYWORDS

genetically engineered pigs, xenotransplantation, immunologic barriers, interspecies chimeras, porcine endogenous retroviruses (PERV)

1 Introduction

Organ transplantation is one of the greatest medical achievements in the 20th century and has saved the lives of thousands of patients who were suffering from organ failure. With the rapid developments in surgical techniques and the utilization of immunosuppressive agents, allotransplantation has become the only available treatment for end-stage organ failure in biomedicine. However, the disparity between organ supply and the demand for human organs is a bottleneck for clinical allotransplantation. According to the statistical results of United States Government Information on Organ Donation and Transplantation, 105,000 patients are currently waiting for transplants in the United States at present, and approximately 17 people die daily whilst waiting for a transplant. The organ supply in developed countries can only meet 15% of the needs, and about one-fifth of patients die while waiting. In China, the ratio of patients on the waiting list to the transplant recipients is 30: 1.6 (Pan et al., 2019). Research on xenotransplantation was brought into being because of the increasingly arresting contradiction between organ supply and the demand for organ resources. Many disorders could be treated with clinical xenotransplantation (Figure 1) (Ekser et al., 2012). At present, various large animals have been used in xenotransplantation, including pigs, monkeys, chimpanzees and baboons. Pigs are considered the most ideal organ xenograft donor because their organ size, physiological metabolism and immune system are similar to those of human beings. However, natural immunologic barriers exist between pig organs and human organs. So how can suitable pig organs be produced for xenotransplantation?

One approach is to genetically modify the donor pigs to reduce or prevent attack by the human immune system, and thus achieve the compatibility with the human body. Another possible approach is the use of interspecies chimeras, in which human stem cells are made chimeric with pigs with specific organ defects, and then developed into a particular organ under a human micro-environment.

2 Genetically modified pigs provide organs for xenotransplantation

In recent years, some non-cellular tissues from pigs have been used in clinical applications, such as pig cardiac valves for plastic surgery, small intestinal submucosa for bladder repair, and dermis for extensive burns (Laurencin and El-Amin, 2008). Meanwhile, the use of pigs with one or more immune-related genes modified has made a significant advance in solid organ transplantation from pigs to other large animals, and has resulted in remarkably long survival times for both recipients and grafts (Cooper, 2003). The survival time of neurons from *CTLA4-Ig* modified pigs reached 549 days after xenotransplantation (Badin et al., 2013). Islet cells xenografted from *hCD46* transgenic pigs survived for 950 days (Shin et al., 2016). The use of genetically modified pigs has greatly addressed the immune barriers to xenotransplantation. Hyperacute rejection and acute cellular rejection have been nearly overcome (Kuwaki et al., 2005), and results from these studies have greatly contributed to research on acute vascular rejection and chronic rejection. With the discovery of an increasing number of immune-related key genes and the rapid development of efficient gene modification methods, the clinical application of xenotransplantation using genetically modified pigs as donors in preclinical application is becoming more feasible (Table 1). The immune barriers to xenotransplantation can be overcome *via* several genetic modification strategies that address the different modes of rejection discussed below.

2.1 Hyperacute rejection

This type of rejection is mediated by the xenoreactive natural antibodies (XNAs) from the recipient and occur within minutes or hours after the restoration of xenograft blood circulation. XNAs bind to the xenoantigens of the xenograft and activate the classical complement pathway in the recipient, resulting in interstitial hemorrhage, edema and thrombosis of the xenograft, and finally leading to inactivation and necrosis of the xenograft within a few minutes or hours (Shimizu and Yamada, 2006). After more than a century of research, various methods to prevent hyperacute rejection have been developed. The first and most essential method is to reduce or eliminate the expression of galactose-α1,3-galactose (α-Gal), which is the main xenoantigen recognized by XNAs. α-Gal is expressed by α-1, 3-galactosyltransferase (*GGTA1*) gene and functions in pigs, but not in human beings, apes, or Old World monkeys (Good et al., 1992; Cooper et al., 1993). In 2002, Lai et al. and Dai et al. first produced clone pigs with *GGTA1* gene deficient, which was seen as a milestone of xenotransplantation field (Dai et al., 2002; Lai et al., 2002). Subsequently, an increasing number of GTKO (*GGTA1* knock out) pigs have been generated and used in xenotransplantation research (Cheng et al., 2016; Feng et al., 2016). When xenograft organs from GTKO pigs were transplanted into non-human primates, the survival times of the xenograft and the recipient were significantly prolonged, and the

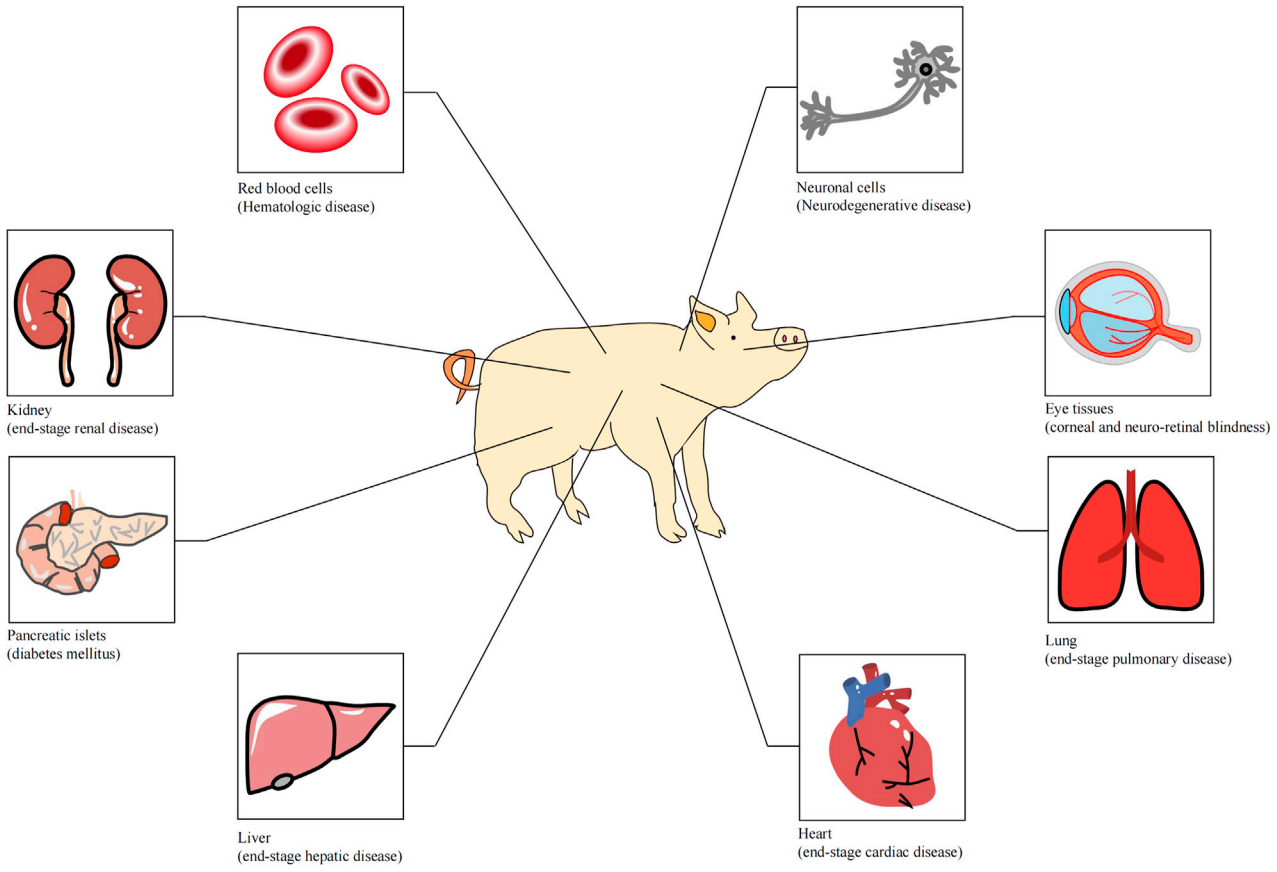

FIGURE 1
Tissues or organs that can be used for xenotransplantation (Ekser et al. 2012).

TABLE 1 Genetically modified pigs for xenotransplantation.

	Target genes	Gene modifications	Functions	References
Incompatible epitopes	*GGTA1*	Gene knockout	Deletion of α-Gal epitope	Cheng et al. (2016); Dai et al. (2002); Feng et al. (2016); Gao et al. (2017); Kolber-Simonds et al., 2004; Lai et al. (2002); Phelps et al., 2003)
	GGTA1/hCD46	Gene knockout & Transgenic	Deletion of α-Gal epitope, inactivation of complement system	Dong et al. (2017); Mohiuddin et al. (2010)
	GGTA1/β4GalNT2	Gene knockout	Deletion of α-Gal epitope and SDa blood group	Adams et al. (2018)
	GGTA1/CMAH	Gene knockout	Deletion of α-Gal epitope and N-glycolylneuraminic acid	Lai et al. (2002); Li et al. (2015); Lutz et al. (2013)
	GGTA1/β4GalNT2/CMAH	Gene knockout	Deletion of α-Gal epitope, N-glycolylneuraminic acid and SDa blood group	Estrada et al. (2015); Zhang et al. (2018)
Immunological cell	*hCTLA4-Ig*	Transgenic	Reduction of the proliferative response of human T lymphocytes	(badin et al., 2010; Martin et al. (2005)
	GGTA1/HLA-G	Gene knockout & Transgenic	Reduction of NK cell attack	Zhou et al. (2022)
	CIITA-DN	Transgenic	Suppression of T-cell activation	Hara et al. (2013)
	HLA-E/β2m	Transgenic	Protection of against human NK cell-mediated cytotoxicity	Weiss et al. (2009)
	A20	Transgenic	Reduction of apoptosis and inflammatory stimuli	Oropeza et al. (2009)
Complement system	*hCD46*	Transgenic	Inactivation of complement system	(Diamond et al., 2001; van der Windt et al. (2009)
	hCD55	Transgenic	Acceleration of complement decay	(Baldan et al., 2004)
PERV	PERV	Gene knockout	Inactivation of porcine endogenous retrovirus	Niu et al. (2017)
Multiple system	PERV/*GGTA1/CMAH/B4GALNT2/hCD46/hCD55/hCD59/hTHBD/hTFPI/hCD39/hB2M/HLA-E/hCD47*	Gene knockout & Transgenic	Inactivation of porcine endogenous retrovirus, deletion of α-Gal epitope, inactivation of complement system	Yue et al. (2021)

frequency of hyperacute rejection was significantly reduced or even disappeared. In other studies, a heart from a GTKO/*hTBM/hCD46* pig survived for 945 days after transplantation into baboons (Mohiuddin et al., 2016), and kidney xenografts from a GTKO/*hCD55* pig survived for 499 days after transplantation into rhesus macaque (Kim et al., 2019).

Except for α-Gal, two other non-Gal epitopes present an additional barrier to xenotransplantation. One is N-glycolylneuraminic acid (Neu5Gc), which is encoded by CMP-N-acetylneuraminic acid hydroxylase (*CMAH*) gene (Song et al., 2010). The other is the SDa blood group, which is produced by beta-1,4-N-acetyl-galactosaminyltransferase 2 (β4GALNT2) (Byrne, Ahmad-Villiers, Du, & McGregor, 2018). Attempts have been made to overcome these new xenoantigens by developing new transgenic pigs. The double or triple knockout pigs, which eliminate a-Gal, Neu5Gc, and the SDa epitopes, exhibited reduced human antibody binding *in vitro* (Lutz et al., 2013; Estrada et al., 2015; Li et al., 2015; Adams et al., 2018).

Another method for preventing hyperacute rejection is to inhibit complement response. Hyperacute rejection is mainly caused by the activation of complement pathway when XNAs bind to α-Gal. Thus, inhibiting the complement response can achieve the same effect. Numerous studies have shown that the frequency of hyperacute rejection during xenotransplantation was significantly reduced when transgenic pigs with human complement regulatory proteins (hCRPs) such as CD46, CD55, or CD59 were used (Huang et al., 2001; Dong et al., 2017; Gao et al., 2017; Zhang et al., 2018). Pancreas grafts from *hCD46* transgenic pigs survived 396 days after transplantation into non-human primates (van der Windt et al., 2009). Kidney grafts from GTKO/*hCD55* pigs survived for 499 days (Kim et al., 2019). Heart grafts from GTKO/*hTBM/hCD46* gene-modified pigs survived for 945 days (Mohiuddin et al., 2016). These results suggest that inhibition of the complement response is another effective way of inhibiting hyperacute rejection.

Other methods can also be used to inhibit hyperacute rejection. For example, the level of α-Gal can be reduced by transducing enzymes that compete with α-1, 3-galactosyltransferase (Sharma et al., 1996). In another study, specific siRNA was used to reduce the expression of α-1, 3 galactosyltransferase *via* RNA interference (Zhu et al., 2005). Plasmapheresis can decrease the level of α-1, 3 galactosyltransferase, which reduces the risk of activation of the complement response and delayed hypersensitivity (Watts et al., 2000).

2.2 Acute vascular rejection

Acute vascular rejection usually occurs two to three days after xenotransplantation. However, a detailed mechanism for this response remains unclear. This rejection may be caused by the interaction between the xenograft and the recipient's xenoantibodies, macrophages, or platelets. The combination of XNAs and xenograft endothelial causes the activation of xenograft endothelial cells and receptor of macrophage, which induces the expression of various specific proteins, including cytokines, endothelial adhesion molecules, and blood coagulation factors. These factors can cause inflammation, thrombosis, cellulose precipitation or diffuse blood clotting in the xenograft, which lead to xenograft loss or inactivation (Gollackner et al., 2004). At present, the main strategies for addressing acute vascular rejection are to inhibit the activities of endothelial cells and macrophage, induce the expression of anticoagulants on the surface of porcine organs, and inhibit NF-kB signaling.

1) Inhibition of activity of endothelial cells and macrophage. Endothelial cells and macrophage release a variety of cytokines after activation. These cytokines participate in inflammation, thrombosis, and coagulation formation. Inhibition of macrophages and endothelial activities helps alleviate acute vascular rejection. Meanwhile, human leukocyte antigen G (HLA-G), a non-classical MHC Ⅰ molecule, is mainly expressed in the extravillous trophoblast cells of the maternal-fetal barrier and plays an significant role in maintaining maternal immune tolerance to the fetus as well as normal pregnancy. In xenotransplantation, the soluble HLA-G can protect porcine endothelial cells from NK cell; thus, *HLA-G* transgenic pigs are a potential option as donors in xenotransplantation (M. H. Zeng et al., 2006). The fibroblasts from the GTKO/*HLA-G5* pigs showed enhanced resistance to complement-mediated lysis ability (Zhou et al., 2022). HLA-E/human beta2-microglobulin transgenic pigs showed the protection against xenogeneic human anti-pig natural killer cell cytotoxicity (Weiss et al., 2009). Signal regulatory protein α (SIRPα), a major macrophage inhibitory receptor, can inhibit the macrophages activity when it binds to CD47. Porcine cells that expressing human CD47 could almost completely resist phagocytosis by macrophages (Ide et al., 2007).
2) Induction of the expression of anticoagulants on the surface of porcine organs. Coagulation dysfunction is an important cause of acute vascular rejection. The expression of one or more anticoagulant substances on the surface of pig organs by genetically modified methods, can significantly inhibit platelet aggregation and activation after xenotransplantation, thus alleviating the acute vascular rejection (Crikis et al., 2010). The same effect can be achieved by reducing the expression of procoagulant substances.
3) Inhibition of NF-kB signaling. Endothelial adhesion factors, cytokines and procoagulant factors mostly function through the NF-kB signaling pathway and participate in the formation of inflammation, thrombosis, and coagulation. The A20 protein can regulate the NF-kB expression, inhibit NF-kB activation and nuclear transfer, prevent endothelial cells activation and prevent the production of related inflammatory molecules such as vascular cell adhesion molecules and interleukins, thus inhibiting acute vascular rejection (Ferran, Stroka, Badrichani, Cooper, & Bach, 1997; Oropeza et al., 2009).

2.3 Acute cellular rejection

Hyperacute rejection and acute vascular rejection are mainly related to humoral immune system, whereas acute cellular rejection is primarily based on cell immunity. The most important cells in acute cellular rejection are NK cells and T lymphocytes. After xenotransplantation, antigen presenting cells present xenoantigen epitopes to recipient $CD4^+$ T Cells *via* xenogeneic MHC class Ⅱ molecules. The xenoantigen of the graft can also be presented to $CD8^+$ T cells *via* the MHC class I molecules of the recipient. The proliferation of $CD4^+$ T cells and $CD8^+$ T cells induces the production of interleukin-2 (IL-2) and interferon-γ (IFN-γ), which induces a series of immune rejection reactions (Maksoud, 2004). At present, T cell response is mainly inhibited by multigenic modifications that reduce acute cellular rejection. Pigs with multigenic GTKO/hCRPs modification were originally developed to overcome primary humoral immunity, however, Gal epitope loss and hCRP expression on porcine cell surfaces can also slow down the T cell proliferation and some cytokine mediated responses, thereby inhibiting acute cellular rejection to a certain extent (Xu, Goodman, Sasaki, Lowell, & Mohanakumar, 2002; Saethre et al., 2008). Cytotoxic effects mediated by human $CD8^+$ T Cells, especially $CD8^+$ CTL cells, mainly occur through the Fas/FasL apoptosis pathway. Kawamoto et al. overexpressed human FasL and Fas in pig islet cells, and found that the overexpression interfered with the apoptotic pathway, resulting in resistance to the cytotoxic effect mediated by $CD8^+$CTL cells (Kawamoto et al., 2006). Recombinant hCTLA4-Ig expressed in piglets induced a 50% reduction in the proliferative response of human T lymphocytes, thus specifically and effectively inhibiting cellular and humoral immunity through negative immune regulation (Martin et al., 2005). Badin et al. transplanted the neuronal cells from *hCTLA4-Ig* transgenic pigs into Parkinson monkeys and observed long-term clinical recovery in the monkeys (Badin et al., 2010). Hara et al. found that the knockdown of CIITA, an MHC class Ⅱ transactivator, can effectively reduce the expression of MHC class Ⅱ molecules in pigs, thereby slowing down the stimulation of $CD4^+$ T cells and reducing xenoantibody-mediated injury and T cell response (Hara et al., 2013).

2.4 Chronic rejection

To date, the chronic rejection in immune disorders has not been convincingly explained. Chronic rejection usually occurs months or years after xenotransplantation and mainly proceeds through humoral immunity, which is mediated by XNAs and the complement system. The low immune response of XNAs in the circulatory system leads to perivascular inflammation and injury to the vascular endothelium of the xenograft, which is accompanied by proliferation of vascular smooth muscle cells that block the blood vessels, and eventually leads to arteriosclerosis and xenograft loss. Chronic rejection may be inhibited by transducing new anti-inflammatory genes, such as *TFPI* (tissue factor inhibitor), *ENTPD1* (*CD39*), and *hHO-1* (human heme oxidase), to GTKO/hCRPs pigs. Of course, it still needs to be strengthened in overcoming chronic rejection before xenotransplantation comes into clinical applications.

Except for reduction or prevention the attack by the human immune system, how to improve the activity of transplanted organ is also a key concern. As reported, deletion of p53 or overexpression of

BCL2 could inhibit cell apoptosis (Masaki et al., 2016; Olbrich et al., 2017; Zhang et al., 2020), which could provide a new different approach to inhibit exnograft cell apoptosis or prolong xenograft cell survival.

3 Interspecies chimeras

Another potential organ source is by creating human organs from human pluripotent stems cells (PSCs) in animal bodies *via* forming interspecies chimeras. Chimeras refer to cells in an organism that are derived from two different zygotes. This phenomenon usually occurs during embryonic development and does not involve immune rejection (or good immune tolerance). Chimerism has been reported in humans under natural conditions (such as in twins) (Dunsford et al., 1953) or during *in-vitro* fertilization (IVF) (Strain, Dean, Hamilton, & Bonthron, 1998). In scientific research, the intraspecies chimerism in lower animals, including drosophila, *xenopus*, zebrafish, birds and other model animals, was first applied in studies on development issues. As an important tool for studying the developmental biology, the use of intraspecies mice chimeras made a very significant contribution to the study of cell fate determination, cell migration, immune system development, organogenesis and stem cells. Therefore, intraspecies chimeras were originally used as a convenient biomarker to study embryonic development (Tarkowski, 1961; Le Douarin and Jotereau, 1975; Le Douarin, Jotereau, Houssaint, & Belo, 1976).

The first reported interspecies chimera that survived to adulthood was a chimera from a goat and a sheep (Fehilly, Willadsen, & Tucker, 1984). That study showed the feasibility of generating interspecies chimeras. In 2001, Mercer et al. reported that human-mouse chimeric liver animals were used as an animal model to study hepatitis C virus infection *in vivo*. Although a high ratio of chimerism was observed in the liver, chimerism in small animals can only be used for human cell level research, and is difficult to use in human organ transplantation (Mercer et al., 2001). In terms of large animals, in 2006, Zeng et al. developed a "human-goat chimera" by injecting bone marrow stem cells at the early stage of goat embryonic development (F. Zeng et al., 2006). However, this process was challenging to do in large animals and easily caused miscarriage, resulting a very low ratio of exogenous cells in animal organs obtained was very low. Only a particular population of cells (e.g., hematopoietic stem cells) can be studied, thus making targeting a specific organ difficult.

With the developments in stem cell research and regenerative medicine, an increasing number of researchers have attempted to use stem cells, particularly patient-derived iPS cells to generate human organs or tissues *in vitro*, which is also one of the ultimate goals of regenerative medicine. In 2016, mouse-rat hetero-diploid embryonic stems cells (ESCs) have been successfully constructed using mouse and rat haploid ESCs. These ESCs had a stable hetero-diploid genome and were able to differentiate into all three germ layers and early germ cells (Li et al., 2016). Given the high complexity of organogenesis, Kobayashi et al. adopted the blastocyst complementation method to mimic the certain microenvironments *in vivo* (Kobayashi et al., 2010). PSCs isolated from a normal mouse or rat were injected into the blastocysts of defective pancreatic development *Pdx1*$^{-/-}$ mice and retransplanted into the uterus of surrogate mice. The newborn mice had a chimeric pancreas and showed normal pancreas function. In 2012, Usui et al. used the same method to obtain allogeneic source compensation in blastocysts from defective renal development *Sall1*$^{-/-}$ mice (Usui et al., 2012). By injecting mouse PSCs into *Pdx1*$^{-/-}$ deficient rat blastocysts, Yamaguchi et al. generated rat-sized pancreata composed of mouse-PSC-derived cells. Islets from these mouse-rat chimaeric pancreata were transplanted into diabetes mice. The transplanted islets successfully normalized and maintained host blood glucose levels for over 370 days in the absence of immunosuppression (Yamaguchi et al., 2017). Aside from the pancreas, many other organs have been generated by blastocyst complementation, including kidney, thymus, blood and vascular endothelial cells, lungs and bronchi, and gametes (Isotani, Hatayama, Kaseda, Ikawa, & Okabe, 2011; Hamanaka et al., 2018; Goto et al., 2019; Mori et al., 2019; Kobayashi et al., 2021). Blastocyst complementation could also generated exogenic pancreas *in vivo* in apancreatic cloned pigs (Matsunari et al., 2013). These studies showed the potential of using xenogeneic animals to generate human organs for clinical application.

However, numerous scientific issues that remain to be addressed before organs can be generated from interspecies chimeras for clinical application: (1) Embryonic mortality is high, and interspecies chimeras such as the *Sall1*$^{-/-}$ mice rarely survive to adulthood. (2) The main barriers to interspecies chimeras, which may be related to the evolutionary distance between species, have not been fully elucidated. (3) Organs are multicellular structures that are organized in three dimensions. Thus, the mechanisms involved in the organ development are immensely complex and multifaceted. (4) The sizes and other morphological characteristics of the chimeric organs are determined by the recipient blastocyst animal, Thus limiting the selection of large animals for clinical application. (5) Primate stem cells are different from rodent stem cells, and their developmental potential, chimerism ability and chimerism timing remain to be determined (Nichols and Smith, 2009). The ratios of chimerism between human ES cells and chicken embryo or human ES cells and mouse blastocyst have been very low (Goldstein, Drukker, Reubinoff, & Benvenisty, 2002; James, Noggle, Swigut, & Brivanlou, 2006). Reports on chimera in rhesus monkeys suggest that these animals require a different approach from that on mice because their cells are heterogeneous at the early stage of blastocyst development (Tachibana et al., 2012). Exhilaratingly, Tan et al. first generated the human-monkey chimeric embryos in 2021, which developed strategies to improve human chimerism in evolutionarily distant species (Tan et al., 2021). Yu et al. derived PSCs from mice, horses, and humans that are permissive for direct PGC-like cell induction *in vitro* and are capable of contributing to intra- or inter-species chimeras *in vivo* (Yu et al., 2021). Currently, many species have been used for the research of interspecies chimerism, including non-human and human related researches (Table 2).

Pigs have always been a good choice as an animal source for xenotransplantation. Chimeric pigs are obtained by injecting inner cell masses into blastocysts (Nagashima, Giannakis, Ashman, & Nottle, 2004). Human-pig chimerism has been reported in human liver cells that had been grafted into pigs *via* intrauterine injection and postnatal injection; the proteins produced by human hepatocytes can be detected in pigs after 6 weeks (Fisher et al., 2013). Of course, such simple grafting, rather than regular chimerism, can produce only certain proteins made by human liver cells, not human cell-derived organs for xenotransplantation. Wu et al. found that instead of naïve hPSCs, an intermediate hPSC type exhibited higher capability to generate differentiated progenies in post-implantation pig embryos

TABLE 2 Interspecies chimerism in different species.

	Chimeric species	Research objects	References
Non-human	Japanese quail-chick	Thymuses and bursa development	Le Douarin and Jotereau, (1975); Le Douarin, Jotereau, Houssaint, and Belo, (1976)
	Goat-sheep	Reproductive incompatibilities	Fehilly, Willadsen, and Tucker, (1984)
	Mouse-rat	Chimeric pancreas	Kobayashi et al. (2010)
	Mouse-rat	Thymus	Isotani, Hatayama, Kaseda, Ikawa, and Okabe, (2011)
	Mouse-rat	Chimeric renal development	Usui et al. (2012)
	Mouse-rat	Hetero-diploid ESCs	Li et al. (2016)
	Mouse-rat	Chimeric pancreata	Yamaguchi et al. (2017)
	Mouse-rat	Pluripotent stem cell-derived mouse kidneys	Goto et al. (2019)
	Monkey-pig	Functional cells derived from monkey	Fu et al. (2020)
	Mouse-rat	Gametes	Kobayashi et al. (2021)
Human related	Human-mouse	Hepatitis C virus infection	Mercer et al. (2001)
	Human-chicken	Integration and differentiation of human embryonic stem cells	Goldstein, Drukker, Reubinoff, and Benvenisty, (2002)
	Human-goat	Multitissue engraftment of human primitive hematopoietic cells and their differentiation	F. Zeng et al. (2006)
	Human-pig	Hepatocytes	Fisher et al. (2013)
	Human-pig	hPSCs derived progenies	Wu et al. (2017)
	Human-monkey	Chimeric competency of human extended pluripotent stem cells	Tan et al. (2021)

(Wu et al., 2017). Fu et al. demonstrated that domesticated cynomolgus monkey embryonic stem cells exhibited the capability to integrate and differentiate into functional cells in a porcine model (Fu et al., 2020). The use of pig-human chimerism still has a long way to go before it can be used in clinical xenotransplantation.

4 Endogenous virus infection in pigs

As an alternative to allotransplantation, xenotransplantation using pig cells, tissues, or organs has made tremendous progress in recent years. However, the clinical use of porcine organs has been hindered by the potential risk of transmission of pig viruses to humans. Although many known potential viruses and microorganisms can be removed by strict feeding conditions, porcine endogenous retroviruses (PERV) are unavoidable. PERV is incorporated into the pig genome in the form of proviral DNA and replicates as the cells proliferate. PERV was integrated into the pig genome more than six million years ago, and formed three subtypes (PERV-A, PERV-B and PERV-C). Two subtypes of PERV-A and -B can be found in the genome of all pigs, and both of which can infect human cells (Patience, Takeuchi, & Weiss, 1997; Takeuchi et al., 1998). By contrast, PERV-C does not ubiquitously appear in the pig genome and only infects pig cells (Jung et al., 2013). PERVs are harmless to pigs, however, whether they are potential harmful to humans remains unclear. PERVs have been verified to be transmitted from pig to human *in vitro* (Denner et al., 2013). Since xenotransplant recipients are under strong immunosuppression, it is desirable to avoid PERV infection.

Scientists have developed various strategies to reduce the risk of PERV transmission to human recipients. These strategies include inhibition of PERV expression using a PERV-specific vaccine (Denner, Mihica, Kaulitz, & Schmidt, 2012; Waechter and Denner, 2014), antiretroviral drugs (Demange et al., 2015; Argaw, Colon-Moran, & Wilson, 2016; Denner, 2017), PERV-specific small interfering RNAs (Ramsoondar et al., 2009; Semaan, Kaulitz, Petersen, Niemann, & Denner, 2012) and PERV gene knockout by genome editing technologies (Semaan, Ivanusic, & Denner, 2015; Yang et al., 2015; Niu et al., 2017). In 2015, Denner et al., 2003 reported that they failed to knock out of PERVs in pig PK15 cells using ZFN technology (Semaan et al., 2015). They found that ZFN is extremely toxic to the transfected cells. In addition, they presumed that the cytotoxic effects are due to the specific cutting of a high copy number of the PERV gene or the non-specific cleavage of off-target sites, which both produce numerous double-stranded DNA breaks in the pig genome. In the same year, Yang et al. reported that they completely eradicated 62 copies of PERV in porcine PK15 using CRISPR/Cas9 (Yang et al., 2015). Two years later, their team successfully generated the PERV knockout pigs (Niu et al., 2017). In 2021, Yang's team generated an extensively edited pigs with inactivated endogenous retroviruses, thus enhancing the compatibility of pig organs with the human immune and coagulation system (Yue et al., 2021). In 2022, the multigene edited pig heart was given to a dying patient (David Bennett Sr). The new pig heart pumped for about 2 months after his transplant surgery, and eventually failed with the patient's death. The cause of his death was not clear, however, the porcine cytomegalovirus (PCMV) were detected in his body, which may have contributed to his death. All

these reports indicated that the potential risk of transmission of pig viruses to humans remains a big obstacle in the clinical use of porcine organs for xenotransplantation.

5 Prospects and challenges

Aside from the inevitable immune obstacles in xenotransplantation, numerous challenges also need to be addressed in the use of genetically modified pigs in clinical application. However, rapid developments in transgenic technology and recent remarkable progress in large-animal cloning, particularly the emergence of GTKO/hCRP genetically modified pigs, bring xenotransplantation a major step closer to clinical application. Although interspecies chimeras meet great challenges, we believe that future research developments will lead to the realization of animal-based transplantation medicine. At present, in some European and American countries, pig hearts, kidneys, and livers have reportedly been transplanted to patients that suffered from advanced organ failure. In 2020, GTKO pigs were approved by the United States Food and Drug Administration (FDA) to be a source of human therapeutics including xenotransplantation. In 2022, the university of Alabama reported that a brain-dead decedent was transplanted a kidney from 10-gene modified pig (Porrett et al., 2022). Furthermore, the University of Maryland Medical Center reported that an extensively edited pig heart was given to a dying patient. All these cases marked the clinical application of xenotransplantation from a pig to a human. Although the survival times of the xenografts were relatively short or xenotransplantation was used only as a transition to allotransplantation, hope remains for the use of xenogeneic organ transplantation in the future. The road toward the introduction of clinical xenotransplantation is proving long and arduous, but progress is steadily being made.

Author contributions

JX was responsible for the writing of the manuscript, WZ for the editing of the graphs, MC for the editing and recording of the tables, QZ for the original revision, CT and XZ for the revision and final review of the manuscript. All authors were involved in the creation and were responsible for the content of the work.

Funding

This research was funded by the Youth Innovation Project of Guangdong Province University (2022KQNCX095), the Science and Technology Planing Project of Jiangmen (2021030101220004887, 2021030101230004833), the Natural Science Foundation of Guangdong Province of China (2019A1515110283).

Conflict of interest

The authors declare that the research was conducted in the absence of any commercial or financial relationships that could be construed as a potential conflict of interest.

Publisher's note

All claims expressed in this article are solely those of the authors and do not necessarily represent those of their affiliated organizations, or those of the publisher, the editors and the reviewers. Any product that may be evaluated in this article, or claim that may be made by its manufacturer, is not guaranteed or endorsed by the publisher.

References

Adams, A. B., Kim, S. C., Martens, G. R., Ladowski, J. M., Estrada, J. L., Reyes, L. M., et al. (2018). Xenoantigen deletion and chemical immunosuppression can prolong renal xenograft survival. *Ann. Surg.* 268 (4), 564–573. doi:10.1097/sla.0000000000002977

Argaw, T., Colon-Moran, W., and Wilson, C. (2016). Susceptibility of porcine endogenous retrovirus to anti-retroviral inhibitors. *Xenotransplantation* 23 (2), 151–158. doi:10.1111/xen.12230

Badin, A. R., Padoan, A., Vadori, M., Boldrin, M., Cavicchioli, L., De benedictis, G. M., et al. (2010). Longterm clinical recovery in parkinsonian monkey recipients of ctla4-ig transgenic porcine neural precursors: 3288. *Transplantation* 90, 47. doi:10.1097/00007890-201007272-00090

Badin, A. R., Vanhove, B., Vadori, M., Fante, F., Boldrin, M., De benedictis, G. M., et al. (2013). Systemic immunosuppression plus local production of CTLA4-Ig to control rejection of transgenic pig neuroblasts in non-human primates, *Retrieved from Joint congress of IXA and organ transplantation in ABO-incompatible and hyperimmunized recipients (IXA 2013)*. Hoboken, New Jersey: Wiley-Blackwell.

Byrne, G., Ahmad-Villiers, S., Du, Z., and McGregor, C. (2018). B4GALNT2 and xenotransplantation: A newly appreciated xenogeneic antigen. *Xenotransplantation* 25 (5)–e12394. doi:10.1111/xen.12394

Cheng, W., Zhao, H., Yu, H., Xin, J., Wang, J., Zeng, L., et al. (2016). Efficient generation of GGTA1-null Diannan miniature pigs using TALENs combined with somatic cell nuclear transfer. *Reprod. Biol. Endocrinol.* 14 (1), 77. doi:10.1186/s12958-016-0212-7

Cooper, D. K. (2003). Clinical xenotransplantion-how close are we? *Lancet* 362 (9383), 557–559. doi:10.1016/s0140-6736(03)14118-9

Cooper, D. K., Good, A. H., Koren, E., Oriol, R., Malcolm, A. J., Ippolito, R. M., et al. (1993). Identification of alpha-galactosyl and other carbohydrate epitopes that are bound by human anti-pig antibodies: Relevance to discordant xenografting in man. *Transpl. Immunol.* 1 (3), 198–205. doi:10.1016/0966-3274(93)90047-c

Crikis, S., Lu, B., Murray-Segal, L. M., Selan, C., Robson, S. C., D'Apice, A. J., et al. (2010). Transgenic overexpression of CD39 protects against renal ischemia-reperfusion and transplant vascular injury. *Am. J. Transpl.* 10 (12), 2586–2595. doi:10.1111/j.1600-6143.2010.03257.x

Dai, Y., Vaught, T. D., Boone, J., Chen, S. H., Phelps, C. J., Ball, S., et al. (2002). Targeted disruption of the alpha1, 3-galactosyltransferase gene in cloned pigs. *Nat. Biotechnol.* 20 (3), 251–255. doi:10.1038/nbt0302-251

Demange, A., Yajjou-Hamalian, H., Gallay, K., Luengo, C., Beven, V., Leroux, A., et al. (2015). Porcine endogenous retrovirus-A/C: Biochemical properties of its integrase and susceptibility to raltegravir. *J. Gen. Virol.* 96 (10), 3124–3130. doi:10.1099/jgv.0.000236

Denner, J. (2017). Can antiretroviral drugs Be used to treat porcine endogenous retrovirus (PERV) infection after xenotransplantation? *Viruses* 9 (8), 213. doi:10.3390/v9080213

Denner, J., Mihica, D., Kaulitz, D., and Schmidt, C. M. (2012). Increased titers of neutralizing antibodies after immunization with both envelope proteins of the porcine endogenous retroviruses (PERVs). *Virol. J.* 9, 260. doi:10.1186/1743-422x-9-260

Denner, J., Specke, V., Thiesen, U., Karlas, A., and Kurth, R. (2003). Genetic alterations of the long terminal repeat of an ecotropic porcine endogenous retrovirus during passage in human cells. *Virology* 314, 125–133. doi:10.1016/S0042-6822(03)00428-8

Dong, X., Hara, H., Wang, Y., Wang, L., Zhang, Y., Cooper, D. K., et al. (2017). Initial study of α1, 3-galactosyltransferase gene-knockout/CD46 pig full-thickness corneal xenografts in rhesus monkeys. *Xenotransplantation* 24 (1), e12282. doi:10.1111/xen.12282

Dunsford, I., Bowley, C. C., Hutchison, A. M., Thompson, J. S., Sanger, R., and Race, R. R. (1953). A human blood-group chimera. *Br. Med. J.* 2 (4827), 81. doi:10.1136/bmj.2.4827.81

Ekser, B., Ezzelarab, M., Hara, H., van der Windt, D. J., Wijkstrom, M., Bottino, R., et al. (2012). Clinical xenotransplantation: The next medical revolution? *Lancet* 379 (9816), 672–683. doi:10.1016/S0140-6736(11)61091-X

Estrada, J. L., Martens, G., Li, P., Adams, A., Newell, K. A., Ford, M. L., et al. (2015). Evaluation of human and non-human primate antibody binding to pig cells lacking GGTA1/CMAH/β4GalNT2 genes. *Xenotransplantation* 22 (3), 194–202. doi:10.1111/xen.12161

Fehilly, C. B., Willadsen, S. M., and Tucker, E. M. (1984). Interspecific chimaerism between sheep and goat. *Nature* 307 (5952), 634–636. doi:10.1038/307634a0

Feng, C., Xi-Rui, L. I., Cui, H. T., Long, C., Liu, X., Tian, X. H., et al. (2016). Highly efficient generation of GGTA1 knockout pigs using a combination of TALEN mRNA and magnetic beads with somatic cell nuclear transfer. *J. Integr. Agric.* 15. doi:10.1016/S2095-3119(16)61347-3

Ferran, C., Stroka, D. M., Badrichani, A. Z., Cooper, J. T., and Bach, F. H. (1997). Adenovirus-mediated gene transfer of A20 renders endothelial cells resistant to activation: A means of evaluating the role of endothelial cell activation in xenograft rejection. *Transpl. Proc.* 29 (1-2), 879–880. doi:10.1016/s0041-1345(96)00184-4

Fisher, J. E., Lillegard, J. B., McKenzie, T. J., Rodysill, B. R., Wettstein, P. J., and Nyberg, S. L. (2013). *In utero* transplanted human hepatocytes allow postnatal engraftment of human hepatocytes in pigs. *Liver Transpl.* 19 (3), 328–335. doi:10.1002/lt.23598

Fu, R., Yu, D., Ren, J., Li, C., Wang, J., Feng, G., et al. (2020). Domesticated cynomolgus monkey embryonic stem cells allow the generation of neonatal interspecies chimeric pigs. *Protein Cell* 11 (2), 97–107. doi:10.1007/s13238-019-00676-8

Gao, H., Zhao, C., Xiang, X., Li, Y., Zhao, Y., Li, Z., et al. (2017). Production of α1, 3-galactosyltransferase and cytidine monophosphate-N-acetylneuraminic acid hydroxylase gene double-deficient pigs by CRISPR/Cas9 and handmade cloning. *J. Reprod. Dev.* 63 (1), 17–26. doi:10.1262/jrd.2016-079

Goldstein, R. S., Drukker, M., Reubinoff, B. E., and Benvenisty, N. (2002). Integration and differentiation of human embryonic stem cells transplanted to the chick embryo. *Dev. Dyn.* 225 (1), 80–86. doi:10.1002/dvdy.10108

Gollackner, B., Goh, S. K., Qawi, I., Buhler, L., Knosalla, C., Daniel, S., et al. (2004). Acute vascular rejection of xenografts: Roles of natural and elicited xenoreactive antibodies in activation of vascular endothelial cells and induction of procoagulant activity. *Transplantation* 77 (11), 1735–1741. doi:10.1097/01.tp.0000131167.21930.b8

Good, A. H., Cooper, D. K., Malcolm, A. J., Ippolito, R. M., Koren, E., Neethling, F. A., et al. (1992). Identification of carbohydrate structures that bind human antiporcine antibodies: Implications for discordant xenografting in humans. *Transpl. Proc.* 24 (2), 559–562.

Goto, T., Hara, H., Sanbo, M., Masaki, H., Sato, H., Yamaguchi, T., et al. (2019). Generation of pluripotent stem cell-derived mouse kidneys in Sall1-targeted anephric rats. *Nat. Commun.* 10 (1), 451. doi:10.1038/s41467-019-08394-9

Hamanaka, S., Umino, A., Sato, H., Hayama, T., Yanagida, A., Mizuno, N., et al. (2018). Generation of vascular endothelial cells and hematopoietic cells by blastocyst complementation. *Stem Cell Rep.* 11 (4), 988–997. doi:10.1016/j.stemcr.2018.08.015

Hara, H., Witt, W., Crossley, T., Long, C., Isse, K., Fan, L., et al. (2013). Human dominant-negative class II transactivator transgenic pigs - effect on the human anti-pig T-cell immune response and immune status. *Immunology* 140 (1), 39–46. doi:10.1111/imm.12107

Huang, J., Gou, D., Zhen, C., Jiang, D., Mao, X., Li, W., et al. (2001). Protection of xenogeneic cells from human complement-mediated lysis by the expression of human DAF, CD59 and MCP. *FEMS Immunol. Med. Microbiol* 31 (3), 203–209. doi:10.1111/j.1574-695X.2001.tb00521.x

Ide, K., Wang, H., Tahara, H., Liu, J., Wang, X., Asahara, T., et al. (2007). Role for CD47-SIRPalpha signaling in xenograft rejection by macrophages. *Proc. Natl. Acad. Sci. U. S. A* 104 (12), 5062–5066. doi:10.1073/pnas.0609661104

Isotani, A., Hatayama, H., Kaseda, K., Ikawa, M., and Okabe, M. (2011). Formation of a thymus from rat ES cells in xenogeneic nude mouse↔rat ES chimeras. *Genes cells.* 16 (4), 397–405. doi:10.1111/j.1365-2443.2011.01495.x

James, D., Noggle, S. A., Swigut, T., and Brivanlou, A. H. (2006). Contribution of human embryonic stem cells to mouse blastocysts. *Dev. Biol.* 295 (1), 90–102. doi:10.1016/j.ydbio.2006.03.026

Jung, Y. D., Ha, H. S., Park, S. J., Oh, K. B., Im, G. S., Kim, T. H., et al. (2013). Identification and promoter analysis of PERV LTR subtypes in NIH-miniature pig. *Mol. Cells* 35 (2), 99–105. doi:10.1007/s10059-013-2289-6

Kawamoto, K., Tanemura, M., Komoda, H., Omori, T., Fumimoto, Y., Shimada, K., et al. (2006). Adenoviral-mediated overexpression of membrane-bound human FasL and human decoy Fas protect pig islets against human CD8+ CTL-mediated cytotoxicity. *Transpl. Proc.* 38 (10), 3286–3288. doi:10.1016/j.transproceed.2006.10.072

Kim, S. C., Mathews, D. V., Breeden, C. P., Higginbotham, L. B., Ladowski, J., Martens, G., et al. (2019). Long-term survival of pig-to-rhesus macaque renal xenografts is dependent on CD4 T cell depletion. *Am. J. Transpl.* 19 (8), 2174–2185. doi:10.1111/ajt.15329

Kobayashi, T., Goto, T., Oikawa, M., Sanbo, M., Yoshida, F., Terada, R., et al. (2021). Blastocyst complementation using Prdm14-deficient rats enables efficient germline transmission and generation of functional mouse spermatids in rats. *Nat. Commun.* 12 (1), 1328. doi:10.1038/s41467-021-21557-x

Kobayashi, T., Yamaguchi, T., Hamanaka, S., Kato-Itoh, M., Yamazaki, Y., Ibata, M., et al. (2010). Generation of rat pancreas in mouse by interspecific blastocyst injection of pluripotent stem cells. *Cell* 142 (5), 787–799. doi:10.1016/j.cell.2010.07.039

Kuwaki, K., Tseng, Y. L., Dor, F. J., Shimizu, A., Houser, S. L., Sanderson, T. M., et al. (2005). Heart transplantation in baboons using alpha1, 3-galactosyltransferase gene-knockout pigs as donors: Initial experience. *Nat. Med.* 11 (1), 29–31. doi:10.1038/nm1171

Lai, L., Kolber-Simonds, D., Park, K. W., Cheong, H. T., Greenstein, J. L., Im, G. S., et al. (2002). Production of alpha-1, 3-galactosyltransferase knockout pigs by nuclear transfer cloning. *Science* 295 (5557), 1089–1092. doi:10.1126/science.1068228

Laurencin, C. T., and El-Amin, S. F. (2008). Xenotransplantation in orthopaedic surgery. *J. Am. Acad. Orthop. Surg.* 16 (1), 4–8. doi:10.5435/00124635-200801000-00002

Le Douarin, N. M., Jotereau, F. V., Houssaint, E., and Belo, M. (1976). Ontogeny of the avian thymus and bursa of Fabricius studied in interspecific chimeras. *Ann. Immunol. Paris.* 127 (6), 849–856.

Le Douarin, N. M., and Jotereau, F. V. (1975). Tracing of cells of the avian thymus through embryonic life in interspecific chimeras. *J. Exp. Med.* 142 (1), 17–40. doi:10.1084/jem.142.1.17

Li, P., Estrada, J. L., Burlak, C., Montgomery, J., Butler, J. R., Santos, R. M., et al. (2015). Efficient generation of genetically distinct pigs in a single pregnancy using multiplexed single-guide RNA and carbohydrate selection. *Xenotransplantation* 22 (1), 20–31. doi:10.1111/xen.12131

Li, X., Cui, X. L., Wang, J. Q., Wang, Y. K., Li, Y. F., Wang, L. Y., et al. (2016). Generation and application of mouse-rat allodiploid embryonic stem cells. *Cell* 164 (1-2), 279–292. doi:10.1016/j.cell.2015.11.035

Lutz, A. J., Li, P., Estrada, J. L., Sidner, R. A., Chihara, R. K., Downey, S. M., et al. (2013). Double knockout pigs deficient in N-glycolylneuraminic acid and galactose α-1, 3-galactose reduce the humoral barrier to xenotransplantation. *Xenotransplantation* 20 (1), 27–35. doi:10.1111/xen.12019

Maksoud, A. J. A. J. o. M. S. (2004). *Cellular and molecular immunology* - 5th Edition [Book Review]. *25*. China

Martin, C., Plat, M., Nerriére-Daguin, V., Coulon, F., Uzbekova, S., Venturi, E., et al. (2005). Transgenic expression of CTLA4-Ig by fetal pig neurons for xenotransplantation. *Transgenic Res.* 14 (4), 373–384. doi:10.1007/s11248-004-7268-4

Masaki, H., Kato-Itoh, M., Takahashi, Y., Umino, A., Sato, H., Ito, K., et al. (2016). Inhibition of apoptosis overcomes stage-related compatibility barriers to chimera formation in mouse embryos. *Cell Stem Cell* 19 (5), 587–592. doi:10.1016/j.stem.2016.10.013

Matsunari, H., Nagashima, H., Watanabe, M., Umeyama, K., Nakano, K., Nagaya, M., et al. (2013). Blastocyst complementation generates exogenic pancreas *in vivo* in apancreatic cloned pigs. *Proc. Natl. Acad. Sci. U. S. A.* 110 (12), 4557–4562. doi:10.1073/pnas.1222902110

Mercer, D. F., Schiller, D. E., Elliott, J. F., Douglas, D. N., Hao, C., Rinfret, A., et al. (2001). Hepatitis C virus replication in mice with chimeric human livers. *Nat. Med.* 7 (8), 927–933. doi:10.1038/90968

Mohiuddin, M. M., Singh, A. K., Corcoran, P. C., Thomas, M. L., Iii, Clark, T., Lewis, B. G., et al. (2016). Chimeric 2C10R4 anti-CD40 antibody therapy is critical for long-term survival of GTKO.hCD46.hTBM pig-to-primate cardiac xenograft. *Nat. Commun.* 7–11138. doi:10.1038/ncomms11138

Mori, M., Furuhashi, K., Danielsson, J. A., Hirata, Y., Kakiuchi, M., Lin, C. S., et al. (2019). Generation of functional lungs via conditional blastocyst complementation using pluripotent stem cells. *Nat. Med.* 25 (11), 1691–1698. doi:10.1038/s41591-019-0635-8

Nagashima, H., Giannakis, C., Ashman, R. J., and Nottle, M. B. (2004). Sex differentiation and germ cell production in chimeric pigs produced by inner cell mass injection into blastocysts. *Biol. Reprod.* 70 (3), 702–707. doi:10.1095/biolreprod.103.022681

Nichols, J., and Smith, A. (2009). Naive and primed pluripotent states. *Cell Stem Cell* 4 (6), 487–492. doi:10.1016/j.stem.2009.05.015

Niu, D., Wei, H. J., Lin, L., George, H., Wang, T., Lee, I. H., et al. (2017). Inactivation of porcine endogenous retrovirus in pigs using CRISPR-Cas9. *Science* 357 (6357), 1303–1307. doi:10.1126/science.aan4187

Olbrich, T., Mayor-Ruiz, C., Vega-Sendino, M., Gomez, C., Ortega, S., Ruiz, S., et al. (2017). A p53-dependent response limits the viability of mammalian haploid cells. *Proc. Natl. Acad. Sci. U. S. A.* 114 (35), 9367–9372. doi:10.1073/pnas.1705133114

Oropeza, M., Petersen, B., Carnwath, J. W., Lucas-Hahn, A., Lemme, E., Hassel, P., et al. (2009). Transgenic expression of the human A20 gene in cloned pigs provides protection against apoptotic and inflammatory stimuli. *Xenotransplantation* 16 (6), 522–534. doi:10.1111/j.1399-3089.2009.00556.x

Pan, D., Liu, T., Lei, T., Zhu, H., Wang, Y., and Deng, S. (2019). Progress in multiple genetically modified minipigs for xenotransplantation in China. *Xenotransplantation* 26 (1)–e12492. doi:10.1111/xen.12492

Patience, C., Takeuchi, Y., and Weiss, R. A. (1997). Infection of human cells by an endogenous retrovirus of pigs. *Nat. Med.* 3 (3), 282–286. doi:10.1038/nm0397-282

Porrett, P. M., Orandi, B. J., Kumar, V., Houp, J., Anderson, D., Cozette Killian, A., et al. (2022). First clinical-grade porcine kidney xenotransplant using a human decedent model. *Am. J. Transpl.* 22 (4), 1037–1053. doi:10.1111/ajt.16930

Ramsoondar, J., Vaught, T., Ball, S., Mendicino, M., Monahan, J., Jobst, P., et al. (2009). Production of transgenic pigs that express porcine endogenous retrovirus small interfering RNAs. *Xenotransplantation* 16 (3), 164–180. doi:10.1111/j.1399-3089.2009.00525.x

Saethre, M., Schneider, M. K., Lambris, J. D., Magotti, P., Haraldsen, G., Seebach, J. D., et al. (2008). Cytokine secretion depends on Galalpha(1, 3)Gal expression in a pig-to-human whole blood model. *J. Immunol.* 180 (9), 6346–6353. doi:10.4049/jimmunol.180.9.6346

Semaan, M., Ivanusic, D., and Denner, J. (2015). Cytotoxic effects during knock out of multiple porcine endogenous retrovirus (PERV) sequences in the pig genome by zinc finger nucleases (ZFN). *PLoS One* 10 (4)–e0122059. doi:10.1371/journal.pone.0122059

Semaan, M., Kaulitz, D., Petersen, B., Niemann, H., and Denner, J. (2012). Long-term effects of PERV-specific RNA interference in transgenic pigs. *Xenotransplantation* 19 (2), 112–121. doi:10.1111/j.1399-3089.2012.00683.x

Sharma, A., Okabe, J., Birch, P., McClellan, S. B., Martin, M. J., Platt, J. L., et al. (1996). Reduction in the level of Gal(alpha1, 3)Gal in transgenic mice and pigs by the expression of an alpha(1, 2)fucosyltransferase. *Proc. Natl. Acad. Sci. U. S. A.* 93 (14), 7190–7195. doi:10.1073/pnas.93.14.7190

Shimizu, A., and Yamada, K. (2006). Pathology of renal xenograft rejection in pig to non-human primate transplantation. *Clin. Transpl.* 20 (Suppl. 15), 46–52. doi:10.1111/j.1399-0012.2006.00550.x

Shin, J. S., Min, B. H., Kim, J. M., Kim, J. S., Yoon, I. H., Kim, H. J., et al. (2016). Failure of transplantation tolerance induction by autologous regulatory T cells in the pig-to-non-human primate islet xenotransplantation model. *Xenotransplantation* 23 (4), 300–309. doi:10.1111/xen.12246

Song, K. H., Kang, Y. J., Jin, U. H., Park, Y. I., Kim, S. M., Seong, H. H., et al. (2010). Cloning and functional characterization of pig CMP-N-acetylneuraminic acid hydroxylase for the synthesis of N-glycolylneuraminic acid as the xenoantigenic determinant in pig-human xenotransplantation. *Biochem. J.* 427 (1), 179–188. doi:10.1042/bj20090835

Strain, L., Dean, J. C., Hamilton, M. P., and Bonthron, D. T. (1998). A true hermaphrodite chimera resulting from embryo amalgamation after *in vitro* fertilization. *N. Engl. J. Med.* 338 (3), 166–169. doi:10.1056/nejm199801153380305

Tachibana, M., Sparman, M., Ramsey, C., Ma, H., Lee, H. S., Penedo, M. C., et al. (2012). Generation of chimeric rhesus monkeys. *Cell* 148 (1-2), 285–295. doi:10.1016/j.cell.2011.12.007

Takeuchi, Y., Patience, C., Magre, S., Weiss, R. A., Banerjee, P. T., Le Tissier, P., et al. (1998). Host range and interference studies of three classes of pig endogenous retrovirus. *J. Virol.* 72 (12), 9986–9991. doi:10.1128/jvi.72.12.9986-9991.1998

Tan, T., Wu, J., Si, C., Dai, S., Zhang, Y., Sun, N., et al. (2021). Chimeric contribution of human extended pluripotent stem cells to monkey embryos *ex vivo*. *Cell* 184 (8), 20202020–20202032.e14. doi:10.1016/j.cell.2021.03.020

Tarkowski, A. K. (1961). Mouse chimaeras developed from fused eggs. *Nature* 190, 857–860. doi:10.1038/190857a0

Usui, J., Kobayashi, T., Yamaguchi, T., Knisely, A. S., Nishinakamura, R., and Nakauchi, H. (2012). Generation of kidney from pluripotent stem cells via blastocyst complementation. *Am. J. Pathol.* 180 (6), 2417–2426. doi:10.1016/j.ajpath.2012.03.007

van der Windt, D. J., Bottino, R., Casu, A., Campanile, N., Smetanka, C., He, J., et al. (2009). Long-term controlled normoglycemia in diabetic non-human primates after transplantation with hCD46 transgenic porcine islets. *Am. J. Transpl.* 9 (12), 2716–2726. doi:10.1111/j.1600-6143.2009.02850.x

Waechter, A., and Denner, J. (2014). Novel neutralising antibodies targeting the N-terminal helical region of the transmembrane envelope protein p15E of the porcine endogenous retrovirus (PERV). *Immunol. Res.* 58 (1), 9–19. doi:10.1007/s12026-013-8430-y

Watts, A., Foley, A., Awwad, M., Treter, S., Oravec, G., Buhler, L., et al. (2000). Plasma perfusion by apheresis through a gal immunoaffinity column successfully depletes anti-gal antibody: Experience with 320 aphereses in baboons. *Xenotransplantation* 7 (3), 181–185. doi:10.1034/j.1399-3089.2000.00068.x

Weiss, E. H., Lilienfeld, B. G., Müller, S., Müller, E., Herbach, N., Kessler, B., et al. (2009). HLA-E/human beta2-microglobulin transgenic pigs: Protection against xenogeneic human anti-pig natural killer cell cytotoxicity. *Transplantation* 87 (1), 35–43. doi:10.1097/TP.0b013e318191c784

Wu, J., Platero-Luengo, A., Sakurai, M., Sugawara, A., Gil, M. A., Yamauchi, T., et al. (2017). Interspecies chimerism with mammalian pluripotent stem cells. *Cell*, 168 (3): 473–486. doi:10.1016/j.cell.2016.12.036

Xu, X. C., Goodman, J., Sasaki, H., Lowell, J., and Mohanakumar, T. (2002). Activation of natural killer cells and macrophages by porcine endothelial cells augments specific T-cell xenoresponse. *Am. J. Transpl.* 2 (4), 314–322. doi:10.1034/j.1600-6143.2002.20405.x

Yamaguchi, T., Sato, H., Kato-Itoh, M., Goto, T., Hara, H., Sanbo, M., et al. (2017). Interspecies organogenesis generates autologous functional islets. *Nature* 542 (7640), 191–196. doi:10.1038/nature21070

Yang, L., Güell, M., Niu, D., George, H., Lesha, E., Grishin, D., et al. (2015). Genome-wide inactivation of porcine endogenous retroviruses (PERVs). *Science* 350 (6264), 1101–1104. doi:10.1126/science.aad1191

Yu, L., Wei, Y., Sun, H. X., Mahdi, A. K., Pinzon Arteaga, C. A., Sakurai, M., et al. (2021). Derivation of intermediate pluripotent stem cells amenable to primordial germ cell specification. *Cell Stem Cell* 28 (3), 550–567.e12. doi:10.1016/j.stem.2020.11.003

Yue, Y., Xu, W., Kan, Y., Zhao, H. Y., Zhou, Y., Song, X., et al. (2021). Extensive germline genome engineering in pigs. *Nat. Biomed. Eng.* 5 (2), 134–143. doi:10.1038/s41551-020-00613-9

Zeng, F., Chen, M. J., Baldwin, D. A., Gong, Z. J., Yan, J. B., Qian, H., et al. (2006). Multiorgan engraftment and differentiation of human cord blood CD34+ Lin-cells in goats assessed by gene expression profiling. *Proc. Natl. Acad. Sci. U. S. A.* 103 (20), 7801–7806. doi:10.1073/pnas.0602646103

Zeng, M. H., Fang, C. Y., Wang, S. S., Zhu, M., Xie, L., Li, R., et al. (2006). A study of soluble HLA-G1 protecting porcine endothelial cells against human natural killer cell-mediated cytotoxicity. *Transpl. Proc.* 38 (10), 3312–3314. doi:10.1016/j.transproceed.2006.10.179

Zhang, R., Wang, Y., Chen, L., Wang, R., Li, C., Li, X., et al. (2018). Reducing immunoreactivity of porcine bioprosthetic heart valves by genetically-deleting three major glycan antigens, GGTA1/β4GalNT2/CMAH. *Acta Biomater.* 72, 196–205. doi:10.1016/j.actbio.2018.03.055

Zhang, W., Tian, Y., Gao, Q., Li, X., Li, Y., Zhang, J., et al. (2020). Inhibition of apoptosis reduces diploidization of haploid mouse embryonic stem cells during differentiation. *Stem Cell Rep.* 15 (1), 185–197. doi:10.1016/j.stemcr.2020.05.004

Zhou, X., Liu, Y., Tang, C., Cheng, L., Zheng, S., Zheng, Y., et al. (2022). Generation of genetic modified pigs devoid of GGTA1 and expressing the human leukocyte antigen-G5. *Sheng Wu Gong Cheng Xue Bao* 38 (3), 1096–1111. doi:10.13345/j.cjb.210655

Zhu, M., Wang, S. S., Xia, Z. X., Cao, R. H., Chen, D., Huang, Y. B., et al. (2005). Inhibition of xenogeneic response in porcine endothelium using RNA interference. *Transplantation* 79 (3), 289–296. doi:10.1097/01.tp.0000148733.57977.fd

frontiers | Frontiers in Cell and Developmental Biology

TYPE Review
PUBLISHED 23 January 2023
DOI 10.3389/fcell.2023.1110551

OPEN ACCESS

EDITED BY
Feng Yue,
Hainan University, China

REVIEWED BY
Maria Victoria Bariani,
University of Buenos Aires, Argentina
Jia Song,
Tianjin University of Science and Technology, China

*CORRESPONDENCE
Da Liu,
liuda_1986@163.com
Yongzhi Deng,
627473544@qq.com

SPECIALTY SECTION
This article was submitted to Stem Cell Research,
a section of the journal
Frontiers in Cell and Developmental Biology

RECEIVED 28 November 2022
ACCEPTED 12 January 2023
PUBLISHED 23 January 2023

CITATION
Cui M, Liu Y, Men X, Li T, Liu D and Deng Y (2023), Large animal models in the study of gynecological diseases.
Front. Cell Dev. Biol. 11:1110551.
doi: 10.3389/fcell.2023.1110551

Large animal models in the study of gynecological diseases

Minghua Cui[1], Yuehui Liu[2], Xiaoping Men[2], Tao Li[3], Da Liu[4]* and Yongzhi Deng[5]*

[1]Gynecology Department, Affiliated Hospital of Changchun University of Chinese Medicine, Changchun, Jilin, China, [2]Laboratory Department, Affiliated Hospital of Changchun University of Chinese Medicine, Changchun, Jilin, China, [3]Department of Acupuncture and Massage, The Third Affiliated Hospital of Changchun University of Chinese Medicine, Changchun, Jilin, China, [4]School of Pharmacy, Changchun University of Chinese Medicine, Changchun, Jilin, China, [5]The Third Affiliated Hospital of Changchun University of Chinese Medicine, Changchun, Jilin, China

Gynecological diseases are a series of diseases caused by abnormalities in the female reproductive organs or breast, which endanger women's fertility and even their lives. Therefore, it is important to investigate the mechanism of occurrence and treatment of gynecological diseases. Animal models are the main objects for people to study the development of diseases and explore treatment options. Large animals, compared to small rodents, have reproductive organs with structural and physiological characteristics closer to those of humans, and are also better suited for long-term serial examinations for gynecological disease studies. This review gives examples of large animal models in gynecological diseases and provides a reference for the selection of animal models for gynecological diseases.

KEYWORDS

gynecological diseases, large animal models, gestational diabetes mellitus, polycystic ovary syndrome, endometriosis

Introduction

Animal models are commonly used in biomedical research as the basis for experimental and clinical hypotheses. The use of animal models is an extremely important experimental method and tool in modern biomedical research, contributing to a more convenient and effective understanding of the developmental patterns of human diseases (Robinson et al., 2019; Lunney et al., 2021). People first used animals as physiological models in ancient Greek times (Ericsson et al., 2013). Since then, animals have been utilized more and more in the study of human diseases and have gradually become an irreplaceable part. Rodents such as mice and rats reproduce rapidly and one can make them present multiple phenotypes by knockout techniques (Filipiak and Saunders, 2006). In the early 20th century, the use of rodents as models for biological research was well established. However, these rodents do not mimic all diseases because some of the physiological characteristics differ significantly from those of humans. In pursuit of higher similarity of physiological structures, large animal models such as pigs (Lunney et al., 2021), sheep (Murray et al., 2019), and horses (Schüttler et al., 2020) and other higher classes of animals have become the choice of models for disease studies.

Gynecological diseases are diseases caused by abnormal development, infections, and tumors of the female reproductive organs and mammary glands. According to the site of the disease, gynecological diseases are mainly divided into: 1) Diseases of the reproductive system such as uterine diseases and vaginal diseases, which are mostly caused by infections, but also some diseases caused by genetic factors and hormonal disorders (Grimbizis et al., 2001; Stewart, 2001; White et al., 2011); 2) breast diseases, which mostly refer to breast inflammation and malignant tumors (Harbeck and Gnant, 2017; Scott, 2022); 3) endocrine

TABLE 1 Reproductive characteristics of humans and some animals. Table content was compiled from Abedal-Majed and Cupp (2019), Lu et al. (2022).

Reproductive characteristics	Women	Cows	Sheep	Mice	Monkeys
Ovarian size	4 × 3 × 1 cm	2–3 × 1–2.5 × 1–1.5 cm	1–1.5 × 0.5–1 × 0.5–1 cm	0.2 × 0.1 × 0.05 cm	1.0–1.8 × 0.4–0.6 × 0.2–0.4 cm
Diameter of ovulatory follicle	18–20 mm	15–20 mm	5–7 mm	0.9–1.1 mm	6–9 mm
Lifespan	70–80 years	10–20 years	5–15 years	1–3 years	20–25 years
Ovulatory cycle	24–30 days	17–24 days	13–19 days	4–6 days	22–33 days
Length of follicular phase	12–14 days	2–3 days	2–3 days	1–3 days	17–19 days
Length of luteal phase	14–16 days	15–18 days	12–14 days	—	13–15 days
Duration of gestation	278–282 days	278–282 days	142–148 days	21 days	156–180 days

disorders due to reproductive abnormalities, such as gestational diabetes (Khalil et al., 2018). In the current research on gynecological diseases, a variety of animals have successfully simulated human diseases, and the research is divided into two main areas. The first is the mechanism of disease onset. Researchers explore the possible causes of disease through the expression of proteins associated with specific signaling pathways. In the study of signaling pathways (Lv et al., 2022), researchers can predict the potential symptoms of a disease and reveal the harm of it to other tissues or organs. The second is the treatment plan for the disease (Tyrrell, 1999). By applying spontaneous disease models or artificially induced disease models, drug efficacy is evaluated, and issues such as drug safety are assessed, which is the basis of preclinical drug research. However, due to the specificity of gynecological diseases, small rodents do not mimic the manifestations of human gynecological diseases very well (Adams et al., 2012). Large animals are often applied in the study of gynecological diseases because of their reproductive characteristics close to those of humans. In this review, we briefly introduce the application of large animal models in gynecologic diseases, using three gynecologic diseases as examples. An in-depth understanding of the application of large animal models will provide more insight into the study of gynecological diseases and enlighten researchers to pay more attention to the selection of animal models in their studies.

Large animal models

For a long time, it has been found that it is difficult to advance medicine by using human subjects as subjects themselves. Not only are the accumulated clinical experiences limited in time and space, but many experiments are morally and methodologically restricted. The attractiveness of animal models lies in the fact that they overcome these shortcomings, and their unique role in biomedical research is being increasingly appreciated by researchers (Banstola and Reynolds, 2022). In order to fully simulate the main clinical manifestations and pathological features of a specific disease, the selection of animal models varies from disease to disease. Although rodents such as mice and rats are widely used in disease research, they have shown many shortcomings in gynecological diseases. Rodents usually have a short ovarian cycle and a luteal phase that only arises during mating, and their gestation period is much smaller than that of humans (Table 1). Their small size is also a problem, and examination of organs by necropsy does not allow for continuous follow-up of disease progression. Although there are instruments for examination of mice, such as Doppler ultrasound, the same instruments used for human examination can be applied to large animals and can be examined by palpation, which are not possible in small rodents. In contrast, gynecological diseases usually develop continuously over a specific period of time, so examination by means of dissection does not contribute to the understanding of the disease. The larger size of large animals facilitates real-time examination of the ovaries and uterus. Researchers used cows as an animal model to study the effects of aging on female reproduction. Changes in plasma estradiol concentrations and luteal phase progesterone concentrations were found to be similar to those in menopausal women (Malhi et al., 2005). Ovary-related endocrine changes in sheep have also been shown to be similar to those in women (de Souza et al., 1998). The results of large animals as models for human gynecological studies are more closely related to those of humans. Smaller animals tend to have shorter lifespans, and obtaining sufficient blood from these small animals for analysis is difficult and does not allow for long-term observation of hormone level. In addition, the pharmacokinetics of small animals differ significantly from those of humans, and the evaluation of drugs in small animals may deviate significantly from reality (Lin, 1995). In a review by Mondal et al. (2022) detailing the comparison of tumor sink between mice and pigs, it was found that using a mouse model would severely underestimate the toxicity of the drug, compared to pigs. This is due to the smaller size of the mouse, where the drug would be more preferentially concentrated at the tumor site, while the pig has higher concentrations in the plasma and greater systemic toxicity. Therefore, large animals are more advantageous in studying gynecological diseases both in terms of physiological similarity and manipulation. This is why researchers have used large animals to construct models of various gynecological diseases for basic and pharmacodynamic studies.

Gestational diabetes

Gestational diabetes (GDM) is a spontaneous hyperglycemia during pregnancy. Gestational diabetes is one of the factors that affect the prognosis of pregnancy, increasing the risk of pregnancy and causing adverse pregnancy outcomes (Bellamy et al., 2009; American Diabetes Association, 2013). In addition, GDM may

TABLE 2 Different large animals for the study of gestational diabetes.

Species	Method	Result	References
Pigs	Alloxan injection	Elevated liver glycogen concentration in offspring of gestational diabetic sows with unaffected prenatal muscle development	Ezekwe and Martin, (1978)
		Maternal diabetes induces increased abundance of IGF-I mRNA in fetal skeletal muscle, liver, heart, kidney and placenta and decreased IGF-I mRNA levels in the brain	Ramsay et al. (1994)
	Streptozotocin injection	The offspring of severely diabetic sows have elevated body lipids, while the offspring of mildly diabetic sows have unaffected body lipids	Ezekwe et al. (1984)
Dogs	High fat/fructose diet	Dogs fed a high-fat/high-fructose diet in late gestation exhibit worsened glucose tolerance and impaired systemic and hepatic insulin sensitivity	Moore et al. (1985)
Sheep	High-fat diet	Fetal insulin is elevated in ewes on a high-fat diet due to increased glucose exposure and cortisol-induced accelerated beta-cell maturation	Ford et al. (2009)
	Streptozotocin injection	Streptozotocin-induced islet beta-cell destruction causes altered maternal glucose and insulin responses and results in elevated fetal glucose, insulin, and body weight levels	Dickinson et al. (1991)
	Alloxan injection	Gestational diabetes mellitus was successfully induced in ewes by alloxan injection, but their fetuses were not significantly affected	Miodovnik et al. (1989)

have an impact on maternal health long after delivery, increasing the risk of type 2 diabetes (Peters et al., 1996) as well as cardiovascular disease (Shostrom et al., 2017; Plows et al., 2018). Therefore, an in-depth study of the pathogenesis of gestational diabetes mellitus and the proposal of targeted therapeutic approaches are of great clinical value. Establishing effective animal models is the basis for understanding GDM. In GDM modeling, chemical induction of toxicity in pancreatic β-cells of rodents is commonly used. However, rodents have a shorter gestation period, and gestational hormones and islet structure are different from humans (Schüttler et al., 2020). This is the main problem of using them for GDM studies (Pasek and Gannon, 2013; Gao et al., 2021). Pigs are similar to humans in terms of anatomy, physiology, and disease mechanisms (Yao et al., 2016). They were used to create a maternal diabetes model to explore the effects of tetraoxacillin diabetes and maternal fasting on fetal development. For the quantitative increase in body fat only in fetuses of diabetic pigs, it was concluded that diabetic pregnancy stimulates the *ab initio* synthesis of fatty acids from fetal fat and is the main mechanism for the increase in fetal body fat accumulation (Kasser et al., 1981). In Ezekwe's study, streptozotocin was administered to pregnant sows during gestation to induce diabetes and to explore changes in fetal growth, energy reserves and body composition in neonatal pigs (Ezekwe et al., 1984). With the rapid development of genetic engineering technology, researchers are using transgenic techniques to manipulate animals and construct the desired models. Mice can be genetically edited and reproduced stably by CRISPR/Cas9 technology (Hall et al., 2018). Gene editing techniques are also used in large animals, and people have successfully used sperm-mediated gene transfer (Umeyama et al., 2012), gene-targeted technique (Watanabe et al., 2010) to get transgenic pigs, which have potential in the research of gynecological diseases. Renner et al. (2019) designed transgenic pigs with INSC93S, a genetic mutation that causes hyperglycemia and insulin resistance in pregnant pigs in late gestation, and the transgenic pigs became a promising model for GDM. In addition to pigs, dogs have also been used to model GDM. Moore et al. (1985) successfully induced a GDM in dogs by feeding them high fat and fructose at weeks six and seven of gestation. Further exploration of hepatic glucose metabolism in dogs during gestation revealed that the hepatic response to hyperglycemia is diminished in normal pregnancy whereas this response is more suppressed in the GDM model. This response may be responsible for exacerbating hyperglycemia and is one of the characteristics of GDM (Coate et al., 2013). Large animals are of greater value in the construction of gestational diabetes models (Table 2), and gene editing technology offers new directions for the construction of such models.

Polycystic ovary syndrome

Polycystic ovary syndrome (PCOS) is a complex endocrine disorder that is characterized by hyperandrogenemia. Hyperandrogenemia leads to abnormal follicular development, obesity, and hirsutism, which cause greater distress for women (Legro et al., 2013; Azziz et al., 2016; Lizneva et al., 2016; Rosenfield and Ehrmann, 2016; Zeng et al., 2020). However, the pathogenesis of PCOS has not yet been fully elucidated, and genetics is thought to be one of the main causes (Kahsar-Miller et al., 2001). Understanding the pathophysiology of PCOS and the methods to predict and prevent it is crucial. Because highly invasive tests are not applicable to humans, studies of PCOS need to be initiated from animal models. Although rodent models are widely used, there are differences in ovulation patterns and growth regulation between rodents and human females. In addition, there are significant differences in placental structure and fetal development between rodents and humans. Most organ development in the mouse fetus occurs after birth, which makes it less accurate to assess the effect of disease on fetal development (Carter, 2020). Because sheep and monkeys are similar to humans in terms of physiology and hormone regulation, several researchers have used these large animals to simulate human PCOS and to explore possible pathogenesis in recent years (Table 3). In a study by Tonellotto Dos Santos et al. (2018), the possible causes of the hypertrichosis symptoms caused by PCOS were investigated by injecting pregnant ewes with androgens to make them androgenic. It was found that increased 5-a-reductase type 1 (SRD5A1) activity may be a cause of hirsutism due to PCOS. PCOS is also induced in sheep by prenatal overtreatment with testosterone, and King et al. (2007)

TABLE 3 Large animal models for the study of polycystic ovary syndrome.

Species	Modeling method	Result	References
Rhesus monkeys	Testosterone propionate injection	Testosterone propionate injections increased serum testosterone and androstenedione levels in maternal and prenatal androgenized fetuses	Abbott et al. (2008)
	Testosterone pellets implanting subcutaneously	Androgens stimulate gonadotropin-independent follicle growth in the primate ovary	Vendola et al. (1998)
Sheep	Testosterone propionate injection	Prenatal androgen injections reduce adipose differentiation during puberty and lead to subcutaneous adipose tissue inflammation in adulthood in sheep	Siemienowicz et al. (2021)
		Pregnant ewes showed increased hair number and diameter, mild hypertension, and impaired placental function after testosterone treatment	King et al. (2007); Tonellotto Dos Santos et al. (2018); Kelley et al. (2019)

TABLE 4 Large animal models for the study of endometriosis.

Species	Modeling method	Result	References
Cynomolgus monkeys	Shredding and transferring endometrial tissue to the peritoneum	GhRhα is therapeutically effective in monkey endometriosis, but ovulation and cessation of menstruation occur in some individuals	Werlin and Hodgen (1983); Mann et al. (1986)
	Perfusing cell suspensions of endometrial tissue into the posterior culde-sac	Intact structure is an important condition for ectopic bed of endometrial fragments, and ectopic growth is inhibited after enzymatic digestion and protease inhibitor treatment of endometrial fragments	Sillem et al. (1996)
Baboons	Intrapelvic injection of menstrual endometrium	Transplantation of menstrual endometrium is more likely to cause endometriosis than transplantation of luteal endometrium, and intraperitoneal seeding is more likely to cause endometriosis than subperitoneal injection	D'Hooghe et al. (1995b)
Marmoset monkeys	Flushing sterile medium through the fallopian tube from the uterus into the abdominal cavity	Endometriosis lesions have high local estradiol synthesis and low estrogen inactivation	Einspanier et al. (2006)
Pigs	Suturing the endometrium to the caudodorsal aspect of the bladder	Endometriosis was successfully induced in dogs, pigs and sheep by surgical transplantation of endometrium, but subsequent lesions could be observed in dogs	Varughese et al. (2018)
Dogs			
Sheep	Suturing the endometrium to caudodorsal aspect of the uterus		

demonstrated mild hypertension in unproductive sheep after overtreatment with testosterone, which is also a symptom of PCOS. The human and sheep placentas have similar villi structures in the stem, middle and terminal vessels (Leiser et al., 1997). Kelley et al. (2019) examined the effects of testosterone treatment on the sheep placenta and demonstrated that PCOS may impair placental function through increased oxidative stress and hypoxia. In general, the higher the evolutionary stage of experimental animals, the more complex their functions and structures are, and the closer their physiological responses are to humans. Non-primate species are widely used in PCOS research (Abbott et al., 1998). In a detailed comparison of multiple animal models of PCOS in a review by Paixao et al, (2017) they concluded that the prenatal administration of androgens in non-human primates was the closest modeling approach to the real. Non-human primates treated with testosterone have the same characteristics as humans with PCOS (Abbott et al., 2016). In addition, the secretory function of the fetus is affected in individuals with PCOS. The secretion of gonadotropins is increased in fetuses of non-human primate models induced with androgens. This also provides a retrospective basis for the developmental origin of luteinizing hormone and androgen overload symptoms in adulthood (Abbott et al., 2008). Although it is costly to use large animals such as sheep and monkeys, they are suitable for androgen injection molding and the disease response is much closer to that of humans.

Endometriosis

Endometriosis is a disease caused by the growth of the endometrial glands and mesenchyme outside the uterine cavity. There are three main types of endometriosis: peritoneal endometriosis, ovarian endometriosis cysts, and deep infiltrating endometriosis (Shafrir et al., 2018; Chapron et al., 2019; Lagana et al., 2019). Li et al. (2022) were able to establish an endometriosis model in nude mice using a mixture of human immortalized endometriosis stromal cells and epithelial cells. The use of rodents to study this disease is not appropriate. In rodents, molting occurs only in the presence of a fertilized egg, whereas in humans this process is automatic. In addition, the receptors that play a dominant role in this process differ between the two (Bulun et al., 2019). However, transgenic mice are reproductively different from humans (Maenhoudt et al., 2022). Because of this, non-human primates play a large role in preclinical disease research (D'Hooghe et al., 2009). Investigators have mastered multiple

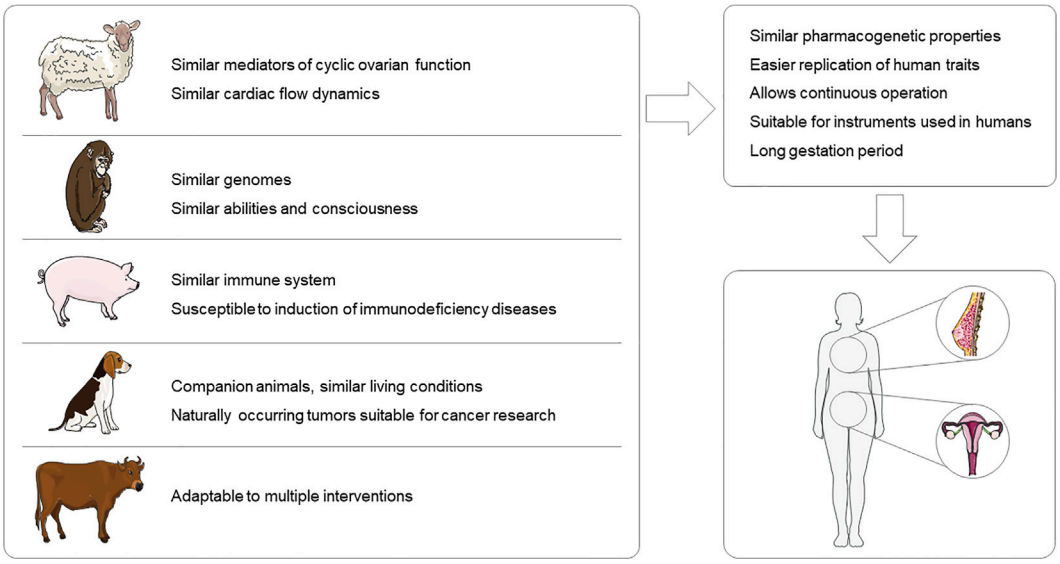

FIGURE 1
Advantages of large animal models for gynecological disease research. This figure was created using images from Servier Medical Art Commons Attribution 3.0 Unported License (http://smart.servier.com).

methods to induce endometriosis in large animals (Table 4). Models of endometriosis formed by induction in non-human primates are highly physiologically similar to humans, and therefore many related studies have been conducted in them. Some researchers have induced endometriosis in baboons by shredding and transferring endometrial tissue to the peritoneum, ovaries, and fallopian tubes (D'Hooghe et al., 1995a). Mann et al. found that intraperitoneal implantation using menstrual endometrium rather than luteal endometrium was more successful in inducing endometriosis compared to retroperitoneal injection. They also demonstrated that continuous infusion of GnRH agonist or levonorgestrel was effective in the treatment of endometriosis in monkeys (Mann et al., 1986; Gu et al., 2020). In addition, the exploration of the molecular mechanisms of endometriosis has revealed abnormal expression of many progesterone and estrogen regulatory genes. Transient pre-disease upregulation of vascular endothelial cell growth factor-A and angiogenic factor CYR61 suggests that symptoms of endometriosis are associated with increased angiogenic capacity and imbalance of hormonal regulation (Hastings and Fazleabas, 2006). The analysis related to endometriosis in the thorax of rhesus monkeys was first reported by Assaf and Miller (2012) Immunohistochemical and other results revealed that the uterine glands and mesenchyme entered the lungs, an extremely rare case that provides a reference for the extrauterine effects of endometriosis. A comparative study of progesterone treatment versus surgical excision in rhesus monkeys showed that subcutaneous implantation is a viable treatment with a shorter recovery period compared to oral versus surgical treatment (Maginnis et al., 2008). Researchers are also using large animals to explore biological therapies for endometriosis. Adipose-Derived Stem Cells (ADSCs) have been used to study the immunomodulatory effects of ADSCs on endometriosis in mares. Although positive effects such as some infiltration of ADSCs into endometrial tissue and upregulation of matrix metalloproteinase-9 expression were observed, the upregulation of interleukin-8 may have a negative effect on the therapeutic effect (Falomo et al., 2015). Nevertheless, this study is instructive for the biological treatment of endometriosis.

Discussion

Large animal models are an important reliance for humans to explore disease principles, discover drug targets, and test new drugs. Small rodents such as mice and rats still account for the majority of preclinical studies in gynecological diseases. These animals are cheaper, reproduce rapidly, and the knockout technique is easier to implement compared to larger animals, allowing study results to be obtained in a short period of time. However, large animals, such as pigs, monkeys, and sheep, have reproductive organs with structures and physiological cycles that are closer to those of humans than to those of rodents. Also, the larger size of large animals and the larger volume of their organs lend themselves to a wider variety of modeling approaches and allow for real-time examination. In the study of gynecological diseases, large animal models are more suitable (Figure 1). However, there are some issues to be noted for the use of large animals. Large animals are subject to more stringent ethical review and have higher requirements for husbandry conditions. Therefore, the selection of animal models requires a comprehensive consideration by the investigator. In this review, the use of large animals in gynecological diseases is presented with three disease examples, but of course, the examples go far beyond that Trus et al. (2020) used pigs to simulate human *in utero* Zika virus infection with a pathological response highly correlated with that of humans Nahmias et al.

(1971) successfully simulated genital infection with genital herpesvirus hominis type 2 virus in macaques. Researchers should be more critical in the selection of experimental animals, and the selection of appropriate animal models according to the study content is already a non-negligible item in the design of experiments.

Undeniably, with the increased use of large animal models in the study of gynecological diseases, there are many accompanying issues that deserve deeper consideration. First, although the characteristics of large animals are closer to those of humans, the issue of heterogeneity should be equally considered. There are also variations in reproductive characteristics between large animals and humans, for example, the trophoblast does not enter the uterine vasculature during pregnancy in sheep. The differences in physiological properties between large animal models and humans should be explored more deeply and these differences should be considered when studying human diseases. Finally, more attention should be paid to the welfare of large animals and to reducing the harm to experimental animals in the process of modeling and experimental validation using large animals. Though large animals are more tolerant of handling, the implementation process should follow the principles of "replace, reduce, optimize". Since it is not feasible to conduct large-scale disease studies with humans, the use of large laboratory animals remains the better option for now. However, there are still some reproductive diseases that lack large animals as models for research, such as multiple bacterial and fungal infection models, where researchers induce infection by inoculating bacteria and fungi in the genitalia. As for large animals, more naturally occurring diseased animals have been collected for research. But there is no denying the advantages of large animals for gynecological disease research, and more modeling protocols being explored will facilitate a deeper understanding of gynecological diseases.

Author contributions

MC wrote the manuscript and drew the pictures with partial help from YL, XM, and TL, DL, and YD edited and revised the manuscript. All authors contributed to the article and approved the submitted version.

Funding

This work was supported by the National Natural Science Foundation of China (Grant No. 81973712), Jilin Province Science and Technology Development Program in China (Grant No. 20210204013YY), Jilin Province Science and Technology Development Plan Program (Grant No. 20210204013YY, 20210101192JC, 20200504005YY) and Jilin Provincial Development and Reform Commission Program (2023C027-3).

Conflict of interest

The authors declare that the research was conducted in the absence of any commercial or financial relationships that could be construed as a potential conflict of interest.

Publisher's note

References

Abbott, D. H., Barnett, D. K., Levine, J. E., Padmanabhan, V., Dumesic, D. A., Jacoris, S., et al. (2008). Endocrine antecedents of polycystic ovary syndrome in fetal and infant prenatally androgenized female rhesus monkeys. *Biol. Reprod.* 79 (1), 154–163. doi:10.1095/biolreprod.108.067702

Abbott, D. H., Dumesic, D. A., Eisner, J. R., Colman, R. J., and Kemnitz, J. W. (1998). Insights into the development of polycystic ovary syndrome (PCOS) from studies of prenatally androgenized female rhesus monkeys. *Trends Endocrinol. Metab.* 9 (2), 62–67. doi:10.1016/s1043-2760(98)00019-8

Abbott, D. H., Levine, J. E., and Dumesic, D. A. (2016). Translational insight into polycystic ovary syndrome (PCOS) from female monkeys with PCOS-like traits. *Curr. Pharm. Des.* 22 (36), 5625–5633. doi:10.2174/1381612822666160715133437

Abedal-Majed, M. A., and Cupp, A. S. (2019). Livestock animals to study infertility in women. *Anim. Front.* 9 (3), 28–33. doi:10.1093/af/vfz017

Adams, G. P., Singh, J., and Baerwald, A. R. (2012). Large animal models for the study of ovarian follicular dynamics in women. *Theriogenology* 78 (8), 1733–1748. doi:10.1016/j.theriogenology.2012.04.010

American Diabetes Association (2013). Diagnosis and classification of diabetes mellitus. *Diabetes Care* 36, S67–S74. doi:10.2337/dc13-S067

Assaf, B. T., and Miller, A. D. (2012). Pleural endometriosis in an aged rhesus macaque (*Macaca mulatta*): A histopathologic and immunohistochemical study. *Vet. Pathol.* 49 (4), 636–641. doi:10.1177/0300985811406890

Azziz, R., Carmina, E., Chen, Z., Dunaif, A., Laven, J. S. E., Legro, R. S., et al. (2016). Polycystic ovary syndrome. *Nat. Rev. Dis. Prim.* 2, 16057. doi:10.1038/nrdp.2016.57

Banstola, A., and Reynolds, J. N. J. (2022). The sheep as a large animal model for the investigation and treatment of human disorders. *Biol. (Basel)* 11 (9), 1251. doi:10.3390/biology11091251

Bellamy, L., Casas, J. P., Hingorani, A. D., and Williams, D. (2009). Type 2 diabetes mellitus after gestational diabetes: A systematic review and meta-analysis. *Lancet* 373 (9677), 1773–1779. doi:10.1016/S0140-6736(09)60731-5

Bulun, S. E., Yilmaz, B. D., Sison, C., Miyazaki, K., Bernardi, L., Liu, S., et al. (2019). *Endometr. Endocr. Rev.* 40 (4), 1048–1079. doi:10.1210/er.2018-00242

Carter, A. M. (2020). Animal models of human pregnancy and placentation: Alternatives to the mouse. *Reproduction* 160 (6), R129–r143. doi:10.1530/REP-20-0354

Chapron, C., Marcellin, L., Borghese, B., and Santulli, P. (2019). Rethinking mechanisms, diagnosis and management of endometriosis. *Nat. Rev. Endocrinol.* 15 (11), 666–682. doi:10.1038/s41574-019-0245-z

Coate, K. C., Smith, M. S., Shiota, M., Irimia, J. M., Roach, P. J., Farmer, B., et al. (2013). Hepatic glucose metabolism in late pregnancy: Normal versus high-fat and -fructose diet. *Diabetes* 62 (3), 753–761. doi:10.2337/db12-0875

D'Hooghe, T. M., Bambra, C. S., Raeymaekers, B. M., De Jonge, I., Lauweryns, J. M., and Koninckx, P. R. (1995). Intrapelvic injection of menstrual endometrium causes endometriosis in baboons (*Papio cynocephalus* and *Papio anubis*). *Am. J. Obstetrics Gynecol.* 173 (1), 125–134. doi:10.1016/0002-9378(95)90180-9

D'Hooghe, T. M., Bambra, C. S., Raeymaekers, B. M., De Jonge, I., Lauweryns, J. M., and Koninckx, P. R. (1995). Intrapelvic injection of menstrual endometrium causes endometriosis in baboons (*Papio cynocephalus* and *Papio anubis*). *Am. J. Obstet. Gynecol.* 173 (1), 125–134. doi:10.1016/0002-9378(95)90180-9

D'Hooghe, T. M., Kyama, C. M., Chai, D., Fassbender, A., VodolAzkAiA, A., Bokor, A., et al. (2009). Nonhuman primate models for translational research in endometriosis. *Reprod. Sci.* 16 (2), 152–161. doi:10.1177/1933719108322430

de Souza, C. J., Campbell, B. K., and Baird, D. T. (1998). Incipient ovarian failure associated with raised levels of follicle stimulating hormone and reduced levels of inhibin A in older sheep. *Hum. Reprod.* 13 (11), 3016–3022. doi:10.1093/humrep/13.11.3016

Dickinson, J. E., Meyer, B. A., Chmielowiec, S., and Palmer, S. M. (1991). Streptozocin-induced diabetes mellitus in the pregnant Ewe. *Am. J. Obstetrics Gynecol.* 165 (6), 1673–1677. doi:10.1016/0002-9378(91)90013-h

Einspanier, A., Bruns, A., Husen, B., Thole, H., and Simon, C. (2006). Induction of endometriosis in the marmoset monkey (*Callithrix jacchus*). *Mol. Hum. Reprod.* 12 (5), 291–299. doi:10.1093/molehr/gal031

Ericsson, A. C., Crim, M. J., and Franklin, C. L. (2013). A brief history of animal modeling. *Mo Med.* 110 (3), 201–205.

Ezekwe, M. O., Ezekwe, E. I., Sen, D. K., and Ogolla, F. (1984). Effects of maternal streptozotocin-diabetes on fetal growth, energy reserves and body composition of newborn pigs. *J. Anim. Sci.* 59 (4), 974–980. doi:10.2527/jas1984.594974x

Ezekwe, M. O., and Martin, R. J. (1978). Influence of maternal alloxan diabetes or insulin injections on fetal glycogen reserves, muscle and liver development of pigs (Sus domesticus). *J. Anim. Sci.* 47 (5), 1121–1127. doi:10.2527/jas1978.4751121x

Falomo, M. E., Ferroni, L., Tocco, I., Gardin, C., and Zavan, B. (2015). Immunomodulatory role of adipose-derived stem cells on equine endometriosis. *Biomed. Res. Int.* 2015, 141485. doi:10.1155/2015/141485

Filipiak, W. E., and Saunders, T. L. (2006). Advances in transgenic rat production. *Transgenic Res.* 15 (6), 673–686. doi:10.1007/s11248-006-9002-x

Ford, S. P., Zhang, L., Zhu, M., Miller, M. M., Smith, D. T., Hess, B. W., et al. (2009). Maternal obesity accelerates fetal pancreatic beta-cell but not alpha-cell development in sheep: Prenatal consequences. *Am. J. Physiol. Regul. Integr. Comp. Physiol.* 297 (3), R835–R843. doi:10.1152/ajpregu.00072.2009

Gao, X., He, J., Zhu, A., Xie, K., Yan, K., Jiang, X., et al. (2021). Modelling gestational diabetes mellitus: Large animals hold great promise. *Rev. Endocr. Metab. Disord.* 22 (2), 407–420. doi:10.1007/s11154-020-09617-x

Grimbizis, G. F., CaMus, M., Tarlatzis, B. C., Bontis, J. N., and Devroey, P. (2001). Clinical implications of uterine malformations and hysteroscopic treatment results. *Hum. Reprod. Update* 7 (2), 161–174. doi:10.1093/humupd/7.2.161

Gu, Z. Y., Jia, S. Z., and Leng, J. H. (2020). Establishment of endometriotic models: The past and future. *Chin. Med. J. Engl.* 133 (14), 1703–1710. doi:10.1097/CM9.0000000000000885

Hall, B., Cho, A., Limaye, A., Cho, K., Khillan, J., and Kulkarni, A. B. (2018). Genome editing in mice using CRISPR/Cas9 technology. *Curr. Protoc. Cell Biol.* 81 (1), e57. doi:10.1002/cpcb.57

Harbeck, N., and Gnant, M. (2017). Breast cancer. *Lancet* 389 (10074), 1134–1150. doi:10.1016/S0140-6736(16)31891-8

Hastings, J. M., and Fazleabas, A. T. (2006). A baboon model for endometriosis: Implications for fertility. *Reprod. Biol. Endocrinol.* 4 (1), S7. doi:10.1186/1477-7827-4-S1-S7

Kahsar-Miller, M. D., Nixon, C., Boots, L. R., Go, R. C., and Azziz, R. (2001). Prevalence of polycystic ovary syndrome (PCOS) in first-degree relatives of patients with PCOS. *Fertil. Steril.* 75 (1), 53–58. doi:10.1016/s0015-0282(00)01662-9

Kasser, T. R., Martin, R. J., and Allen, C. E. (1981). Effect of gestational alloxan diabetes and fasting on fetal lipogenesis and lipid deposition in pigs. *Biol. Neonate* 40 (3-4), 105–112. doi:10.1159/000241478

Kelley, A. S., Puttabyatappa, M., Ciarelli, J. N., Zeng, L., Smith, Y. R., Lieberman, R., et al. (2019). Prenatal testosterone excess disrupts placental function in a sheep model of polycystic ovary syndrome. *Endocrinology* 160 (11), 2663–2672. doi:10.1210/en.2019-00386

Khalil, I., Aziz, S. E., Bensbaa, S., and Chadli, A. (2018). Grossesse diabétique et diabète gestationnel: Situations gestationnelles à haut risque. *Ann. d'Endocrinologie* 79 (4), 470–471. doi:10.1016/j.ando.2018.06.906

King, A. J., Olivier, N. B., Mohankumar, P. S., Lee, J. S., Padmanabhan, V., and Fink, G. D. (2007). Hypertension caused by prenatal testosterone excess in female sheep. *Am. J. Physiol. Endocrinol. Metab.* 292 (6), E1837–E1841. doi:10.1152/ajpendo.00668.2006

Lagana, A. S., Garzon, S., Gotte, M., Vigano, P., Franchi, M., Ghezzi, F., et al. (2019). The pathogenesis of endometriosis: Molecular and cell Biology insights. *Int. J. Mol. Sci.* 20 (22), 5615. doi:10.3390/ijms20225615

Legro, R. S., Arslanian, S. A., Ehrmann, D. A., Hoeger, K. M., Murad, M. H., Pasquali, R., et al. (2013). Diagnosis and treatment of polycystic ovary syndrome: An endocrine society clinical practice guideline. *J. Clin. Endocrinol. Metabolism* 98 (12), 4565–4592. doi:10.1210/jc.2013-2350

Leiser, R., Krebs, C., Ebert, B., and Dantzer, V. (1997). Placental vascular corrosion cast studies: A comparison between ruminants and humans. *Microsc. Res. Tech.* 38 (1-2), 76–87. doi:10.1002/(SICI)1097-0029(19970701/15)38:1/2<76:AID-JEMT9>3.0.CO;2-S

Li, L. P., Li, Z. M., Wang, Z. Z., Cheng, Y. F., He, D. M., Chen, G., et al. (2022). A novel nude mouse model for studying the pathogenesis of endometriosis. *Exp. Ther. Med.* 24 (2), 498. doi:10.3892/etm.2022.11425

Lin, J. H. (1995). Species similarities and differences in pharmacokinetics. *Drug Metab. Dispos.* 23 (10), 1008–1021.

Lizneva, D., Suturina, L., Walker, W., Brakta, S., Gavrilova-Jordan, L., and Azziz, R. (2016). Criteria, prevalence, and phenotypes of polycystic ovary syndrome. *Fertil. Steril.* 106 (1), 6–15. doi:10.1016/j.fertnstert.2016.05.003

Lu, H., Zhang, Y., Feng, Y., Zhang, J., and Wang, S. (2022). Current animal model systems for ovarian aging research. *Aging Dis.* 13 (4), 1183–1195. doi:10.14336/AD.2021.1209

Lunney, J. K., Van Goor, A., Walker, K. E., Hailstock, T., Franklin, J., and Dai, C. (2021). Importance of the pig as a human biomedical model. *Sci. Transl. Med.* 13 (621), eabd5758. doi:10.1126/scitranslmed.abd5758

Lv, H., Zhao, G., Jiang, P., Wang, H., Wang, Z., Yao, S., et al. (2022). Deciphering the endometrial niche of human thin endometrium at single-cell resolution. *Proc. Natl. Acad. Sci. U. S. A.* 119 (8), e2115912119. doi:10.1073/pnas.2115912119

Maenhoudt, N., De Moor, A., and Vankelecom, H. (2022). Modeling endometrium Biology and disease. *J. Pers. Med.* 12 (7), 1048. doi:10.3390/jpm12071048

Maginnis, G., Wilk, J., CaRRoll, R., and Slayden, O. D. (2008). Assessment of progestin-only therapy for endometriosis in macaque. *J. Med. Primatol.* 37 (1), 52–55. doi:10.1111/j.1600-0684.2007.00262.x

Malhi, P. S., Adams, G. P., and Singh, J. (2005). Bovine model for the study of reproductive aging in women: Follicular, luteal, and endocrine characteristics. *Biol. Reprod.* 73 (1), 45–53. doi:10.1095/biolreprod.104.038745

Mann, D. R., Collins, D. C., Smith, M. M., Kessler, M. J., and Gould, K. G. (1986). Treatment of endometriosis in monkeys: Effectiveness of continuous infusion of a gonadotropin-releasing hormone agonist compared to treatment with a progestational steroid. *J. Clin. Endocrinol. Metab.* 63 (6), 1277–1283. doi:10.1210/jcem-63-6-1277

Miodovnik, M., Mimouni, F., Berk, M., and Clark, K. E. (1989). Alloxan-induced diabetes mellitus in the pregnant Ewe: Metabolic and cardiovascular effects on the mother and her fetus. *Am. J. Obstetrics Gynecol.* 160 (5), 1239–1244. doi:10.1016/0002-9378(89)90203-2

Mondal, P., Bailey, K. L., Cartwright, S. B., Band, V., and Carlson, M. A. (2022). Large animal models of breast cancer. *Front. Oncol.* 12, 788038. doi:10.3389/fonc.2022.788038

Moore, M. C., Menon, R., Coate, K. C., Gannon, M., Smith, M. S., Farmer, B., et al. (1985). Diet-induced impaired glucose tolerance and gestational diabetes in the dog. *J. Appl. Physiol.* 110 (2), 458–467. doi:10.1152/japplphysiol.00768.2010

Murray, S. J., Black, B. L., Reid, S. J., Rudiger, S. R., Simon Bawden, C., Snell, R. G., et al. (2019). Chemical neuroanatomy of the substantia nigra in the ovine brain. *J. Chem. Neuroanat.* 97, 43–56. doi:10.1016/j.jchemneu.2019.01.007

Nahmias, A. J., London, W. T., Catalano, L. W., Fuccillo, D. A., Sever, J. L., and Graham, C. (1971). Genital herpesvirus hominis type 2 infection: An experimental model in cebus monkeys. *Science* 171 (3968), 297–298. doi:10.1126/science.171.3968.297

Paixao, L., Ramos, R. B., Lavarda, A., Morsh, D. M., and Spritzer, P. M. (2017). Animal models of hyperandrogenism and ovarian morphology changes as features of polycystic ovary syndrome: A systematic review. *Reprod. Biol. Endocrinol.* 15 (1), 12. doi:10.1186/s12958-017-0231-z

Pasek, R. C., and Gannon, M. (2013). Advancements and challenges in generating accurate animal models of gestational diabetes mellitus. *Am. J. Physiol. Endocrinol. Metab.* 305 (11), E1327–E1338. doi:10.1152/ajpendo.00425.2013

Peters, R. K., Kjos, S. L., XiAng, A., and Buchanan, T. A. (1996). Long-term diabetogenic effect of single pregnancy in women with previous gestational diabetes mellitus. *Lancet* 347 (8996), 227–230. doi:10.1016/s0140-6736(96)90405-5

Plows, J. F., Stanley, J. L., Baker, P. N., Reynolds, C. M., and Vickers, M. H. (2018). The pathophysiology of gestational diabetes mellitus. *Int. J. Mol. Sci.* 19 (11), 3342. doi:10.3390/ijms19113342

Ramsay, T. G., Wolverton, C. K., and Steele, N. C. (1994). Alteration in IGF-I mRNA content of fetal swine tissues in response to maternal diabetes. *Am. J. Physiol.* 267 (5), R1391–R1396. doi:10.1152/ajpregu.1994.267.5.R1391

Renner, S., Martins, A. S., Streckel, E., Braun-Reichhart, C., Backman, M., Prehn, C., et al. (2019). Mild maternal hyperglycemia in INS (C93S) transgenic pigs causes impaired glucose tolerance and metabolic alterations in neonatal offspring. *Dis. Model Mech.* 12 (8), dmm039156. doi:10.1242/dmm.039156

Robinson, N. B., Krieger, K., Khan, F. M., Huffman, W., Chang, M., Naik, A., et al. (2019). The current state of animal models in research: A review. *Int. J. Surg.* 72, 9–13. doi:10.1016/j.ijsu.2019.10.015

Rosenfield, R. L., and Ehrmann, D. A. (2016). The pathogenesis of polycystic ovary syndrome (PCOS): The hypothesis of PCOS as functional ovarian hyperandrogenism revisited. *Endocr. Rev.* 37 (5), 467–520. doi:10.1210/er.2015-1104

Schüttler, D., Bapat, A., Kaab, S., Lee, K., Tomsits, P., Clauss, S., et al. (2020). Animal models of atrial fibrillation. *Circ. Res.* 127 (1), 91–110. doi:10.1161/CIRCRESAHA.120.316366

Scott, D. M. (2022). Inflammatory diseases of the breast. *Best. Pract. Res. Clin. Obstet. Gynaecol.* 83, 72–87. doi:10.1016/j.bpobgyn.2021.11.013

Shafrir, A. L., Farland, L. V., Shah, D. K., Harris, H. R., Kvaskoff, M., Zondervan, K., et al. (2018). Risk for and consequences of endometriosis: A critical epidemiologic review. *Best Pract. Res. Clin. Obstetrics Gynaecol.* 51, 1–15. doi:10.1016/j.bpobgyn.2018.06.001

Shostrom, D. C. V., Sun, Y., Oleson, J. J., Snetselaar, L. G., and Bao, W. (2017). History of gestational diabetes mellitus in relation to cardiovascular disease and cardiovascular risk factors in US women. *Front. Endocrinol. (Lausanne)* 8, 144. doi:10.3389/fendo.2017.00144

Siemienowicz, K. J., Coukan, F., Franks, S., Rae, M. T., and Duncan, W. C. (2021). Aberrant subcutaneous adipogenesis precedes adult metabolic dysfunction in an ovine model of polycystic ovary syndrome (PCOS). *Mol. Cell Endocrinol.* 519, 111042. doi:10.1016/j.mce.2020.111042

Sillem, M., Hahn, U., Coddington, C. C., Gordon, K., RunneBaum, B., and Hodgen, G. D. (1996). Ectopic growth of endometrium depends on its structural integrity and proteolytic activity in the cynomolgus monkey (*Macaca fascicularis*) model of endometriosis. *Fertil. Steril.* 66 (3), 468–473. doi:10.1016/s0015-0282(16)58521-5

Stewart, E. A. (2001). Uterine fibroids. *Lancet* 357 (9252), 293–298. doi:10.1016/S0140-6736(00)03622-9

Tonellotto Dos Santos, J., Escariao da Nobrega, J., Serrano Mujica, L. K., Dos Santos Amaral, C., Machado, F. A., Manta, M. W., et al. (2018). Prenatal androgenization of ewes as a model of hirsutism in polycystic ovary syndrome. *Endocrinology* 159 (12), 4056–4064. doi:10.1210/en.2018-00781

Trus, I., Walker, S., Fuchs, M., Udenze, D., Gerdts, V., and Karniychuk, U. (2020). A porcine model of Zika virus infection to profile the in utero interferon alpha response. *Methods Mol. Biol.* 2142, 181–195. doi:10.1007/978-1-0716-0581-3_15

Tyrrell, C. J. (1999). Gynaecomastia: Aetiology and treatment options. *Prostate Cancer Prostatic Dis.* 2 (4), 167–171. doi:10.1038/sj.pcan.4500314

Umeyama, K., Saito, H., Kurome, M., Matsunari, H., Watanabe, M., Nakauchi, H., et al. (2012). Characterization of the ICSI-mediated gene transfer method in the production of transgenic pigs. *Mol. Reprod. Dev.* 79 (3), 218–228. doi:10.1002/mrd.22015

Varughese, E. E., Adams, G. P., Leonardi, C. E., Malhi, P. S., Babyn, P., Kinloch, M., et al. (2018). Development of a domestic animal model for endometriosis: Surgical induction in the dog, pigs, and sheep. *J. Endometr. Pelvic Pain Disord.* 10 (2), 95–106. doi:10.1177/2284026518773942

Vendola, K. A., Zhou, J., Adesanya, O. O., Weil, S. J., and Bondy, C. A. (1998). Androgens stimulate early stages of follicular growth in the primate ovary. *J. Clin. Invest.* 101 (12), 2622–2629. doi:10.1172/JCI2081

Watanabe, M., Umeyama, K., Matsunari, H., Takayanagi, S., Haruyama, E., Nakano, K., et al. (2010). Knockout of exogenous EGFP gene in porcine somatic cells using zinc-finger nucleases. *Biochem. Biophys. Res. Commun.* 402 (1), 14–18. doi:10.1016/j.bbrc.2010.09.092

Werlin, L. B., and Hodgen, G. D. (1983). Gonadotropin-releasing hormone agonist suppresses ovulation, menses, and endometriosis in monkeys: An individualized, intermittent regimen. *J. Clin. Endocrinol. Metab.* 56 (4), 844–848. doi:10.1210/jcem-56-4-844

White, B. A., Creedon, D. J., Nelson, K. E., and Wilson, B. A. (2011). The vaginal microbiome in health and disease. *Trends Endocrinol. Metab.* 22 (10), 389–393. doi:10.1016/j.tem.2011.06.001

Yao, J., Huang, J., and Zhao, J. (2016). Genome editing revolutionize the creation of genetically modified pigs for modeling human diseases. *Hum. Genet.* 135 (9), 1093–1105. doi:10.1007/s00439-016-1710-6

Zeng, X., Xie, Y. J., Liu, Y. T., Long, S. L., and Mo, Z. C. (2020). Polycystic ovarian syndrome: Correlation between hyperandrogenism, insulin resistance and obesity. *Clin. Chim. Acta* 502, 214–221. doi:10.1016/j.cca.2019.11.003

frontiers | Frontiers in Cell and Developmental Biology

TYPE Original Research
PUBLISHED 24 January 2023
DOI 10.3389/fcell.2022.1115348

OPEN ACCESS

EDITED BY
Feng Yue,
Hainan University, China

REVIEWED BY
Xing Guo,
Nanjing Medical University, China
Shang-Hsun Yang,
National Cheng Kung University, Taiwan

*CORRESPONDENCE
Shihua Li,
lishihualis@jnu.edu.cn
Sen Yan,
231yansen@163.com

†These authors contributed equally to this work and share first authorship

SPECIALTY SECTION
This article was submitted to Stem Cell Research, a section of the journal Frontiers in Cell and Developmental Biology

RECEIVED 03 December 2022
ACCEPTED 13 December 2022
PUBLISHED 24 January 2023

CITATION
Lin Y, Li C, Wang W, Li J, Huang C, Zheng X, Liu Z, Song X, Chen Y, Gao J, Wu J, Wu J, Tu Z, Lai L, Li X-J, Li S and Yan S (2023), Intravenous AAV9 administration results in safe and widespread distribution of transgene in the brain of mini-pig.
Front. Cell Dev. Biol. 10:1115348.
doi: 10.3389/fcell.2022.1115348

Intravenous AAV9 administration results in safe and widespread distribution of transgene in the brain of mini-pig

Yingqi Lin[1†], Caijuan Li[1†], Wei Wang[1], Jiawei Li[1], Chunhui Huang[1], Xiao Zheng[1], Zhaoming Liu[2], Xichen Song[1], Yizhi Chen[1], Jiale Gao[1], Jianhao Wu[1], Jiaxi Wu[1], Zhuchi Tu[1], Liangxue Lai[2], Xiao-Jiang Li[1], Shihua Li[1]* and Sen Yan[1]*

[1]Guangdong Key Laboratory of Non-human Primate Research, Guangdong-Hongkong-Macau Institute of CNS Regeneration, Jinan University, Guangzhou, China, [2]Key Laboratory of Regenerative Biology, South China Institute for Stem Cell, Biology and Regenerative Medicine, Guangzhou Institutes of Biomedicine and Health, Chinese Academy of Sciences, Guangzhou, China

Animal models are important for understanding the pathogenesis of human diseases and for developing and testing new drugs. Pigs have been widely used in the research on the cardiovascular, skin barrier, gastrointestinal, and central nervous systems as well as organ transplantation. Recently, pigs also become an attractive large animal model for the study of neurodegenerative diseases because their brains are very similar to human brains in terms of mass, gully pattern, vascularization, and the proportions of the gray and white matters. Although adeno-associated virus type 9 (AAV9) has been widely used to deliver transgenes in the brain, its utilization in large animal models remains to be fully characterized. Here, we report that intravenous injection of AAV9-GFP can lead to widespread expression of transgene in various organs in the pig. Importantly, GFP was highly expressed in various brain regions, especially the striatum, cortex, cerebellum, hippocampus, without detectable inflammatory responses. These results suggest that intravenous AAV9 administration can be used to establish large animal models of neurodegenerative diseases caused by gene mutations and to treat these animal models as well.

KEYWORDS

AAV9, CNS, large animal, pig, neurodegeneration

Introduction

Animal models are indispensable in scientific research and often used in the study of disease mechanisms, drug development, and therapeutics. Many animal models of neurodegenerative diseases have been established and thoroughly investigated in the past. These include invertebrate (Lee et al., 2018) and rodent models (Levine et al., 2004; Ashe and Zahs, 2010; Epis et al., 2010; McWilliams et al., 2018), and provide valuable information for understanding how neuropathology and neurological symptoms are

developed. However, the genomic homology and complexity (Kwon and Ernst, 2021), the size and structure of the brain (Laramée and Boire, 2015), and the life span (Dutta and Sengupta, 2016) as well as various physiological aspects are noticeably different between small animals and humans, which hampers small animal models in fully modeling the complex pathological features in neurodegenerative diseases, especially in selective neurodegeneration. Therefore, there is an apparent need to establish large animal models that can more closely mimic important pathological and clinical features because of they are more similar to humans in anatomy, physiology and development.

Compared to small animal models, pigs are highly similar to humans in genetics, anatomy, physiology, and neural network complexity (Wernersson et al., 2005; Chen et al., 2007). In addition, the pregnancy period of pigs is short, the number of offspring born in a litter is large, and sexual maturity can be achieved in 5–6 months. These advantages are superior to non-human primates, which normally produce single fetus and have long sexual maturity time with a long pregnancy period. Transgenic pig models for a variety of neurodegenerative diseases have been established, including Alzheimer's diseases (Kragh et al., 2009; Søndergaard et al., 2012; Jakobsen et al., 2013), Huntington's disease (Yang et al., 2010; Baxa et al., 2013; Yan et al., 2018), Parkinson's disease (Yao et al., 2014; Zhou et al., 2015), amyotrophic lateral sclerosis (Chieppa et al., 2014; Yang et al., 2014), spinal muscular atrophy (Lorson et al., 2011), and ataxia–telangiectasia (Kim et al., 2014). Our previous studies have shown that pigs expressing full-length mutant HTT at endogenous levels exhibit neuropathologic and behavioral characteristics similar to the HD patients (Yan et al., 2018). Therefore, pigs have become an attractive large animal model for studying neurodegenerative diseases or other neurological disorders.

Viral vectors are often used to deliver transgenes into the central nervous system to generate neurodegenerative disease models or to treat neurodegenerative diseases. Adeno-associated virus (AAV) is one of the most studied gene therapy tool. So far, multiple AAV serotypes have been characterized, including AAV1-5 and AAV7-9 (Wu et al., 2006). A variety of AAV-based treatments have already been used in clinical research, including Alipogene tiparvovec (Glybera®; AMT-011, AAV1-LPLS447X), an adeno-associated virus serotype 1-based gene therapy for adult patients with familial lipoprotein lipase (LPL) deficiency (LPLD) (Scott, 2015), AAV-2 vector for Neurosurgical Delivery of Aspartoacylase Gene (ASPA) to treat Canavan Disease (Janson et al., 2002), a serotype 2 adeno-associated virus expressing CLN2 cDNA for treating late infantile neuronal ceroid lipofuscinos (Worgall et al., 2008), and the voretigene neparvovec gene therapy for patients with RPE65-mediated inherited retinal dystrophy (Russell et al., 2017).

Although AAV has become one of the key tools for preclinical and clinical gene therapy research, how to deliver these AAV carrying the transgenes to the affected brain regions remains a challenge (Mingozzi and High, 2011). To bypass the blood-brain barrier (BBB), intraparenchymal or intrathecal delivery is usually used in current research. However, permanent effects normally cannot be achieved by single AAV administration, and multiple or regular administrations are usually required to produce desired effects (Broekman et al., 2007; Herzog et al., 2007; Worgall et al., 2008; Hudry et al., 2010; Hocquemiller et al., 2016). Although direct injection of AAV into the brain has made great progress, craniotomy still faces many risks and challenges, such as postoperative nausea, vomiting, pain, venous thromboembolism and so on (Anthofer et al., 2016; Fang et al., 2017; Tsaousi et al., 2017). Therefore, there is a need to find an efficient, safe, and simple delivery method of AAVs.

AAV9 is one of the most studied AAV serotypes recently in gene therapy. Compared with other AAV serotypes, AAV9 targets the central nervous system with a higher efficiency and can cross the blood-brain barrier (Duque et al., 2009; Penzes et al., 2021). In addition, AAV9 has a low seropositive rate in the population, which has a significant advantage in gene therapy for humans (Boutin et al., 2010). However, the efficiency of intravenous delivery of adeno-associated virus to the central nervous system in large animals remains to be fully investigated. In the current study, we investigated the efficacy and safety of intravenous delivery of AAV9 in pigs. Our results demonstrated that intravenous administration of AAV9 that expresses GFP did not cause significant inflammatory response and allowed GFP to be widely distributed in the central nervous system in the pigs. These findings provided experimental evidence from large animals for using AAV9 in the preclinical treatment of human brain diseases.

Results

Expression of GFP in the central nervous system and peripheral tissues after auricular vein injection of AAV-CMV-GFP in pigs

The purpose of this study is to find an efficient, safe, and simple way of AAV virus delivery to the brain in mini pigs, allowing transgene to cross the blood brain barrier for the gene therapy on neurodegenerative diseases. To this end, AAV-CMV-GFP was injected into mini pigs through the ear vein. The subsequent experiments were then performed to verify the expression of GFP in the pig brain and to explore whether this therapeutic approach yielded any obvious neurotoxicity and inflammatory response.

As a disease model, pigs have been widely used in the study of central nervous system diseases. AAV, as a delivery tool for foreign genes, is also widely used in the study of central nervous

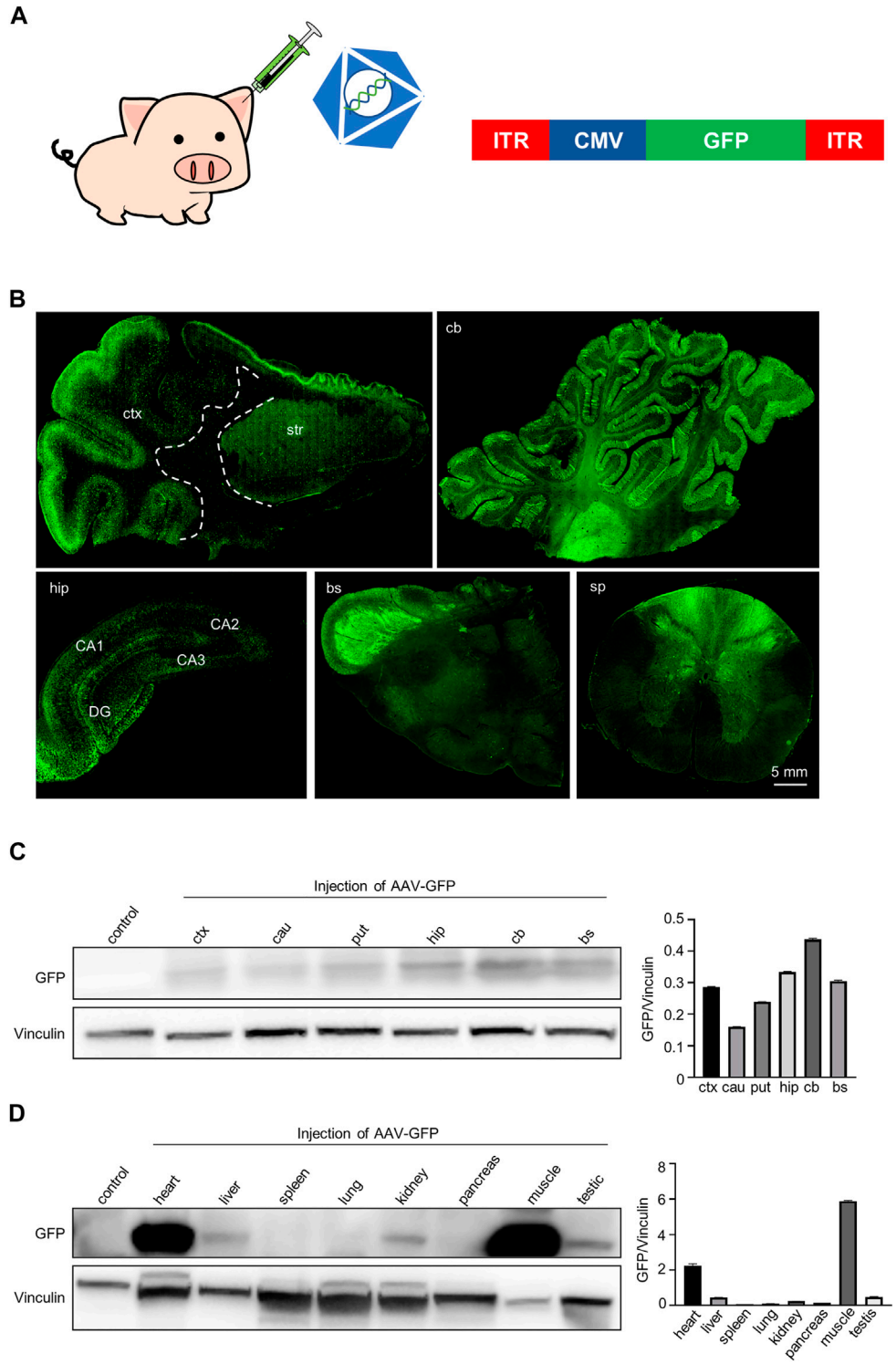

FIGURE 1
GFP expression in the pig brain, spinal cord and periphery tissues following intravascular administration. **(A)** Injection of AAV-CMV-GFP into 7-day-old Bama pigs *via* auricular vein. Saline served as a control. AAV9 serotype was used to package viruses. **(B)** Immunofluorescent staining showed that GFP was expressed in various brain regions and spinal cord of pigs after AAV-CMV-GFP injection. Regions are (clockwise from upper left) cortex and striatum (ctx and str), cerebellum (cb), hippocampus (hip), brain stem (bs), spinal cord (sp). **(C)** Western blotting demonstrates that GFP was expressed in various brain regions of pigs. Vinculin served as a loading control (left). Quantification of the GFP expression in each brain region. Data are analyzed by Student's T-test and presented as mean ± SEM (right). N = 3 animals per group. **(D)** Western blotting of GFP expression in various peripheral tissues of pigs. Vinculin served as a loading control (left). Quantification of GFP expression in each type of peripheral tissues. Data are analyzed by Student's T-test and presented as mean ± SEM (right). N = 3 animals per group.

system diseases. But how to safely and efficiently deliver AAV to the central nerve system of pigs has not been studied. Because the blood-brain barrier of newborn piglets is not fully established, AAV-9 virus has been proved that it can cross the blood-brain barrier relatively easily and can be distributed widely in the brain after intravenous injection of newborn pigs (Foust et al., 2009). Therefore, we injected the AAV-CMV-GFP through auricular vein into 7-day-old piglets at a dose of 1.2×10^{13} genome copies/kg (Figure 1A). GFP was expressed by AAV9 vector under the control of the CMV promoter (AAV-CMV-GFP). This virus can be widely expressed in a variety of cell types and was selected for intravenous injection such that GFP represents transgene expression that can be readily detected.

We first evaluated the expression of GFP in the mini-pig. We detected the expression of GFP in the central nervous system, including the cortex, striatum, cerebellum, hippocampus and spinal cord by using immunofluorescent staining with anti-GFP antibody (Figure 1B). GFP-positive cells were widely distributed in the cortex and were more abundant in the gray matter region where neuronal cells are enriched. GFP-positive cells were also frequently seen in the striatum (Figure 1B, top left panels). The cerebellum contained abundant GFP-positive neurons and glia cells, and most Purkinje cells expressed GFP (Figure 1B, top right panels). We also observed a large number of GFP-positive cells in the hippocampus (Figure 1B, bottom right panel). Many GFP-positive fibers were observed mainly in the brainstem and spinal cord, potentially reflecting fibers in afferent and efferent brain regions (Figure 1B, bottom, center, right panel). Consistently, western blotting results showed that GFP was wildly expressed in the brain regions, including the cortex, caudate, putamen, cerebellum and hippocampus (Figure 1C). In addition, GFP was also expressed in the peripheral tissues of pig, especially in heart and muscle. Interestingly, we found that GFP was expressed in the testis, which means that the virus can enter the seminiferous ducts through the blood-testis barrier when being injected through the auricular vein in newborn animals (Figure 1D). Taken together, a single intravenous injection of AAV-CMV-GFP into the newborn pigs allowed GFP expression throughout the pig body.

Effects of AAV-GFP transduction on the expression of neuronal and glial proteins

To assess the effect of AAV-GFP transduction on neuronal and glial cells, we used antibodies against neuronal protein (NeuN) for detecting neurons (Gusel'nikova and Korzhevskiy, 2015), glial fibrillary acidic protein (GFAP) for astrocytes (Baba et al., 1997; Eng et al., 2000; Li et al., 2020), ionized calcium binding adapter molecule 1 (Iba1) for microglia (Ito et al., 1998; Sasaki et al., 2001), and oligodendrocyte lineage transcription factor 2 (Olig2) for oligodendrocytes (Zhou et al., 2000). The number s of neurons, astrocytes, microglia and oligodendrocytes in the cortex of wild type (WT) pigs injected with virus did not change, compared with WT pigs injected with saline. (Figures 2A–L). Similarly, the results of western blotting demonstrated that synapsin-1, which is involved in regulation of neurotransmitter release, NeuN, GFAP and Iba1 were unchanged in cortex (Figure 2M, N). In brain regions where numerous cell bodies were also GFP-labeled, including the striatum (Figure 3), hippocampus (Figure 4) and cerebellum (Figure 5), cell numbers and synapsin-1 staining did not change, consistent with the results observed in the cortex. Similarly, there were also no changes in the above-mentioned neuropathology-related markers in the brain stem (Supplementary Figure S1) and spinal cord (Supplementary Figure S2), though GFP-tagged fibers were present in these two regions. We then compared GFP expression in the cortex (Figure 2), striatum (Figure 3), and hippocampus (Figure 4) using double immunohistochemical staining and found that AAV-CMV-GFP was more abundant in neurons (Figure 2B; Figure 3B; Figure 4B) and astrocytes (Figure 2E; Figure 3E; Figure 4E) than microglia (Figure 2H; Figure 3H; Figure 4H) and oligodendrocytes (Figure 2K; Figure 3K; Figure 4K). A qualitative analysis of transduction levels of each cell type is in Supplementary Table S1. What is strikingly noticeable is that in the cerebellum the virus basically infected neurons, especially Purkinje cells, and did not infect glial cells (Figure 5). Taken together, injecting the AAV-CMV-GFP into pigs through auricular vein did not cause neuronal damage and glial cell activation, and the virus infected basically neurons and astrocytes.

AAV-CMV-GFP injection in pigs *via* auricular vein does not cause inflammatory response

Inflammation within the central nervous system can damage neurons (Herz et al., 2010; Ashraf et al., 2021). In addition, the degree of inflammatory response in the central nervous system is associated with systemic inflammation. Inhibiting the inflammatory response in the peripheral tissues can improve inflammation in the central nervous system (Campbell et al., 2007, 2008; Anthony and Couch, 2014; Clausen et al., 2014). To test the safety of intravenous administration of AAV, we next investigated whether intravenous injection of AAV-CMV-GFP could cause inflammatory responses in the central nervous system and peripheral tissues. Because the expression of inflammatory cytokines is a pathological feature of inflammation in the brain, spinal cord, and periphery (Zhang and An, 2007; Becher et al., 2017), we chose to examine the expression of several typical inflammatory cytokines, including TGFβ, IL17, IL6, IL4, IL1β, TNFα, in the AAV-GFP-injected pigs and compare them with those in the saline-injected pigs. Western blotting results showed no significant changes in the expression of inflammatory cytokines detected in the cortex of pigs after

10.3389/fcell.2022.1115348

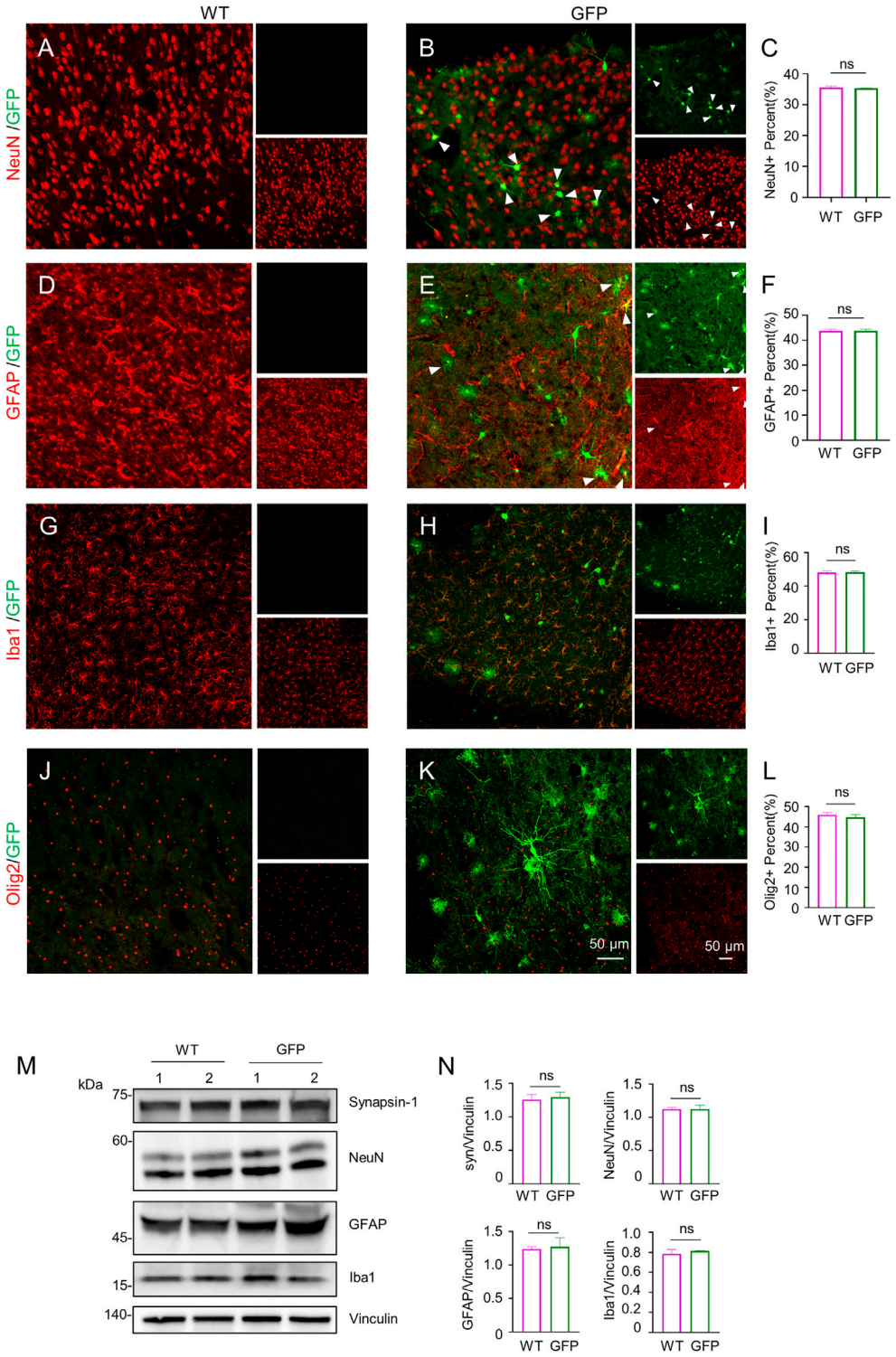

FIGURE 2
Immunofluorescent staining of the pig's cortex injected with AAV-GFP or saline. **(A–C)** Double immunofluorescent labeling **(A,B)** and quantification **(C)** of neurons (NeuN) of saline- or AAV-GFP-injected-wild type pigs. GFP positive cells are shown in green (small images in the upper right), NeuN positive cells are shown in red (small images in the lower right). The triangles indicate cells that are positive for both GFP and NeuN. **(D–F)** Double-immunofluorescent labeling **(D,E)** and quantification **(F)** of astrocytes (GFAP) in saline control or AAV-GFP injected pigs. Small images in the upper right are GFP positive cells and in the lower right are GFAP positive cells. **(G–I)** Double-immunofluorescent labeling **(G,H)** and quantification **(I)** of microglial cells (Iba1) in saline control or AAV-GFP injected pigs. Small images in the upper right are GFP positive cells and in the

(*Continued*)

FIGURE 2 (Continued)
lower right are Iba1 positive cells. **(J–L)** Double-immunofluorescent labeling **(G,H)** and quantification **(L)** of oligodendrocytes (Olig2) cells in the saline control or AAV-GFP injected pigs. Small images in the upper right are GFP positive cells and in the lower right are Olig2 positive cells. Quantification of the numbers of neuronal or glial cells was performed using three animals per group. Data are analyzed by Student's T-test and presented as mean ± SEM. **(M)** Western blotting of the cortex of the saline- or AAV-GFP-injected pigs with antibodies against synapsin-1, NeuN, GFAP, and Iba1. Vinculin served as a loading control. **(N)** Quantitation of the ratios of synapsin-1, NeuN, GFAP and Iba1 to vinculin on the western blots. Data are analyzed by student's T-test and presented as mean ± SEM. n = 3 animals per group.

virus injection (Figure 6A). Similar, similar results were observed in the striatum (Figure 6B), hippocampus (Figure 6C), cerebellum (Figure 6D), and brain stem (Supplementary Figure S3A). The expression of these inflammatory cytokines was also largely unchanged in the spinal cord (Supplementary Figure S3B) and peripheral tissues (Supplementary Figure S4). The above results indicate that intravenous injection of AAV-CMV-GFP is safe and does not cause severe inflammatory reactions in any major organ.

AAV-CMV-GFP injection in pigs *via* auricular vein does not cause transcriptome alternation

To further determine the effect of intravenous AAV9 on the central nervous system, we performed RNA-seq analysis of the cortical tissues, which has high GFP expression and contains major part of the brain. The results showed that the transcriptomes of in the cortex of pigs receiving intravenous AAV-CMV-GFP (GFP) were very similar to those of pigs receiving saline treatment (WT) (Figure 7A; Supplementary Figure S5). Further analysis of the differential expression at the same difference threshold (log2FC > 2, Padj<.01) revealed no significant difference between WT and AAV-GFP groups (Figure 7B), though slight but not significant differences may exist. We also examined 20 genes associated with inflammation between WT and GFP groups and found no significant changes in these genes (Figure 7C), suggesting that intravenous administration of AAV9 in large animals did not induce a strong inflammatory response. RNA-seq showed that intravenous administration of AAV9 did not cause changes in the transcriptional regulation or inflammatory response in the cortical tissues of pigs injected with AAV-GFP.

Discussion

Intravenous delivery of AAV9 to target specific genes in the central nervous system has great therapeutic potential for a variety of neurodegenerative diseases, such as Alzheimer's, Huntington's, Parkinson's diseases, amyotrophic lateral sclerosis, spinal muscular atrophy, ataxia telangiectasia *etc.* Currently, not many studies have evaluated the transduction efficiency, distribution pattern, and safety of AAV9 after direct intravenous delivery in the central nervous system of large animals such as pigs. Our results demonstrated the ability of AAV9 to transduce neurons and glial cells in various brain regions and spinal cord of pigs by injecting AAV-CMV-GFP into the auricular vein.

Many neurodegenerative diseases often start with selective specific brain regional cell death (Double et al., 2010; Reith, 2018), and as diseases progress, neurodegeneration becomes more severe and extends to other brain regions. Brain regional administration can be used to treat brain-region specific damage but would be difficult to reach to the large area of brain parenchyma. However, AAV9 can spreading to various brain regions and is able to pass blood brain barrier, providing a possibility for the treatment of disease that affects large areas in brain.

In our study, neuronal cells in both the cortex and striatum were found to express transgene GFP after intravenous injection of AAV-CMV-GFP. The widespread expression of transgene in these two brain regions is important for treating Huntington disease (HD), which is caused by polyglutamine repeat expansion in the Huntingtin (HTT) protein and display neurodegeneration that is most severe in the striatum and cortex (Bates et al., 2015). In both HD patients and HD KI pig models, the medium spiny neurons in the striatum undergo preferential neurodegeneration. With the development of the disease, the cortex and other brain regions will also be involved (Waldvogel et al., 2015; Yan et al., 2018). Because HD is caused by a single gene mutation, using gene therapy to inhibit the expression of mutated HTT is one of the attractive strategies to treat HD. Previous study has used HDKI-140Q mice to test gene therapy because they express mutant HTT in the same manner as patients with HD. However, rodents cannot truly mimic the neuropathology seen in HD patients, and HD KI mice expressing full-length mutant HTT at endogenous level lack significant pathological features of neuronal loss (Levine et al., 2004; Yang et al., 2017). On the other hand, HD KI pigs we established previously show striking neuronal loss as HD patients (Yan et al., 2018), providing a valuable model to evaluate the effects of gene therapy on neurodegeneration. Thus, it is important to use pigs as a model to examine whether AAV administration can effectively deliver transgene into the pig brain.

Previous studies have used intracranial or intratarsal injection of AAV into the pig brain to suppress HTT

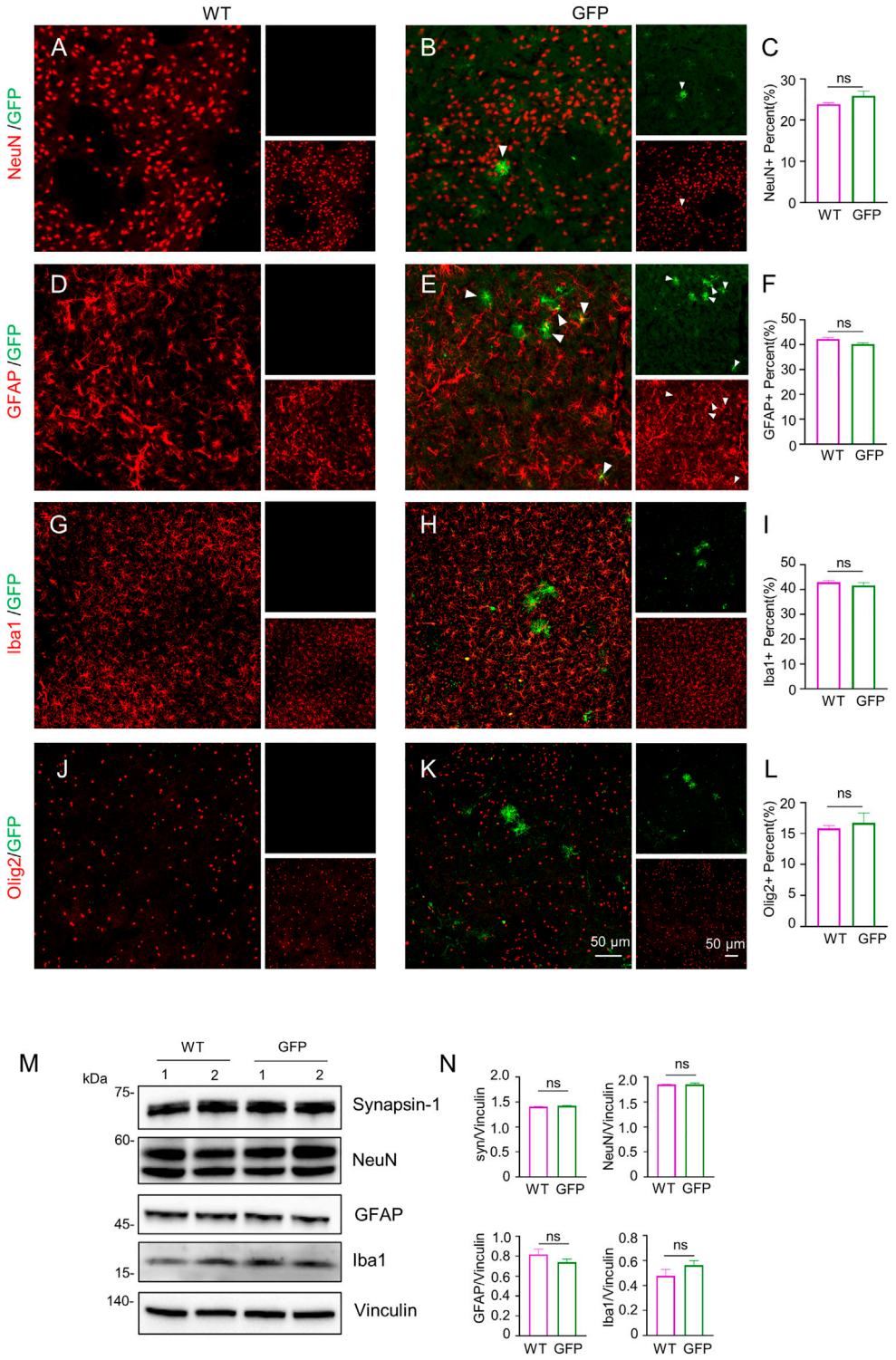

FIGURE 3
Immunofluorescent staining of the pig's striatum injected with AAV-GFP or saline. **(A–L)** Double immunofluorescent labeling and quantification of neurons (NeuN) **(A–C)**, astrocytes (GFAP) **(D–F)**, microglial (Iba1) **(G–I)** and oligodendrocytes (Olig2) **(J–L)** of saline- or AAV-GFP-injected-wild type pigs. GFP positive cells are shown in green, NeuN, GFAP, Iba1 and Olig2 positive cells are shown in red. Data are analyzed by Student's T-test and presented as mean ± SEM. *n* = 3 animals per group. **(M)** Western blotting of the striatum of saline- or AAV-GFP-injected pigs with antibodies against synapsin-1, NeuN, GFAP and Iba1. Vinculin served as a loading control. **(N)** Quantitation of the ratios of synapsin-1, NeuN, GFAP or Iba1 to vinculin on the western blots. Data are analyzed by student's T-test and presented as mean ± SEM. *n* = 3 animals per group.

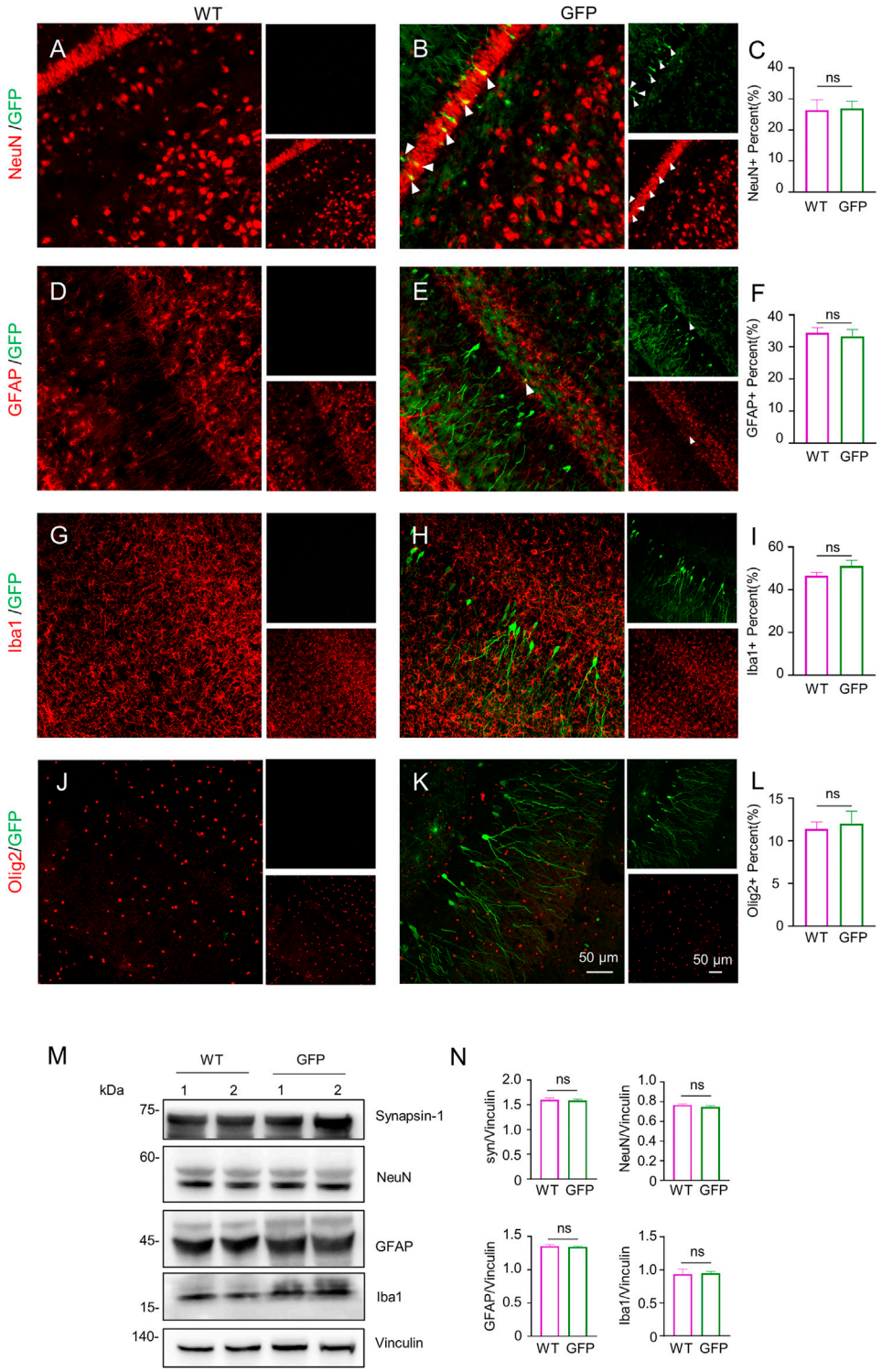

FIGURE 4
Immunofluorescent staining of the pigs' hippocampus injected with AAV-GFP or saline. **(A–L)** Double immunofluorescent labeling and quantification of neurons (NeuN) **(A–C)**, astrocytes (GFAP) **(D–F)**, microglial (Iba1) **(G–I)** and oligodendrocytes (Olig2) **(J–L)** of saline- or AAV-GFP-injected-wild type pigs. GFP positive cells are shown in green, NeuN, GFAP, Iba1 and Olig2 positive cells are shown in red. Data are analyzed by Student's T-test and presented as mean ± SEM. *n* = 3 animals per group. **(M)** Western blotting of the hippocampus of saline- or AAV-GFP-injected pigs with antibodies against synapsin-1, NeuN, GFAP and Iba1. Vinculin served as a loading control. **(N)** Quantitation of the ratios of synapsin-1, NeuN, GFAP or Iba1 to vinculin on the western blots. Data are analyzed by student's T-test and presented as mean ± SEM. *n* = 3 animals per group.

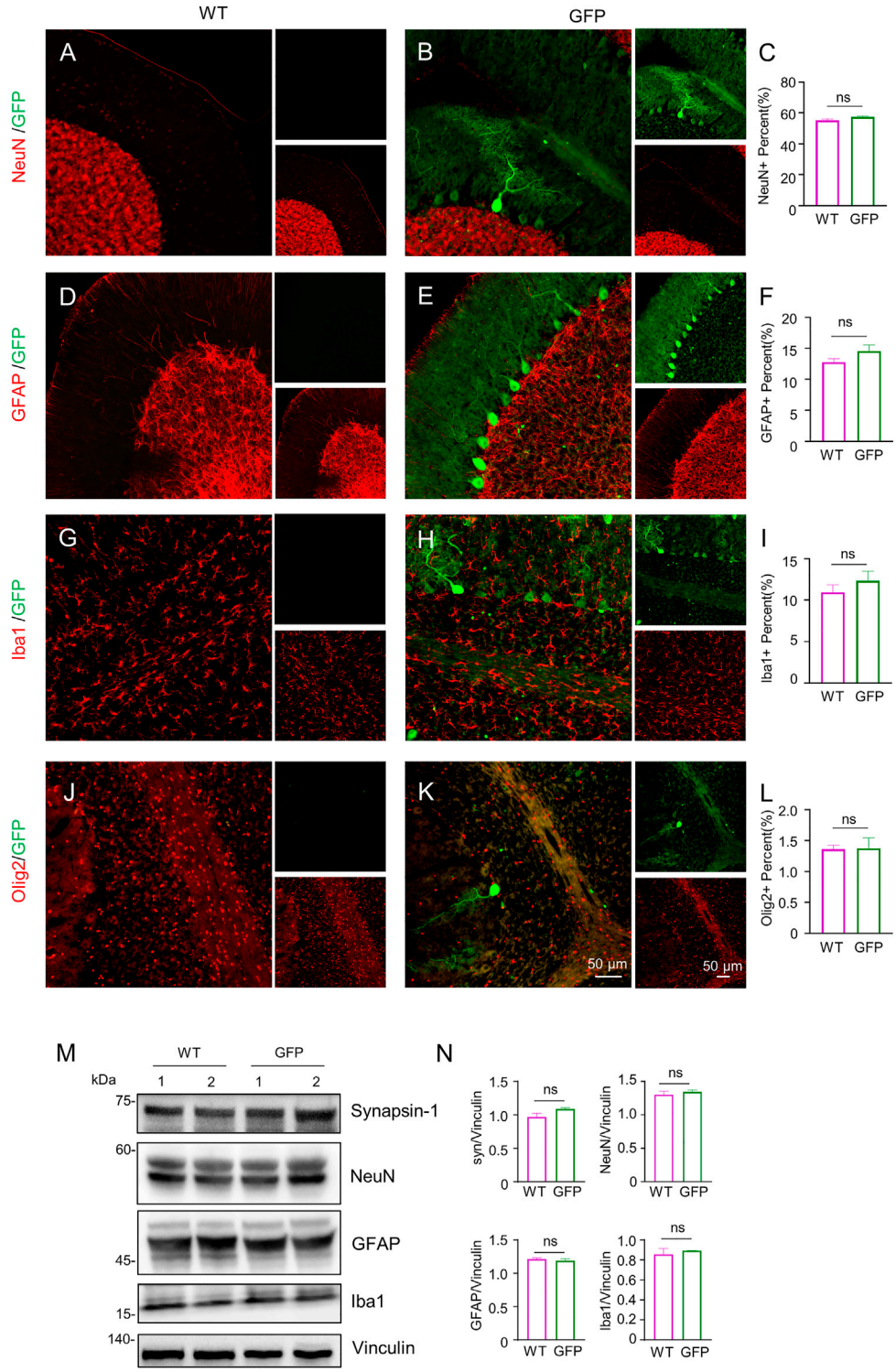

FIGURE 5
Immunofluorescent staining of the pigs' cerebellum injected with AAV-GFP or saline. **(A–L)** Double immunofluorescent labeling and quantification of neurons (NeuN) **(A–C)**, astrocytes (GFAP) **(D–F)**, microglial (Iba1) **(G–I)** and oligodendrocytes (Olig2) **(J–L)** of saline- or AAV-GFP-injected-wild type pigs. GFP positive cells are shown in green, NeuN, GFAP, Iba1 and Olig2 positive cells are shown in red. Data are analyzed by Student's T-test and presented as mean ± SEM. *n* = 3 animals per group. **(M)** Western blotting of the cerebellum injected with saline or AAV-GFP using antibodies against synapsin-1, NeuN, GFAP and Iba1. Vinculin served as a loading control. **(N)** Quantitation of the ratios of synapsin-1, NeuN, GFAP or Iba1 to vinculin on the western blots. Data are analyzed by student's T-test and presented as mean ± SEM. *n* = 3 animals per group.

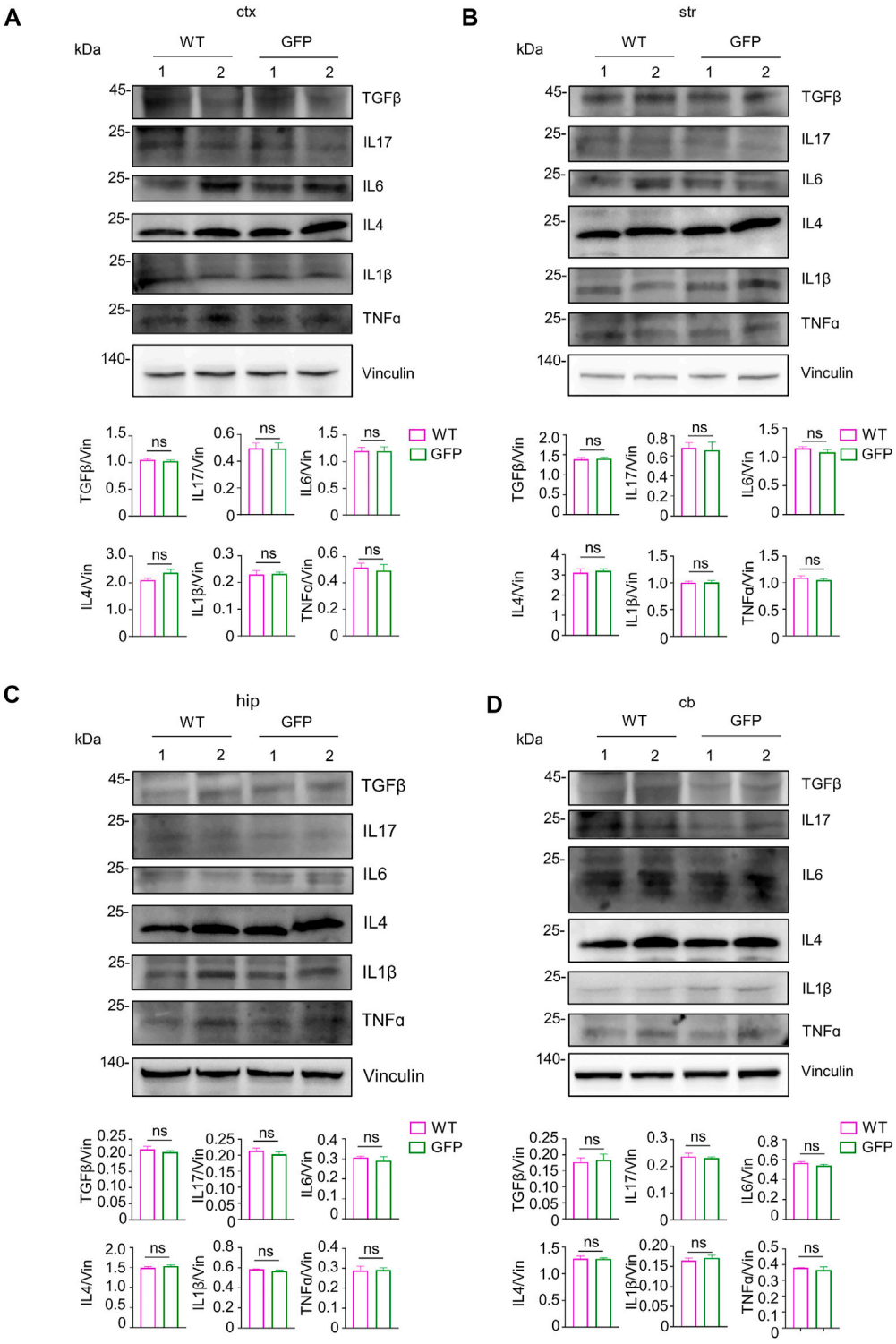

FIGURE 6
Examination of inflammatory factors in the pig's central nervous system after intravenous injection of saline or AAV-GFP. **(A–D)** Western blotting of the cortical tissue **(A)**, striatum **(B)**, hippocampus **(C)** and cerebellum **(D)** of saline-or AAV GFP-injected pigs with antibodies against TGFβ, IL17, IL6, IL4, IL1β and TNFα. Vinculin served as a loading control. Quantitation of the ratios of TGFβ, IL17, IL6, IL4, IL1β and TNFα to vinculin on the western blots are presented beneath the blots. Data are analyzed by Student's T-test and presented as mean ± SEM. *n* = 3 animals per group.

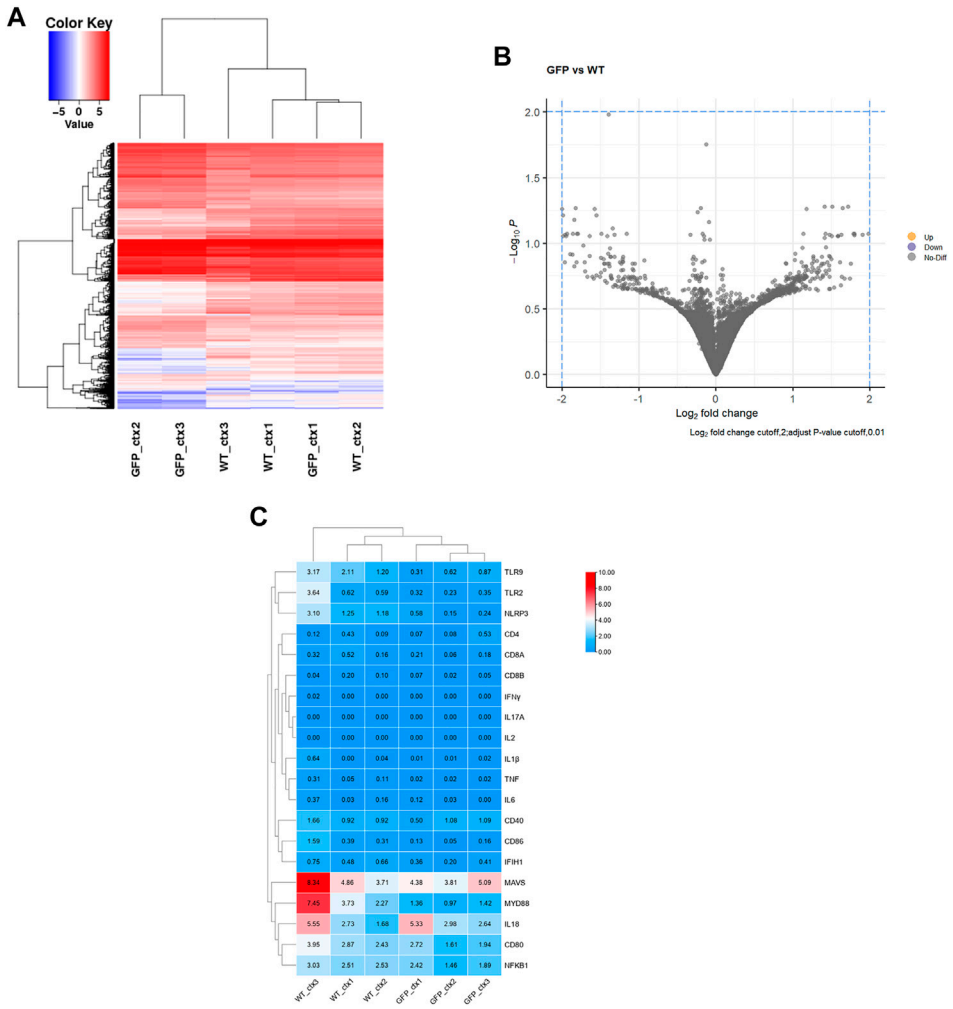

FIGURE 7
Transcriptome analysis of the intravenous AAV9-injected pig cortical tissues. **(A)** Heatmap of differential gene expression, blue and red color intensities represent gene downregulation and upregulation, respectively. **(B)** GFP vs. WT differential gene volcano plot, Log_2 fold change cutoff,2; adjust *p*-value cutoff,0.01. **(C)** Heatmap of expression of 20 common genes associated with inflammatory responses.

expression (Evers et al., 2018; Vallès et al., 2021). It remains unknown whether a single intravenous injection of AAV into large animals can lead to the broad distribution of transgene in various brain regions. We used AAV9-GFP for intravenous injection in pigs so that the expression of transgene (GFP) could be identified in the pig brain. In addition to the striatum and cortex that are most affected in HD, GFP was expressed in the hippocampus, cerebellum (especially in Purkinje cells), brainstem, and spinal cord. These brain regions have been reported to be affected in a number of neurodegenerative diseases. For example, in patients with Alzheimer's disease, the abnormal accumulation of Aβ plaques and Tau tangles leads to neuronal cell death in the entorhinal cortex and hippocampus first, with plaques and tangles gradually being spread in the frontal lobe, parietal lobe, globus pallidus and other brain regions (Čaušević et al., 2010; Latimer et al., 2019). A common and fatal heritable spinal muscular atrophy in infants is caused by the loss of alpha motor neurons in the spinal cord (Crawford and Pardo, 1996), and amyotrophic lateral sclerosis (ALS) is a fatal neurodegenerative disease with the degeneration of motor neurons in the brain stem of the motor cortex and spinal cord (Wang et al., 2015; Bonafede and Mariotti, 2017). SCA3 is caused by an abnormal CAG repeat expansion in exon 10 of the ATXN3 gene with progressive motor and neuronal dysfunction, in the somatosensory and motor nuclei spanning brainstem, cerebellum, midbrain, spinal cord, striatum, and thalamus (McLoughlin et al., 2020). For all the brain disordered in the above-mentioned classes, intravenous injection has an advantage in the treatment, and once AAV9 passes through the blood-brain barrier, the transgene

can be expressed in the specific populations of cells or selective brain regions under the control of specific promoters.

It should be point out that intravenous AAV delivery can induce immune and inflammatory responses, which would also be dependent on animal size, brain anatomy, and physiology in different species. Our findings demonstrated the efficacy and safety of intravenous injection of AAV-CMV-GFP in transducing the central nervous system of piglet. Currently, lipid nanoparticles (LNPS) have become an attractive treatment tool due to their low immunogenicity, low production costs, and the capability to deliver various goods. However, LNPS tend to target peripheral tissue, as they are difficult to pass the blood brain barrier to deliver the cargoes to the brain, and do not yield long-term transgene expression. Therefore, the gene expression of AAV is currently a more effective treatment for neurodegenerative diseases.

We found that a single intravenous injection of AAV-CMV-GFP can lead to a widespread expression of GFP in the central nervous system in a large animal model. Because the sizes of brain and body of pigs are similar to those of humans, the non-invasive nature of intravenous injection of AAV and widespread expression of transgene in pigs reinforce the therapeutic potential of intravenous injection of AAV to treat neurological disorders in humans.

Materials and methods

Animals and ethics statement

Bama pigs are local strains from Southern China. The pigs were breed at the animal Facility of the Guangzhou Institute of Biomedicine and Health (GIBH), Chinese Academy of Sciences (Animal Welfare Assurance #N2019083). Animal use and care followed the NIH Guide for the Care and Use of Laboratory Animals. The Institutional Animal Care and Use Committees (IACUC) at Guangzhou Institute of Biomedicine and Health (GIBH), Chinese Academy of Sciences approved the animal use protocol. This study carried out in strict compliance with the "Guide for the Care and Use of Laboratory Animals (2011)" to ensure the safety of personnel and animal welfare. The pigs used in the current experiments were wild-type pigs, and maintained under in-door housing conditions at room temperature in the Animal Center of Guangzhou Institutes of Biomedicine and Health. Regular food and water were provided *ad libitum*.

Virus production and injection

GFP-expressing viral vector was obtained from Addgene (plasmid# 67634). The vector was packaged by PackGene Biotech with the AAV9 serotype. Purified viruses were stored at -80°C. The genomic titer of the purified viruses (vg) (approximate 10^{13} vg/mL) was determined by PCR method.

The same litter of 7-day-old Bama pigs were injected with AAV-CMV-GFP or saline as the experimental group or the control group. The pigs were anesthetized with 1.5% isoflurane, and the surgical site was sterilized with a betadine solution (10% povidone-iodine) followed by 75% ethanol. A 30G needle attached to a 1 ml Hamilton syringe was inserted into the auricular vein. Viruses (300 ml of 10^{13} vg/ml diluted in 1 ml saline) or the same volume of saline were injected through the auricular vein into each pig over the course of 5 min. After the infusion is complete, the needle was left in place for 3 min and then slowly removed from the pigs. Pigs were placed on a warm cuddy after surgery to allow them to recover from anesthesia. After the piglets woke up, they were sent back to their mothers.

Necropsy and tissue collection

Two months after the virus injection, the pigs were euthanized by deep anesthesia with intraperitoneal injection of .3–.5 ml of atropine, followed by 10–12 mg of ketamine per kg body weight and perfused with 3 L of a sterile .9% sodium chloride solution through the left ventricle of the heart. The brain was removed from the skull, the left hemisphere was immediately frozen on dry ice after the brain regions were separated, and the right hemisphere was emersed in 10 volumes of 4% paraformaldehyde (PFA) for fixation for 48 h.

Western blot analysis and immunohistochemistry

The primary antibodies against the following proteins were used in the study: synapsin-1 (Cell Signaling, 5297 S), NeuN (Abcam, ab177487), GFAP (Abcam, ab7260), IBA1 (WAKO, 019-19741), Olig2 (Milipore, MABN50), GFP (Invitrogen, A11122), TGFβ (Abcam, ab215715), IL17 (Santa Cruz, sc-374218), IL6 (abcam, ab6672), IL4 (Proteintech, 66142-1-Ig), IL1β (abcam, ab9722), TNF (abcam, ab1793). Secondary antibodies were all from Jackson ImmunoResearch laboratories, INC, Abcam and Invitrogen.

For western blot analysis, pig brain tissues were lysed in ice-cold RIPA buffer (50 mmol/L Tris, pH 8.0, 150 mmol/L NaCl, 1 mmol/L EDTA pH 8.0, 1 mmol/L EGTA pH 8.0, .1% SDS, .5% DOC, 50 mmol/L NaF and 1% Triton X-100) containing Halt protease inhibitor cocktail (Thermo Scientific) and PMSF (Sigma). The pig brain tissues were grinded by using a Luka Grinding instrument (LUKYM-II, China) and the tissue lysates were incubated on ice for 30 min, centrifuged at 12,000 rpm for 10 min. Protein concentrations in the supernatants were determined by BCA assay (Bio-Rad), and equal amount of proteins were loaded to SDS-PAGE and subsequently

transferred to a nitrocellulose membrane. The membrane was blocked with 5% milk/TBST for 1 h at room temperature. Primary antibodies were diluted in 3% BSA/TBST and incubated with the membrane overnight at 4°C. The membranes were then washed 3 times with TBST and incubated with HRP-conjugated secondary antibodies in 5% milk/TBST for 1 h at room temperature. After washing with TBST, the signals on the membrane were detected with the ECL Prime (GE Healthcare) kit.

For immunofluorescent study, the isolated pig brain tissues were fixed for 48 h in 4% paraformaldehyde/0.01 M PBS and then transferred into 30% sucrose to dehydrate at 4°C until the brain completely sank to the bottom of the tube. The tissues embedded in Tissue-Tek®O.C.T.Compound (Tissue-Tek, Sakura Finetek) and frozen in liquid nitrogen with an isopentane interphase. The consecutive pig brain coronal sections of 30 μm were cut with freezing microtome. The pig tissue slides were fixed in 4% paraformaldehyde in .01 M PB for 10 min, and pre-blocked with 4% normal goat serum in .1% Triton X-100/PBS for 1 h. Slides were incubated with primary antibodies in 3% BSA/2%NGS/TBST overnight at 4°C. Secondary antibodies were added after three washes with PBS. Microscopic images were acquired by TissueFAXS PLUS (TissueGnostics, Vienna, AUT) and a confocal imaging system ((Olympus FV3000 Microscope).

RNA-seq and data analysis

Total RNA of the cortex in WT pigs injected with saline or WT pigs injected with AAV-CMV-GFP through the auricular vein were isolated using RNAiso Plus (TaKaRa). The RNAs were sent to HeQin Biotechnology Corporation (Guangzhou) for RNA-seq analysis and database construction. A total of 2 mg of RNAs per sample were used for analysis. NEBNext Ultra RNA Library Prep Kit for Illumina (E7530L; NEB) was used for sequencing according to the manufacturer's recommendations. After cluster generation, the libraries were sequenced and 150-bp paired-end reads were generated using Illumina platform. After obtaining the raw sequencing data, Trimmomatic software was used to control the quality of raw RNA-seq data and remove the sequencing adapter (Bolger et al., 2014). We then used STAR software (STAR: ultrafast universal RNA-seq aligner - PMC) to map the clean data to the pig genome, which was downloaded from the Ensembl website (Howe et al., 2020), to obtain the sam files. The samtools (Li et al., 2009) was used to convert sam files into bam files, sort and build index files. We used stringtie (Pertea et al., 2015) and its script 'prepDE.py' to quantify genes and convert them into read counts matrix. Finally, the R package DESeq2 (Love et al., 2014) was used for gene differential expression analysis, and the read counts matrix was used as the input file. Genes with adjusted *p*-value <.01 and an absolute fold change >2 were considered as DEGs. GO enrichment analysis for DEGs in a group was carried out using TBtools (Chen et al., 2020). GO terms with a *p*-value <.01 and a hit rate >.05 were considered significantly enriched. In addition, PCA analysis and heat map were also performed using carrieUBC. The RNAseq data have been deposited with the GEO number PRJNA911021.

Statistical analysis

When every two groups were compared, statistical significance was assessed with the two-tailed Student's t-test. Data are presented as mean ± SEM. For pathological examination, western blotting, and RNA-seq, at least three animals per group were used. Calculations were performed with GraphPad Prism software (GraphPad Software). A *p*-value of .05 was considered statistically significant.

Data availability statement

The data presented in the study are deposited in the NCBI Trace Archive NCBI SequenceRead Archive repository, accession number PRJNA911021.

Ethics statement

The animal study was reviewed and approved by the Guangzhou Institute of Biomedicine and Health (GIBH), Chinese Academy of Sciences (Animal Welfare Assurance N2019083).

Author contributions

SY, X-JL, and SL designed the research; SY, YL, CL, WW, JL, CH, XZ, ZL, XS, YC, JG, JW, and JW performed the research; SY, X-JL, SL, and YL analyzed the data; JL performed bioinformatics analysis; SY, X-JL, and SL wrote the paper with input from all authors.

Funding

This work was supported by the National Key Research and Development Program of China (2021YFA0805300), The National Natural Science Foundation of China (81922026, 82171244, 81830032, 31872779, 82071421 and 32170981), Guangzhou Key Research Program on Brain Science (202007030008, 202007030003), Key Field Research and Development Program of Guangdong province (2018B030337001) and Department of Science and Technology of Guangdong Province (2021ZT09Y007, 2020B121201006).

Acknowledgments

We thank Mrs. Du Wu, Yunpeng Ai for animal care.

Conflict of interest

The authors declare that the research was conducted in the absence of any commercial or financial relationships that could be construed as a potential conflict of interest.

Publisher's note

All claims expressed in this article are solely those of the authors and do not necessarily represent those of their affiliated organizations, or those of the publisher, the editors and the reviewers. Any product that may be evaluated in this article, or claim that may be made by its manufacturer, is not guaranteed or endorsed by the publisher.

Supplementary material

The Supplementary Material for this article can be found online at: https://www.frontiersin.org/articles/10.3389/fcell.2022.1115348/full#supplementary-material

SUPPLEMENTARY MATERIAL S1
Three brain regions were chosen (cortex, striatum and hippocampus) for qualitative rating of cell type transduction. Scale ranges from – to ++++, with – indicating no double labeling of GFP and the cell specific marker and ++++ indicating the highest level of double labeling observed.

SUPPLEMENTARY MATERIAL S1
Three brain regions were chosen (cortex, striatum and hippocampus) for qualitative rating of cell type transduction. Scale ranges from – to ++++, with – indicating no double labeling of GFP and the cell specific marker and ++++ indicating the highest level of double labeling observed.

SUPPLEMENTARY FIGURE S1
Immunofluorescent staining of the pig's brain stem injected with AAV-GFP or saline. **(A–L)** Double immunofluorescent labeling and quantification of neurons (NeuN) **(A–C)**, astrocytes (GFAP) **(D–F)**, microglial (Iba1) **(G–I)** and oligodendrocytes (Olig2) **(J–L)** of saline- or AAV-GFP-injected-wild type pigs. GFP positive cells are shown in green, NeuN, GFAP, Iba1 and Olig2 positive cells are shown in red. Data are analyzed by Student's T-test and presented as mean ± SEM. n = 3 animals per group. **(N)** Western blotting of the brain stem of saline- or AAV-GFP-injected pigs with antibodies against synapsin-1, NeuN, GFAP and Iba1. Vinculin served as a loading control. **(N)** Quantitation of the ratios of synapsin-1, NeuN, GFAP or Iba1 to vinculin on the western blots. Data are analyzed by student's T-test and presented as mean ± SEM. n = 3 animals per group.

SUPPLEMENTARY FIGURE S2
Immunofluorescent staining of the pig's spinal cord injected with AAV-GFP or saline. **(A–L)** Double immunofluorescent labeling and quantification of neurons (NeuN) **(A–C)**, astrocytes (GFAP) **(D–F)**, microglial (Iba1) **(G–I)** and oligodendrocytes (Olig2) **(J–L)** of saline- or AAV-GFP-injected-wild type pigs. GFP positive cells are shown in green, NeuN, GFAP, Iba1 and Olig2 positive cells are shown in red. Data are analyzed by Student's T-test and presented as mean ± SEM. n = 3 animals per group. **(M)** Western blotting of the spinal cord of saline- or AAV-GFP-injected pigs with antibodies against synapsin-1, NeuN, GFAP and Iba1. Vinculin served as a loading control. **(N)** Quantitation of the ratios of synapsin-1, NeuN, GFAP or Iba1 to vinculin on the western blots. Data are analyzed by student's T-test and presented as mean ± SEM. n = 3 animals per group.

SUPPLEMENTARY FIGURE S3
Examination of inflammatory factors in the pig's brain stem and spinal cord after intravenous injection of saline or AAV-GFP. **(A,B)** Western blotting of the brain stem **(A)** and spinal cord **(B)** of saline-or AAV GFP-injected pigs with antibodies against TGFβ, IL17, IL6, IL4, IL1β and TNFα. Vinculin served as a loading control. Quantitation of the ratios of TGFβ, IL17, IL6, IL4, IL1β and TNFα to vinculin on the western blots are presented beneath the blots. Data are analyzed by Student's T-test and presented as mean ± SEM. n = 3 animals per group.

SUPPLEMENTARY FIGURE S4
Examination of inflammatory factors in the pig's peripheral tissues after intravenous injection of saline or AAV-GFP. **(A,C)** Western blotting of the heart, muscle, spleen, testis, liver, lung, kidney of saline-or AAV GFP-injected pigs with antibodies against TGFβ, IL17, IL6, IL4, IL1β and TNFα. Vinculin served as a loading control. **(B,D)** Quantitation of the ratios of TGFβ, IL17, IL6, IL4, IL1β or TNFα to vinculin on the western blots. Data are analyzed by student's T-test and presented as mean ± SEM. n = 3 animals per group.

SUPPLEMENTARY FIGURE S5
Heat map of correlation of expression levels between WT and GFP.

References

Anthofer, J., Wester, M., Zeman, F., Brawanski, A., and Schebesch, K.-M. (2016). Case-control study of patients at risk of medical complications after elective craniotomy. *World Neurosurg.* 91, 58–65. doi:10.1016/j.wneu.2016.03.087

Anthony, D. C., and Couch, Y. (2014). The systemic response to CNS injury. *Exp. Neurol.* 258, 105–111. doi:10.1016/j.expneurol.2014.03.013

Ashe, K. H., and Zahs, K. R. (2010). Probing the biology of Alzheimer's disease in mice. *Neuron* 66, 631–645. doi:10.1016/j.neuron.2010.04.031

Ashraf, U., Ding, Z., Deng, S., Ye, J., Cao, S., and Chen, Z. (2021). Pathogenicity and virulence of Japanese encephalitis virus: Neuroinflammation and neuronal cell damage. *Virulence* 12, 968–980. doi:10.1080/21505594.2021.1899674

AuthorAnonymous (2022). Star: Ultrafast universal RNA-seq aligner - PMC. Available at: https://www.ncbi.nlm.nih.gov/pmc/articles/PMC3530905/(Accessed April 17, 2022).

Baba, H., Nakahira, K., Morita, N., Tanaka, F., Akita, H., and Ikenaka, K. (1997). GFAP gene expression during development of astrocyte. *Dev. Neurosci.* 19, 49–57. doi:10.1159/000111185

Bates, G. P., Dorsey, R., Gusella, J. F., Hayden, M. R., Kay, C., Leavitt, B. R., et al. (2015). Huntington disease. *Nat. Rev. Dis. Primer* 1, 15005–15021. doi:10.1038/nrdp.2015.5

Baxa, M., Hruska-Plochan, M., Juhas, S., Vodicka, P., Pavlok, A., Juhasova, J., et al. (2013). A transgenic minipig model of huntington's disease. *J. Huntingt. Dis.* 2, 47–68. doi:10.3233/JHD-130001

Becher, B., Spath, S., and Goverman, J. (2017). Cytokine networks in neuroinflammation. *Nat. Rev. Immunol.* 17, 49–59. doi:10.1038/nri.2016.123

Bolger, A. M., Lohse, M., and Usadel, B. (2014). Trimmomatic: A flexible trimmer for Illumina sequence data. *Bioinformatics* 30, 2114–2120. doi:10.1093/bioinformatics/btu170

Bonafede, R., and Mariotti, R. (2017). ALS pathogenesis and therapeutic approaches: The role of mesenchymal stem cells and extracellular vesicles. *Front. Cell. Neurosci.* 11, 80. doi:10.3389/fncel.2017.00080

Boutin, S., Monteilhet, V., Veron, P., Leborgne, C., Benveniste, O., Montus, M. F., et al. (2010). Prevalence of serum IgG and neutralizing factors against adeno-

associated virus (AAV) types 1, 2, 5, 6, 8, and 9 in the healthy population: Implications for gene therapy using AAV vectors. *Hum. Gene Ther.* 21, 704–712. doi:10.1089/hum.2009.182

Broekman, M. L. D., Baek, R. C., Comer, L. A., Fernandez, J. L., Seyfried, T. N., and Sena-Esteves, M. (2007). Complete correction of enzymatic deficiency and neurochemistry in the GM1-gangliosidosis mouse brain by neonatal adeno-associated virus–mediated gene delivery. *Mol. Ther.* 15, 30–37. doi:10.1038/sj.mt.6300004

Campbell, S. J., Deacon, R. M. J., Jiang, Y., Ferrari, C., Pitossi, F. J., and Anthony, D. C. (2007). Overexpression of IL-1beta by adenoviral-mediated gene transfer in the rat brain causes a prolonged hepatic chemokine response, axonal injury and the suppression of spontaneous behaviour. *Neurobiol. Dis.* 27, 151–163. doi:10.1016/j.nbd.2007.04.013

Campbell, S. J., Zahid, I., Losey, P., Law, S., Jiang, Y., Bilgen, M., et al. (2008). Liver Kupffer cells control the magnitude of the inflammatory response in the injured brain and spinal cord. *Neuropharmacology* 55, 780–787. doi:10.1016/j.neuropharm.2008.06.074

Čaušević, M., Farooq, U., Lovestone, S., and Killick, R. (2010). β-Amyloid precursor protein and tau protein levels are differently regulated in human cerebellum compared to brain regions vulnerable to Alzheimer's type neurodegeneration. *Neurosci. Lett.* 485, 162–166. doi:10.1016/j.neulet.2010.08.088

Chen, C., Chen, H., Zhang, Y., Thomas, H. R., Frank, M. H., He, Y., et al. (2020). TBtools: An integrative toolkit developed for interactive analyses of big biological data. *Mol. Plant* 13, 1194–1202. doi:10.1016/j.molp.2020.06.009

Chen, K., Baxter, T., Muir, W. M., Groenen, M. A., and Schook, L. B. (2007). Genetic resources, genome mapping and evolutionary genomics of the pig (*Sus scrofa*). *Int. J. Biol. Sci.* 3, 153–165. doi:10.7150/ijbs.3.153

Chieppa, M. N., Perota, A., Corona, C., Grindatto, A., Lagutina, I., Costassa, E. V., et al. (2014). Modeling amyotrophic lateral sclerosis in hSOD1 transgenic swine. *Neurodegener. Dis.* 13, 246–254. doi:10.1159/000353472

Clausen, B. H., Degn, M., Martin, N. A., Couch, Y., Karimi, L., Ormhøj, M., et al. (2014). Systemically administered anti-TNF therapy ameliorates functional outcomes after focal cerebral ischemia. *J. Neuroinflammation* 11, 203. doi:10.1186/s12974-014-0203-6

Crawford, T. O., and Pardo, C. A. (1996). The neurobiology of childhood spinal muscular atrophy. *Neurobiol. Dis.* 3, 97–110. doi:10.1006/nbdi.1996.0010

Double, K. L., Reyes, S., Werry, E. L., and Halliday, G. M. (2010). Selective cell death in neurodegeneration: Why are some neurons spared in vulnerable regions? *Prog. Neurobiol.* 92, 316–329. doi:10.1016/j.pneurobio.2010.06.001

Duque, S., Joussemet, B., Riviere, C., Marais, T., Dubreil, L., Douar, A.-M., et al. (2009). Intravenous administration of self-complementary AAV9 enables transgene delivery to adult motor neurons. *Mol. Ther. J. Am. Soc. Gene Ther.* 17, 1187–1196. doi:10.1038/mt.2009.71

Dutta, S., and Sengupta, P. (2016). Men and mice: Relating their ages. *Life Sci.* 152, 244–248. doi:10.1016/j.lfs.2015.10.025

Eng, L. F., Ghirnikar, R. S., and Lee, Y. L. (2000). Glial fibrillary acidic protein: GFAP-thirty-one years (1969-2000). *Neurochem. Res.* 25, 1439–1451. doi:10.1023/a:1007677003387

Epis, R., Gardoni, F., Marcello, E., Genazzani, A., Canonico, P. L., and Di Luca, M. (2010). Searching for new animal models of Alzheimer′s disease. *Eur. J. Pharmacol.* 626, 57–63. doi:10.1016/j.ejphar.2009.10.020

Evers, M. M., Miniarikova, J., Juhas, S., Vallès, A., Bohuslavova, B., Juhasova, J., et al. (2018). AAV5-miHTT gene therapy demonstrates broad distribution and strong human mutant huntingtin lowering in a huntington's disease minipig model. *Mol. Ther.* 26, 2163–2177. doi:10.1016/j.ymthe.2018.06.021

Fang, C., Zhu, T., Zhang, P., Xia, L., and Sun, C. (2017). Risk factors of neurosurgical site infection after craniotomy: A systematic review and meta-analysis. *Am. J. Infect. Control* 45, e123–e134. doi:10.1016/j.ajic.2017.06.009

Foust, K. D., Nurre, E., Montgomery, C. L., Hernandez, A., Chan, C. M., and Kaspar, B. K. (2009). Intravascular AAV9 preferentially targets neonatal neurons and adult astrocytes. *Nat. Biotechnol.* 27, 59–65. doi:10.1038/nbt.1515

Gusel'nikova, V. V., and Korzhevskiy, D. E. (2015). NeuN as a neuronal nuclear antigen and neuron differentiation marker. *Acta Naturae* 7, 42–47. doi:10.32607/20758251-2015-7-2-42-47

Herz, J., Zipp, F., and Siffrin, V. (2010). Neurodegeneration in autoimmune CNS inflammation. *Exp. Neurol.* 225, 9–17. doi:10.1016/j.expneurol.2009.11.019

Herzog, C. D., Dass, B., Holden, J. E., Stansell, J., III, Gasmi, M., Tuszynski, M. H., et al. (2007). Striatal delivery of CERE-120, an AAV2 vector encoding human neurturin, enhances activity of the dopaminergic nigrostriatal system in aged monkeys. *Mov. Disord.* 22, 1124–1132. doi:10.1002/mds.21503

Hocquemiller, M., Giersch, L., Audrain, M., Parker, S., and Cartier, N. (2016). Adeno-associated virus-based gene therapy for CNS diseases. *Hum. Gene Ther.* 27, 478–496. doi:10.1089/hum.2016.087

Howe, K. L., Achuthan, P., Allen, J., Allen, J., Alvarez-Jarreta, J., Amode, M. R., et al. (2020). Ensembl 2021. *Nucleic Acids Res.* 49, D884–D891. doi:10.1093/nar/gkaa942

Hudry, E., Van Dam, D., Kulik, W., De Deyn, P. P., Stet, F. S., Ahouansou, O., et al. (2010). Adeno-associated virus gene therapy with cholesterol 24-hydroxylase reduces the amyloid pathology before or after the onset of amyloid plaques in mouse models of alzheimer's disease. *Mol. Ther.* 18, 44–53. doi:10.1038/mt.2009.175

Ito, D., Imai, Y., Ohsawa, K., Nakajima, K., Fukuuchi, Y., and Kohsaka, S. (1998). Microglia-specific localisation of a novel calcium binding protein, Iba1. *Mol. Brain Res.* 57, 1–9. doi:10.1016/S0169-328X(98)00040-0

Jakobsen, J. E., Johansen, M. G., Schmidt, M., Dagnæs-Hansen, F., Dam, K., Gunnarsson, A., et al. (2013). Generation of minipigs with targeted transgene insertion by recombinase-mediated cassette exchange (RMCE) and somatic cell nuclear transfer (SCNT). *Transgenic Res.* 22, 709–723. doi:10.1007/s11248-012-9671-6

Janson, C., McPhee, S., Bilaniuk, L., Haselgrove, J., Testaiuti, M., Freese, A., et al. (2002). Clinical protocol. Gene therapy of canavan disease: AAV-2 vector for neurosurgical delivery of aspartoacylase gene (ASPA) to the human brain. *Hum. Gene Ther.* 13, 1391–1412. doi:10.1089/104303402760128612

Kim, Y. J., Ahn, K. S., Kim, M., Kim, M. J., Park, S.-M., Ryu, J., et al. (2014). Targeted disruption of Ataxia-telangiectasia mutated gene in miniature pigs by somatic cell nuclear transfer. *Biochem. Biophys. Res. Commun.* 452, 901–905. doi:10.1016/j.bbrc.2014.08.125

Kragh, P. M., Nielsen, A. L., Li, J., Du, Y., Lin, L., Schmidt, M., et al. (2009). Hemizygous minipigs produced by random gene insertion and handmade cloning express the Alzheimer's disease-causing dominant mutation APPsw. *Transgenic Res.* 18, 545–558. doi:10.1007/s11248-009-9245-4

Kwon, S. B., and Ernst, J. (2021). Learning a genome-wide score of human–mouse conservation at the functional genomics level. *Nat. Commun.* 12, 2495. doi:10.1038/s41467-021-22653-8

Laramée, M.-E., and Boire, D. (2015). Visual cortical areas of the mouse: Comparison of parcellation and network structure with primates. *Front. Neural Circuits* 8, 149. doi:10.3389/fncir.2014.00149

Latimer, C. S., Shively, C. A., Dirk Keene, C., Jorgensen, M. J., Andrews, R. N., Register, T. C., et al. (2019). A nonhuman primate model of early Alzheimer's disease pathologic change: Implications for disease pathogenesis. *Alzheimers Dement. J. Alzheimers Assoc.* 15, 93–105. doi:10.1016/j.jalz.2018.06.3057

Lee, J. J., Sanchez-Martinez, A., Martinez Zarate, A., Benincá, C., Mayor, U., Clague, M. J., et al. (2018). Basal mitophagy is widespread in Drosophila but minimally affected by loss of Pink1 or parkin. *J. Cell Biol.* 217, 1613–1622. doi:10.1083/jcb.201801044

Levine, M. S., Cepeda, C., Hickey, M. A., Fleming, S. M., and Chesselet, M.-F. (2004). Genetic mouse models of huntington's and Parkinson's diseases: Illuminating but imperfect. *Trends Neurosci.* 27, 691–697. doi:10.1016/j.tins.2004.08.008

Li, D., Liu, X., Liu, T., Liu, H., Tong, L., Jia, S., et al. (2020). Neurochemical regulation of the expression and function of glial fibrillary acidic protein in astrocytes. *Glia* 68, 878–897. doi:10.1002/glia.23734

Li, H., Handsaker, B., Wysoker, A., Fennell, T., Ruan, J., Homer, N., et al. (2009). The sequence alignment/map format and SAMtools. *Bioinformatics* 25, 2078–2079. doi:10.1093/bioinformatics/btp352

Lorson, M. A., Spate, L. D., Samuel, M. S., Murphy, C. N., Lorson, C. L., Prather, R. S., et al. (2011). Disruption of the Survival Motor Neuron (SMN) gene in pigs using ssDNA. *Transgenic Res.* 20, 1293–1304. doi:10.1007/s11248-011-9496-8

Love, M. I., Huber, W., and Anders, S. (2014). Moderated estimation of fold change and dispersion for RNA-seq data with DESeq2. *Genome Biol.* 15, 550. doi:10.1186/s13059-014-0550-8

McLoughlin, H. S., Moore, L. R., and Paulson, H. L. (2020). Pathogenesis of SCA3 and implications for other polyglutamine diseases. *Neurobiol. Dis.* 134, 104635. doi:10.1016/j.nbd.2019.104635

McWilliams, T. G., Prescott, A. R., Montava-Garriga, L., Ball, G., Singh, F., Barini, E., et al. (2018). Basal mitophagy occurs independently of PINK1 in mouse tissues of high metabolic demand. *Cell Metab.* 27, 439–449. e5. doi:10.1016/j.cmet.2017.12.008

Mingozzi, F., and High, K. A. (2011). Therapeutic *in vivo* gene transfer for genetic disease using AAV: Progress and challenges. *Nat. Rev. Genet.* 12, 341–355. doi:10.1038/nrg2988

Penzes, J. J., Chipman, P., Bhattacharya, N., Zeher, A., Huang, R., McKenna, R., et al. (2021). Adeno-associated virus 9 structural rearrangements induced by endosomal trafficking pH and glycan attachment. *J. Virol.* 95, e0084321–21. doi:10.1128/JVI.00843-21

Pertea, M., Pertea, G. M., Antonescu, C. M., Chang, T.-C., Mendell, J. T., and Salzberg, S. L. (2015). StringTie enables improved reconstruction of a transcriptome from RNA-seq reads. *Nat. Biotechnol.* 33, 290–295. doi:10.1038/nbt.3122

Reith, W. (2018). Neurodegenerative diseases. *Neurodegener. Erkrank. Radiol.* 58, 241–258. doi:10.1007/s00117-018-0363-y

Russell, S., Bennett, J., Wellman, J. A., Chung, D. C., Yu, Z.-F., Tillman, A., et al. (2017). Efficacy and safety of voretigene neparvovec (AAV2-hRPE65v2) in patients with RPE65-mediated inherited retinal dystrophy: A randomised, controlled, open-label, phase 3 trial. *Lancet lond. Engl.* 390, 849–860. doi:10.1016/S0140-6736(17)31868-8

Sasaki, Y., Ohsawa, K., Kanazawa, H., Kohsaka, S., and Imai, Y. (2001). Iba1 is an actin-cross-linking protein in macrophages/microglia. *Biochem. Biophys. Res. Commun.* 286, 292–297. doi:10.1006/bbrc.2001.5388

Scott, L. J. (2015). Alipogene tiparvovec: A review of its use in adults with familial lipoprotein lipase deficiency. *Drugs* 75, 175–182. doi:10.1007/s40265-014-0339-9

Søndergaard, L. V., Ladewig, J., Dagnæs-Hansen, F., Herskin, M. S., and Holm, I. E. (2012). Object recognition as a measure of memory in 1–2 years old transgenic minipigs carrying the APPsw mutation for Alzheimer's disease. *Transgenic Res.* 21, 1341–1348. doi:10.1007/s11248-012-9620-4

Tsaousi, G. G., Pourzitaki, C., and Bilotta, F. (2017). Prophylaxis of postoperative complications after craniotomy. *Curr. Opin. Anesthesiol.* 30, 534–539. doi:10.1097/ACO.0000000000000493

Vallès, A., Evers, M. M., Stam, A., Sogorb-Gonzalez, M., Brouwers, C., Vendrell-Tornero, C., et al. (2021). Widespread and sustained target engagement in Huntington's disease minipigs upon intrastriatal microRNA-based gene therapy. *Sci. Transl. Med.* 13, eabb8920. doi:10.1126/scitranslmed.abb8920

Waldvogel, H. J., Kim, E. H., Tippett, L. J., Vonsattel, J.-P. G., and Faull, R. L. (2015). "The neuropathology of huntington's disease," in Behavioral Neurobiology of huntington's Disease and Parkinson's disease *current topics in behavioral neurosciences.* Editors H. H. P. Nguyen and M. A. Cenci (Berlin, Heidelberg: Springer), 33–80. doi:10.1007/7854_2014_354

Wang, G., Yang, H., Yan, S., Wang, C.-E., Liu, X., Zhao, B., et al. (2015). Cytoplasmic mislocalization of RNA splicing factors and aberrant neuronal gene splicing in TDP-43 transgenic pig brain. *Mol. Neurodegener.* 10, 42. doi:10.1186/s13024-015-0036-5

Wernersson, R., Schierup, M. H., Jørgensen, F. G., Gorodkin, J., Panitz, F., Stærfeldt, H.-H., et al. (2005). Pigs in sequence space: A 0.66X coverage pig genome survey based on shotgun sequencing. *BMC Genomics* 6, 70. doi:10.1186/1471-2164-6-70

Worgall, S., Sondhi, D., Hackett, N. R., Kosofsky, B., Kekatpure, M. V., Neyzi, N., et al. (2008). Treatment of late infantile neuronal ceroid lipofuscinosis by CNS administration of a serotype 2 adeno-associated virus expressing CLN2 cDNA. *Hum. Gene Ther.* 19, 463–474. doi:10.1089/hum.2008.022

Wu, Z., Asokan, A., and Samulski, R. J. (2006). Adeno-associated virus serotypes: Vector toolkit for human gene therapy. *Mol. Ther.* 14, 316–327. doi:10.1016/j.ymthe.2006.05.009

Yan, S., Tu, Z., Liu, Z., Fan, N., Yang, H., Yang, S., et al. (2018). A huntingtin knock-in pig model recapitulates features of selective neurodegeneration in Huntington's disease. *Cell* 173, 989–1002. e13. doi:10.1016/j.cell.2018.03.005

Yang, D., Wang, C.-E., Zhao, B., Li, W., Ouyang, Z., Liu, Z., et al. (2010). Expression of Huntington's disease protein results in apoptotic neurons in the brains of cloned transgenic pigs. *Hum. Mol. Genet.* 19, 3983–3994. doi:10.1093/hmg/ddq313

Yang, H., Wang, G., Sun, H., Shu, R., Liu, T., Wang, C.-E., et al. (2014). Species-dependent neuropathology in transgenic SOD1 pigs. *Cell Res.* 24, 464–481. doi:10.1038/cr.2014.25

Yang, S., Chang, R., Yang, H., Zhao, T., Hong, Y., Kong, H. E., et al. (2017). CRISPR/Cas9-mediated gene editing ameliorates neurotoxicity in mouse model of Huntington's disease. *J. Clin. .* 127, 2719–2724. doi:10.1172/JCI92087

Yao, J., Huang, J., Hai, T., Wang, X., Qin, G., Zhang, H., et al. (2014). Efficient bi-allelic gene knockout and site-specific knock-in mediated by TALENs in pigs. *Sci. Rep.* 4, 6926. doi:10.1038/srep06926

Zhang, J.-M., and An, J. (2007). Cytokines, inflammation and pain. *Int. Anesthesiol. Clin.* 45, 27–37. doi:10.1097/AIA.0b013e318034194e

Zhou, Q., Wang, S., and Anderson, D. J. (2000). Identification of a novel family of oligodendrocyte lineage-specific basic helix–loop–helix transcription factors. *Neuron* 25, 331–343. doi:10.1016/S0896-6273(00)80898-3

Zhou, X., Xin, J., Fan, N., Zou, Q., Huang, J., Ouyang, Z., et al. (2015). Generation of CRISPR/Cas9-mediated gene-targeted pigs via somatic cell nuclear transfer. *Cell. Mol. Life Sci.* 72, 1175–1184. doi:10.1007/s00018-014-1744-7

frontiers | Frontiers in Cell and Developmental Biology

TYPE Original Research
PUBLISHED 15 May 2023
DOI 10.3389/fcell.2023.1111684

OPEN ACCESS

EDITED BY
Yongye Huang,
Northeastern University, China

REVIEWED BY
Alexandre R. Colas,
Sanford Burnham Prebys Medical Discovery Institute, United States
Chikai Zhou,
Chinese Academy of Agricultural Sciences, China
Loukia Yiangou,
Leiden University Medical Center (LUMC), Netherlands

*CORRESPONDENCE
Alessandra Moretti,
amoretti@mytum.de
Monika Nowak-Imialek,
monika.nowak-imialek@tum.de

†These authors have contributed equally to this work

RECEIVED 29 November 2022
ACCEPTED 21 April 2023
PUBLISHED 15 May 2023

CITATION
Rawat H, Kornherr J, Zawada D, Bakhshiyeva S, Kupatt C, Laugwitz K-L, Bähr A, Dorn T, Moretti A and Nowak-Imialek M (2023), Recapitulating porcine cardiac development *in vitro*: from expanded potential stem cell to embryo culture models.
Front. Cell Dev. Biol. 11:1111684.
doi: 10.3389/fcell.2023.1111684

Recapitulating porcine cardiac development *in vitro*: from expanded potential stem cell to embryo culture models

Hilansi Rawat[1,2,3†], Jessica Kornherr[1,2,3†], Dorota Zawada[1,2,3], Sara Bakhshiyeva[1,2,3], Christian Kupatt[1], Karl-Ludwig Laugwitz[1], Andrea Bähr[1], Tatjana Dorn[1,2,3], Alessandra Moretti[1,2,3,4*] and Monika Nowak-Imialek[1,2,3*]

[1]First Department of Medicine, Cardiology, Klinikum Rechts der Isar, School of Medicine and Health, Technical University of Munich, Munich, Germany, [2]German Center for Cardiovascular Research (DZHK), Munich Heart Alliance, Munich, Germany, [3]Regenerative Medicine in Cardiovascular Diseases, First Department of Medicine, Klinikum Rechts der Isar, School of Medicine and Health, Technical University of Munich, Munich, Germany, [4]Department of Surgery, Yale University School of Medicine, New Haven, CT, United States

Domestic pigs (*Sus scrofa*) share many genetic, anatomical, and physiological traits with humans and therefore constitute an excellent preclinical animal model. Fundamental understanding of the cellular and molecular processes governing early porcine cardiogenesis is critical for developing advanced porcine models used for the study of heart diseases and new regenerative therapies. Here, we provide a detailed characterization of porcine cardiogenesis based on fetal porcine hearts at various developmental stages and cardiac cells derived from porcine expanded pluripotent stem cells (pEPSCs), i.e., stem cells having the potential to give rise to both embryonic and extraembryonic tissue. We notably demonstrate for the first time that pEPSCs can differentiate into cardiovascular progenitor cells (CPCs), functional cardiomyocytes (CMs), epicardial cells and epicardial-derived cells (EPDCs) *in vitro*. Furthermore, we present an enhanced system for whole-embryo culture which allows continuous *ex utero* development of porcine post-implantation embryos from the cardiac crescent stage (ED14) up to the cardiac looping (ED17) stage. These new techniques provide a versatile platform for studying porcine cardiac development and disease modeling.

KEYWORDS

pig, heart development, porcine expanded pluripotent stem cells, cardiac progenitor cells, epicardial cells, cardiomyocyte, cardiac differentiation

Introduction

Cardiovascular diseases including congenital heart defects remain the leading cause of mortality worldwide. Our current knowledge of cardiogenesis is largely based on studies performed in rodents, owing to their accessibility, rapid reproducibility, and relatively low cost. However, results from these models do not always translate to humans due to significant differences in cardiac development and physiology (Maselli et al., 2022). There is an urgent need to establish alternative model systems more closely related to humans in terms fetal development, organ size, anatomy, and physiology. Large animal models offer a clear advantage compared to rodents. Non-human primates have the closest

phylogenetic relationship to humans, but these models are limited due to their high costs, prolonged breeding time, and high ethical concerns (Stirm et al., 2022). However, pigs represent a valuable alternative, since important physiological parameters such as heart rate, cardiac structure, and contractile function closely resemble those of an adult human (Hughes, 1986; Lelovas et al., 2014; Romagnuolo et al., 2019).

Although anatomical atlases of both human and mouse heart development have been published, only two recent studies have investigated embryonic cardiac development of pigs (Gabriel et al., 2021; Lauschke et al., 2021). However, *in vitro* models of porcine cardiogenesis are still limited due to the lack of *bona fide* pluripotent stem cells (PSCs) in this species. Recently, we established porcine expanded potential stem cells (pEPSCs) (Gao et al., 2019), which possess long-term self-renewal, allow precise genome editing, and have the ability to contribute to both embryonic and extraembryonic lineages *in vitro* and *in vivo*, thereby representing a major advance for differentiation studies and future cell therapy applications. However, the efficient generation of cardiac lineages from pEPSCs has not been yet investigated.

Here, we provide an anatomical and molecular characterization of *in vivo* porcine cardiogenesis at embryonic days ED13, ED14, ED15, ED17 and ED19. We also established an *ex utero* culture system allowing faithful monitoring of porcine embryonic cardiac development. Finally, we describe protocols for the directed differentiation of pEPSCs into CPCs, CMs, epicardial cells, smooth muscle cells (SMCs), endothelial cells (ECs) and cardiac fibroblasts (FBs). These platforms open new possibilities for the development of autologous or allogeneic cell-based cardiac regenerative therapies.

Materials and methods

Animals

German Landrace gilts (7–9 months) from an approved local farm facility were used as embryo donors. Animals were transported to the Technical University Munich, Klinikum rechts der Isar animal facility for sample isolation. Embryos were harvested in the accordance with §4 German Animal Welfare legislation. Pregnant sows were euthanized using pentobarbital (Euthadorm, CP-Pharma, Germany) according to the manufacturer's specifications and the uterus was explanted immediately after cardiac arrest. All experiments were performed with permission from the local regulatory authority.

pEPSCs culture

Porcine EPSCs were maintained on 0.1% gelatin-coated plates (Sigma-Aldrich®, G1890) with mitotically inactivated mouse SNL76/7 feeder cells in porcine EPSC medium (pEPSCM) as previously described by Gao et al. (2019). The N2B27 basal media was supplemented with 0.2 μM CHIR99021 (Tocris, 4423), 0.02 μM A-419259 trihydrochloride (Tocris, 3914), 2.5 μM XAV939 (Sigma-Aldrich®, X3004), 50 μg/mL ascorbic acid (Sigma-Aldrich®, 49752-100G), 10 ng/mL LIF (Millipore, LIF1050), 20 ng/mL Activin A (Stemcell Technologies, 78001.1). Cells were enzymatically passaged every 4 days using TrypLE™ (Thermo Fisher Scientific, 12605010). To promote cell survival, Rho-associated coiled kinase (ROCK) inhibitor Y-27632 (Tocris, 1254) was added at a concentration of 5 μM for 24 h after passaging. Two different pEPSCs lines (pEPSCs-T4 and pEPSCs-T6) at different passages were used for differentiation experiments.

hESCs culture

Human ESC line used in these studies was approved by the Ethics Commission of the TUM Faculty of Medicine (# 447/17S). Authorization to use the hESC-TN was granted by the Central Ethics Committee for Stem Cell Research of the Robert Koch Institute to AM (AZ 3.04.02/0131). Generation of the hESC-TN line was described in Zawada et al. (2023). hESCs were maintained on Matrigel-coated plates (Corning, 354277) in Essential 8 medium (Thermo Fisher Scientific, A1517001) containing 0.5% penicillin/streptomycin (Thermo Fisher Scientific, 15140-122) under standard culture conditions (37°C, 5% CO_2); medium was refreshed every day. Cells were passaged every 4 days with 0.5 mM EDTA (Invitrogen, AM92606) in PBS without Ca^{2+} and Mg^{2+} ($PBS^{-/-}$; Thermo Fisher Scientific, 10010023). To promote better cell survival, 2 μM ROCK inhibitor Thiazovivin (Sigma-Aldrich®, SML1045) was added for 24 h after passaging. Cells were differentiated according to differentiation protocols described below.

Cardiac differentiation

The cardiac differentiation protocol was adapted from well-established protocols (Mendjan et al., 2014; Hofbauer et al., 2021; Zawada et al., 2023). Briefly, pEPSCs were passaged using TrypLE™ and were pre-plated on a gelatinized 6-well tissue culture plates in pEPSCM for 30 min at 37°C and 5% CO_2 to remove SNL76/7 feeder cells. Thereafter, 240,000 pEPSCs were seeded per well of a 24-well plate in pEPSCM containing 5 μM Y-27632 (day −1). Differentiation was initiated (day 0) by changing the EPSCM to CDM-BSA medium (CDM-BSA: 1:1 DMEM/F-12 with Glutamax (Thermo Fisher Scientific, 31331028) and IMDM (Thermo Fisher Scientific, 21980032) containing 0.1 g/mL BSA (Sigma-Aldrich®, A9647), 30 mg/mL transferrin (Sigma-Aldrich®, T1147), 1% chemically defined lipid concentrate (Thermo Fisher Scientific, 11905031), ~0.46 mM (0.004%) of monothioglycerol (Sigma-Aldrich®, M6145), supplemented with 10 ng/mL BMP4 (R&D, 314-BP), 1.5 μM CHIR99021 (R&D, 4423), 50 ng/mL Activin A (Sigma-Aldrich®, SRP3003), 30 ng/mL bFGF (R&D, 233-FB) and 5 μM LY 294002 hydrochloride (R&D, 1130). Thereafter medium was replaced with CDM-Meso medium [CDM-BSA supplemented with 10 ng/mL BMP4, 8 ng/mL bFGF, 10 μg/mL insulin (Sigma-Aldrich®, 11376497001), 5 μM IWP2 (Stemcell Technologies, 72122) and 0.5 μM retinoic acid (RA; Sigma-Aldrich®, R2625)] for 4 days with medium change every 24 h. Subsequently, the medium was replaced with CDM-Myo medium (CDM-BSA medium supplemented with 10 ng/mL BMP4, 8 ng/mL bFGF, and 10 μg/mL insulin) for 2 days with medium change every 24 h. The cardiomyocytes were cultured in CDM-Maintenance medium

(CDM-BSA supplemented with 10 μg/mL insulin). The medium was replaced every second day. Human ESCs were differentiated into CPCs as described in Zawada et al. (2023).

Cardiomyocytes dissociation and replating

Five days before dissociation, maintenance medium was changed to EB2 medium consisting of DMEM/F12 (Thermo Fisher Scientific, 21331-020) supplemented with 2% fetal bovine serum (FBS; Sigma-Aldrich®, F7524, batch 044M3395), 1% L-glutamine (Thermo Fisher Scientific, 25030-081), 1% non-essential amino acids (Thermo Fisher Scientific, 11140-050), 0.5% penicillin/streptomycin and 0.1 mM beta-mercaptoethanol. Cells were subjected to papain-based dissociation as described by Fischer et al. (2018). Briefly, cells were incubated with papain solution (Worthington Biochemical Corporation, LS003124) for 20 min at 37°C. The enzymatic reaction was stopped with 1 mg/mL trypsin inhibitor (Sigma-Aldrich®, T9253) in $PBS^{-/-}$. Cells were reseeded at a density of 100,000-120,000 cells on 12-well chamber slides (Ibidi, 81201) coated with 2 μg/cm² fibronectin (Sigma-Aldrich®, F1141) for immunofluorescence analysis or at a density of 50,000-70,000 cells in 3.5 cm glass-bottom cell culture microdishes (MatTek Corporation, P35G-1.5 14-C) coated with 2 μg/cm² fibronectin for calcium and action potential analysis. Cells were incubated for 24 h in EB20 medium consisting of DMEM/F12, 20% FBS, 1% L-glutamine, 1% non-essential amino acids, 0.5% penicillin/streptomycin and 0.1 mM beta-mercaptoethanol. The next day media was changed to EB2 and changed daily till day 65.

Epicardial and endothelial differentiation of CPCs

Porcine EPSCs were differentiated into epicardial cells as previously described (Bao et al., 2017b; Zawada et al., 2023). On day 6, pEPSC-derived CPCs were detached with Accutase (Thermo Fisher Scientific, A1110501) at 37°C for 5 min and seeded in a density of 20,000 cells/cm² onto 0.1% gelatin-coated wells of 12-well chamber slide or 48-well plates for long-term culture in LaSR medium (Advanced DMEM/ F12 containing Glutamax (Thermo Fisher Scientific, 12634010), 0.1 mg/mL ascorbic acid (Sigma-Aldrich®, A5960) and 0.5% penicillin/streptomycin) supplemented with 1% FBS and 10 μM of Y- 27632 for 24 h. On days 7 and 8, the medium was replaced with LaSR medium containing 3 μM CHIR99021. From day 9 to day 12 LaSR medium without additional supplementation was replaced every day. From day 12, epicardial cells were maintained in LaSR medium containing 2 μM SB431542 (R&D, 1614/1) to prevent spontaneous differentiation. For long-term maintenance, cells were passaged 1:4 onto gelatin-coated plates in LaSR medium supplemented with 2 μM SB431542. hESCs were differentiated as described in Zawada et al. (2023).

For endothelial differentiation modified protocol described by Wei et al. (2020) was used. Briefly, d4.5 CPCs were seeded in a density of 20,000 cells/cm² on 12-well chamber slides in LaSR medium containing 50 ng/mL VEGF (R&D, 293-VE-010) and 25 ng/mL BMP4 (R&D, 314-BP). After 8 days, cells were fixed for immunofluorescence staining.

Differentiation of epicardial cells into ECs, SMCs and cardiac FBs

Porcine EPSC-derived epicardial cells were differentiated into SMCs and FBs as previously described by Bao et al. (2017b). On day −1, pEPSCs were dissociated with Accutase and reseeded onto gelatin-coated plates at a density of 30,000 cells/cm² in LaSR medium containing 5 μM Y27632. From day 0 to day 8, medium was replaced every day with LaSR medium containing 5 ng/mL TGF-β1 (R&D, 7754-BH-005) for SMCs differentiation or with 10 ng/mL bFGF (R&D, 233-FB-025/CF) for FBs differentiation. Epicardial cells were differentiated into ECs as previously described by Bao et al. (2017a) with some modifications. After maintenance in LaSR medium containing 0.5 μM A83-01 for several passages, confluent pEPSC-derived epicardial cells were reseeded at a density of 40,000 cells/cm² on 12-well chamber slides in EGM-2 medium (Lonza, CC-3162) supplemented with 100 ng/mL VEGF. After 8 days cells were fixed for immunostaining.

RNA isolation, reverse transcription PCR (RT-PCR), and quantitative real-time PCR (qRT-PCR)

Total RNA was isolated from cells using the Absolutely RNA Microprep kit (Agilent, 400805) following manufacturer's instructions. cDNA was prepared using the High Capacity cDNA RT kit (Applied Biosystems, 4368814) according to the manufacturer's instructions, and a FlexCycler2 PCR thermal cycler (Analytik Jena, Germany). For long-term storage, RNA was kept at −80°C and cDNA at −20°C. Quantitative real-time PCR (qRT-PCR) was performed using the Power SYBR Green PCR Master Mix (Applied Biosystems, 4367659), 1 μL cDNA, and the gene-specific primers (Table 1). Reactions were run on a 7,500 Fast Real-Time PCR instrument (Applied Biosystems, Germany). The mRNA expression levels of genes of interest were quantified relative to *GAPDH* expression using the ΔCt method.

Immunofluorescence staining of cells

For immunostaining, cells were washed with PBS with Ca^{2+} and Mg^{2+} ($PBS^{+/+}$; Sigma-Aldrich®, D8662) and fixed with 4% PFA (Sigma-Aldrich®, 158127) for 15 min at room temperature (RT). After washing three times with $PBS^{+/+}$, cells were blocked for 1 h at RT in 0.1% Triton X-100 (Sigma-Aldrich®, X100) in $PBS^{+/+}$ containing 3% BSA. Appropriate primary antibodies (Table 2) were then added at the indicated dilutions in $PBS^{+/+}$ containing 0.1% Triton-X-100 and 0.5% BSA and incubated overnight at 4°C. After washing with 0.1% Triton-X-100 in $PBS^{+/+}$, samples were incubated with appropriate secondary antibodies (Table 3) diluted in 0.1% Triton-X-100 PBS containing 0.5% BSA for 1 h at RT. After three washing steps with 0.1% Triton-X-100 in $PBS^{+/+}$, Hoechst 33258 (Sigma-Aldrich®, 94403) was added at a final concentration of

TABLE 1 Quantitative RT (qRT)-PCR primers used for gene expression analysis of porcine cardiac and epicardial cells.

Primer name	Forward sequence	Reverse sequence	References
ALDH1A2	AGCTCTGTGCTGTGGCAATAC	AAAGCCAGCCTCCTTGATG	
BNC2	CTGAGGACTTGCGATCAGTGT	GTATAGGTGCTGCGTGCTGA	
TBXT	TCAAGGAGCTCACCAACGA	AGACACGTTCACCTTCAGCAC	
EOMES	ACTCCCATGGACCTCCAGAA	TCGCTTACAAGCACTGGTGT	Zhi et al. (2022)
GAPDH	CTCAACGGGAAGCTCACTGG	CATTGTCGTACGAGGAAATGAGC	Gao et al. (2019)
ID2	TCGCACCCCACTATTGTCAG	TTCAGAAGCCTGCAAGGACA	Wei et al. (2020)
ISL1	CACTGTGGACATTACTCCCTGTT	AACCAACACATAGGGAAATCAGAC	
KDR	GAGCCCCTGATTACACCACC	GCAGATACTGACTGATTCCTGCT	Wei et al. (2020)
MESP1	CGTCTTGGGGGTCTCCTTCTG	GGGGCCAATATTCCACCGTC	Wei et al. (2020)
MYH6	TCCATCTCTGACAACGCCTA	TGGCGAAGTACTGGATGACA	
MYH7	AAGGCCAAGATTTTGTCTCG	CTTGTCGAACTTGGGTGGAT	
MYL2	GGGACACCTTTGCTGCTCT	ATTGGACCTGGAGCTTCCTT	
MYL7	ATGGCATCATCTGCAAGTCA	AACGTGAGGAAGACGGTGAA	
NKX2.5	CCCTCGAGCCGATAAGAAAG	ACCTGTGCCTGCGAAAAG	Das et al. (2020)
SEMA3D	CACGCTGTTTCTTCCAGTCA	CAGCTATTTGAAAGCAGCAAGTC	
TBX1	GTGAAGAAGAACGCGAAGGT	ATGCCGAAAAGCTTCACTTG	
TBX5	CACGAAGTGGGCACAGAAA	TTTGGGATTAAGGCCAGTCA	
TBX18	TTCACTACGGACTCTCACCTTTG	CATTCCCAGAACCTTGGAGTAA	
TCF21	CAACGACAAGTACGAGAATGGTT	TCAGGTCACTTTCGGGTTTC	
TNNT2	CCGGAAGAAGAAGGCTCTGT	CCGTCTGCCTCTTTCCACT	
WNT5A	CGCGAAGACAGGCATCAAAG	CCTATCTGCATGACCCTGCC	
WT1	GTCTACGGATGCCACACCTC	AAGCTGGGAGGTCATTTGGT	

5 μg/mL in $PBS^{+/+}$ for 15 min at RT. After washing once with $PBS^{+/+}$, slides with cells were then covered with fluorescence mounting medium (Dako, S3023) and coverslip and stored at 4°C until imaging.

Microscopy and image analysis

Stained cells were imaged using confocal laser scanning microscope (TCS SP8; Leica Microsystems, Wetzlar, Germany). Images were acquired and processed using the Leica Application Suite X software (v3.5.7.23225). To quantify the relative distribution of CM subtypes, the number of ventricular ($MLC2v^+$), immature ventricular ($MLC2v^+/a^+$) and atrial CMs ($MLC2a^+$) was counted using ImageJ (National Institutes of Health).

Flow cytometry analysis

At day 30 of cardiac differentiation, cells were detached using papain-based dissociation as previously described (Fischer et al., 2018; Zawada et al., 2023). 2×10^6 cells per sample were fixed with 4% PFA for 7 min at RT. After washing three times for 5 min with $PBS^{+/+}$, cells were permeabilized/blocked with 0.1% Triton-X-100, 10% FCS, for 1 h at RT. The primary antibody for cardiac Troponin T (Table 2) was diluted in 1% FCS, with 0.1% Triton-X-100 in $PBS^{+/+}$, and incubated with cells overnight at 4°C. After washing three times for 15 min with $PBS^{+/+}$ containing 0.1% Triton-X-100, an appropriate secondary antibody diluted in 1% FCS in $PBS^{+/+}$ with 0.1% Triton-X-100 was added for 1 h at RT (Table 3). After repeating the previous washing steps with $PBS^{+/+}$ containing 0.1% Triton-X-100 cells were re-suspended in 100 μL $PBS^{+/+}$ supplemented with 2% FCS. Cells were then filtered with a 40 μm filter (Sartorius, 16555-K) and subjected to flow cytometry analysis on Gallios (Beckman Coulter). Data were analyzed using Kaluza software (Beckman Coulter). No-primary antibody, no-secondary antibody, IgG antibody and undifferentiated pEPSCs were performed as controls.

Calcium imaging

For calcium imaging, day 65 pEPSC-CMs were incubated with calcium indicator Fluo-4 AM (Thermo Fisher, F14201) at a concentration of 1 μM in Tyrode's solution supplemented with

TABLE 2 Primary antibodies used for immunostaining.

Target	Host species	Manufacturer	Catalog number	Concentration
α-SMA	Mouse	Sigma-Aldrich®	A2547	1:100
ALDH1A2	Rabbit	Abcam	ab96060	1:100
BNC1	Rabbit	Sigma-Aldrich®	HPA 063183	1:100
TBXT	Rabbit	R&D Systems	MAB20851-100	1:100
CALPONIN	Mouse	Abcam	AB700	1:100
Cardiac TROPONIN T (cTNT)	Rabbit	Abcam	ab92546	1:500
CD31	Mouse	Bio-Rad	MCA1746GA	1:50
EOMES	Rabbit	Abcam	ab23345	1:100
ISL1	Mouse	Developmental Studies Hybridoma Bank	39.4D5	1:100
KDR/FLK-1/VEGFR2	Rabbit	Cell Signaling	2479	1:100
KRT18 (CK18)	Mouse	Abcam	ab668	1:100
MLC2a	Mouse	Synaptic systems	311 011	1:100
MLC2v	Rabbit	ProteinTech	10906-1-AP	1:100
NANOG	Rabbit	Peprotech	500-p236	1:100
NKX2.5	Rabbit	Invitrogen	PA5-49431	1:100
OCT4	Mouse	Santa Cruz Biotechnology	sc-365509	1:100
SOX2	Goat	R&D Systems	AF2018	1:100
SSEA1	Mouse	Stemcell Technologies	60060AD.1	1:100
SSEA4	Mouse	Stemcell Technologies	60062FI.1	1:100
TBX5	Rabbit	Sigma-Aldrich®	HPA064683	1:100
VE-CADHERIN	Mouse	Invitrogen	14-1449-82	1:100
VIMENTIN	Chicken	Abcam	ab24525	1:400
WT1	Rabbit	Abcam	ab89901	1:100
ZO-1	Mouse	Thermo Fischer	33-91010	1:100

TABLE 3 Secondary antibodies used for immunostaining.

Target species	Host species	Conjugate	Manufacturer	Catalog number	Concentration
Chicken	Goat	Alexa Fluor 594	Invitrogen	A11042	1:500
Goat	Donkey	Alexa Fluor 647	Invitrogen	A32849	1:500
Mouse	Goat	Alexa Fluor 594	Invitrogen	A11005	1:500
Mouse	Goat	Alexa Fluor 488	Invitrogen	A11001	1:500
Mouse	Goat	Alexa Fluor 647	Invitrogen	A21235	1:500
Rabbit	Goat	Alexa Fluor 488	Invitrogen	A11008	1:500
Rabbit	Goat	Alexa Fluor 647	Invitrogen	A32733	1:500

Ca^{2+} as previously described (Moretti et al., 2020). Briefly, field stimulation electrodes (RC-37FS, Warner Instruments, Hamden, CT, United States) were connected to a stimulus generator (HSE Stimulator P, Hugo Sachs Elektronik, March-Hugstetten, Germany) providing depolarizing pulses (50 V, 5 ms duration) at the frequencies indicated. ImageJ (National Institutes of Health,

Bethesda, MD) was used to quantify fluorescence over single cells and background regions. Thereafter, analysis was performed in RStudio using custom-written scripts (RStudio, 2020). After subtraction of background fluorescence, the time course of Fluo-4 fluorescence was normalized to the initial value (F/F0). After manual selection of the starting points and peaks of the calcium transients, the transient duration at 50% decay (TD_{50}) and 90% decay (TD_{90}) was automatically determined by the script. The amplitude of calcium transients was calculated by subtracting the basal fluorescence value from the peak value.

Optical action potential measurements

For optical action potential imaging a genetically encoded Förster resonance energy transfer (FRET)-mediated membrane potential sensor (voltage-sensitive fluorescent protein, VSFP) was used as previously described (Chen et al., 2017). Briefly, day 58 porcine CMs were reseeded on a 3.5 cm glass-bottom cell culture dishes (MatTek Life Science) using papain-based dissociation and 2 days later transduced with a lentiviral vector encoding the VSFP sensor under the control of the ubiquitous phosphoglycerate kinase 1 (PGK) promoter. Five days after infection, CMs were incubated with Tyrode's solution and subjected to imaging at 100 frames per second on an inverted epifluorescence microscope (DMI6000B, Leica Microsystems) equipped with a Zyla V sCMOS camera (Andor Technology). Electrical stimulation was performed at 0.5 Hz using field stimulation electrodes as described above. The VSFP was excited at 480 nm, and the emitted GFP and RFP fluorescence signals were separated using an image splitter (OptoSplit II, Caim Research) equipped with CAIRN HQ535.50 566DCXR E570LP filters (Chen et al., 2017; Goedel et al., 2018). The fluorescence over cells and over background regions was quantified in GFP and RFP channels using ImageJ (National Institutes of Health). Custom-written scripts were applied for further analysis in RStudio Team (2020). After background correction, the RFP/GFP ratio corresponding to APs was derived. Cardiomyocytes based on their action potentials were classified into 2 groups: Ventricular-like cardiomyocytes (V-CMs), and immature ventricular-like cardiomyocytes (iV-CMs) based on $APD_{90}/_{50}$ ratio. iV-CMs = APD_{90}/APD_{50} ratio between 1.4 and 1.8. V-CMs = APD_{90}/APD_{50} ratio between 1.0 and 1.4.

Porcine *in vivo* embryos

Porcine embryos were obtained at ED13, ED14, ED15, ED17, and ED19 of gestation following insemination on two subsequent days. The sows were slaughtered and the uterus was excised and flushed with $PBS^{-/-}$. Collected embryos (11-16 embryos per stage) were fixed in 4% PFA. After washing with $PBS^{+/+}$, the embryos were subjected to a sucrose gradient (5–20%) and embedded in a 1:1 mixture of Tissue-Tek O.C.T. (Sakura, 4583) and 20% sucrose (Sigma-Aldrich®, S9378). Samples were frozen in a bath of 2-methylbutane (Sigma-Aldrich®, M32631) with liquid nitrogen and stored at −80°C or directly cryosectioned into 8 µm-thick sections using cryotome (Microm HM560, Thermo Fisher). Sections were collected onto polylysine-coated slides and stored at −80°C until staining.

Whole embryo culture *ex utero*

Porcine embryos at ED14 were dissected from uterus and transferred to culture dish with prewarmed $PBS^{-/-}$. Approximately 2 cm of chorioamniotic membrane attached to both ends of each embryo were kept. Immediately after dissection, a single intact embryo was transferred into one glass culture bottle (B.T.C. Engineering, Cullum Starr Precision Engineering Ltd.) in a pre-equilibrated culture medium containing 50% porcine serum (prepared in-house) and 50% DMEM (Thermo Fisher Scientific, 31966). The bottles were placed on a rotating incubator (B.T.C. Engineering) and the complete medium was changed every 24 h. At the end of the culture, embryos were removed from the yolk sac, allantois, and amnion and evaluated in terms of morphological development. Subsequently, embryos were fixed with 4% PFA and processed for cryopreservation as described above.

Immunofluorescence staining of cryosections

Tissue slides were re-fixed with 3.7% formaldehyde for 15 min at RT. After washing three times with 0.05% Tween-20 in $PBS^{+/+}$ (PBST), sections were permeabilized with 0.1% TritonX-100 for 10 min at RT. After washing briefly with PBST sections were blocked with 10% FBS in PBST for 1 h at RT. The slides were incubated with primary antibodies (Table 2) in $PBS^{+/+}$ containing 1% FBS and 0.1% TritonX-100 at 4°C overnight. Subsequently, sections were washed three times with PBST, incubated with appropriate secondary antibodies (Table 3) for 1 h at RT. After washing three times with PBST, samples were counterstained with Hoechst 33258 at a final concentration of 5 µg/mL in $PBS^{+/+}$ for 15 min at RT. After a final wash with $PBS^{+/+}$, sections were covered with fluorescence mounting medium (Dako, S3023) and stored at 4°C until imaging with confocal laser scanning microscopy (TCS SP8; Leica Microsystems, Wetzlar, Germany) or Leica THUNDER system.

Statistical analysis

Statistical analyses were performed with GraphPad Prism 9.1.0 (La Jolla California, United States). Bar graphs indicate the mean ± SEM with all data points displayed separately. For calcium imaging, a p-value < 0.05 was considered statistically significant.

Results

Anatomical and molecular profile of porcine heart development

Porcine preclinical models are now considered the gold standard for studying congenital heart diseases (CHDs) (Buijtendijk et al., 2020; Gabriel et al., 2021), as numerous recent studies have highlighted the anatomical and molecular similarities in cardiac development between pigs and humans (Lelovas et al., 2014; Lauschke et al., 2021). However, a detailed characterization of the

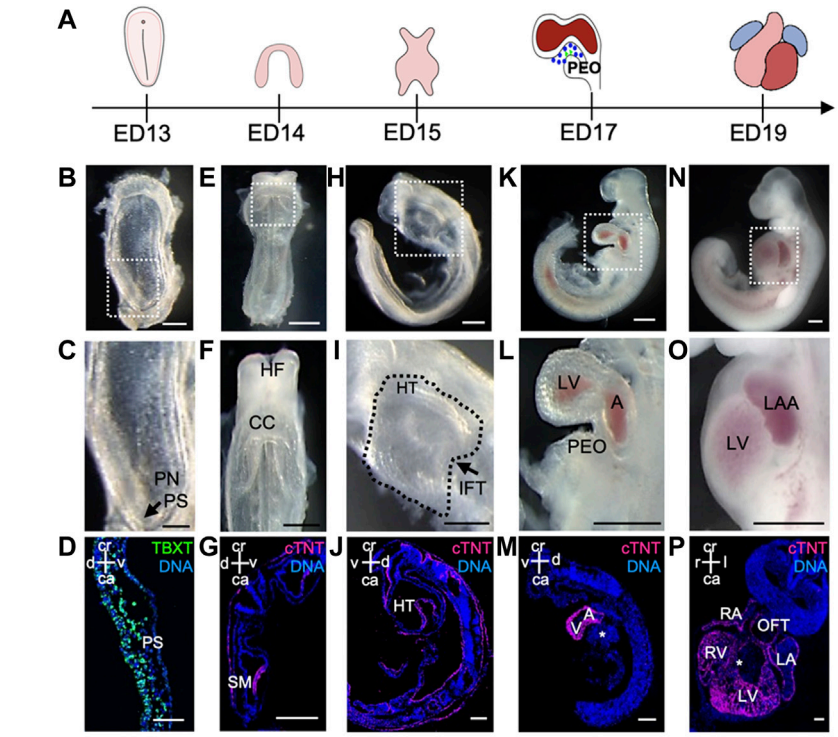

	Primitive streak	Cardiac crescent	Heart tube	Pro-epicardium	Four-chambered
Mouse	ED6.5	ED7.5	ED8.0	ED9.5	ED14.5
Pig	ED13	ED14	ED15	ED17	ED19
Human	Unknown	~ED14	ED21	Unknown	~ED42

FIGURE 1
Porcine heart development from ED13 to ED19. **(A)** Graphical representation of different stages of porcine cardiac development. **(B, C)** Frontal view of ED13 porcine embryo displaying primitive streak (arrow). The boxed region in **(B)** is shown at higher magnification in **(C)**. **(D)** Representative image of sagittal section of ED13 embryo after immunofluorescence analysis of TBXT (green). Nuclei were labeled with Hoechst 33528 (blue). **(E, F)** Frontal view of ED14 embryo depicting the cardiac crescent. The boxed region in **(E)** is shown at higher magnification in **(F)**. **(G)** Representative image of transverse section of ED14 embryo after immunofluorescence analysis of cTNT (magenta). Nuclei were labeled with Hoechst 33528 (blue). **(H, I)** Left view of ED15 embryo showing the primitive heart tube. The boxed region in **(H)** is shown at higher magnification in **(I)**. **(J)** Representative image of sagittal section of ED15 embryo after immunofluorescence analysis of cTNT (magenta). Nuclei were labeled with Hoechst 33528 (blue). **(K, L)** Left view of ED17 embryo displaying the proepicardium, common atrium, and left ventricle. The boxed region in **(K)** is shown at higher magnification in **(L)**. **(M)** Representative image of sagittal section of ED17 embryo after immunofluorescence analysis of cTNT (magenta). Nuclei were labeled with Hoechst 33528 (blue). **(N, O)** Left view of ED19 embryo with four-chambered heart. The boxed region in **(N)** is shown at higher magnification in **(O)**. **(P)** Representative image of frontal section of ED19 embryo after immunofluorescence analysis of cTNT (magenta). Nuclei were labeled with Hoechst 33528 (blue). **(Q)** Table summarizing major events during heart development in pig, mouse and human. A, atrium; ca, caudal; CC, cardiac crescent; cr, cranial; d, dorsal; HT, heart tube; IFT, inflow tract; l, left; LA, left atrium; LAA, left atrial appendage; LV, left ventricle; OFT, outflow tract; PEO, proepicardial organ; PN, primitive node; PS, primitive streak; r, right; SM, splanchnic mesoderm; v, ventral; V, ventricle. Asterix indicates interventricular septum. Scale bars for bright-field images 1 mm, for immunostaining images: 10 µm.

early stages of porcine cardiogenesis is still lacking. Here, we examined the porcine heart development from the primitive streak stage (ED13) to the four-chambered beating heart (ED19). The embryos were collected at five different time points (ED13, ED14, ED15, ED17, and ED19) (Figure 1A) and subjected to anatomical and immunohistochemical analyses (Figures 1B–P; Supplementary Figure S1).

At ED11-12, the porcine spherical blastocyst starts to elongate and forms a filamentous structure (Hyttel et al., 2011). This process is accompanied by the initiation of gastrulation, establishing the primitive streak. At ED13, the primitive streak was visible at the caudal end of the porcine embryo (Figures 1A–D), which was marked by the expression of mesodermal T-box transcription factor TBXT (BRACHYURY) (Figure 1D) and cardiac mesoderm-specific marker KDR (Supplementary Figures S2A–C) corresponding to the stage ED6.5 in the mouse (Krishnan et al., 2014). The first cells expressing cardiac troponin T (cTNT) were detected at ED14 (ED7.5 in mouse and approximately week 2 of human gestation) (Krishnan et al., 2014; Buijtendijk et al., 2020) in splanchnic mesoderm forming the cardiac crescent (Figures 1E–G, Q). At ED15, a faintly beating linear heart tube could be visualized (ED8.0 in mouse and week 3 of human gestation) (Figures 1H–J, Q),

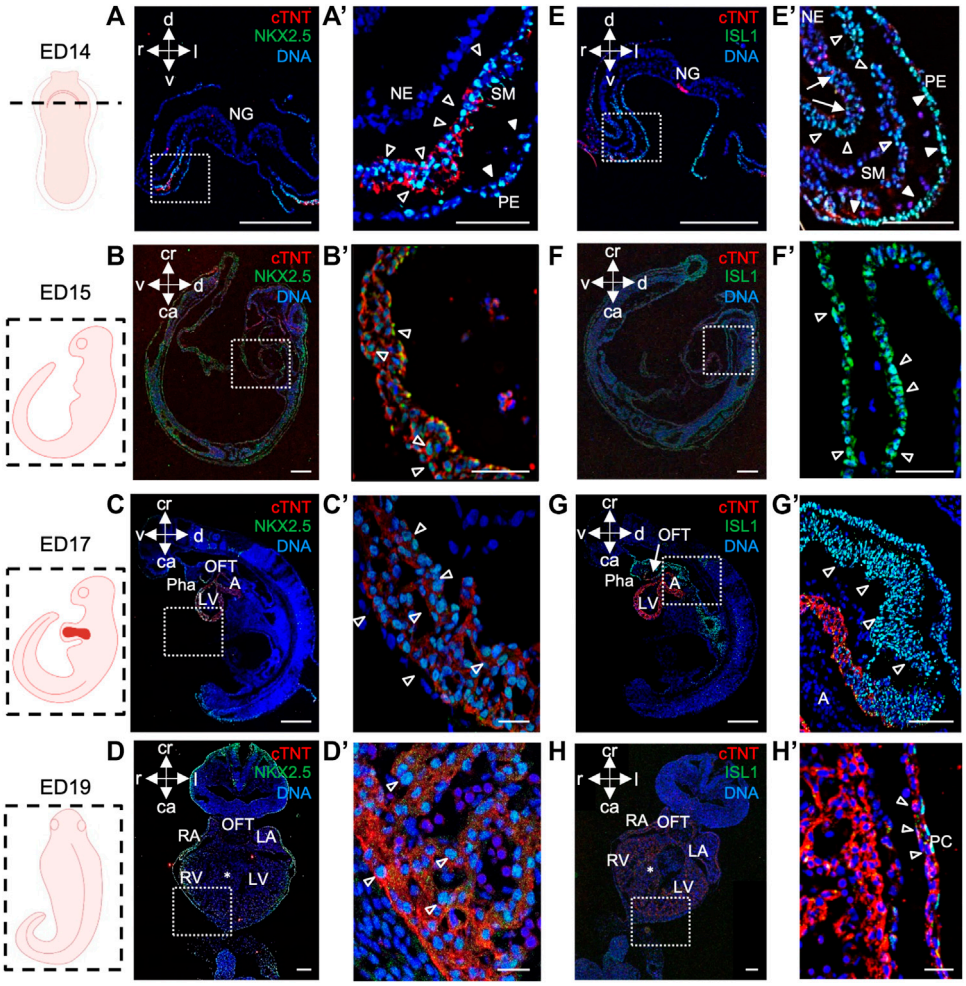

FIGURE 2
NKX2.5 and ISL1 expression during porcine heart development from ED14 to ED19. **(A–D')** Representative images of ED14 **(A, A')**, transverse, ED15 **(B, B')**, sagittal, ED17 **(C, C')**, sagittal, and ED19 **(D, D')**, frontal embryo sections after immunofluorescence analysis of NKX2.5 (green) and cTNT (red). Nuclei were labeled with Hoechst 33528 (blue). At ED14, NKX2.5$^+$ cells were detected in the splanchnic mesoderm (empty arrowheads) and pharyngeal endoderm (filled arrowheads) **(A, A')**. At ED15, ED17, and ED19, NKX2.5 expression was observed in cardiomyocytes of the developing heart (empty arrowheads) **(B'–D')**. **(E–H')** Representative images of ED14 **(E, E')**, transverse, ED15 **(F, F')**, sagittal, ED17 **(G, G')**, sagittal, and ED19 **(H, H')**, frontal embryo sections after immunofluorescence analysis of ISL1 (green) and cTNT (red). Nuclei were labeled with Hoechst 33528 (blue). At ED14, ISL1$^+$ cells were found in splanchnic mesoderm (empty arrowheads), pharyngeal endoderm (filled arrowheads), and neuroectoderm (arrows) **(E, E')**. At ED15, ISL1 expression was detected in SHF (filled arrowheads) and outflow tract (empty arrowheads) of the primitive heart tube **(F, F')**. At ED17, ISL1 expression was detected in cells of OFT **(G)**, arrow and SHF **(G')**, empty arrowheads. At ED19, ISL1$^+$ cells were sparsely detected in the pericardium (empty arrows) **(H, H')**. Sections correspond to the position indicated by the plane drawn through the adjacent embryo view. The white boxes indicate a region of higher magnification shown in adjacent panels. A, atrium; ca, caudal; cr, cranial; d, dorsal; IFT, inflow tract; l, left; LA, left atrium; LV, left ventricle; NE, neuroectoderm; NG, neural groove; OFT, outflow tract; Pha, pharyngeal arch; PC, pericardium; r, right; RA, right atrium; RV, right ventricle; SHF, second heart field; SM, splanchnic mesoderm; v, ventral; asterix indicates interventricular septum. Scale bars: 10 μm.

which subsequently underwent looping and around ED17 (ED9.5 in mouse) common atrium and ventricle could be distinguished (Krishnan et al., 2014; Buijtendijk et al., 2020) (Figures 1K–M, Q). Notably, at ED17 an extracardiac cluster of cells was detectable at the base of the venous pole of the embryonic heart resembling the proepicardial organ (PEO) in mouse at ED9.5 (Figures 1L, Q) (Krishnan et al., 2014). By ED19 the embryo and extraembryonic membranes increased in size (Figures 1N, O, Q; Supplementary Figures S1J–N). The heart had developed a four-chambered structure, and the heartbeat became more prominent (Figures 1N–P). The interventricular septum, atrial septum, atrial appendages, compact myocardium, and trabecular myocardium were also clearly visible at ED19 (Figure 1P; Supplementary Figure S1).

Next, we sought to provide a more comprehensive characterization of the porcine cardiac precursors giving rise to the various cardiac lineages. In mouse embryo, three spatially and temporarily distinct populations of cardiac progenitors have been identified and described in detail: the cardiogenic mesoderm cells, which encompasses first and second heart field (FHF and SHF), precursors of the PEO, and cardiac neural crest cells (Brade et al., 2013). Here, we focussed primarily on the cardiogenic mesoderm and PEO (Moretti et al., 2006; Zhou et al., 2008; Buijtendijk et al., 2020).

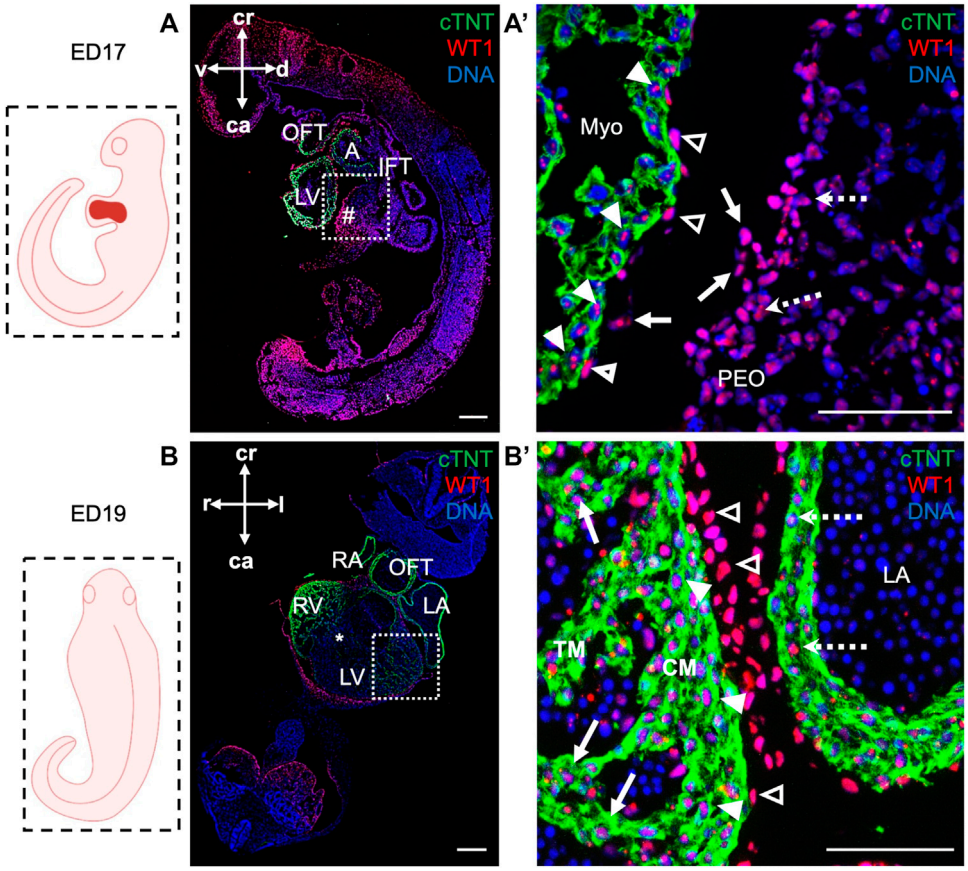

FIGURE 3
WT1 expression in proepicardium and epicardium of ED17 and ED19 porcine hearts. **(A, A′)** Representative images of sagittal section of ED17 embryo after immunofluorescence analysis of cTNT (green) and WT1 (red) depicting WT1 expression in proepiardial (dashed arrows), in PEO-derived translocating cells (arrows), epicardial (empty arrowheads) cells and cardiomyocytes (filled arrowheads). Nuclei were labeled with Hoechst 33528 (blue). The boxed region in **(A)** is shown at higher magnification in **(A′)**. Scale bars: 10 μm. **(B, B′)** Representative images of frontal section of ED19 embryo after immunofluorescence analysis of cTNT (green) and WT1 (red) showing WT1 expression in epicardial cells (empty arrowheads), ventricular cardiomyocytes in compact (filled arrowheads) and trabecular myocardium (arrows) and in atrial cardiomyocytes (dashed arrows). Nuclei were labeled with Hoechst 33528 (blue). The boxed region in **(B)** is shown at higher magnification in **(B′)**. Scale bars: 10 μm. Sections correspond to the position indicated by the plane drawn through the adjacent embryo view. A, atrium; ca, caudal; CM, compact myocardium; cr, cranial; d, dorsal; l, left; LV, left ventricle; Myo, myocardium; OFT, outflow tract; PEO (#), proepicardial organ; r, right; RV, right ventricle; TM, trabecular myocardium; v, ventral; asterix indicates interventricular septum.

Within the cardiogenic mesoderm, FHF progenitors reside in the cardiac crescent and form a linear heart tube, which later becomes the left ventricle, whereas SHF precursors are located posteriorly and medially to the FHF and give rise to the outflow tract, right ventricle, a subset of left ventricular cells, and atria (Brade et al., 2013; Paige et al., 2015; Meilhac and Buckingham, 2018; Ivanovitch et al., 2021). NKX2.5 and ISL1 are the key cardiac-specific transcription factors that mark FHF and SHF and play a pivotal role in early heart development (Lyons et al., 1995; Cai et al., 2003; Moretti et al., 2006). While NKX2.5 is expressed in cardiac precursors of both heart fields and differentiated CMs (Lints et al., 1993; Kasahara et al., 1998), ISL1 shows transient expression in FHF and is mainly restricted to the SHF progenitors. Furthermore, it is absent in differentiated states (Moretti et al., 2006).

In porcine embryos at ED14, we detected NKX2.5^{+} and ISL1^{+} cells in splanchnic mesoderm, where cardiogenic progenitors reside, and in pharyngeal endoderm (Figures 2A, A′, E, E′). ISL1^{+} cells were also present in neuroectoderm (Figure 2E′). Co-staining of both proteins allowed us to identify a population of NKX2.5^{high}/ISL1^{low}- and NKX2.5^{high}/ISL1^{high}-expressing progenitors, resembling FHF and SHF precursors in mouse, respectively (Mommersteeg et al., 2010) (Supplementary Figures S2D–G). At later stages ED15, ED17, and ED19, NKX2.5 was expressed in CMs of the developing heart (Figures 2B–D′), whereas ISL1^{+} cells were detected in SHF and outflow tract (OFT) at ED15 and ED17 (Figures 2F–G′), which is similar to the mouse (Kasahara et al., 1998; Cai et al., 2003). By ED19, no more ISL1^{+} cells could be found within the heart (Figure 2H), although very few cells in the pericardium persisted to express ISL1 (Figure 2H′).

Next, we took advantage of ED17 porcine embryos to examine and further characterize the PEO, which gives rise to the epicardium, the outermost mesothelial layer of the heart (Cao et al., 2020). In mouse, the PEO is a transient extra-cardiac structure that arises at the septum transversum of the venous pole at ED9.0 -ED10.5 and is derived from NKX2.5/ISL1 expressing progenitors. PEO is marked by the expression of several

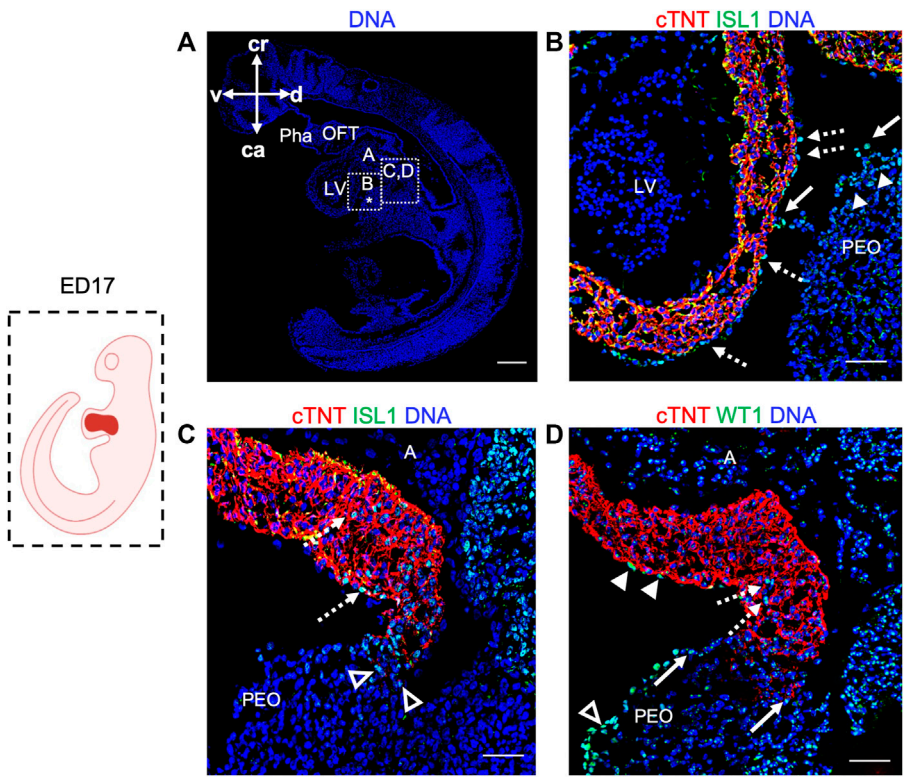

FIGURE 4
Expression of ISL1 and WT1 in ED17 porcine hearts. **(A)** Representative image of sagittal section of ED17 embryo stained with Hoechst 33528 (blue). The white boxes indicate regions of higher magnification shown in **(B–D)** **(B–D)** Representative images of sagittal section of ED17 embryo after immunofluorescence analysis of cTNT (red), ISL1 (green), and WT1 (green). ISL1 expression was detected in cells emerging from the proepicardium (filled arrowheads), translocating towards epicardium (arrows), in the newly formed epicardium (dashed arrows) **(B)**, at the junction of the PEO and the base of the atrium (empty arrowheads), and atrium (dashed arrows) **(C)**. $WT1^+$ cells were present at the PEO-atrium junction (arrows), atrium (dashed arrows), epicardium (filled arrowheads), and PEO (empty arrowheads). Scale bars: 10 μm. A, atrium; ca, caudal; cr, cranial; d, dorsal; l, left; LV, left ventricle; OFT, outflow tract; PEO (*), proepicardial organ; Pha, pharyngeal arch; v, ventral.

transcription factors, including Wilm's Tumor 1 (WT1), which continues to be expressed in the epicardium (Wagner et al., 2005). Immunofluorescence analysis of ED17 porcine hearts demonstrated WT1 expression in the cell cluster at the ventro-caudal base of the developing heart corresponding to PEO (Figures 3A, A′). Importantly, we could capture single cells in the PEO translocating across the pericardial cavity and adhering to the myocardial layer of the developing heart (Figure 3A′). At this stage $WT1^+$ epicardial cells were sparsely scattered around the heart (Figure 3A′) and by ED19 they uniformly enveloped the myocardium (Figures 3B, B′). Strikingly, few cells emerging from the PEO and attaching to the myocardium also expressed ISL1 (Figures 4A, B), as well as cells at the junction of PEO and base of the atrium (Figure 4C), the area that was positive for WT1 (Figure 4D). This differs from the mouse, where ISL1 is not expressed in these cells at comparable stages (Ruiz-Villalba et al., 2013; Zhuang et al., 2013; Niderla-Bielinska et al., 2019). At ED19, ISL1 expression was lost in the porcine epicardium and became restricted to the pericardium, which was negative for WT1 (Supplementary Figure S3). Interestingly, we observed WT1 expression in the cardiomyocytes of the developing heart at ED17 (Figure 3A′) as well as in the compact and trabecular myocardium and atria at ED19 (Figure 3B′), which is in line with the recent reports describing WT1 expression in cardiomyocytes in mice at ED10.5 (Diaz Del Moral et al., 2021; Wagner et al., 2021).

Ex utero culture of porcine embryos from cardiac crescent to proepicardial organ specification

Recent studies using *ex utero* culture of mouse embryos have recapitulated *in utero* development and thus opened new possibilities to study mammalian development and disease (Aguilera-Castrejon et al., 2021; Zawada et al., 2023). Here, we report for the first time the culture of porcine embryos at cardiac crescent stage for up to 4 days using a rotating incubator (Figure 5A). We applied the same conditions as for the mouse embryo culture (20% O_2, 5% CO_2, 30 rpm, 37°C) (Aguilera-Castrejon et al., 2021) and observed similar development in terms of morphology, initiation of heartbeat and growth compared to the *in utero* situation (Figures 5B, C). Embryos were examined after 24, 48, 72, and 96 h of *ex utero* culture. The beating of the heart was detected after 48 h and persisted at 96 h of culture, although weaker. Morphological and

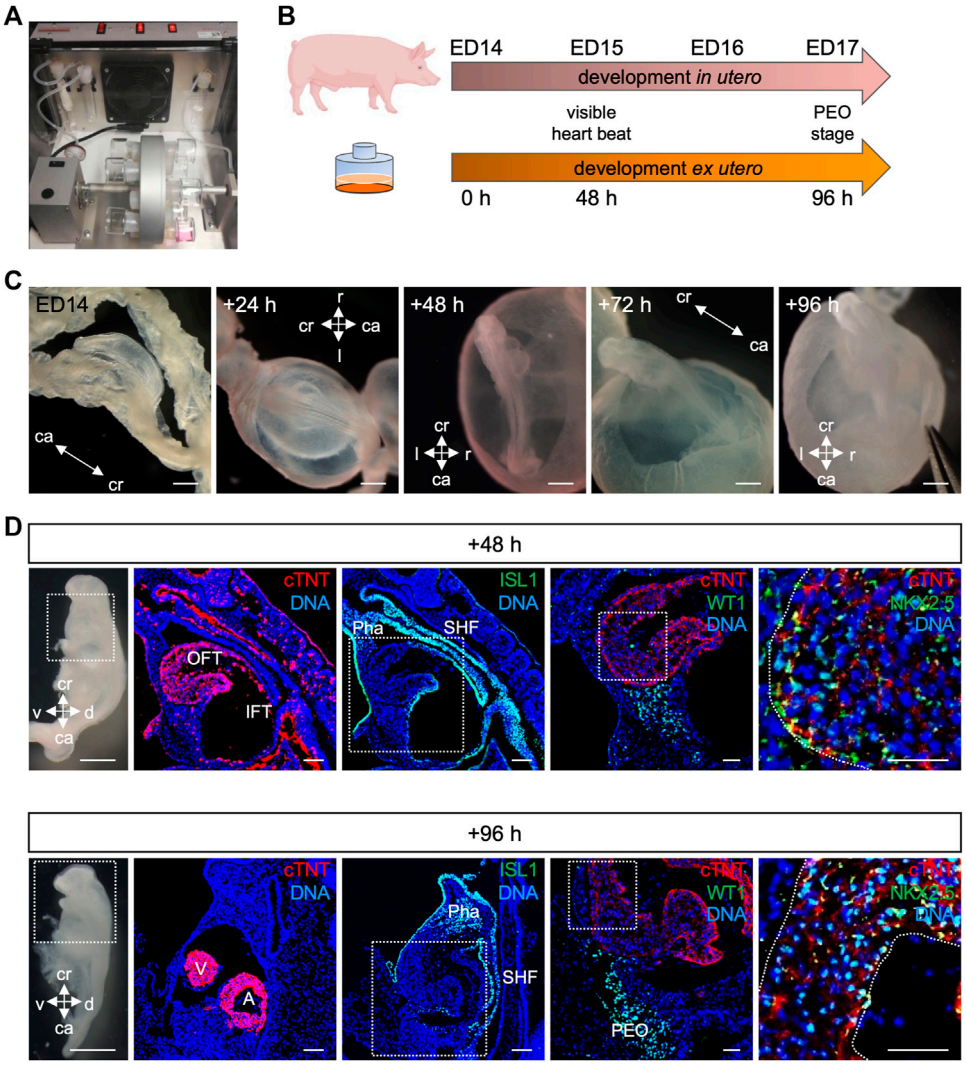

FIGURE 5
Culture of porcine embryos *ex utero*. **(A)** Picture depicting rotating incubator used for porcine embryo culture *ex utero*. **(B)** Schematic comparison of porcine embryonic development *in utero* and *ex utero* based on two developmental hallmarks (heart beat and PEO formation). **(C)** Bright-field images of embryo at ED14, after 24, 48, 72, and 96 h *ex utero* culture. **(D)** On the left, bright-field images of the dissected *ex utero* cultured embryos after 48 h (top) and 96 h (bottom) are shown. Right beside corresponding representative images of sagittal sections after immunofluorescence analysis for cTNT (red), ISL1 (green), WT1 (green), and NKX2.5 (green). Nuclei were labeled with Hoechst 33528 (blue). The white box indicates a region of higher magnification shown in the adjacent right panel. Scale bars for bright-field images: 500 µm, for immunostaining images: 50 µm. A, atrium; ca, caudal; cr, cranial; d, dorsal; IFT, inflow tract; OFT, outflow tract; Pha, pharyngeal arch; PEO, proepicardial organ; SHF, second heart field; v, ventral; V, ventricle.

immunohistochemical analyses revealed development of a primitive heart tube within 48 h and PEO within 96 h of culture, resembling ED15 and ED17 embryos *in vivo*, respectively (Figure 5D). At these stages, ISL1 was expressed in the second heart field and NKX2.5 was present in CMs of the developing heart, similarly to the *in utero* counterpart. WT1 could be detected after 48 h of culture and after 96 h WT1 expressing cells were identified underneath the atrioventricular cavity forming the PEO as seen *in vivo*. Together, we could culture porcine embryos from cardiac crescent up to PEO stage, and recapitulate porcine early embryonic development *ex utero*. This system offers new possibilities for genetic manipulation of porcine embryos and for life-monitoring of developing structures.

Porcine CPCs and CMs derived from pEPSCs express key lineage commitment markers

The availability of functional porcine CPCs and CMs is essential for cardiac disease modeling or testing of autologous cell therapy in the preclinical pig model. However, differentiation of porcine PSCs into the numerous cardiac lineages has not yet been achieved.

To investigate whether CMs can be derived from pEPSCs, we utilized a stepwise 2D differentiation protocol for directed differentiation of human PSCs towards CMs using low/mid-dose dosage of retinoic acid (Zawada et al., 2023) (Figure 6A). This protocol is based on temporal control of key cardiogenic signaling pathways, including Activin/Nodal, bone morphogenic protein (BMP), fibroblast growth factor (FGF), Wnt and retinoic acid (RA),

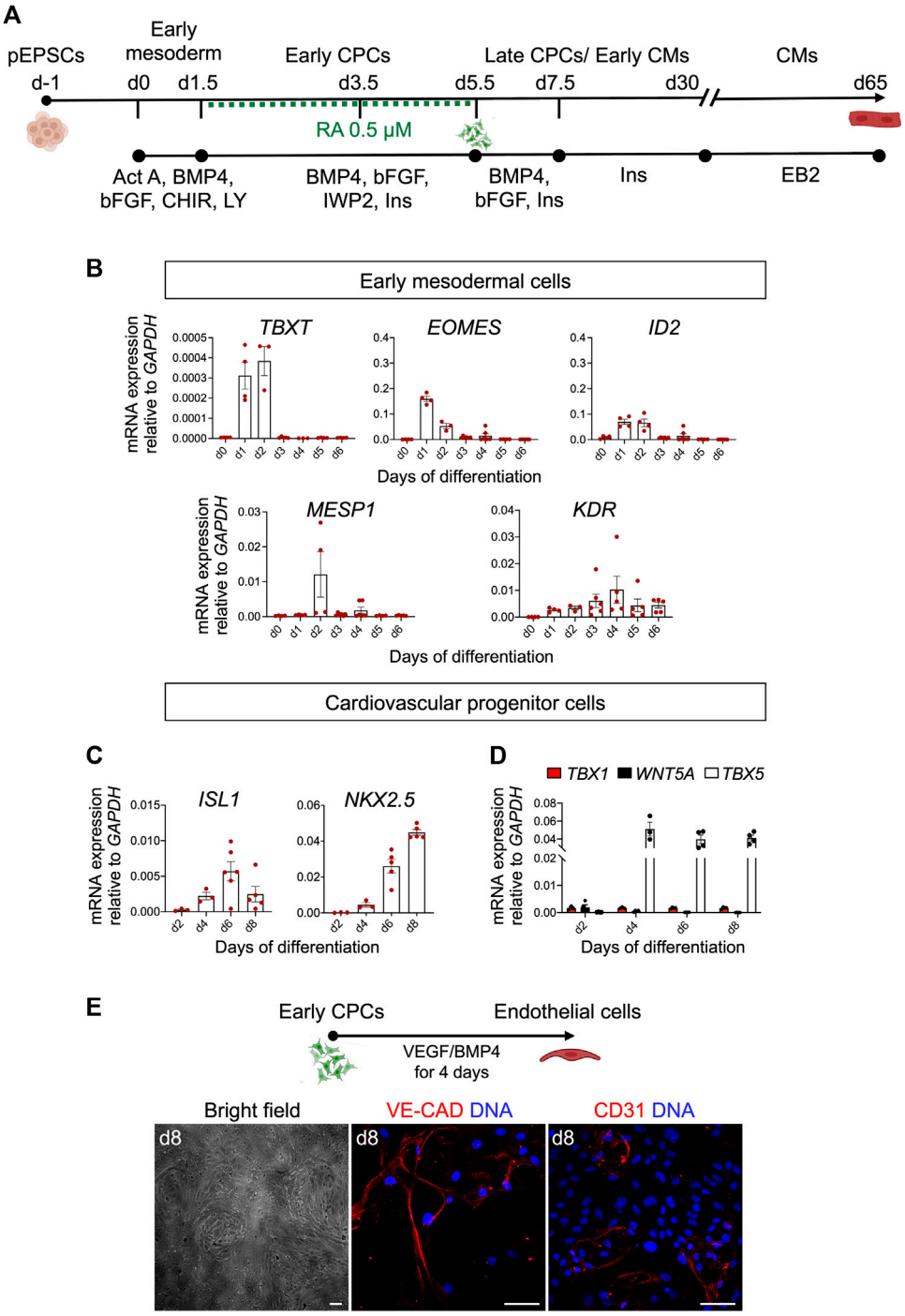

FIGURE 6
Differentiation of pEPSCs into early mesodermal cells. **(A)** Schematic representation of the protocol used to differentiate porcine expanded potential stem cells (EPSCs) into cardiomyocytes (CMs) through defined steps of early mesoderm and cardiovascular progenitor cells (CPCs). Act A, Activin A; CHIR, CHIR99021, LY, LY-29004, RA, retinoic acid, Ins, Insulin. **(B)** mRNA expression levels of *TBXT*, *EOMES*, *ID2*, *MESP1* and *KDR* relative to *GAPDH* during the first 6 days of cardiac differentiation. Data are mean ± SEM; n = 3–6 differentiations. **(C)** mRNA expression level of *ISL1*, *NKX2.5* in CPCs. **(D)** mRNA expression of FHF marker *TBX5* and anterior SHF markers *TBX1* and *WNT5A* relative to *GAPDH* during 8 days of cardiac differentiation. Data are mean ± SEM; n = 3–6 differentiations. **(E)** Top panel: Schematic representation of the protocol used to differentiate day 4.5 cardiovascular progenitor cells (CPCs) into endothelial cells (ECs). Bottom panel: Representative bright-field and immunofluorescence images of CPC-derived ECs stained for CD31 (red) and VE-CADHERIN (red) at day 8 of differentiation. Nuclei were labeled with Hoechst 33258 (blue). Scale bars: 50 μm. Images are representative of three independent differentiations.

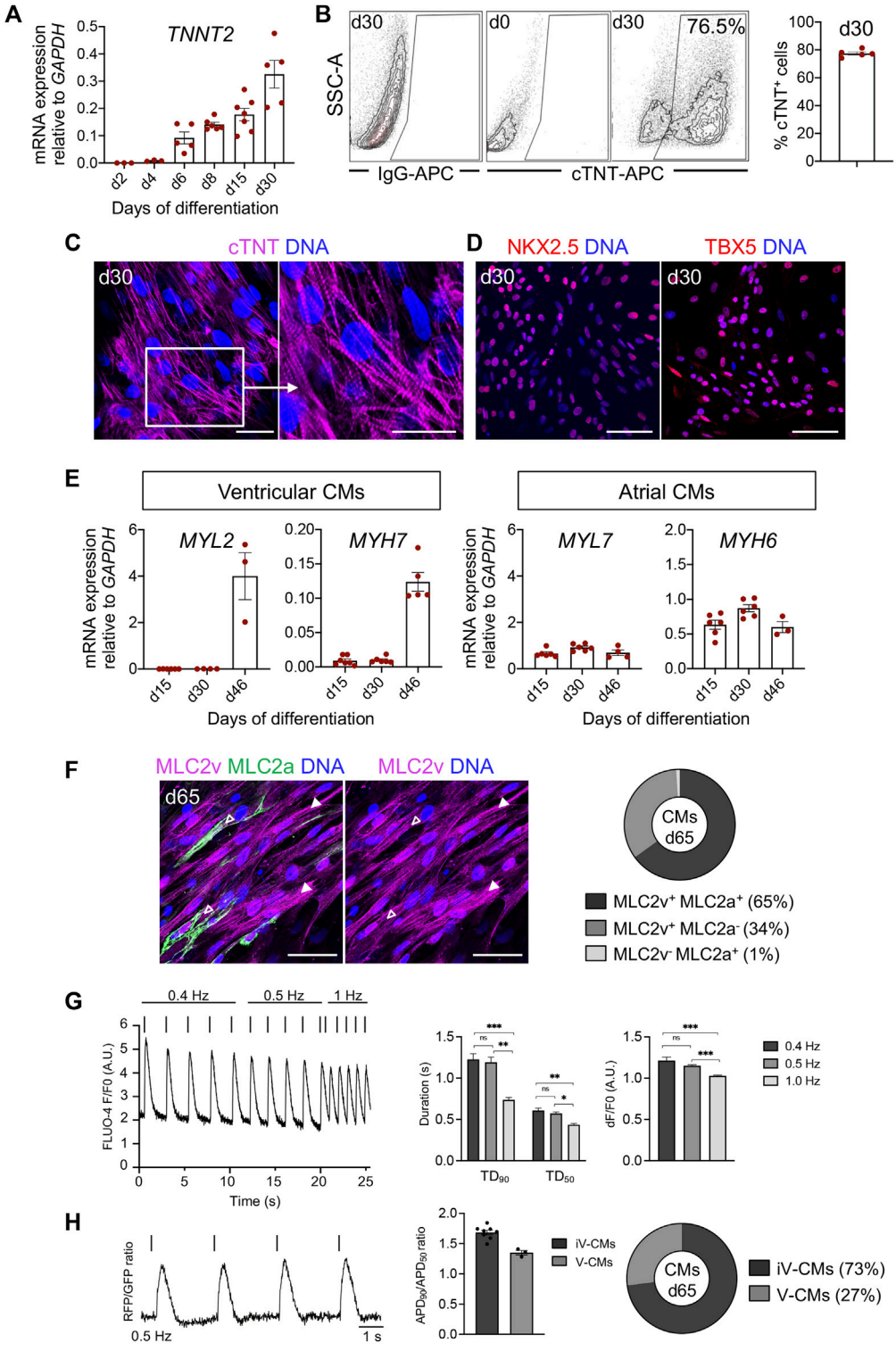

FIGURE 7
Characteristics of pEPSC-derived CMs. **(A)** mRNA expression level of *TNNT2* relative to *GAPDH* during 30 days of the differentiation. Data are mean ± SEM; *n* = 3–6 differentiations. **(B)** Representative plots of flow cytometry analysis (left) and percentage of cells positive for cTNT at day 30 of differentiation (right); *n* = 4 independent differentiations. **(C)** Representative immunofluorescence images for the cTNT (magenta) in CMs at d30. The white box indicates a region of higher magnification shown in the adjacent right panel. Nuclei were labeled with Hoechst 33258 (blue). Scale bars: 50 μm. *n* = 8 independent differentiations. **(D)** Representative images of immunostaining for NKX2.5 (red), TBX5 (red) in CMs at day 30. Nuclei were labeled with Hoechst 33258 (blue). Scale bars: 50 μm. *n* = 8 independent differentiations. **(E)** mRNA expression level of markers specific for ventricular (*MYL2*, *MYH7*) and atrial (*MYL7*, *MYH6*) CMs relative to *GAPDH*. Data are mean ± SEM, *n* = 3–6 independent experiments. **(F)** Left panel: Representative immunofluorescence images of CMs stained for MLC2v (magenta) and MLC2a (green) at day 65. Immature CMs expressing both MLC2v$^+$ and MLC2a$^+$ were marked with empty arrows and mature CMs expressing only MLC2v$^+$ with filled arrowheads. Nuclei were labeled with Hoechst 33258 (blue). Scale
(*Continued*)

FIGURE 7 (Continued)
bars: 50 μm, n = 4 independent differentiations. Right panel: Percentage of CMs expressing MLC2a$^+$ and MLC2v$^+$ (65%), MLC2v$^+$ (34%) and MLC2a$^+$ (1%) at day 65, N = 579 cells, n = 2 differentiations. **(G)** Left panel: Representative trace of Fluo-4-based intracellular calcium transient of porcine CMs at day 65 with increasing pacing rates (0.4–1 Hz). Middle panel: Ca^{2+} transient duration at 90% and 50% decay (TD_{90} and TD_{50}). Right panel: Calcium transient amplitudes. Data are mean ± SEM; N = 42 cells, n = 3 independent differentiations. *$p < 0.05$, **$p < 0.01$, ***$p < 0.0001$ (Kruskal–Wallis test with a Dunn's multiple comparisons test). **(H)** Left panel: Representative optical AP traces of porcine CMs transduced with a lentiviral vector encoding PGK-voltage-sensitive fluorescent protein at 0.5 Hz stimulation at day 65. Middle panel: Ratio of APD_{90}/APD_{50} at 0.5 Hz. Data are mean ± SEM; N = 11 cells,
n = 2 independent differentiations. Right panel: Percentage of cardiomyocyte subtypes at day 65 of differentiation based on the ratio of APD_{90}/APD_{50}. iV-CMs immature ventricular cardiomyocytes, V-CMs ventricular cardiomyocytes.

recapitulating induction of FHF-like cells and (left) ventricular-like CMs (Zawada et al., 2023).

The differentiation of pEPSCs into CMs progresses through multiple steps of cell-fate determination, and each stage can be captured by the expression of identity-specific marker genes. Porcine EPSCs, which expressed pluripotency markers, including OCT4, NANOG, SOX2, SSEA1 and SSEA4 (Supplementary Figure S4A), differentiated in the first step into primitive streak/early mesoderm-like cells upon activation of Wnt pathway by GSK-3β inhibition using CHIR99021 (CHIR) and phosphatidylinositol 3-kinase inhibitor LY294002 (Ly), and parallel stimulation of FGF and Activin/Nodal pathways by basic FGF (bFGF) and Activin A, respectively. At day 1, we detected expression of *TBXT* (*BRACHYURY*), indicative of the primitive streak stage *in vivo*, as well as *EOMES*, *ID2*, and *KDR* marking the earliest cardiac mesodermal cells, followed by upregulation of *MESP1* at day 2 (Figure 6B). Subsequent Wnt inhibition from day 1.5 to day 5.5 by IWP2 and supplementation with BMP4, bFGF and RA induced expression of CPCs markers *ISL1*, *NKX2.5* and *TBX5* (Figures 6C, D). Timing and patterns of gene expression corresponded to those described recently by our group during *in vitro* differentiation of hPSCs (Zawada et al., 2023). With the progression of differentiation, we observed a downregulation of *ISL1* and increased expression of *NKX2.5* (Figure 6C). Thereafter we analysed the expression of key FHF marker *TBX5* and anterior SHF markers *TBX1* and *WNT5A*. Notably, we confirmed only an abundant presence of *TBX5* transcripts in the porcine CPCs suggesting FHF-like fate acquisition similar to hPSCs (Figure 6D) (Zawada et al., 2023). Interestingly, porcine CPCs arising at day 4.5 of differentiation had also the potential to differentiate into ECs upon treatment with VEGF and BMP4, as indicated by expression of CD31 and VE-CADHERIN as well as cobblestone-like morphology (Figure 6E).

During differentiation, upregulation of *TNNT2* gene was observed from day 6 onward (Figure 7A), which corresponds to the first observed cTNT expression in the porcine cardiac crescent at ED14 (Figure 1G). Importantly, we validated our mRNA results using immunofluorescence analysis showing a similar expression pattern of TBXT, EOMES and KDR (Supplementary Figure S4B). Porcine CPCs were stained positive for ISL1 and early CMs for NKX2.5 (Supplementary Figure S4C). Spontaneously contracting porcine CMs emerged in 80% of differentiation experiments at day 8 and in around 20% of experiments at days 9 and 10 (n = 8) (Supplementary Video). Using flow cytometry analyses we detected ~76% of cTNT$^+$ cells at day 30 of differentiation (Figure 7B). The CMs had elongated morphology and showed well-organized sarcomeres, as visualized by immunostaining for cTNT at day 30 (Figure 7C). Furthermore, immunofluorescence analysis revealed that they expressed TBX5 and NKX2.5 at day 30 (Figure 7D).

Next, we examined the expression of cardiac subtype-specific markers during differentiation. Transcripts for myosin light chain 2v (*MYL2*) and myosin heavy chain 7 (*MYH7*)—markers that are specific for ventricular CMs—increased during differentiation, whereas expression of markers typical of atrial or immature CMs, such as myosin light chain 2a (*MYL7*) and myosin heavy chain 6 (*MYH6*) remained constant over time (Figure 7E).

Immunofluorescence analysis for the ventricular and atrial-specific myosin light chain isoforms (MLC2v and MLC2a) indicated that most of the CMs at day 65 (99%) were positive for MLC2v, implying a ventricular-like identity. Many of them still expressed MLC2a and represented immature ventricular CMs. We observed only around 1% of MLC2a$^+$/MLC2v$^-$ CMs, likely corresponding to an atrial population (Figure 7F).

We further validated the functionality of the pEPSC-derived CMs at day 65 using calcium and optical action potential (AP) imaging. The porcine CMs responded to electrical stimulation and demonstrated a reduction in Ca^{2+} transient duration at 50% and 90% decay (TD_{50} and TD_{90}) as well as in calcium transient amplitude at increasing pacing frequencies (0.4 Hz–1.0 Hz), indicative of normal Ca^{2+} handling (Figure 7G). Optical AP traces obtained from porcine CMs were comparable to those previously recorded from human CMs (Chen et al., 2017). CMs demonstrated a ratio of AP duration at 90% and 50% repolarization (APD_{90} and APD_{50}) typical of the ventricular CM lineage (APD_{90}/APD_{50} = 1.0–1.8) (Figure 7H). In line with immunofluorescence results, AP measurements indicated a primarily immature ventricular-like profile of porcine CMs (Figures 7F, H).

In summary, we could demonstrate that porcine CPCs in our differentiation conditions acquired a FHF-like fate and gave rise to ventricular-like CMs similar to hPSCs (Zawada et al., 2023). Overall, these findings confirm that the developmental pathways that take place in the embryonic porcine heart *in vivo* can be replicated during cardiogenesis *in vitro* using pEPSCs.

Differentiation and long-term maintenance of pEPSC-derived epicardial cells

The epicardium, as an outer mesothelial layer of the heart, plays a crucial role during heart development by providing the majority of cardiac FBs and vascular SMCs. It is also essential for myocardial growth and repair, making epicardial cells a relevant population for preclinical testing (Cai et al., 2003; Cai et al., 2008; Bao et al., 2016).

Having succeeded in applying hPSC-directed cardiac differentiation protocol to pEPSCs, we decided to use a similar approach to generate epicardial cells. We again used the protocol published by Zawada et al. (2023) [based on a modified protocol of Bao et al. (2016)]. This protocol is

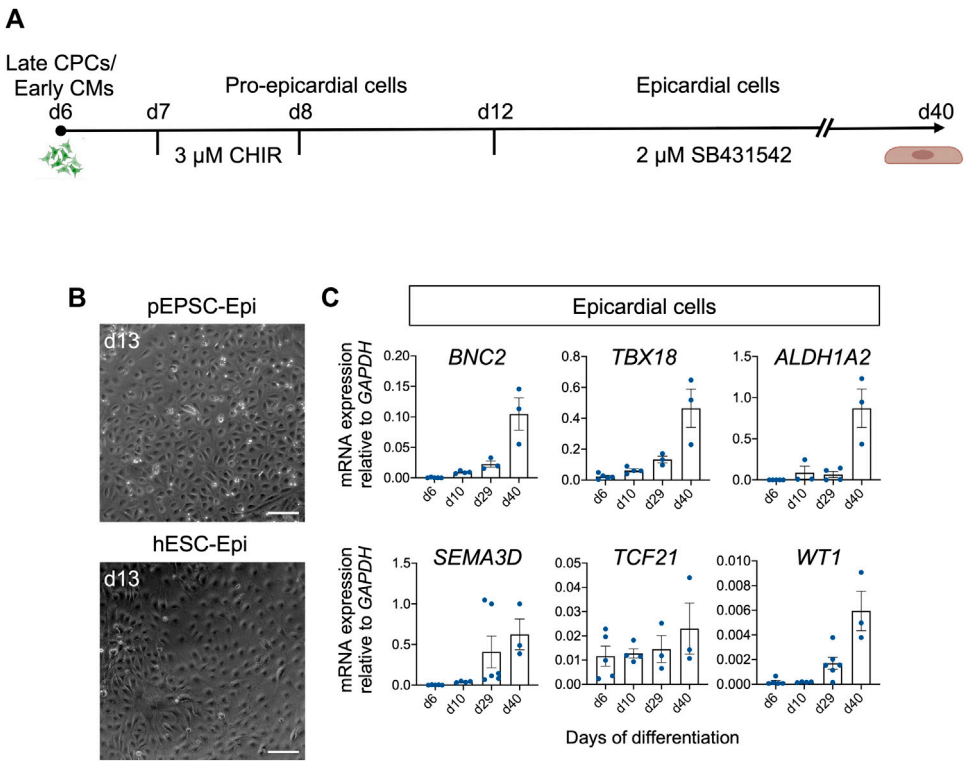

FIGURE 8
Differentiation of pEPSCs and hESCs into epicardial cells. **(A)** Graphical representation of the protocol used to differentiate pEPSCs and hESCs into epicardial cells. CHIR: CHIR99021. CPCs: cardiovascular progenitors, CMs: cardiomyocytes. **(B)** Representative bright-field images of hESC- and pEPSC-derived epicardial cells displaying typical cobblestone morphology at day 13 of differentiation. Scale bars: 100 μm. hESC-Epi: human embryonic stem cell-derived epicardial cells; pEPSC-Epi: porcine expanded potential stem cell-derived epicardial cells. **(C)** mRNA expression levels of markers specific for epicardial cells *BNC2*, *TBX18*, *ALDH1A2*, *SEMA3D*, *TCF21* and *WT1* relative to *GAPDH* at days 6, 10, 29, and 40 of differentiation. Data are mean ± SEM; *n* = 3–6 differentiations.

based on the induction of CPCs from pEPSCs as described above. On day 7, pEPSC-derived CPCs were directed to proepicardial cells by activation of Wnt signaling using GSK-3β inhibitor CHIR for 48 h (Figure 8A). At day 13, pEPSC-derived epicardial cells adopted typical epithelial cobblestone-like morphology similar to human cells (Figure 8B). Molecular analysis revealed progressive induction of well-established epicardial markers *BNC2*, *TBX18*, *ALDH1A2*, *SEMAD3*, *TCF21* and *WT1* during differentiation (Figure 8C), which was consistent with the expression pattern seen in hESC-derived epicardial cells (Bao et al., 2016; Iyer et al., 2016; Guadix et al., 2017). Immunofluorescence analysis showed that pEPSC-derived epicardial cells expressed WT1, cytokeratin 18 (CK18), and BNC1 proteins and formed tight junctions marked by ZO-1 expression along cell borders (Figure 9A). Furthermore, they also expressed aldehyde dehydrogenase enzyme retinaldehyde dehydrogenase 2 (ALDH1A2) (Figure 9A) indicating that these cells could synthesize retinoic acid, which is a sign of more mature functional epicardial cells (Witty et al., 2014). Of note, at day 12, some porcine $WT1^+$ cells co-expressed ISL1, resembling the expression pattern of hESC-derived epicardial cells *in vitro* (Figures 9A, B) (Sun et al., 2007). This was in line with our results from the native pig embryos at ED19 (Supplementary Figures S3A, A′) and with recent findings in the early developing epicardium of human embryos and hPSC-derived epicardioids (Meier et al., 2023), confirming a higher degree of similarity between pig and human cardiac development when compared to the mouse. Inhibition of TGF-β signaling by SB431542 enabled expansion of pEPSC-derived epicardial cells, which maintained their epithelial characteristics for more than 40 days (14 passages) (Figure 9A).

The *in vitro* generation of epicardial cells from pEPSCs provides a source of porcine epicardial cells for functional studies aimed at harnessing the regenerative capacity of the epicardium for therapeutic purposes.

Porcine epicardial cells undergo EMT to differentiate into SMCs, ECs and cardiac FBs

During cardiac development *in vivo*, a subset of epicardial cells undergo epithelial-to-mesenchymal transition (EMT) to become epicardial-derived cells (EPDCs) that migrate into the myocardium and give rise to several differentiated non-myocardial cell types including mural cells (vascular smooth muscle cells and pericytes) and cardiac FBs (Cai et al., 2003; Cai et al., 2008; Bao et al., 2016). However, differentiation into CMs and coronary endothelial cells is still debated (Quijada et al., 2020). Previous studies have shown that both mouse and human *in vitro*-derived epicardial cells possess the same potential (Witty et al., 2014; Iyer et al., 2016; Bao et al., 2017b; Meier et al., 2023).

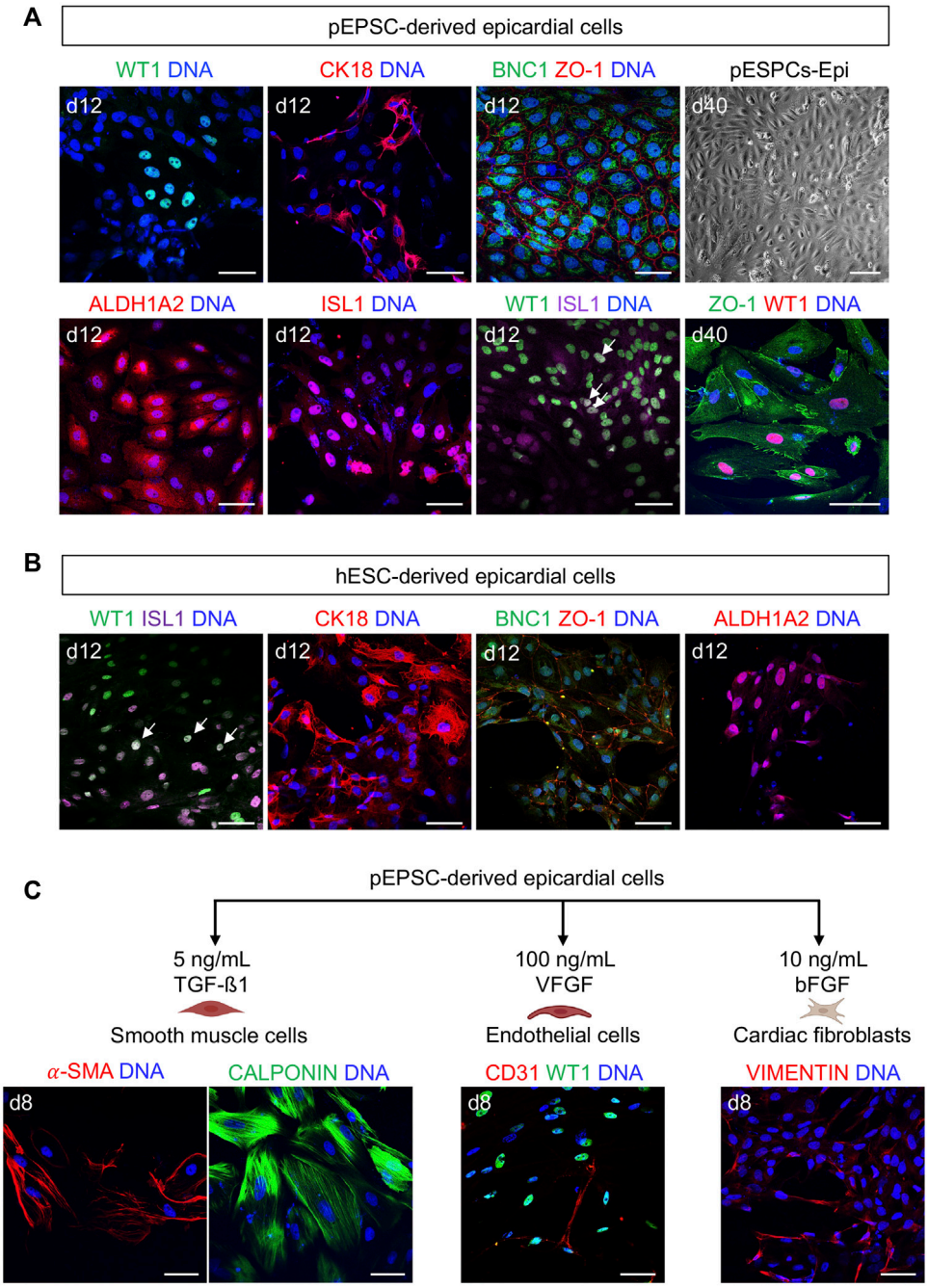

FIGURE 9
pEPSC-derived epicardial cells express similar epicardial markers to humans. **(A)** Representative bright-field image of pEPSC-derived epicardial cells at day 40 of differentiation displaying typical cobblestone morphology and immunofluorescence images after staining for WT1 (green), CK18 (red), BNC1 (green), ZO-1 (red), ALDH1A2 (red) and ISL1 (red) derived from pEPSCs. Nuclei were labeled with Hoechst 33528 (blue). WT1 (green)/ISL1 (magenta) co-expressing cells are marked with arrows. Scale bars: 50 µm. pEPSCs: porcine expanded potential stem cells. Scale bar: 100 µm, *n* = 6 independent differentiations. **(B)** Representative images of hESC-derived epicardial cells immunostained for ISL1 (magenta), WT1 (green), CK18 (red), BNC1 (green), ZO-1 (red) and ALDH1A2 (red). Nuclei were labeled with Hoechst 33528 (blue). Arrows: cells co-expressing WT1/ISL1. Scale bars: 50 µm, *n* = 1 differentiation. **(C)** Graphical representation of the protocols used to differentiate pEPSC-derived epicardial cells into SMCs, ECs and cardiac FBs. Representative images of SMCs immunostained for CALPONIN (green) and ALPHA SMOOTH MUSCLE ACTIN (α-SMA) (red), ECs stained for CD31 (red) together with epicardial cells stained for WT1 (green) and cardiac FBs stained for fibroblast marker VIMENTIN (red). Scale bars: 50 µm, *n* = 3 independent differentiations.

We adopted the protocol published by Bao et al. (2017a, b) to initiate epicardial EMT *in vitro* from pEPSC-derived epicardial cells and induce SMCs, ECs and FBs differentiation (Figure 9C). SMCs could be differentiated upon TGF-β1 treatment and expressed both CALPONIN and ALPHA SMOOTH MUSCLE ACTININ (α-SMA). Maintaining cultures in the presence of bFGF led to a generation FBs-

like cells expressing VIMENTIN, whereas angiogenic growth factor VEGF promoted emergence of ECs expressing CD31 (Figure 9C).

Discussion

The pig represents one of the large animal models currently used in human disease-related translational research (Romagnuolo et al., 2019; Zhao et al., 2021; Poch et al., 2022). Several studies in the past described pre-gastrulation and gastrulation processes in pigs (Flechon et al., 2004; Oestrup et al., 2009); however, little is known about porcine heart development. Recently, a developmental profile of the cardiovascular system in porcine embryos has been described by Gabriel et al. (2021) and Lauschke et al. (2021), providing the first insights into porcine cardiogenesis. Still, the knowledge of early porcine heart development is very limited and a more detailed, comprehensive, stage-by-stage characterization of molecular determinants is needed. Our study provides a detailed anatomical and molecular analysis of porcine development from the primitive streak stage to the four-chambered beating heart. For the first time, we identified and molecularly characterized porcine proepicardium and epicardium during embryonic development. Our findings highlight previously unappreciated differences between porcine and murine epicardium, which are conserved in human.

In pig, gastrulation starts with the appearance of the primitive streak marked by the expression of TBXT at ED13/ED14 (Hyttel et al., 2011). The earliest cardiac mesoderm progenitors migrate from the primitive streak to form the cardiac crescent (Lescroart et al., 2014; Ivanovitch et al., 2021). We found the first cells marked by cTNT in splanchnic mesoderm in the porcine embryo at ED14, which formed a horseshoe-shaped structure resembling the cardiac crescent. We observed the generation of a linear heart tube at ED15, which is in line with the results published by Lauschke et al. (2021). Porcine ED17 was marked by the presence of PEO, which has not been previously characterized in porcine embryos. By ED19, the porcine heart showed tremendous growth and became four-chambered, corresponding to ED20/ED22 as described by Lauschke et al. (2021).

The expression of pan-cardiac markers ISL1 and NKX2.5 observed in porcine ED14, ED15, ED17 and ED19 overlapped with mouse and human expression pattern (Elliott et al., 2003; Kelly et al., 2014; Zhang et al., 2014; Ren et al., 2021). Importantly, for the first time, we identified and characterized porcine PEO cells expressing WT1 at ED17, showing similar WT1 expression dynamics to humans and mice (Zhou et al., 2008; Risebro et al., 2015). Intriguingly, at ED17 we observed some $WT1^+$ and $ISL1^+$ cells migrating toward the myocardium and forming the epicardium of the developing heart. This data highlights previously unappreciated differences between pig and mouse epicardial cells, as the latter do not express ISL1 (Sun et al., 2007), and similarity to the human counterpart (Meier et al., 2023). A more detailed analysis will be necessary to fully characterize the origin and differentiation potential of these cells in the pig. It has been shown in mouse that $WT1^+$ PEO progenitors are derived from $ISL1^+/NKX2.5^+$ precursors (Zhou et al., 2008) and that epicardial cells give rise to the coronary vasculature and potentially to a small population of myocytes during embryonic and postnatal development (Dorn et al., 2018; Wagner et al., 2021). In human fetal and adult heart $WT1^+$ cells were found in epicardium, sub-epicardium, and myocardial layer (Duim et al., 2016).

An improved understanding of porcine cardiac development is essential not only for studying cardiac physiology but also for developing cell-based therapies for preclinical testing. The limited regenerative capacity of the adult heart is insufficient to replace damaged CMs leading to heart failure (Eschenhagen et al., 2017; Tzahor and Poss, 2017). Heart transplantation is usually the only available treatment option for patients with end-stage heart failure but it is limited by the discrepancy between the availability of donors and recipients (Boilson et al., 2010; Tzahor and Poss, 2017). Therefore, there is enormous interest in tissue-engineered porcine biomaterials or cell replacement-based therapies aimed at the repopulation of damaged cardiac tissue in the pig as preclinical model (Cui et al., 2005; Foo et al., 2018; Miia et al., 2021; Maselli et al., 2022). From a clinical perspective, allogeneic and autologous cell therapies may provide a better understanding of the respective immunological responses and the corresponding immunosuppression regimens for future PSC-derived cell therapies in humans (Wu et al., 2012; Stauske et al., 2020). Until now, for testing of allogenic therapies in the porcine heart infarct model, CPCs derived directly from heart biopsy were used (Crisostomo et al., 2015; Prat-Vidal et al., 2021). The disadvantage of these cells is their limited proliferation potential *in vitro* and, thus constant need of replacement by new donor animals. Therefore, exploring the prospects and safety of preclinical cell therapy creates interest in the establishment of cardiac cells directly from pESCs. In the present study, for the first-time pEPSCs could be directed to differentiate into functional cardiac and epicardial lineages, *in vitro*, recapitulating the differentiation potential of hPSCs towards ventricular-like CMs and epicardial cells. Thus, these cells offer a valuable source of pEPSC-derived CPCs, CMs and epicardial cells for future preclinical testing of autologous and allogeneic cardiac cell therapies and would be an authentic reflection of human physiology in preclinical studies. Furthermore, pEPSC-derived CPCs can be functionally validated using *ex utero* porcine embryo culture platform, allowing for faithful recapitulation of porcine cardiac development outside the uterus.

Data availability statement

The original contributions presented in the study are included in the article/Supplementary Material, further inquiries can be directed to the corresponding authors.

Ethics statement

The animal study was reviewed and approved by local regulatory authority.

Author contributions

MN-I and TD conceived the study and interpreted the data. MN-I designed and performed all of the experiments using

pEPSCs, analysed data, prepared figures, and wrote the draft. TD and MN-I performed functional assays. SB supported the maintenance and differentiation of pEPSCs, some molecular assays, and immunostainings. DZ provided hPSC-derived CPCs, experimental suggestion/advice, and supported data analysis and interpretation. HR and JK performed embryo analysis, *ex utero* pig experiments, and prepared embryo figures. AB supported the organization of animals and the isolation of pig embryos. AM, K-LL, and CK funded the research. TD, DZ, HR, JK, and AM revised and edited the draft. All authors have read and agreed to the published version of the manuscript.

Funding

This work was supported by the European Research Council (ERC) (grant 788381 to AM and grant 101021043 to CK). Several authors of this study are principal investigators of the Transregio Research Units 152 and 267 funded by the German Research Foundation.

Acknowledgments

We would like to acknowledge Birgit Campbell, Christina Scherb, and Marco Crovella for their technical assistance.

All figures were created using Prism 9 (GraphPad Software) or BioRender (https://biorender.com) with appropriate licenses.

Conflict of interest

The authors declare that the research was conducted in the absence of any commercial or financial relationships that could be construed as a potential conflict of interest.

Publisher's note

All claims expressed in this article are solely those of the authors and do not necessarily represent those of their affiliated organizations, or those of the publisher, the editors and the reviewers. Any product that may be evaluated in this article, or claim that may be made by its manufacturer, is not guaranteed or endorsed by the publisher.

Supplementary material

The Supplementary Material for this article can be found online at: https://www.frontiersin.org/articles/10.3389/fcell.2023.1111684/full#supplementary-material

References

Aguilera-Castrejon, A., Oldak, B., Shani, T., Ghanem, N., Itzkovich, C., Slomovich, S., et al. (2021). Ex utero mouse embryogenesis from pre-gastrulation to late organogenesis. *Nature* 593 (7857), 119–124. doi:10.1038/s41586-021-03416-3

Bao, X. P., Lian, X., Hacker, T. A., Schmuck, E. G., Qian, T., Bhute, V. J., et al. (2016). Long-term self-renewing human epicardial cells generated from pluripotent stem cells under defined xeno-free conditions. *Nat. Biomed. Eng.* 1, 0003. doi:10.1038/s41551-016-0003

Bao, X., Bhute, V. J., Han, T., Qian, T., Lian, X., and Palecek, S. P. (2017a). Human pluripotent stem cell-derived epicardial progenitors can differentiate to endocardial-like endothelial cells. *Bioeng. Transl. Med.* 2 (2), 191–201. doi:10.1002/btm2.10062

Bao, X. P., Lian, X. J., Qian, T. C., Bhute, V. J., Han, T. X., and Palecek, S. P. (2017b). Directed differentiation and long-term maintenance of epicardial cells derived from human pluripotent stem cells under fully defined conditions. *Nat. Protoc.* 12 (9), 1890–1900. doi:10.1038/nprot.2017.080

Boilson, B. A., Raichlin, E., Park, S. J., and Kushwaha, S. S. (2010). Device therapy and cardiac transplantation for end-stage heart failure. *Curr. Probl. Cardiol.* 35 (1), 8–64. doi:10.1016/j.cpcardiol.2009.09.001

Brade, T., Pane, L. S., Moretti, A., Chien, K. R., and Laugwitz, K. L. (2013). Embryonic heart progenitors and cardiogenesis. *Cold Spring Harb. Perspect. Med.* 3 (10), a013847. doi:10.1101/cshperspect.a013847

Buijtendijk, M. F. J., Barnett, P., and van den Hoff, M. J. B. (2020). Development of the human heart. *Am. J. Med. Genet. C Semin. Med. Genet.* 184 (1), 7–22. doi:10.1002/ajmg.c.31778

Cai, C. L., Liang, X., Shi, Y., Chu, P. H., Pfaff, S. L., Chen, J., et al. (2003). Isl1 identifies a cardiac progenitor population that proliferates prior to differentiation and contributes a majority of cells to the heart. *Dev. Cell* 5 (6), 877–889. doi:10.1016/s1534-5807(03)00363-0

Cai, J., DeLaForest, A., Fisher, J., Urick, A., Wagner, T., Twaroski, K., et al. (2008). "Protocol for directed differentiation of human pluripotent stem cells toward a hepatocyte fate," in *StemBook* (Cambridge (MA).

Cao, Y., Duca, S., and Cao, J. (2020). Epicardium in heart development. *Cold Spring Harb. Perspect. Biol.* 12 (2), a037192. doi:10.1101/cshperspect.a037192

Chen, Z., Xian, W., Bellin, M., Dorn, T., Tian, Q., Goedel, A., et al. (2017). Subtype-specific promoter-driven action potential imaging for precise disease modelling and drug testing in hiPSC-derived cardiomyocytes. *Eur. Heart J.* 38 (4), 292–301. doi:10.1093/eurheartj/ehw189

Crisostomo, V., Baez-Diaz, C., Maestre, J., Garcia-Lindo, M., Sun, F., Casado, J. G., et al. (2015). Delayed administration of allogeneic cardiac stem cell therapy for acute myocardial infarction could ameliorate adverse remodeling: Experimental study in swine. *J. Transl. Med.* 13, 156. doi:10.1186/s12967-015-0512-2

Cui, J. H., Li, J. H., Mathison, M., Tondato, F., Mulkey, S. P., Micko, C., et al. (2005). A clinically relevant large-animal model for evaluation of tissue-engineered cardiac surgical patch materials. *Cardiovasc. Revasc. Med.* 6 (3), 113–120. doi:10.1016/j.carrev.2005.07.006

Das, S., Koyano-Nakagawa, N., Gafni, O., Maeng, G., Singh, B. N., Rasmussen, T., et al. (2020). Generation of human endothelium in pig embryos deficient in ETV2. *Nat. Biotechnol.* 38 (3), 297–302. doi:10.1038/s41587-019-0373-y

Diaz Del Moral, S., Barrena, S., Hernandez-Torres, F., Aranega, A., Villaescusa, J. M., Gomez Doblas, J. J., et al. (2021). Deletion of the wilms' tumor suppressor gene in the cardiac troponin-T lineage reveals novel functions of WT1 in heart development. *Front. Cell Dev. Biol.* 9, 683861. doi:10.3389/fcell.2021.683861

Dorn, T., Kornherr, J., Parrotta, E. I., Zawada, D., Ayetey, H., Santamaria, G., et al. (2018). Interplay of cell-cell contacts and RhoA/MRTF-A signaling regulates cardiomyocyte identity. *EMBO J.* 37 (12), e98133. doi:10.15252/embj.201798133

Duim, S. N., Smits, A. M., Kruithof, B. P., and Goumans, M. J. (2016). The roadmap of WT1 protein expression in the human fetal heart. *J. Mol. Cell Cardiol.* 90, 139–145. doi:10.1016/j.yjmcc.2015.12.008

Elliott, D. A., Kirk, E. P., Yeoh, T., Chandar, S., McKenzie, F., Taylor, P., et al. (2003). Cardiac homeobox gene NKX2-5 mutations and congenital heart disease: Associations with atrial septal defect and hypoplastic left heart syndrome. *J. Am. Coll. Cardiol.* 41 (11), 2072–2076. doi:10.1016/s0735-1097(03)00420-0

Eschenhagen, T., Bolli, R., Braun, T., Field, L. J., Fleischmann, B. K., Frisen, J., et al. (2017). Cardiomyocyte regeneration: A consensus statement. *Circulation* 136 (7), 680–686. doi:10.1161/CIRCULATIONAHA.117.029343

Fischer, B., Meier, A., Dehne, A., Salhotra, A., Tran, T. A., Neumann, S., et al. (2018). A complete workflow for the differentiation and the dissociation of hiPSC-derived cardiospheres. *Stem Cell Res.* 32, 65–72. doi:10.1016/j.scr.2018.08.015

Flechon, J. E., Degrouard, J., and Flechon, B. (2004). Gastrulation events in the prestreak pig embryo: Ultrastructure and cell markers. *Genesis* 38 (1), 13–25. doi:10.1002/gene.10244

Foo, K. S., Lehtinen, M. L., Leung, C. Y., Lian, X. J., Xu, J. J., Keung, W., et al. (2018). Human ISL1(+) ventricular progenitors self-assemble into an *in vivo* functional heart patch and preserve cardiac function post infarction. *Mol. Ther.* 26 (7), 1644–1659. doi:10.1016/j.ymthe.2018.02.012

Gabriel, G. C., Devine, W., Redel, B. K., Whitworth, K. M., Samuel, M., Spate, L. D., et al. (2021). Cardiovascular development and congenital heart disease modeling in the pig. *J. Am. Heart Assoc.* 10 (14), e021631. doi:10.1161/JAHA.121.021631

Gao, X., Nowak-Imialek, M., Chen, X., Chen, D., Herrmann, D., Ruan, D., et al. (2019). Establishment of porcine and human expanded potential stem cells. *Nat. Cell Biol.* 21 (6), 687–699. doi:10.1038/s41556-019-0333-2

Goedel, A., Zawada, D. M., Zhang, F., Chen, Z., Moretti, A., and Sinnecker, D. (2018). Subtype-specific optical action potential recordings in human induced pluripotent stem cell-derived ventricular cardiomyocytes. *J. Vis. Exp.* 139, 58134. doi:10.3791/58134

Guadix, J. A., Orlova, V. V., Giacomelli, E., Bellin, M., Ribeiro, M. C., Mummery, C. L., et al. (2017). Human pluripotent stem cell differentiation into functional epicardial progenitor cells. *Stem Cell Rep.* 9 (6), 1754–1764. doi:10.1016/j.stemcr.2017.10.023

Hofbauer, P., Jahnel, S. M., Papai, N., Giesshammer, M., Deyett, A., Schmidt, C., et al. (2021). Cardioids reveal self-organizing principles of human cardiogenesis. *Cell* 184 (12), 3299–3317.e22. doi:10.1016/j.cell.2021.04.034

Hughes, H. C. (1986). Swine in cardiovascular research. *Lab. Anim. Sci.* 36 (4), 348–350.

Hyttel, P., Kamstrup, K. M., and Hyldig, S. M. W. (2011). From hatching into fetal life in the pig. *Acta Sci. Veterinariae* 39, 203–221.

Ivanovitch, K., Soro-Barrio, P., Chakravarty, P., Jones, R. A., Bell, D. M., Mousavy Gharavy, S. N., et al. (2021). Ventricular, atrial, and outflow tract heart progenitors arise from spatially and molecularly distinct regions of the primitive streak. *PLoS Biol.* 19 (5), e3001200. doi:10.1371/journal.pbio.3001200

Iyer, D., Gambardella, L., Bernard, W. G., Serrano, F., Mascetti, V. L., Pedersen, R. A., et al. (2016). Robust derivation of epicardium and its differentiated smooth muscle cell progeny from human pluripotent stem cells. *Development* 143 (5), 904. doi:10.1242/dev.136143

Kasahara, H., Bartunkova, S., Schinke, M., Tanaka, M., and Izumo, S. (1998). Cardiac and extracardiac expression of Csx/Nkx2.5 homeodomain protein. *Circ. Res.* 82 (9), 936–946. doi:10.1161/01.res.82.9.936

Kelly, R. G., Buckingham, M. E., and Moorman, A. F. (2014). Heart fields and cardiac morphogenesis. *Cold Spring Harb. Perspect. Med.* 4 (10), a015750. doi:10.1101/cshperspect.a015750

Krishnan, A., Samtani, R., Dhanantwari, P., Lee, E., Yamada, S., Shiota, K., et al. (2014). A detailed comparison of mouse and human cardiac development. *Pediatr. Res.* 76 (6), 500–507. doi:10.1038/pr.2014.128

Lauschke, K., Volpini, L., Liu, Y., Vinggaard, A. M., and Hall, V. J. (2021). A comparative assessment of marker expression between cardiomyocyte differentiation of human induced pluripotent stem cells and the developing pig heart. *Stem Cells Dev.* 30 (7), 374–385. doi:10.1089/scd.2020.0184

Lelovas, P. P., Kostomitsopoulos, N. G., and Xanthos, T. T. (2014). A comparative anatomic and physiologic overview of the porcine heart. *J. Am. Assoc. Lab. Anim. Sci.* 53 (5), 432–438.

Lescroart, F., Chabab, S., Lin, X., Rulands, S., Paulissen, C., Rodolosse, A., et al. (2014). Early lineage restriction in temporally distinct populations of Mesp1 progenitors during mammalian heart development. *Nat. Cell Biol.* 16 (9), 829–840. doi:10.1038/ncb3024

Lints, T. J., Parsons, L. M., Hartley, L., Lyons, I., and Harvey, R. P. (1993). Nkx-2.5: A novel murine homeobox gene expressed in early heart progenitor cells and their myogenic descendants. *Development* 119 (3), 969. doi:10.1242/dev.119.3.969

Lyons, I., Parsons, L. M., Hartley, L., Li, R., Andrews, J. E., Robb, L., et al. (1995). Myogenic and morphogenetic defects in the heart tubes of murine embryos lacking the homeo box gene Nkx2-5. *Genes Dev.* 9 (13), 1654–1666. doi:10.1101/gad.9.13.1654

Maselli, D., Matos, R. S., Johnson, R. D., Martella, D., Caprettini, V., Chiappini, C., et al. (2022). Porcine organotypic epicardial slice protocol: A tool for the study of epicardium in cardiovascular research. *Front. Cardiovasc Med.* 9, 920013. doi:10.3389/fcvm.2022.920013

Meier, A. B., Zawada, D., De Angelis, M. T., Martens, L. D., Santamaria, G., Zengerle, S., et al. (2023). Epicardioid single-cell genomics uncovers principles of human epicardium biology in heart development and disease. *Nat. Biotechnol.* doi:10.1038/s41587-023-01718-7

Meilhac, S. M., and Buckingham, M. E. (2018). The deployment of cell lineages that form the mammalian heart. *Nat. Rev. Cardiol.* 15 (11), 705–724. doi:10.1038/s41569-018-0086-9

Mendjan, S., Mascetti, V. L., Ortmann, D., Ortiz, M., Karjosukarso, D. W., Ng, Y., et al. (2014). NANOG and CDX2 pattern distinct subtypes of human mesoderm during exit from pluripotency. *Cell Stem Cell* 15 (3), 310–325. doi:10.1016/j.stem.2014.06.006

Miia, K. S. F., Leung, C. Y., Lian, X. J., Xu, J. J., Keung, W., Geng, L., et al. (2021). Human ISL1(+) ventricular progenitors self-assemble into an *in vivo* functional heart patch and preserve cardiac function post infarction (vol 26, pg 1644, 2018). *Mol. Ther.* 29 (1), 409. doi:10.1016/j.ymthe.2020.11.015

Mommersteeg, M. T., Dominguez, J. N., Wiese, C., Norden, J., de Gier-de Vries, C., Burch, J. B., et al. (2010). The sinus venosus progenitors separate and diversify from the first and second heart fields early in development. *Cardiovasc Res.* 87 (1), 92–101. doi:10.1093/cvr/cvq033

Moretti, A., Caron, L., Nakano, A., Lam, J. T., Bernshausen, A., Chen, Y., et al. (2006). Multipotent embryonic isl1+ progenitor cells lead to cardiac, smooth muscle, and endothelial cell diversification. *Cell* 127 (6), 1151–1165. doi:10.1016/j.cell.2006.10.029

Moretti, A., Fonteyne, L., Giesert, F., Hoppmann, P., Meier, A. B., Bozoglu, T., et al. (2020). Somatic gene editing ameliorates skeletal and cardiac muscle failure in pig and human models of Duchenne muscular dystrophy. *Nat. Med.* 26 (2), 207–214. doi:10.1038/s41591-019-0738-2

Niderla-Bielinska, J., Jankowska-Steifer, E., Flaht-Zabost, A., Gula, G., Czarnowska, E., and Ratajska, A. (2019). Proepicardium: Current understanding of its structure, induction, and fate. *Anat. Rec. Hob.* 302 (6), 893–903. doi:10.1002/ar.24028

Oestrup, O., Hall, V., Petkov, S. G., Wolf, X. A., Hyldig, S., and Hyttel, P. (2009). From zygote to implantation: Morphological and molecular dynamics during embryo development in the pig. *Reprod. Domest. Anim.* 44, 39–49. doi:10.1111/j.1439-0531.2009.01482.x

Paige, S. L., Plonowska, K., Xu, A., and Wu, S. M. (2015). Molecular regulation of cardiomyocyte differentiation. *Circ. Res.* 116 (2), 341–353. doi:10.1161/CIRCRESAHA.116.302752

Poch, C. M., Foo, K. S., De Angelis, M. T., Jennbacken, K., Santamaria, G., Bahr, A., et al. (2022). Migratory and anti-fibrotic programmes define the regenerative potential of human cardiac progenitors. *Nat. Cell Biol.* 24 (5), 659–671. doi:10.1038/s41556-022-00899-8

Prat-Vidal, C., Crisostomo, V., Moscoso, I., Baez-Diaz, C., Blanco-Blazquez, V., Gomez-Mauricio, G., et al. (2021). Intracoronary delivery of porcine cardiac progenitor cells overexpressing IGF-1 and HGF in a pig model of sub-acute myocardial infarction. *Cells* 10 (10), 2571. doi:10.3390/cells10102571

Quijada, P., Trembley, M. A., and Small, E. M. (2020). The role of the epicardium during heart development and repair. *Circ. Res.* 126 (3), 377–394. doi:10.1161/CIRCRESAHA.119.315857

Ren, J., Miao, D., Li, Y., and Gao, R. (2021). Spotlight on Isl1: A key player in cardiovascular development and diseases. *Front. Cell Dev. Biol.* 9, 793605. doi:10.3389/fcell.2021.793605

Risebro, C. A., Vieira, J. M., Klotz, L., and Riley, P. R. (2015). Characterisation of the human embryonic and foetal epicardium during heart development. *Development* 142 (21), 3630–3636. doi:10.1242/dev.127621

Romagnuolo, R., Masoudpour, H., Porta-Sanchez, A., Qiang, B. P., Barry, J., Laskary, A., et al. (2019). Human embryonic stem cell-derived cardiomyocytes regenerate the infarcted pig heart but induce ventricular tachyarrhythmias. *Stem Cell Rep.* 12 (5), 967–981. doi:10.1016/j.stemcr.2019.04.005

Ruiz-Villalba, A., Ziogas, A., Ehrbar, M., and Perez-Pomares, J. M. (2013). Characterization of epicardial-derived cardiac interstitial cells: Differentiation and mobilization of heart fibroblast progenitors. *PLoS One* 8 (1), e53694. doi:10.1371/journal.pone.0053694

Stauske, M., Rodriguez Polo, I., Haas, W., Knorr, D. Y., Borchert, T., Streckfuss-Bomeke, K., et al. (2020). Non-human primate iPSC generation, cultivation, and cardiac differentiation under chemically defined conditions. *Cells* 9 (6), 1349. doi:10.3390/cells9061349

Stirm, M., Fonteyne, L. M., Shashikadze, B., Stockl, J. B., Kurome, M., Kessler, B., et al. (2022). Pig models for Duchenne muscular dystrophy - from disease mechanisms to validation of new diagnostic and therapeutic concepts. *Neuromuscul. Disord.* 32 (7), 543–556. doi:10.1016/j.nmd.2022.04.005

Sun, Y., Liang, X., Najafi, N., Cass, M., Lin, L., Cai, C. L., et al. (2007). Islet 1 is expressed in distinct cardiovascular lineages, including pacemaker and coronary vascular cells. *Dev. Biol.* 304 (1), 286–296. doi:10.1016/j.ydbio.2006.12.048

Tzahor, E., and Poss, K. D. (2017). Cardiac regeneration strategies: Staying young at heart. *Science* 356 (6342), 1035–1039. doi:10.1126/science.aam5894

Wagner, N., Wagner, K. D., Theres, H., Englert, C., Schedl, A., and Scholz, H. (2005). Coronary vessel development requires activation of the TrkB neurotrophin receptor by the Wilms' tumor transcription factor Wt1. *Genes Dev.* 19 (21), 2631–2642. doi:10.1101/gad.346405

Wagner, N., Ninkov, M., Vukolic, A., Cubukcuoglu Deniz, G., Rassoulzadegan, M., Michiels, J. F., et al. (2021). Implications of the wilms' tumor suppressor Wt1 in cardiomyocyte differentiation. *Int. J. Mol. Sci.* 22 (9), 4346. doi:10.3390/ijms22094346

Wei, R., Lv, J., Li, X., Li, Y., Xu, Q., Jin, J., et al. (2020). Derivation of endothelial cells from porcine induced pluripotent stem cells by optimized single layer culture system. *J. Vet. Sci.* 21 (1), e9. doi:10.4142/jvs.2020.21.e9

Witty, A. D., Mihic, A., Tam, R. Y., Fisher, S. A., Mikryukov, A., Shoichet, M. S., et al. (2014). Generation of the epicardial lineage from human pluripotent stem cells. *Nat. Biotechnol.* 32 (10), 1026–1035. doi:10.1038/nbt.3002

Wu, Y., Mishra, A., Qiu, Z., Farnsworth, S., Tardif, S. D., and Hornsby, P. J. (2012). Nonhuman primate induced pluripotent stem cells in regenerative medicine. *Stem Cells Int.* 2012, 767195. doi:10.1155/2012/767195

Zawada, D., Kornherr, J., Meier, A. B., Santamaria, G., Dorn, T., Nowak-Imialek, M., et al. (2023). Retinoic acid signaling modulation guides *in vitro* specification of human heart field-specific progenitor pools. *Nat. Commun.* 14 (1), 1722. doi:10.1038/s41467-023-36764-x

Zhang, L., Nomura-Kitabayashi, A., Sultana, N., Cai, W., Cai, X., Moon, A. M., et al. (2014). Mesodermal Nkx2.5 is necessary and sufficient for early second heart field development. *Dev. Biol.* 390 (1), 68–79. doi:10.1016/j.ydbio.2014.02.023

Zhao, M., Nakada, Y., Wei, Y., Bian, W., Chu, Y., Borovjagin, A. V., et al. (2021). Cyclin D2 overexpression enhances the efficacy of human induced pluripotent stem cell-derived cardiomyocytes for myocardial repair in a swine model of myocardial infarction. *Circulation* 144 (3), 210–228. doi:10.1161/CIRCULATIONAHA.120.049497

Zhi, M., Zhang, J., Tang, Q., Yu, D., Gao, S., Gao, D., et al. (2022). Generation and characterization of stable pig pregastrulation epiblast stem cell lines. *Cell Res.* 32 (4), 383–400. doi:10.1038/s41422-021-00592-9

Zhou, B., von Gise, A., Ma, Q., Rivera-Feliciano, J., and Pu, W. T. (2008). Nkx2-5- and Isl1-expressing cardiac progenitors contribute to proepicardium. *Biochem. Biophys. Res. Commun.* 375 (3), 450–453. doi:10.1016/j.bbrc.2008.08.044

Zhuang, S., Zhang, Q., Zhuang, T., Evans, S. M., Liang, X., and Sun, Y. (2013). Expression of Isl1 during mouse development. *Gene Expr. Patterns* 13 (8), 407–412. doi:10.1016/j.gep.2013.07.001

Frontiers in
Cell and Developmental Biology

Explores the fundamental biological processes of life, covering intracellular and extracellular dynamics.

The world's most cited developmental biology journal, advancing our understanding of the fundamental processes of life. It explores a wide spectrum of cell and developmental biology, covering intracellular and extracellular dynamics.

Discover the latest Research Topics

See more →

Frontiers

Avenue du Tribunal-Fédéral 34
1005 Lausanne, Switzerland
frontiersin.org

Contact us

+41 (0)21 510 17 00
frontiersin.org/about/contact